AED R-3318F
April 23, 1970

ITOS
Meteorological Satellite System

TIROS M Spacecraft (ITOS 1) Final Engineering Report

Volume III

Prepared for
Goddard Space Flight Center
National Aeronautics and Space Administration
Washington, D.C.
Contract No. NAS5-10306

RCA

RCA | Defense Electronic Products
Astro Electronics Division | Princeton, New Jersey

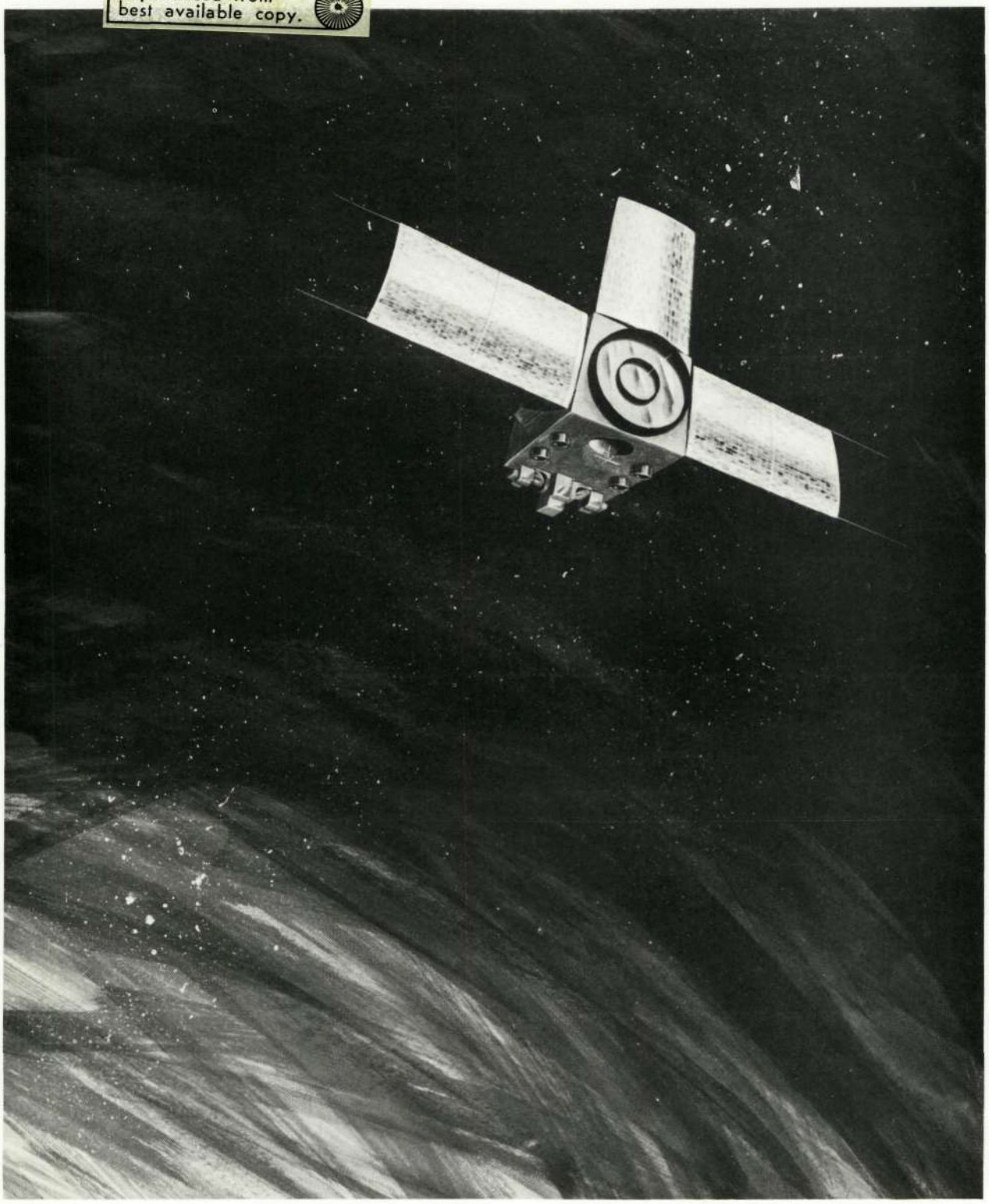

Artist's Concept of the ITOS Spacecraft

PREFACE

The TIROS M (ITOS 1) spacecraft was developed and built by the Astro-Electronics Division of RCA Corporation for the Goddard Space Flight Center of the National Aeronautics and Space Administration, under NASA Contract NAS5-10306. The TIROS M (ITOS 1) spacecraft was developed to meet the requirements of an Improved TIROS Operational System (ITOS) mission, and became, upon attaining successful operation in orbit, the first of the second-generation operational meteorological satellites.

This document provides system, subsystem, and component descriptions for the spacecraft and ground support equipment, and documents the design, development, testing, and integration phases of the program. It also describes the prelaunch and launch activities in which RCA personnel participated.

TABLE OF CONTENTS

TABLE OF CONTENTS (Continued)

PART 2. SPACECRAFT DESIGN

TABLE OF CONTENTS (Continued)

TABLE OF CONTENTS (Continued)

TABLE OF CONTENTS (Continued)

Section Page

Section Page

Section Page

Section Page

Section

Page

Section Page

TABLE OF CONTENTS (Continued)

Section Page

VOLUME III

PART 3. TEST HISTORIES

TABLE OF CONTENTS (Continued)

Section Page

Section Page

Section Page

VOLUME III

PART 4. TIROS M LAUNCH-SUPPORT OPERATIONS

TABLE OF CONTENTS (Continued)

TABLE OF CONTENTS (Continued)

TABLE OF CONTENTS (Continued)

TABLE OF CONTENTS (Continued)

LIST OF ILLUSTRATIONS

LIST OF ILLUSTRATIONS (Continued)

LIST OF ILLUSTRATIONS (Continued)

VOLUME II

PART 2 (Cont'd)

LIST OF ILLUSTRATIONS (Continued)

LIST OF ILLUSTRATIONS (Continued)

LIST OF ILLUSTRATIONS (Continued)

LIST OF ILLUSTRATIONS (Continued)

VOLUME III

PART 3. TEST HISTORIES

LIST OF ILLUSTRATIONS (Continued)

LIST OF ILLUSTRATIONS (Continued)

LIST OF ILLUSTRATIONS (Continued)

LIST OF ILLUSTRATIONS (Continued)

LIST OF ILLUSTRATIONS (Continued)

LIST OF TABLES

LIST OF TABLES (Continued)

VOLUME II

PART 2 (Cont'd)

LIST OF TABLES (Continued)

VOLUME III

PART 3. TEST HISTORIES

LIST OF TABLES (Continued)

LIST OF TABLES (Continued)

PART 3. TEST HISTORIES

PART 3. TEST HISTORIES

SECTION I. DESCRIPTION OF TEST PROGRAM

The test program documented in this report included the detailed flight acceptance and calibration program for the TIROS M spacecraft as well as the testing of full-scale spacecraft mechanical, thermal, antenna, and electrical models, and testing of engineering models and prototypes of the spacecraft components. The TIROS M portion of the test program consisted of subsystem and component testing of flight units during the subsystem qualification phase, and test operations on the integrated flight model spacecraft from the time that the subsystems were mounted on the spacecraft up to the time that the qualified spacecraft was launched.

The TIROS M program was subdivided into three major phases, as follows:

- Phase A, Component Testing
  - I. Board and Component Testing
  - II. Individual Component Qualification
- Phase B, Subsystem Testing
  - I. AVCS Subsystem
  - II. Pitch Control Subsystem
- Phase C, Spacecraft System Tests
  - I. Initial Assembly, Debugging and Interface Verification
  - II. System Evaluation and Prequalification Calibration Cycle
  - III. Environmental Qualification
  - IV. Final Calibration
  - V. Launch Site Testing

Phase A consisted of the qualification and testing of individual components (units and black boxes). A performance specification and test procedure detailed the tests necessary to qualify each component for prototype or flight use. Phase B consisted of the qualification and testing of certain individual subsystems prior to their integration into the spacecraft. A subsystem test plan detailed the various tests to be accomplished. Phase C I was a complete and systematic evaluation of the various

subsystem interfaces on the integrated flight model spacecraft. Phase C II was an evaluation of the spacecraft to ensure that it operated the same in a closed-up configuration as in an open configuration. A spacecraft Standard Electrical Performance Evaluation Test (SEPET) was performed to assure proper performance. The spacecraft received a prequalification calibration of the primary and secondary sensors during this testing phase. Phase C III was a detailed engineering demonstration of the operation and performance of the spacecraft system and a quantitative evaluation of its performance with respect to established parameters. In addition, it demonstrated the ability of the spacecraft to survive the launch and to operate reliably in the space environment. In Phase C IV, calibrated transfer functions were obtained for NASA and ESSA for use in deriving accurate meteorological information from the video and telemetry data being transmitted by the spacecraft in orbit. Phase C V consisted of the final tests and evaluations performed at the launch site.

Operating trends were noted through the comparison of sets of test data obtained throughout the program, as well as by comparing individual sets of data to a set of nominally established specifications. The results of the comparisons of sets of data verified the need for maintaining system integrity after the completion of Phase C III. Any equipment changes in the system tended to reduce or destroy the value of subsequent data. The use of data comparison accented the necessity for recording data in a quantitative form wherever possible, and provided for a positive and objective comparison of successive measurements.

Test data collected during the ITOS testing program was handled as follows:

- Data recorded during Phase A and Phase B was recorded on test data sheets during the test, which were monitored by Product Quality Control (PQC). The data sheets were retained in individual documentation folders.
- All test data obtained during Phase C was recorded on the data sheets provided. Test deviations, discrepancies, test history, and other pertinent test information were recorded in an engineer logbook. In addition, test discrepancies were written up on Test Discrepancy Reports (TDR's). Test data and logbooks were retained by Spacecraft Integration and made available for PQC and GSFC resident review.
- At the completion of Phase C I and prior to Flight Qualification Phase C III, a review of data was made by Spacecraft Qualification, Project Engineers, Product Assurance, and the GSFC resident to ensure satisfactory answers to all test discrepancy reports and satisfactory performance of the spacecraft. A review of spacecraft performance was held with the ITOS Environmental Committee.

- At the conclusion of Phase C II through Phase C IV, data and spacecraft performance were evaluated and critiqued prior to proceeding with the following phase. During these phases, all spacecraft failures were reviewed with the ITOS Environmental Committee to determine the necessity for additional spacecraft testing.
- During all phases, malfunctions were analyzed and reported in accordance with the ITOS Reliability Program Plan.
- During Phase A, individual component histories were maintained in separate documentation folders under the control of PQC to ensure adherence to the predetermined flow charts and checklists prepared for this program. These folders contain the following documents:

  Unit Evaluation Record (Inspection)

  Material Review Board Actions

  Flow Charts

  Checklists

  Test Discrepancy Reports

  Test Data Sheets

  Test Review Board Actions

This documentation was retained by the PQC activity for review during the manufacturing and testing of the components. It is now maintained in the library and handled as explained above.

In the following sections, the test program is divided into discussions of mechanical test model testing, thermal test model testing, antenna test model testing, electrical test model testing, component testing, and TIROS M spacecraft integration and testing, in that order.

SECTION II

MECHANICAL TEST MODEL TESTING

A. INTRODUCTION

The Mechanical Test Model (MTM) has had a three-fold function. It was used to:

- Verify the structural design.
- Verify, via fit checks, that mechanical tolerances are adequate
- Determine, via vibration testing, spacecraft resonances and transmitted vibration levels at various points in the spacecraft.

The purpose of the vibration tests was to meet the following requirements:

- To evaluate the structural integrity of the spacecraft separation ring and Douglas Aircraft Corporation (DAC) attach fitting,
- To evaluate the vibration response of several typical components,
- To observe RCA separation ring/DAC attach fitting interface area and note any unusual disturbances, and
- To measure dynamic response functions at a number of selected locations on the spacecraft structure.

The MTM was also used for measurements of moments of inertia, center of gravity, and axes of inertia. The MTM vibration tests were performed during November and December 1967, in accordance with Test Procedure ET-Y-3835, with minor deviations. Figures 3-II-1, 3-II-2, and 3-II-3 are photographs of the MTM. The test transducers used were strain gages and accelerometers.

A list of the components used in the MTM configuration, whether authentic flight version or dummy, is given in Table 3-II-1.

Data from the strain gages and accelerometers was reduced to X-Y plots, for both filtered and unfiltered responses. Low-level sine survey vibration tests preceded the full level prototype tests in all three axes. Data from the sine survey runs was not reduced to plots if the same channels were recorded during the prototype level tests. The lateral prototype input sinusoidal G-levels were notched in the vicinity of the fundamental frequencies to protect the DAC attach fitting from excessive loads. The test results are summarized in this section.

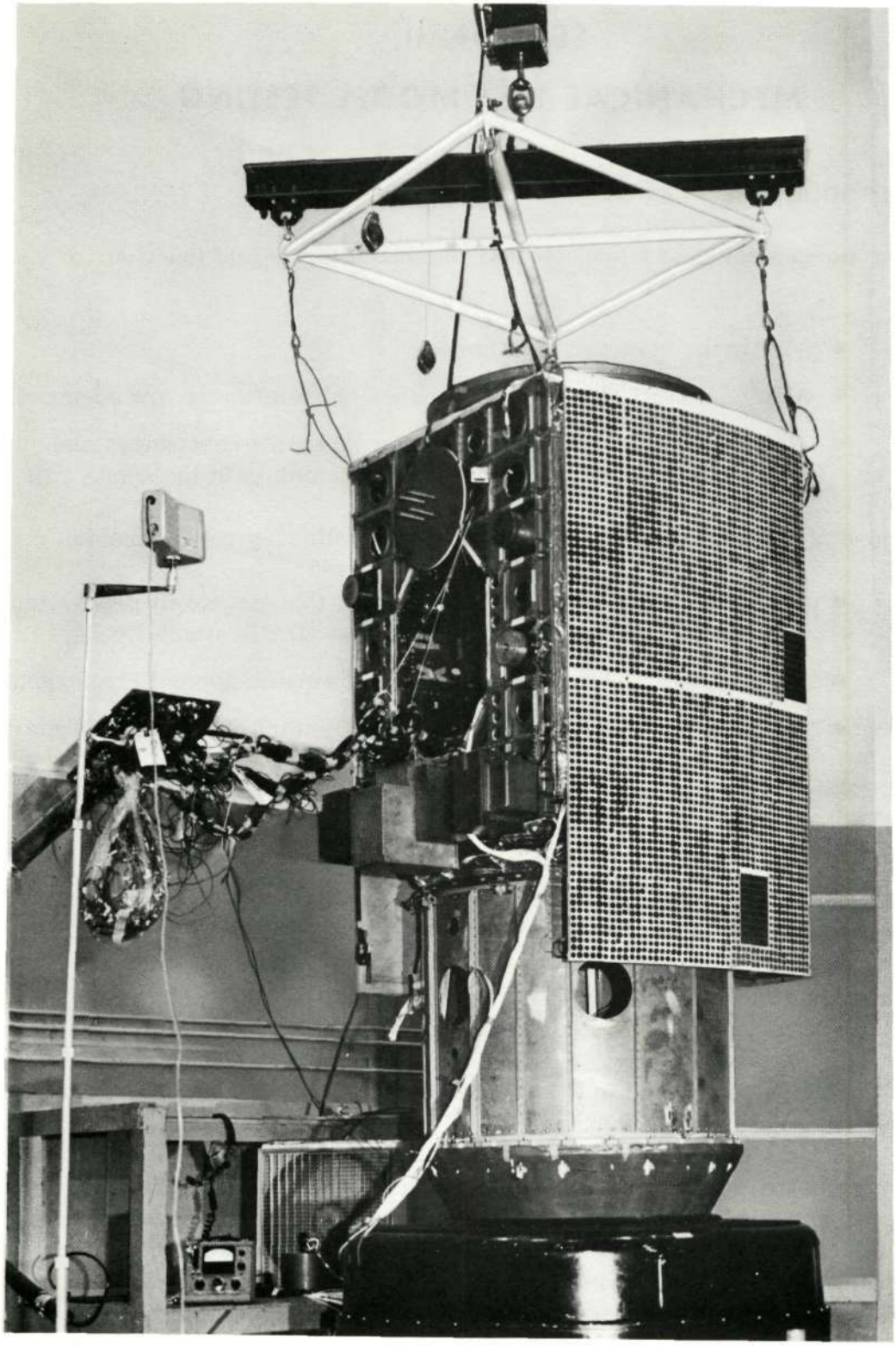

Figure 3-II-1. Mechanical Test Model with DAC Attach Fitting on the Vibration Test Fixture

Figure 3-II-2. MTM on Dynamic Balance Machine

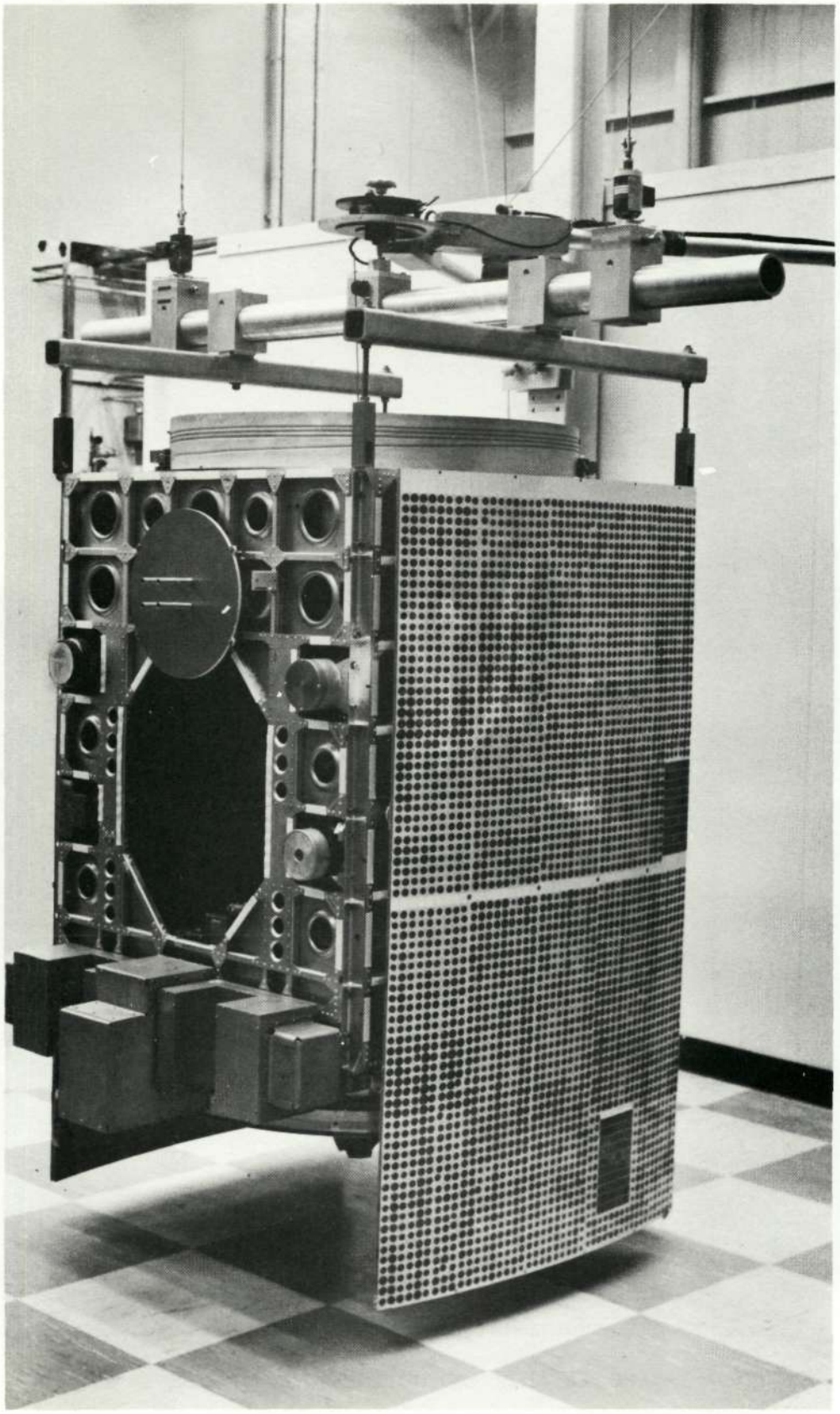

Figure 3-II-3. MTM Suspended in Bifilar Pendulum for Moments of Inertia Measurement

B. MTM TESTS

1. Summary

The MTM spacecraft structure successfully withstood the vibration tests. No evidence of damage was found except for these minor items:

(1) Flexing of a solar panel during the vibration test caused the two halves of a hinge to interfere with each other, which resulted in minor damage to one solar panel hinge bracket.

(2) The despin cables, which were not fully prestretched before installation, lost part of their preload. However, the weights freely released from the spacecraft with no entanglement of the cable or damage to the craft. Despin devices were subsequently eliminated from the TIROS M.

(3) The first sinusoidal survey (Y-axis) indicated that the anti-earth solar panel was not properly snubbed even though the recommended procedure had been followed. A new procedure was instituted, and the solar panels were readjusted to modified preload levels prior to subsequent vibration runs.

The condition of the structure before and after the vibration test is discussed in Paragraph 3.II.B.3.

A comparison between vibration test results and the pretest stress analysis revealed the following deviations:

(1) The calculated thrust spacecraft resonant frequency was higher than calculated, primarily because the DAC attach fitting was more compliant than estimated in the analysis. With the introduction of a modified compliancy constant into the calculations, natural frequencies were in good agreement with the test data, in all three directions.

(2) The baseplate showed edge fixity that was not accounted for in the analysis, which resulted in a higher baseplate natural frequency and bending stresses in the ribs that were 25 percent less than calculated.

(3) Bending stresses in the equipment panel were 25 percent higher than anticipated because of higher overall loading on the equipment panels. Nevertheless, the test stresses were within one half of the design values because of G-level notching during the lateral vibration tests. Induced stresses with an unnotched spectrum probably would not exceed the design values because of the normal drop in transmissibility at higher G-loadings. Finally, the unnotched responses could only be determined by test.

A comparison of the relative severity between black box test levels and vibration levels recorded on the structure indicated that the component test levels were adequate to verify the integrity of the black boxes. See the discussion in Paragraph 3.II.B.4.

NOTE

All the foregoing remarks apply to the 720-pound MTM configuration which included 25 pounds additional weight over the flight configuration. This weight represented future payload expansion in the form of growth boxes. Flight weight of the TIROS M is 682 pounds.

2. Mechanical Test Model Configuration

Table 3-II-1 lists the type of components employed during MTM vibration tests. The right-hand column states whether the components were of authentic flight configuration or dummy simulated.

3. Condition of Structure Before and After Vibration Test

a. GENERAL

After completion of vibration tests, the MTM was subjected to a thorough inspection. Areas of the structure, especially the center of the AVCS and APT equipment panels and the baseplate, were inspected for fatigue cracks using a Turco Dye check kit No. 15. The edges of the access holes in the access panels, solar panel hinges and the separation ring and spring pads were also tested using the same test kit. No stress or fatigue damage was noted in the above areas of the spacecraft due to its vibration exposure.

Torques on all structural bolts were measured with no change from the original readings noted. The torques on all accessible black box mounting hardware were also measured and no change from the original torque settings was noted.

The structure was also inspected for (1) the momentum wheel impacting the structure or separation spring brackets, (2) separation ring and separation spring damage, and (3) nutation damper oil leakage. No evidence of damage was found.

Contrary to the usual galling evidenced during TIROS/ TOS prototype level vibration tests at the separation plane, the mating surfaces on the new enlarged 37-inch diameter interface appeared absolutely clean.

TABLE 3-II-1. MTM COMPONENT TEST VERSIONS

Item	Test Version
Structure	Flight configuration
Solar Panels (3)	
Substrate	Flight configuration
Array	One with glass chips plus two 6x10 live circuits; two with metal chips
Solar Panel Harness	None
Shunt Limiters	Flight configured components on solar panels
Marman Clamp	Flight configuration
DAC Attach Fitting	Flight configuration
Liftoff Springs (4) and Brackets	Flight configuration
Thermal Fence	Flight configuration
Alzak Reflectors	Flight configuration
Despin Mechanism (2)	Flight configuration (without squibs)
Solar Panel Deployment and Latching Mechanism	
Actuator (ADEL)	Flight configuration
Pin Puller	Simulated flight-configured dummy
Lateral Restraints	Flight configuration
Center Snubber Supports	Flight configuration
Thermal Blankets	Flight configuration
Spacecraft Harness	Flight configuration (no connectors)
Balance Weights	None
RF Cabling and Misc. RF Components	None
ATC Louvers (4)	Flight configuration
Momentum Wheel	Flight configuration
Separation Switch (2)	Flight configuration
Real-Time Antennas (2)	Flight configuration
Beacon and Command Antenna	Flight configuration
AVCS Camera (1 only)	Simulated flight-configured dummy
APT Camera (1 only)	Simulated flight-configured dummy
Dummy Growth Boxes*	To bring spacecraft weight to nominal 720 lb

* Growth boxes represented future payload expansion.

TABLE 3-II-1. MTM COMPONENT TEST VERSIONS (Continued)

Black Boxes Simulated by Dummy Weights	
Incremental tape recorder	Digital solar aspect sensor (authentic bracket)
Battery (2)	Digital solar aspect electronics
Power supply electronics	Scanning radiometer (SR)
ATC actuator (4)	SR electronics
AVCS camera (1 only)	SR recorder (2)
APT camera (1 only)	SR recorder electronics (2)
AVCS electronics (2)	Dual command receiver
APT electronics (2)	Beacon transmitter & SCO
AVCS recorder (2)	S-band transmitter
AVCS recorder electronics (2)	Flat plate radiometer
Solar proton sensors	Acquisition sensor
Solar proton electronics	Dual decoder
Real-time transmitter	Command distribution units A& B
Dual multiplexer	Dual programmer
Signal cond. & telemetry unit	Dual IR processor
S-band array	Data format converter
Pitch control electronics	
Magnetic bias switch	

Only one instance of minor damage became apparent during the post test examination. Flexing of the solar panel during the vibration tests caused the two halves of the hinge bracket to interfere. A chamfer on both pieces removed this minor interference.

b. ALIGNMENT

To assure that the MTM structure would not be disturbed as a result of the imposed vibration levels, match marks were put precisely on the structure prior to vibration; in addition, discrete surfaces were measured with respect to the separation plane.

Vertical perpendicularity measurements taken after vibration indicated an average difference of 0.003-inch variation, compared to the measurements taken before vibration. The largest shift in perpendicularity was in the upper portion of the APT equipment panel and earth panel. This difference was measured at 0.006 inch. Measurements were obtained using a 4-foot precision height gage and a 0- to 1-inch dial indicator. These measurements were taken using the base of the spacecraft as the reference point and measuring at precisely 12-inch intervals. The cameras were measured also using the base of the spacecraft as the reference

point and measuring to the top of the cameras. There was a 0.004-inch difference noted after vibration as compared to the measurements taken before vibration. These values are well within acceptable limits (± 0.020-inch at camera and ± 0.032-inch at top of structure).

c. SOLAR PANEL PRELOAD

Inspection of data during the Y-axis sine survey indicated that the anti-earth solar panel was not properly snubbed even though the recommended procedure had been followed.

The preload was adjusted on the anti-earth solar panel between the Y-axis survey tests. When the proper adjustment was obtained for this panel, the remaining solar panels were adjusted to the proper value during the change of axis of the spacecraft. Preloads before and after vibration are given in Table 3-II-2.

TABLE 3-II-2. PRELOADING OF PANELS

Units	Before Vibration (lb)		After Vibration (lb)	
	Bumper	Jacks	Bumper	Jacks
APT Solar Panel	40	26-35	38 & 42	25
AVCS Solar Panel	40	26-35	47 & 45	24
Anti-Earth Solar Panel	40	26-35	38 & 40	20

The torque on the turnbuckles after vibration measured 8 to 10 in-lb. Torque measurements on the turnbuckles were not taken prior to vibration.

Review of test data indicates that the modified procedure properly meets the solar panel preloading requirements. The revised procedure for solar panel preloading will be incorporated on the proper drawings.

d. SOLAR PANEL DEPLOYMENT

Time measurements were made for the deployment of each of three solar panels before and after vibration. The time recorded starts when the pin is pulled until the panel deployment is stopped by bottoming in the actuator (Table 3-II-3).

TABLE 3-II-3. PANEL DEPLOYMENT TIMES

Unit	Before Vibration(s)	After Vibration(s)
APT Solar Panel	61	70
AVCS Solar Panel	59	65
Anti-Earth Solar Panel	65	70
Note: These values are within acceptable limits (52 to 72 s at 70°F).		

e. REAL-TIME ANTENNA DEPLOYMENT

Antenna deployment tests were conducted before and after the vibration test. Fast-action films of the previbration deployment tests revealed that excessive whipping of the antennas resulted in the antennas hitting one another during deployment. The addition of 0.010-inch thick beryllium-copper banking strips, at the base of the antenna, considerably retarded the whipping action. Fast action film was again taken of the antenna deployment after completion of vibration tests. Over-travel of the antennas beyond the normal deployed position was kept to a minimum, and the two antennas did not contact each other.

f. ACTIVE THERMAL CONTROLLER

The active thermal control louvers were successfully deployed both before and after the vibration test. High speed film was taken of the louver motion before the vibration test. The deployment action was normal.

4. List of Components With Responses Over 10 G

TIROS M/ITOS components are qualified to a component prototype sinusoidal vibration level of 10 G in each of three axes from 5 Hz to 2000 Hz. To ensure that these components will not experience a more severe vibration environment when mounted on the spacecraft, the vibration response test data was reviewed for items which exceed 10 G. These items and their G levels are listed in Table 3-II-4.

The momentum wheel assembly was vibrated to the component specification levels prior to the MTM vibration test. The responses from the component test are much higher than those recorded on the MTM test. The MTM test was therefore less severe than the component test for this assembly.

Black boxes usually have resonant frequencies well above the spacecraft structure resonant frequencies. The G-level to which these black boxes are exposed during vibration tests, as they pass through their resonant frequencies, is more severe than the exposure they will experience during spacecraft vibration.

The AVCS camera had a measured natural frequency over 150 Hz. The camera electronics will have a natural frequency of about 180 Hz compared with a similar tested unit. No test data is available for the pitch control electronics and the radiometer, but they are estimated to have natural frequencies of at least 120 Hz.

The command distribution unit A (CDU-A) had a response of 15 G at 280 Hz and a response of 13.6 G at 730 Hz during prototype sinusoidal vibration in the thrust direction. An accelerometer was located on the top of the dummy black box and the response of 13.6 G and 15 G is believed to be due to the dummy box resonance. The input levels at CDU-A are expected to be less than 10 G and therefore less severe than the component test level.

TABLE 3-II-4. COMPONENTS WITH RESPONSES OVER 10 G

(Sinusoidal Prototype Levels)

Accelerometer	Component	Reading
	Y Excitation - Run 3	
17Y	Live Camera, AVCS	13.2 G at 76 Hz
15Y	Bolometer Housing	33.0 G at 88 Hz
51Y	Momentum Wheel Housing, Brg.	10.5 G at 75 Hz
	X Excitation - Run 2	
No component exceeded the 10-G level.		
	Z Excitation - Run 15	
9Z	Pitch Control Electronics	21 G at 53 Hz, 10.5 G at 87 Hz
12Z	Command Dist. Unit A, Top	15 G at 280 Hz, 13.6 G at 730 Hz
15Z	Bolometer Housing	25 G at 52 Hz
16Z	Camera Electronics, Top	21 G at 73 Hz, 18 G at 125 Hz
17Z	Live Camera, AVCS	16 G at 73 Hz, 17 G at 83 Hz
21Z	AVCS Recorder, Foot	15 G at 77 Hz, 16 G at 82 & 93 Hz
51Z	Momentum Wheel Housing	30 G at 53 Hz
59Z	Radiometer, Near Support	13 G at 74 Hz, 14.7 G at 84 Hz
69Z	Flywheel	47 G at 55 Hz, 22.0 G at 90 Hz

5. Other MTM Test Results

a. GENERAL

The MTM was used for other tests in addition to vibration tests. Measurements were made of the mass moments of inertia, center of gravity location, and principal axes of inertia. Results compared favorably with calculated data. The MTM was dynamically balanced prior to the mass inertia tests. The deflection of the spacecraft during vibration can be determined from the measured G levels. This has been done for locations on the spacecraft that could interfere with the shroud. Test results are presented below.

b. MOMENT OF INERTIA

Moment of inertia tests were conducted, in accordance with RCA procedure TP-SE-1975000 using the 56-inch bifilar torsional pendulum. The natural period of pendulum oscillation was used in measuring inertias, weight and center of mass of the MTM in various orientations and configurations.

The data obtained was used to calculate the following spacecraft parameters: spacecraft weight, moments of inertia in each of the three spacecraft coordinate axes, principal inertia in the X-Y plane and the location of the principal X-Y axes with respect to the spacecraft coordinate axes, inertia ratio, and location of the center of mass above the separation plane.

In addition, spacecraft parameters were determined for computer analysis of inertia and mass properties of the spacecraft in the orbit configurations. Launch configuration is defined as a complete spacecraft with the solar array, ATC louvers, and antennas folded, and only flight hardware aboard. The orbit configuration is defined as a complete spacecraft with the solar array, louvers and antennas unfolded, and only flight hardware aboard. The mechanical parameters determined are given in Table 3-II-5. The measured data showed good agreement with pretest computer calculated values. Figure 3-II-4 is a sketch of the axes.

NOTE

Growth boxes, which were added during the vibration tests for qualifying the structure to the desired 720 pounds, maximum, were removed during the moment of inertia measurements to correlate measured and calculated data.

TABLE 3-II-5. MTM MOMENT OF INERTIA TESTS DATA

Parameter	Measured Data		Units	Calculated Data	
	Launch	Orbit		Launch	Orbit
Weight*	656.37	652.41	pounds	672.55	666.48
I zz	639.57	982.81	lb-in-sec^2	638.23	988.89
I xx	754.24	967.91	lb-in-sec^2	762.40	959.02
I yy	829.44	1129.32	lb-in-sec^2	830.16	1163.85
I max	829.92	1129.54	lb-in-sec^2	830.93	
I xy	5.95	5.96	lb-in-sec^2		3.68
O xy**	4.5	2.2	degrees	6.1	
I Ratio	1.30	1.15		1.30	
Z Bar***	22.26	24.34	inches	21.85	24.26

* Dummy growth boxes removed before this test.
** Counterclockwise from Y axis viewing aft.
*** Above Separation Plane.

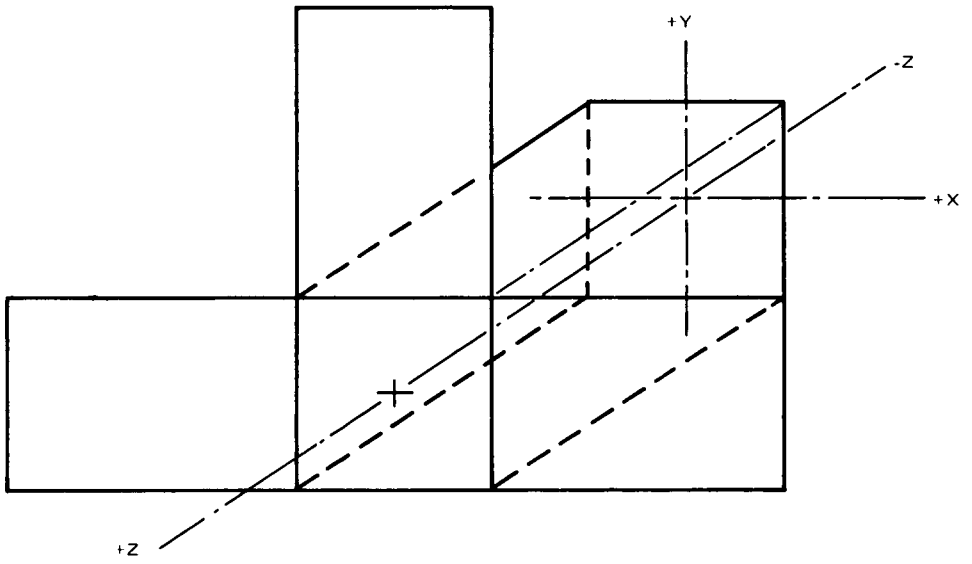

Figure 3-II-4. Moments of Inertia Axes

c. DYNAMIC BALANCE

The MTM was dynamically balanced in accordance with RCA procedure TP-SD-1975000 except that the imbalance level was left at 4000 oz-in^2, for expediency. To accomplish balance, a total of 6.86 pounds of lead weights were affixed to the baseplate and 4.28 pounds to the cross brace.

The purpose of a fine balance was to set up the RCA balancing machine computer so so that future balancing operations could be accomplished more expeditiously. Also, the test determines the threshold of imbalance which the balancing machine can discern.

d. DYNAMIC DEFLECTIONS

The deflections during vibration can be computed from the vibration test data by assuming sinusoidal responses. The deflection is then given by the expression:

$$y = \frac{386\ g}{(2\pi)2f^2} = \frac{9.78\ g}{f^2}$$

where

y is deflection (inches),

g is acceleration level, and

f is frequency (Hz).

These deflections are at prototype vibration levels. Ample clearance is provided between the spacecraft and fairing for the above-calculated spacecraft excursions under vibratory inputs. See Table 3-II-6.

TABLE 3-II-6. DYNAMIC DEFLECTION

Acceler-ometers	Location	Frequency (Hz)	Acceleration Level (G's)	Deflection (Inches)
5Y	Top of AVCS Equipment Panel at Corner	31	9.4	0.10
6Y	Top of APT Equipment Panel at Corner	30	9.0	0.10
36Y	Back Solar Panel-Bottom Center	54	28.0	0.09
37Y	Back Solar Panel-Bottom Corner	48	60.0	0.25

TABLE 3-II-6. DYNAMIC DEFLECTION (Continued)

Acceler-ometers	Location	Frequency (Hz)	Acceleration Level (G's)	Deflection (Inches)
5X	Top of AVCS Equipment Panel at Corner	20	7.9	0.19
34X	AVCS Solar Panel-Bottom Corner	52	49.0	0.18
49X	Back Solar Panel-Bottom Corner	20	6.4	0.16
66X	Back Solar Panel-Bottom Corner	52	14.5	0.05

SECTION III

THERMAL TEST MODEL TESTING

Thermal control of the ITOS spacecraft is achieved by a combination of passive and active control elements which function to ensure favorable temperatures for the electronic equipment and which provide a small capacity for future growth in terms of accommodating higher power and realizing more precise temperature control.

The passive elements include a variable solar-absorptance thermal fence and fixed radiator surfaces. The fence consists of concentric rings or fins, finished with a 3M 400 series black velvet coating, projecting above Alzak reflector plates which they bound. The solar absorptance of the fence varies as a function of solar radiation incidence angle.

The active elements are temperature-controlled, moving louvers, two per equipment panel, which cover or expose radiator surface as required. The louvers are driven by active temperature controllers (ATC's), which consist of hydraulic reservoirs coupled to bellows. A change in reservoir temperature causes a related change in the liquid volume, which results in an expansion or contraction of the bellows. The motion of the bellows is transmitted through mechanical linkages to the equipment panel louvers. A detailed description of the spacecraft thermal control design is contained in Part 2 of this report.

A. THERMAL TEST MODEL

The thermal test model (TTM), which comprised a full-scale configuration of the spacecraft and components, incorporated the following features. (See Figure 3-III-1.)

1) Structure — actual flight design.

2) Solar panels — for injection mode tests, folded flight units without cells or shunt dissipator components installed; for operational mode tests, deployed dummy panels. Dimensions of the vacuum chamber limited the size of these panels to simulated sections 3 feet long on spacecraft equipment sides and 2 feet long on anti-Earth side. Sheet metal was single sheet instead of the flight design honeycomb material.

3) Electronic equipment — cameras, tape recorders, batteries, and control boxes, and other internal black boxes simulated with aluminim models of equivalent size and thermal mass. Internal power dissipation levels were achieved with resistance heaters within each unit.

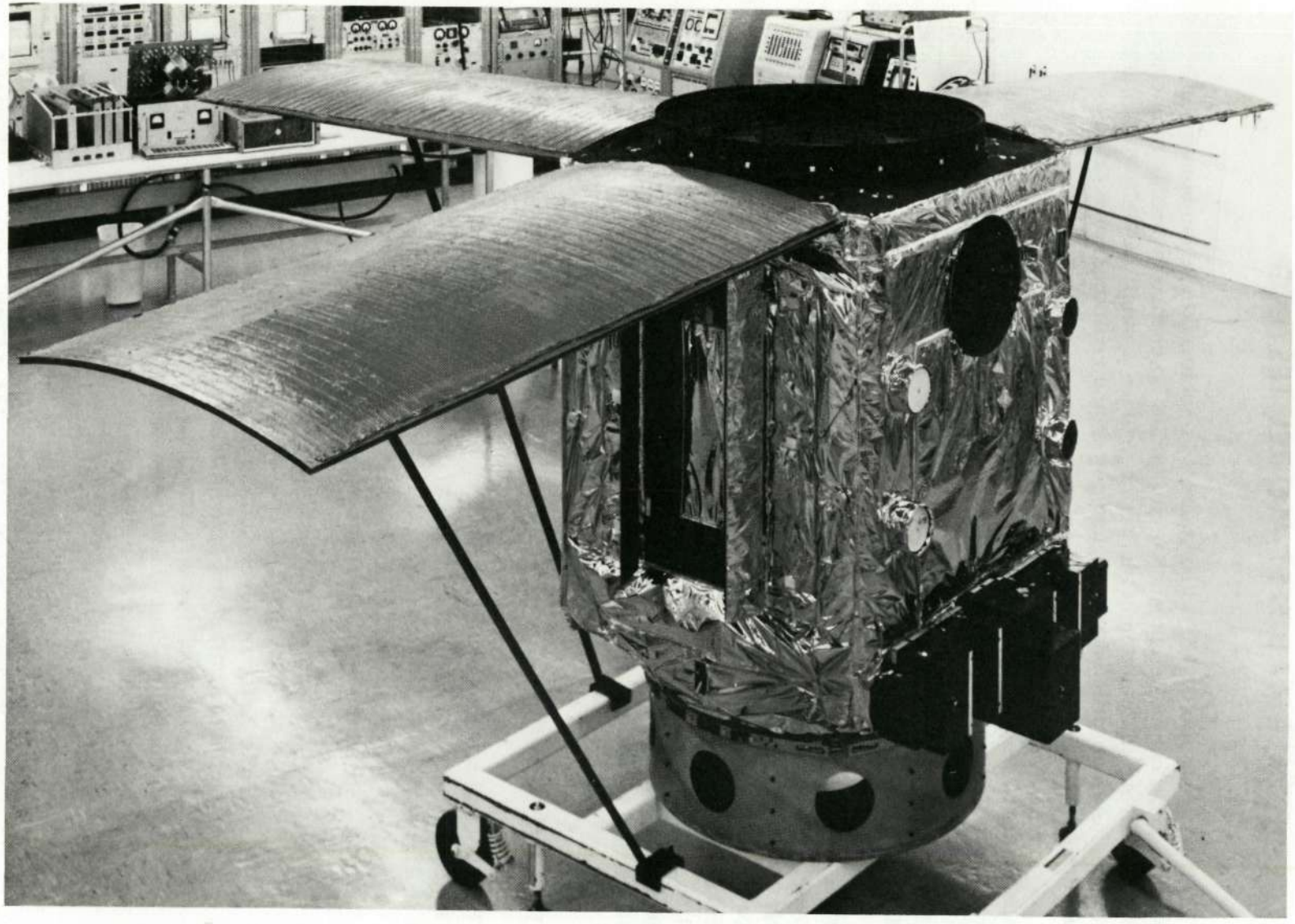

Figure 3-III-1. ITOS Thermal Test Model

4) Scanning radiometer — a dummy model mounted in the flight configuration with an internal resistance heater for power dissipation simulation.

5) Flat plate radiometer — same as for the SR.

6) Solar proton monitor — a dummy model.

7) Active thermal controller — operational flight units.

8) Momentum wheel assembly — an operational unit, in both a rotating and a static condition (see Paragraph E.).

9) Finishes and insulation — flight configuration finishes and insulation blanketing.

10) Antennas — a dummy S-band antenna only.

B. TEST SIMULATION

1. Solar Input

The thermal fence plate, facing the interior of the spacecraft, is the sole fence influence on equipment temperatures. Since solar simulation testing indicated the fence plate would experience only moderate thermal gradients in flight, it was considered valid to induce like average temperatures on the plate by uniformly heating the fence fins. Heating to represent solar, albedo and earthshine inputs was induced by resistance heaters applied both to the fences and to the Alzak reflectors.

The solar panels were heated uniformly at levels determined by factors of solar flux, sun angle, and surface absorptivity. The emissivity of the surfaces was the same as that for flight configuration, resulting in temperatures analogous to those anticipated in flight. Heaters were applied over the entire sun-facing surface of each panel. The total heat input simulated the operational thermal loading due to the solar, albedo, and earthshine radiation incedent on both faces of the panels.

Initially, solar input to the insulated areas was simulated by resistance heaters. However after the insulation was redesigned, (a modification made necessary because of excessive heat losses through the material), these heaters were omitted to avoid introduction of an indeterminant factor in the insulation quality. This omission was accounted for in the analytical model used for correlation of the test data.

At times during each orbit the side radiators will be exposed to solar radiation. This heat input will directly affect the equipment and, therefore, cannot be ignored. Heaters bonded to the outside of the radiator were powered to simulate the levels

of solar input consistent with the calculated values for solar flux, area illuminated, sun angle, and surface absorptivity; heat inputs were varied in a stepped profile according to the anticipated flight changes.

2. Power Dissipation

As stated, power dissipation in the onboard electronic units was simulated by resistance heaters in individual dummy boxes. The level of simulated dissipations followed the power profiles of the equivalent flight equipment with regard to operating mode, equipment life, and orbit geometry.

3. Instrumentation

Copper-constantan thermocouples were used to monitor temperatures within the thermal model during testing. Instrumented areas included each electronic box and related mountings, the structure, the solar panels, the outlying equipment, the thermal fence, the active thermal controllers, the momentum wheel assembly, and the insulation.

4. Control

Heater power application was controlled by two methods. The input to the areas illuminated by the sun in orbit was controlled in increments by utilizing variacs, equal in number to the steps required. The variacs were set at appropriate voltage levels and selected via a programming switch. The simulated electrical power dissipation in the dummy boxes was controlled by switching the heaters within the units, increasing or decreasing the internal dissipation as required.

C. THE TTM TESTING (INITIAL)

1. Test Objectives

a. INJECTION MODE SIMULATION

This portion of the test program had as its objective the evaluation of the thermal behavior of the spacecraft in the operational injection mode. External heat inputs and internal power dissipation during simulated orbits were derived from resistance heaters. Results of this testing served to verify the analytical methods of temperature determination. Selection of a range of simulated orbits provided data for all expected flight conditions. This simulation was conducted in a thermal-vacuum chamber.

b. OPERATIONAL MODE SIMULATION

The objective of this portion of the test program was the evalution of the thermal behavior of the orbiting spacecraft in an operational mode. Solar and power dissipation inputs were simulated as in the injection mode simulation. The results corrobbrated the analytical methods for temperature determination. This simulation was also conducted in a thermal-vacuum chamber.

2. Test Procedure

Five flight orbital conditions were simulated in vacuum chamber testing of the TTM. These were the worst case hot and cold operational cases (i.e., a 30-degree orbit sun angle at beginning-of-life and a 60-degree orbit sun angle at end-of-life) and three possible worst cold injection cases (i.e., a 38-degree orbit sun angle with a 150-degree spacecraft sun angle and a 60-degree orbit sun angle with 30- and 90-degree spacecraft sun angles). The hot injection mode case (i.e., a 38-degree orbit sun angle with a 60-degree spacecraft sun angle) was not simulated, because the mounting point temperatures predicted for all injection mode cases were well below the specified maximum values.

The data derived from each simulation provided:

- Electronics box and mounting point temperatures
- Structure temperatures
- Active controller temperatures and louver positions

3. Initial Test Results

As a result of initial testing of the TTM, design modifications were made on the test model. These changes were necessitated by virtue of the prevailing low temperatures for the components mounted on or near the baseplate. For the 60-degree orbit sun angle EOL simulation, units were as much as 10°C below analytical temperature predictions. Battery temperatures were 0° to 10°C below specification. However, for the 30-degree orbit sun angle BOL simulation unit, temperatures were within 3°C of the predictions. The test was interrupted to allow the data to be evaluated and design modifications to be considered.

Results of the initial temperature testing indicated that the insulation design was not equal to the task of maintaining spacecraft temperatures within the desired range due in large part to the bending and fastening of the blankets around the spacecraft corners. As a result, a multilayer insulation testing program was initiated to find an adequate design. Prior testing of spacecraft equipment panels

had not indicated any insulation deficiencies primarily attributable to bending and fastening of the insulating blankets, since the method of insulation attachment was not as complex as for the TTM. The insulation design was revised to incorporate nylon mesh separators between the Mylar layers prior to resuming the TTM test (see paragraph D). The improved insulating characteristics of the blanket necessitated the reconfiguration of the spacecraft radiator surfaces.

4. Test Results for Reconfigured Model

Good correlation between the test results for the reconfigured model and the analytical predictions was obtained. Area temperature averages were excellent; however, the test model results indicated the existence of thermal gradients within the structure which were not apparent in the analytical mode. Resolution of this inconsistency entailed a revision of the analytical model.

As a result of the revisions deriving from the testing of the modified thermal model, the analytical model was made to more closely correspond with the physical model.

D. INSULATION EVALUATION TEST

The objectives of this series of tests were to determine the effective emissivity of various insulating blanket configurations and to arrive at an optimum design based upon physical and thermal properties. Eleven configurations were tested. In each case, the specimen enclosed a 12 by 12 by 1/8-inch copper plate weighing 6 pounds. The multilayer insulating blanket, with nylon mesh separators between the individual Mylar layers, and the singly and doubly stitched Velcro hook and eye fasteners shown in Figure 3-III-2, was selected.

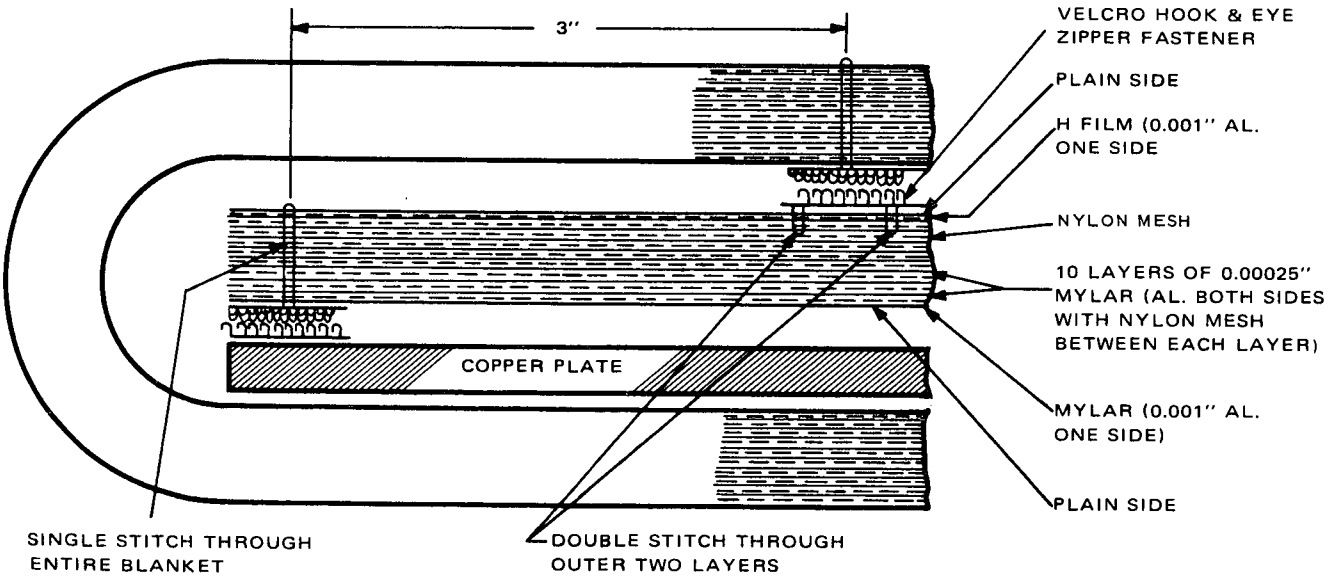

Figure 3-III-2. Thermal Blanket Test Configuration

E. EMITTANCE TEST

1. Test Program

A thermal vacuum development test was performed on key elements of the spacecraft in order to evaluate the thermal characteristics of these items. The testing was performed before assembly of the complete Thermal Test Model. The elements that were thermally evaluated were:

- Thermal control fence assembly
- ATC/Side equipment panel assembly
- Baseplate equipment panel
- Momentum wheel assembly

An individual test plan was written for each test item. All tests were performed in parallel.

2. IR Simulation of the Thermal Fence

a. TEST OBJECTIVES

The objectives of the test program were to evaluate the behavior of the revised thermal fence in a simulated space environment, using heaters to simulate the solar energy input, and to compare the results with solar simulation test data. The test program yielded the following design information:

(1) The distributed solar heater inputs required to closely duplicate solar simulation temperature test data.

(2) The feasibility of obtaining a close duplication of solar simulation temperature test data* by application of uniform surface heating with the heaters, rather than applying the actual heater input distribution.

(3) The temperature distribution on the thermal fence that results from addition of computed flight albedo and earth IR energy to the solar heat inputs determined from items 1 or 2. This temperature distribution corresponds to the anticipated flight values, and the resulting heater settings will be those used during the TTM spacecraft test program.

*Temperatures on the internal plate of the thermal fence.

b. TEST THEORY

The results of solar simulation of a thermal fence configuration agreed closely with analytical predictions. The solar inputs computed for the predictions, when applied to the appropriate surfaces in the form of heat by resistance heaters, should yield a close approximation of the solar simulation temperature distribution data.

The first phase of the thermal fence test program, identified as test sequence FA, this concept was evaluated. Thermal fence heater circuits were adjusted to the predicted solar heat input values and a thermal equilibium condition was established.

The resulting temperatures were compared with solar simulation test results. Some deviation from the predicted heater settings were required to reproduce the desired temperature distribution, since any single heater covered a relatively large surface area. Average heater settings for a surface area zone simulated the input rather than the continuously variable heat input that occurred during the solar test. The heater input adjustments that resulted in the best temperature distribution match were recorded and the test concluded. Test sequence FA was performed for the following thermal fence environments:

- Test FA-1: Spacecraft simulation shroud adjusted to 20°C uniformly, heater input energy corresponding to a 30-degree sun angle.
- Test FA-2: Spacecraft simulation shroud adjusted to 20°C, heater input energy corresponding to a 45-degree sun angle.
- Test FA-3: Spacecraft simulation shroud adjusted to 20°C, heater input energy corresponding to a 60-degree sun angle.

In the second phase of the thermal fence test program, identified as test sequence FB the magnitude of the temperature discrepancy was evaluated with average uniform heater power applied to the fence (rather than the distributed heater settings obtained from test sequence FA). Test sequence FB was performed for the following thermal fence environments:

- Test FB-1: Spacecraft simulation shroud adjusted to 20°C, heater input energy corresponding to a 30 degree sun angle.
- Test FB-2: Spacecraft simulation shroud adjusted to 20°C, heater input energy corresponding to a 45 degree sun angle.
- Test FB-3: Spacecraft simulation shroud adjusted to 20°C, heater input energy corresponding to a 60 degree sun angle.

In the third phase of the thermal fence test program, identified as test sequence FC the anticipated flight temperature distribution of the fence due to solar, albedo, and earth IR heat flux was evaluated. The heater settings of test sequences FA and FB were a simulation of only the solar heat input component. During test series FC, the additional predicted components of albedo and earth IR heating were added to the solar component determined in tests FA or FB and the thermal fence was allowed to reach thermal equilibrium. The resulting total heater input settings were used during TTM testing and the measured temperature distributions corresponded to the anticipated flight levels. Test sequence FC was performed for the following conditions:

- FC-1: Spacecraft simulation shroud adjusted to 20°C, heater input energy corresponding to a 30-degree sun angle.
- FC-2: Spacecraft simulation shroud adjusted to 20°C, heater input energy corresponding to a 45-degree sun angle.
- FC-3: Spacecraft simulation shroud adjusted to 20°C, heater input energy corresponding to a 60-degree sun angle.

c. TEST RESULTS

Temperatures close to those obtained in the solar-simulation testing were accomplished by applying the computed inputs to the resistance heaters on the fence surfaces. Adjustments on the order of 1 percent on the large fence and 10 percent on the small fence enabled the temperature match to be very close to the values obtained in the simulation testing.

Addition of the albedo and earthshine values provided the heater settings to be used for the TTM test sequence.

3. Active Thermal Controller (ATC) Effective Emissivity Evaluation

a. GENERAL

The test item was one equipment panel of the TIROS M spacecraft, which included two of the ATC devices and their related flaps. A single solar cell panel, less cells, was attached at the appropriate location on the equipment panel. The outside surface of the panel was insulated as designed for flight with the normally inside surface insulated with multilayer aluminized Mylar blanket.

b. TEST OBJECTIVE

The objective of the test was to determine, empirically, the effective emissivity of the the active thermal controller as a function of flap angular position.

The effective emissivity of the ATC varies, dependent upon the position of the radiator flaps. At any position, the effective emissivity can be determined when the temperature of the system is at equilibrium. At this condition, the energy input equals the energy emitted from the space-exposed surfaces of the ATC when losses of the normally unexposed surfaces are controlled to negligible quantities. The flap position is dependent upon the structure temperature. Flap position was determined by read-out from the flap angle indicator.

c. TEST RESULTS

Emissivity versus flap-angle results were utilized to adjust and verify the analytical model. The analytical model was the basis for temperature predictions in the TTM test.

4. Baseplate Effective Emissivity Test

a. GENERAL

The test item was an assembly consisting of the baseplate, separation ring and the momentum wheel assemby, insulated as illustrated in Figure 3-III-3. A portion of the baseplate was exposed for thermal radiation: the remaining area was covered with multilayer aluminized insulation blanket.

b. TEST OBJECTIVE

The objective of the test program was to determine empirically the effective emissivity of the baseplate.

c. TEST THEORY

The effective emissivity obtained from the data in this test was utilized in the development of an analytical model of the baseplate. The analytical model is the basis for predictions of temperatures for the TTM.

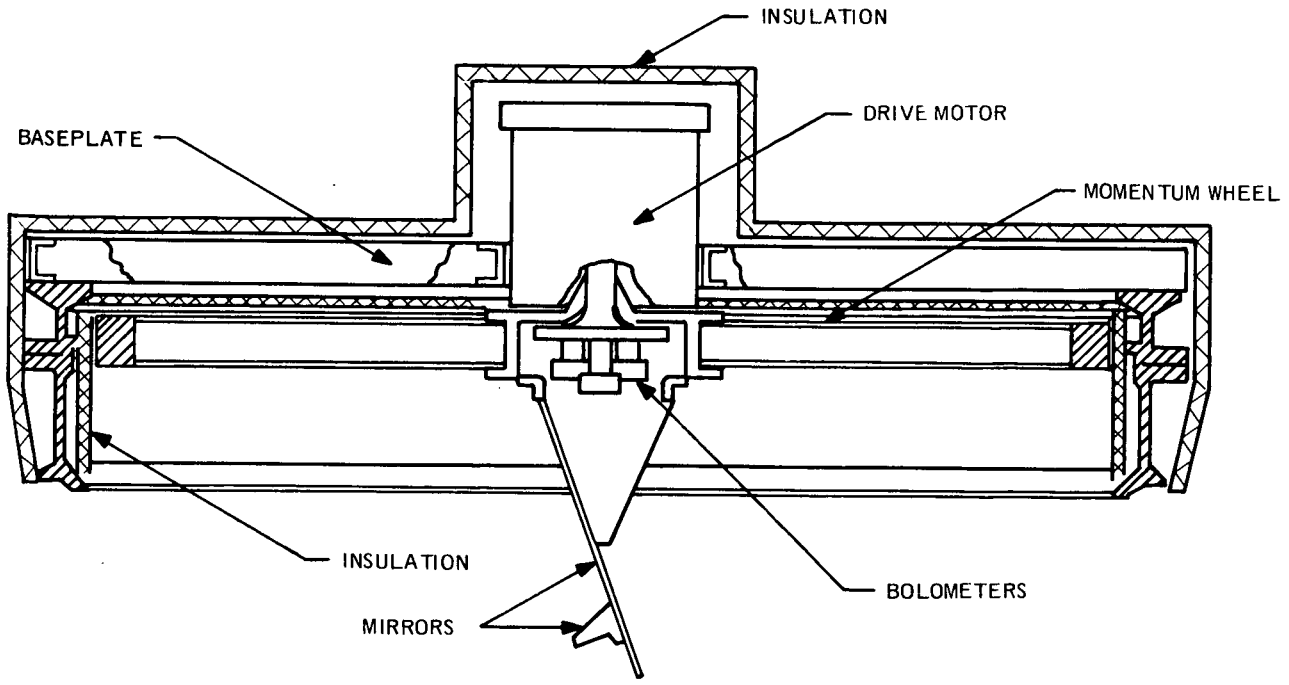

Figure 3-III-3. Baseplate Test Assembly

F. MOMENTUM WHEEL ASSEMBLY TESTS

The momentum wheel assembly (MWA) was utilized in three separate exercises in connection with TTM testing.

These exercises included:

- Baseplate emissivity testing
- Initial TTM testing
- Retest of TTM

A different test configuration was used on each occasion.

1. Baseplate Emissivity Testing

a. TEST PLAN

The purposes of this test program included the acquisition of information relating the applied thermal loads on the rotating and static elements of the MWA, and the determination of the temperature gradients across the bearing and the labyrinth seals. The specific objective was to examine steady state thermal performance under eight different combinations of motor power

dissipation and baseplate temperature.

The MWA was mounted on a test baseplate with a representative effective emissivity. The side of the baseplate which would view the interior of the spacecraft was covered with a blanket of multilayer insulation, as was the MWA housing. The MWA wheel and rotating number assembly viewed the liquid nitrogen shroud of the test chamber.

Externally, the test unit was a duplicate of the flight assembly. Internally, the test unit included both motors, both labyrinth seals, the bearing, the bolometer stem and bolometer head, with actual sensors and empty electronics boxes. Absent from the unit were the electronics packages inside the bolometer head boxes, the Nylasint lubricant reservoirs and the encoder. These items were omitted since their presence was not likely to affect the steady-state temperature levels of other components of the assembly. For this test, the unit was in a locked-rotor condition, in order to accommodate adequate instrumentation. Employing a heat-conducting epoxy, two heaters were attached around the periphery of the MWA housing to simulate, in conjunction with the power dissipation the two motor windings, the expected heating levels, and heat flow paths. A third heater was epoxied to the back of the large mirror, under the insulation, to simulate the orbital heating load on the outside of the unit.

From the instrumented, locked-rotor momentum wheel assembly test, it was provisionally concluded that the thermal design was satisfactory, with sufficient capacity to accommodate the increased power loads present in the rotating subassembly.

On consideration of the data from this first test phase, no insulation modifications were felt necessary for the next phase, in which a rotating assembly attached to the TTM was to be subjected to representative launch and orbital conditions in a thermal vacuum chamber.

2. Initial TTM Testing

This discussion concerns the initial testing and the retesting of the TTM, as related to the MWA. The fact that different test configurations were utilized in the respective test phases was exploited to gain further insight into the thermal performance of the MWA. During initial testing, the MWA was permitted to rotate, whereas during retest, the rotor was locked, affording the opportunity of further instrumentation in key areas.

a. TEST PLAN

The purpose of the initial testing program was to operate a representative momentum wheel assembly under simulated orbital conditions, while attached to the TTM baseplate. Temperature points on the nonrotating portion

of the assembly along with readings of the voltage and current supplied to the active motor, were recorded. In addition, the MWA spin rate was derived from the shaft encoder. The MWA tested was the same model used for baseplate emissivity testing. Only one circuit of the encoder was required for the angular velocity signal, and the unit was run in open-loop configuration. The electronics modules associated with the boxes at the head of the bolometer stem were not present. Thermocouples were positioned on the housing end cap near the center, along the length of the housing at the motor 1 and motor 2 levels, on the bolometer head box under the shield, and on the MWA mounting flange.

After the TTM had been installed in the chamber, the instrumentation and power supply connections were made and the thermocouples were checked. The motor leads were connected to two power packs, each equipped with an ammeter. A digital voltmeter was arranged to read the supply voltage to either motor. The encoder pulse signal was displayed on an oscilloscope along with a fixed pulse equivalent to that available from the encoder at 150 rpm. By synchronizing the scope time base to the fixed pulse, any change in wheel speed was made immediately evident. The wheel was checked for correct direction of rotation using each motor.

Initially, the chamber was brought to the required environmental conditions for TTM testing. Shortly after the testing had begun, power was applied to the MWA. At this time, all the operating test data appeared satisfactory. Upon termination of the TTM testing, the MWA was dismounted from the TTM. This same MWA was subsequently reattached to the TTM, in the same configuration, but in a locked-rotor condition, for the retesting of the TTM.

b. TEST RESULTS

The variations in wheel speed, temperature fluctuations at the mounting flange, and switching from one motor to the other, resulted in no measurable change in motor performance. From this result, it was inferred that the frictional characteristics of the motor assembly did not significantly change during the test.

3. TTM Retesting

TTM retesting afforded an opportunity to monitor in greater detail the thermal performance of the MWA during the various operational conditions simulated. With the rotor in a locked condition, a representative level of heat loading was provided by applying power to the motor windings, the mirror assembly, the wheel rim, and the bolometer head, as required. Results were to be correlated with results derived from previous testing to more precisely define the temperature gradients across the bearing under representative operating conditions. Information on the thermal performance of the solar

proton monitors, the bolometer head sensors, the scanning flat plate radiometers and the S-band antenna was to be obtained as well.

a. TEST SIMULATION

Although the wheel was stationary during retesting, permitting more instrumentation, it was not possible to place thermocouples inside the unit, nor was it practicable to add small heaters to the housing. Accordingly, heating was provided by the I^2R losses of the two motors, a heater on the bolometer head, a heater attached to the rear of the large (pitch) mirror, under the thermal insulation, and a heater attached to the inside of the flywheel rim.

The heaters were utilized to simulate the orbital heat flux loads on the MWA and were energized, via rotary switches, to realize the day and night variations attending each of the simulated orbits.

Thermocouples were located at the flywheel hub (on the outer vertical surface), on the pitch mirror (on the back at the upper end under the insulation), on the bolometer head (on the fiberglass thermal shield), on the mirror support cylinder (at the top center), on the MWA housing (at the center of the end cap and along the length at the motor No. 1 and motor No. 2 levels), on the bolometer head (on the electronics box), and on the spacecraft MWA mounting flange.

Apart from the extra heaters and thermocouples, the MWA configuration during retesting was exactly the same as it had been during the initial testing. The bolometers were actual sensors and the head assembly with sensors and thermal shield duplicated that of a flight unit.

It was not possible to use scanning radiometer and solar proton monitor flight units in this test. Therefore, dummy models were employed whose primary purpose was to provide heat leakage paths and thermal loads equivalent to those of the actual sensors. As an ancillary benefit, use of these models provided sensor mounting-point temperature gradient information.

For this test, the S-band antenna was duplicated with a dummy having the same diameter reflector plate, but without the peripheral ring. A heater was attached between the antenna disc and the spacecraft insulation blanket, and the thermocouple was attached to the disc. The dummy antenna was installed on the spacecraft earth-facing side of the structure, using the appropriate fiberglass-epoxy standoffs.

b. TEST PROCEDURE

During retest of the TTM, the following sequence was observed:

1) The TTM was installed in the thermal vacuum test chamber.

2) The MWA flywheel was secured to the adapter ring, to prevent rotation.

3) Thermocouples and heaters were connected to their respective circuits and checked for correct performance.

4) The test chamber environmental conditions were brought to required levels and heater power levels adjusted to values appropriate for simulating the end-of-life, 60-degree orbit sun angle, operational mode. Refer to Table 3-III-I.

5) After spacecraft thermal equilibrium was achieved, a two-orbit continuous printout of thermocouple temperature data was taken; heater power level readings were recorded before and after the printout.

6) Steps 4) and 5) were repeated for the 30- and 90-degree orbit sun angle injection modes simulations.

c. TEST RESULTS

As regards the momentum wheel assembly, conditions during TTM retest differed from those of previous static MWA testing as follows: no internal instrumentation was employed; no heaters were installed on the housing; heaters were installed on the bolometer head and the wheel rim; the housing was thermally coupled to the interior of the spacecraft, and baseplate temperatures were representative of actual operational conditions. This test provided the opportunity of measuring MWA external temperatures under various conditions suitable for comparison with those obtained during previous static testing.

Table 3-III-1 summarizes the temperatures and power levels prevailing during the TTM retesting.

For the two operational mode cases, with a single exception, the maximum orbital temperature variation for all items was ±1°C. The exception was the solar proton monitor bracket which fluctuated ±4°C for the 60-degree orbit sun angle case. This fluctuation is attributable to the relatively small thermal mass of the element, its high thermal resistance path to the spacecraft and the fact that for the orbit in question, the external heat flux input has a 73-percent orbital duty cycle.

TABLE 3-III -1. TEMPERATURE AND POWER LEVELS FOR TTM RETEST

Thermocouple or Heater* Location	Operation Mode Sun Angle		Injection Mode Sun Angle			Units
	30° BOL	60° EOL	30°	90°	150°	
Momentum Wheel						
Hub	-13.5	-21.5	-32.0	-29.0	+5.5	°C
Mirror	-21.5	-29.0	-36.0	-35.0	+1.0	
Bolometer head	+3.5	-5.5	-19.0	-19.0	+34.0	
Mirror support	-19.0	-25.5	-35.0	-32.0	+2.5	
Housing end cap	+20.0	+9.0	-9.0	-9.0	+23.5	
Motor No. 2 housing	+20.0	+10.0	-7.0	-6.5	+22.5	
Motor No. 1 housing	+17.0	+7.5	-10.5	-9.0	+20.0	
Bolometer head	+8.0	-1.5	-17.0	-16.5	+32.5	
Spacecraft base flange	+21.0	+10.0	+9.5	+7.5	+19.5	
Wheel spoke, midpoint	-75.0	-81.5	-78.0	-69.5		
Wheel rim	-43.5	-49.5	-65.0	-62.5		
I^2R motor No. 2	2.58	2.64	2.70	2.70	2.67	Watts
	(2.70)	(2.70)	(2.70)	(2.70)	(2.70)	
I^2R motor No. 2	1.04	1.10	1.12	1.12	1.13	
	(1.12)	(1.12)	(1.12)	(1.12)	(1.12)	
Mirror heater	0	0	0	0	2.11	
	(0)	(0)	(0)	(0)	(2.13)	
Bolometer head	0	0	0	0	4.39	
heater	(0)	(0)	(0)	(0)	(4.25)	
Wheel rim heater	5.9	6.0	1.6	1.6	92.4	
	(5.9)	(6.4)	(1.6)	(1.6)	(86.4)	
Flat Plate Radiometer						
Body	+16.0	+4.5	-20.0	-19.0	8.0	°C
Mounting	+24.5	+12.5	-12.0	-10.0	+14.0	°C
Heater	1.0	1.0	0	0		
	(1.0)	(1.0)	(0)	(0)		
Scanning Radiometers						
Radiometer bodies (average)	+24.0	0.0	-31.0	-22.5	+34.0	°C
Radiometer mtg. plate ends	+25.0	+14.0	-9.5	-7.5	+14.0	°C
Radiometer heater	50.4	32.5	16.4	21.2	64.8	Watts
Solar Proton Monitor						
SPM Bracket	-27.0	-15.5	-3.2	-2.1	+4.0	°C
Base Plate Node 61	+30.5	+14.5	-2.0	+2.5	+10.0	°C
SPM bracket heater	0 (0)	1.90 (73% sun time)	0	0	1.16 (88% sun time)	Watts
S-Band Antenna						
S-band antenna plate	+21.0	+0.5	-22.0	+16.0	-23.0	°C
S-band heater	40.5 (40.0)	-29.8 (31.1)	22.1 (22.3)	37.7	25.2 (88% sun time) (24.7)	Watts

*Required power levels are shown in parentheses below measured values where applicable

No case in the TTM retest coincided exactly, as regards both power levels and general temperatures, with any case set up in previous static test. However, four of the five cases in the TTM retest closely approximated cases simulated in previous static testing. Table 3-III-2 shows correlation of the test data for the first and second tests.

4. Conclusions

The results of the thermal tests of the MWA and other external components established the necessary confidence that these components will maintain temperatures and gradients within specified limits under injection and operational mode conditions.

G. THERMAL FENCE TEST

1. Test Program

The objective of this test was to evaluate the behavior of a thermal fence model in a simulated solar space environment for comparison with the analytical predictions made for the flight units. The thermal fence, illustrated in Figure 3-III-4, was mounted over a "sandbox" shaped aluminum structure in order to simulate the heat exchange between the fence and the spacecraft. The assembly was tested in the JPL 10-foot solar simulator, chosen because of requirements for uniform radiation intensity, and authentic spectral energy match. The fence assembly was rotated about an axis normal to the simulator reflector plates while displaced at various angles with respect to the artificial sun. The range of sun angles simulated extended from 15 to 75 degrees in 15 degree increments. The test assembly was instrumented with 100 thermocouples the outputs of which were recorded on printed tape. Heaters maintained the temperature of the "sandbox" shaped spacecraft simulator at 20°C.

2. Test Results

Results for the 30-, 45-, and 60-degree orbit sun angle tests were compared with predicted fence temperatures obtained with the aid of a 71-node analytical model. This analytical model consisted of an 18-node large fence, a 9-node small fence, an 8-node large diameter reflector, an 8-node small diameter reflector, 3-node insulation segments at each of four corners, and a 16-node interior thermal control plate.

TABLE 3-III-2. CORRELATION OF TEST DATA, FIRST AND SECOND TTM TESTS

Case No.	Power (w)	Mean Housing Temp. (°C)*	Corrected Bearing Temp. (°C)	Temperature Differences (°C)		
				Housing and Bolometer Head	Housing and Hub	Bolometer Head and Hub
BP1	4.42	3.1	-4.5	10.1	27.1	17.0
2	0	12.1	-4.6	11.1	29.1	18.0
MWA1	3.87	30.4	-3.9	11.9	34.4	22.5
2A	4.34	31.4	-3.5	11.4	32.4	21.0
2B	5.42	32.0	-3.2	11.0	32.0	21.0
3A	4.35	45.8	-5.3	16.3	37.3	21.0
3B	6.03	47.5	-4.6	15.5	37.0	21.5
3C	8.40	51.9	-3.0	15.9	39.9	24.0
4A	0	-12.8	-4.5	9.7	25.7	16.0
4C	5.96	- 0.8	-1.5	7.7	31.2	23.5
30° BOL	3.62	19.5	-3.7	11.5	33.0	21.5
60° EOL	3.74	9.1	-4.6	10.6	30.6	16.0
$30°_N$ INJ	3.82	-9.0	-4.5	8.0	23.0	15.0
$90°_N$ INJ	3.82	-8.0	-4.5	8.5	21.0	12.5
$150°_N$ INJ	3.80 +6.5 (88% time)	21.4	+16	-11.1	15.9	27.0

*The "mean housing temperature" is the mean of four values, the two housing temperatures, the housing cap temperature, and the mounting flange temperature.

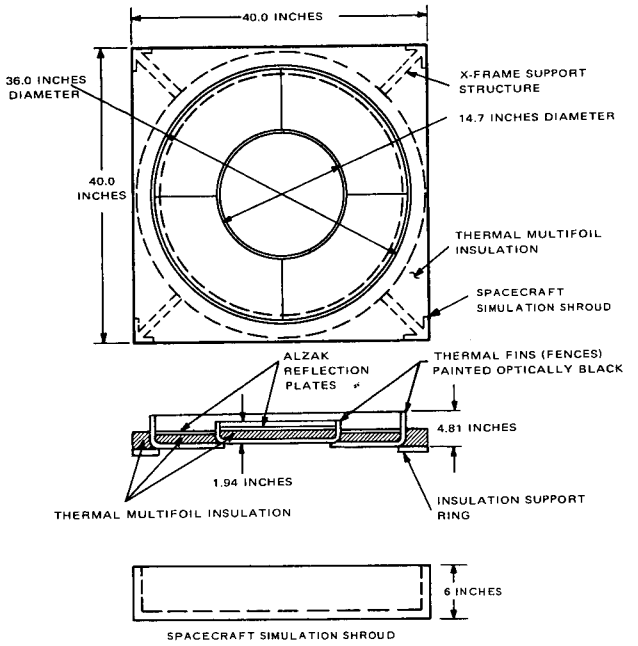

Figure 3-III-4. Thermal Control Fence Design

On the large fence, the predicted temperatures were approximately 15 percent higher than those realized in test. Upon further examination of the analytical model, it was inferred that the choice of nodal centers can cause a large variation in the predicted temperature due to the conductive coupling between the thermal control plate and the adjacent fence member. A computer run was made to substantiate this inference.

The predicted temperatures for nodes on the small fence deviated less than 10 percent from test values. As for the large fence, the observed discrepancy was ascribed to the effect of nodal location which in this case was reduced by virtue of the diminished size of the nodes. Ideally, the number of nodes of the analytical model should be as large as practical in order to minimize the size of each node and, consequently, the effect of small changes in the conductive coupling factor. The memory capacity of the computer on which the model is simulated may limit the nodes to less than an ideal number; however, some reduction in the size of the larger nodes is always possible.

On the large diameter reflection, temperature comparisons between predicted and test values vary with sun angle, shadow pattern and rotation angle. The reflective nature of the Alzak plate is manifest in a marked sensitivity to the radiation from other members of the assembly and environmental chamber

areas as well as surface shadowing. Since the reflector is simulated by a small number of large nodes, the averaging of intrinsic thermal gradients, with the two thermocouples allocated to each node, is a difficult undertaking. However, the temperatures of these nodes are relatively unimportant to the thermal design and agreement between predicted and test values within 10 to 15 percent is considered adequate. Generally, the test temperature results were 10 to 15 percent lower than predicted values. In cases where one thermocouple temperature deviated significantly from that of the second sensor located on the same node, examination of shadow pattern drawings indicated that one sensor was shadowed. A number of the discrepancies between predicted and test temperature values were resolved is this manner.

For the small diameter reflector, the comparison of predicted and test temperatures yielded results similar to those obtained for the large reflector. An additional factor is the difficulty in accurately determining the absorptivity and emmissivity on the surface contributing to the discrepancies between predicted and test results. For example, if the emmissivity of the reflector is greater than the postulated value used in the analytical exercises, the reflector temperature will be cooler than predicted, a condition which was indeed observed in certain cases.

The temperature of the interior surface of the corner insulator (i.e., the surface facing the simulated spacecraft interior) was found to be within a few degrees Fahranheit of the predicted temperatures. The external temperature is inconsequential to the thermal design, provided it does not exceed the limits of the material.

The interior thermal control plate is a most critical area since it is the only portion of the thermal fence assembly which can directly affect the internal spacecraft temperatures. In many cases, the temperatures derived from the thermocouples mounted on the thermal control plate were found to be within 1°F or less of the predicted values; in the worst cases, the observed discrepancies were no greater than 3°F. The anticipated temperature gradients were observed in the control plate, as were the predicted sun-angle dependent variations in average temperature level.

H. CONCLUSIONS

Based on the analyses and testing documented herein, it is concluded that the spacecraft thermal design meets or exceeds all design requirements and will successfully achieve its mission performance goals.

SECTION IV

ANTENNA TEST MODEL TESTING

A. GENERAL

This section describes the testing program performed on the antenna test model (ATM). (See Figures 3-IV-1 and 3-IV-2.) The ATM was used to verify the transmitted RF signal patterns and the overall adequacy of the RF system design. The S-band antenna included on the ATM spacecraft was a prototype of the initial four-dipole S-band design for ITOS. The transmitted wave using this antenna had RHC or LHC polarization, depending on which S-band transmitter was coupled to the antenna. This design was superseded by a single-element turnstile configuration that has identical radiation characteristics to the earlier configuration except that the transmitted wave has RHC polarization regardless of which transmitter is in use. This change was occasioned by a system study which showed that RHC polarization would be necessary for compatibility with all the NASA ground stations. Radiation pattern measurements, VSWR, isolation, and insertion loss measurements for the turnstile were performed during the engineering design phase of the program and are documented in Part 2 of this report (Section VII, paragraph E).

The program was divided into two phases which differed in the type of test performed. Phase I was a test to measure the performance of the antenna subsystems on an accurate representation of the flight spacecraft. Phase II was a test of the compatibility of the RF equipment in a model of the operating configuration. These tests verified the operation of the command system for all operating modes of the spacecraft, and tested the S-band data link through the ground station.

The tests were conducted with the ATM in the RCA metal-free, RF tower outside the main plant (shown in Figure 3-IV-3).

B. EQUIPMENT TESTED

The following is a list of the equipment tested on the ATM.

Real-time transmitter	1975130, Ser. No. 4-454-51P
S-band transmitter	1975128-1, Ser. No. 001

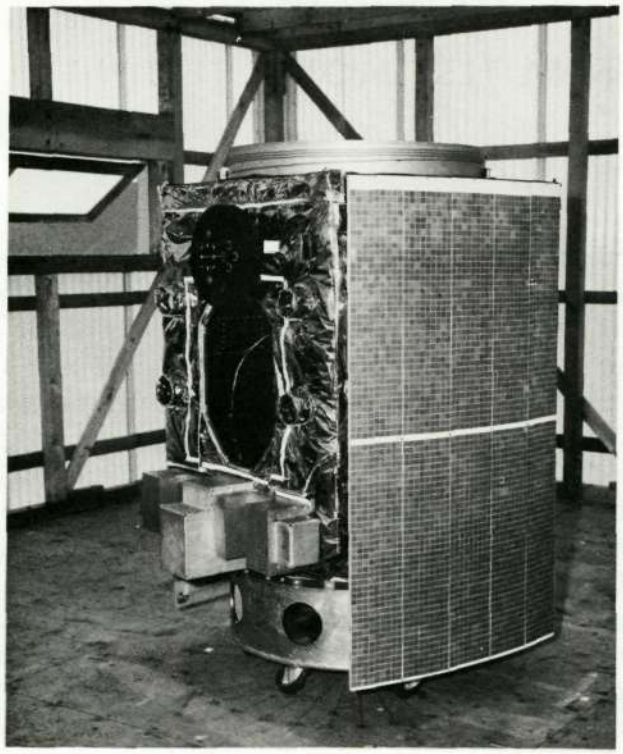

Figure 3-IV-1. Antenna Test Model in RF Test Building

Beacon transmitter	1975143-501, Ser. No. 04
Dual SCO transmitter	1975144-1, Ser. No. 2502
Command receiver	1975123-501, Ser. No. 01 (proto)
Dual multiplexer	1975133-501, (ETM)
Charge controller	1956912-501, Ser. No. 4-843-05
Voltage regulator	1755774-502, Ser. No. 4-844-17
Telemetry signal conditioner	1755736-501, Ser. No. 3-924-04
Command and control unit, side 1	1755183-501, 3-621-4
Command and control unit, side 2	1755183-503, 3-622-03
S-band antenna	1975148 (prototype)
Real-time antenna	1975146 (ETM, MTM)
Beacon-command antenna	1969056 (ETM)

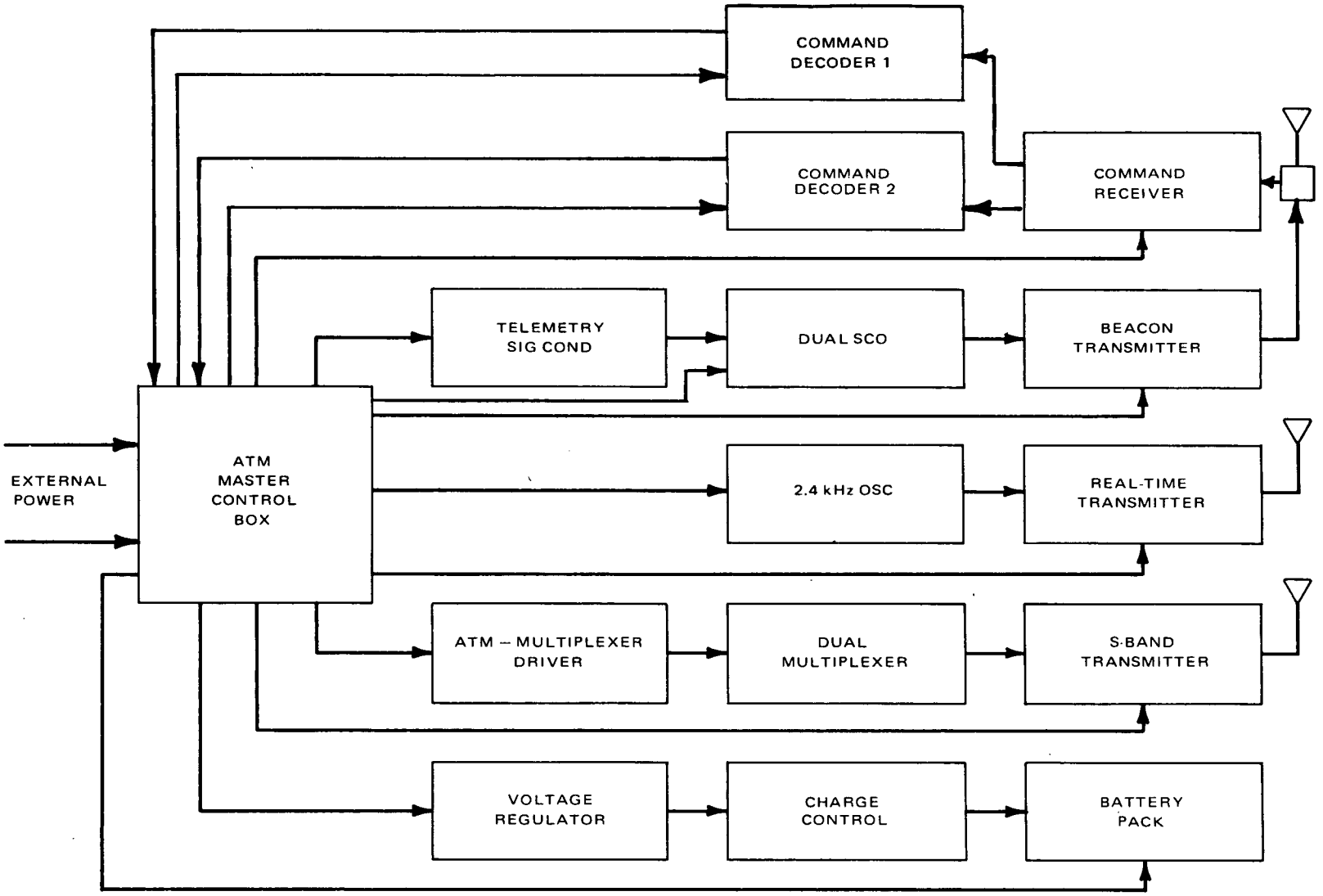

Figure 3-IV-2. ATM Spacecraft, Block Diagram

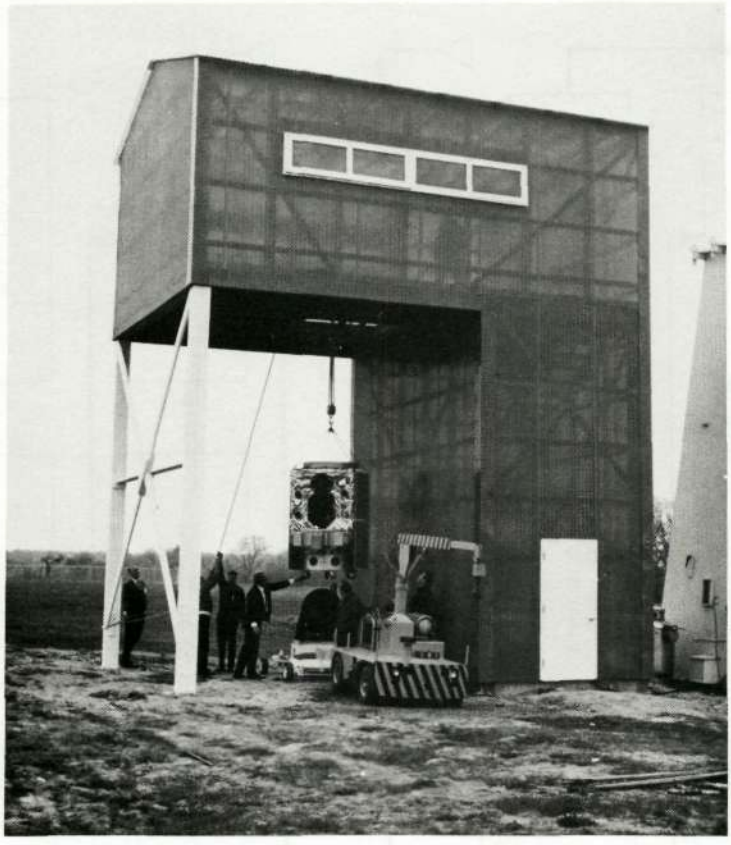

Figure 3-IV-3. RF Test Tower at RCA Premises (ATM is being hoisted into building)

C. TEST OBJECTIVES

The ATM test objectives were:

(1) To measure VSWR of each antenna subsystem with solar panels deployed and stowed.

(2) To measure isolation between antenna subsystems with solar panels deployed and stowed.

(3) To measure insertion loss of each antenna subsystem between input and output ports.

(4) To calibrate the ground-station-to-antenna-test-site range at the three frequencies using permanently installed test antennas.

(5) To measure the S-band data link performance through the ground station equipment, with "hard-line" connections simulating the space transmission path.

(6) To measure the S-band data link, but at the antenna test site.

(7) To measure the performance of the command system with the RF equipment operating in the launch and orbit configurations.

(8) To check the performance of the real-time link through the ground station.

(9) To measure the radiated power and spurious outputs from the three transmitter systems.

(10) To measure antenna patterns in a single plane.

(11) To measure spurious signals in command receiver.

(12) To measure signal-to-noise ratios in S-band multiplex channels.

D. SUMMARY OF ATM TEST RESULTS

The Phase I tests for VSWR's, losses and radiation patterns of the various antenna systems were performed as specified in TP-1970284. All measurements were found to be within applicable specification limits. Path losses from the test building to the ground station were found to be dependent on antenna position, and the antenna patterns were found to be different from the free-space patterns, as expected. In the Phase II equipment tests, a staircase signal transmitted through the real-time system remained linear within the limits of measurement of the test, or about ±5 percent. Quality of the multiplexer/demultiplexer link was slightly impaired by introduction of the S-band system using an RHG receiver. (The Goddard S-band receiver was not available.)

Operation of spacecraft equipment did not affect command receiver sensitivity in any way. Spacecraft equipment did not interact except for the generation of third-order intermodulation products between the beacon transmitter and real-time transmitter. Coupling between these transmitters was through the antennas, which have a measured isolation of 25 dB. These products are less than 0 dBm and present no problem.

E. PHASE I TEST RESULTS

1. S-Band Antenna System

a. S-BAND VSWR

The VSWR measured 1.10 to 1 ±0.02 for both transmitter ports with the unused port terminated in 50 ohms. Specification limit is 1.50 maximum.

b. S-BAND ISOLATION

Isolation between S-band transmitter ports measured 20.5 dB; specification limit is 18 dB minimum.

c. S-BAND INSERTION LOSS

Insertion losses are given in Table 3-IV-1. Specification limit is 7.3 dB maximum loss. Ports other than input and output were terminated in 50 ohms.

TABLE 3-IV-1. S-BAND INSERTION LOSS

Input	Output	Loss (dB)
TX1 (W5)	W1	7.0
TX1	W2	6.8
TX1	W3	7.0
TX1	W4	6.8
TX2 (W6)	W1	7.0
TX2	W2	6.8
TX2	W3	6.8
TX2	W4	7.0

2. Real-Time Antenna System

In general, the procedure used for antenna system loss measurements makes use of a modulated signal generatork crystal detector and video amplifier/ indicator (Hewlett-Packard 415B). Ten-dB pads were used to buffer the generator and detector from the antenna system where a close match was necessary.

Errors due to nonlinear detection were eliminated by maintaining a constant signal level at the detector.

a. REAL-TIME VSWR

With the solar panels deployed, side 1 VSWR was 1.3 to 1. Side 2, using mechanical test model antennas which had not been adjusted electrically, measured 1.4 to 1. Specification limit is 1.5 to 1.

Because power reflected from the real-time antennas may be directed into a dummy load by the hybrid, an indication of system efficiency may be obtained by measuring the amount of power absorbed by the load. On side 1, level at the load was -14 dB with respect to the transmitter port. No specification limit exists for this measurement.

The VSWR with panels stowed was highly dependent on the points of contact between the antenna and thermal blanket. It is expected that flight models will have the blanket dressed away from the antennas, but this was not possible with the ATM. As the blanket was moved, VSWR varied between 1.1 and 3 to 1. Specification limit is 2.0 maximum. The measurements were made at 137.56 MHz.

b. REAL TIME ANTENNA INSERTION LOSS

The insertion loss of both real-time antenna systems was measured at 137.56 MHz and at 148.56 MHz. The results are presented in Table 3-IV-2.

TABLE 3-IV-2. REAL-TIME ANTENNA INSERTION LOSS

Input	Output	Frequency (MHz)	Specification (dB)	Measured (dB)
No. 1 (W6)	No. 1 (W4)	137.56	4.8 max	3.8
(W6)	No. 2 (W2)	137.56	4.8 max	4.8
(W6)	No. 1 (W4)	148.56	20 min	29
(W6)	No. 2 (W2)	148.56	20 min	34
No. 2 (W10)	No. 1 (W4)	137.56	4.8 max	4.0
(W10)	No. 2 (W2)	137.56	4.8 max	4.5
(W10)	No. 1 (W4)	148.56	20 min	30.5
(W10)	No. 2 (W2)	148.56	20 min	31

c. REAL-TIME ANTENNA PHASE MEASUREMENT

The relative phase of the real-time antenna was measured by inserting a T connector between the W1 cables and either the antennas or 50-ohm loads. The measurement gave readings of 88 degrees with 50-ohm loads and 95 degrees with the antennas. In both cases, the earth-facing side lagged the space-facing side.

3. Beacon and Command Antenna System

a. BEACON AND COMMAND VSWR

The VSWR of the beacon and command antenna system was measured with all unused ports terminated in 50 ohms. The specification calls for a maximum of 1.5:1 deployed and 2:1 when the panels are stowed. The measurements are given in Table 3-IV-3.

TABLE 3-IV-3. BEACON AND COMMAND VSWR

Input	Frequency (MHz)	VSWR Deployed	VSWR Stowed
BEA No. 1	136.77	1.43	1.8
BEA No. 2	136.77	1.43	1.8
COM No. 1	148.56	1.22	1.25
COM No. 2	148.56	1.22	1.25

b. BEACON AND COMMAND ISOLATION

The results of the tests of isolation between beacon and command ports are given in Table 3-IV-4.

TABLE 3-IV-4. BEACON AND COMMAND ISOLATION

Input Port	Output Port	Frequency (MHz)	Specification (dB)	Actual (dB)
BEA No. 1	BEA No. 2	136.77	15	30
BEA No. 1	COM No. 1	136.77	64	75
BEA No. 1	COM No. 2	136.77	64	75
BEA No. 1	COM No. 1	148.56	25	40
BEA No. 1	COM No. 2	148.56	25	40
BEA No. 1	COM No. 1	108.56	25	75
BEA No. 1	COM No. 2	108.56	25	75

c. BEACON AND COMMAND INSERTION LOSS

The insertion loss of the beacon and command antenna system was measured. The results are given in Table 3-IV-5.

TABLE 3-IV-5. BEACON AND COMMAND INSERTION LOSS

Input Port	Frequency (MHz)	Specification Max (dB)	Actual (dB)
BEA No. 1	136.77	2.0	1.0
BEA No. 2	136.77	2.0	1.0
COM No. 1	148.56	8.0	7.0
COM No. 2	148.56	8.0	7.0

4. Isolation Between Input Ports

Isolation measurements between RF input ports were made. The HP 614 generator was used for S-band and the HP 608 generator with internal modulation was used for the VHF range. The results are in Table 3-IV-6.

5. Range Calibration

These tests compare signal strengths received from spacecraft antennas with those received from appropriately polarized permanent antennas. Transmitter levels were held constant when switching between the spacecraft and reference antennas, and received signal strengths were measured at the input to a 10-dB pad preceding the receiver input by direct comparison with a generator at the ground station.

a. REAL-TIME LINK CALIBRATION

For this test, the permanent antennas were horizontally polarized.

Frequency: 137.56 MHz
Transmitter Level: 0 dBm
Received level, spacecraft: -56 dBm
Received level, fixed antenna: -50.5 dBm
Spacecraft level relative to fixed antenna: -5.5 dB
Reference antenna gain: +5 dBi relative to isotropic (dBi)

b. BEACON LINK CALIBRATION

The permanent antennas were vertically polarized.

Frequency: 136.770 MHz
Transmitter level: 0 dBm

TABLE 3-IV-6. ISOLATION BETWEEN INPUT PORTS

Input Port	Output Port	Frequency (MHz)	Specification Limits	Isolation (dB)	
				Deployed	Stowed
BEA	COM	148.56	25	40	37
BEA	COM	108.56	25	75	75
BEA	COM	136.77	64	75	65-67
R-T No. 1	COM	148.56	35	55	65
R-T No. 1	COM	108.56	40	75	75
R-T No. 1	COM	137.56	67	75	75
R-T No. 2	COM	148.56	35	55	65
R-T No. 2	COM	108.56	40	75	75
R-T No. 2	COM	137.56	67	70	75
S-Band	COM	148.56	35	65	65
S-Band	COM	108.56	35	75	75
R-T No. 1	BEA	136.77	--	24	65
R-T No. 1	BEA	137.56	--	25	45
R-T No. 1	S-Band	137.56	--	75	75
S-Band	R-T	1697.5	--	60	60
S-Band	BEA	1697.5	--	60	60
S-Band	COM	1697.5	--	60	60
BEA	R-T	136.77	--	25	--

Received level, spacecraft: -58.5 dBm
Received level, fixed antenna: -54.5 dBm
Spacecraft level relative to fixed antenna: -4.0 dB
Reference antenna gain: +5 dBi

c. COMMAND LINK CALIBRATION

The permanent antennas were vertically polarized.

Frequency: 148.56 MHz
Transmitter level: 0 dBm
Received level, spacecraft: -68 dBm
Received level, fixed antenna: -52 dBm
Spacecraft level relative to fixed antenna: -16 dB
Reference antenna gain: +5 dBi

Comparison of Paragraph b, above, with this section indicates a possible difference in the radiation efficiency of the beacon and command antenna for the beacon and command frequencies. This difference is greater than the 6 dB additional loss within the spacecraft (Paragraph 3.IV. E.3.c) at the command frequency. The test was repeated using a dipole in place of the spacecraft antenna, and similar results were obtained. When the dipole was located in place of the reference antenna (which was removed when the dipole was radiating), there was no difference in the radiation efficiency at the two frequencies. As the dipole was moved, a null in signal strength was found near the position normally occupied by the spacecraft. This position exhibited a null at the command frequency but not at the beacon frequency.

d. S-BAND LINK CALIBRATION

The permanent antennas were vertically polarized.

Frequency: 1697.5 MHz
Transmitter level: +15 dBm
Received level, spacecraft: -74 dBm
Received level, fixed antenna: -68.5 dBm
Spacecraft level relative to fixed antenna: -5.5 dB
Reference antenna gain: +12.2 dBi

6. Antenna Pattern Checks

The antenna patterns were taken by transmitting at a known signal level and measuring the received signal level as a function of position. Rotation was clockwise from 0 to 360 degrees, with 0 degree corresponding to the direction of the earth in orbital configuration. The antenna patterns are plotted in terms of total loss from the spacecraft transmitter port to ground station antenna port (on the patch panel).

a. BEACON ANTENNA PATTERN

The beacon antenna pattern was +0, -3.0 dB from the 0-degree reference at all angles, and hence was not plotted. Transmitter power was +25 dBm (316 milliwatts) and received power was -36 to -39 dBm, for a total path loss of 61 to 64 dB in both deployed and stowed condition.

b. REAL-TIME ANTENNA PATTERN

The real-time patterns were plotted deployed and stowed. Data was taken at 10-degree increments. Transmitter power output was +37.0 dBm (6 watts) when the antennas were deployed, and +37.0 dBm (5 watts) when they were stowed. The real-time antennas of side 1 and side 2 were interchanged, and the pattern of side 2 was also measured in the deployed configuration. The real-time antenna patterns are shown in Figures 3-IV-4, -5, and -6. The total path loss includes cable system.

c. S-BAND ANTENNA PATTERN

The S-band pattern was essentially identical in the deployed and stowed configurations. Readings were taken in 5-degree increments. A signal generator and TWTA were used in place of the S-band transmitter, and output power level was +23.3 dBm. The S-band antenna pattern is shown in Figure 3-IV-7. The total path loss includes antenna and cable system.

F. PHASE II TEST RESULTS - RF EQUIPMENT

1. Bench Tests

a. S-BAND LINK

For the S-band link, the tests were made at a received signal level of approximately -55 dBm. The video gain on the receiver was adjusted to give 45 mV for the 300-kHz TBU tone into the demultiplexer.

The amplitude response (Table 3-IV-7 below) and phase response (not tabulated) tests using the S-band link did not show any significant deviation from the corresponding direct back-to-back tests.

The test for crosstalk between channels through the S-band transmitter and receiver (Table 3-IV-8, column 4) shows decreased (S + N)/N compared to the direct back-to-back tests (column 2). However, data taken with no signals in the multiplexer (columns 1 and 3) indicates the (S + N)/N is generally limited by noise introduced by the receiver rather than crosstalk. Receiver noise is highest in the DFC channel (440 to 480 kHz at the input to the DEMUX), as would be expected from FM noise characteristic.

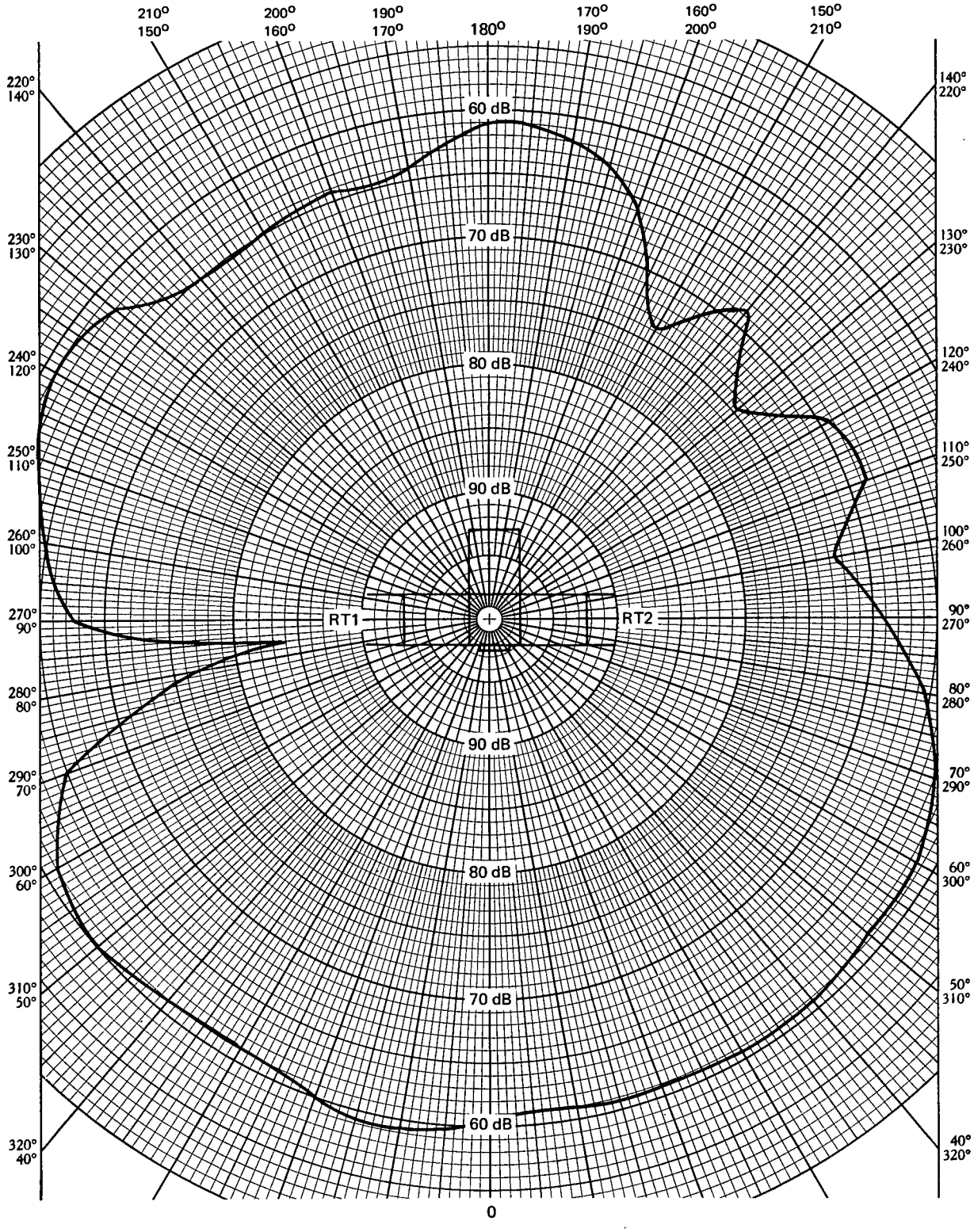

Figure 3-IV-4. Real-Time Antenna 1 Pattern, Panels Deployed

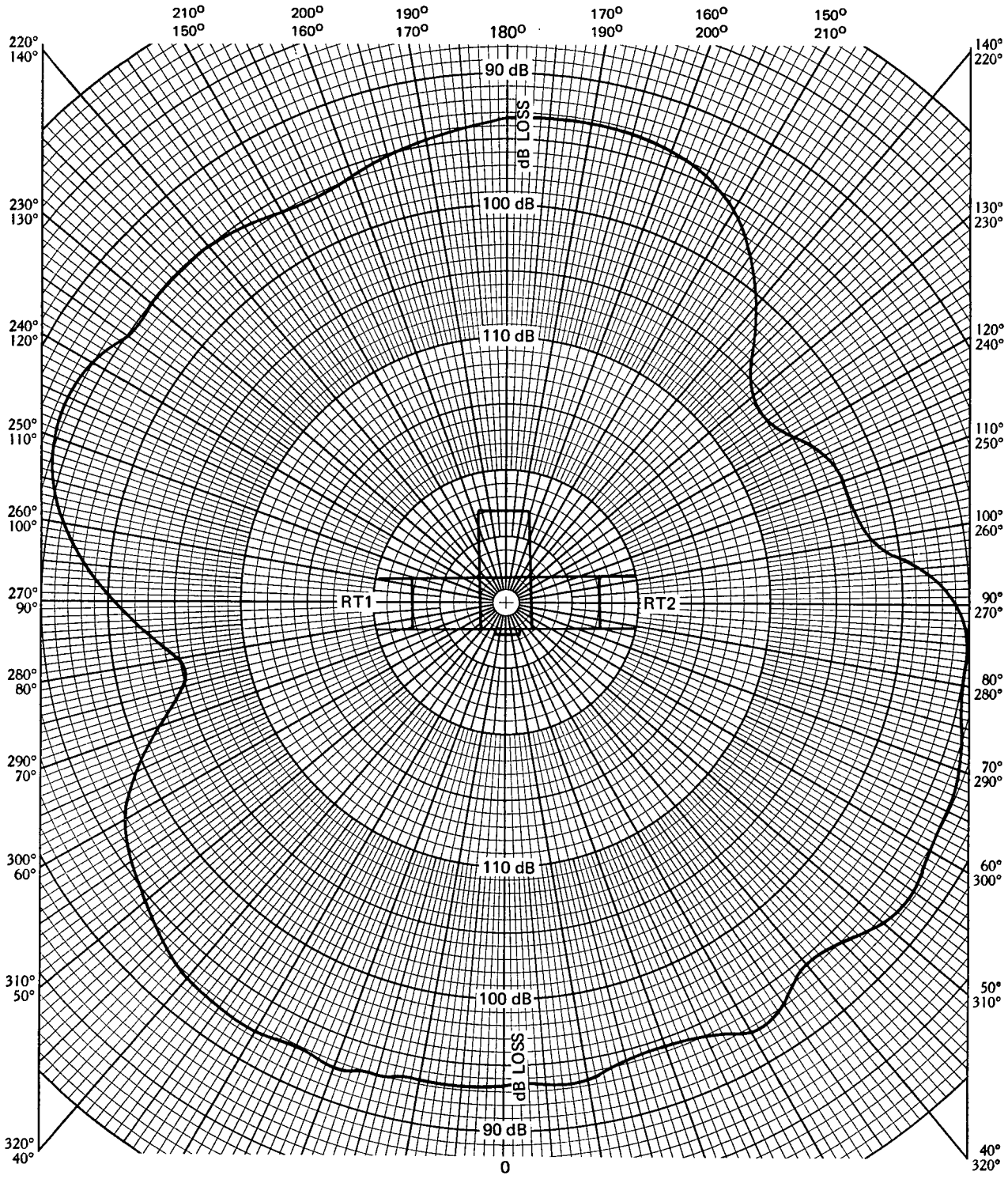

Figure 3-IV-5. Real-Time Antenna 1 Pattern, Panels Stowed

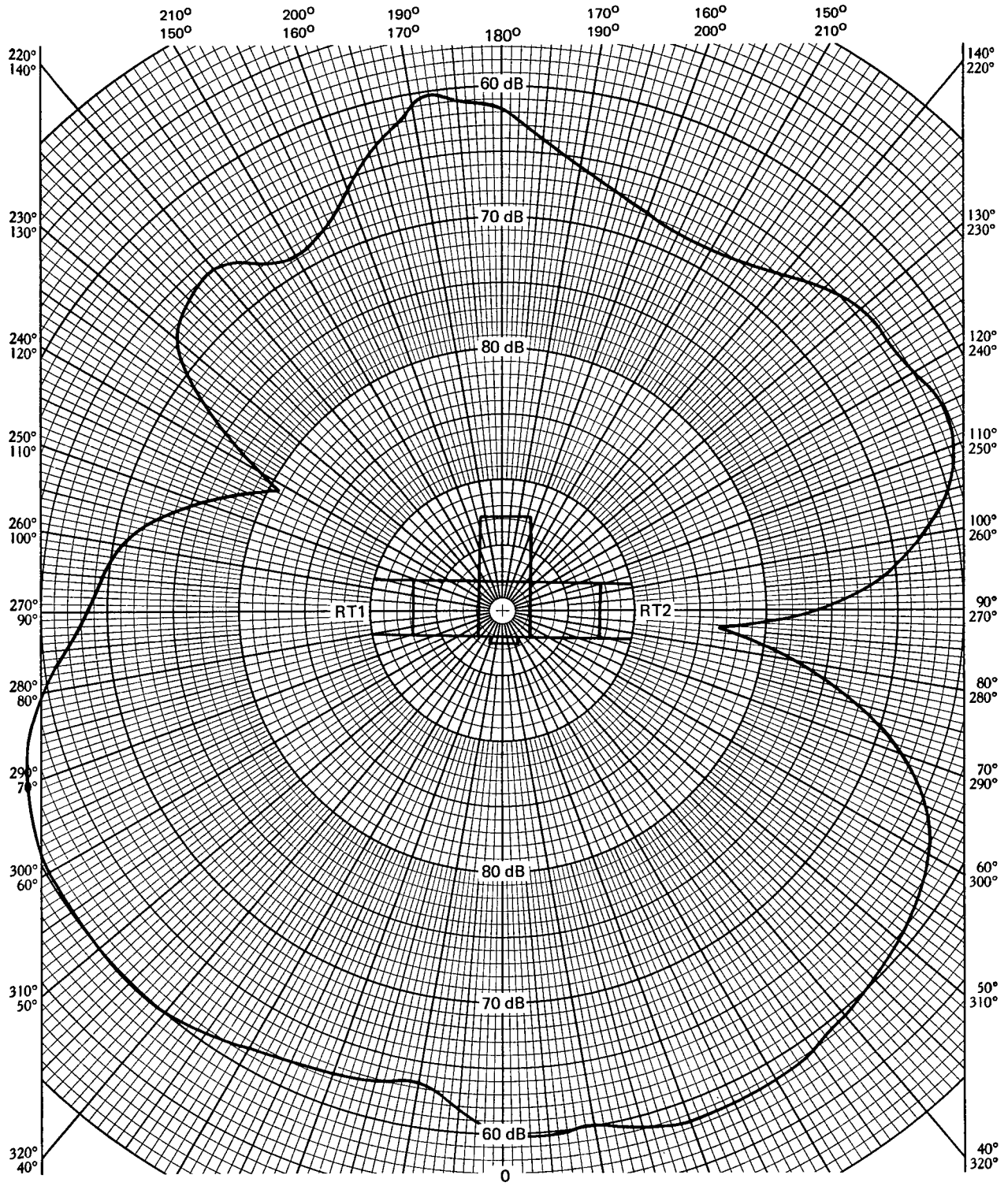

Figure 3-IV-6. Real-Time Antenna 2 Pattern, Panels Deployed

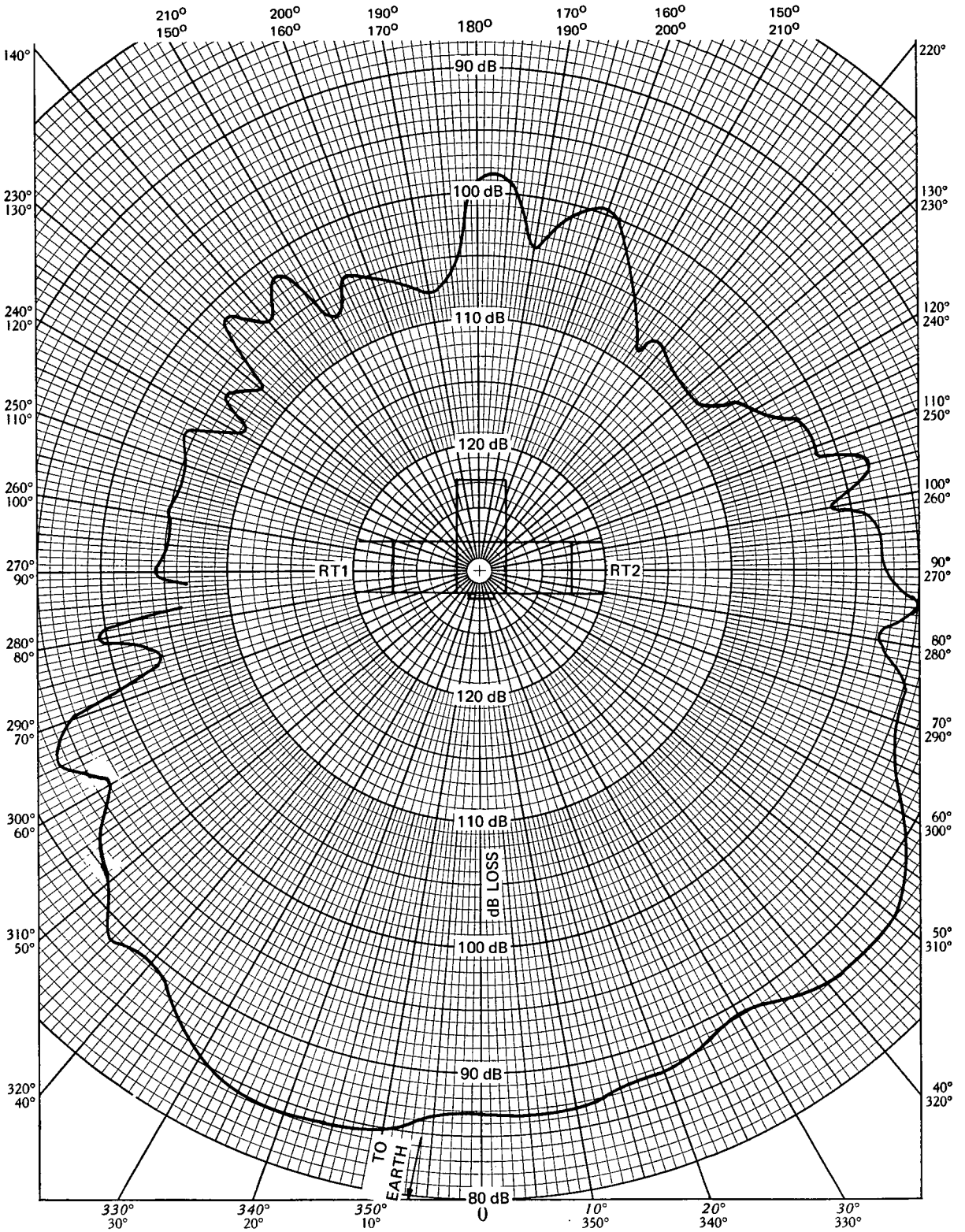

Figure 3-IV-7. S-Band Antenna Pattern

TABLE 3-IV-7. S-BAND LINK AMPLITUDE RESPONSE

MUX	Channel	Direct Ripple (dB)	S-Band Ripple (dB)
1	AVCS Video	3.5	3.0
1	SRR-A Video	0.8	0.9
1	SRR-B Video	0.6	0.7
2	DFC	2.0	1.7
2	AVCS W&F*	2.6	1.3
2	SRR No. 1 W&F*	0.5	0.3
1	SRR No. 2 W&F*	2.4	0.9

*Direct back-to-back measurements were made with ±1.5-kHz channel bandwidth; S-band measurements were made with ±1.0-kHz channel bandwidth because of a change in specification.

TABLE 3-IV-8. S-BAND LINK SIGNAL AND NOISE-TO-NOISE RATIOS (RMS/RMS)

Channel	1	2	3	4
	DIRECT		S-BAND	
	Noise (dB)	Crosstalk (dB)	Noise (dB)	Crosstalk (dB)
AVCS Video	72	66	66	64
SRR-A Video	60	50	43	42
SRR-B Video	60	50	42	41
DFC	61	49	38	38
AVCS W&F	62.5	44	46	40
SRR No. 1 W&F	49.5	38	45	34
SRR No. 2 W&F	65	47	44	43

b. REAL-TIME STAIRCASE TEST

Breadboards of the SR processor and commutator were used to generate an 8-level staircase, which was transmitted through the real-time link using a ground station Nems-Clarke receiver. Ground-loops made it necessary to insert a 300-Hz (active) high-pass filter between the receiver and oscilloscope. Within the limits of the test equipment, (±5 percent of maximum output amplitude) no significant degradation of the signal is evident.

2. RF Subsystem Test

a. COMMAND SENSITIVITY

Using as the command signal a carrier modulated 80 percent with a single tone, -109 dBm was found to be the command sensitivity of the receiver/decoder system at the receiver input port. The spacecraft was then installed in metal-free building with the solar panels deployed. Command signals were generated by a HP 608C at the ground station, (80-percent modulation) and transmitted over its vertically polarized antenna. It was found that under these conditions, -44 dBm was required from the generator to activate the command and control system. This sensitivity was found to be unaffected with all spacecraft transmitters on and fully modulated, and with various combinations of transmitters turned on. A TOS command decoder was used for these tests.

b. COMMAND SIGNAL SPURIOUS OBSERVATIONS

The video output of the command receiver was observed on an oscilloscope and with a wave analyzer as the various transmitters were turned on and modulated. With each combination of operating spacecraft equipment, receiver input was varied from no signal to -70 dBm. No effects of spacecraft equipment on the output of the command receiver were noted at any time. This test was performed with the panels stowed and deployed.

c. SPURIOUS OUTPUTS

In the absence of the GSFC electronics van, spurious output checks were made using an HP 8551B/851B spectrum analyzer. The spectrum of the spacecraft was found to be free of spurious outputs down to -55 dB from the beacon transmitter with the following exceptions:

(1) The second harmonic of the real-time transmitter was observable at least 54 dB down from the fundamental. The exact result could not be measured because an antenna calibrated at both the fundamental and harmonic frequencies was not available.

(2) When both the beacon and real-time transmitters are on, odd-order products are generated due to the relatively low (25-dB) isolation between the two transmitters. The strongest spur is 136.04 MHz, which is generated in the beacon transmitter and is -32 dB relative to the beacon signal. A spur at 138.23 MHz is 52 dB down from the real-time transmitter, in which it originates.

SECTION V

ETM SPACECRAFT TEST PROGRAM

A. ETM TEST PHILOSOPHY

The Electrical Test Model (ETM) spacecraft was used to verify all system interfaces, both within the spacecraft and between the spacecraft and ground equipment. It was used also to check the test facilities and to debug the handling and test procedures intended for use on flight spacecraft. The overall ETM spacecraft test program was conducted in three phases as follows:

- Phase I, System Interface Verification. This phase includes harness ringout, power turn-on, functional check, detailed electrical tests, a dynamic suspension test, and RFI tests.
- Phase II, Procedure and Facility Check. During this phase, the flight test procedures were debugged and the test facilities checked for compatibility.
- Phase III, Program Support. The ETM spacecraft was used to verify mechanical, electrical, and RF compatibility with the launch vehicle at the Western Test Range. In addition, it was used as an RF model during the launch operation. Major system changes were checked on the ETM spacecraft.

B. ETM SPACECRAFT TEST CHRONOLOGY

1. Harness Ringout

The harness ringout of the ETM spacecraft began on May 13, 1968. Two harness wiring errors were detected and corrected.

2. Initial Power and Functional Checkout (IPFC)

The electrical integration of the ETM spacecraft commenced with the IPFC on May 27, 1968. The harness interface with command distribution unit (CDU) B did not mate properly as the connectors were incorrectly oriented. This was remedied by reorientating all the CDU-B harness connectors.

On May 29 a broken wire at pin 19 of connector P1 on CDU-B was discovered and immediately repaired.

Functional checkout of the units on the ETM spacecraft continued satisfactorily until June 3 when an abnormality in the performance of the telemetry conditioner and commutators was detected. The commutators did not provide full external clock width for channel 1. Vendor modification of the commutators was required so that they could meet the performance requirements. However, the commutators were usable until a new modified set was supplied by the manufacturer. Also on June 3, it was discovered that the programmer did not provide continuous telemetry power, as required. This problem was remedied by adding a jumper wire inside the programmer which resulted in continuous telemetry power when the programmer was on.

On June 4, a discrepancy report indicated that it was not possible to load either programmer from either decoder. Investigation revealed a printed circuit trace was missing on the A3 and A6 boards in the decoder. A jumper wire was installed to correct the deficiency and all A3 and A6 boards in the decoders were reworked to correct this deficiency.

A second anomaly occurred on June 4 during functional checkout of the ETM spacecraft. It was discovered that the output DC level from the acquisition altitude sensor (AAS) Ser. No. 01P was -15 volts instead of the required value of -2.5 volts. Investigation revealed that the test output and operational output pins (pins 13 and 14) were reversed inside the AAS unit. The AAS was repaired and tested to confirm its satisfactory operational performance.*

Satisfactory checkout of the ETM spacecraft continued until June 10 when three discrepancies occurred. The first discrepancy involved the solar proton monitor (SPM) simulator. When commanded on, no output appeared at P1-14 or P1-5 of the SPM. Investigation revealed that the 15-Hz clock signal from the time base unit (TBU) was incompatible with the SPM requirements. The TBU was modified by adding a 1.6-kilohm clamping resistor to the SPM 15-Hz interface circuit. This change was incorporated on all A4 boards of the TBU.

The second June 10 discrepancy involved the incremental tape recorder (ITR) motor. During initial power turn-on (in record mode), the ITR motor was stepping backward instead of forward. The problem was resolved by reversing the motor power wires in the harness.

The third June 10 discrepancy involved the abnormally low 300-kHz input signal to the multiplexer from the TBU, causing the 300-Hz pilot tone to be low and out of specification. A decision was made to increase the amplitude of the 300-kHz signal from the TBU (A6 board) to provide a desired MUX output amplitude of 106 millivolts (p-p) instead of 95 millivolts (p-p).

* The AAS was later deleted from the ITOS design.

Functional checkout progressed satisfactorily until June 20. It was discovered that the push-to-talk (PTT) operation did not stop the scanning radiometer recorder No. 1 (SRR1) playback. Investigation revealed that the impedance to ground on the S-band switched ground lines from the CDU was 20 kilohms. This impedance kept SSR1 playback relay K3 (in CDU-A) energized after the S-band transmitter switched ground was opened. A sneak electrical path was found which caused K3 to remain energized when the S-band transmitter was turned off. To correct this anomaly, two isolating diodes (CR13 and CR14) were added to the A4 board in CDU-B to eliminate the sneak path. Necessary design and drawing changes were implemented.

During July 1968, four IPFC discrepancies were resolved. On July 2, improper dual SR processor power interface caused a power short to ground, resulting in a blown fuse (F19) in the power supply electronics (PSE). Subsequent troubleshooting disclosed that -24.5-volt power from the PSE was erroneously routed via the harness to the dual SR processor power ground lines. Though the erroneous interconnection existed for each processor, power was applied to only one and it was inoperative. This problem was remedied by modifying the spacecraft harness for correct interface with the SR processor wiring and fuse F19 in the PSE was replaced.

On July 11, a point-to-point check of the PSE outputs was made before any loads were attached. Initial measurements indicated -24.5 volts on pin 1 of the output connector, but subsequent tests revealed that fuse F18 on the A4 board was open, resulting in loss of -24.5 volts at pin 1. The only logical explanation for this anomaly was that pin 1 was accidentally shorted to ground during the output measurements. After completing the initial spacecraft electrical check, the PSE was removed from the spacecraft, and the open fuse was replaced.

On July 22 it was discovered that the AVCS camera performed improperly due to effects of power transients on the video clamp (camera video driven into the black clamp) only when the camera was operated with the AVCS recorder. Analysis revealed that the run tape power transient, originating from the A3 board in the camera electronics, caused the problem. The A3 board in the AVCS camera electronics assembly was modified to reduce clamp susceptibility to power transients.

The last IPFC discrepancy occurred on July 26, involving the pitch control electronics (PCE) unit. Incorrect closed/coarse telemetry (normal pitch loop gain mode having two states with same telemetry value) on channel 108 was obtained. Investigation revealed that this condition was due to improper interface impedance. The telemetry signal conditioner requires that the two-level signals have a source impedance of 15 kilohms ±10 percent. Back-biasing of two series diodes in the PCE caused improper impedances and the closed/coarse telemetry to be incorrect. The problem was resolved by a design change in the values of resistors R8 and R9 of the telemetry signal conditioner.

3. Detailed Electrical Test

a. GENERAL

The detailed electrical test of the ETM spacecraft units and subsystems began on June 19, 1968 with the test of the power subsystem. The units of the power subsystem included the power supply electronics, two batteries, and three solar panels. The series of tests performed included (1) PSE bus voltage verification, (2) PSE diode losses, (3) command operations, (4) battery charge characteristics, (5) solar bus characteristics, and (6) power subsystem profile and telemetry verification. All of the above tests were performed satisfactorily and the following objectives were established:

- Verify the interface compatibility of the individual units comprising the power subsystem with each other and with the other spacecraft units.
- Compare performance parameters with original unit test data to search out signs of degradation.
- Establish a performance reference at the spacecraft level against which later test data may be compared for historical trend analysis.
- Determine suitability of telemetry calibration curves supplied from unit test data for use at the spacecraft level.

b. RF DATA LINK TEST

On June 26, the detailed electrical test of the RF data link was satisfactorily completed. This test was restricted primarily to (1) the beacon and command links, (2) the real-time RF link, and (3) the S-band link. The test setup configuration for each of these tests is shown in Figures 3-V-1, 3-V-2, and 3-V-3 respectively.

c. APT CAMERA SUBSYSTEM TEST

On July 15, the APT camera subsystem detailed electrical test was successfully completed. The object of this test was to check out the performance of the APT camera subsystem when integrated with the other ETM spacecraft units. A secondary purpose of this test was to obtain duplicate data from the camera video detector and the demodulated video at the ground station from which a correlation could be established from the two points. This correlation was of importance since the camera video detector would be unavailable for future testing; all subsequent measurements would be made on the demodulated video at the ground

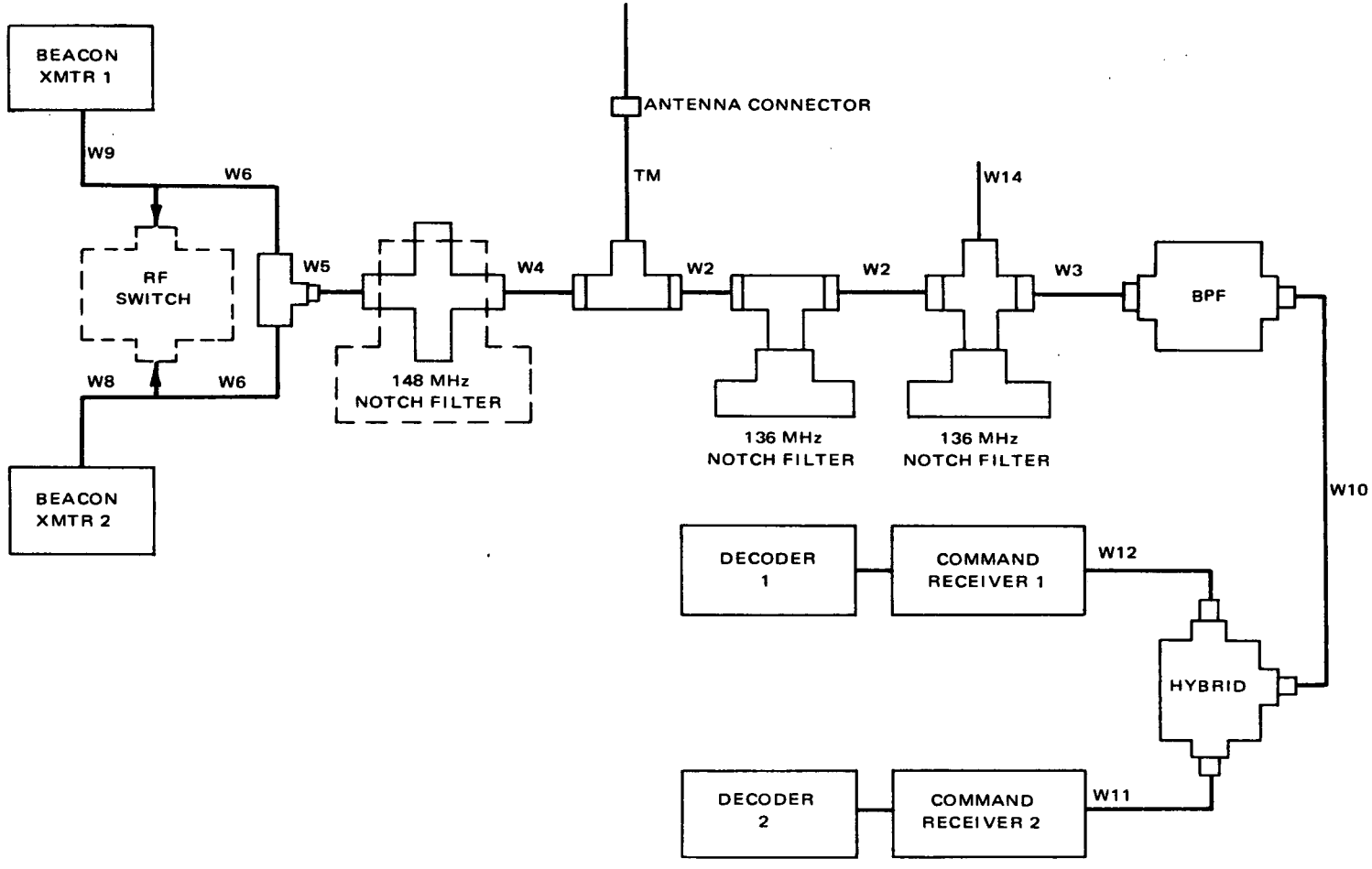

Figure 3-V-1. Beacon and Command Link (RF Data Link Test)

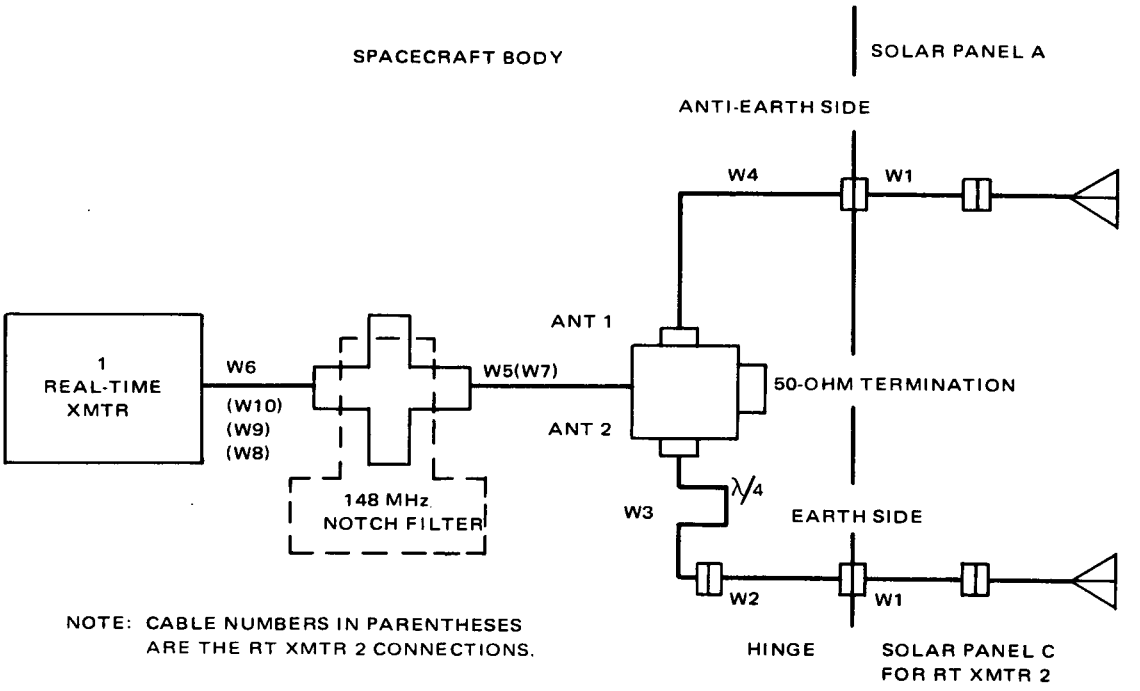

Figure 3-V-2. Real-Time RF Link (RF Data Link Test)

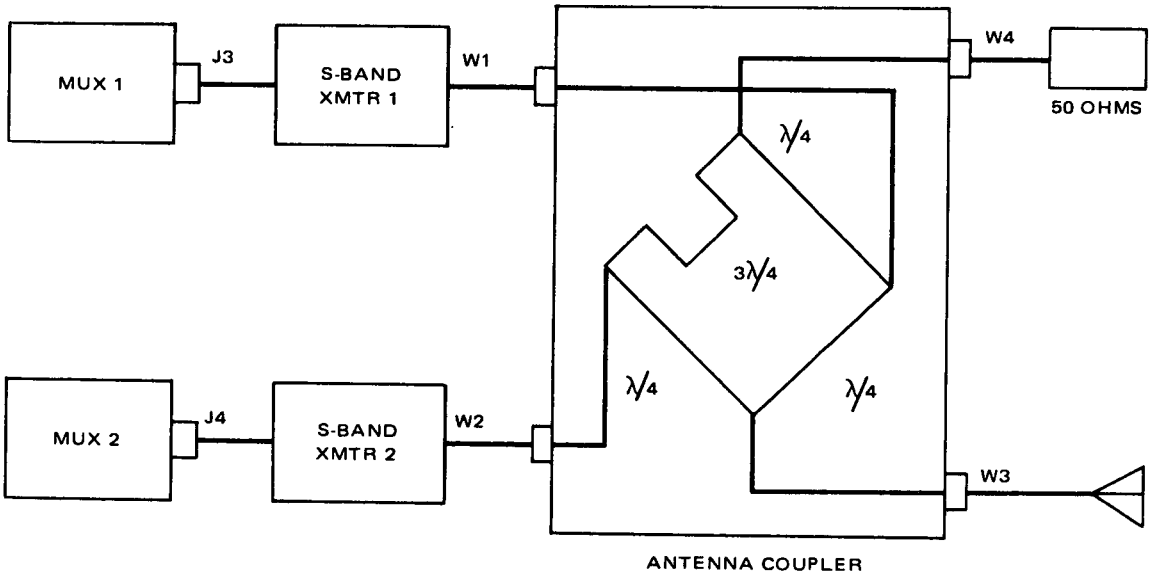

Figure 3-V-3. S-Band Link (RF Data Link Test)

station. The series of tests completed on the APT camera subsystem included the following:

- Shading measurements
- Resolution
- Signal-to-noise ratio
- Residual signal
- Phasing measurements
- Contrast ratio
- Gray scale measurements
- 300-Hz start tone measurements
- Angular rotation and deflection skew
- Picture size
- Picture evaluation

d. DYNAMICS SUBSYSTEM TEST

On July 17, the detailed electrical test of the ETM spacecraft dynamics subsystem was performed. The units involved for evaluating the performance characteristics of the various subsystems associated with the dynamic control and monitoring of the ETM spacecraft include the following:

- Momentum coils
- Magnetic bias coils and switch
- QOMAC coil
- Solar panel deployment squibs and associated firing circuitry
- Separation switches
- Accelerometer assembly and control unit
- Digital solar aspect sensor,
- Thermal controllers
- Structure temperature sensors

Testing of the above units was directed towards establishing operation and compatibility in association with their spacecraft interfaces. The various tests performed included the following:

- Momentum control
- Attitude control subsystem

- Pyrotechnics subsystem
- Separation switch control (including pitch loop motor power control)
- Accelerometer telemetry
- Digital solar aspect sensor
- Miscellaneous telemetry checkout

All tests were performed satisfactorily with the exception of the first. A logic error caused the wrong polarity on momentum coil 1. This was resolved by changing the logic and wiring the appropriate leads in the spacecraft harness.

e. SR, AVCS, AND SECONDARY SENSOR (SS) SUBSYSTEM TESTS

By July 22, detailed electrical tests were completed on the SR subsystem, AVCS subsystem, and the SS subsystem. The latter two were completed with no problems. However, before the SR subsystem was completed, a wiring error in the IR channel of the SR recorder produced excessive capacitance in the input line causing frequency roll-off of the input signal. The sync pulses were rounded off compared to the visible data and the amplitude of the marker tone on the IR channel was reduced from 3.8 volts (p-p) to 1.2 volts (p-p). This problem was resolved with correction of the wiring error in the SR recorder.

The various tests performed on July 22 for each of the three subsystems are summarized below:

SR Subsystem

- S-band receiver calibration
- SR mirror rotation
- Visible SR output into SR processor
- IR SR output into SR processor
- Visible real-time output
- IR real-time output

AVCS Subsystem

- Camera 1/camera 2 - recorder 1 parameter test
- Camera 2/recorder 2 parameter test

- Shading measurements
- Resolution
- Signal-to-noise ratio
- Gray scale
- Horizontal line measurements
- Vertical line and time code measurements
- Residual image
- Vidicon rotation
- Interframe gap
- Flutter-and-wow measurements
- Picture capacity
- S-band amplitude
- Picture evaluation

SS Subsystem (SSS)

- SSS testing (flight FPR sensors installed)
- SPM functional test
- SSS testing (FPR dummy head installed)
- SSS playback data reduction (analog and digital methods)
- Removal of FPR flight sensor and installation of FPR dummy head

f. PITCH CONTROL SYSTEM TEST

As a function of the phase II and III concepts, the ETM spacecraft was used to verify the flight test and launch checkout procedures developed for the dynamics subsystem and the pitch control system. On January 28, 1969 a detailed electrical test was performed on the dynamics subsystem. An external short caused fuse F-23 on the A4 board in the power supply electronics to blow. This was caused by a clip lead touching the baseplate. The fuse was replaced, and the test was completed satisfactorily. On February 18, after alignment of the pitch control system, a detailed electrical test was performed on this system with satisfactory results.

4. Go/No-Go- Electrical Test

On August 29, 1968, a go/no-go test was performed on the ETM spacecraft to provide a quick-look survey to check the basic operations of the various spacecraft subsystems. During this test, it was discovered that the pitch loop control motor would not stabilize at 75 rpm. Investigation revealed that the speed was dependent on the unregulated bus voltage, indicating a defect in the PCE. A leaky transistor (Q1 on the A7 board) in the PCE was found and replaced. The go/no-go test was then resumed and completed satisfactorily.

5. Measurement of Magnetic-Dipole Moments (Partial)

The ETM spacecraft was subjected to a partial magnetic dipole test on September 6, 1968 which was completed with satisfactory results. The test consisted of measuring the magnetic dipole moment using the magnetometer test stand and adding the required magnet to bring the dipole moment within controllable range. Further magnetic determinations included dipole measurements for each of the electrical modes of the spacecraft, including the quarter orbit magnetic attitude coil (QOMAC), magnetic bias coil, and the momentum coils. (The procedures for measuring and adjusting the magnetic-dipole moments are described in RCA test procedure TP-MD-1975000.)

6. Dynamic Suspension Test (Test No. 1)

On September 17, the ETM spacecraft was subjected to a dynamic suspension test which comprises a complete simulation of in-orbit, closed-loop performance of the pitch axis control system during initial spacecraft stabilization. The two main objectives of this test were:

(1) To demonstrate the control capacity of the pitch loops by establishing the ability of the spacecraft to lock-on to a heated target for a variety of values of initial system momentum and angular position.

(2) To ascertain the dynamic behavior of the spacecraft during the precapture transient, including the time from initiation of closed-loop operation to target lock-on.

Tests in both air and vacuum were performed. Test results were generally satisfactory. In the in-air tests, lock-on of the spacecraft was achieved in eight test runs during which high-speed telemetry data was recorded. The in-vacuum tests resulted in lock-on during three test runs with recorded telemetry data. On the basis of the test results, the dynamic suspension rig was modified to minimize the momentum added by the suspension system during the "follow" mode.

This test was then continued but later interrupted because of two discrepancies. The first anomaly was a change in amplitude of the pitch index pulse and roll sensor pulse on the beacon subcarrier oscillator (SCO) which caused a change in bias level during one capture run. This part of the test was rerun but the anomaly could not be reproduced. The second discrepancy was an unexpected reversal in motor acceleration causing additional revolution of the spacecraft before capture. This was caused by loss of a horizon pulse during the switch from coarse to fine gain. This problem was resolved by providing a permanent 330-degree backup pulse per spin period in the coarse mode. This necessitated a change to board A1 in the PCE. After this change, the spacecraft was again mounted in the suspension rig for continuation and satisfactory completion of the test. The ETM spacecraft is shown on the dynamic suspension rig in Figure 3-V-4.

7. Standard Electrical Performance Evaluation Test (SEPET)

The ETM SEPET, orbit 1 through orbit 8, was performed from September 26 through 28, with overall satisfactory results. During this test, both pitch loops were operated, using the onboard sensors. Three data anomalies were observed during the SEPET and were resolved as follows.

The first anomaly occurred during the APT readout in which discontinuities in the vertical deflection appeared on the Mufax printouts. This anomaly was believed to be externally induced since repeated operation of the system failed to reproduce the anomaly.

The second data anomaly involved the out-of-specification width of the data "1" verification pulse. Investigation revealed that this was caused by an open resistor (R35) on board A7 in the decoder. Resistor R35 was replaced and initial retest of the A7 board returned the pulse to normal.

The third anomaly proved to be the result of an incorrect performance specification for the TBU. Applications of -24.5 volts on the time code lock test point did not cause the time code to alternate from all "1's" to all "0's" frame by frame, as required by the SEPET procedure and TBU performance specification. No component or wiring change was required since the system requirement to shut down the real-time transmitter was met. The wording of both the TBU performance specification and SEPET procedure were changed.

The SEPET on the ETM spacecraft was completed during the first week of October 1968. The spacecraft is shown mounted in the SEPET fixture in Figure 3-V-5.

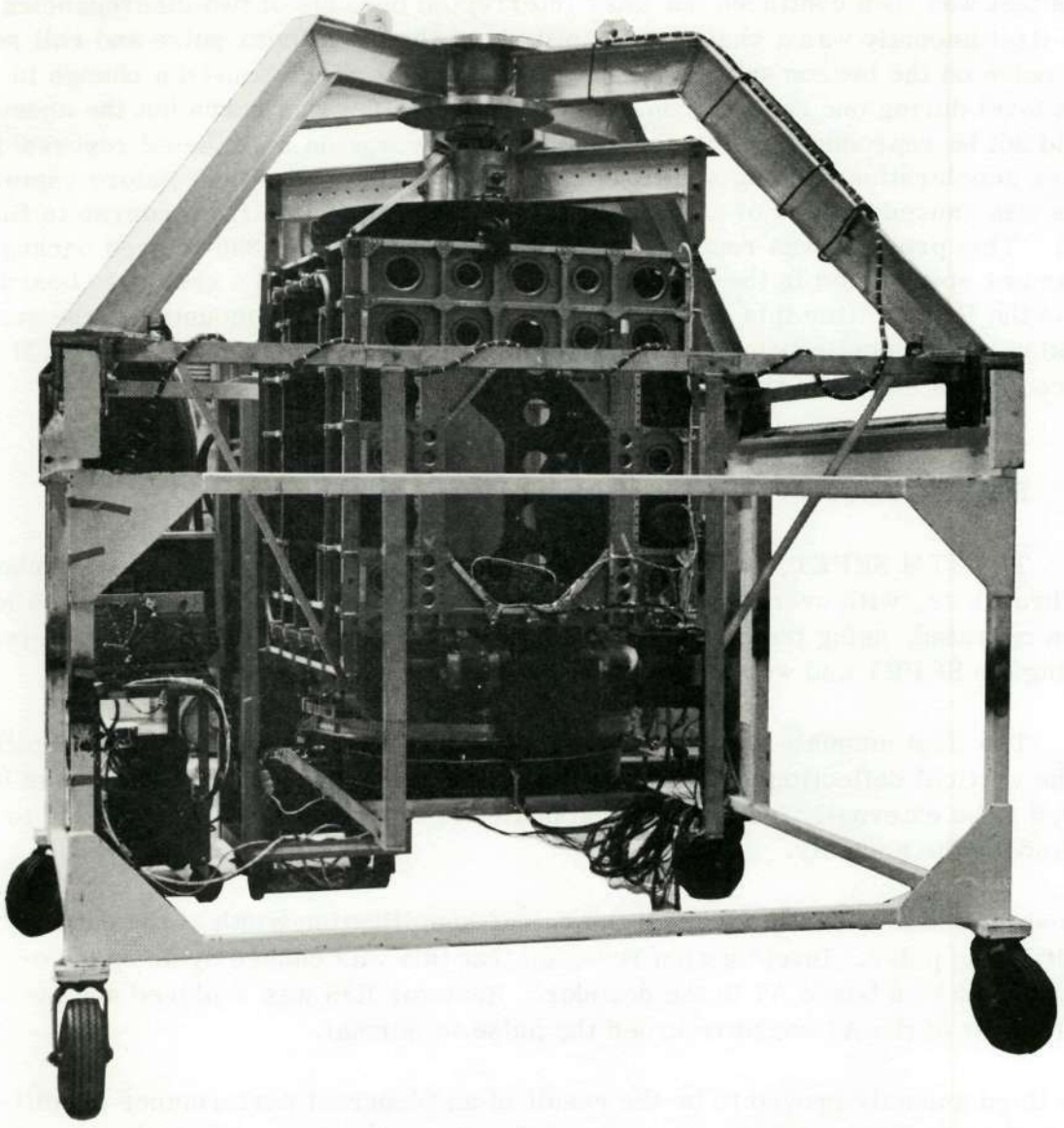

Figure 3-V-4. ETM Spacecraft Suspended from Dynamic Suspension Rig

8. Special Scanning Radiometer Test

On October 8, 1968, the ETM spacecraft was subjected to a partial scanning radiometer subsystem calibration check. This check involved IR and visible spartial resolution measurements and adjustments using a special parabolic collimator supplied by ESSA. The test was performed satisfactorily.

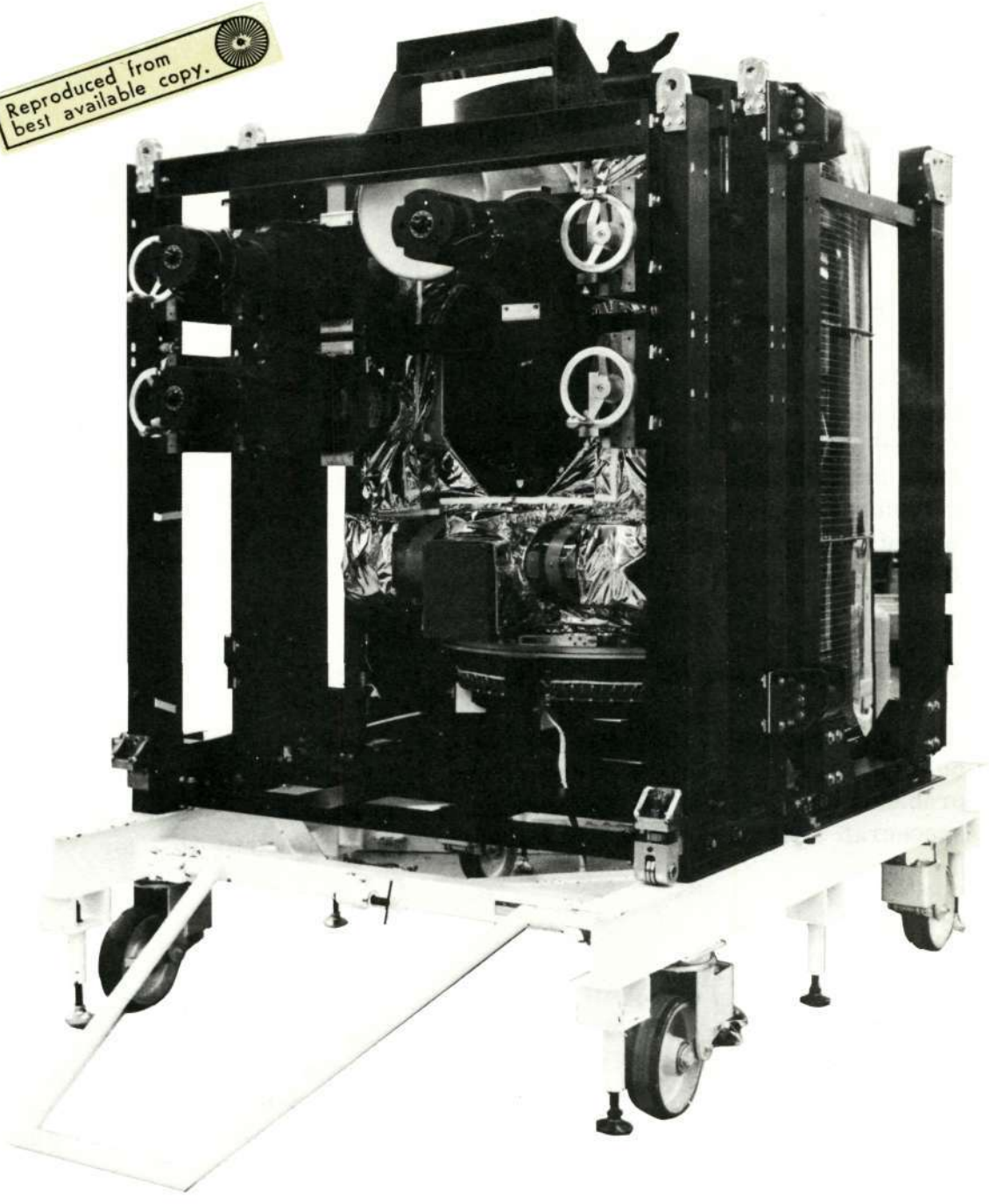

Figure 3-V-5. ETM Spacecraft on SEPET Fixture

9. RFI Test (Test No. 1)

An RFI test was performed on the ETM spacecraft on October 9 to demonstrate the ability of the spacecraft to operate in its own RF field without degradation of the command and primary or secondary sensor subsystems. During

this test it was noted that the S-band signal strength measured at the GSE* S-band receiver was fluctuating and that the pitch sensor telemetry at PS1 on SCO-1 was noisy. Investigation of these two anomalies revealed that they were not spacecraft problems, but test equipment and ground station receiver problems. The test equipment was repaired and proper tuning of the beacon receiver eliminated these anomalies. Figure 3-V-6 shows the ETM spacecraft undergoing the RFI test.

10. Special Power System Test

On October 17 during an outdoor solar array check, oscillations across the shunt dissipator resistors on the outer rib of anti-earth solar panel occurred only during operation of the beacon transmitter. Subsequent investigations isolated the oscillations to the power switch elements of the shunt limiter circuitry. The shunt dissipator/ PSE loop and spacecraft harness were redesigned to eliminate the oscillations and increase the overall stability of the loop.

11. Solar Proton Monitor Test

On October 21, the APL solar proton monitor (Ser. No. 002) was tested on the ETM spacecraft. There were some IC (open metallization) circuit problems encountered, but this unit was temporarily bypassed to continue ETM spacecraft testing. This unit was subsequently returned to APL for retrofit.

12. Transient Test

As a follow-up to circuit changes in the shunt dissipator/PSE loop to eliminate oscillations and ETM spacecraft harness modifications (including relocation of connectors), on November 13 a transient test was performed on the ETM spacecraft to determine if switching the S-band transmitter on and off would affect the power bus. The transient test was completed with no power bus discrepancies.

13. Balance and Moment-of-Inertia Measurements

On December 6, rough and fine balancing of the ETM spacecraft was satisfactorily completed, followed by satisfactory completion of the moment-of-inertia measurements.

---

* Ground Station Equipment

Figure 3-V-6. RFI Test of ETM Spacecraft

The weight and location of the balancing weights for the ETM were representative of the mass distribution for the final flight configuration. This task consisted of (1) removing each black box (functional or dummy) from the ETM spacecraft, (2) weighing the box, (3) adjusting its weight to conform to the weight of the flight unit, and (4) reassembling the box to the spacecraft.

The moment-of-inertia measurements were made to determine the moment and products of inertia in both the launch and operational configurations. Figure 3-V-7 shows the ETM spacecraft suspended from the bifilar pendulum used for moment-of-inertia measurements.

14. Spacecraft Console No. 2 Operational Check

On December 17 the ETM spacecraft was employed to verify the operation of spacecraft checkout console No. 2. During this check, two discrepancies occurred.

When the S-band transmitter was commanded on, the unregulated voltage dropped to approximately -21 volts DC, resulting in execution of several erroneous commands. When the unregulated bus recovered to a normal voltage of

Figure 3-V-7. ETM Spacecraft Suspended from Bifilar Pendulum

-30.5 volts DC, the spacecraft commands could be sent and executed normally. No units were removed from the spacecraft and testing was resumed.

The second discrepancy also resulted in the generation of several erroneous commands from the spacecraft. This occurred when console No. 2 ground and spacecraft ground were connected at the console. Investigation of this problem was isolated to a wiring error in the console power supply. The defective power supply was replaced and the test was satisfactorily completed. No damage or overstress condition to the spacecraft equipment resulted.

15. Dynamic Suspension Test (Test No. 2)

A second dynamic suspension test was performed on the ETM spacecraft on December 26 and yielded satisfactory results. However, there was a problem of test rig leveling. Leveling of the rig was subsequently refined by modifying the dynamic suspension console which included spacecraft interface connectors and a high-resolution synchro bias adjustment.

16. Spacecraft Optical Alignment

On January 8, 1969, a check of the ETM spacecraft optical alignment was made to determine the pointing accuracy of all primary sensors and the fiducial center of the camera optical axis. During this check, it was discovered that there was no video output from the ETM APT camera. The APT camera was removed from the spacecraft for troubleshooting and the vidicon tube socket was found to be loose from the tube. The tube socket was repaired, the camera reinstalled on the spacecraft, and the optical alignment resumed and checked out satisfactorily. Figure 3-V-8 shows the optical alignment set-up for the ETM spacecraft.

17. Secondary Sensor Subsystem Data Reduction Debugging

On January 31, during debugging of the ETM spacecraft, it was observed that the clock frequency pulse on channel 2 of the ITR (Ser. No. 02P) was unstable (out-of-spec) during playback. This unit was removed from the spacecraft and an investigation revealed that the playback motor was not operating properly. The motor was replaced, the unit retested, and the performance was found to be satisfactory. The ITR was reinstalled on the spacecraft and the frequency of the clock pulse measured 1.09 kHz, which met the specification requirement of 1.0 kHz ±15 percent.

18. Abbreviated SEPET

Prior to using the ETM spacecraft to verify the procedures for the thermal-vacuum programs, an abbreviated SEPET was performed on the ETM and satisfactorily completed on February 1, 1969.

19. Thermal-Vacuum Facility Check

As a function of the phase II concept, the ETM spacecraft was subjected to a thermal-vacuum procedural facility check on February 3 for compatibility.

During this check it was discovered that on commanding the TBU-2 time code, the resulting time code readout appeared as all data "0's" and would not advance its count beyond zero. The unit was removed from the spacecraft and checked. The IC on board A3 was found to malfunction at cold temperatures (-10° C). The IC was replaced and the TBU retested. The TBU was reinstalled on the ETM spacecraft and the thermal-vacuum test was successfully completed.

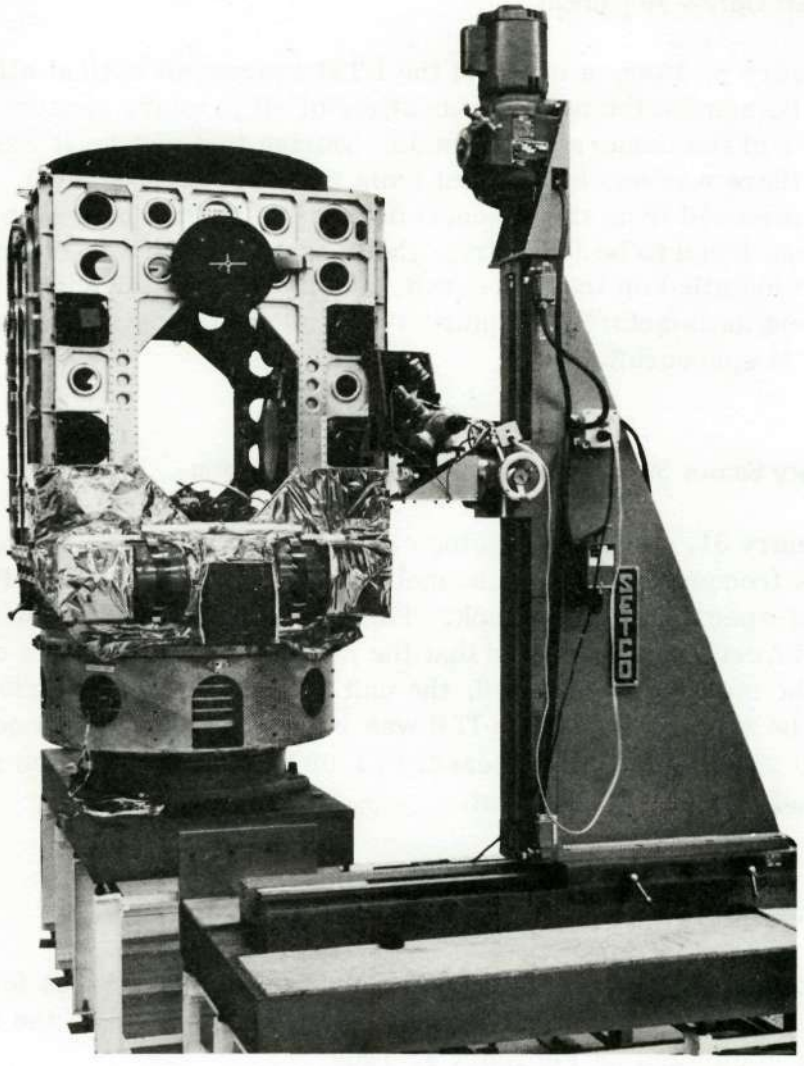

Figure 3-V-8. Optical Alignment Setup for ETM Spacecraft

20. Training Tape Test

On February 8, during checkout of the ETM spacecraft training tape, two discrepancies occurred, one with the prototype APT camera and one with the prototype AVCS recorder. During the readout of the APT camera, it was discovered that a portion of the picture broke up into a random pattern. It was also noted during playback of the AVCS recorder that the video as monitored on the A scan suffered severe frequency distortion and that the recorder startup occurred after the AVCS shutter. The APT camera problem was isolated to a previous 2N4008 transistor problem caused by a ball bond failure in the transistor. A new more reliable version of the 2N4008 transistor was ordered from the vendor for replacement of the defective type and for subsequent retrofit of all flight cameras.

The AVCS recorder problem was resolved by replacing the discovered defective A5 board in the tape recorder electronics.

21. RFI Test (Test No. 2)

The ETM spacecraft was subjected to a second RFI test on February 15, 1969. During this test the real-time output of the prototype scanning radiometer was observed to be varying arbitrarily between the black and white levels, intermittently missing the sync pulse and the calibration step. This anomaly was still present when the RFI environment was removed, and thus not RF related. Subsequent testing isolated one problem caused by an intermittent solder joint at the cathode of CR21. The second problem proved to be a leaky capacitor (C2) in the bias power supply, causing instability of the supply. CR21 was resoldered and C2 was replaced with a wet slug tantalum type capacitor. The RFI test was then completed with no RFI apparent.

22. Indoor Solar Array/PSE Test

On February 17, the power supply subsystem was tested after the solar array panels and PSE were modified to eliminate oscillations. No oscillations occurred during this test.

23. Launch Checkout

The launch checkout procedure was performed on the ETM spacecraft on February 17. During this test it was discovered that the unipolar torquing "on" time as recorded on console No. 2 events recorder was too long. Investigation of this problem revealed that the QOMAC events recorder had an erratic display, although spacecraft operation was normal. It was concluded that consol No. 2 events display was at fault. The threshold level of the events recorder driver circuit was readjusted. During the interim, console No. 3 events recorder was used to complete the launch checkout with no further anomalies.

24. Dynamic Suspension Test (Test No. 3)

A third dynamic suspension test was performed on the ETM spacecraft on February 27, 1969. This test was performed in vacuum and a discrepancy was discovered in the pitch control electronics (PCE) assembly (Ser. No. 05). The capture time was 7 minutes. This problem was caused by the loss of index pulses due to the wheel dropping to a low speed in going from coarse mode

to the closed loop mode. This was corrected by increasing the motor speed clamp circuit to obtain a higher speed (115 rpm instead of 75 rpm). This was accomplished by changing the values of R49, R57, R65, and R73 on board A6 in the PCE assembly.

25. Thermal-Vacuum Check and Thermal Cycle

On March 3, 1969 the ETM spacecraft was installed in the 8-foot thermal-vacuum chamber to verify the compatibility of the spacecraft, its thermal-vacuum fixture, the electrical interface, and the chamber. During this check, the thermal inertia of the spacecraft and fixture was determined. With spacecraft power off and sensor exciters off, it required 8 hours to lower the temperature of the spacecraft and fixture from +50° C to -10° C. This check was completed with no problems.

26. Outdoor Solar Array Check

On April 3, 1969 an outdoor solar array and spacecraft check was performed on the ETM spacecraft to verify power subsystem stability. During the solar array check, it was discovered that the shunt dissipator elements were inoperative because of a wiring error; the effect was to cut off transistor pairs Q1, Q2 and Q3, Q4 by interchanging the base and emitter leads. The wiring error was corrected, and the solar array check was completed satisfactorily.

27. RF Tests

On April 8, 1969, the ETM spacecraft was subjected to RF tests to verify proper performance of the spacecraft antennas, transmitters, and command receiver. Test results showed all RF parameters to be as specified. The ETM spacecraft was housed in the AED RF tower during the tests. (See Figure 3-V-9)

Figure 3-V-9. ETM Spacecraft in the AED RF Tower

SECTION VI

COMPONENT TEST HISTORIES

A. INTRODUCTION

The test histories in this section describe briefly the testing of three categories of components; i.e., engineering test models of new or revised circuits, prototypes of units that had not previously qualified for the TOS program, and flight units for the TIROS M spacecraft. The designs of new or revised components were verified by fabricating and testing engineering models of the units to demonstrate specified electrical performance. Prototypes of the units were constructed for environmental testing at prototype acceptance levels, which exceeded the flight levels. The flight units were subjected to environmental levels more severe than launch and orbital environments.

The prototype units were later mounted on the ETM spacecraft for the testing described in Section V above. The flight units described are those that made up the final complement of the TIROS M spacecraft.

Two components that were included in the preliminary design of the spacecraft were later deleted from the design when the decision was made to use a two-stage rather than a three-stage launch vehicle. These components, the attitude acquisition sensor and the despin mechanism, were designed for use in the initial orientation maneuver, in which the spacecraft, after separation from the launch vehicle, was required to perform an attitude reorientation of approximately 80 degrees and a despin from approximately 120 rpm to the very low mission rate. These two components because unnecessary with the use of the two-stage vehicles, which, before separation, places the spacecraft in the approximate orbital attitude and at the approximate mission spin rate, to within the control capabilities of the pitch control system, requiring the use of neither of these components.

Some testing, although included under the generic term of "component", was actually performed on boards or subassemblies. During this phase, module boards and subassemblies were "debugged", and "select at test" components were determined and assembled. This testing started with a circuit check (when applicable) of assembled parts and wiring. Following acceptance by Product Quality Assurance (PQA), initial power was applied and initial tests performed. These tests, investigative in nature, were made in accordance with test procedures prepared for this purpose. After conformal coating, the boards and subassemblies were assembled into the final subsystem configuration, sealed by Product Quality Control (PQC), and considered ready for qualification testing.

Except as modified by special directive from NASA or in Table 3-VI-1, each TIROS M component was subjected to the following test sequences:

PROTOTYPE

- Initial Electrical Performance Test
- Vibration at Prototype Levels
- Abbreviated Electrical Performance Test
- Acceleration
- Abbreviated Electrical Performance Test
- Thermal-Vacuum at Prototype Levels
- Final Electrical Performance Test

FLIGHT ACCEPTANCE

- Initial Electrical Performance Test
- Vibration
- Abbreviated Electrical Performance Test
- Thermal-Vacuum
- Final Electrical Performance Test

The listings in Table 3-VI-1 show the tests to which each prototype and flight component was subjected and provide a summary of test completion dates. Qualification tests were not performed on GFE units including the flat plate radiometers and solar proton monitors, which were delivered to RCA pretested at the University of Wisconsin and ESSA/APL, respectively.

Each prototype and flight component was functionally tested in accordance with its individual Initial Electrical Performance Test Procedure, as shown in Table 3-VI-1. Detailed quantitative measurements were made. This testing was designed to demonstrate thermal stability and was performed at room ambient temperature and at temperature extremes from -10°C to +55°C using the Tenney box facility.

Typically, each prototype and flight component of the TIROS M spacecraft was exposed to vibration levels designed to demonstrate its ability to perform following launch and to reveal any latent workmanship defects in parts and subassemblies. Those components that would be operating during launch had power applied, and performance was monitored while vibration tests were being conducted.

TABLE 3-VI-1. HISTORY OF COMPONENT TESTING

Nomenclature	Part Number	Prototype				Flight Acceptance		
		Acc.	Vib.	Tenney	T/V	Vib.	Tenney	T/V
COMMAND GROUP								
CDU-A	1975101-501		5/17/68	5/17/68	5/23/68	8/28/68	8/27/68	9/6/68
CDU-B	1975101-501		5/17/68	5/17/68	5/23/68	1/24/69	1/24/69	1/28/69
Dual SR Processor	1975102-501		6/28/68	6/20/68	7/12/68	4/16/69	4/15/69	4/19/69
Data Format Converter	1975103-501		7/10/68	7/10/68	7/19/68	12/7/68	12/7/68	12/10/68
Dual Programmer	1975104-501	5/21/68	5/20/68	5/18/68	7/31/68	4/1/69	4/1/69	4/3/69
Dual Time Base Unit	1975105-501		8/20/68	5/20/68	1/30/69	3/25/69	2/17/69	3/3/69
Dual Decoder	1975106-501*		5/9/68	5/8/68	5/17/68	4/26/69	5/14/69	1/27/69
STRUCTURE GROUP								
Spacecraft Structure	Various		**		***	S/C	S/C	S/C
Spacecraft Harness	1975052-501					S/C	S/C	S/C
Solar Panel Actuator****	1975044-501					S/C		S/C
Solar Panel Pin Puller****	1967591-501					S/C	S/C	S/C
CAMERA GROUP								
APT Camera Sensor No. 1	1975200-503		7/2/68	6/5/68	7/16/68	3/14/69	8/22/69	8/15/69
APT Camera Elec. No. 1	1975202-503					4/19/69		
APT Camera Sensor No. 2	1975200-503					5/7/69	5/7/69	6/2/69
APT Camera Elec. No. 2	1975202-503					5/7/69		
AVCS Camera Sensor No. 1	1975203-501		7/15/68	7/8/68	11/11/68	3/11/69	3/9/69	***** 3/19/69
AVCS Camera Elec. No. 1	1975205-501					3/11/69		
AVCS Camera Sensor No. 2	1975203-501					12/11/68	12/4/68	***** 1/20/69
AVCS Camera Elec. No. 2	1975205-501					12/11/68		
COMMUNICATIONS GROUP								
Real-Time Antenna No. 1	1975146-501					S/C		S/C
Command Receiver	1975123-501			4/16/68		4/26/68	4/25/68	4/30/68
Bandpass Filter (148 MHz)	1840332-2					9/16/68 Ⓧ	9/13/68 Ⓧ	S/C
Notch Filter (136 MHz)	1842378-502					1/26/68	S/C	S/C
Hybrid Coupler, Real-Time****	1975126-1					7/16/68	7/2/68	7/27/68
S-Band Transmitters	1975128-1	4/5/68			7/22/68	1/3/69	1/2/69	1/14/69
S-Band Antenna Coupler	1975147-501							
Real-Time Transmitter	1975130-501		†	5/10/68	†	8/14/68	8/14/68	8/28/68
Real-Time Transmitter	1975130-502					10/1/68	10/1/68	10/18/68
RF Switch	1964670-501		1/23/69	1/21/69	1/27/69	1/31/69	1/30/69	S/C

* 1975106-502 through -507 indicate dual decoder units with different command addresses.
** Mechanical Test Model Tests
*** Thermal Test Model Tests
**** Vendor-tested
***** AVCS Subsystem Thermal-Vacuum Test
Ⓧ Indicates testing by RCA after delivery.
† Qualified under Contract No. NAS5-9034
†† Waived
††† Pitch Control Subsystem Thermal-Vacuum Tests

TABLE 3-VI-1. HISTORY OF COMPONENT TESTING (Continued)

Nomenclature	Part Number	Prototype				Flight Acceptance		
		Acc.	Vib.	Tenney	T/V	Vib.	Tenney	T/V
COMMUNICATIONS GROUP (continued)								
Notch Filters (148 MHz)	1848920-501		†	†	†	2/15-2/18/68	S/C	S/C
Dual Multiplexer	1975133-501		9/5/68	8/29/68	9/13/68	10/4/68	10/4/68	10/8/68
Telemetry Cond. & Comm.	1975134-501		5/22/68	5/21/68	††	7/30/68	12/23/68	3/28/69
Beacon Command Antenna	1969056-501							
Beacon Command R-F Cabling	1975136-501							
Hybrid Coupler****	1975138-1					12/21/67	12/18/67	1/17/68
Beacon Transmitter No. 1	1975143-1		6/10/68	6/7/68	6/17/68	6/10/68	6/6/68	6/14/68
No. 2	1975143-1					4/18/68	4/9/68	4/24/68
Dual SCO Assembly****	1975144-1					1/30/68	1/30/68	1/31/68
Coaxial Termination	19626841-1							
Real-Time R-F Cabling	1975245-501							
S-Band R-F Cabling	1975246-501							
Real-Time Antenna No. 2	1975146-502							
S-Band Antenna	1975149-501		8/28/68	8/68		9/18/68	9/17/68	
S-Band Coupler	1975150-501		8/28/68	8/68		9/18/68	9/17/68	
Coaxial Cable	1964700-501							
POWER GROUP								
Solar Panel Cell Assembly	1975005-501		**			S/C	9/19/68	6/10/69
Solar Panel Cell Assembly	1975003-501		**	4/26/68	4/6/68	S/C	11/25/68	6/10/69
Solar Panel Cell Assembly	1975003-501		**			S/C	6/4/69	6/6/69
Power Supply Electronics	1975158-501		8/5/68	7/31/68	8/12/68	2/12/69	4/29/69	2/13/69
Battery	1975160-501		7/2/68	6/28/68	8/8/68	8/15/68	8/14/68	8/20/68
RECORDER GROUP								
SR Recorder No. 1	1975225-501	**	1/69	12/22/68	2/69	2/27/69	2/25/69	2/28/69
SR Recorder Elec. No. 1	1975228-501					2/27/69		
SR Recorder No. 2	1975225-501					4/2/69	3/29/69	4/10/69
SR Recorder Elec. No. 2	1975228-501					4/2/69		
AVCS Recorder No. 1	1975226-501	11/1/68	1/8/69	12/23/68	*****	3/12/69	2/14/69	3/25/69
AVCS Recorder Elec. No. 1	1975230-501					2/15/69		*****
AVCS Recorder No. 2	1975226-501					3/1/69	2/27/69	*****
AVCS Recorder Elec. No. 2	1975230-501					3/1/69		3/14/69
Incremental Recorder	1975227-501	8/26/68	6/21/68	6/20/68	8/23/68	9/13/68	9/13/68	9/17/68

* 1975106-502 through -507 indicate dual decoder units with different command addresses.
** Mechanical Test Model Tests
*** Thermal Test Model Tests
**** Vendor-tested
***** AVCS Subsystem Thermal-Vacuum Test
Ⓧ Indicates testing by RCA after delivery.
† Qualified under Contract No. NAS5-9034
†† Waived
††† Pitch Control Subsystem Thermal-Vacuum Tests

TABLE 3-VI-1. HISTORY OF COMPONENT TESTING (Continued)

Nomenclature	Part Number	Prototype				Flight Acceptance		
		Acc.	Vib.	Tenney	T/V	Vib.	Tenney	T/V
INFRARED GROUP								
DSAS	1975254-1, -2	4/1/68	3/29/68	3/26/68	4/7/68	5/14/68	5/13/68	5/17/68
SR Sensor & Elec. No. 1	1975255-1, -2	7/23/68	7/2/68	7/24/68	7/19/68	2/6/69	2/3/69	2/10/69
SR Sensor & Elec. No. 2	1975255-1, -2					12/11/68 (Scanner) 12/30/68 (Elec.)	12/5/68	1/17/69
DYNAMICS GROUP								
Dual Momentum Coil	1975175-501					S/C	2/23/68	S/C
Nutation Damper	1975176-501		**		***	S/C	S/C	S/C
Momentum Wheel Assembly	1975177-501	7/11/68	7/3/68		†††	8/1/69	S/C	†††
Momentum Wheel Assembly	1975177-501		5/17/69		6/19/69			(Life Test)
Pitch Control Electronics	1975178-501		8/12/68	8/9/68	†††	5/7/69	5/7/69	†††
Magnetic Bias Switch	1975179-501		5/10/68	5/17/68		6/4/68	6/3/68	S/C
Attitude Control Coil	1975180-501					S/C	2/23/68	S/C
THERMAL GROUP								
Active Thermal Controller (Right)	1975082-501		**		***	S/C	S/C	S/C
Actuator/Sensor Assembly	1975304-501		5/23/68	5/21/68	5/29/68	5/14/68 & 3/15/68		6/24/68
Active Thermal Controller (Left)	197509-501					S/C	S/C	S/C
Thermal Blankets	1975080-501				***	S/C		

* 1975106-502 through -507 indicate dual decoder units with different command addresses.
** Mechanical Test Model Tests
*** Thermal Test Model Tests
**** Vendor-tested
***** AVCS Subsystem Thermal-Vacuum Test
Ⓧ Indicates testing by RCA after delivery.
† Qualified under Contract No. NAS5-9034
†† Waived
††† Pitch Control Subsystem Thermal-Vacuum Tests

Table 3-VI-2 shows the exposure levels used in vibration and acceleration testing.

TABLE 3-VI-2. COMPONENT VIBRATION AND ACCELERATION TEST REQUIREMENTS

PROTOTYPE COMPONENT VIBRATION TEST LEVELS		
Parameter	A	B
	Random** (All axes)	Sinusoidal* (All axes)
Bandwidth	20 - 2000 Hz	5 - 2000 Hz
Duration	4 minutes	2 octaves/min.
Vibration Level	0.2 g^2/Hz (20 g rms)	10 g, 0 to peak

FLIGHT COMPONENT VIBRATION TEST LEVELS		
Parameter	A	B
	Random** (All axes)	Sinusoidal* (All axes)
Bandwidth	20 - 2000 Hz	5 - 2000 Hz
Duration	2 minutes	4 octaves/min.
Vibration Level	0.05 g^2/Hz (10 g rms)	5 g, 0 to peak

PROTOTYPE COMPONENT SUSTAINED ACCELERATION TEST				
Description	Level (g)	Duration (minutes)	No. of Tests	AED Centrifuge Speed (rpm)
Positive, in each of 3 axes	22	5	3	Measure radius to c.g. and determine required speed.
Negative, in each of 3 axes	22	5	3	

* Displacement must be maintained 0.500 inch, double amplitude when designated g levels cannot be attained due to armature displacement limitations.

** A 12 dB/octave minimum roll-off shall be applied at both ends of the frequency bandwidth.

An abbreviated electrical test was performed after vibration and acceleration tests. Its purpose was to demonstrate basic functional operation of the unit.

Typically, each component of the TIROS M spacecraft was operated while exposed to the thermal-vacuum conditions shown in Figure 3-VI-1. Like the vibration tests, these tests were designed to demonstrate the ability of the individual components to perform in the space environment and to reveal any latent workmanship defects in parts and subassemblies. The individual thermal-vacuum profiles for the scanning radiometer, scanning radiometer recorder, incremental tape recorder, and APT camera, which differed from the typical profiles of Figure 3-VI-1, are shown in Figures 3-VI-2 through 3-VI-5.

Any test discrepancies that occurred during the individual component qualification testing were reported in accordance with the ITOS Reliability Program Plan. Each anomaly was investigated and a Test Review Board, in accordance with the ITOS Quality Control Plan, determined the extent of retesting required.

B. SUBSYSTEM TESTING

Tests on integrated components of the AVCS Subsystem and Pitch Control Subsystem were performed to ensure that these subsystems met their design specifications prior to integration with the spacecraft. The tests included thermal-vacuum, alignment, performance, and calibration testing.

1. AVCS Subsystem

The components of the AVCS subsystem are the AVCS camera and camera electronics, and the AVCS recorder and recorder electronics. The individual components were separately tested through component vibration before beginning the subsystem test. The subsystem tests were composed of integration tests and performance tests. The integration test was performed on the AVCS subsystem to assure that no component interface problems existed and to verify that the integrated camera and recorder combination would operate in accordance with the camera and recorder performance specifications. Performance tests were performed to provide a complete test of AVCS operation prior to installation of the subsystem into the spacecraft. Thermal-vacuum tests were performed at anticipated orbital environmental levels to prove that subsystem performance would meet the required test parameters. The tests were also performed at environmental exposure levels that exceeded those anticipated; the subsystem at these times was required to perform properly in accordance with an abbreviated list of test parameters. The thermal-vacuum profile for this testing is shown in Figure 3-VI-6.

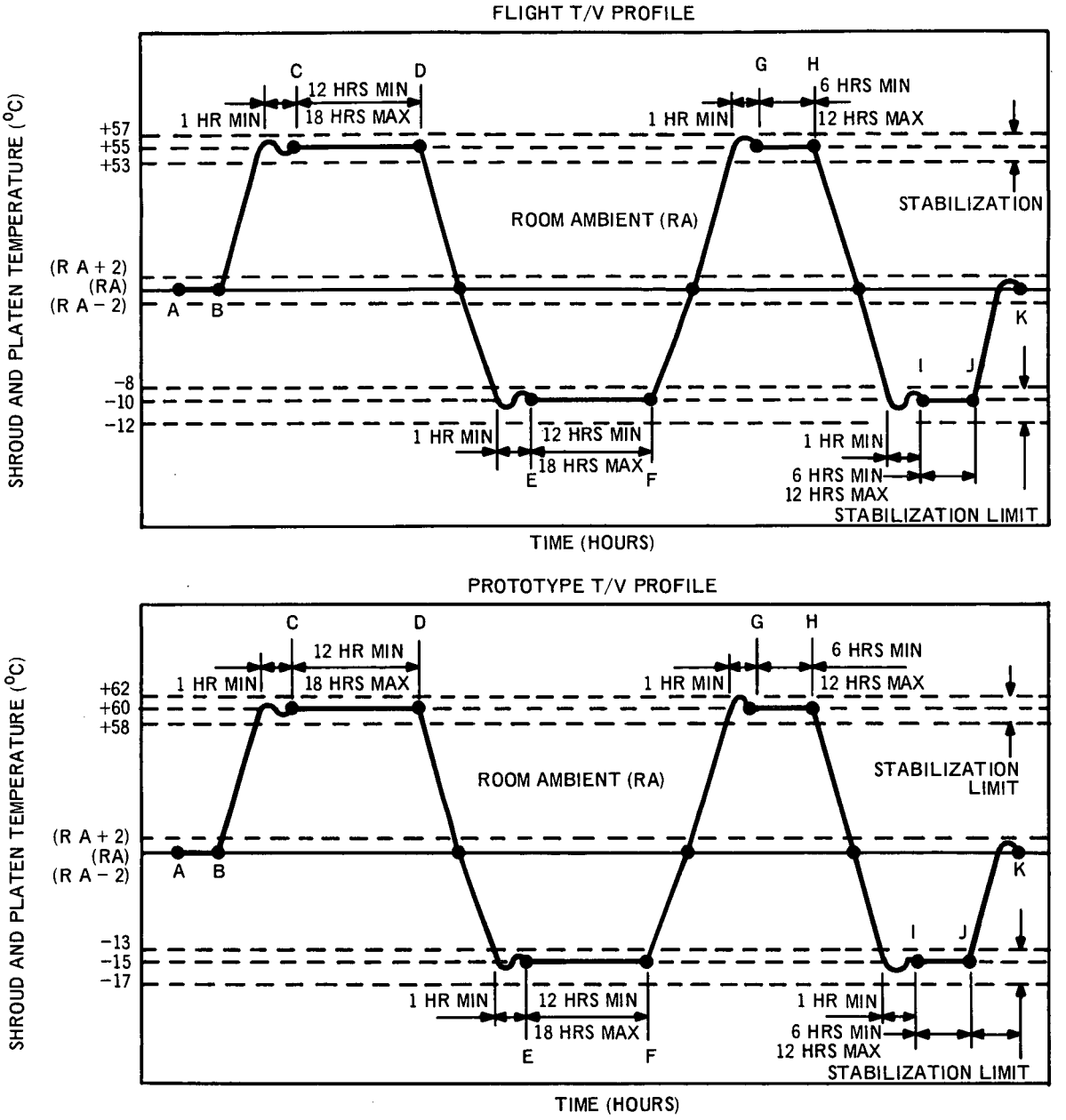

LEGEND

I. PERFORM ELECTRICAL TEST AS DETAILED IN THE COMPONENT TEST PROCEDURE.
   1. DURING PUMPDOWN AT 1×10^{-4} mm Hg (OR LESS) BETWEEN A AND B.
   2. AFTER TEMPERATURE STABILIZATION OF MONITORING T/C's AT POINTS C, E, G, I, AND K, AND BEFORE PLATEAU TERMINAL POINTS D, F, H, AND J, FOLLOWING EACH STABILIZATION POINT.

II. MAINTAIN 5×10^{-5} mm Hg* FROM POINT C THROUGH REMAINDER OF TEST.

III. BREAK VACUUM WHEN ELECTRICAL CHECK AT POINT K IS COMPLETE.

IV. RATE OF CHANGE OF TEMPERATURE SHALL BE THE MAXIMUM OF THE PARTICULAR BELL JAR CAPABILITY WITHOUT EXCEEDING THE INDICATED LIMITS.

*OR LESS

Figure 3-VI-1. Flight-Model and Prototype Thermal-Vacuum Test Profile for Components (Except Recorders and Sensors)

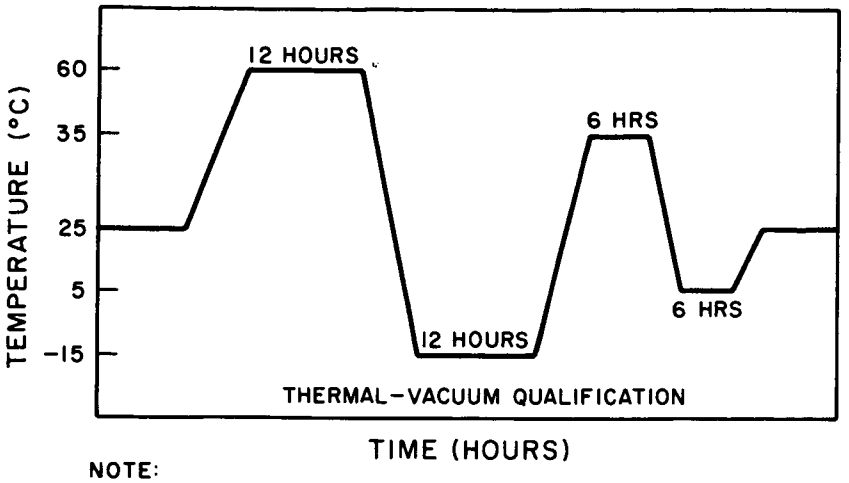

NOTE:
MAXIMUM TRANSITION RATE
IS 10°C PER HOUR.

Figure 3-VI-2a. Thermal-Vacuum Test Profiles for the Prototype Scanning Radiometer

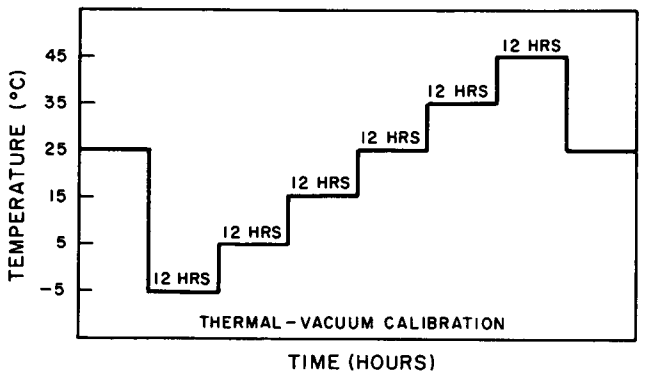

NOTE:
MAXIMUM TRANSITION RATE
IS 10°C PER HOUR.

Figure 3-VI-2b. Thermal-Vacuum Test Profiles for the Prototype Scanning Radiometer

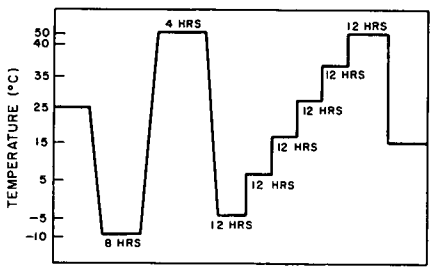

NOTES:
1. TIMES AT PLATEAUS ARE MINIMUM.
2. MAXIMUM TRANSITION RATE IS 10°C PER HOUR.
3. RADIOMETER IS TO OPERATE CONTINUOUSLY.

Figure 3-VI-3. Thermal-Vacuum Test Profile for the Flight Scanning Radiometer

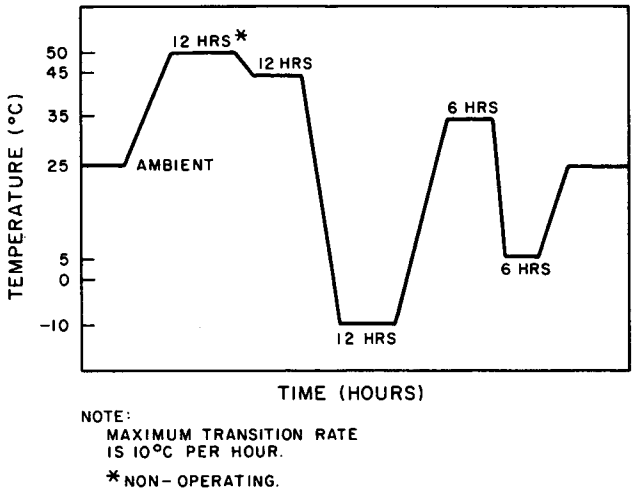

Figure 3-VI-4. Thermal-Vacuum Test Profile for the Scanning Radiometer Recorder and Incremental Tape Recorder (Prototype and Flight Units)

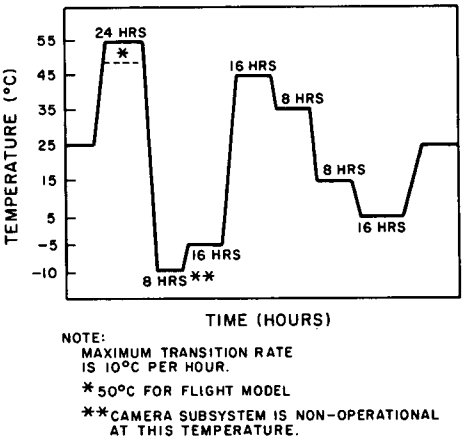

Figure 3-VI-5. Thermal-Vacuum Test Profile for the APT Subsystem

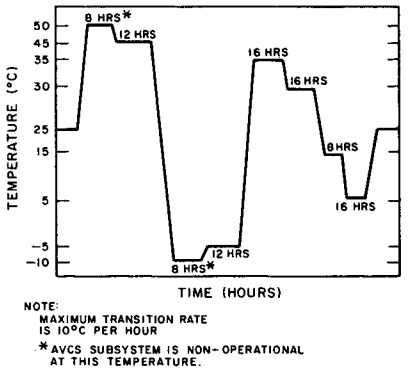

Figure 3-VI-6. Thermal-Vacuum Test Profile for the AVCS Subsystem (Prototype and Flight Units)

A camera distortion test was performed following the thermal-vacuum tests. During the distortion test, the optical alignment of the camera was checked, and the size and field of view were measured.

A sensitivity test was performed on the subsystem prior to its integration on the spacecraft for system testing. The light input to the camera was varied and a plot of input light versus output voltage was obtained. A plot was also made for a variety of power supply operating voltage levels.

2. Pitch Control Subsystem

The components of the pitch control subsystem; i.e., the pitch control electronics (PCE) and the momentum wheel assembly (MWA), were tested by performing checks on the subassemblies that make up the subsystem, and then testing the integrated subsystem.

The following tests were accomplished on the MWA prior to integration of the subsystem:

- Motor-Encoder Test (including bake-in and run-in)
- T-Plate Horizon Crossing Sensor Tests
- Pre-vibration Alignment and Performance Test
- Vibration
- Post-vibration Performance Test and Alignment Check

Prior to integration with the MWA, the PCE was exposed to the following tests:

- Pre-vibration Performance Test
- Vibration Test
- Post-vibration Performance Test

The pre-vibration test assured that the PCE operated to the test procedure requirements prior to the vibration test. The vibration test exposed the PCE to vibration in all axes. The post-vibration performance test verified proper operation of the PCE after vibration.

Pitch control subsystem tests were performed to verify that the subsystem performed to the electrical and environmental design specifications prior to its integration into the spacecraft. The tests consisted of the following:

- Integrated Performance Test — Assured correct harness interfacing between the MWA and PCE.

- Pre-thermal-Vacuum Setup and Go/No-Go Test — Assured that all major subsystems were operating properly.
- Thermal-Vacuum Test — Verified that the subsystem met test parameters at the anticipated orbital environment.
- Abbreviated Post-Thermal-Vacuum Test - Verified proper operation of the subsystem after the thermal-vacuum test.

The subsystem, after exhibiting acceptable performance for the pitch control subsystem tests, was integrated with the other subsystems of the spacecraft.

C. COMPONENT TESTING

1. Dual Command Decoder

a. PROTOTYPE

Qualification testing of the prototype dual command decoder (Ser. No. 01P) was performed as described below.

Test	Date Performed (1968)
Post-potting	May 8
Vibration	May 9
Acceleration	May 10

During thermal-vacuum testing on May 14, decoder 1 failed to latch. The vendor-supplied FSK discriminator filter was replaced and a special series of qualification tests was performed, including bench and vibration tests. The vibration portion of these special tests revealed a defective vendor-supplied DC/DC converter, which was replaced. During thermal testing on May 22, the replacement DC/DC converter again proved defective and it was replaced. Failure analysis at the vendor revealed failure to be due to a bad solder joint in the converter. During these special tests, decoder 2 required the replacement of an open resistor and three integrated circuit modules.

Prototype testing of the dual command decoder was completed on August 7, 1968.

Test	Date Performed (1969)
Pre-vibration	January 23
Vibration	January 24
Post-vibration	January 24
Thermal-vacuum	January 27
Post-thermal-vacuum	January 27

In April, 1969, the DC/DC converters were replaced by two improved units having the new 12E109 transistors. Pre-vibration operational testing followed on April 25, and vibration testing on April 26. The dual decoder then started on the 168 hour box-level survival tests requested by NASA. These tests were completed in early May.

2. Dual Command Programmer

a. PROTOTYPE

The individual printed circuit boards in the DCP, upon which the integrated circuits and the minimod buffers are mounted, were tested separately at room temperature and pressure. The tested boards were then assembled into a DCP unit. This unit underwent a series of tests both at room temperature and pressure, and at high, nominal, and low temperatures in a vacuum. Included were tests after the unit was subjected to vibration. The tests performed were electrical, designed to detect flaws in manufacturing and assembly and also any discrepancies between the actual and specified performance of the unit.

Qualification testing of the prototype dual command programmer (Ser. No. 01P) was accomplished as tabulated below.

Test	Date Performed (1968)
Post-potting	May 18
Vibration	May 20
Acceleration	May 21
Thermal-vacuum	July 31*

*Replacement of defective diode in minimod buffer required retesting over temperature range.

b. FLIGHT MODEL

The dual command programmer (Ser. No. 02) successfully completed the following tests on the dates indicated: pre-vibration test, vibration test, and post-vibration test on April 1, 1969; and thermal-vacuum and post-thermal-vacuum tests on April 3, 1969. On April 24, the DC/DC converters were replaced with two improved units having the new 12E109 transistors.

Box-level, special operational confidence tests, requested NASA, were performed during the period of April 25 to May 5, 1969.

3. Dual Time Base Unit

a. ELECTRICAL TEST MODEL

Breadboard testing of the time base unit (TBU) logic circuits was completed in June, 1967. The TBU breadboard circuitry was modified to incorporate several improvements and, except for a new 300 kHz buffer circuit, testing of the modified circuitry was completed by July, 1967.

b. PROTOTYPE

Testing of the prototype dual time base unit (Ser. No. 01P) began with pre-acceptance testing and debugging, performed from May 14 through 17, 1968. This testing disclosed an inoperative integrated circuit module and a shorted component board. After corrective action, the tests were repeated. Postpot testing was completed on May 20, 1968. Qualification vibration testing on May 21 revealed that the location of the oscillators resulted in a vibrational overstress. The oscillators were relocated and the vibration tests successfully completed on June 18, 1968.

On August 21, 1968, during a vibrational retest, the DC/DC converter experienced a malfunction which was traced to a defective 12E109 output regulator transistor. This transistor was responsible for the DC/DC converter failures detected on two other subassemblies during prototype vibration testing.* As a result, several meetings were held with the component suppliers, and a new improved version of the 12E109 transistor was developed and used. Thermal-vacuum testing was completed on January 30, 1969.

*See dual command decoder and SR processor testing.

c. FLIGHT MODEL

A pre-vibration test was performed on the dual time base unit, Ser. No. 02, on February 17, 1969. Vibration testing on February 18 revealed an out-of-specification low voltage reading with ripple from the DC/DC converter. The converter was replaced by a new flight unit, and a full flight-acceptance test performed on the dual time base unit.

During vibration testing on February 20, a crystal oscillator unit on one side broke loose from its shock mounting. This was considered a unique case and attributed to a faulty bond. Repairs were made, and vibration testing continued. Vibration and post-vibration testing were completed on March 1, 1969. Thermal-vacuum testing was performed on March 3, and post-thermal-vacuum testing was successfully completed on March 4, 1969.

On March 25, pre-vibration and vibration testing of the time base unit were repeated following rework of component board assembly A2A8. Rework was required to eliminate a shorting problem found on other similar units. Post-vibration tests were successfully completed on March 26. On April 24, 1969, the DC/DC converters were replaced by improved units having the new 12E109 transistors. Box-level special operation confidence tests, required by NASA, were performed from April 25 to May 9, 1969.

4. Command Distribution Units (CDU) A and B

a. PROTOTYPE

Qualification tests of the prototype command distribution units (CDU's) A and B (Ser. No. 01P) were accomplished as tabulated below.

Test	Date Performed (1968) CDU A	Date Performed (1968) CDU B
Post-potting	May 17	May 17
Vibration	May 17	May 17
Post-vibration	May 17	May 17
Acceleration	May 18	May 18
Post-acceleration	May 20	May 18
Thermal-vacuum	May 23	May 23
Final Electrical	May 23	May 23

During spacecraft level testing in June, 1968, "push-to-talk" (PTT) operation disclosed a playback relay hangup. Corrections were made to eliminate a sneak electrical path that kept the relay energized. The unit were given a performance test at +60°C and -15°C, and a complete electrical test at ambient conditions.

b. FLIGHT MODEL

Command distribution unit A, Ser. No. 03, and command distribution unit B, Ser. No. 02, were tested as indicated below:

Test	Date Performed	
	Ser. No. 03	Ser. No. 02
Pre-vibration operational	August 27, 1968	December 31, 1968
Vibration	August 28, 1968	January 2, 1969
Post-vibration operational	August 28, 1968	January 6, 1969

Post-vibration electrical testing on January 6 indicated that latching relays K3 and K4 (board A1) on CDU Ser. No. 02 had changed states. Subsequent analysis indicated that this could only result from mechanical vibration. The relays were replaced and on January 20, pre-vibration and vibration testing were repeated. On January 21, during post-vibration testing, transistor driver Q6 on relay driver A6 was accidentally damaged. After replacement of the damaged transistor, pre-vibration operational testing and vibration testing were performed on January 24, and post-vibration operational testing was successfully completed on January 25, 1969.

Further testing on both CDU's was performed as shown below.

Test	Date Performed	
	Ser. No. 03	Ser. No. 02
Thermal-vacuum	September 6, 1968	January 28, 1969
Post-thermal-vacuum	September 6, 1968	January 28, 1969
NASA 168-hour confidence	April 30, 1969	May 7, 1969

5. AVCS Camera Subsystem

a. ELECTRICAL TEST MODEL

The electrical test model camera subsystem was tested and evaluated against specified performance at -5°, +5°, +25°, +30°, +35°, and +50°C. A

summary of the results is contained in Table 3-VI-3, which indicates conformance with all specification parameters.

In additional testing, the camera shutter was checked for uniformity of exposure across the vidicon format and for shock transmission. The maximum variation of exposure was ±1.5 percent when checked at both ends and at the center. For testing shock transmission, a dummy vidicon was mounted in the camera sensor assembly and instrumented with two accelerometers: one on the assembly near the shutter and the other on the dummy vidicon faceplate. The accelerometer on the housing recorded the specified maximum of 7 g's which was attenuated to 3 g's at the vidicon faceplate.

b. PROTOTYPE

Prototype hybrid AVCS camera Ser. No. 01P underwent qualification testing as indicated below.

Test	Date Performed
Operational (including thermal)	July 8, 1968
Acceleration	July 8, 1968
Go/No-Go	July 9, 1968
Distortion	July 10, 1968
RFI	July 12, 1968
Magnetic Susceptibility	July 12, 1968
Special Go/No-Go	July 12, 1968
Vibration	July 17, 1968
Go/No-Go Vibration (between axes 1 and 2)	July 17, 1968*
Operational (Post-vibration)	July 19, 1968**
Distortion	July 22, 1968
Operational	October 31, 1968

*Vidicon faceplate cleaned to remove spot. This was a retest of the portion that had been dismantled.

**Retest of camera electronic unit after redressing of wires which had caused improper video output.

TABLE 3-VI-3. SUMMARY OF ETM AVCS CAMERA TEST RESULTS

Test Parameter	Initial Specification Limits (+5° C to +30° C)	Variation* Due to Input Voltage Change; ±0.5V	Test Temperatures				
			Specified Range				
			+5°C	+30°C	-5°C	35°C	50°C
Raster Size	±1.5%						
Horiz		$^{-0.88}_{+0.74}$%	+0.41%	-0.03%	+0.40%	+0.24%	+0.93%
Vert		$^{-1.35}_{+0.72}$%	0%	-0.25%	-0.20%	-0.26%	+0.22%
Raster Centering	+1.0%						
Horiz		$^{-0.35}_{+0.44}$%	+0.04%	-0.06%	+0.20%	-0.60%	-0.4%
Vert		$^{-0.48}_{+0.64}$%	+0.24%	+0.24%	+0.19%	+0.24%	+0.10%
Deflection Linearity	+1.0%						
Horiz		—	0.21%	0.15%	0.13%	0.15%	0.27%
Vert		—	0.05%	0.08%	0.27%	0.08%	0.03%
Resolution							
Center 800 TV Lines	>15%	36.7%	37.5%	32.8%	35.9%	30.4%	48%

TABLE 3-VI-3. SUMMARY OF ETM AVCS CAMERA TEST RESULTS (Continued)

Test Parameter	Initial Specification Limits (+5°C to +30°C)	Variation* Due to Input Voltage Change; ±0.5V	Test Temperatures				
			Specified Range				
			+5°C	+30°C	-5°C	35°C	50°C
Resolution (continued)							
600 TV Lines	>30%	65%	69.4%	62.0%	63.6%	58.0%	95%
400 TV Lines	>50%	93%	99%	95.6%	96.5%	90.7%	114.0%
Corner (min.)							
600 TV Lines	>20%	39.4%	50.5%	44.0%	52.3%	42.6%	56.4%
400 TV Lines	>35%	81%	89.0%	80.6%	93.0%	77.0%	90.0%
Shading**							
Horiz White	<30%						
Top		25.3%	14.8%	24.9%	20.1%	21.9%	23.0%
Center		19%	19.0%	22.4%	13.2%	19.3%	23.0%
Bottom		29.5%	22%	20.4%	20.4%	24.0%	11.9%
Horiz Black	<15%						
Top		1.0%	2.0%	2.5%	2%	4%	13%
Center		↓	↓	↓	↓	↓	25.2%
Bottom		↓	↓	↓	↓	↓	7.0%

TABLE 3-VI-3. SUMMARY OF ETM AVCS CAMERA TEST RESULTS (Continued)

Test Parameter	Initial Specification Limits (+5°C to +30°C)	Variation* Due to Input Voltage Change; ±0.5V	Test Temperatures				
			Specified Range				
			+5°C	+30°C	-5°C	35°C	50°C
Shading** (continued)							
Vert White	<30%	12.2%	12.2%	18.3%	17.0%	16.8%	12.5%
Vert Black	<15%	1.3%	0%	1.7%	0%	1.8%	21.8%
Noise							
S/N	>32 dB	—	50.4 dB	46.6 dB	47.3 dB	***	***
Microphonics and Converter Spikes	<10%	—	0%	0%	4.6%	0%	0%
Mesh	<15%	10%	12.5%	11.9%	10.5%	11.0%	24.0%
Video Levels							
Horiz Sync Tip Level	-6.5 +120 mV	-17 mV	0 mV	-18 mV	+6 mV	-4 mV	-18 mV
Black Clip Level	-7.3 ±120 mV	+10 mV	+28 mV	+24mV	+29mV	+35 mV	+30 mV

TABLE 3-VI-3. SUMMARY OF ETM AVCS CAMERA TEST RESULTS (Continued)

Test Parameter	Initial Specification Limits (+5°C to +30°C)	Variation* Due to Input Voltage Change; ±0.5V	Test Temperatures				
			Specified Range				
			+5°C	+30°C	-5°C	35°C	50°C
Video Levels (continued)							
Horiz Back Porch Level	-7.75 +120 mV	+9 mV	0 mV	-2 mV	-5 mV	-10 mV	-12 mV
Black Level	-7.75 +200 mV -400						
Top		-31 mV	+20 mV	-30 mV	+28 mV	-80 mV	-26 mV
Center		-46 mV	0	-62 mV	+31 mV	-110 mV	-212 mV
Bottom		$^{-26}_{+21}$ mV	+30 mV	-20 mV	+18 mV	-60 mV	-112 mV
White Clip Level	-11.45 +120 mV	+50 mV	+30 mV	+44 mV	+90 mV	+90 mV	+30 mV
Time Code							
"1"	$-8.50^{+0.3}_{-0.08}$ V	$^{-0.23}_{+0.05}$V	-0.11V	-0.05V	-0.12V	-0.06V	-0.06V
No Data	-9.75±0.7V	+0.39V	+0.24V	+0.26V	+0.23V	+0.27V	+0.29V
"0"	$^{-10.75}_{\pm 0.7}$V	+0.31V	+0.35V	+0.38V	+0.35V	+0.39V	+0.42V

TABLE 3-VI-3. SUMMARY OF ETM AVCS CAMERA TEST RESULTS (Continued)

Test Parameter	Initial Specification Limits (+5°C to +30°C)	Variation* Due to Input Voltage Change; ±0.5V	Test Temperatures				
			Specified Range				
			+5°C	+30°C	-5°C	35°C	50°C
Video Levels (continued)							
Horiz Sync Rise and Fall Times	8 to 24 μs	13 μs	11 μs	11 μs	13 μs	13 μs	13 μs
Gray Scale	>7 steps	—	9 steps	9 steps	10 steps	9	*
Residual Signal	<10%	—	2.4%	4.9%	2.3%	5.7%	8.3%
Change in Sensitivity	<40%	-2.8% $+4.9$%	-13.3%	+3.1%	-23%	+4.9%	-60%
Tracking of Peak White Signals (Gray Scale versus Scene)	±2%@25°C	—	-1.4%	+0.7%	-1.8%	+1.3%	
Telemetry	***						
Filament	—	-0.07V	+0.16V	-0.14V	+0.28V	-0.15V	-0.32V
Standby	±200 mV	-90 $+97$ mV	+3 mV	-3mV	+5 mV	+2 mV	-6 mV

TABLE 3-VI-3. SUMMARY OF ETM AVCS CAMERA TEST RESULTS (Continued)

Test Parameter	Initial Specification Limits (+5°C to +30°C)	Variation* Due to Input Voltage Change; ±0.5V	Test Temperatures				
			Specified Range				
			+5°C	+30°C	-5°C	35°C	50°C
Telemetry (continued)							
Main and +13V	±200 mV	$^{-75}_{+87}$mV	-0.1 mV	-0.4 mV	-0.5 mV	+4 mV	-8 mV
Turn-on Transient	<3 A peak						
	<50 mA/μs						
Standby		—	0.55A	0.44A	0.50A	0.52A	0.54A
		—	<15 mA/μs	< 15 mA/μs	<15 mA/μs	<15 mA/μs	15 mA/μs
Main		—	1.45A	1.45A		1.77A	1.84A
		—	<9 mA/μs	< 9 mA/μs	<9 mA/μs	<9 mA/μs	9.2 mA/μs
Overvoltage Operation	—	OK	OK	OK	OK	OK	OK
Deflection Skew	+1.0°	0.4° at 25°C only					
Power Consumption							
Quiescent	12 mA	10 mA at 25°C only					
Standby Operation	120 mA	72 mA at 25°C only					
Main Power Operation	410 mA	380 mA at 25°C only					

TABLE 3-VI-3. SUMMARY OF ETM AVCS CAMERA TEST RESULTS (Continued)

Test Parameter	Initial Specification Limits (+5°C to +30°C)	Variation* Due to Input Voltage Change; ±0.5V	Test Temperatures				
			Specified Range				
			+5°C	+30°C	-5°C	35°C	50°C
Power Consumption (continued)							
Peak Shutter	7.0A	4.5A at 25°C only					
RFI Immunity	—	Camera's performance was within specification at 25°C.					

NOTES:

*The change in the camera subsystem input voltage is made up of two factors: the spacecraft voltage regulator end-of-life value, which is ±0.25 volt; and the maximum line drop between the regulator and the camera, which is 0.25 volt. Once the camera subsystem is on the spacecraft, the input voltage variation will be ±0.25 volt, which is one-half the value that was used for this testing.

**Shading correction was not used with this camera because it was not needed to meet the specified shading.

***Due to the increase in mesh noise, these readings could not be made (not required by the specification).

The percentage shown is made up of microphonics only.

Specified at end-of-life value only.

Temperature limits -5°C to +50°C.

Test	Date Performed
Thermal-vacuum	November 11, 1968
Optical Alignment Check	November 12, 1968
Distortion	November 12, 1968
Operational	November 18, 1968
Sensitivity	January 10, 1969

c. FLIGHT MODEL

Two AVCS camera subsystems are carried aboard the TIROS M spacecraft: AVCS camera subsystem No. 1 designated Ser. No. 05, and AVCS camera subsystem No. 2 designated Ser. No. 03. Until May 1969, camera assemblies designated Ser. No. 02 (sensor and electronics) were associated with camera subsystem No. 1. However, at that time camera sensor Ser. No. 02 began to exhibit an undesirable and pronounced warmup characteristic and was replaced by Ser. No. 05 assemblies.

(1) AVCS CAMERA SUBSYSTEM NO. 1

AVCS camera sensor and electronics Ser. No. 05 successfully completed the following subsystem operational tests.

Test	Date Completed (1969)
Previbration	March 9
Vibration	March 11
Postvibration	March 12
Thermal-vacuum	March 19
Post-thermal-vacuum	March 27

Retesting of the camera subsystem was performed on March 27 after repositioning and adjusting the Gray scale calibrator to reduce the amount of video. The camera sensor was retested on April 1 after removal of some lint observed on the vidicon faceplate.

The 168-hour operational survival test on the camera subsystem, requested by NASA, was completed on May 20, 1969.

On May 6 a capacitor was added to camera electronics power supply board A6. Operational tests were then performed. These tests consisted of observing current profiles and monitor photographs at several temperatures and checking the vidicon electrode voltage and camera resolution at 25°C.

(2) AVCS CAMERA SUBSYSTEM NO. 2

During previbration acceptance testing of camera subsystem No. 2 (Ser. No. 03) on November 13, 1968, the baseline shading correction circuit of board A4 did not function correctly. Investigation revealed a defective tantalum capacitor (C14). The capacitor was replaced, and the board checked and reinstalled in the camera sensor. The camera sensor was returned to acceptance testing and on December 9, operational testing (including thermal) on this unit was completed. The camera subsystem then successfully completed the following acceptance tests on the dates indicated:

Test	Date Completed
Vibration	December 11, 1968
Distortion	December 18, 1968
Magnetic Susceptibility	December 20, 1968
Operational	December 24, 1968
Pre-thermal-vacuum	January 12, 1969
Thermal-vacuum	January 20, 1969
Post-thermal-vacuum	January 22, 1969
Camera Calibration	January 22, 1969

On April 7, 1969, two 1N944B diodes (VR1 in the A1 circuit board and VR5 in the A3 circuit board) in the camera electronics unit were replaced with newly preconditioned diodes. These replacements were considered necessary since it was discovered that the original AED preconditioning of this type of diode may have resulted in incipient damage due to excessive power dissipation during the "burn-in" period. The camera subsystem was then exposed to, and successfully passed, a pre-vibration operational test on April 9. The camera electronics unit only was then subjected to, and passed, a random vibration test (thrust axis only) on the same date. On April 10, 1969, the camera subsystem successfully completed a post-vibration operational test.

As directed by NASA, on April 24, 1969 a 168-hour continuous test of the AVCS cameras subsystem, operating in the normal orbital mode, was started. A complete operational test was performed at the beginning, middle, and end of the 168-hour period. The test was satisfactorily completed on May 1, 1969.

On May 5, 1969, a capacitor was added to board A6 of the camera electronics power supply. Subsequent operational testing was completed on May 6, 1969. These tests consisted of taking current profiles and monitor photographs at several temperatures and checking the vidicon electrode voltage and camera resolution at 25°C.

6. AVCS Tape Recorder

a. ELECTRICAL TEST MODEL

In general, the ETM signal electronics circuitry on boards A1 and A2 was checked and the potentiometers adjusted to perform within specified limits with regard to record head current, FM modulator deviations, and playback signal limiting. The command and control, drive, and telemetry circuits were also checked for functional and operational integrity against the requirements of the performance specification (No. 1975231). The transport was aligned for satisfactory operation.

Table 3-VI-4 summarizes the conformance of the test results to the performance specifications.

b. PROTOTYPE

Qualification testing on the prototype AVCS tape recorder (Ser. No. 01P) was performed as indicated below.

Test	Date Performed
Operational	December 21, 1968
Vibration	December 23, 1968
Postvibration	December 27, 1968*
Acceleration (Transport only)	November 1, 1968
Pressurization	January 6, 1969
Confidence	January 7, 1969
Vibration	January 8, 1969

*Post-vibrational testing disclosed broken signal lead wires due to too short service loop and movement of the stacked preamp blocks. Corrective action was taken, and the unit was retested.

TABLE 3-VI-4. SUMMARY OF ETM AVCS RECORDER SPECIFICATION LIMITS AND TEST RESULTS

Function	Spec. Limit	Test Data	Notes
Video Input of -6.5 V	72.0 kHz ±1%	72.022 kHz	At 25°C
Video Input of -11.5V	120.0 kHz ±1%	120.060 kHz	At 25°C
Modulator Linearity	Not to deviate from best-fit straight line by more than ±1%	Not tested	Same modulator as used on another successful classified program
Output Signal Voltage (Data Channel)	2.0 volts ±1dB square wave	2.0 volts square wave	
Output Signal Harmonic Content (Data Channel)	2nd harmonic at least 35 dB below fundamental	Max 2nd harmonic found is -40 dB @ 65 kHz	
Signal-to-Noise Ratio (Data Channel)	Peak-to-peak signal-to-rms noise shall be a minimum of 35 dB	38 dB	S/N is specified at the output of a std. demod.
FM Frequency Response	Constant ±2 dB from 100 Hz to 20 kHz. From 20 kHz to 60 kHz 9.0 dB down	4 dB down at 60 kHz	Freq. response is specified at the output of a std. demod.
FM Transient Response	Level - f(demod) Rise time -15 μs max. Width - 50 μs max Overshoot - 20% max.	Not measured (Proto met spec.)	Transient response is specified at the output of a std. demod.
Output Voltage (F & W Channel)	2.0 Volts ±1 dB square wave	2.0 Volts square wave	

TABLE 3-VI-4. SUMMARY OF ETM AVCS RECORDER SPECIFICATION LIMITS AND TEST RESULTS (Continued)

Function	Spec. Limit	Test Data	Notes
Harmonic Content (F & W Channel)	2nd harmonic at least 30 dB below fundamental	-43 dB during pbk. -21 dB during direct record	Actual system requirement is for a fundamental amplitude of 2.55 ± .3 volts. This requirement is satisfied.
Power Drain	<56 watts <14.5 watts <54.6 watts <13.2 watts <0.7 watts <0.1 watt	Rec. start: 53.9 watts Rec. run: 13.9 watts Pbk. start: 52.6 watts Pbk. start: 12.7 watts Standby: 0.6 watt Telemetry not measured.	All data was taken using a sample motor. TLM power was not measured because temp and pressure sensors were not available.
Current Transients	Slope < 50 ma/ μs	< 5.0 ma/<s	
Power Line Current	1 to 100 kHz random peak current fluctuation not to exceed 10 mA. Repetitive switching transients shall not exceed 20 mA peak	Freq range 10 Hz to 30 Hz. Peak-to-peak ripple of 20 mA. At the 400 Hz rate there were 5 mA peak spikes.	
Residual Angular Momentum	Uncompensated angular momentum shall be less than 0.02 in-lb-sec.	Not measured	

TABLE 3-VI-4. SUMMARY OF ETM AVCS RECORDER SPECIFICATION LIMITS AND TEST RESULTS (Continued)

Function	Spec. Limit	Test Data	Notes
Weight	Transport <11.75 lb Electronics <5.0 lb	13.35 lb 4.5 lb	1.6 lb heavy 0.5 lb light. Weight reduction program underway.
Flutter-and-Wow	0.5 to 30 Hz: 0.1% rms 30 to 300 Hz: 0.08% rms 300 Hz to 5 kHz: 0.2% rms 0.5 Hz to 5 kHz: 0.3% rms	0.5 to 30 Hz: .04% rms 30 to 300 Hz: .03% rms 300 Hz to 5 kHz: .25% rms .5 Hz to 5 kHz: .25% rms	At -10°C At -10°C At -10°C Slightly high At -10°C
Usable Tape Length	1360 ft	1360 ft ±1 ft	
Number of Tracks	3	3	
Number of Heads	3	3	Rcd, Pbk, Erase
Tape Speed	30 ips	30.1 ips	
Tape Speed Variations	±0.3% max	±0.125%	
Playback Time	1360 ft in less than 9.1 min	1360 ±1 ft in 539.5 or 8.98 min	
Record Time	Start in less than 1.5 s. Record for 8.75 s. No spec. stop time.	Start time 0.6 s. Record time can be set to any value. Stop time is 5.0 s.	

During vibration testing on January 8, the head cover mounting hardware loosened. The mounting method was changed, and the unit was subjected to extensive qualification vibrational testing. On January 14, 1969, the test results were considered satisfactory. On January 17, 1969, the prototype AVCS tape recorder was used in conjunction with the Ser. No. 03 camera subsystem for thermal-vacuum testing which was completed on January 20, 1969.

c. FLIGHT MODEL

(1) AVCS TAPE RECORDER SUBSYSTEM NO. 1

AVCS tape recorder subsystem No. 1 is composed of tape recorder assembly Ser. No. 02 and tape recorder electronics Ser. No. 03.

A tape recorder assembly confidence test was performed on January 14, 1969. On January 17, subsystem performance tests involving tape recorder assembly Ser. No. 02 and tape recorder electronics Ser. No. 02 were initiated. These tests revealed the necessity for a voltage regulating diode in the modulator current source to correct a temperature drift problem. All flight recorders now include this regulating diode.

Pre-vibration testing of the recorder assembly was successfully completed on January 21, and vibration testing on January 22, 1969.

On January 22, tape recorder electronics Ser. No. 02 was replaced by tape recorder electronics Ser. No. 03. This replacement recorder assembly was then subjected to a series of board-level tests. Initial subsystem performance and pre-vibration operational testing of this new configuration was completed on January 25, 1969.

After pre-vibration testing of the tape recorder electronics on January 31, the AVCS recorder subassembly underwent pre-vibrational testing on February 14.

AVCS recorder electronics (Ser. No. 03) successfully completed vibration testing on February 15, a post-vibration test on AVCS tape recorder system No. 1 was performed on February 16, 1969.

On February 20, while undergoing operational testing, this same subsystem showed dropouts in the 35-mm playback pictures. Analysis showed damage to the oxide coating of the tape which was attributed to handling. While changing the tape, the magnetic head preamplifier assembly was also replaced. Operational testing was completed on March 11, 1969.

The recorder assembly successfully completed vibration testing on March 12, post-vibration testing on March 14, and pre-thermal-vacuum testing on March 16.

The AVCS camera subsystem (Ser. No. 05) and recorder subsystem No. 1 completed thermal-vacuum testing on March 25, 1969.

Post-thermal-vacuum testing on the recorder electronics was completed on March 26. On April 10, a retrofit was made to this unit involving the replacement of a diode possibly damaged during burn-in. Operational testing was then performed and completed by April 11, 1969.

On April 30, 1969, the AVCS camera, tape recorder, and recorder electronics completed the 168-hour survival test in compliance with NASA special directive.

(2) AVCS TAPE RECORDER SUBSYSTEM NO. 2

AVCS tape recorder subsystem No. 2 is composed of tape recorder assembly Ser. No. 03 and tape recorder electronics assembly Ser. No. 04.

Confidence level testing was performed on the AVCS recorder electronics assembly on January 27, 1969, and on the AVCS recorder assembly on February 18, and 19, 1969. Testing of the recorder electronics assembly was repeated on February 22 after relocating a filter assembly board. The recorder and electronics assemblies were pre-vibration tested together on February 24 to 27. During vibration testing on February 28, an end-of-tape switch mounting bracket screw and washers loosened. After inspection, correction, and retesting, the recorder subassembly vibration testing (March 1, 1969) was considered successfully completed. On March 2 post-vibration testing of the subassembly was initiated. However, because of test equipment error, retesting had to be performed and was successfully completed on March 7, 1969. Thermal-vacuum testing was completed on March 14, and post-thermal-vacuum testing on March 15.

In early April, a retrofit was made on the A5 board of the recorder electronics assembly to change a diode possibly damaged during burn-in. This assembly then completed a modified pre-vibration test on April 10, a modified vibration test on April 11, and post-vibration testing on April 13, 1969.

On April 30, the AVCS tape recorder, recorder electronics, and camera were survival tested on a subsystem basis for 168 hours in compliance with NASA special directive.

7. APT Camera Subsystem

a. ELECTRICAL TEST MODEL

Breadboarding and debugging of all new circuits except the digital-to-analog (D/A) converter was completed in June, 1967, with excellent results.

Thermal tests on the new circuits were conducted in early July, followed by successful breadboard testing of the D/A converter.

In August, 1967, breadboard testing of all circuit modifications was completed. The modifications comprised the initial TIROS M adaption, changes necessary for the inclusion of overvoltage protection circuits, telemetry changes, and reduction of the vertical frame time.

b. PROTOTYPE

Prototype APT camera Ser. No. 01P underwent qualification testing as indicated below.

Test	Date Completed
Tenney Box	
Alignment	June 4, 1968
Operational	June 5, 1968
Initial Operational (bench test)	July 1, 1968
Vibration	July 2, 1961
Post-vibration	
Go/No-Go	July 3, 1968
Operational	July 8, 1968
Thermal-vacuum	July 16, 1968
Post-thermal-vacuum	July 17, 1968
Magnetic Susceptibility	July 17, 1968
RFI	July 18, 1968
Distortion	July 19, 1968
Sensitivity	July 22, 1968
Final Operational	July 29, 1968

c. FLIGHT MODEL

Two APT camera subsystems are carried aboard the TIROS M spacecraft: APT camera subsystem No. 1 designated Ser. No. 05 and APT camera subsystem No. 2 designated Ser. No. 06.

In September, 1969, because of an open vidicon filament, Ser. No. 02 camera units were replaced by Ser. No. 05 in APT camera subsystem 1.

Initially, APT camera assemblies designated Ser. No. 03 (sensor and electronics) were associated with APT camera subsystem No. 2. In early April, Ser. No. 02 camera assemblies were replaced by Ser. No. 04. However, due to a shift in camera sensitivity in May, 1969, Ser. No. 04 was replaced by Ser. No. 05. In June, 1969, Ser.No. 05 was replaced by the present flight model, Ser. No. 06.

(1) APT CAMERA SUBSYSTEM NO. 1

APT camera sensor and electronics Ser. No. 05 successfully completed the following qualification tests on the dates indicated.

Test	Date Completed (1969)
Pre-vibration	March 14
Vibration (sensor only)	March 14
Abbreviated operational	March 21
Post-vibration	March 26
Thermal-vacuum	April 9
Post-thermal-vacuum	April 10
Leak Test	April 11

Following these tests, a retrofit was made to the 1968035 and 1968024 boards involving the 2N4008 transistors and the 1N944B diodes, respectively. The transistors were replaced because of a bonding problem. The new transistors bear a white dot to indicate that they have been x-rayed, and have a To 46 instead of a To 18 case size. The diodes were replaced because of possible damage during preconditioning power "burn-in". Pre- and post-potting tests were made on these boards before replacement in the camera electronics assembly. Pre-vibration testing on the camera electronics assembly was performed on April 16, 1969. During a special post-vibration test on April 17, it was disclosed that a resistor had been broken by the force and heat applied in the potting procedure. After correction, the test procedure was repeated, and vibration testing performed on April 19. This special camera sensor and electronics test (including satisfactory Mufax printouts at several temperature ranges) was completed on April 21, 1969.

Camera subsystem post-vibration testing was successfully completed on April 23, 1969.

The NASA-requested 168 hour survival test was started on May 12.

During detailed electrical testing of the camera subsystem on May 23, 1969, large changes in video amplitude were noted which were attributed to a resistor (R 66 on D/A converter board 1968035) which was cracked during troubleshooting of the D/A converter, influencing the -18-volt regulator. Following rework and acceptance by quality assurance, the subsystem was retested. This testing included:

- Vibration random thrust at flight level (electronics only)
- Low light-level Mufax printouts
- Cycle tests at 55° and -5°C
- Operational, sensitivity, and DC testing.

These tests were completed on July 10, 1969.

At NASA direction, camera subsystem Ser. No. 05 was released from spacecraft integration for special thermal-vacuum testing prior to installation aboard the TIROS M spacecraft. These tests were aimed at minimizing changeover time and exposing this camera subsystem to additional thermal-vacuum testing. On August 17, a black line was noticed in the Mufax printouts. Investigation determined that the cause originated from a defective D/A converter board.

After correction, the camera subsystem completed flight acceptance testing and a distortion and sensitivity test on August 27. In addition, the subsystem was subjected to a series of thermal cycle performance tests and confirming distortion and sensitivity tests. Testing was completed on September 2, 1969.

(2) APT CAMERA SUBSYSTEM NO. 2

APT camera subsystem No. 2 completed the following qualification tests on the dates indicated.

Test	Date Completed (1969)
Pre-vibration	May 7
Vibration	May 7
Post-vibration	May 12
Thermal-vacuum	June 2
Post-thermal-vacuum	June 3

On June 25, 1969, this camera subsystem was removed from the TIROS M spacecraft for the addition of diode CR-9 (1968025 Rev. D) to correct a -18-volt regulator problem and the precautionary replacement of Q3 transistor 2N722. In addition, the iris was adjusted to correct the sensitivity of the camera. After these tasks were completed, operational testing (TP-OT-1975208) was performed at +5°C and +45°C.

8. Scanning Radiometer Assembly

a. ELECTRICAL TEST MODEL

The scanning radiometers were tested and calibrated at Santa Barbara Research Center, California. Alignment and calibration were performed before environmental testing. The parameters that could change were either monitored during environmental testing or measured at the conclusion of environmental testing to detect any degradation due to the testing environment.

Scan mirror drive assembly performance was measured using a linearity and a jitter test. The linearity test measured the time between an optically stimulated signal and a synchronization pulse for eleven different view scan angles. From this repetitive data, scan linearity error was determined. Sync pulse jitter, due to electrical and mechanical causes, was determined by measuring the time between successive sync pulses.

The spatial resolution, a combination of optical and electrical characteristics, was evaluated using a square wave modulation transfer test. This involved rotating a series of test targets at the focal point of a collimator and comparing the upper and lower spatial resolutions.

Radiance calibration measurements were made at six different radiometer temperatures under precisely controlled conditions.

The sun exposure test, using controlled sunlight as the light source, provided a means for predicting performance in the event the radiometer accidentally scans through the sun in space.

For a quick check on radiometer performance at Santa Barbara Research Center (SBRC), a bench check was run using the radiance calibration test fixture in the unevacuated vacuum chamber.

b. PROTOTYPE

A summary of the qualification test history of Ser. No. P1 prototype scanning radiometer assembly is contained in Table 3-VI-5.

TABLE 3-VI-5. PROTOTYPE SCANNING RADIOMETER ASSEMBLY TEST HISTORY

Test	Date	Results
Acceptance Test	Start 5/01/68	
	5/05/68	Scan mirror stopped rotating.
	5/13/68	Scan mirror assembly returned to scanner housing.
Circuit Performance	Start 5/23/68	Noise in video channels increased at low temperature.
	Completed 5/28/68	Some portions of test were repeated on 7/24/68 after circuit modifications were made.
Jitter	Completed 5/28/68	Successful
	5/29/68	Radiometer returned to vacuum chamber for further test for noise on video channels.
	6/11/68	Testing completed. Radiometer sent for rewiring.
	6/11/68	Scan assembly removed and seal box pinned.
	6/12/68	Scan assembly replaced in scanner housing.
Spectral Bandwidth	6/15/68	Successful
Elemental Field-of-View	6/17/68	Successful
Spatial Resolution (modulation transfer function)	6/17/68	Successful
Scan Field-of-View	6/17/68	Successful
Scan Linearity	6/18/68	Successful
	6/18/68	Preparing to put radiometer in thermal-vacuum chamber, no telemetry output from bolometer temperature sensor was present.

TABLE 3-VI-5. PROTOTYPE SCANNING RADIOMETER ASSEMBLY TEST HISTORY (Continued)

Test	Date	Results
Calibration	Started 6/18/68 Completed 6/22/68	Test was completed though following discrepancies were detected. 1. Random dropout of sync pulse, voltage calibration signal, and telemetry start pulse at +45°C. 2. Signal level from thermal channel dropped to 1/4 amplitude for a period during test at 15°C. Preamp changed from P-1 to P-1A. Gain adjusted to give same calibration as earlier.
	6/27/68	Recheck of calibration made in thermal-vacuum at 25°C.
Vibration	Started 7/01/68 Completed 7/02/68	Postvibration showed: 1. Rattle inside scanner housing. 2. No output from telemetry output for temperature sensors A and B
Post-vibration (jitter, scan linearity, field- of-view, and alignment)	7/03/68	Successful
Vibration	7/06/68	Scanner unit only
Calibration Recheck	7/08/68	Successful
Thermal-vacuum	Stopped 7/10/68	Discontinued when scan drive stopped.
		Scan drive assembly reworked. It was revibrated in X-1 housing, then reinstalled in P-1 scanner.
Field-of-View and Alignment	7/15/68	Successful (These readings supersede all others as alignment is affected by removing mirror drive).

TABLE 3-VI-5. PROTOTYPE SCANNING RADIOMETER ASSEMBLY TEST HISTORY (Continued)

Test	Date	Results
Thermal-vacuum	Started 7/16/68 Completed 7/19/68	Data obtained to complete calibration. Vacuum chamber sprung leak. Only effect was to delay completion of test. Scan indicator telemetry output gave false rotation indication when operated off backup power.
Acceleration	7/23/68	Successful Mirror balance caused mirror to stop at 30-G level but started up when acceleration dropped below this level.
Post-acceleration Optical test	Started 7/24/68 Completed 7/25/68	Successful
Sun Exposure	7/25/68 7/26/58	Successful RFI filter installed
Circuit Performance (partial)	7/29/68	No telemetry start pulse signal.
RFI	7/30/69	Successful
Test Data Design Review	Started 8/01/68 Completed 8/3/68	Changes to be made to pip amplifier
Bench Test	8/09/68	Successful
Radiometer Delivered to RCA for shipment to AED	8/09/68	
RADIOMETER MALFUNCTIONED AT RCA-AED RETURNED TO SBRC FOR EVALUATION 2/18/69		
Evaluation Test	Start 2/20/69	Problem reported by RCA not detected. IR channel noisy.
Special Tests	2/27/69	RFI Filter Retrofitted
	Start 3/21/69 Comp. 5/12/69	Test to determine long-term stability of targets. Excessive noise detected.

TABLE 3-VI-5. PROTOTYPE SCANNING RADIOMETER ASSEMBLY TEST HISTORY (Continued)

Test	Date	Results
	5/15/69	Capacitors C1 through C4 removed from bias supply.
	8/12/69	Capacitors replaced
Bench Test	Start 8/18/69 Comp. 8/19/69	Successful (total operating time at SBRC 372 hours)
Data Review	8/19/69	Successful
Radiometer Delivered to RCA for shipment to AED	8/19/69	

c. FLIGHT MODEL

Scanning radiometer assemblies, Ser. Nos. F3 and F5, were installed aboard the TIROS M spacecraft. Ser. No. F5 is associated with scanning radiometer subassembly No. 1; Ser. No. F3 with scanning radiometer No. 2. These assemblies successfully completed the following flight-level qualification test on the dates indicated.

Test	Ser. No. F3	Ser. No. F5
Pre-vibration	December 5, 1968	January 21, 1969*
		February 3, 1969
Vibration (scanner)	December 11, 1968	February 6, 1969
(electronics)	December 19, 1968	February 6, 1969
Post-vibration	December 19, 1968	February 7, 1969
Thermal-vacuum	January 12, 1969	February 16, 1969
Post-thermal-vacuum	January 17, 1969	February 19, 1969

*Increase in thermal channel noise isolated to poor solder joint. Repaired and retested. Tests on Ser. No. F5 after January 21 included scanner and electronics.

9. Dual Scanning Radiometer Processor

a. ELECTRICAL TEST MODEL

In July, 1967, temperature tests were performed on breadboards from the real-time channel and commutator portions of the SR processor. Real-time channel testing included linearity, gain, limiting, carrier injection, carrier suppression, and carrier duty cycle. Commutator testing covered such characteristics as offset, scatter, linearity, crosstalk, gain, and source impedance sensitivity.

(1) REAL-TIME CHANNEL

Tables 3-VI-6 and 3-VI-7 list the real-time channel signal conditioner and the real-time channel limiter as a function of temperature for a visual input and an IR input, respectively. Figures 3-VI-7 and 3-VI-8 illustrate the overall linearity of the real-time channel for visual and IR data inputs, respectively.

TABLE 3-VI-6. OUTPUT OF SIGNAL CONDITIONER AND LIMITER VERSUS TEMPERATURE FOR VISUAL INPUT

Visual Input (Volts, D C)	Signal Conditioner Output (Volts, DC)			Limiter Output (Volts, DC)		
	+75°C	+20°C	-30°C	+75°C	+20°C	-30°C
0	-0.00216	-0.00153	-0.00130	+0.795	+0.794	+0.793
-1	-1.0025	-1.0020	-1.0018	+1.924	+1.924	+1.922
-2	-2.0010	-2.0005	-2.0002	+3.042	+3.049	+3.029
-3	-3.0014	-3.0009	-3.0007	+4.174	+4.175	+4.152
-4	-4.0015	-4.0009	-4.0003	+5.319	+5.310	+5.286
-5	-5.0015	-5.001	-5.001	+6.452	+6.448	+6.428
-6	-6.0025	-6.002	-6.002	+7.565	+7.569	+7.564
-7	-7.002	-7.002	-7.001	+7.824	+7.820	+7.814
-8	-8.0025	-8.003	-8.002	+7.861	+7.851	+7.841

TABLE 3-VI-7. OUTPUT OF SIGNAL CONDITIONER AND LIMITER VERSUS TEMPERATURE FOR IR INPUT

IR Input (Volts, DC)	Signal Conditioner Output (Volts, DC)			Limiter Output (Volts, DC)		
	+75 C	+20°C	-30°C	+75°C	+20°C	-30°C
0	-6.0030	-6.004	-6.0015	+7.565	+7.571	+7.563
-1	-5.0045	-5.005	-5.002	+6.446	+6.451	+6.425
-2	-4.0080	-4.0073	-4.0031	+5.304	+5.313	+5.287
-3	-3.0095	-3.0077	-3.0027	+4.166	+4.1786	+4.152
-4	-2.0115	-2.0090	-2.0030	+3.041	+3.0539	+3.031
-5	-1.0130	-1.0096	-1.0026	+1.916	+1.9303	+1.922
-6	-0.0145	-0.0097	-0.00190	+0.086	+0.076	+0.073
-7	+0.9836	+0.9891	+0.9977	-0.035	-0.036	-0.037
-8	+1.9820	+1.9883	+1.9977	-0.073	-0.074	-0.076

Harmonic suppression of the real-time channel is a function of the symmetry of the carrier. Table 3-VI-8 is a listing of the harmonic distortion components in the real-time channel output when modulated by a 400-Hz sinusoidal input. Figures 3-VI-9 and 3-VI-10 show the effect on the output frequency spectrum from changing the duty cycle.

TABLE 3-VI-8. REAL-TIME CHANNEL HARMONIC DISTORTION COMPONENTS (ATTENUATION)

Signal	Output Level (dB)	Frequency
Carrier	0 - Ref	2.4 kHz
USB	-9.0	2.8 kHz
LSB	-9.0	2.0 kHz
Modulating Input	-47	400 kHz
2nd	-50	4.8 kHz
Harmonic	-48	4.4 kHz
Components	-55	5.2 kHz
3rd	-63	6.8 kHz
Harmonic	-53	7.2 kHz
Components	-66	7.6 kHz

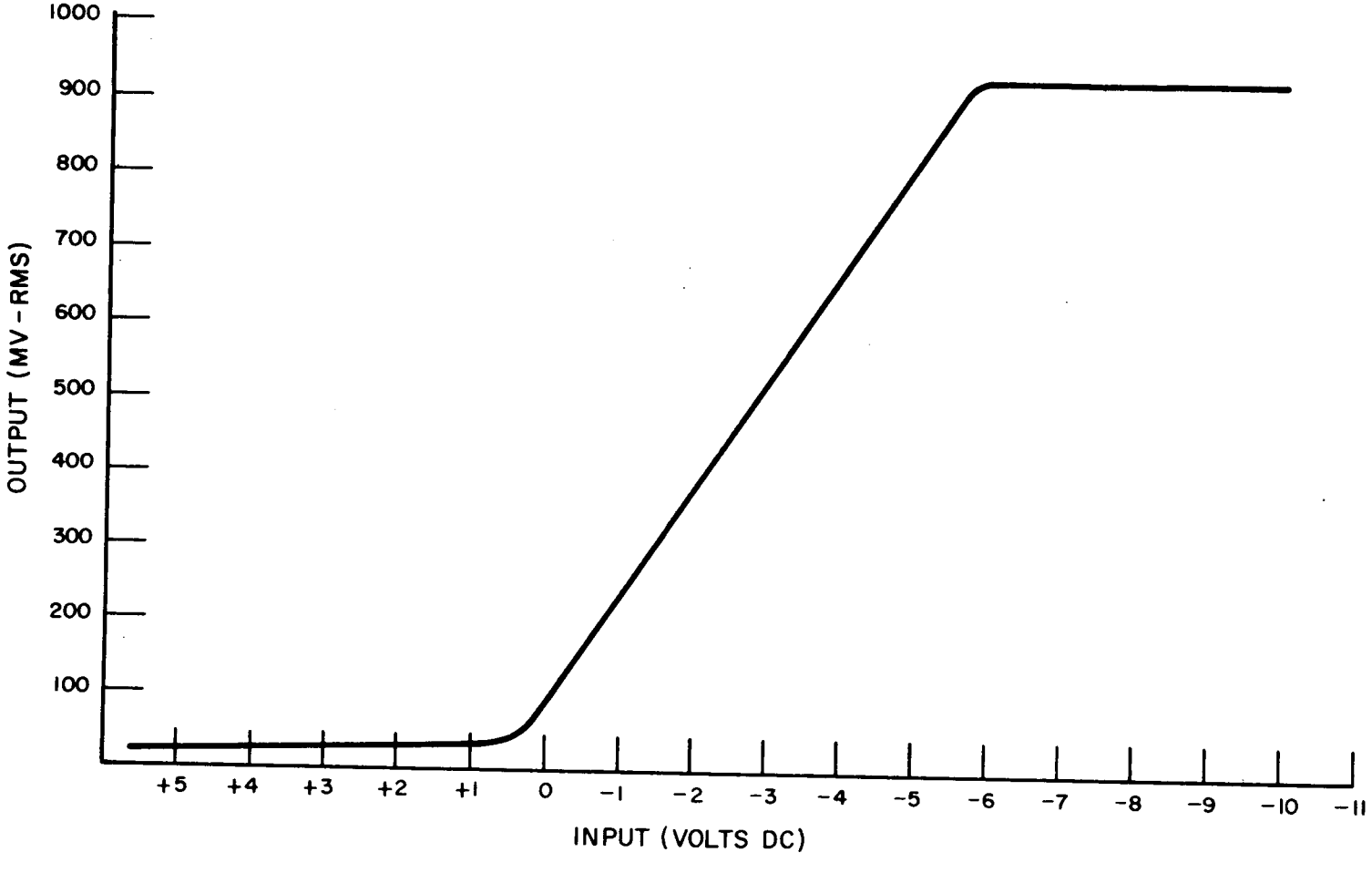

Figure 3-VI-7. Real-Time Channel Response for Visual Data Inputs

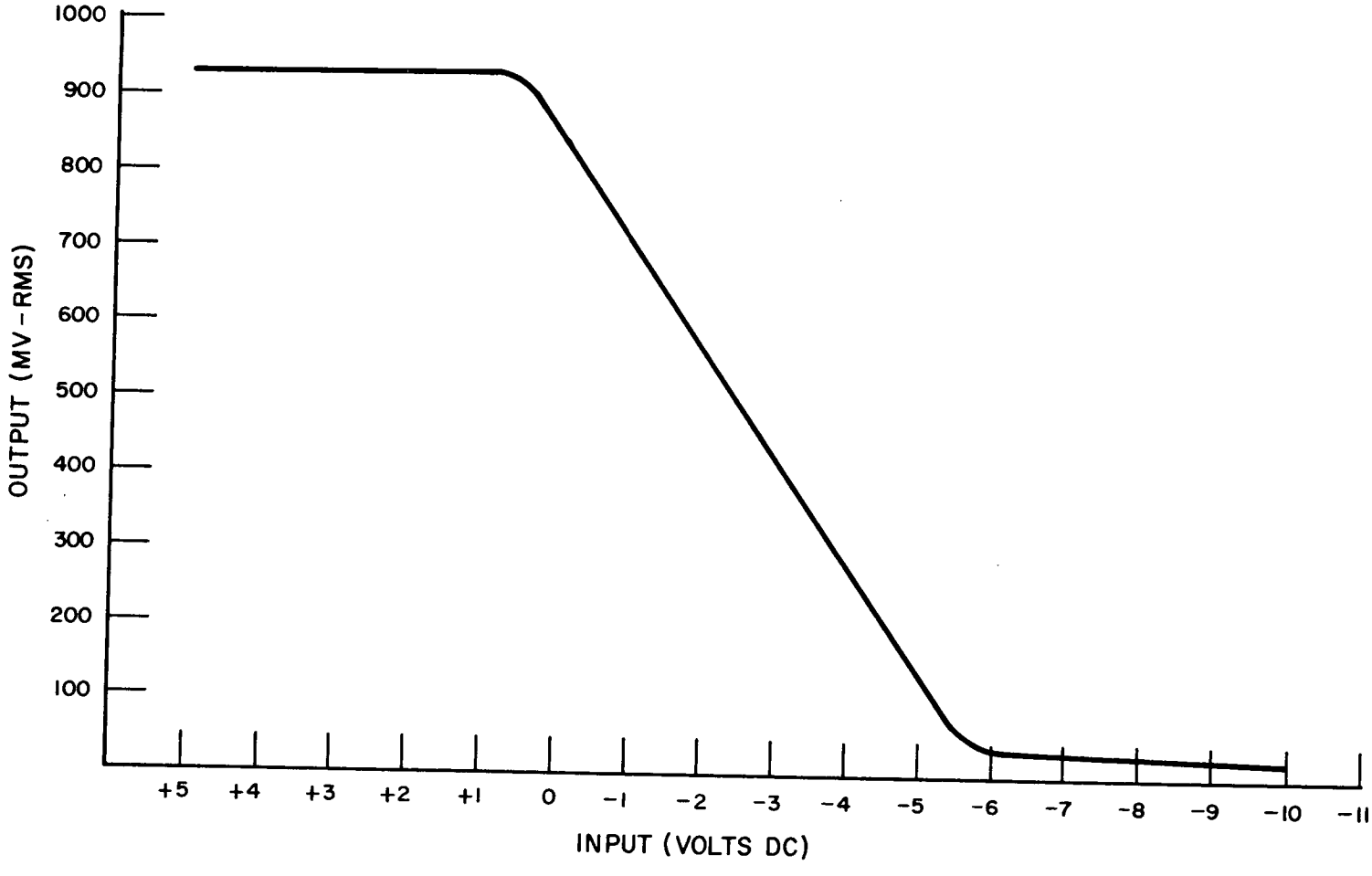

Figure 3-VI-8. Real-Time Channel Response For IR Data Inputs

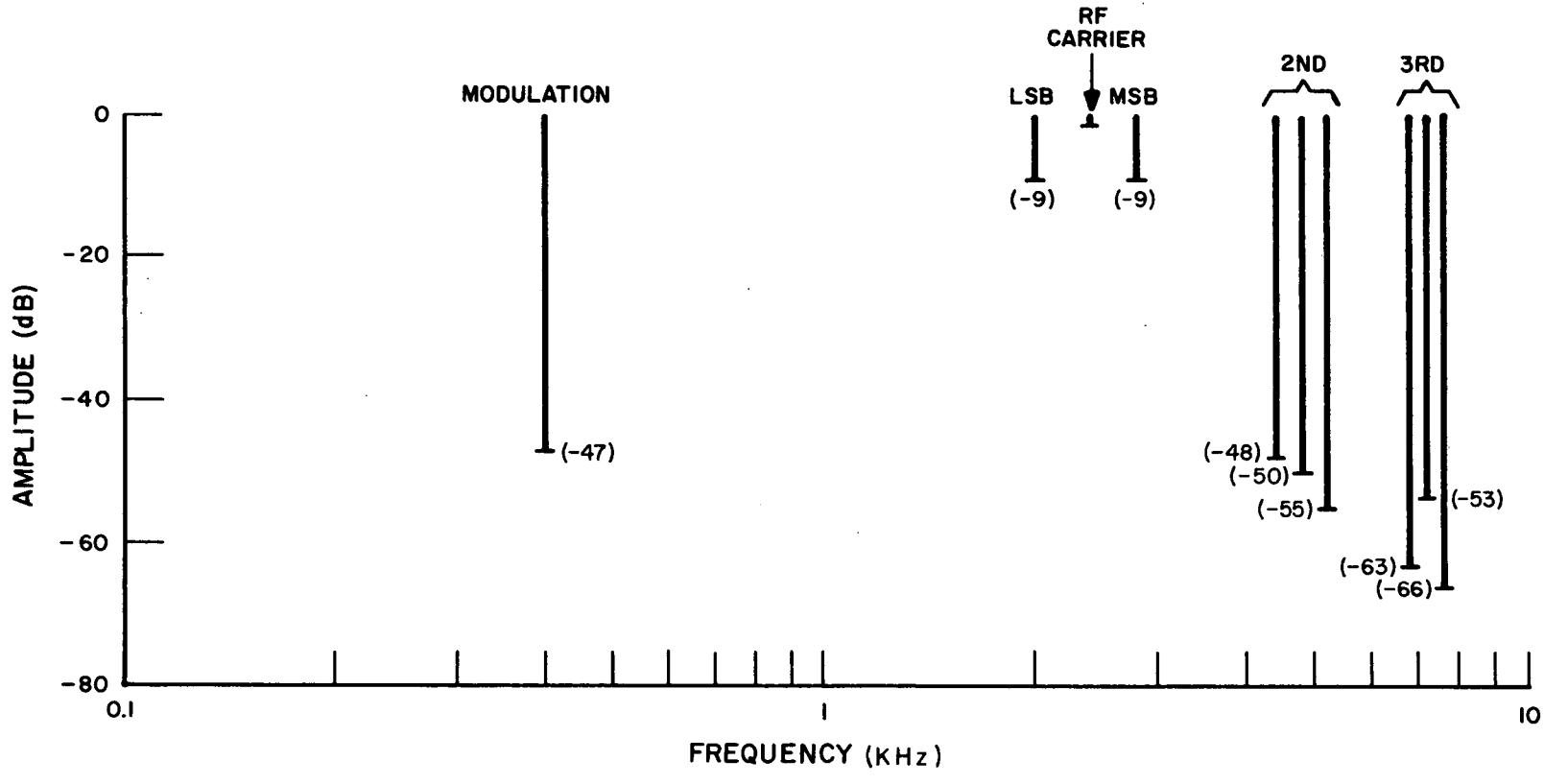

Figure 3-VI-9. Real-Time Channel Frequency Spectrum For 50-Percent Duty Cycle Carrier

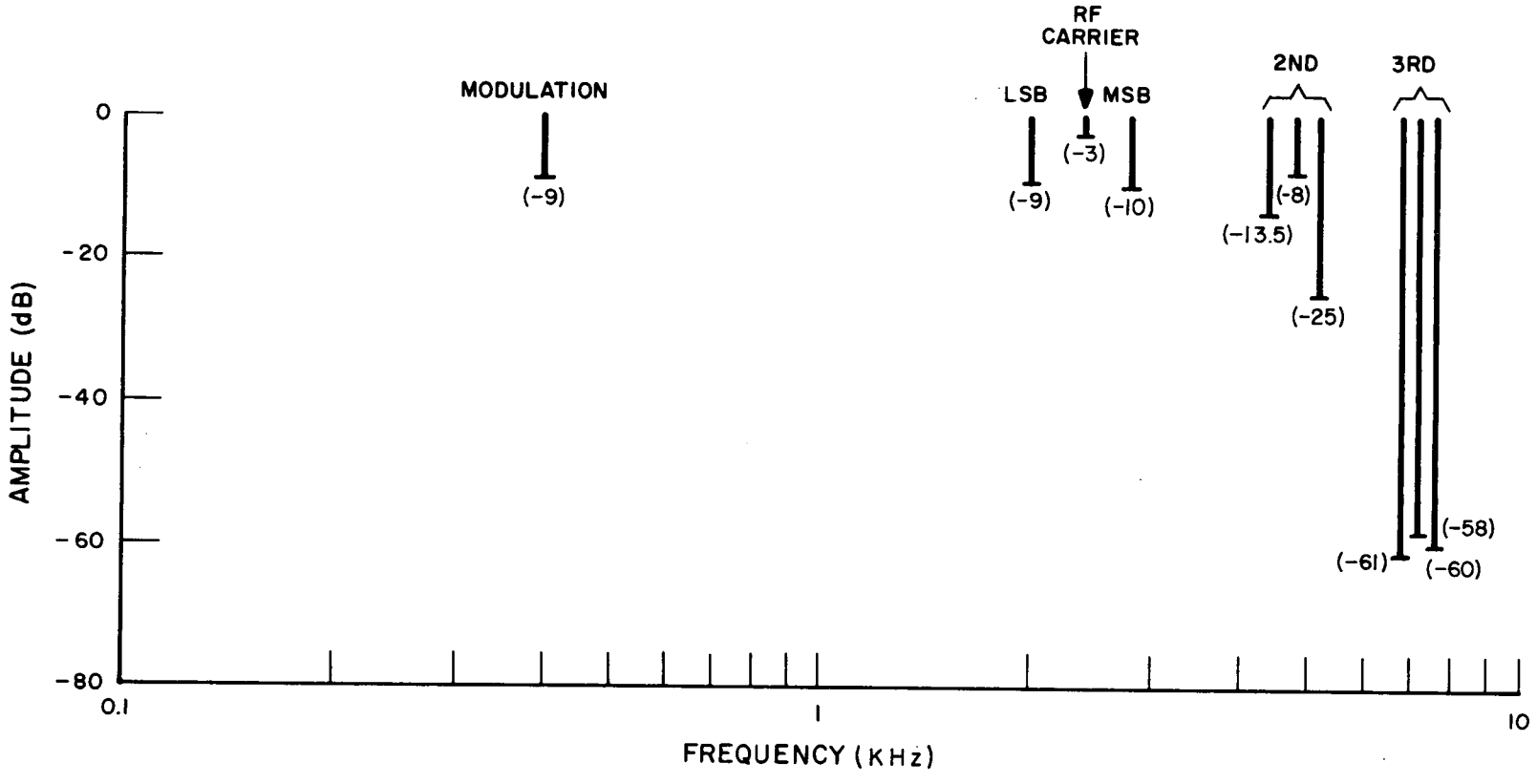

Figure 3-VI-10. Real-Time Channel Frequency Spectrum For 25-Percent Duty Cycle Carrier

(2) COMMUTATOR

SR processor commutator offset for three temperatures is illustrated in Figure 3-VI-11. This figure is a plot of the variation of the commutator output (offset) for each channel, with the input at ground, at three different temperatures.

Since the commutator output is an operational amplifier in the voltage follower configuration, it exhibits small variations in gain with mismatches between input source impedance and amplifier feedback resistance. Figure 3-VI-12 illustrates this variation, referred to as source impedance sensitivity, for a single channel. For this test, an external resistor was placed in series with the input to vary the source impedance, and the output was measured with the input voltage held constant. This test was performed for a source impedance range of 0 to 30 kilohms at full-scale input voltage.

b. PROTOTYPE

Following conformal coating of the circuit boards in early June, 1968, the dual SR processor, Ser. No. 01P, successfully completed post-potting and vibration tests on June 20, 1968. However, during post-vibration testing the following day, the vendor-supplied DC/DC converter failed to start during low temperature operation.* Vendor failure analysis revealed that a change in resistor value would correct the problem and all converters were scheduled for rework by the vendor.

It was decided to continue testing with the spacecraft using two DC/DC converters that had not been reworked, and to test the reworked converters when they were returned.

Thermal-vacuum testing of the SR processor was completed on July 12. On August 28, the reworked DC/DC converters were successfully vibration tested. Post-vibration testing of the prototype dual SR processor was successfully completed on August 30, 1968.

c. FLIGHT MODEL

SR processor Ser. No. 04 was subjected to successful pre-vibration, vibration, and post-vibration tests on January 4, 1969. On January 7, during

*Another DC/DC converter was installed and full qualification testing of the SR processor started. On July 1, during post-vibration testing the replacement DC/DC converters failed.

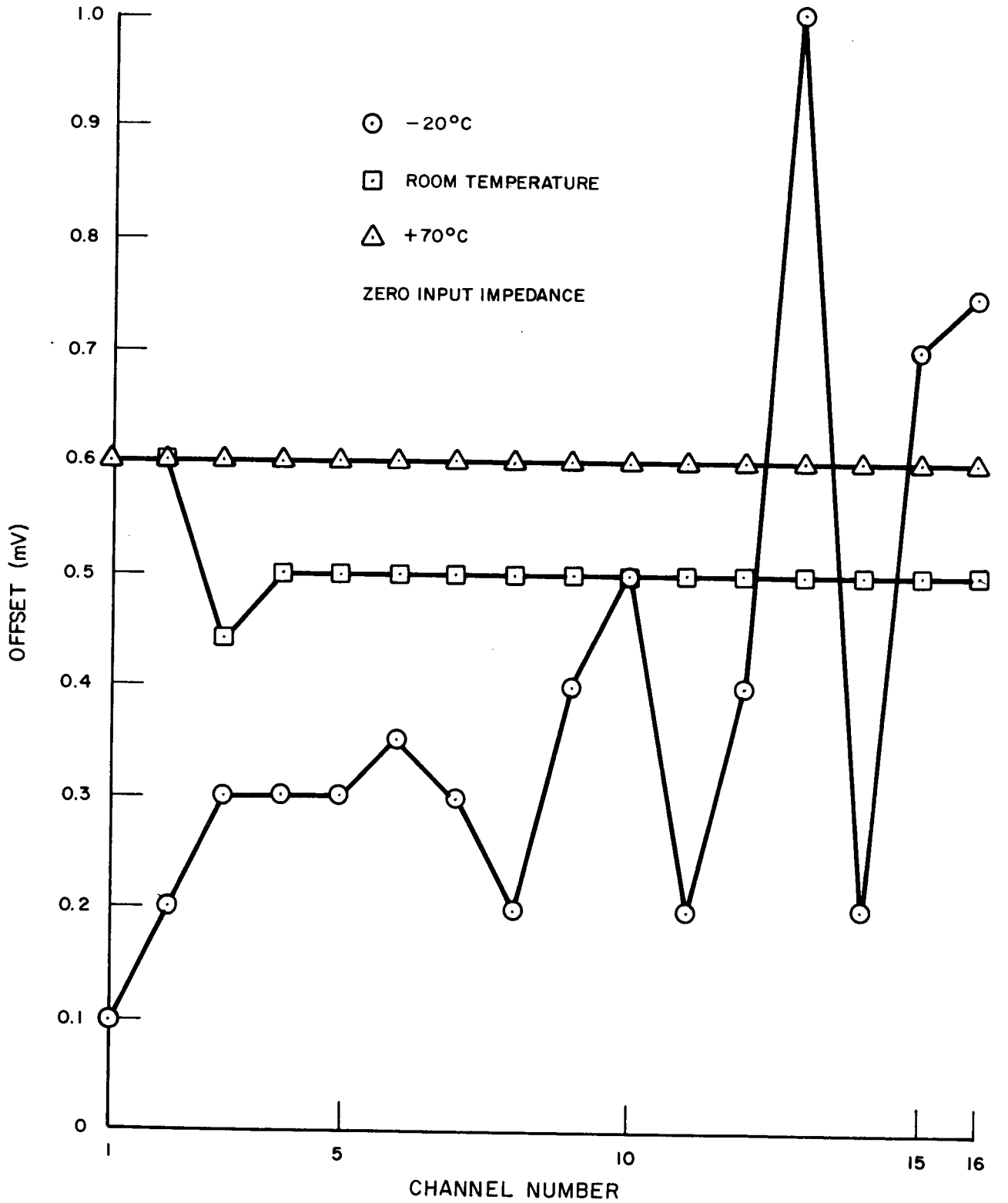

Figure 3-VI-11. Commutator Offset at Ground Input for all Channels Versus Temperature

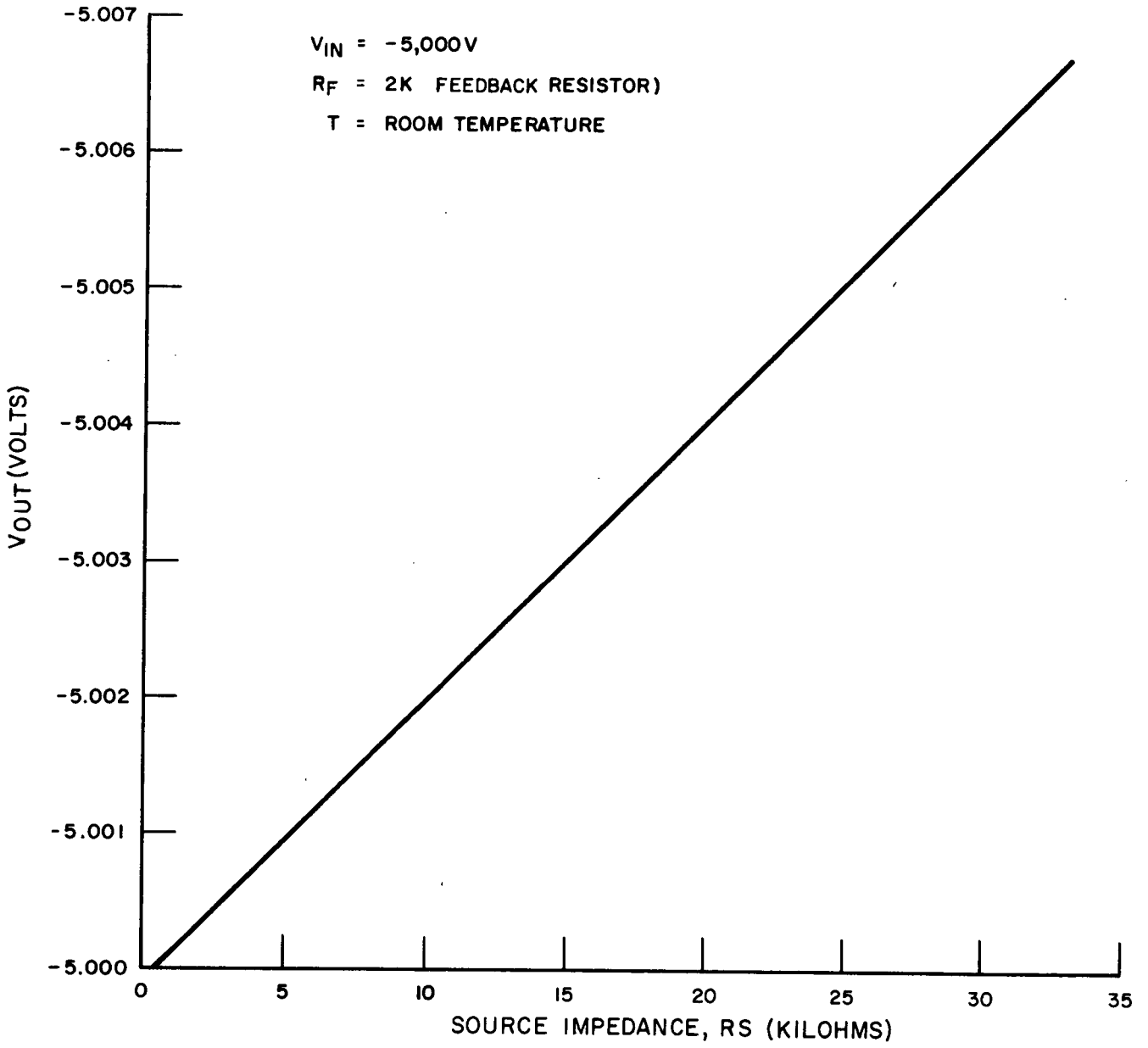

Figure 3-VI-12. Commutator Source Impedance Sensitivity For One Channel at Full-Scale Input

the first hot run of thermal-vacuum testing, side 2 did not cycle properly; marker frequencies not being present in channels 12 through 15.

After extensive testing of those boards which could have caused this anomaly, no defects were located nor did the anomaly recur. The failure was attributed to the test equipment. Flight acceptance testing of the SR processor was repeated with a new marker board (1975411). Pre-vibration, vibration, and post-vibration tests were successfully completed on February 25. During thermal-vacuum testing on February 27, which involved the same bell jar and test cable as used in the previous thermal-vacuum tests, the anomaly described above recurred. It was found that the test cable had been shorted to the bell jar by the shroud when the bell jar was closed. The test cable was repaired and the following tests successfully completed.

Test	Date Completed (1969)
Pre-thermal-vacuum	February 28
Thermal-vacuum	March 1
Post-thermal-vacuum	March 3

The newly designed sync generator board, A8, was then installed in the processor to provide a new sync pulse format at the start of each scan line of real-time IR and visible data. Successful retesting of the SR processor was completed as shown in the following listing.

Test	Completion Date (1969)
Pre-vibration	April 15
Vibration	April 16
Post-vibration	April 17
Thermal-vacuum	April 19
Post-thermal-vacuum	April 20

On April 24, the DC/DC converters in the processor were replaced with units having new 12E109 transistors. Successful tests were then completed as follows:

Test	Completion Date (1969)
Operational (ambient conditions only)	April 25
Vibration (flight level random, all 3 axes)	April 25

Test	Completion Date (1969)
Operational (-10°C and +55°C only)	April 26
168-hour confidence	May 4

10. Scanning Radiometer Recorder and Recorder Electronics

a. ELECTRICAL TEST MODEL

Testing of the electrical test model of the scanning radiometer recorder (SRR) assembly was performed using a control box to simulate spacecraft functions when required. The testing was accomplished as chronologically detailed below.

During functional checkout and power turn-on, transients were observed and measured on April 17, 1968. Command and control circuitry was checked at board level for compliance with the logic diagram and found to be correct. Voltage levels, and rise and fall times were within IC specification limits. Voltage drop across the power switches was 0.3 volt. Turn-on rise time was 6 milliseconds for the servo power switch and 10 milliseconds for the record power switch. The 5-second delay was measured to ± 5 percent.

Measurements of power consumption was made at 25°C with the following results:

Power Mode	Specified	Measured
Record	7.5 W	4.19 W
Playback	10 W	5.62 W
Standby	0.6 W	0.56 W

Turn-on current transients were measured across a 1-ohm resistor with a rise rate of 40 milliamperes per microsecond. A voltage of -24.5 was applied to the SRR in the playback mode. Ripple current taken from the -24.5-volt supply line measured 6 milliamperes peak-to-peak at 12 kHz, and 90 milliamperes peak-to-peak at 10 Hz.

During the period April 17 through 26, 1968, testing on the servo loop circuitry was performed. The procedures and results are discussed in the following paragraphs.

The encoder shaper was tested by injecting a 600-Hz, 20-microampere sine wave current into the input. The output was a 5.5-volt square wave (50-percent duty cycle) maintained over the input current range of 4 to 80 microamperes. Acceptable square wave outputs were obtained when the input frequency was increased to 15 kHz.

The motor driver was tested at board level using 1-ampere average current. The 12-kHz pulse current rise and fall times were less than 1 microsecond, and total delay from input voltage to output current pulse was 1.2 microseconds (calculated worst-case delay is 4 microseconds). The nominal motor record current is 80 milliamperes and playback current 250 milliamperes.

Closed loop servo stability tests were conducted by injecting a sine wave voltage from a low-frequency oscillator maintained at a minimum level to keep the servo loop operating in a linear mode. Valid output readings were taken using a Solartron Resolved Component Indicator. Figure 3-VI-13 is an inverse plot of the closed-loop record mode operation. This illustration shows a 40-degree phase margin and a 3-dB gain margin. Closed-loop playback inverse plot is included as Figure 3-VI-14, and shows a 38-degree phase margin. Playback gain margin was not established due to limitations in the test equipment, but theoretically should be 18 dB. The digital phase detector output was recorded and, in the record mode, the delay was 300 microseconds and the jitter about 40 microseconds.

Theoretical record delay, D

$$= \text{phase detector pulse interval} \frac{\text{Dc offset volts}}{\text{correction swing}} + \frac{\text{torque required}}{\text{torque developed with correction voltage}}$$

$$= 835 \frac{0.9}{5} + \frac{2}{10} = 318\ \mu s$$

Theoretical jitter

$$= \text{encoder jitter and jitter caused by T (0.2 oz-in)}$$

$$= (2\% \text{ of } 2 \times 835\ \mu s) + \frac{0.2\ (\Delta T) \times 2 \times 835}{10(T) \times 10\ (\text{attn})}$$

$$= 33.4\ \mu s + 3.3 \mu s = 36.7\ \mu s$$

Record mode measured torque capability was 8.0 ounce-inches. Record mode nominal torque was 2.0 ounce-inches and calculated worst-case transport torque at -10°C was 4.15 ounce-inches. Playback mode measured torque capability was 15 ounce-inches. Playback mode calculated worst-case transport torque at -10°C was 6.42 ounce-inches.

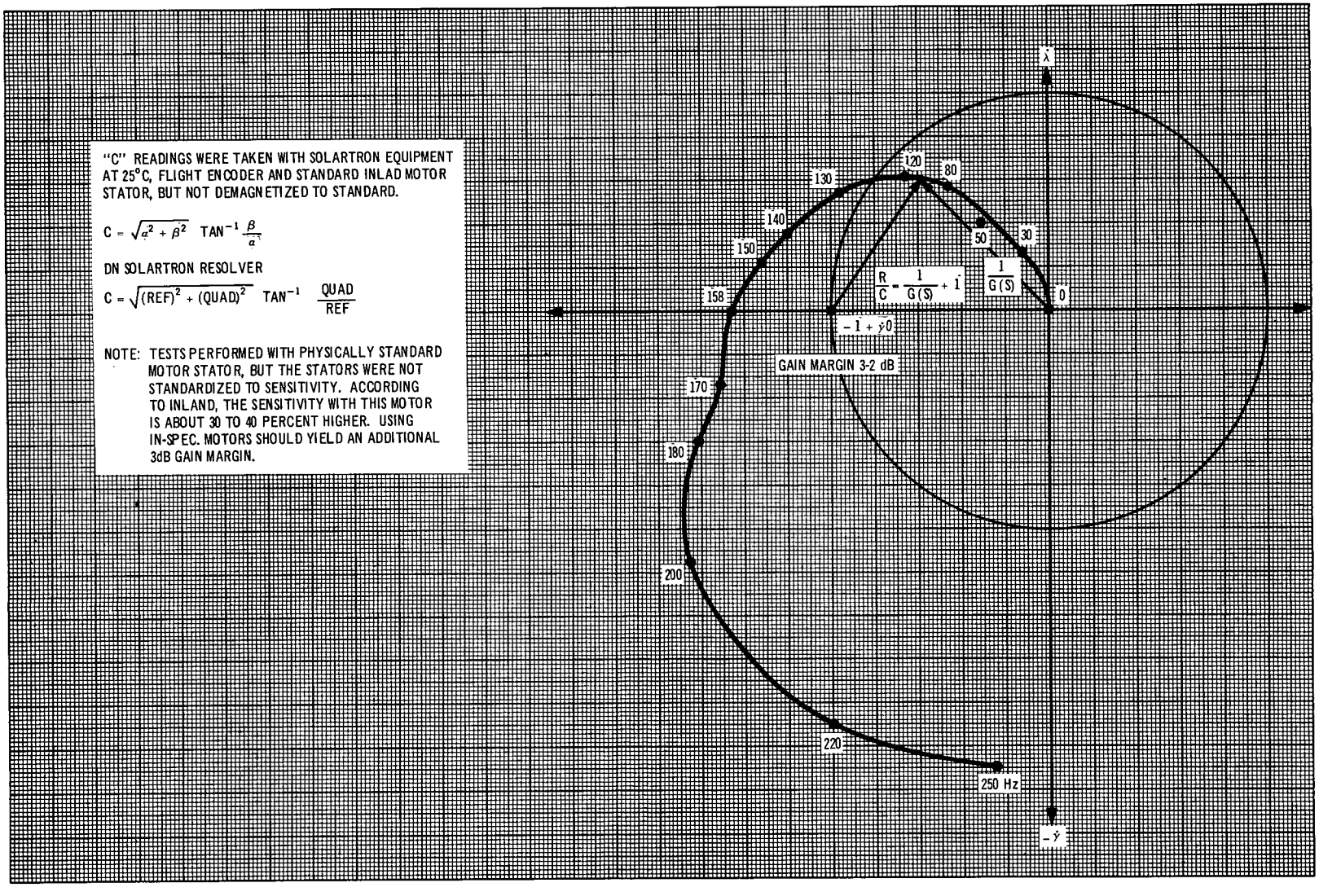

Figure 3-VI-13. SRR ETM Servo Inverse Plot, Record Mode

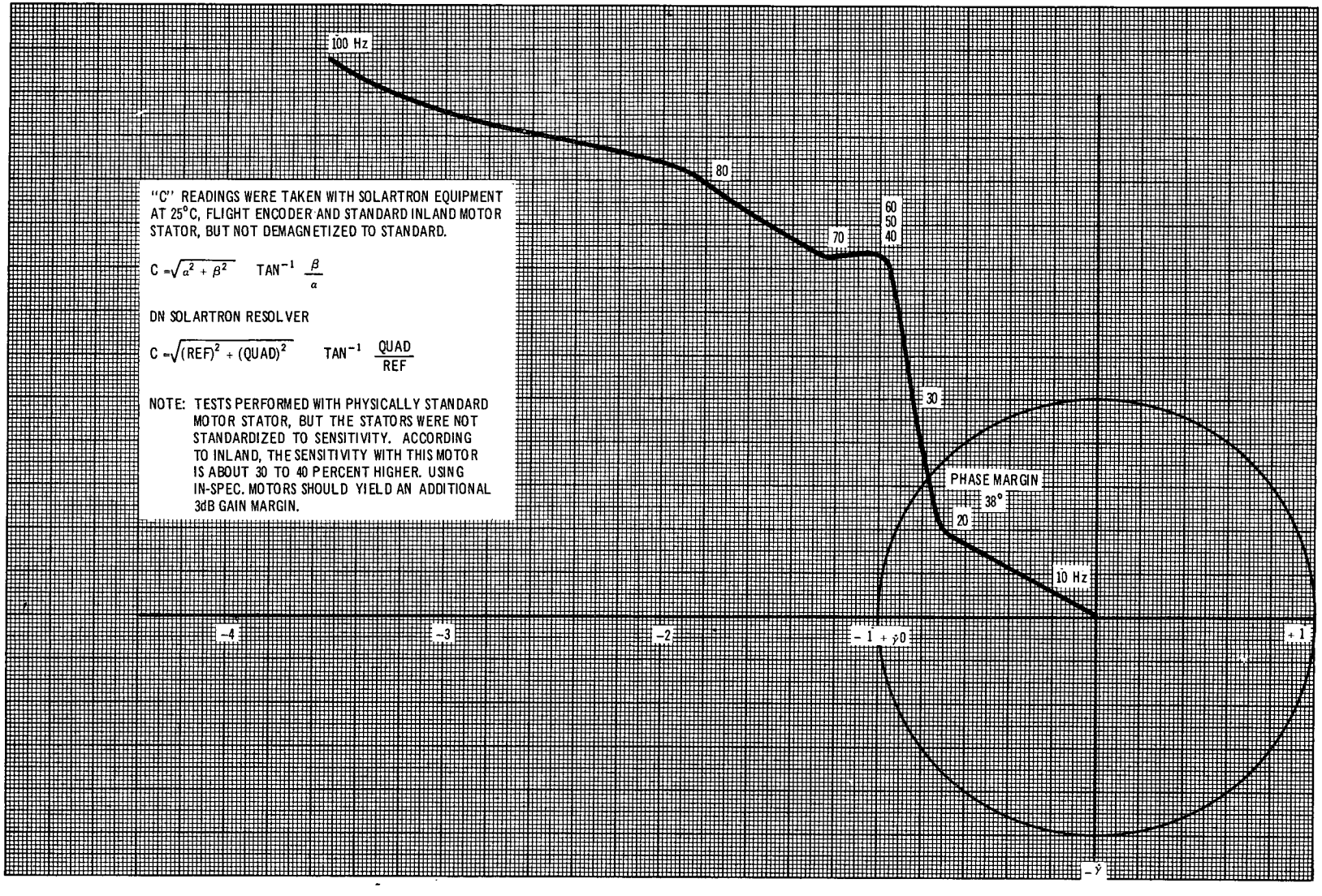

Figure 3-VI-14. SRR ETM Servo Inverse Plot, Playback Mode

Tape tension was measured as 6 ounces on the empty reel, 4 ounces on the full reel, and 3 ounces when both reels were half full.

Tape tracking was measured from one end of the tape to the other, and the tracking, including the tape edge irregularities, was within 0.005 inch.

A resistor was inserted in series with the end-of-tape record (EOTR) and end-of-tape playback (EOTP) line, and increased until the end-of-tape just malfunctioned. The resistance required to produce a malfunction was 75 ohms, whereas normally the resistance is about 1 ohm.

Tape travel past the EOTR was 0.2 inch. The tape travel past the EOTP was 9 inches. The supply line was varied between -18 and -35 volts while the entire system was still operating at a degraded performance level. From this, the servo drive system is considered to be compatible with the calculations and is able to produce the desired signal integrity.

During the period May 13 through 16, 1968, testing on the signal electronics portion of the SR recorder assembly was performed as discussed in the following paragraphs.

Adjustments were made and "select on test" components were installed in the IR and visual FM modulators so that the output frequency at 3.3 kHz, 2.85 kHz, and 2.4 kHz was ±1.5 percent (-10°C to +50°C) when inputs of 0, -4, and -8 volts were applied.

Playback flutter measurements were conducted at +25°, +51°, and -10°C. Figures 3-VI-15, 3-VI-16 and 3-VI-17 are plots of the flutter spectrum and cumulative flutter. A value of 0.3-percent flutter corresponds to a 40-dB peak-to-peak signal-to-rms noise figure. The illustrations show results well within specifications (0.2 percent) for temperatures of 25° and 51°C, but show flutter in excess of 0.3 percent at one part of the tape at -10°C. Indications point to the cause of higher flutter as a result of the different channeling of G6 grease when the direction of rotation is reversed.

Frequency change was measured at 25°C on flutter-and-wow channels over the entire tape length using a carrier frequency of 38 kHz. Taking samples every 3 seconds, the change in frequency was 33 Hz, or a total measured tape "creep" of 0.087 percent.

The system frequency response was measured (using the TIROS M SR tape recorder STE demodulator) from 5 to 650 Hz at 75-percent modulation level. The response was flat to 200 Hz, down 1.2 dB at 450 Hz, and down 14 dB at 650 Hz with reference to the record mode.

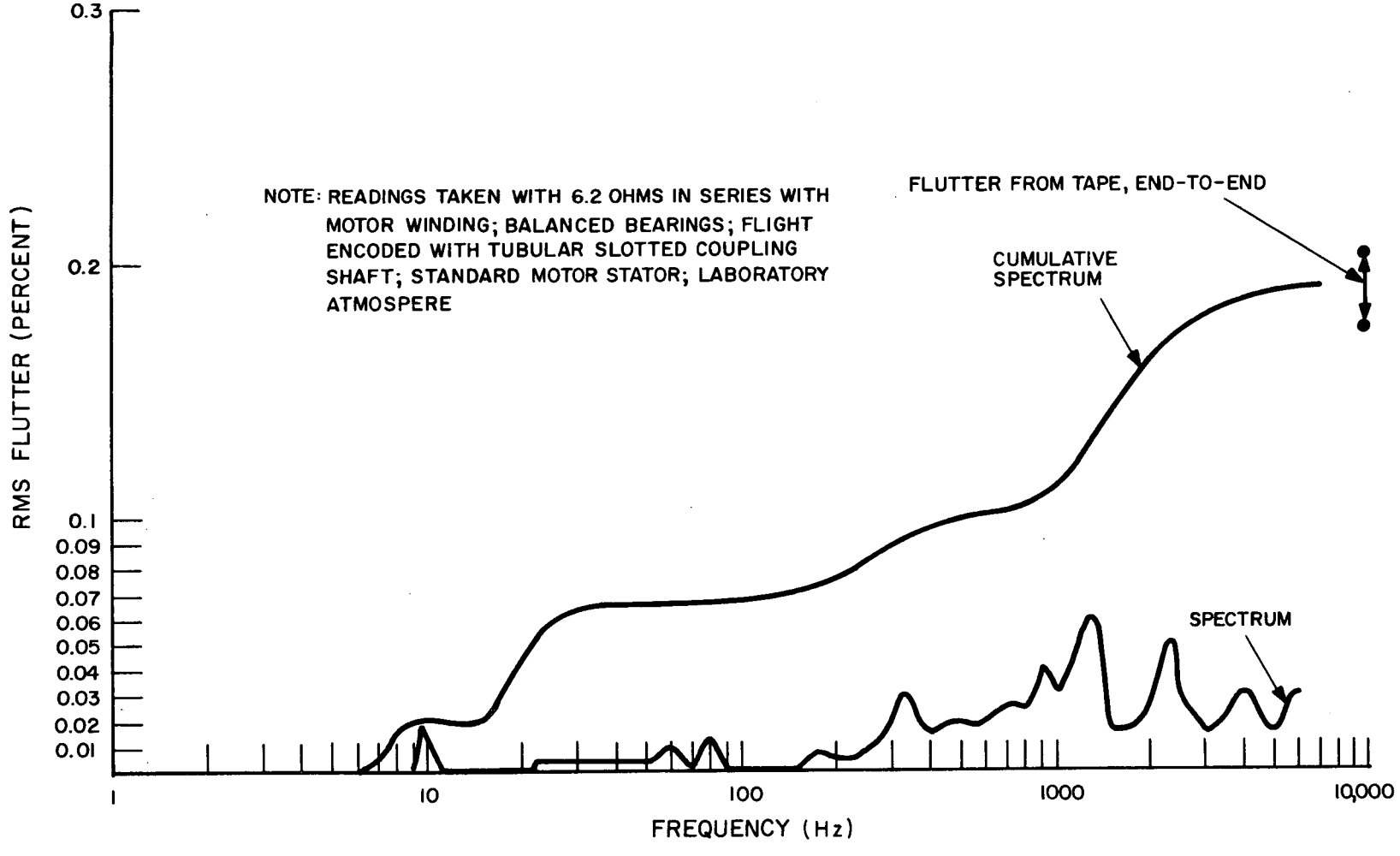

Figure 3-VI-15. SRR ETM Flutter Characteristics at 25°C

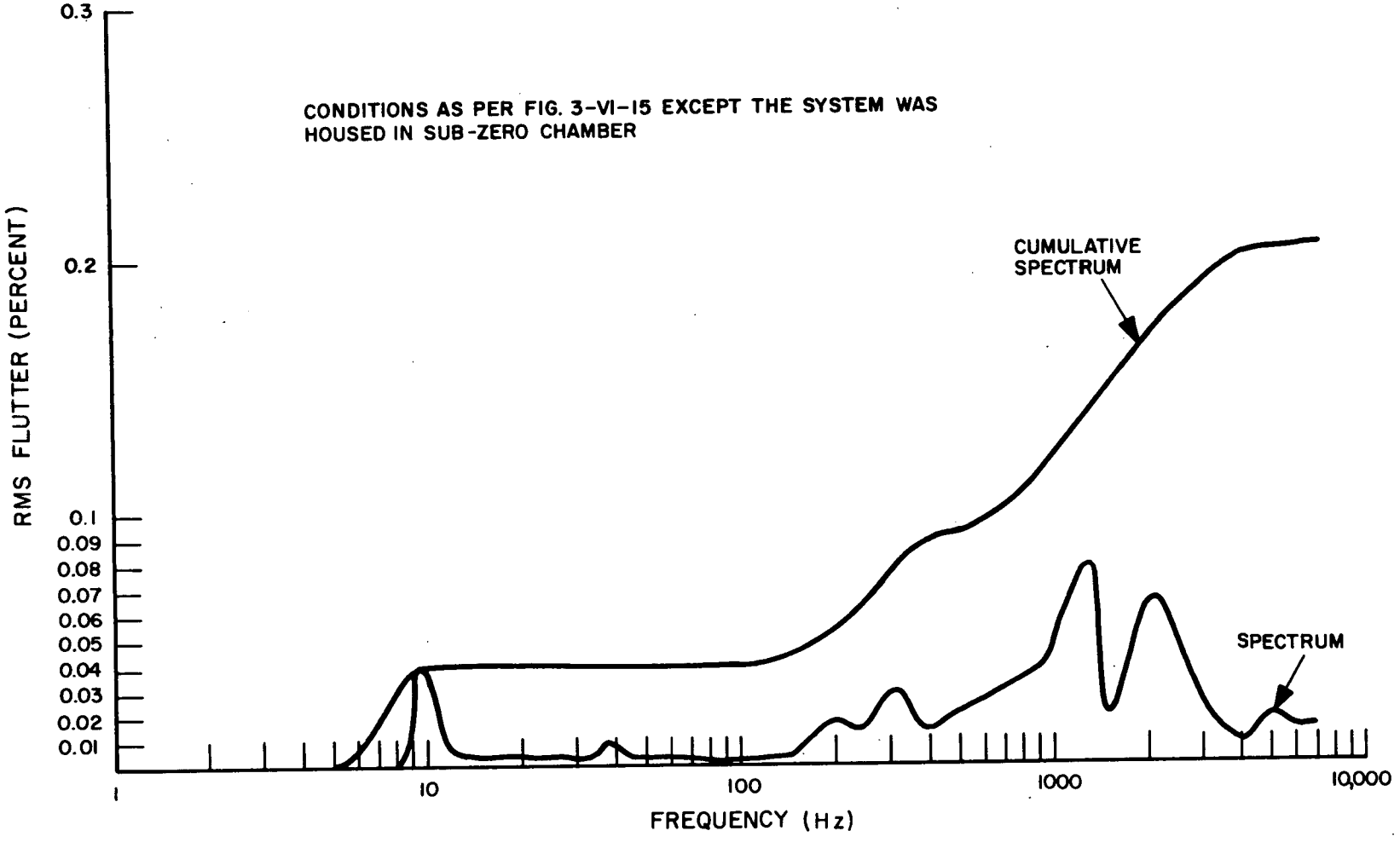

Figure 3-VI-16. SRR ETM Flutter Characteristic at 51°C

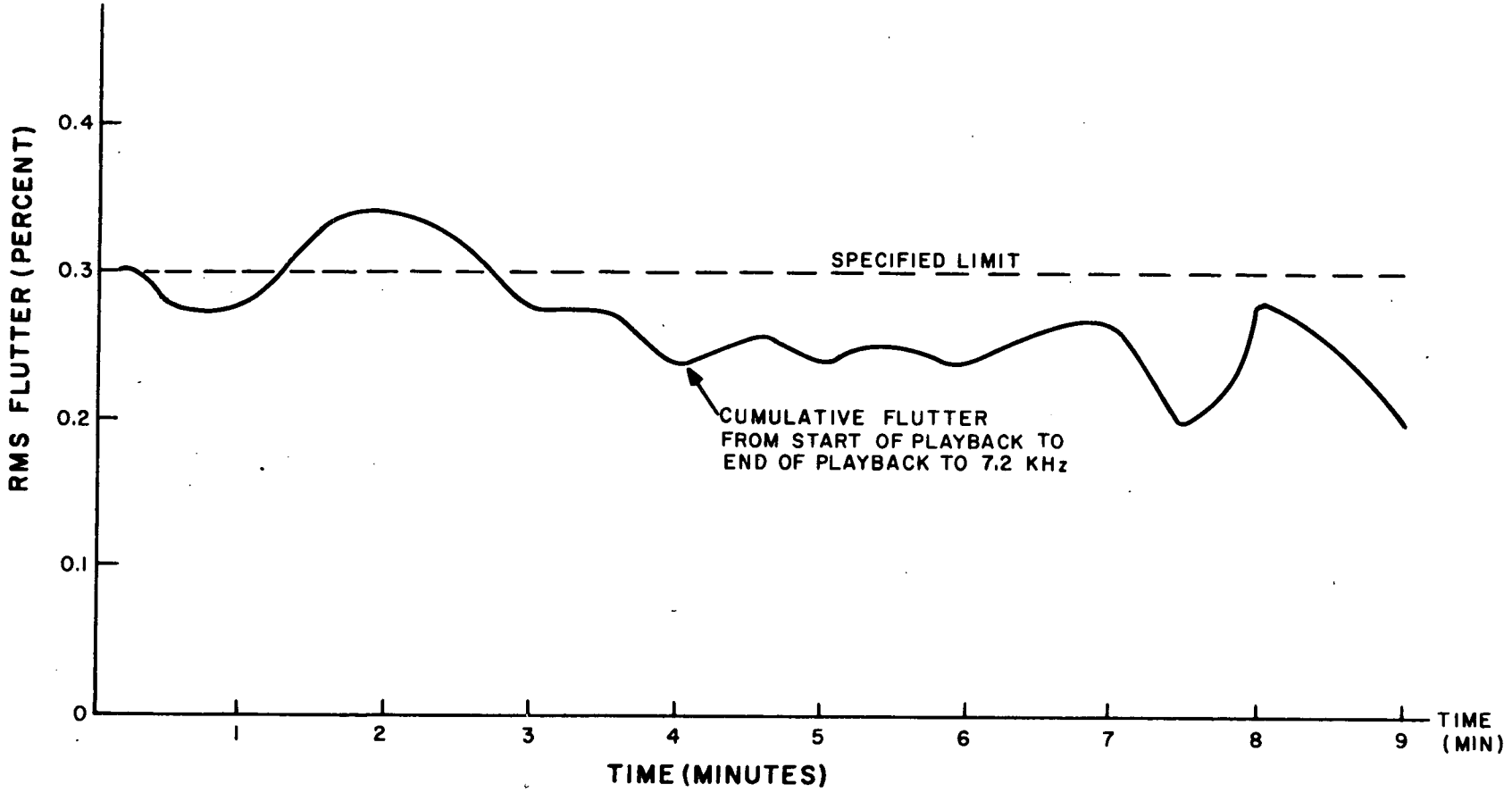

Figure 3-VI-17. SRR ETM Flutter Characteristics at -10°C

The signal-to-noise measurements were made using the same demodulator mentioned in the preceding paragraph. The results showed a 43-dB peak-to-peak signal-to-rms noise ratio at carriers of 45.6, 38.4, and 52.8 kHz.

The SR tape recorder modulator was tested using a 10-Hz square wave as a modulation source with an amplitude of 0 to -8 volts. Rise and fall times were 14 microseconds, with practically no overshoots. The TIROS M SR tape recorder STE demodulator peak-to-peak output voltage was 20 volts, rise and fall times 100 microseconds, and measured overshoot of 7 percent. The duration of the overshoots was about 50 microseconds (specified maximum overshoot is 5 percent). The dynamic behavior of the system is considered to be almost entirely governed by the response of the demodulator.

Vibration testing was performed during May, 1968 by mounting the tape transport (only) to its base and subjecting it to prototype level vibrations on 3 planes. The transport suffered no major failure. However, the following problem areas were uncovered:

- Tendency of the metalized portion of the tape (EOT) to move off the flat idler onto the capstan,
- Loosening of the screws holding the negator storage drums and arms, and
- Loosening of the capstan nut.

These areas were reworked and corrective action taken.

Following the vibration test, the bearing axial clearances were measured and found to be within specification. Motor and encoder areas were disassembled, examined, and reassembled. Electrical tests were performed covering servo operation, flutter spectra, and cumulative flutter, and compared to pre-vibration test results. No deterioration of performance was observed.

Table 3-VI-9, comparing the measured ans specified values, was prepared to summarize the ETM testing, and is included herein.

b. PROTOTYPE

The scanning radiometer recorder (Ser. No. 01P) consists of two units: the tape transport in a hermetically sealed enclosure and the recorder electronics. Unless otherwise specified, the following discussion of the testing program includes both units.

During October, the SR recorder was assembled and temperature cycling tests performed in preparation for qualification testing.

TABLE 3-VI-9. SCANNING RADIOMETER RECORDER SUMMARY OF SPECIFICATION LIMITS AND ETM TEST RESULTS

Function	Specification	Test Results
Tape Travel		
Record	145 min	145.7 min } 16 ÷ 1 Ratio
Playback	9.1 min	9.11 min }
Data Bandwidth		
Subcarrier	(2.85 ± 0.45 kHz)	±1.5%
Deviation	±1.85%	
Channels 1 and 3	Linearity + Drift with temperature	
Demodulated Baseband		
Cumulative Flutter to 7.2 kHz	0.3% rms	0.2% rms at 25°C and at 50°C 0.3% rms at -10°C*
Power Consumption		
Standby	0.6 W max	0.56 W
Record	7.5 W max	4.19 W 25°C
Playback	10.0 W max	5.62 W +20% at -10°C
SR Recorder Status		
OFF	OFF $^{+0}_{-0.5V}$	0
Standby	-0.9 ± 0.1V	-0.8V
Record	-1.8 ± 0.2V	-1.65V
Playback	-2.7 ± 0.3V	-2.55V
Playback & Record	-3.6 ± 0.4V	-3.3V
Data Channel Amplitude	2 V p-p ± 5%	2 V
Transient Response	5% overshoot max	7%**
Signal-to-Noise	40 dB p-p/rms	43 dB at 25°C, 50°C 40 dB at -10°C

*Flutter is shown in Figure 3-VI-17 and shows 0.34 percent over 1.5 minutes of playback. Most of the time flutter was 0.275 percent.

**The overshoot is mainly due to the dynamic behavior of the demodulator. Hence, it is not controlled by the SRR.

Note: Capstan "creep" was measured over record and playback cycle by sampling flutter-and-wow channel frequency every 3 seconds, and was 0.087 percent.

TABLE 3-VI-9. SCANNING RADIOMETER RECORDER SUMMARY OF SPECIFICATION LIMITS AND ETM TEST RESULTS (Continued)

Function	Specification	Test Results
Turn-on Transients	50 mA/μs V_S = -36V	40 mA/μs No breakdowns
Ripple Current		
1 Hz to 1 kHz	20% (80 mA)	90 mA***
1 kHz to 15 kHz	2% (9 mA)	6 mA
15 kHz to 100 kHz	0.1% (0.4 mA)	Not Measurable
Recorder Temperature, Telemetry		
Amplitude Range	-0.5 to -4.5V	-2.85V at +23°C
Recorder Pressure, Telemetry		
Amplitude Range	-0.5 to -4.5V	-2.85V at 1 atmosphere
Weight		
Electronics and Container	5.5 lb	5.326 lb
Transport and Assembly	11.75 lb	14.034 lb****
	Record/Playback	Record/Playback
Acceleration	1.0 s 3.0 s	0.3 s 1.8 s
Deceleration	1.0 s 5.0 s	0.3 s 2.2 s

***Measured with a nonstandard encoder which had once-around position variation. Using flight encoder, this value should not exceed 10 percent (40 mA).

****Weight reduction program was initiated.

Confidence testing was performed on October 25, 1968. On this date a leak (pressurization) test was also completed on the tape transport.

During qualification testing on October 27, high and erratic motor current was evident when in the record mode. Analysis revealed the cause to be an oscillation at the encoder shaper. Low-pass filtering and decoupling was added to suppress the oscillation. While troubleshooting the encoder shaper board on October 29, the frequency and phase detection circuits of the A6 board (1975414) did not function properly and the board was replaced. During troubleshooting of the recorder electronics unit on December 9, the frequency and phase detection circuits appeared unstable. By relocating the test point to a terminal, the problem was eliminated.

Alignment testing was performed on December 18, and component qualification testing completed on December 22, 1968.

During January, 1969, following completion of thermal testing, vibration testing of qualification levels was performed. As a result, several changes were implemented:

- A set of flanges was installed to prevent disturbance of the tape stack.
- The encoder cover was reinstalled with locking compound.
- The encoder shaft setscrews were changed to a type that permitted greater tightening torque to be applied.

Thermal-vacuum testing was performed in early February, 1969, and qualification of the prototype SR recorder was considered completed.

c. FLIGHT MODEL

Two scanning radiometer recorder and recorder electronic assemblies are carried aboard the TIROS M spacecraft: scanning radiometer recorder assembly No. 1 designated Ser. No. 02 and scanning radiometer recorder assembly No. 2 designated Ser. No. 05. Until August, 1969, testing on SR recorder assembly No. 2 was performed using Ser. No. 04.

(1) SCANNING RADIOMETER RECORDER ASSEMBLY SER. NO. 02

SR recorder tape transport Ser. No. 02 underwent pressurization (leak) testing on February 15, 1969. During SR recorder assembly pre-vibration testing on February 17, the measured frequencies during the data acquisition portion of the playback did not meet specifications. Troubleshooting

revealed a temperature-sensitive A3 modulator board which was replaced. Continued testing on February 18 showed that the flutter-and-wow noise readings exceeded specifications. The cause was traced to a small burr on the tape transport capstan shaft between the inner and outer encoder shaft assemblies. After correction, the tape transport was successfully leak-tested. Confidence testing of the SR recorder assembly was completed on February 24, 1969.

Performance testing on the SR recorder assembly was initiated as shown below.

TEST	DATE (1969)
Pre-vibration	February 25
Vibration	February 27
Post-vibration	February 28
Thermal-vacuum	February 28
Post-thermal-vacuum	March 4

In compliance with an instruction by the Test Review Board, all Motorola 1N944B diodes date-coded 6750 were to be changed. This retrofit was performed on the SR recorder electronics unit. The SR recorder assembly was then given an abbreviated performance test on April 12. Post-vibration testing was performed on the SR recorder electronics unit on April 13.

The 168-hour confidence test on the SR recorder assembly was successfully completed on April 29, 1969.

(2) SCANNING RADIOMETER RECORDER ASSEMBLY SER. NO. 05

Testing on the SR recorder assembly Ser. No. 05 was performed as listed below.

TEST	DATE PERFORMED (1969)
Pre-vibration	March 29
Leak Test	April 2
Vibration	April 2
Post-vibration	April 2
Thermal-vacuum	April 10
Post-thermal-vacuum	April 10
Leak Test	April 10

The diode retrofit ordered for SR recorder electronic unit Ser. No. 02 was performed on this unit and retesting of the recorder assembly completed on April 18, 1969.

The 168-hour survival test on the SR recorder assembly Ser. No. 05 was initiated on May 26, 1969.

11. Data Format Converter

a. ELECTRICAL TEST MODEL

Although the TIROS M data format converter (DFC) was a new design, the digital logic circuitry was composed of elements which have been used on earlier projects. Therefore, no ETM breadboard was constructed for the complete unit. Specific sections, however, were tested to determine if they would meet the requirements of the system.

The VCO summing amplifier was assembled from standard components and tested for frequency response with and without capacitive loading, and over a temperature range of -20 to +60°C. Gain linearity at a frequency of 150 kHz was also measured over this temperature range. Test results indicated that the amplifier operation was well within specification limits.

Harmonic content of the amplifier output signal was measured. With an input of 1.5 volts peak-to-peak, and an output of 3.6 volts peak-to-peak, the following data was recorded:

- With each input frequency applied separately, harmonics up to the fifth were measured and were down at least 45 dB.
- With all three inputs applied simultaneously, the same harmonics of each input frequency were measured and were at least 45 dB down.
- With all three inputs applied simultaneously the harmonics of the sums and differences of the input frequencies were measured and found to be at least 50 dB down.

A test model of the DFC commutator was assembled, using a type uA709 integrated circuit operational amplifier. Comparisons of output voltage versus commutator channel showed variations of 0.16 millivolt at 25°C, 0.9 millivolt at -20°C, and no variation at +70°C.

When the source resistance was matched to the feedback resistor of the uA709, gain versus linearity variation was less than ±1.5 millivolts over the temperature range from -20° to +70°C.

With a feedback resistor of 2 kilohms, and the input voltage held constant at 5.000 volts, the output varied from 5.000 to 5.006 volts as the source resistance was varied from 2 to 30 kilohms.

The switching point error of the A/D converter was measured at temperatures of -15°, +25°, and +70°C. Variations was less than 4 millivolts over the temperature range. Differential linearity variation over a range of 125 counts did not exceed 4.0 millivolts, over the full test temperature range.

b. PROTOTYPE

Digital format converter (DFC) Ser. No. 01P completed the following qualification tests.

Test	Date Performed (1968)
Post-potting*	July 10
Vibration	July 10
Post-vibration	July 11
Acceleration	July 11
Prethermal-vacuum	July 15
Thermal-vacuum	July 19
Final Electrical	July 19

c. FLIGHT MODEL

Data format converter Ser. No. 03 was subjected to, and successfully passed, the following tests on December 7, 1968: pre-vibration operational test, vibration test, and post-vibration operational test. The unit was subjected to, and successfully passed, thermal-vacuum testing on December 10 and post-thermal-vacuum testing on December 12, 1968.

In April 1969, the DC/DC converter (RCA Drawing No. 1960870) was replaced with a new subassembly using new General Electric 12E109 transistors. Then, in accordance with a NASA directive, the modified unit was subjected to a special 168-hour confidence test which was completed on May 9, 1969.

*Failure on this test was due to an open connection on pin 6 of IC Z14. This was categorized as an isolated case of poor vendor workmanship. After replacement of Z14, testing continued.

12. Incremental Tape Recorder

a. ELECTRICAL TEST MODEL

A test program was initiated in August 1967, to determine if the recorder could operate successfully over the temperature range of -15° to 60°C. The basis for the test rested not on worst-case available torque margins, but on tape qualification over this temperature range. In September, soak tests of a recorder model were conducted with the tape in a fixed position at 60°C for about 53 hours. The recorder was then started in the record mode. Near the end of the record cycle, the stepper motor began to slip. Preliminary analysis showed indications of tape stiction. Even after complete cleaning, installation of a new tape, purging, and pressurization, the tape stiction condition persisted. In October, the transport was cleaned and a slightly thicker tape installed. Retesting was successfully accomplished. However, testing on the engineering model revealed that a support post interfered with a negative spring buildup, and a relief notch was machined in the post to provide the necessary clearance.

b. PROTOTYPE

Incremental tape recorder Ser. No. 02P was subjected to the following tests. Initial electrical performance testing was concluded on June 20, 1968, and vibration testing completed on June 21. Thermal-vacuum testing was initiated on June 23, 1968, but erratic playback operation was observed. A series of thermal-vacuum retests were run to determine the cause of tape deposits, motor stalling, and EOT malfunctions. Testing continued into July to evaluate the cause of these elusive anomalies. As a result, the one-way idler was modified into a two-way idler, a tape having a segment of fine abrasive (green tape) to clean friction surfaces during operation was installed, and the recorder was run and monitored for extended periods. Thermal-vacuum testing was considered successful on August 23, 1968.

Acceleration testing was completed on August 26, and post-acceleration performance testing on August 27, 1968.

Leak rate tests were performed before and after vibration, and after thermal-vacuum testing.

c. FLIGHT MODEL

Incremental tape recorder Ser. No. 03 was subjected to, and successfully completed, the following tests:

Test	Date Completed
Pre-vibration	September 13, 1968
Vibration	September 13, 1968
Post-vibration	September 13, 1968
Thermal-vacuum	September 17, 1968
Post-thermal-vacuum	September 24, 1968
168-hour survival	April 23, 1969

An instance of track-to-track jitter observed during pre-vibration testing was attributed to the jitter error counter. Apparent anomalies involving turn-on transients and bit-to-bit and track-to-track jitter during thermal-vacuum testing were attributed to the test equipment. An oscilloscope was substituted for the track-to-track and bit-width counters to measure the applicable parameters, and the test procedure was modified accordingly. During the 168-hour survival test, non-repeatable instances of crosstalk and bit-to-bit and track-to-track jitter occurred. Analysis of test data, however, indicated that the recorder had performed within the specified limits.

13. Beacon and Command Antenna Group

The beacon and command antenna group is comprised of the antenna structure itself, and the following major electronic components: a bandpass filter*, a 148-MHz notch filter*, two 136-MHz notch filters*, a command hybrid coupler*, and an RF switch.

A 2-1/2:1 scale model of the beacon and command antenna was fabricated, and in April 1967, field patterns were measured.

During July 1967, electrical testing of a breadboard version of the single dipole antenna was performed. The antenna was matched at both beacon and command frequencies and isolation tests completed in September 1967.

Vibration testing was performed on the antenna and the results showed that the design was satisfactory at component vibration levels.

*These components are vendor supplied and only flight model testing occurred at AED.

a. BANDPASS FILTER

Bandpass filter Ser. No. 04 successfully passed a pre-vibration operational test September 13, a vibration test on September 16, and a post-vibration operational test on September 17, 1968.

b. 148-MHz NOTCH FILTER

The 148-MHz notch filters Ser. Nos. 04, 05, and 06 successfully passed the following flight-level tests on the dates indicated.

	Date Completed		
Test	Ser. No. 04.	Ser. No. 05.	Ser. No. 06.
Pre-vibration	Feb. 12, 1968	Feb. 12, 1968	Feb. 12, 1968
Vibration	Feb. 16, 1968	Feb. 18, 1968	Feb. 15, 1968
Post-vibration	Feb. 20, 1968	Feb. 20, 1968	Feb. 20, 1968

NOTE: Only one 148-MHz notch filter is used with the beacon and command antenna group/ - the other two filters are associates with the real-time antenna group.

c. 136-MHz NOTCH FILTERS

The 138-MHz notch filters Ser. Nos. 02 and 03, were subjected to, and successfully passed the following flight-level tests on the dates indicated.

	Date Completed	
Test	Ser. No. 02	Ser. No. 03
Pre-vibration	January 26, 1968	January 25, 1968
Vibration	January 27, 1968	January 26, 1968
Post-vibration	January 26, 1968	January 26, 1968

d. COMMAND HYBRID COUPLER

Command Hybrid coupler Ser. No. 193 successfully completed the following flight-level tests on the dates indicated.

Test	Date Completed
Pre-vibration	December 18, 1967
Vibration	December 21, 1967
Post-vibration	January 15, 1968
Thermal-vacuum	January 17, 1968
Post-thermal-vacuum	January 18, 1968

e. RF SWITCH ASSEMBLY

(1) PROTOTYPE

Qualification testing of the RF switch assembly Ser. No. 011 was performed as delineated below.

Initial electrical performance testing was accomplished on January 9, 1969. The following tests were performed as indicated:

Test	Date Completed (1969)	Temperatures (°C)
Conducted RF	January 9	+25
Alignment	January 9	+25
Overvoltage	January 21	+25
Surge Current	January 21	+60, +25, -15
VSWR	January 21	+61, +25, -15
Insertion Loss	January 21	+60, +25, -15
Isolation	January 21	+60, +25, -15
Current Drain	January 21	+60, +25, -15
RF Power	January 21	+25

Vibration testing was accomplished on January 23, and post-vibration testing on January 24. Thermal-vacuum testing was completed on January 27, 1969.

(2) FLIGHT MODEL

RF switch Ser. No. 02 successfully completed a pre-vibration operational test on January 30, a vibration test on January 31, and a post-vibration operational test on February 3, 1969.

14. Dual Command Receiver

a. PROTOTYPE

Qualification testing on the dual command receiver Ser. No. 01P consisted of thermal profiles at +25°, +55°, and -10° C taken at ambient pressures. Prototype testing was completed on April 16, 1968.

b. FLIGHT MODEL

Dual command receiver Ser. No. 02 was subjected to, and successfully passed, the following tests on the dates indicated: pre-vibration - April 25, 1968; vibration - April 26, 1968; and post-vibration - April 29, 1968. On April 30, 1968, during thermal-vacuum testing at -10° C, the bandwidth of side 1 (J1 and J2) read 49.8 kHz and the bandwidth of side 2 (J3 and J4) read 49.6 kHz instead of the specified requirement of > 50 kHz.

An investigation into this anomaly indicated that the receiver crystal filters were specified for a bandwidth of 50 kHz. Since the maximum available bandwidth is limited by the crystal filter, some degradation of bandwidth is to be expected due to other circuit factors. Since no significant degradation of system performance would result, the bandwidth requirement was changed to be greater than 48 kHz. On May 2, 1969, the dual command receiver successfully completed a special 168-hour survival test initiated by NASA directive and was ordered delivered to spacecraft integration.

15. Beacon Transmitter

a. PROTOTYPE

Beacon transmitter Ser. No. 01 successfully completed the following tests on the dates indicated.

Test	Date Completed
Acceptance Temperature	June 7, 1968
Vibration	June 10, 1968

Thermal-vacuum	June 17, 1968
Post-thermal-vacuum	June 17, 1968

A data verification test failure during spacecraft testing in December 1968, prompted an investigation into beacon transmitter operation. Tests indicated that some transmitters had spurious outputs at turn-on and oscillated when operating into a short or open circuit. As a result, the "select-on-test" capacitor (C31) in the power amplification section was changed and the section retuned.

b. FLIGHT MODEL

Beacon transmitters Ser. Nos. 08 and 010 were utilized on the TIROS M spacecraft. These transmitters were subjected to, and successfully completed the following tests:

	Date Completed	
Test	Ser. No. 08	Ser. No. 010
Pre-vibration	June 6, 1968	April 9, 1968
Vibration	June 10, 1968	April 18, 1968
Post-vibration	June 10, 1968	April 18, 1968
Thermal-vacuum	June 14, 1968	April 24, 1968
Post-thermal-vacuum	June 17, 1968	April 26, 1968

Following the circuit modification discussed in the preceding section (Prototype) the design review board recommended the addition of resistor R23 to the power amplifier section and the removal of capacitor C31. This change required retesting of the transmitters as shown in the following tabulation. Both transmitters (Ser. Nos. 08 and 010) completed the tests on the same date.

Test	Date Completed
Temperature	April 17, 1969
Modified Vibration	April 23, 1969
Post-vibration	April 25, 1969

16. Dual Subcarrier Oscillators (SCO's)

a. ELECTRICAL TEST MODEL

None. Item supplied by vendor.

b. PROTOTYPE

Tested by vendor.

The dual SCO is a vendor-supplied and tested item. The flight model was delivered to RCA on February 23, 1968.

The dual SCO assembly Ser. No. 05 was subjected to, and successfully completed, the following tests at the vendor's plant on the dates indicated:

Test	Date Completed
Pre-vibration	January 30, 1968
Vibration	January 30, 1968
Post-vibration	January 31, 1968
Thermal-vacuum	January 31, 1968

The dual beacon transmitter and SCO assembly were tested as a unit on May 2, 1969.

17. Signal Condition

a. PROTOTYPE

Testing of the signal conditioner (Ser. No. 01P) was performed as indicated below.

Test	Date Completed
Acceptance	May 21, 1968
Vibration	May 22, 1968
Post-vibration	May 22, 1968

During initial power application and functional checkout of the pitch control electronics on July 26, 1968, incorrect closed/coarse telemetry values were obtained. Investigations revealed an incompatibility in the interface impedance which was corrected by a design change in the values of two resistors in the telemetry signal conditioner. Retesting for proper performance was effected on November 25, 1968, and on January 2, 1969, the unit was turned over to integration.

b. FLIGHT MODEL

Telemetry signal conditioner Ser. No. 02 mates with vendor-supplied and qualified telemetry commutators Ser. Nos. 2489 and 2481 (discussed in the following subsection) to form a complete unit.

Telemetry signal conditioner Ser. No. 02 was given a pre-vibration test on July 25, 1968, a vibration test on July 30, and a post-vibration test on July 31, 1968.

During initial power application to the spacecraft on August 14, routine ground checks revealed a direct short between commutator signal and case grounds. The cause was ascertained as originating from a manufacturing defect in the commutator which, along with several others, was returned to the manufacturer for repair and retesting. After a good commutator was installed in the signal conditioner, the assembly was retested: pre-vibration, Tenney box, and modified vibration tests were performed on September 4, and a post-vibration test on September 5, 1968.

Following the correction of the interface incompatibility with the pitch control electronics discussed in the preceding subsection (Prototype), the conditioner was given a temperature test on December 23, 1968.

Thermal-vacuum and post-thermal-vacuum testing were successfully on March 28, 1969, and on April 30, 1969, telemetry signal conditioner Ser. No. 02 completed the box-level, special operational survival test requested by NASA.

On June 26, 1969, the signal conditioner A2 board (1975551) was modified to permit channel 55 of commutator 1 to handle telemetry inputs from strain gage 1 and channel 55 of commutator 2 to handle telemetry inputs from strain gage 2. A complete electrical check at ambient temperature was performed on June 27, 1969.

c. PROTOTYPE

Qualified by vendor.

18. Telemetry Commutators

The telemetry commutators are vendor-supplied and tested items. The flight models were delivered to RCA on July 17, 1968.

Commutators Ser. Nos. 2481 and 2480 were installed on the TIROS M spacecraft. The commutators were exposed to, and successfully completed, the following tests at the vendor's plant on the dates indicated.

	Date Completed (1968)	
Test	Ser. No. 2481	Ser. No. 2489
Pre-vibration	July 10	March 20
Vibration	July 11	March 22
Post-vibration	July 11	March 23
Thermal-vacuum	July 16	March 27
Post-thermal-vacuum	July 17	March 29

19. Real-Time Transmitter

a. PROTOTYPE

Since vibration and thermal-vacuum testing were performed on real-time transmitter Ser. No. 01P during the FOTOS program, qualification testing of this unit for the TIROS M spacecraft was confined to performance at ambient pressures, and temperatures of -55°, +25°, +10°, and -10°C. These tests were performed between May 2 to May 10, 1968.

b. FLIGHT MODEL

Real-time transmitters Ser. Nos. 03 and 05 were used aboard the TIROS M spacecraft. Qualification testing was performed as described below.

(1) REAL-TIME TRANSMITTER SER. NO. 03

Real-Time transmitter Ser. No. 03 completed pre-vibration acceptance testing on July 17, 1968. However, during vibration testing on July 18, the incidental FM exceeded the specified limits. Investigations revealed that transformer T1 on the first doubler board (A3) broke its bond and imposed

a variable load on the VCXO board. The transformer was rebonded and full retesting initiated. During cold temperature acceptance testing on August 5, 1968, the output power dropped below the minimum specified value. The transmitter was completely realigned and tuned and completed acceptance testing as shown in the following tabulation:

Test	Date Completed (1968)
Pre-vibration	August 14
Vibration	August 14
Post-vibration	August 23
Thermal-vacuum	August 28
Post-thermal-vacuum	August 28

Several JAN 1N944B diodes were overstressed during preconditioning, and it was suspected that one of these diodes was included in this transmitter. Therefore, this diode (CR1 on board 2 assembly, 1967593) was replaced and the unit was temperature tested and given a modified vibration test on April 17, 1969. In accordance with a NASA directive, the unit successfully completed the 168-hour operational test on May 16, 1969.

(2) REAL-TIME TRANSMITTER SER. NO. 05

During initial acceptance testing on September 20 to 24, 1968, two poorly soldered connections were detected. After repair, the unit underwent full flight acceptance tests as indicated in the following listing.

Test	Date Completed
Pre-vibration	October 1, 1968
Vibration	October 1, 1968
Post-vibration	October 15, 1968
Thermal-vacuum	October 18, 1968

An overstressed JAN 1N944-B diode (see description in preceding subsection) was replaced and the unit retested. Electrical testing at ambient and extreme temperatures, and thrust axis random vibration testing were performed on April 11, 1969. In accordance with a NASA directive, the unit completed 168-hour operational testing on April 27, 1969.

20. Real-Time Antenna Group

a. REAL-TIME ANTENNA

(1) ELECTRICAL TEST MODEL

During April 1967, a deployable real-time transmission antenna design was initiated, and testing on a scale model completed. Antenna pattern measurements were completed on the scale model in July 1967. In September 1967, stress analysis was completed with acceptable results pending completion of vibration tests. In addition, the first ETM dipole was fabricated, assembled, and used for electrical testing.

(2) PROTOTYPE

This unit was tested on the ETM and MTM spacecraft. Refer to Part 3, Sections II and IV, of this report.

(3) FLIGHT MODEL

The real-time antennas, Ser. Nos. 10 and 09, were subjected to and successfully passed acceptance testing on April 14, and April 16, 1969, respectively.

b. 148-MHz NOTCH FILTERS

TIROS M uses three 148-MHz notch filters: two in the real-time antenna group and one in the beacon and command antenna group. See Section 3.VI.B.13 for writeups on these filters.

c. ANTENNA HYBRID COUPLERS

Antenna hybrid couplers Ser. Nos. 50 and 71 were utilized aboard the TIROS M spacecraft. The couplers successfully completed the following tests on the dates indicated.

	Completion Date	
Test	Ser. No. 50	Ser. No. 71
Pre-vibration	January 23, 1968	July 2, 1968
Vibration	January 24, 1968	July 7, 1968

Results from the mux only and mux-demux testing are listed in tables 3-VI-10 and 3-VI-11, respectively.

21. Dual Multiplexer

a. ELECTRICAL TEST MODEL

For expository purposes, testing on the electrical test model dual multiplexer is separated into those tests involving the multiplexers (mux) alone and those tests performed in conjunction with the demultiplexer (demux) breadboard; these are referred to as mux-demux back-to-back tests.

The mux-only tests were confined to:

(1) DC power dissipation

(2) Turn-on transients

(3) Regulated bus overvoltage and transient survival

(4) Noise feedback into power subsystem

(5) Stability of output levels with temperature

(6) Amplitude response of individual channels

(7) AVCS video channel envelope delay

(8) Total harmonic distortion and output clipping level

(9) Crosstalk

Testing of the mux-demux back-to-back consisted of:

(1) Amplitude responses of individual channels

(2) Phase response

(3) Crosstalk - noise loading

(4) Crosstalk - discrete frequencies

All tests were performed on both redundant multiplexer sections and most tests were performed at ambient temperatures and pressures, and repeated at $-15^{o}C$ and $+60^{o}C$.

b. PROTOTYPE

The dual multiplexer Ser. No. 01P was received for testing on June 4, 1968. On June 10, during acceptance testing level adjustment, the center value of the adjustment range was found to be improper. New values for the output resistor networks were computed and new resistors were installed. In addition, these tests revealed an open P-C trace on board A16 which was repaired. Retesting was successfully performed on June 21, 1968.

During operational testing on July 1, both multiplexers exhibited low output readings at several frequencies resulting from pickup of power line noise. On July 24, after circuit modifications, the dual multiplexer successfully completed the operational test.

Operational testing of the multiplexer and demultiplexer as a single unit was successfully completed on August 9, 1968.

Thermal testing was completed on August 29, 1968.

Vibration testing was initiated on August 30, but during post-vibration testing on September 3, the output levels were out of specification at 250 kHz and 350 kHz and readjustment was performed. Level adjustment tests were rerun on September 4 and vibration testing repeated on September 5, 1968. After minor difficulty in achieving the proper vacuum conditions, thermal-vacuum testing was completed on September 13, 1968.

c. FLIGHT MODEL

Pre-vibration testing on dual multiplexer Ser. No. 02 was successfully completed October 4, 1968. The multiplexer successfully passed the following tests on the dates indicated.

Test	Date
Vibration	October 4, 1968
Post-vibration	October 6, 1968
Thermal-vacuum	October 8, 1968

The 168-hour special operational survival testing, as requested by NASA, was performed on April 22, 1969.

22. S-Band Transmitter

a. ELECTRICAL TEST MODEL

The S-band transmitter is a vendor item; testing at the breadboard level performed at the vendor's plant.

b. PROTOTYPE

Testing of the Ser. No. 001P prototype S-band transmitter was performed at the vendor's plant during the period April 5 to July 22, 1968. The following major tests were successfully completed:

- Performance tests at +25°, +60°, and -15°C
- Vibration
- Temperature cycle
- Acceleration
- Thermal-vacuum

c. FLIGHT MODEL

S-band transmitters Ser. Nos. 010 and 013 underwent flight acceptance tests as indicated below:

Test	Ser. No. 010	Ser. No. 013
Pre-vibration	January 2, 1969	January 3, 1969
Vibration	January 3, 1969	January 3, 1969
Post-vibration	Janaury 3, 1969	January 3, 1969
Thermal-vacuum	January 14, 1969	January 14, 1969
Post-thermal-vacuum	January 14, 1969	January 14, 1969

Special thermal-vacuum operational test were performed on both transmitters on March 20, 1969.

As a result of performance data collected during operation of the Nimbus project, the transmitters were removed from the TIROS M spacecraft and given a special thermal-vacuum operational test on June 25, 1969.

23. S-Band Antenna and Couplers

a. ELECTRICAL TEST MODEL

Two S-band antennas were developed for the TIROS M spacecraft. In the first design, the radiators consisted of a four-pole array configuration over a circular base with the two transmitters coupled to the antenna via a printed stripline hybrid. Transmitter 1 radiated a RHC polarization and transmitter 2 a LHC polarization due to the coupler itself. An in-depth system study indicated that this antenna would not be compatible with all NASA ground stations.

On the first antenna design, experimental testing was conducted in July 1967. During tests at large look angles in August, antenna gain was lower than predicted due primarily to the finite diameter of the ground plane. Addition of a "fence" on the ground plane substantially improved the gain. At this time the optimum fence configuration was under study. Continued testing in September resulted in the selection of a 14-inch diameter ground plane with a single 1-3/4-inch fence around the periphery. Breadboard coupler tests indicated satisfactory power splitter and isolation characteristics. Basic electrical tests were completed in October 1967, on a matched dipole array and matched coupler.

The second and final antenna configuration employs a single-port RHC polarized turnstile over a circular base. The radiator is fed by a printed stripline hybrid which couples both transmitters to the antenna. Radiation from either transmitter is RHC.

The redesign was initiated in January 1968, and in February, pattern and impedance measurements were begun on a test configuration containing a scaled version of an existing turnstile design. Range testing on a breadboard model was performed in March and stress and thermal analyses completed in April 1968.

An electrical test model of the new S-band antenna was completed in May, and pattern and impedance tests performed.

b. PROTOTYPE

Qualification testing on the S-band antenna and coupler Ser. No. 01P was performed as indicated below.

Test	Date (1968)
Pre-potting (coupler)	July 2
Post-potting temperature	August

Test	Date (1968)
Pattern tests	August 21, 22
Vibration	August 28
Post-vibration	September 9
Special critical pressure	October 9

c. FLIGHT MODEL

S-band antenna and antenna coupler Ser. No. 03 successfully completed the following operational tests on the dates indicated: pre-vibration testing on September 17, vibration testing on September 18, and post-vibration testing on September 24, 1968.

24. Digital Solar Aspect Sensor (DSAS) and Electronics

a. PROTOTYPE

Qualification testing on digital solar aspect sensor (DSAS) Ser. No. 01P was performed as delineated below.

Test	Date (1968)
Radiated EMI	March 19
Conductive EMI	March 28
Vibration	March 29
Post-vibration	March 30
Acceleration	April 1
Abbreviated electrical test	April 2
Thermal-vacuum	April 4 through 7*

*During thermal-vacuum testing the output of bit No. 1 was not constant. This originated from a burned edge on this cell which had chipped during the testing process. Testing continued after corrective action.

b. FLIGHT MODEL

Qualification testing on the DSAS and DSAS electronics Ser. No. 02 was performed as tabulated below.

Test	Sensor	Date (1968) Electronics
Initial electrical	May 13	May 10
Vibration	May 14	May 14
Post-vibration	May 15	May 15
Thermal-vacuum	May 17	May 17
Post-thermal-vacuum	May 17	May 17
Subsystem*	May 20	May 20

25. Nutation Dampers

Nutation dampers Ser. Nos. 24 and 25 were both subjected to leak tests on December 4, 1968. Operational testing was performed on January 7 and 10, 1969, for Ser. Nos. 25 and 24, respectively.

26. Attitude Control Coil Unit

The attitude control coil unit serial No. 005 was subjected to and successfully completed the pre-vibration operational test on February 23, 1968. The unit was ordered delivered to spacecraft integration on that date.

27. Magnetic Bias Coil (MBC) Switch

a. PROTOTYPE

Testing of the prototype magnetic bias coil switch Ser. No. 02P was accomplished as shown below.

Test	Date (1968)
Completed assembly	May 6
Bench vibration	May 8 through 10

*Subsystem testing with sensor and electronics as one unit.

Test	Date (1968)
Vibration	May 10
Temperature	May 10 through 17

b. FLIGHT MODEL

Magnetic bias coil switch Ser. No. 01 successfully passed the pre-vibration operational test on June 3, and the vibration and post-vibration tests on June 4, 1968.

28. Dual Momentum Coil

Component testing on the dual momentum coil Ser. No. 004 was confined to an operational test on February 23, 1968.

29. Pitch Control Electronics

a. ELECTRICAL TEST MODEL

By April 1967, electrical tests of the breadboard pitch control electronics at ambient temperature were successfully completed. In April and May of 1967, thermal testing on this unit at temperatures between -15° to +60° C were performed in the Tenney box.

b. PROTOTYPE

Testing on the pitch control electronics Ser. No. 01P was performed as described below.

Test	Date (1968)
Post-potting Box	August 9
Vibration	August 12
Post-vibration	August 13

During the 280° K IR equivalent sky-to-earth test on August 13, a spurious threshold pulse was observed. Investigations revealed the need for a change in the time constant of the input circuitry. The circuitry was corrected by increasing the coupling time constant between sensor preamplifier and threshold amplifier, and the 280° K IR equivalent testing repeated.

On August 19, while in thermal-vacuum test, a DC/DC converter failed to operate. It was determined that this converter was one that had not been retrofitted with the new 12E109 transistor which had caused malfunctions on other subassemblies (see Paragraph 3VIB3, Dual Time Base Unit). The converters were replaced by two which had the new transistors and the thermal-vacuum testing was repeated. Qualification testing was completed on August 26, 1968.

While performing a go/no-go test with the spacecraft on August 30, the motor speed of loop 1 became unstable. The trouble was traced to a leaky capacitor (Q1 on board A7, 1975756-501) in the prototype unit. The capacitor was replaced and testing resumed.

During dynamic suspension testing of the pitch control electronics prototype unit with the spacecraft on October 31, 1968, post-analysis of the capture sequencing indicated that 3 of the 18 capture runs showed an unexplained reversal in motor acceleration. It was found that a situation can occur where an HCI pulse can be blanked out. The problem was corrected by using redundant deblanking pulses in the coarse mode.

c. FLIGHT MODEL

Qualification testing on pitch control electronics Ser. No. 04 was accomplished as described below.

Pre-vibration testing was accomplished on February 4, 1969, and vibration and post-vibration testing on February 6, 1969.

Following spacecraft dynamic suspension tests in March, it was found necessary to modify the clamp circuits on PCE board A6 to increase its operating speed. An operational electrical check, a flight level vibration test, and full electrical tests (post-vibration) were completed on May 7, 1969. Thermal-vacuum and post-thermal-vacuum tests were completed on May 10. In accordance with a NASA directive, PCE Ser. No. 04 was subjected to a special 120-hour per side operational test at box level on May 26, 1969.

On June 13, 1969, during spacecraft level testing, pitch loop 1 failed to enter dual motor mode of operation when commanded. Telemetry indicated that the dual motor mode was enabled but not on. It was found that a resistor was too large resulting in marginal bias conditions which, under certain conditions, prevented the CDU enable command from being executed. Resistors R28 and R68 on board A7 were replaced. Operational testing was repeated on June 20, 1969.

30. Momentum Wheel Assembly

a. ELECTRICAL TEST MODEL

RFI testing on the momentum wheel assembly (MWA) DC torque motor was completed in April, 1967. Six flight quality motors were received in June and were inspected and tested using a dynamometer specifically constructed for checking TIROS M motors. In June 1967, two motors, one four-point contact bearing with bronze retainer, and dioctyl adipate lubricant stored in a Nylasint ring were tested in a magnesium housing at a pressure below 10^{-5} torr. Motor housing temperature varied from room conditions to prototype minimum (-15°C). Decreasing housing temperatures resulted in increases in motor current; probably caused by less lubricity at the lower temperatures. Even at the extreme prototype ambient temperature of -15°C, the assembly ran satisfactorily, and at various temperatures, speed step commands resulted in satisfactory and consistent responses. When motor power was restored after an intentional motor stoppage of 1 hour at an ambient temperature of -15° C and a bell-jar pressure of 1.7×10^{-6} torr, the unit accelerated normally to 150 rpm within about 1 minute.

The same setup as previously tested, except using only one motor unit, was subjected to the thermal-vacuum environment after lubricating surface films were removed from the bearing and the commutator by repeated washing with filtered Freon. After about 2 hours of pumpdown (5×10^{-5} torr), application of power resulted in normal acceleration to the 150 rpm design speed, although motor current was higher and more erratic than usual. Five hours after pumpdown, motor current dropped rapidly and leveled out at about 120 mA, which is reasonable for a single-motor configuration at room temperature. Apparently, the vapor lubrication provided by the Nylasint oil reservoir was at this time able to establish an adequate film on the originally dry commutator and bearing race surfaces, thus demonstrating the effectiveness of the lubrication process. A chemical analysis of the bearing races at the conclusion of the test indicated traces of dioctyl adipate oil. Bearing races and balls were pitted, no doubt from originally running completely dry.

Vibration testing of the MWA (without IR horizon sensors) was performed during July 1967. The test results indicated that the IR horizon sensors would be exposed to an acceleration of more than 100 G's when the vibration frequency of the assembly passed through a resonant point. Although the sensors had successfully withstood accelerations as high at 100 G's on other pgorams, the sensor mounting flange was modified to reduce the input acceleration. The sensor mounting flange was modified to reduce the input acceleration. The bearings and motors successfully passed this preliminary vibration testing.

Additional vibration testing was performed in August 1967, to ascertain the effectiveness of damping materials bonded to the mounting plate and installed

between the horizon sensor assembly (tee plate) mount and the main housing. Test results showed that a titanium sheet bonded to the existing mounting plate by a viscous urethane material (with aluminum screening imbedded in the viscous material) and a tee plate end cap washer of a fiberglass mesh imbedded in urethane, reduced the axial accelerations of the horizon sensor assembly from about 120 G's to 80 G's with qualification inputs of 10-G sinusoids.

b. PROTOTYPE

The testing associated with the Ser. No. 02P momentum wheel assembly was performed as described below.

Initial assembly and testing was accomplished during the period April 15 through May 6, 1968. Vibration testing of Ser. No. 01P MWA revealed a failure involving the separation of the roll mirror from the mirror support, the breaking of two encoder wires at their terminals, and the cracking of a flywheel spoke. Corrective action, which applied to both prototypes, included larger mounting screws in the mirror assembly, additional shear pins, thread inserts in the support piece, and the encapsulation of encoder wire terminations.

After this rework, Ser. No. 02P was reassembled and retested during the period May 16 through July 2, 1968.

The following tests were performed as indicated below:

Test	Date (1968)
Final electrical (bench)	July 3
Vibration	July 3
Post-vibration	July 9*
Acceleration	July 11
Post-acceleration	July 12
Thermal-vacuum	August 26
Post-thermal-vacuum	August 28

*Roll scan mirror cracked during vibration. Investigation revealed that supplier used too high a temperature for heat treatment after nickel plating, with resultant degradation in hardness of substrate. The Test Review Board decided to perform thermal-vacuum testing before disassembling Ser. No. 02P for failure analysis.

Following reassembly after the failure analysis, the MWA underwent an abbreviated bench check and performance test on May 13, 1969, and optical alignment on May 15, 1969.

Following prototype vibration on May 17, visual inspection revealed loose mounting screws and a black powdery residue on the MWA mounting flange. The primary purpose of the test was to confirm the adequacy of a thermal fix in which the thermal washers were increased from 1/8 to 1/2 inch. This purpose was accomplished. However, a correction to the test procedure was prepared specifying the use of new locking ring hardware prior to vibration, and the inspection and control of the depth of the locking ring with respect to the flange (the cause of the black residue).

Post-vibration testing was completed on May 20, 1969, and thermal-vacuum testing completed about June 19, 1969.

A test procedure covering a 6-month life test was prepared, and the MWA underwent an extensive thermal-vacuum test program according to this procedure. The life test was completed in October 1969.

c. FLIGHT MODEL

Qualification testing of the momentum wheel assembly (MWA) Ser. No. 06 was performed as discussed below.

The MWA successfully completed its initial electrical operational test on June 18, 1969. During a pre-thermal-vacuum subsystem test on July 11, 60-Hz pickup was detected and its origin narrowed down to the T-plate being used. Another T-plate was substituted, thermal-vacuum testing was completed on July 20, and post-thermal-vacuum testing was completed on July 21, 1969.

Pre-vibration testing was completed on July 31, and vibration and post-vibration testing on August 1, 1969. Alignment tests were performed on September 3, 1969.

31. Strain Gage Amplifier

a. ELECTRICAL TEST MODEL

Preliminary testing was performed on the strain gage/power supply assembly shown in block diagram form in Figure 3-VI-18. The results of circuit analysis and performance testing are summarized in Table 3-VI-10.

Tests were completed on May 5, 1969.

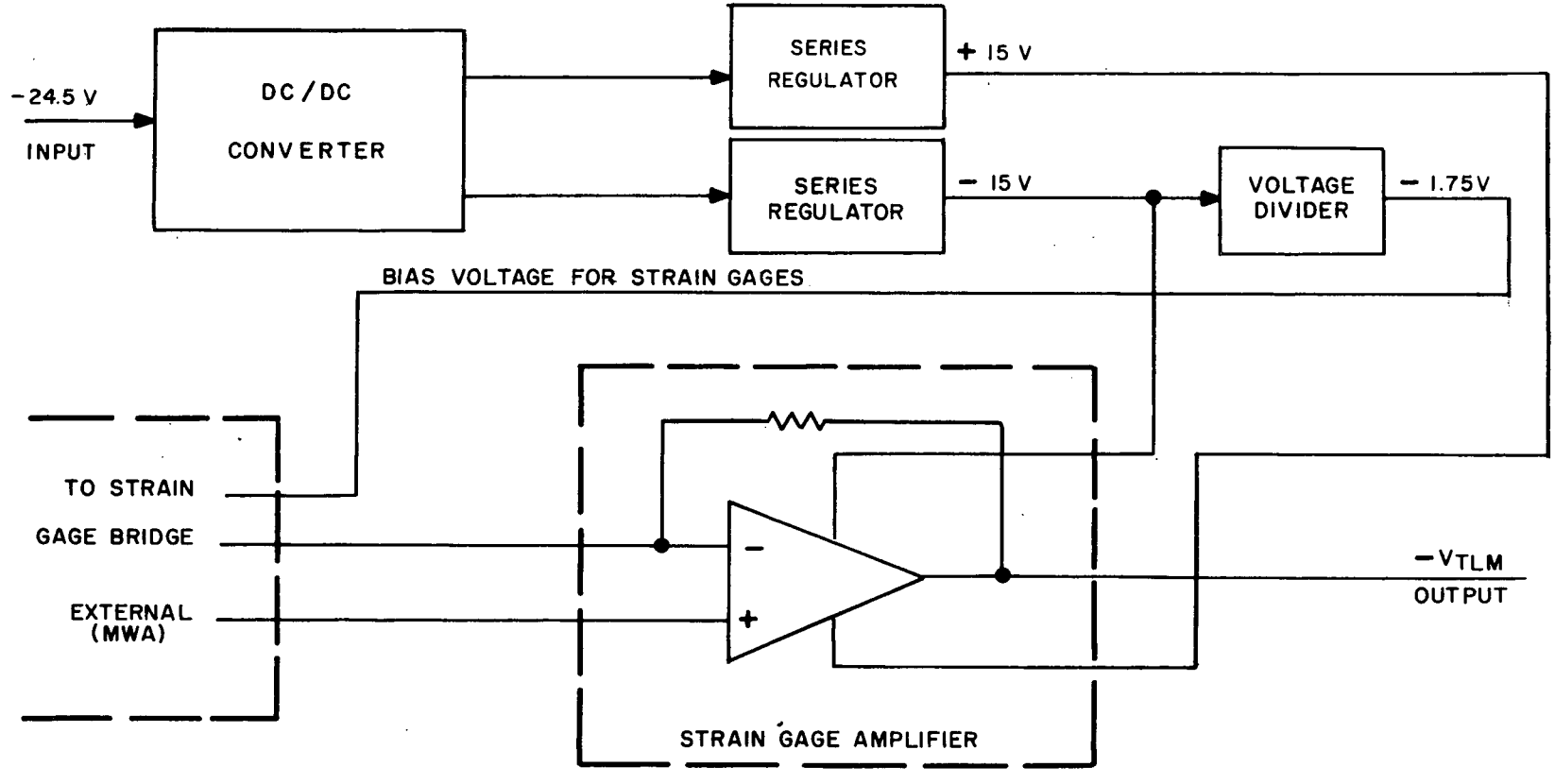

Figure 3-VI-18. Strain Gage Amplifier and Power Supply, Functional Block Diagram

TABLE 3-VI-10. SUMMARY OF INITIAL PERFORMANCE TESTING (ETM) ON STRAIN GAGE AMPLIFIER CIRCUITRY

Parameter	Specification	EOL WC* Prediction	BOL WC** Prediction	Conditions of Test	Test Results
Telemetry Accuracy	± 2 mils (15° to 35°C)	± 1.25 mils	± 0.5 mils	+15° to +35°C	+ 0.22 / - 0.44 mils
	(-10° to +60°C)	± 2 mils	± 1.25 mils	-15° to +65°C	+ 0.105 / - 0.000 mils
Average Input Current	80 mA	70 mA		+15° to +35°C	47.4 mA to 50.7 mA
Ripple Current	5 mA (p-p)	1.5 mA		+25°C	< 0.2 mA
Inrush Current	4 Amps	4 Amps		+35°C	1.87 Amps.
Current Rate of Change	50 mA/μs	50 mA/μs		+35°C	7.6 mA/μs
Turn-on Time	2 seconds			+25°C	2 s to 99.8 percent of final value
+15V Regulator		± 0.6 percent		+15° to +35°C	0 percent
-15V Regulator		± 0.6 percent		+15° to +35°C	+ 0.1 percent / - 0
-1.75V Supply	2.0 percent (15° to 35°C)	± 0.85 percent	± 0.3 percent	+15° to 35°C	+ 0.2 percent / - 0.0

*EOL WC - End-of-Life, Worst Case
**BOL WC - Beginning-of-Life, Worst Case

b. PROTOTYPE

Component selection, testing and calibration of the prototype strain gage amplifier Ser. No. 01P was completed on September 1969.

c. FLIGHT MODEL

Qualification testing on strain gage amplifier Ser. No. 02 was performed as described below.

On August 21, 1969, initial electrical performance, vibration, and post-vibration testing was performed. During thermal-vacuum testing on August 22, difficulty was encountered in starting the unit at a temperature of -10°C. However, testing was permitted to continue until completion. After thermal-vacuum testing, the unit was placed in the Tenney box to investigate the anomaly under stabilized temperatures. The unit would always start at 0°C, but would start intermittently at -5°C. The starting problem is a function of transformer characteristics and matched gain in a set of transistors. After review, a test review board authorized delivery and use of strain gage amplifier Ser. No. 02 on the TIROS M spacecraft without modification. Design modifications were made to enhance starting of other units.

The strain gage amplifier spacecraft installation and subsequent alignment test was performed on August 27, 1969. A test of the strain gage telemetry polarity showed reverse readings. A wiring change was made in the momentum wheel assembly harness to reverse the polarity of the strain gage to the amplifier unit. This permitted negative telemetry readings with increasing brush wear.

32. Solar Array Panels

a. PROTOTYPE

Qualification testing of the prototype solar array panels, Ser. No. 01P, was performed according to the following schedule.

Test	Date (1968)
Initial illumination and electrical test	March 4
Vibration testing while affixed to MTM spacecraft	March 12 through 15
Post-vibration illumination and electrical test	March 21 through 22
Pre-thermal-vacuum electrical test	April 2 through 4

Test	Date (1968) Cont.
Thermal-vacuum test	April 5 through 6
Post-thermal-vacuum illumination and electrical test	April 8 through 9
Thermal cycling test	April 16 through 26
Post-thermal cycle illumination and electrical tests*	April 30 through May 1
Pre-thermal-vacuum (retest)	August 29
Thermal-vacuum (retest)	September 2
Post-thermal-vacuum electrical test (retest)	September 3
Thermal-vacuum retest	June 4 through 7, 1969
Electrical retest	August 22 through September 2, 1969
Thermal-vacuum retest	September 5, 1969

(1) INITIAL ILLUMINATION TEST

The prototype panel was secured in a special illumination fixture and placed under the illuminator installation. Using a specially calibrated standard cell, the panel height and illumination intensity were adjusted to the standard illumination level of 139.6 mW/sq cm at the panel center.

Due to the size of the panel, only one-half of the panel was tested at a time. The two halves were designated "inboard" and "outboard", the inboard section being nearest the hinge brackets.

The curvature of the solar array panel prevented the illumination of all five circuit sections (A, B, C, D, and E) at the same intensity. Therefore, a procedure was adopted to compensate for the results of the power readings from each individual circuit section.

The standard cell was placed on the inboard section of the panel in each of five positions on circuit C, the center circuit, with the output current (Iscm) being

*Several cells were cracked during installation of accelerometers prior to vibration testing.

measured at each point. An average figure was obtained which was equal to the calibrated output of the standard cell (Isco). This procedure was repeated on each remaining circuit, A, B, D, and E. By comparing results of these average readings it was found that circuits A and E gave readings 10 percent below circuit C, and circuits B and D gave readings 2 percent below circuit C. To compensate for the variation in light intensity due to panel curvature, when a reading was made of circuits A or E, a compensation factor of 10 percent was added. On circuits B and D, 2 percent was added. Temperature was controlled to 35° C by adjusting air flow during this test.

When illumination testing on these five circuit sections was completed, the panel in its holding fixture was moved to bring the outboard section under the illumination area. Circuit C was scanned with the standard cell, and the average readings (Iscm) of the five positions were equal to the standard cell value (Isco). The procedure for obtaining the compensation factor was repeated and found to be applicable to the outboard panel section.

Open-circuit voltage (V_{oc}), short-circuit current (I_{sc}), load current (I_l) at a specified voltage, and current/voltage (IV) curves were obtained for each half circuit. Circuit D inboard showed a dip in the IV characteristics though the current was within specification limits for the load current. The cell which was bad was identified, and a judgment was made to keep the cell on the panel so that the effects of the qualification environment could be determined on a known defective cell.

(2) ELECTRICAL COMPONENT TESTS

After completion of the illumination measurements, the shunt dissipator amplifier gain and amplifier leakage, isolation diode forward voltage drop and diode reverse leakage, isolation of circuits from the substrate, thermistor resistance, and current telemetry sensor resistances were measured with a special test using auxiliary power supplies and meters. In addition, the VSWR of the two antenna cables connected to the solar panel were measured with a time-domain reflectometer.

The tests revealed wrong values of current sensor resistors installed on the solar panel. The correct resistors were installed and the test series resumed.

(3) VIBRATION

Vibration testing was performed at the RCA - AED Environmental Test Facility with the solar array panel mounted on the mechanical test model (MTM) spacecraft.

The purposes of the tests were to:

- Evaluate the structural integrity of the solar array panel, including the real-time antenna and RF cable mounted to the panel,
- Measure dynamic response functions at a number of selected locations, and
- Test specific structural components not qualified during the MTM qualification testing (e.g., prototype nutation damper and two "live" solar panel deployment pin pullers).

Test results were considered normal and no evidence of solar array panel structural failure was evident during the prototype sine and random vibration exposure in three axes.

A part of the vibration testing program on the solar array panels was the testing of the spacecraft separation switches. Each switch was wired with the normally open switch contacts in series with a power supply and resistor. Across each resistor was an Ograph strip chart recorder channel to monitor the switch contacts continuously. When the spacecraft was mated to the adapter ring the switch plungers operated, closing the power circuits. No discontinuity was noted in either switch for the entire series of vibration tests.

Following vibration, each normally closed contact was subjected to a short high-current pulse by blowing a 2-ampere fuse through each pair of contacts. All contacts performed correctly under load. No electrical tests were performed on the solar array panel during vibration.

(4) POST-VIBRATION ILLUMINATION AND ELECTRICAL TEST

To check possible deterioration in performance, the panel was again subjected to illumination and electrical component measurements.

Prior to vibration, physical damage was caused to solar cells in outboard circuits C and E during installation of accelerometers. This showed up as an irregular trace on the I/V curves; all other circuits remained unchanged. The electrical parameters were also tested, with results indicating no damage.

(5) PRE-THERMAL-VACUUM TEST

The solar array panel was fitted with a series of thermocouples, and mounted in the "Clam shell" thermal-vacuum chamber (see Figure 3-VI-19). The thermocouples were connected to recorders and the solar array panel output leads connected to the solar array panel test set via the chamber feedthroughs. A short operational test of the panel components was made, the chamber closed, and then pumped down to a pressure of 1×10^{-4} torr.

(6) THERMAL-VACUUM TESTING

The first test under vacuum consisted of passing maximum current through the first shunt dissipator circuit after temperatures of the panel rib were stabilized at +42 degrees with power off. Local heat rise was allowed to stabilize and temperatures were measured. The two other shunt dissipators were similarly tested. Current was then altered to half current (rib quarter power) and after stabilization, the temperatures were again measured. This test provided check of panel operation in continuous sun-simulated conditions.

The second test in vacuum consisted of stabilizing the panel at -8°C and dropping the temperature to -88°C for four thermal cycles. This test checked panel operation in a simulated orbit with a long eclipse or night. Test results were compared to computer predicted results of the test condition because the test conditions cannot simulate orbital conditions close enough (due to test chamber limitations) to compare test results directly to orbital predictions.

The third test was a repeat of the test sequence in the first test to verify that cold temperature cycles did not disturb continuous sun conditions.

(7) POST-THERMAL-VACUUM TEST

Sun side thermocouples were removed and an illumination and electrical parameter test was performed, using the same procedure as previously described. All results corresponded closely to those previously obtained.

(8) THERMAL CYCLING TEST

The sun side thermocouples were replaced on the panel, and the panel placed in the AED Environmental LEM-Bethlehem thermal chamber test

facility. Abbreviated operational test were made followed by a simulated continuous sun temperature rise test (as performed in the thermal-vacuum test) to determine if three shunt dissipators could be correctly tested in a one atmosphere gas environment.

The panel was thermally cycled fifty times between +52°C and -98°C using forced convection gaseous nitrogen. No tests were made on the panels during cycling, but power was applied to the shunt dissipators to keep them above -65°C when required.

At the conclusion of the fifty thermal cycles, the three shunt dissipators were again tested for temperature rise in a simulated continuous sun temperature environment. Post-test analysis indicated that vacuum conditions are required during the simulated continuous sun temperature rise test to properly test and check assembly of the three shunt dissipators.

(9) POST-THERMAL CYCLING ILLUMINATION AND ELECTRICAL PARAMETERS

The panel was removed from the thermal test chamber and all thermocouples removed. A final illumination test was made to previous procedures, and comparable results were obtained. Electrical parameters of all circuit components were also measured and were normal.

(10) ANTENNA CABLE TESTS (THERMAL CYCLING)

During thermal cycling of the prototype solar array panel, checks were made of the antenna cables. Over one temperature cycle each 24 hours, the cable temperatures and VSWR were measured at quarter-hour intervals. Each cable was fitted with four thermocouples to measure the temperature variation while the panel experienced a range of +52° to -98°C. The cable temperatures closely followed the panel temperatures, and the VSWR varied less than 15 percent over the total panel temperature range.

(11) THERMAL-VACUUM RETEST

A full thermal-vacuum test with heat rise checks and ten thermal cycles was ordered by a test review board to qualify drawing changes made to ensure better transistor heat sinking and to prevent local oscillations in the shunt limiter legs. The design changes brought the solar panels within the required design limits during the test. One circuit showed electrical leakage in a transistor.

(12) ELECTRICAL RETEST

An electrical test was performed after replacement of the suspected bad transistor. The circuit again indicated that it was leaky. All other parameters were normal.

(13) THERMAL-VACUUM RETEST

After replacement of the same transistor for a second time, a thermal-vacuum retest was performed successfully. During this test sequence, it was discovered that one of the two solar panel test sets was intermittently faulty and had caused an erroneous transistor leakage indication.

(14) PROTOTYPE TEST RESULTS

The prototype panel was considered to have successfully completed the qualification test.

b. FLIGHT MODEL

The three flight model solar array panels, Ser. Nos. 002, 003, and 005, used aboard the TIROS M spacecraft, underwent flight acceptance qualification testing as delineated below.

(1) SOLAR ARRAY PANEL SER. NO. 002

During flight acceptance testing on September 10, 1968, voltage at the shunt dissipator monitor point (Q3 and Q4, rib 2) was found to be too low. A minor wiring correction was made and initial electrical performance testing was completed on the same data. The panel then completed thermal-vacuum testing on September 19, and post-thermal-vacuum testing on September 25, 1968.

After incorporation of the design changes required to prevent local oscillations in the shunt dissipators, illumination retesting was completed on January 14, 1969; thermal-vacuum retesting was completed on January 18, and a post-thermal-vacuum illumination test was completed on January 25, 1969.

A retrofit was required involving a redesigned power transistor heat sink (see solar array panel Ser. No. 005, this subsection). After completing this retrofit on solar array panel Ser. No. 002, the following tests were performed.

Test	Date (1969)
Electrical performance and Illumination	June 4
Thermal-vacuum	June 6
Electrical performance and Illumination	June 10

During spacecraft level testing on July 11, 1969, solar array panel current telemetry indicated voltages less than -0.5 volt when the panel was illuminated. A hardwire was discovered which was shorting out the sampling resistors. The wire was removed and the solar array panel retested at spacecraft level. Because these resistors have very low values and are not specifically tested, this anomaly was not detected at the black-box level. While still mounted on the spacecraft, the solar array panel was subjected to a vibration test during July 15 through 17, 1969. Panel deployment tests were conducted on July 14 and 18, 1969. Vibration and deployment tests were completed satisfactorily.

At NASA's request, full flight acceptance testing was repeated to ensure that adequate testing time had been logged. Accordingly, the following tests were performed:

Test	Date (1969)
Electrical performance and Illumination	July 28
Thermal-vacuum	August 15
Electrical Performance and Illumination	August 18

(2) SOLAR ARRAY PANEL SER. NO. 003

On July 25, 1968, during initial electrical performance testing on solar array panel Ser. No. 003, it was found that transistor Q2 collector was not fully isolated from the substrate. Investigations revealed that the Q2 mounting plate, which is isolated from the array structure flange by a mica washer, was slightly oversize and allowed contact with the flange. The Q2 plate size was reduced. Electrical performance testing was repeated on September 19, 1968.

During the thermal-vacuum test on September 19, a resistance check revealed an open circuit on the thermistor used to monitor the temperature of the power transistor radiator (heat sink) during electrical operation. This condition was corrected and thermal-vacuum retesting was performed on September 21, 1968 with satisfactory results.

During spacecraft level testing on October 17, 1968, undesirable oscillations appeared on the solar array bus and across the shunt dissipator resistors on the outer rib of the anti-earth panel. Subsequent investigations carried out on the ETM spacecraft isolated the oscillations to the power "switch" elements of the shunt limiter circuitry, and disclosed that the particular oscillator condition could be remedied by adding a capacitor directly across the base-emitter junction of the first stage of each of the nine legs of the power switch. To further ensure against unwanted oscillations, the shields of the switch drive signals from the PSE to each leg of the dissipator were disconnected in the wire harness. In addition, the PSE isolation resistance in the drive lines was divided so that approximately half is located at the base input of the nine legs of the array panel power switches.

On January 8, 1969, prior to repeating the thermal-vacuum testing, three solar cells were accidently cracked while turning the panel. The three cells were replaced and testing continued. During subsystem testing of the panel on January 28, it was discovered that one of the cells (J20) had lifted on the positive side. This cell was removed and replaced. Thermal-vacuum testing was continued, but on February 4, it was found that the RTV layer between the mica washer and the rib was not uniform, causing poor thermal conduction. As a result, the transistor washer configuration was changed to improve the conductive heat path. The maximum shunt power dissipation portion of the thermal-vacuum test was repeated and completed on February 24, 1969. Post-thermal-vacuum illumination tests were completed on February 25, 1969.

A retrofit was made, relative to a redesigned power tansistor heat sink (see solar array panel Ser. No. 005, this section). Following this retrofit, the following testing program was completed:

Test	Date (1969)
Pre-cycling heat dissipation	June 9
Flight level thermal-vacuum	June 10
Post-thermal-vacuum	June 12
Illumination	June 13

While still mounted on the spacecraft, the solar array panel was subjected to a vibration test during July 15 through 17, 1969. Panel deployment tests were conducted on July 14 and 18, 1969. Vibration and deployment tests were completed satisfactorily.

At NASA's request, flight acceptance testing was repeated to ensure that adequate testing time had been logged. Therefore, the following tests were performed:

Test	Date (1969)
Electrical performance and Illumination	August 12
Thermal-vacuum	August 14
Electrical performance and Illumination	August 15

(3) SOLAR ARRAY PANEL SER. NO. 005

Initial electrical performance testing on solar array panel Ser. No. 005 was accomplished on November 25, 1968. Abbreviated electrical testing was completed and thermal-vacuum testing initiated on January 18, 1969, and post-thermal-vacuum testing performed on January 30, 1969. Thermal-vacuum retest of the shunt dissipators was specified after design changes to prevent oscillation. This test was completed satisfactorily. On May 1, 1969, during heat dissipation testing, thermocouple No. 3 on the stud of transistor Q2 (rib 1) register temperatures above the specified limit. A redesign was necessary to provide better heat sink arrangements on the solar array panel power transistors; this redesign affected the solar panel, solar panel substrate, radiator, bushing insulator, insulator, plate mounting, and the solar panel cell assembly of all flight and prototype models. After implementation of these changes, the panels underwent the following tests:

Test	Date (1969)
Pre-cycling heat dissipation tests	June 9
Flight level thermal-vacuum cycle testing	June 10
Post-cycling heat dissipation test	June 12
Illumination test	June 13

Post-test analysis of illumination data revealed three bad cells. Microscopic examination attributed the defects to the effects of peeling off the positive portion of the cell contact material. The cells were replaced and illumination testing repeated.

While still mounted on the spacecraft, the solar array panel was subjected to a vibration test during July 15 through 17, 1969. Panel deployment tests were conducted on July 14 and 18, 1969. Vibration and deployment tests were completed satisfactorily.

As requested by NASA, flight acceptance testing was repeated to ensure that adequate testing time had been logged. Accordingly, the following tests were performed:

Test	Date (1969)
Electrical performance and Illumination	August 12
Thermal-vacuum	August 13
Electrical performance and Illumination	August 15

33. Solar Array Panel Actuators

Solar array panel actuators are vendor items tested at the vendor's facility. The solar array panel actuators Ser. Nos. 103G, 104G and 105G underwent the following tests:

- Loaded and unloaded actuator time
- Static forces
- Dynamic forces
- Compression - loading and retraction
- High temperature timing
- Low temperature timing

The units were accepted by RCA on December 27, 1967.

34. Battery Pack Assembly

a. ELECTRICAL TEST MODEL

Testing on the batteries at this level was confined to overcharge and life cycling tests on 40 vendor-supplied nickel cadmium cells. (A full report on the battery capacity test is included in Appendix B.)

The objective of the life cycling tests was to confirm that a 23-cell, 4-ampere-hour nickel cadmium storage battery would maintain a minimum voltage of 26.5 volts when subjected to cycling requirements as detailed in the battery performance specifications, PS 1975160. In addition, information was desired on the cell charging characteristics as a function of time, with an aim toward improving the data used in the computer analysis of the power subsystem.

The storage cells are identified by serial number and date of manufacture in Table 3-VI-11. The cells were subjected to a reconditioning cycle and the RCA acceptance tests. An overcharge test was performed to verify the maximum overcharge currents specified in Revision A of the battery performance specification prior to the start of the cycling program.

The cycling program is summarized in Table 3-VI-12. Each month of testing consisted of 381 electrical cycles at the cell temperature indicated. These temperatures are 5° above the base plate temperatures originally predicted by the spacecraft thermal analysis.

The test results are presented in Figures 3-VI-20, 3-VI-21, and 3-VI-22. Figure 3-VI-20 is an overall summary of the test data with the various parameters shown as a function of cycle number. Between cycles 500 and 600 there were several instances when the temperatures exceeded 34° C by as much as 6° C due to equipment malfunctions. The equipment was repaired and the subsequent temperature control was restored to maintain ±2°C. Although these temperature variations did affect the end-of-discharge voltages for the specific cycles where they occurred, it was judged that they had no significant permanent effect.

At the beginning of month 6, the discharge current was inadvertently allowed to remain at the value used during month 5 and the depth of discharge was at 19.5 percent instead of 18.9 percent. This additional discharge can be seen reflected in lower average end-of-discharge cell voltage in this figure and the Figure 3-VI-21 for cycles 1905 to 1973. The correction of the discharge current produced higher average end-of-discharge cell voltages and it appears that there was no significant effect on the program.

The end-of-charge current is a measured variable, and it can be observed that the current for the old cells is less than for the new cells. During the first month, the end-of-charge current was increasing, but during the second month this trend reversed. This current is not only affected by cell aging, but also by temperature changes.

At orbit number 2387 there was a malfunction of the Talley timing equipment. The discharge continued beyond the scheduled time and the cells discharged about 30 percent of their rated capacity. The lowest cell reading when this discharge was manually terminated was 1.08 volts. After repair of the equipment the cells were recharged for 234 minutes in place of the noraml 82 minutes, and the test resumed the normal schedule.

The extended discharge and extended recharge appear to have had a radical effect on the end-of-discharge voltages for the subsequent cycles as plotted on Figures 3-VI-20 and 3-VI-21. The end-of-discharge voltages reverted back to levels seen during month 2 of the test program, but it can also be observed that the voltages decreased more rapidly than they did during month 2.

TABLE 3-VI-11. IDENTIFICATION OF BATTERY STORAGE CELLS

Cell Position	"New" Cells		Date (yr/wk)	"Old" Cells		Date (yr/wk)
	Channel	Ser. No.		Channel	Ser. No.	
1	1	1-33	6706	29	5-10	6506
2	2	1-44	6706	30	5-20	6506
3	3	2-7	6706	31	5-28	6506
4	4	2-11	6706	32	5-45	6506
5	5	2-32	6706	33	5-128	6511
6	6	3-16	6706	34	7-53	6521
7	7	3-33	6720	35	9-22	6525
8	8	3-35	6720	36	9-25	6525
9	9	3-36	6720	37	14-17	6533
10	10	4-21	6720	38	14-19	6533
11	11	4-25	6720	39	25-8	6615
12	12	4-28	6720	40	25-9	6615
13	13	5-1	6720	41	25-12	6615
14	14	5-25	6720	42	25-14	6615
15	15	6-2	6720	43	25-17	6615
16	16	6-3	6720	44	25-19	6615
17	17	6-4	6720	45	25-22	6615
18	18	6-5	6720	46	25-23	6615
19	19	6-7	6720	47	25-26	6615
20	20	6-9	6720	48	25-28	6615

TABLE 3-VI-12. BATTERY CYCLING SCHEDULE

Cycle No.	Temp. (°C)	Discharge		Charge		Voltage Limit
		Time (min)	Rate (A)	Time (min)	Rate (A)	
1-381	35	22	1.64	91.5	0.95	27.50
382-762	34	23.5	1.56	90.0	0.95	27.96
763-1143	33	24.5	1.52	89.0	0.95	28.04
1144-1524	32	26.2	1.51	87.3	0.95	28.12
1525-1905	28	29.0	1.51	84.5	0.95	28.46
1906-2286	25	31.0	1.46	82.5	0.95	28.64
2287-2667	25	31.0	1.46	82.5	0.95	28.64

As a result of this test interruption, the average end-of-discharge cell voltages were higher at the end of month 7 than at the end of month 6: 1.212 volts for the new cells and 1.208 volts for the old cells. The minimum requirement for the TIROS M mission with a 22-cell battery is 1.205 volts, and with a 23-cell battery 1.152 volts. The range of end-of-discharge cell voltages for the new cells after 7 months was 1.184 to 1.231 and the range for the old cells was 1.145 to 1.222.

The data shown on Figure 3-VI-21 is identical to the bottom graph on Figure 3-VI-20 except that the voltage is based on either a 22-cell battery or a 23-cell battery. A curve is also shown to represent the original engineering estimate for the 6-month mission. A 23-cell battery was chosen for TIROS M.

The percent recharge, which was calculated for each of the sample cycles at both the lower voltage limit and the upper voltage limit, is shown in Figure 3-VI-22 as a function of the cycle number. In addition to the total recharge, the percent recharge of the cells was also calculated for the time period before the cells reached the imposed voltage limit.

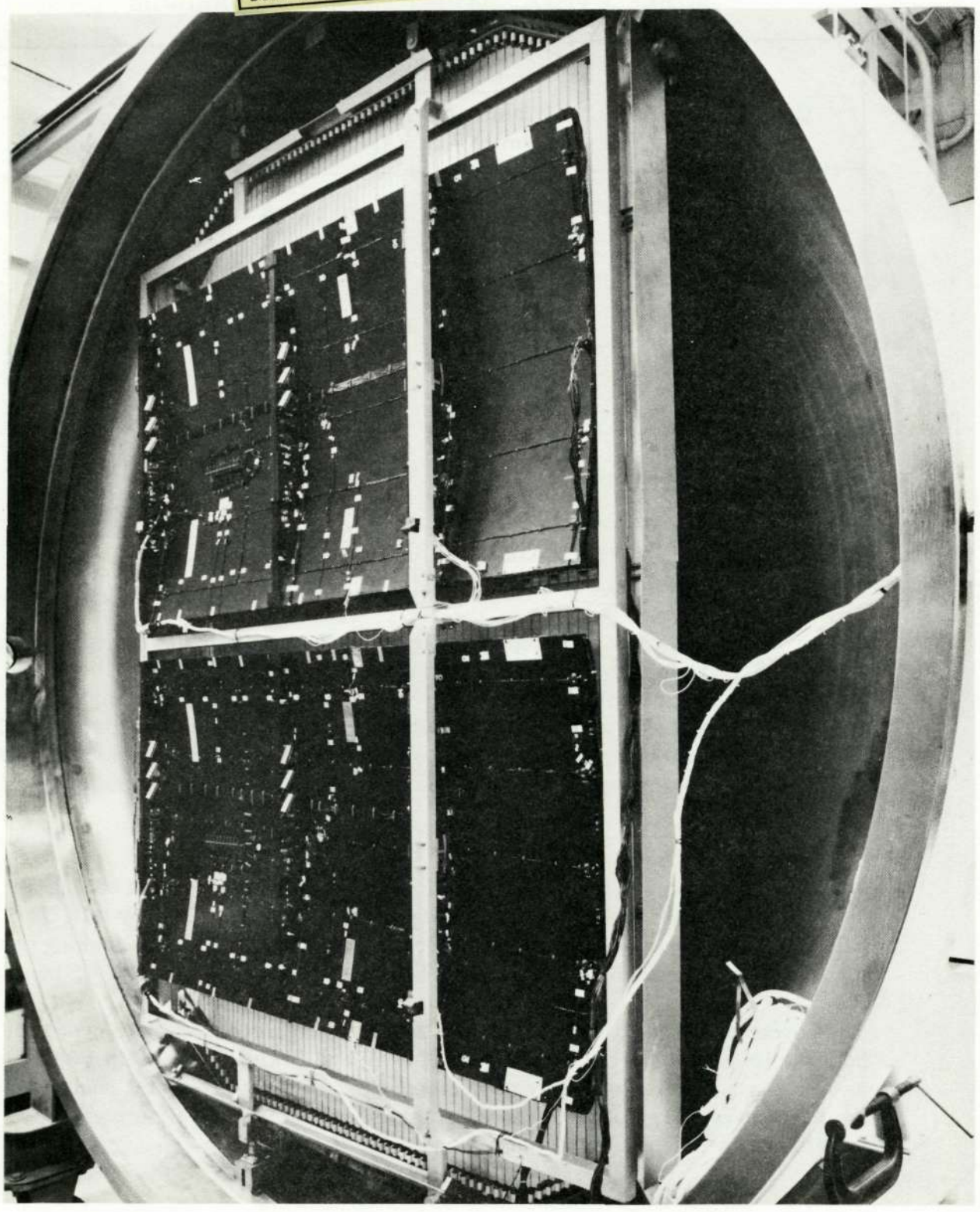

Figure 3-VI-19. Solar Panel Mounted in Clamshell Chamber

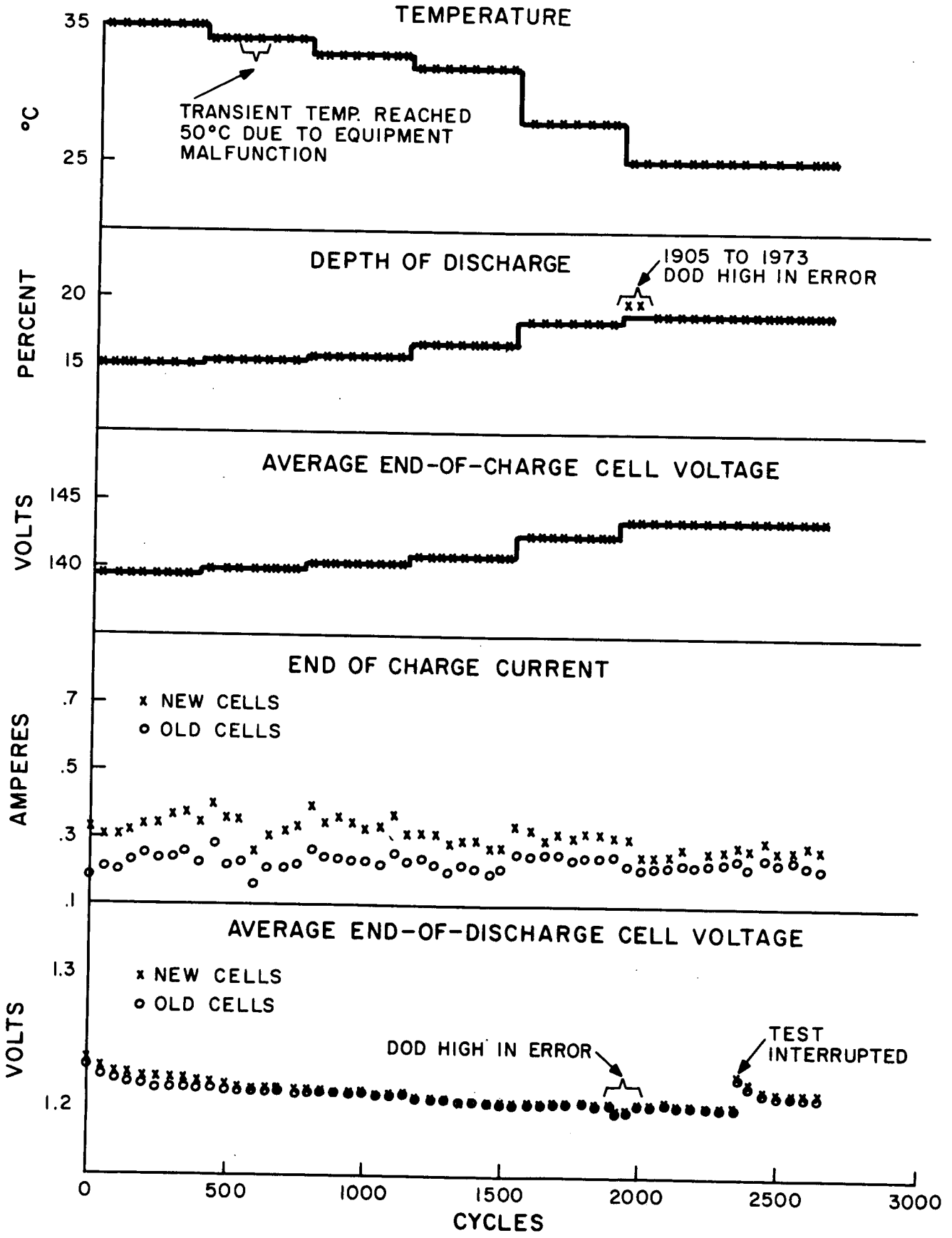

Figure 3-VI-20. Nickel Cadmium Battery Life Cycling Test

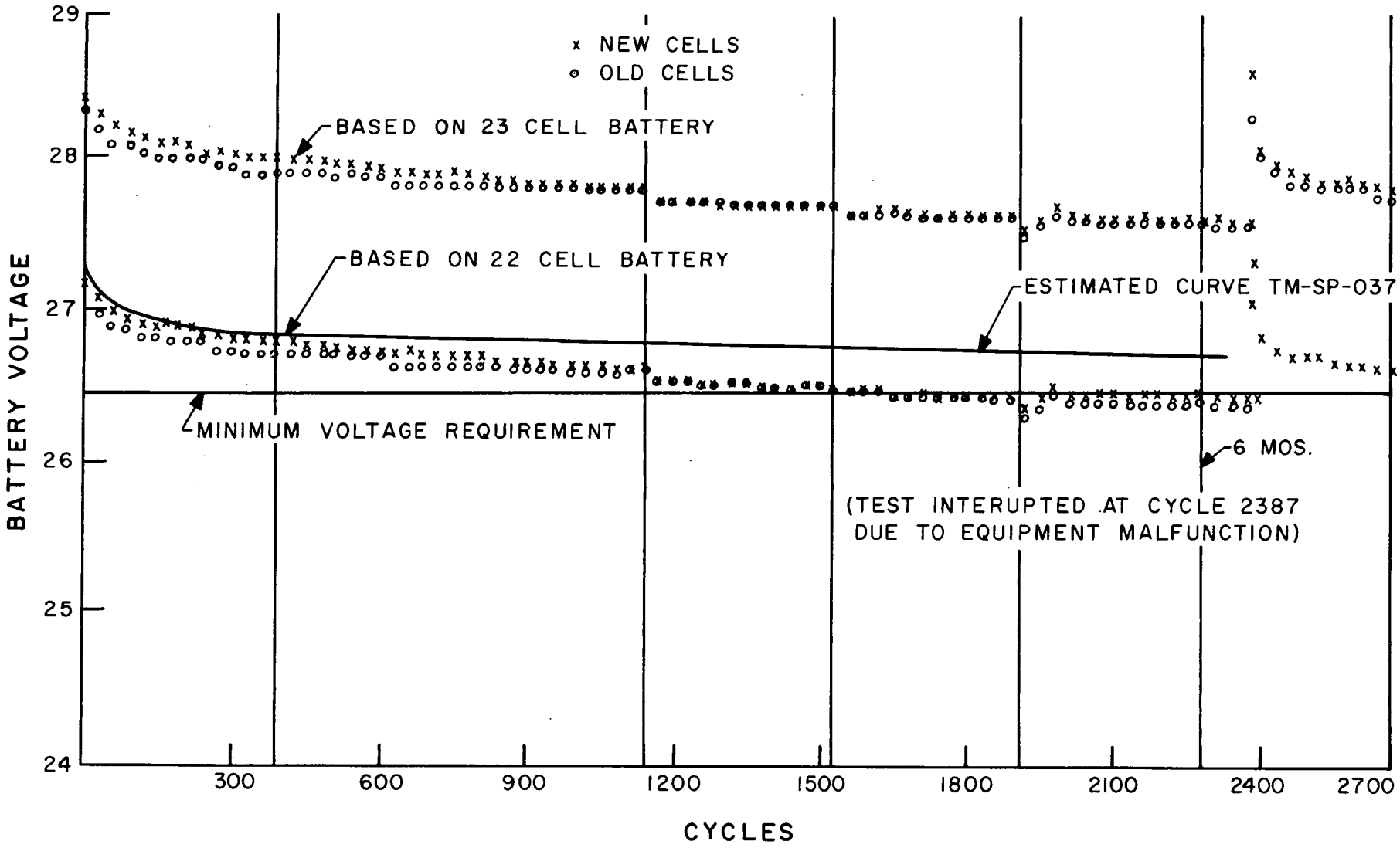

Figure 3-VI-21. Nickel Cadmium Battery Life Cycling Test, Battery End-of-Discharge Voltage Versus Cycle

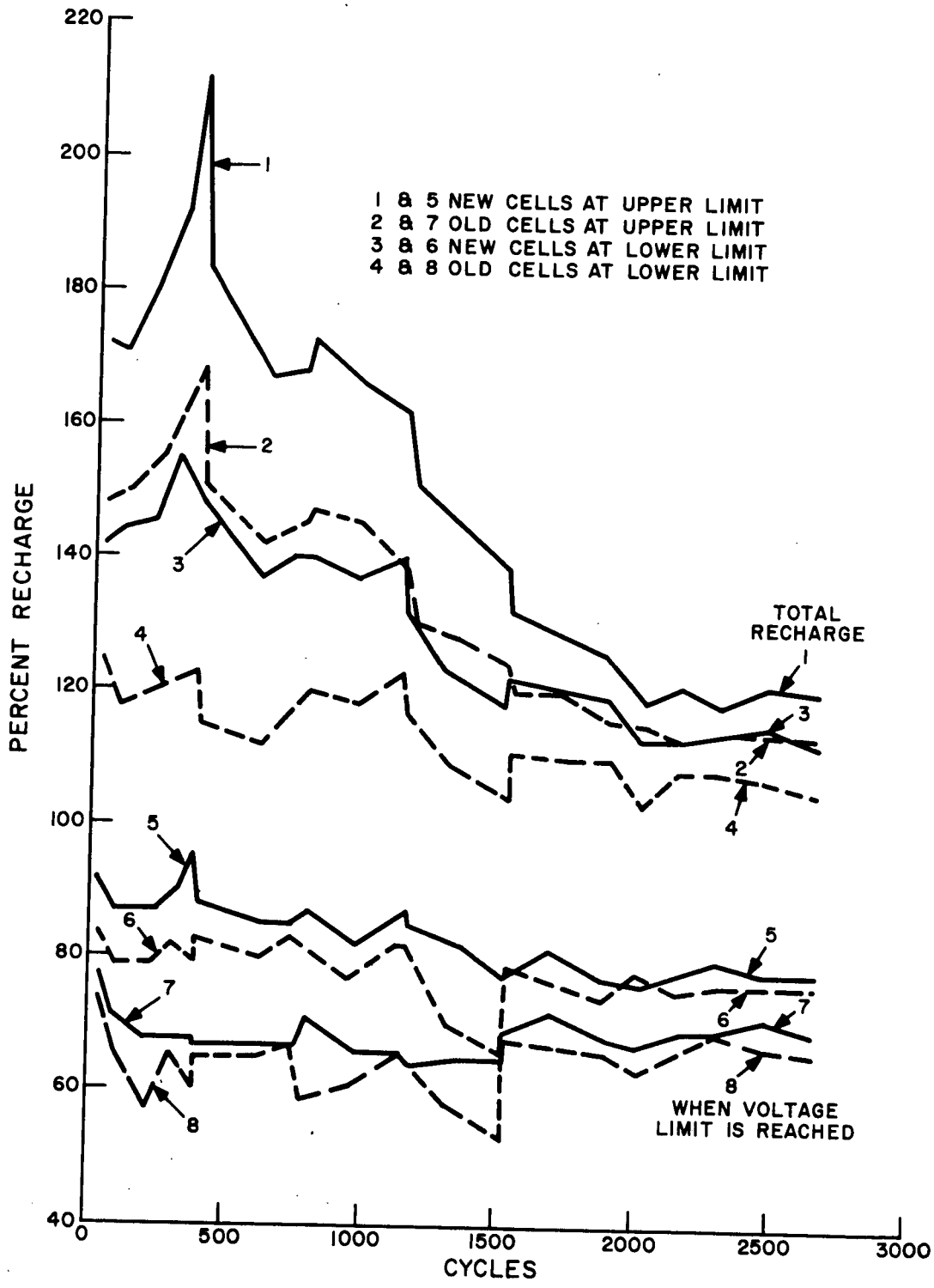

Figure 3-VI-22. Nickel Cadmium Battery Life Cycling Test, Percent Recharge Versus Cycle

b. PROTOTYPE

Battery pack assembly Ser. No. 01P underwent qualification testing as indicated in the following paragraphs.

Test	Date (1968)
DC isolation	June 24
Thermistor resistance	June 24
Preconditioning	June 26
0 °C capacity	June 27
25 °C capacity	June 27
40 °C capacity	June 28
Vibration*	July 2
DC isolation+	July 23
Thermistor resistance+	July 23
Preconditioning+	July 25
25 °C capacity+	July 25
Vibration+	July 30
Electrolyte leakage	July 30
25 °C capacity	July 31
Thermal-vacuum	August 8
Internal self discharge	August 9
Electrolyte leakage	August 9
DC isolation	August 9

*Battery could not be mounted on vibration table because of fixture bolt misalignment. After correction, battery had to be preconditioned and tests marked with a + repeated.

c. FLIGHT MODEL

Flight acceptance testing on battery pack assemblies Ser. Nos. 02 and 03 was performed as tabulated below:

Test	Date (1968)
Pre-vibration	August 14
Vibration	August 15
Post-vibration	August 16
Thermal-vacuum	August 20

Following completion of flight acceptance testing, it was discovered that the hold-down inserts had backed out. Repair consisted of removing the baseplate, repairing the faulty inserts, and reassembling the base. Heat-sinking of each individual battery cell is through direct physical contact with the baseplate. On October 4, 1968 the unit was installed in the thermal-vacuum chamber and charge/overcharge/discharge tests performed. The overcharge test objective was to verify proper heat-sinking of individual cells to the baseplate.

35. Power Supply Electronics

The power supply electronics subsystem major components are two identical voltage regulators, a shunt limiter, two battery charge controllers, and telemetry circuitry.

a. ELECTRICAL TEST MODEL

In general, the PSE subsystem was tested as a completely assembled unit with simulated solar arrays or batteries (or both) as inputs and dynamic loads or resistances (or both) as outputs. Electrical testing was performed at -20°, 25°, and 60°C. Certain deviations from the performance specifications were made as described in the following breakdown.

(1) Control amplifiers were tested as part of the entire shunt limiter circuit (including the remote shunt dissipators) instead of separate circuits with test loads as described in the performance specifications.

(2) The tempterature telemetry circuits (except the PSE and shunt dissipator current) were tested as simple divider circuits with the remote temperature sensing thermistor position shorted out. This was consistent with flight unit test plans, but did not allow for measurement of total circuit accuracy since thermistor errors were not included. No component failures were detected during testing, but the following components failed during the debugging phase.

- The thermofilm insulator used in mounting transistor Q4 (A11) was found to be punctured by a solder particle.
- Transistors Q1 on boards A14 and A15 had open emitter leads.

Following initial unit assembly, all circuits were found operable with the following exceptions. The regulated bus voltage telemetry had a printed circuit board which was shorting out a transistor junction. After removal of the error-causing trace, the circuit performed normally. The voltage regulators had the following malfunctions:

- A connections list error resulted in reversed connections on one coil of the regulator switching relay.
- Wire inductance associated with the input wiring from the external power source caused regulator loop instability.
- Cross coupling in the unit wire harness and between components on the regulator amplifier board caused oscillations during regulator switching.
- An AC ground loop between the amplifier sensing return and the regulator driver stage return contributed to the regulator instability.

Design changes were required to eliminate the above defects. After incorporation of the changes, all circuits performed within the specification limits.

The test parameters and results are summarized in Table 3-VI-13.

b. PROTOTYPE

The TIROS M power supply electronics (PSE) Ser. No. 01P was bench-tested at temperature extremes, vibration tested, and thermal-vacuum tested.

TABLE 3-VI-13. SUMMARY OF ETM PERFORMANCE TESTING ON POWER SUPPLY ELECTRONICS

Parameter	BOL* Spec	Results		
		-20°C	+25°C	+60°C
Shunt Limiter Circuit				
Solar Bus Voltage Overshoot (4 amp, 50 μs unloading)	0.65 V max	0.11 V	0.07 V	0.10 V
Recovery Time	1 ms max	< 0.4 ms	< 0.4 ms	< 0.4 ms
Solar Bus Cut-In Voltage				
Ampl No. 1	36.25 ± 0.1 V	36.24 V	36.26 V	36.25 V
Ampl No. 2	36.25 ± 0.1 V	36.24 V	36.26 V	36.25 V
DC Regulation I shunt = 0.1 to 15.6 A	0.15 V max	0.05 V	0.04 V	0.04 V
AC Impedance, Shunt Limiter Off	2.2 ohm max 100 Hz	0.8	0.8	0.8
Failure Defection Voltage	30.0 V max 28.0 V min	29.28 V 29.24 V	29.04 28.94	28.86 28.83
AC Impedance, Shunt Limiter ON	Not spec (ohms)			
Freq. 20 Hz		< .002	< .002	< .002
100 Hz		< .002	< .002	< .002
500 Hz		.005	.003	.005
1 kHz		.008	.004	.009
10 kHz		.088	.027	0.1
100 kHz		0.41	0.16	0.38
Charge Controllers				
Full Charge Current	0.931 A min 0.969 A max	0.950 0.957	0.950 0.953	0.950 0.953
Trickle Charge Current	0.130 A min 0.171 A max	0.150 0.160	0.146 0.155	0 147 0.158
Insertion Voltage Drop	1.6 V max	1.48 V	1.40 V	1.26 V
Batt Voltage-Temp Detection Band				
Batt T = 0°C	35.21 V max 34.87 V min	35.00 34.98	35.0 35.0	35.03 35.03
Bat T = +25°C	33.24 V max 32.89 V min	33.04 33.03	33.06 33.05	33.08 33.07
Bat T = +40°C	32.07 V max 31.73 V min	31.90 31.90	31.93 31.90	31.94 31.93
Series Regulators				
Line and Load Regulation	± 0.045 V max	+.034 -.039	± .04	
Temp Regulation	± 0.060 V max	-.025	0	

*Beginning-of-Life

TABLE 3-VI-13. SUMMARY OF ETM PERFORMANCE TESTING ON POWER SUPPLY ELECTRONICS (Continued)

Parameter	BOL Spec	Results		
		-20°C	+25°C	+60°C
Series Regulators (cont'd.)				
Transient Sensitivity				
Max Deviation	4.0 V	3.6	3.5	
Recovery to 24.50 ± 1.0 V	4 μsec max	1.5	1.5	
Recovery to 24.50 ± 0.250 V	20 μsec max	16	16	
Output Impedance				
1 - 10 Hz	0.02 ohm max	0.014	0.01	
10.1 Hz - 1 kHz	0.06 ohm max	0.046	0.036	
1.1 - 10 kHz	0.15 ohm max	0.095	0.085	
10.1 - 50 kHz	0.60 ohm max	0.32	0.32	
50.1 - 100 kHz	2.20 ohm max	0.90	1.10	
Regulator Switchover Recovery Time	250 ms max	230	220	
10 A, 1 ms Load Transient Peak Deviation	None	0.32 V	0.30 V	
Overall Performance Excluding 10 A Load Transient	24.75 V max 24.25 V min		24.574 V 24.442 V	
Overall Performance Including 10 A Load Transient	24.95 V max 24.05 V min		24.674 V 24.148 V	
Ripple and Noise Voltage	40 mV (p-p)	10 mV	10 mV	
Solar Bus Diodes				
Voltage Drop at 10 A (Note (1)	1.0 V max +25°C	1.116	1.087	
Reverse Leakage at 36 V	4.0 mA max	0.1 mA	0.25 mA	
Battery Discharge Diodes				
V Drop at 1.5 mA No. 1	0.460 V max	0.532	0.442	0.399
Note (1) No. 2	+25°C	0.470	0.436	0.392
Reverse Leakage at 36 V No. 1	6.0 mA max	0.09 mA	0.16 mA	2.25 mA
No. 2		0.11 mA	0.37 mA	2.50 mA
Shutter Bus Diodes				
Voltage Drop at 6.0 A No. 1	1.1 V max	1.015	0.883	0.944
Note (1) No. 2	+25°C	1.010	0.924	0.946
Reverse Leakage at 36 V No. 1	2.0 mA max	0.00017 mA	<0.0001 mA	0.0005 mA
No. 2		0.00011 mA	<0.0001 mA	0.0003 mA

TABLE 3-VI-13. SUMMARY OF ETM PERFORMANCE TESTING ON POWER SUPPLY ELECTRONICS (Continued)

Parameter	BOL Spec	Results		
		-20°C	+25°C	+60°C
Telemetry				
Accuracies				
Solar Panel I Tlm	± 2.0% max			
Panel 1		± 0.2%	+0.5 % -0.7	± 0.3%
Panel 2		± 0.2%	+0.5 % -0.9	+0.1 % -0.3
Panel 3		+0.3 % -0.5	+0.5 % -0.9	+0.2 % -0.4
Note (2)				
Shunt Limiter I Tlm	Not Applicable		± 1.5%	
Note (3)				
Battery Charge I Tlm	± 1.3%			
Battery 1		+0.7 % -0.4	+0.6 % -0.5	+0.7 % -0.5
Battery 2		+0.7 % -0.4	+0.6 % -0.4	+0.6 % -0.4
Solar Bus Voltage Tlm	± 0.6% max		+0.1 % -0.03	
Battery Voltage Tlm	± 0.6% max			
Battery 1			± 0.16%	
Battery 2			+0.02 % -0.16	
Unregulated Bus Voltage Tlm	± 0.6% max		+0.25 % -0.0	
Regulated Bus Voltage Tlm	± 0.5%		+0.35% -0.2% at 24.50 V	
Battery Temperature Tlm Note (3)	Not Applicable		± 1.5%	
Shunt Dissipator Temperature Tlm Note (3)	Not Applicable		± 1.5%	
PSE Temperature Tlm	± 3.0°C			
Solar Panel Temperature Tlm Note (3)	Not Applicable		± 1.5%	

TABLE 3-VI-13. SUMMARY OF ETM PERFORMANCE TESTING ON POWER SUPPLY ELECTRONICS (Continued)

Parameter	BOL Spec	Results
Control Ampl. On-Off Tlm		
Ampl No. 1 On alone	±3.9% max	$^{+0.4}_{-0.0}$ %
Ampl No. 2 On alone	±3.4% max	$^{+0.1}_{-0.05}$ %
Both On, Coils A & C	±3.4% max	$^{+0.5}_{-0.0}$ %
Both On, Coils B & D	±3.5% max	$^{+0.35}_{-0.0}$ %
Regulator and Charge Mode Selector Tlm		
Reg 1 On, Trickle Charge On	±4.6%	$^{+0.6}_{-0.0}$ %
Reg 1 On, Charge I Normal	±3.6%	$^{+1.8}_{-0.9}$ %
Reg 2 On, Trickle Charge On	±6.4% max	$^{+0.0}_{-2.8}$ %
Reg 2 On, Charge I Normal	±6.6%	$^{+0}_{-2.0}$ %

Notes:

(1) The diode voltage drop results include the drop in the PSE unit wiring.

(2) The solar panel I telemetry results do not take into account the variations of the current sensing resistors normally located on the solar panels. An additional ± 0.7-percent error should be added to the results shown to obtain the worst case beginning-of-life overall circuit accuracy.

(3) The temperature telemetry measurements were made with the remote sensors shorted out. The readings shown indicate the voltage divider outputs from the PSE unit. The shunt limiter current telemetry readings were taken with remote sensor connections open.

The prototype test levels were more severe than the mission requirements to assure that the tested unit would meet the design requirements. The test history for the prototype PSE is delineated below.

Test	Date (1968)
Initial electrical performance test at 25°, -15°, +60°C	July 25
Vibration	August 5

At the start of thermal-vacuum testing, regulation sensing on control amplifiers No. 1 and 2 was out of specification. Investigation revealed that slight flexing of the board affected the output. Microscopic examinations disclosed the need for stress relief loops in the leads to the diodes. New diodes with stress relief loops in the leads were installed and thermal-vacuum testing started. Thermal-vacuum testing was completed on August 12, and post-thermal-vacuum completed on August 14, 1968.

During thermal-vacuum testing on August 6, control amplifier No. 1 regulation sensing was slightly out of specification. Since the aleviation was so marginal and the unit had been successfully bench tested, the test was allowed to continue in the belief that the fault lay in the STE. However, the problem was not in the test equipment and the circuitry was modified. Consequently, after correction, retesting in the Tenney box was performed at -15°, 25°, and 60°C and completed on September 6, 1968. The STE was modified to accommodate the new fuse test currents and the PSE was thermal-vacuum tested for 6 hours at 60°C and 6 hours at -15°C, with fuse tests performed at 1-hour intervals. Testing was completed on September 9, 1968.

Table 3-VI-14 summarizes important test results (after retest, if repaired).

c. FLIGHT MODEL

Qualification testing on power supply electronics Ser. No. 03 was performed as follows:

Test	Date (1969)
Initial electrical performance	Feburary 12
Vibration	February 12
Post-vibration	February 12
Thermal-vacuum	February 13
Post-thermal-vacuum	February 20

TABLE 3-VI-14. TEST RESULTS OF SIGNIFICANT PARAMETERS, POWER SUPPLY ELECTRONICS

Function	Test Limits	Test Results	Unit Number
Battery Charge Current	931 to 969 mA	945 to 965 mA	No. 1
		944 to 965 mA	No. 2
Battery Trickle Charge	120 to 171 mA	158 to 171 mA	No. 1
		154 to 170 mA	No. 2
Regulated Bus Voltage including 10 A transient.	24.10 to 24.90 V	24.15 to 24.55 V	No. 1
		24.17 to 24.54 V	No. 2
Regulated Bus DC Regulation at any one temperature only (0.4 to 6 A)	±0.045 V	0.04 V	No. 1
		0.03 V	No. 2
Regulated Bus Output Impedance:			
1 to 10 Hz	0.02 ohm	0.01 ohm	No. 1
		0.01 ohm	No. 2
10 to 1000 Hz	0.06 ohm	0.02 ohm	No. 1
		0.03 ohm	No. 2
1.01 to 10 kHz	0.15 ohm	0.08 ohm	No. 1
		0.08 ohm	No. 2
10.1 to 50 kHz	0.6 ohm	0.28 ohm	No. 1
		0.28 ohm	No. 2
50.1 to 100 kHz	2.2 ohm	0.34 ohm	No. 1
		0.30 ohm	No. 2
Regulated Bus Recovery on Switchover	0.25 s	0.15 s	No. 1
		0.15 s	No. 2
Solar Bus Cut-in Voltage			
Amplifier No. 1	36.15 to 36.35 V	36.20 to 36.29 V	
Amplifier No. 2	36.15 to 36.35 V	36.22 to 36.30 V	
Solar Bus Voltage Change	0.15 V	0.11 V	No. 1
		0.09 V	No. 2
Failure Detection Cut-in	29.0 %1.0 V	28.8 to 29.3 V	No. 1
		28.9 to 29.3 V	No. 2

TABLE 3-VI-14. TEST RESULTS OF SIGNIFICANT PARAMETERS, POWER SUPPLY ELECTRONICS (Continued)

Function	Test Limits	Test Results	Unit Number
Solar Panel Current Tlm (Nos. 1, 2, 3)	±2%	2%	
Shunt Limiter Current Tlm	±3.3%	1.2%	
Battery Charge Current Tlm	±1.3%	1.2%	
Solar Bus Voltage Tlm	±0.6%	0.2%	
Battery Voltage Tlm	±0.6%	0.2%	
Unregulated Bus Voltage Tlm	±0.6%	0.1%	
Regulated Bus Voltage Tlm	±0.5%	0.2%	
Battery Temperature Tlm Resistors	±3%	0.1%	
Shunt Dissipator Temp Tlm Resistors	±3%	0.2%	
PSE Temperature Tlm difference to heatsink	10 °C	4°C	
Solar Panel Temp Tlm Resistors	±3%	0.2%	
Control Amplifier ON-OFF Tlm			
Amplifier No. 1 ON Alone	±3.9%	0.2%	
Amplifier No. 2 ON Alone	±3.4%	0.5%	
Both ON, Coils A and C	±3.4%	0.5%	
Both ON, Coils B and D	±3.5%	0.6%	
Regulator and Chg. Current Mode Selector Tlm			
Regulator No. 1 ON, Trickle Chg ON	±4.6%	0.5%	
Regulator No. 1 ON, Chg. Current Normal	±3.6%	1.2%	

TABLE 3-VI-14. TEST RESULTS OF SIGNIFICANT PARAMETERS, POWER SUPPLY ELECTRONICS (Continued)

Function	Test Limits	Test Results	Unit Number
Regulator No. 2 ON, Trickle Chg ON	±6.4%	2.5%	
Regulator No. 2 ON, Chg. Current Normal	±6.6%	2.8%	
Battery Isolation-Diode Reverse Leakage at 36.0 V	6.0 mA (max)	1.6 mA 1.5 mA	No. 1 No. 2
Shutter Bus Diode Reverse Leakage at 36.0 V	2.0 mA (max)	0.001 mA 0.001 mA	No. 1 No. 2
Shunt Limiter Control Amplifier Isolation-Diode Reverse Leakage at 36.0 V	25 mA (max)	0	
Solar Bus Isolation-Diode Reverse Leakage at 36.0 V	4.0 mA (max)	.001 mA	
External Power Diode	6.0 mA	.001 mA	
Fuses	Continuity at 1/2 rated current - 150% of applicative current	ALL OK	

On March 21, 1969, during initial power application and functional checkout while temporarily associated with the ITOS A spacecraft, the fuse from the regulated bus to the taper charger No. 2 clamp reference voltage was found to be open. While the PSE box was off the spacecraft to replace the fuse, replacement diodes (Dickson 1N944B) were installed on VR1 and VR2 (boards A14 and A15). After reassembly and sealing, retesting was initiated.

On April 10, electrical operational tests at several temperature levels and a modified random thrust flight level vibration test were performed. Post-vibration testing was completed on April 11, 1969.

In accordance with a NASA directive, the PSE Ser. No. 03 was subjected to a special 240-hour operational test at the box level starting April 29, 1969.

During secondary sensor calibration tests on May 20, a fuse failed as a result of a short circuit in the flat plate radiometer test equipment. After replacement and resealing, fuse resistance checks and electrical operational tests were performed on May 28.

Due to a shorting problem on other PSE units, Ser. No. 03 had fiberglass insulation installed in its base as a precautionary measure. During the low temperature performance retest, fuse A5-F21 indicated "open" on the DVM regulated voltage bus. It was decided to institute an investigation into the possibility of shorting the fuse lead wire from the terminal of F21 to the connector shell. This action was confirmed and, by mutual consent, the A5 board from PSE Ser. No. 03 was replaced by the A5 board from PSE Ser. No. 04. Investigations continued on the cause of the shorting on the Ser. No. 03 board. Electrical performance retesting at assembly level was performed at 25°C on August 27, vibration tested (random thrust only) on August 28, and at +55°C and -10°C on August 29, 1969. Delivery was then made to spacecraft integration for reassembly to the TIROS M spacecraft.

36. Active Thermal Controller

The active thermal controller (ATC) is composed of two major subassemblies: four actuator/sensors, and four louver and hinge assemblies.

a. ACTUATOR/SENSORS

(1) ELECTRICAL TEST MODEL

A simulated 1-year life cycle test on the actuator/sensor was completed at the end of May, 1969, with excellent results.

The tested unit was of flight design; one of the four used on the thermal test model of the spacecraft. An illustration of the test assembly along with the location of the thermocouples is shown in Figure 3-VI-23. The objective of the test was to cycle the sensor unit from one end of its range to the other by repetitive heating and cooling for a period equivalent to 1-year of orbital operation. The test was conducted under ambient conditions, rather than in a vacuum environment, for reasons of practicality and economy. However, the unit was checked for leakage before and after the test by soaking in a vacuum chamber and comparing the operating range.

The unit was instrumented with thermocouples (as shown in Figure 3-VI-25) and the potentiometer supplied with a constant -24.5-volt DC input. Thermocouple outputs were recorded on a 24-channel temperature recorder and the potentiometer output, in the form of a variable voltage linearly dependent upon the shaft extension of the sensor, was recorded throughout the test on a roll chart.

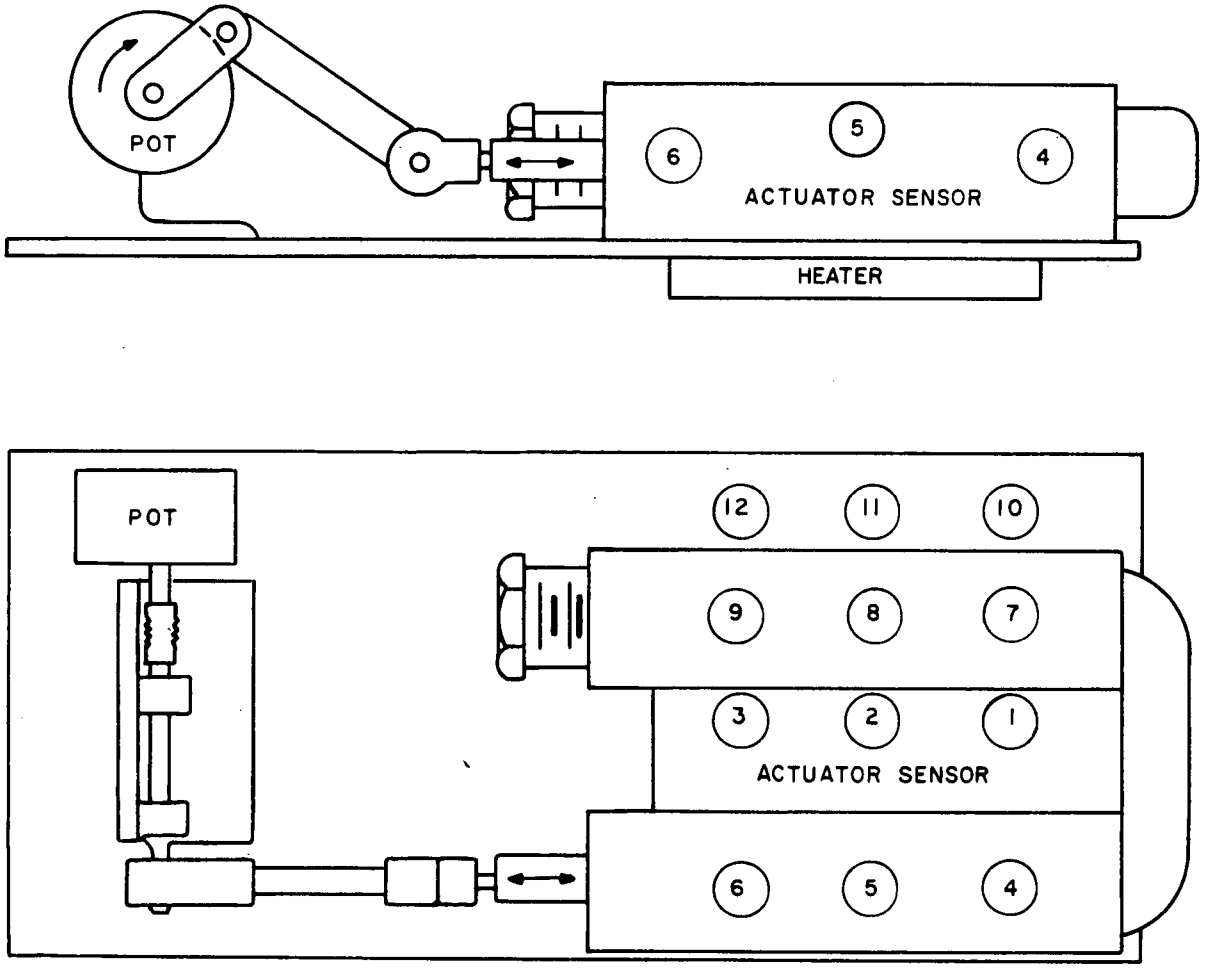

Figure 3-VI-23. Actuator Sensor Life Test Assembly

(2) PROTOTYPE

Actuator/sensor assembly Ser. No. 05P underwent prototype qualification testing as delineated below.

Test	Date (1968)
Leak Rate	February 23
Initial temperature Operational	March 6
Leak rate (retest)	May 17
Performance	May 20
Tenney box	May 21
Post-Tenney box leak rate	May 22
Vibration	May 23
Post-vibration operational test in Tenney box	May 23
Post-vibration leak rate	May 23
Thermal - vacuum	May 29
Post-thermal vacuum operational in Tenney box	May 29
Post-thermal-vacuum leak rate	May 29

(3) FLIGHT MODEL

Four actuator/sensor subassemblies are employed aboard the TIROS M spacecraft: Ser. Nos. 07, 08, 09 and 10. Flight acceptance qualification tests were performed as tabulated below.

	Date (1968)			
Test	Ser. No. 07	Ser. No. 08	Ser. No. 09	Ser. No. 10
Leak rate	February 23	February 23	April 11	April 11
Temperature operational	March 7	March 7	May 6	May 6*
Temperature operational (retest)			May 8	May 8

*During initial setup an external retaining ring popped off. A new ring was installed and the unit returned to test. Other actuators were checked and rings corrected or replaced as necessary.

Test	Date (1968) Ser. No. 07	Ser. No. 08	Ser. No. 09	Ser. No. 10
Pre-vibration	March 12	March 12	May 14	May 14
Vibration	March 15	March 15	May 14	May 14
Thermal-vacuum	June 24	June 24	June 24	June 24
Post-thermal-vacuum operational	June 24	June 24	June 24	June 24

b. LOUVER AND HINGE ASSEMBLIES, FLIGHT MODEL

Flight acceptance qualification testing on the louver and hinge assemblies was confined to operational testing performed on the dates shown below. Two sets of louver and hinge assemblies are carried aboard the TIROS M spacecraft:

AVCS PANEL

1975343-501 Ser. No. 07

1975343-502 Ser. No. 07

APT PANEL

1975343-501 Ser. No. 08

1975343-502 Ser. No. 09

Operational testing was performed on both Ser. No. 07 assemblies on May 7, 1968; on Ser. No. 08 on May 9, 1968; and on Ser. No. 09 on October 11, 1968.

37. Accelerometer Assembly and Acceleration Control Unit, Flight Model

Component testing on the accelerometer assembly and accelerometer control unit Ser. No. 02 was confined to initial electrical and subsystem performance testing.

Initial electrical testing was performed on the accelerometer control unit on December 12, 1968. During subsystemperformance testing of both units together on February 4, 1969, incorrect wiring on the accelerometer assembly was discovered. After correction, performance testing of the integrated units was successfully completed on February 17, 1969.

38. Separation Switches, Flight Model

Separation switches Ser. Nos. 0009 and 0012 were subjected to and successfully completed initial electrical, vibration, and post-vibration testing on May 16, 1969.

SECTION VII

TIROS M SPACECRAFT FLIGHT ACCEPTANCE TESTING

The integrated TIROS M spacecraft, with flight qualified components and subsystems, underwent flight acceptance tests during the period July 1968 to October 1969. The test program (see Table 3-VII-1) consisted of:

- Assembly, debugging and interface verification,
- System evaluation and prequalification calibration cycle,
- Environmental qualification, and
- Final calibration.

The TIROS M spacecraft passed these tests successfully, with some discrepancies, as described in the following paragraphs.

A. ASSEMBLY, DEBUGGING AND INTERFACE VERIFICATION

This test phase was investigative in nature and consisted primarily of discrete problem solving. The purpose was to test TIROS M for the first time after installation of flight accepted units, and also to briefly demonstrate satisfactory operation of these units in an integrated spacecraft. The test sequence consisted of verifying spacecraft harness correctness, connecting together a selected group of interrelated units, and applying spacecraft power to these units. Proper functioning of equipment was then confirmed (on a superficial basis) by monitoring available spacecraft outputs, including test points, telemetry, RF communications data and, where required, internal harness signals.

1. Power Interface

On July 24 to 29, 1968, prior to initial power application and functional checkout (IPFC) a harness "ringout" was performed. Eight wiring discrepancies were discovered during point-to-point continuity tests. They were corrected by the RCA wiring shop.

2. Power Application

On July 30, IPFC began and continued until October 8. During the first day's testing, the telemetry signal conditioner ground was found not to be isolated from the case ground. This was repaired by the vendor. During the next day's

TABLE 3-VII-1. CHRONOLOGY OF TIROS M FLIGHT ACCEPTANCE TESTS

Test	Date
Assembly, Debugging and Interface Verification	
Power Interface	July 24-29, 1968
IPFC	July 30
Bus Functional Checkout	October 17-31
Sensor Mounting, Functional Checkout & DET	January 8- February 25, 1969
Operational Mode Tests	March 4-22
Thermal Tests	March 22-30
Battery Capacity Test	April 28-May 2
Abbreviated SEPET	May 8
Final Mechanical Assembly	May 9-12
System Evaluation and Prequalification Calibration	
Abbreviated SEPET	May 14-15
Solar Panel Checkout	May 17
Camera Calibration	May 17-19
SR Calibration	May 19-20
Secondary Sensor Calibration	May 20-21
Dynamic Suspension	June 3-5
SEPET	June 11-13
Solar Panel Deployment	July 10
Separation Shock	July 15
Environmental Qualification	
Vibration	July 17
Post-Vibration SEPET	July 19-20
Thermal-Vacuum Tests	July 22- August 26
Special Blanket Thermal Tests	September 7
Final Calibration	
Magnetic Dipole Check	September 20-21
SEPET	September 22
Battery Capacity Test	September 24
Camera Calibration	September 24-25
Scanning Radiometer Calibration	September 25
SPM and FPR Calibration	September 26
Sensor Alignment Check	September 27-29
RF Tests	September 30
Final Balancing	October 2
M-I, C-G and Final Weighing	October 4

testing, the decoder turn-on generated undesired data "0's". These caused the telemetry commutator in the manual mode to advance two channels each time the decoder was enabled. The fault was corrected by modification of the power-on reset logic.

On the fourth day of testing, harness plugs for the S-band transmitters would not mate with their corresponding connectors. The plugs were the wrong parts and were returned to the vendor for replacement. Following this a decoder verification dropout on invalid commands occurred. The decoder should have maintained data verification until after the 13th bit to permit easy identification of invalid commands. This situation was remedied by incorporating additional logic to ensure that data verification was maintained. On August 14, during real-time transmitter (RTT) tests, RTT No. 2 did not turn off with real-time night pulse. This was due to a fault in the test console design, which was corrected.

Automatic picture transmission (APT) and scanning radiometer (SR) side 2 detailed electrical tests (DET) were carried out on August 16 to 20 without incident.

On October 7, during DET, the beacon transmitter exhibited spurs at turn-on causing the receiver to miss the command termination bit. A remedial modification of all beacon transmitters followed. Beacon DET was resumed on February 24, 1969 and successfully completed.

Real-time transmitter No. 1 power output measured 30 dB on October 8, due to a faulty attenuator pad in the test equipment. The attenuator was replaced. On October 15, command receiver No. 2 exhibited an incorrect IF passband. This problem resulted from a faulty generator, which was replaced.

3. Bus Functional Checkout

This checkout consisted of connecting limited groups of units and then applying spacecraft power. The operation of these units was evaluated principally from a functional standpoint by monitoring appropriate outputs from the spacecraft test points. The bus DET was performed during the period October 17 to 31, 1968. On the first day, the solar array coupling diode drop measured larger than expected (1.05 volts while the procedure allows only 1.0 volt maximum). Both batteries also had discharge diode losses. Investigation showed that the measurements, per procedure, were made at a point far removed from the diode junction whose drop was to be measured. The procedure was changed and the faults corrected. On October 30, a special scanning radiometer collimator test showed the visible output of the collimator to be low. As a result, ESSA changed the collimator design.

4. Sensor Mounting, Functional Checkout and DET

Following the bus functional checkout, the three primary sensors (AVCS, APT, and SR) and the two secondary sensors [flat plate radiometer (FPR) and solar proton monitor (SPM)], along with their associated electronics, recorders, and data processing units, were mounted onto their appropriate panels.

The functional checkout consisted of connecting each sensor subsystem into the spacecraft system and then applying spacecraft power. The sensor operation was then evaluated primarily from a functional standpoint by monitoring appropriate outputs.

The DET consisted of performing most of each sensor calibration test.

The APT subsystems were subjected to detail electrical testing on January 8, 1969 with no malfunctions.

On January 10, IPFC was performed on the solar proton monitor and the flat plate radiometer. The SPM No. 2 ground line was found to be not isolated from the case ground. It was returned to APL for repair. Minor FPR test procedure difficulties were encountered and resolved.

Secondary sensor DET was begun on January 13 but not completed due to test equipment problems. Tests were resumed later, on March 15, and successfully completed.

IPFC was conducted on the AVCS on January 29, with the only trouble being in the tape recorder playback enable drive. A faulty transistor in the CDU was located and replaced.

The AVCS received detailed electrical testing beginning on January 31. During data analysis, scene video appeared in the gray scale calibration area; an adjustable cover plate in the camera sensor was readjusted to correct the anomaly. On February 25, AVCS camera No. 2 exhibited 0 volt in the head temperature telemetry. Investigation revealed a cracked metal film resistor on the temperature sensor on the outside of the camera sensor. The resistor was replaced.

5. Operational Mode Tests

These tests provided evaluation of combinations of systems in modes similar to those operating in orbit. The purpose of the tests was to demonstrate the ability of the various subsystems to perform efficiently in conjunction with one another.

Dynamics system DET commenced on March 4. On March 5, checkout of the active thermal control position telemetry revealed incorrect wiring. The wiring harness was changed to correct this. On March 7, the thermal fence temperature sensor gave an incorrect output. X-ray analysis revealed a cracked thermistor. The sensor was replaced.

IPFC tests on the momentum wheel assembly were conducted on March 12. On March 15, DET tests were sucessfully run on the prototype pitch control electronics.

Standard electrical performance evaluation testing (SEPET) of the open spacecraft was performed on March 20 to 22 with no problems.

6. Thermal Tests

Temperature tests were conducted to demonstrate spacecraft performance by:

- Evaluating spacecraft performance at temperatures beyond those expected in orbit,
- Evaluating spacecraft performance over the expected temperature range in orbit,
- Establishing confidence in the ability of the spacecraft to perform during the thermal-vacuum tests later.

Spacecraft thermal tests in the Tenney chamber were carried out during March 22 to 30. The tests consisted of:

Temperature	Duration (Hours)
+35°C	56
- 5°C	48
+ 5°C	12
+15°C	12
+50°C	7
-10°C	7

Seven anomalies were recorded.

(1) AVCS recorder No. 2 exhibited dropouts at +35°C and later a loose S-band transmission link cable was discovered. This loose cable probably caused the dropouts.

(2) Beacon transmitter No. 1 subcarrier oscillator No. 2 became inoperative during the transition from +35° to -5°C. The SCO package was replaced; a loose connection in an SCO socket was found to have caused the problem.

(3) The DC restore on both scanning radiometers was seen to be unstable. Investigation showed this to be due to air currents and, therefore, not a failure since it cannot occur in space (or in thermal vacuum).

(4) Both APT cameras exhibited shift of the 300-Hz start tone. This was attributed to a race condition on the reset line in the countdown chain and inherent in all APT cameras. It was not considered to be a malfunction.

(5) Command receiver No. 2 AGC telemetry was out of specification. This was caused by a procedural error, which was corrected.

(6) Beacon transmitter No. 2 SCO assembly showed a frequency drift up from lower band during transition from -10° to +25°C. The cause was not confirmed and the SCO package was replaced.

(7) S-band transmitter No. 2 frequency was out of specification. The anomaly was due to an incorrect measuring technique.

On March 30, the Tenney chamber thermal tests were finished.

Retest of certain boxes removed for reworking took place during April 9 to 16. On April 15, SPM Ser. No. 03 began to yield incorrect data. The fault was isolated to detector No. 5, a GFE item. The SPM and its harness were returned to APL for repairs. On the next day, SR processor No. 2, side 2, back scan calibrator read zero. This malfunction was corrected by replacing the suspected components.

On April 28, battery capacity testing began. These tests are designed to (1) prevent irreversible, high end-of-charge voltage buildup and (2) evaluate battery packs and cells for electrical capacity, internal self-discharge, and end-of-charge voltage limits. The tests were conducted successfully through May 2.

During May 1 to 7, a retest of boxes removed for "burn-in" was performed successfully, with one exception. In programmer No. 2, during AVCS picture sequence, a high voltage test point became inoperative. A 100-kilohm resistor was found to be open-circuited and was replaced.

During the abbreviated SEPET run on May 8, dual decoder No. 2 generated a spurious data "0" output upon power turn-on. It was determined that a voltage

transient by capacitive coupling affected a fast-acting relay. Decoder logic was changed to correct the fault.

On May 9, the spacecraft was turned over the mechanical integration group for final mechanical assembly.

7. Final Mechanical Assembly

This task consisted of permanently securing all units, closing up the spacecraft, performing a sensor optical alignment, performing rough balance, and measuring the spacecraft moment-of-inertia, center-of-gravity, and weight.

B. SYSTEM EVALUATION AND PREQUALIFICATION CALIBRATION CYCLE

For this evaluation the spacecraft was in closed configuration; the purpose was to ensure that operation was essentially the same as in open configuration. An abbreviated SEPET was performed before any other electrical test. The abbreviated SEPET is divided into two principal parts:

(1) Quantitative measurements of the principal electrical parameters of each subsystem

(2) A checkout of the different operational combinations of the various spacecraft subsystems.

Following the abbreviated SEPET, the flight solar panels were mounted on the spacecraft. The solar array was then checked to ensure operation of the solar array/electronics interface and to obtain power system telemetry signatures. The spacecraft was then subjected to a series of checks for RF interference with the flight solar panels. The dynamic suspension test, which provided a check of the pitch control subsystem, was then performed without solar panels.

From the prequalification calibration cycle, data was obtained for comparison with that obtained in the final calibration. This comparison ensured that no degradation occurred during environmental testing.

In the closed configuration, an abbreviated SEPET was conducted on May 14 and 15. The only discrepancy occurred when programmer No. 2 apparently failed to toggle the scanning radiometer recorders. Investigation showed that the problem was a noise-sensitive programmer, which caused toggling of recorders whenever a commutator "on" transient occurred. Replacing the resistors resulted in satisfactory operation by making the programmer less sensitive.

On May 17, the solar panels were mounted on the spacecraft and checked out successfully for RFI with the spacecraft and solar array/electronics interface.

Camera calibration was carried on from May 17 to 19. On May 17, APT camera No. 2 (Ser. No. 04) exhibited a high output. The camera was removed and the vidicon tube was replaced.

On May 19 and 20, the scanning radiometers were calibrated with no problems.

Secondary sensor subsystem calibration was performed on May 20 and 21, with two discrepancies. Solar proton monitor Ser. No. 04 generated internal noise; the SPM electronics unit was removed and repaired. The flat plate radiometer test set blew a fuse due to a frayed wire and the wire was replaced.

On May 22, AVCS camera 1 (Ser. No. 05) was subjected to detailed electrical tests with no problems. The next day, APT camera No. 2 (Ser. No. 05) underwent DET. It produced "noisy" pictures, traced to a cracked resistor in the 18-volt regulator. The unit was removed from the spacecraft and repaired.

On May 29, DET was conducted on the pitch control subsystem with one problem. The momentum wheel assembly (MWA) (Ser. No. 03) had a broken wire on a plug, resulting in faulty operation of pitch loop 2. The plug was replaced.

On June 3 to 5, the dynamic suspension test was successfully performed. See Figure 3-VII-1.

Brightness tests were successfully conducted on AVCS Ser. No. 05 and APT Ser. No. 06 on June 7.

A separation switch checkout on June 9 revealed a blown fuse in the squib power enable box. The trouble was traced to a bad solder connection in the power enable box. A relay in the power enable box and two fuses in the spacecraft were replaced and normal operation was obtained.

During June 9 and 10, alignment checks of APT No. 2, AVCS No. 1, and the MWA were completed with no problems.

On June 11 to 13, full SEPET was performed. Three anomalies occurred.

(1) Pitch control electronics failed to respond to the Enable Dual Motor Mode command. This was remedied by a circuit design change.

(2) Roll sensor and selected pitch index telemetry did not record on the SR recorder unless selected for real-time transmission. Minor design change of the CDU corrected the fault.

(3) Minor procedure errors were noted and corrected.

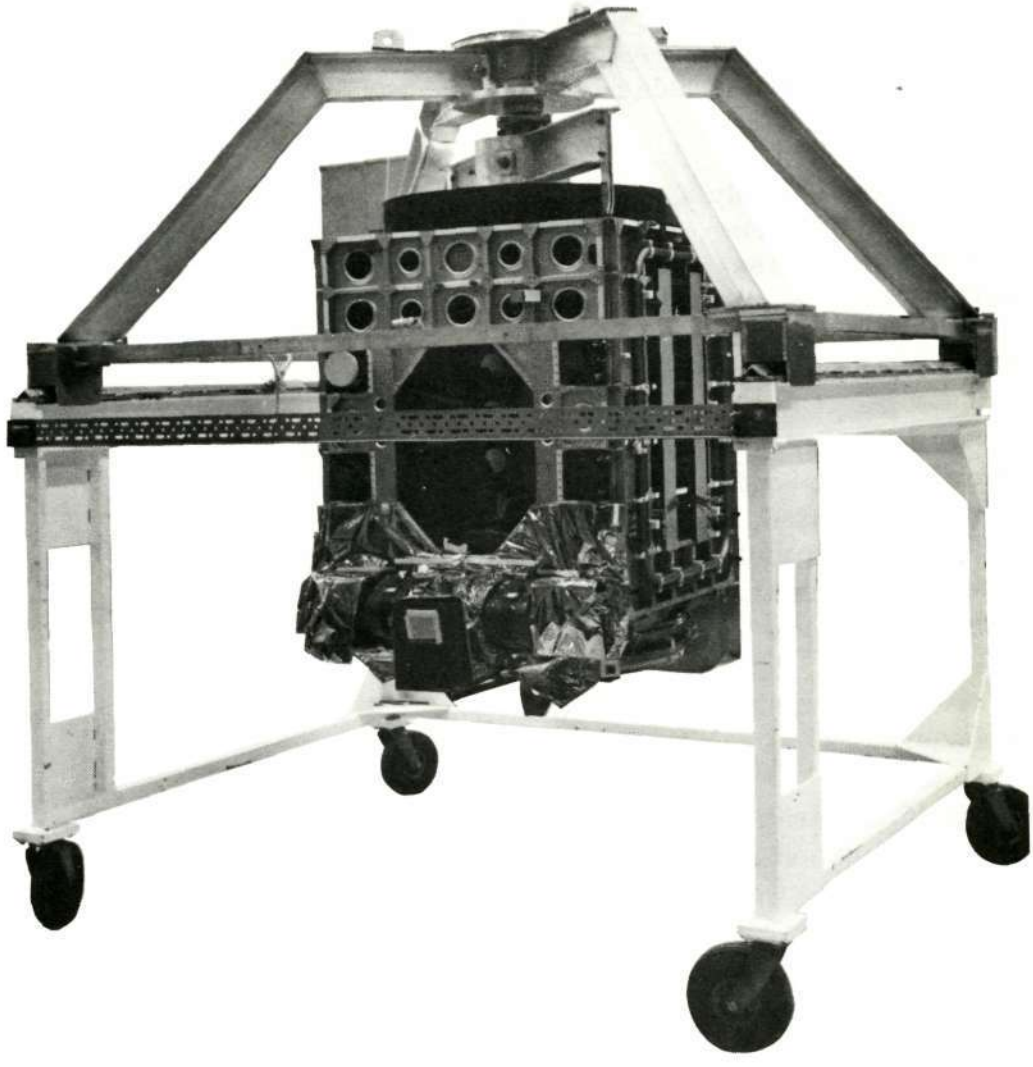

Figure 3-VII-1. TIROS M Spacecraft in Dynamic Suspension Test Fixture

On June 19 and 20, special tests revealed that SR1, Ser. No. 04, was noisier than Ser. No. 05. Therefore, Ser. No. 05 was installed in the spacecraft as SR1.

On June 24, S-band transmitters Ser. Nos. 10 and 13 were removed for a special 5-day thermal-vacuum cycling test.

Momentum wheel assembly (Ser. No. 03) was removed for installation of an additional oil reservoir.

Performed satisfactorily on June 27 were SR Ser. No. 05 calibration, APT Ser. No. 06 calibration, APT Ser. No. 06 DET, and APT Ser. No. 02 functional check.

On June 30, the spacecraft was released to Mechanical Integration for installation in SEPET fixture, alignment of collimators, and installation of the S-band transmitters (which had been removed for 5-day thermal-vacuum cycling).

During June 30 to July 3, a pre-environmental SEPET was conducted, with one discrepancy occurring. In SPM electronics Ser. No. 005, word 61 yielded random values. Test cable capacitance caused the suitcase test set to give spurious outputs. Test set cabling from APL was replaced.

RFI tests were run during July 9 and 10 with no interference detected.

On July 10, solar panel deployment tests were performed. During panel C deployment, the bonding on the RF cables tie-down block failed. The tie-down block was rebonded, and an additional tie-down block was installed. On the next day, solar panel checkout was conducted. Panel 1 (Ser. No. 002) failed to yield array current telemetry because a sampling resistor had been shorted out by a superfluous wire. The wire was removed.

The spacecraft was turned over to environmental test for installation of accelerometers.

On July 15, separation shock tests were completed. Two firings of the Marmon clamp bolt cutters were satisfactorily performed. See Figure 3-VII-2.

The data obtained from the prequalification calibration cycle was compared with similar data recorded earlier during functional checkout. The reference calibration levels for the spacecraft were established and the spacecraft was ready for qualification. It was released to the mechanical group for vibration on July 15.

C. ENVIRONMENTAL QUALIFICATION

The first qualification operation is the vibration of the spacecraft after it has been assembled into the launch configuration. Electrical operation during vibration is identical to that of the launch configuration. Following vibration testing, an abbreviated SEPET is performed to ensure that vibration did not degrade the operation of the spacecraft. Also following vibration, the thermal blankets and flight solar panel assemblies are removed and a solar panel illumination test is performed while the spacecraft thermal-vacuum test is under way.

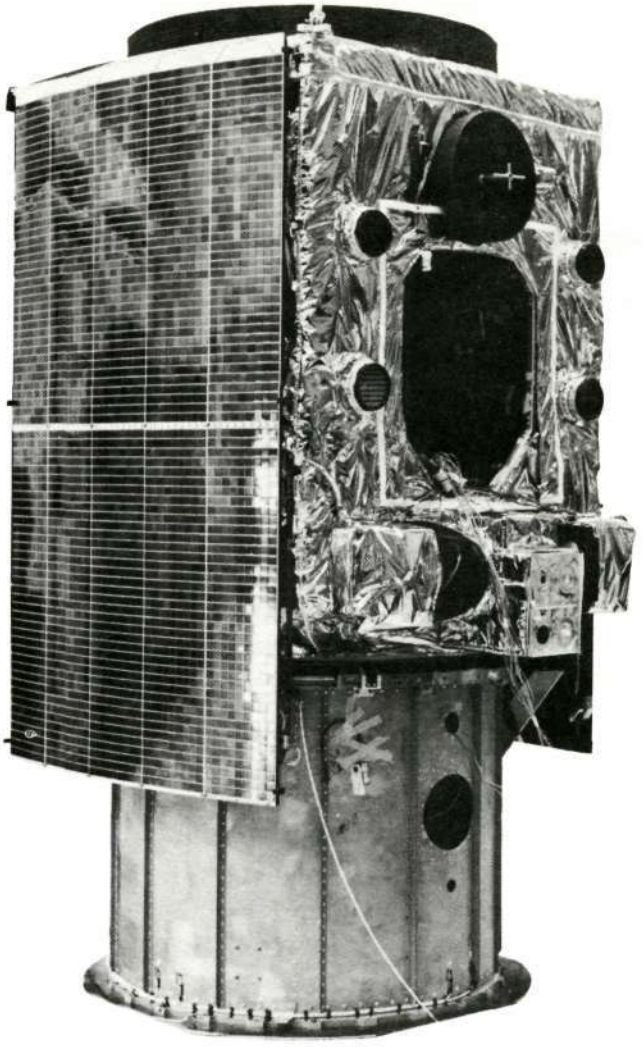

Figure 3-VII-2. TIROS M in Separation Shock Test

For flight acceptance the spacecraft must pass both vibration and thermal-vacuum testing. The spacecraft must be subjected to a three-phase vibration test: resonant survey, sinusoidal sweep, and random exposure. The resonant survey test is conducted at a relatively low level to study the response characteristics of the overall spacecraft, and, specifically, certain critical components within the integrated vehicle. Then the spacecraft is exposed to the flight acceptance test levels; the spacecraft is subjected to an acceptance level vibration test and a thermal-vacuum test cycle to ensure against latent material and manufacturing process defects. Successful completion of these two test phases results in acceptance of the spacecraft for launch. Sinusoidal and vibration test levels are given in Table 3-VII-2. The spacecraft is shown in Figure 3-VII-3 mounted on the vibration test fixture.

TABLE 3-VII-2. SPACECRAFT VIBRATION TEST REQUIREMENTS

FLIGHT ACCEPTANCE SINE LEVELS IN THRUST, (Z-Z), AXIS			
Frequency (Hz)	Duration (min)	Level rms (0 to pk)	Sweep Rate (oct/min)
5-11	0.28	0.48 in. da.	4
11-17	0.16	2.1 ±3.0 g	4
17-23	0.18	3.2 ±4.5 g	3
23-200	0.78	1.6 ±2.3 g	4

FLIGHT ACCEPTANCE SINE LEVELS IN LATERAL AXES, (X-X)* AND (Y-Y)*			
Frequency (Hz)	Duration (min)	Level rms (0 to pk)	Sweep Rate (oct/min)
5-7.5	0.15	0.53 in. da.	4
7.5-200	1.18	1.1 ±1.5 g	4

FLIGHT ACCEPTANCE RANDOM VIBRATION LEVELS FOR EACH OF THREE AXES (Y-Y), (X-X), and (Z-Z)			
Frequency (Hz)	PSD Level (g^2/Hz)	Acceleration g-rms	Duration (min/axis)
20-275	0.0023 to** 0.068	11.2	2
275-2000†	0.068	11.2	2

* The maximum input level is limited by response accelerometers located near the cg of the spacecraft. The accelerometers are connected into the servo loop. During the sweep, if any one of the selected accelerometers reaches the pre-set response limit, it assumes control of the exciter input. The limit accelerometers control the response through the first major structure resonance,

** Increasing from 20 Hz at a rate of 4 dB per octave,

† The filter roll-off characteristic above 200 Hz is at a rate of 40 dB per octave or greater.

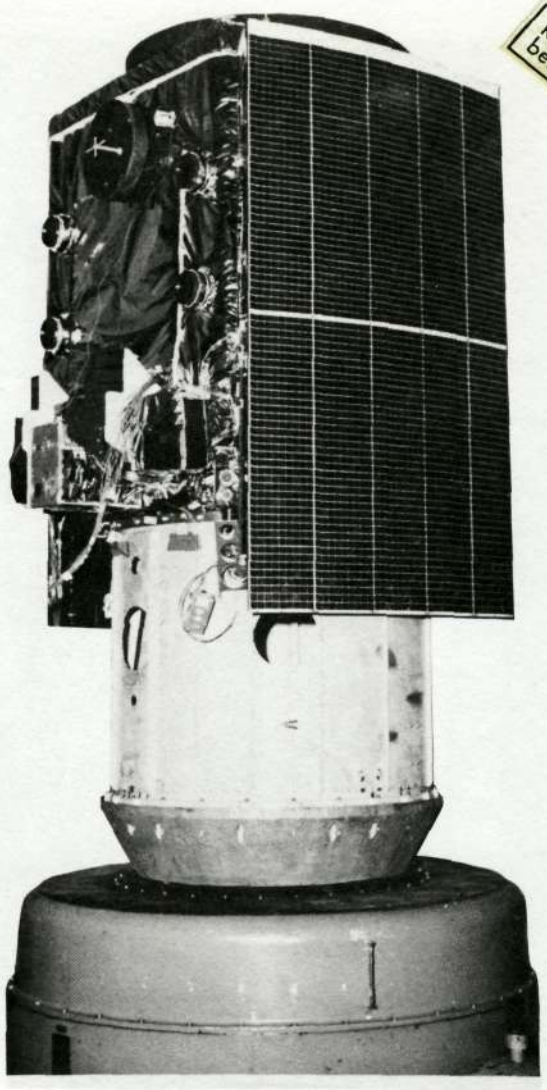

Figure 3-VII-3. TIROS M on Vibration Table

1. Vibration

Vibration of the spacecraft was performed on July 17, with one malfunction; scanning radiometer processor 2, Ser. No. 04, had a shorted 5-volt calibrator. The box cover nut plate was shorting a 5-volt zener diode. The cover was replaced with a modified one, which corrected the fault. After spacecraft vibration, a solar panel deployment test was performed. Following the deployment test, the panels were removed from the spacecraft and thermal-vacuum and illumination testing of the three solar panels was conducted. Figure 3-VII-4 shows the solar panels in the thermal-vacuum chamber.

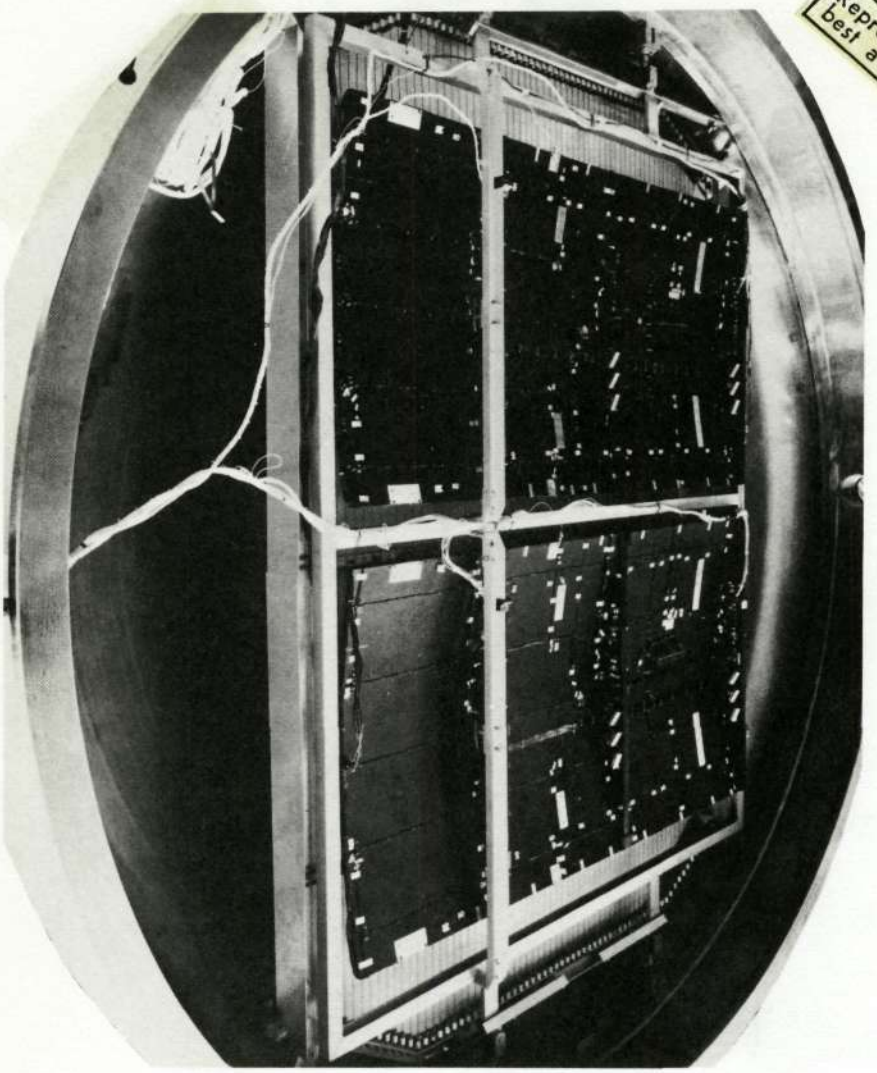

Figure 3-VII-4. Flight Model Solar Panels in Thermal-Vacuum Chamber

Post-vibration abbreviated SEPET was performed on July 19 and 20. During this test, AVCS recorder 2 exhibited 1-millisecond dropouts on picture 12. These dropouts were not repeatable, and recorder performance was considered satisfactory.

2. Thermal-Vacuum Tests

To ensure qualification, the spacecraft is exposed to a thermal-vacuum profile that subjects it to thermal stress. The profile is shown in Figure 3-VII-5.

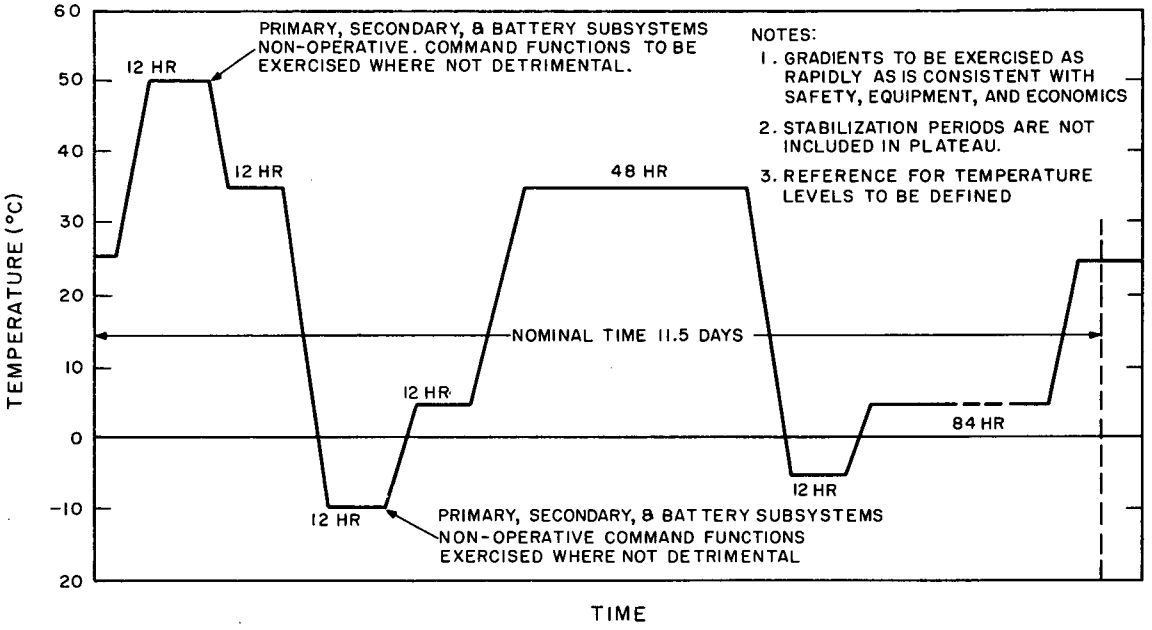

Figure 3-VII-5. Thermal-Vacuum Test Profile

As a preliminary to the thermal vacuum tests, a pin-puller firing test was successfully performed in vacuum using the spacecraft command and firing circuitry.

a. THERMAL SURVEY

The first thermal sequence was a thermal survey on July 22 and 23. The following anomalies were encountered.

(1) The real-time output of the SPM (Ser. No. 04) count for word 65 ranged from 26 to 42. The specification called for 224 ± 160. The fault was electromagnetic interference into the SPM test suitcase.

(2) S-band transmitter 2 (Ser. No. 013) had an indicated power drop due to faulty instrumentation.

(3) Beacon transmitter 2 (Ser. No. 010) power measured 13 dB below normal. This was caused by the regulator selection switch toggling the beacon RF switch so that the selected beacon became uncoupled from the beacon and command antenna, thus causing the low output. Repeated tests of beacon selection showed that no damage resulted from this event and that there was no tendency for the problem to recur, as long as regulator switching did not take place. Since regulator switching is an infrequent operation in orbit, and since the anomaly can be easily remedied in orbit if it should occur, no changes were made as a result of this investigation. The problem was, however, duly noted in the Programming and Control Handbook.

b. FLIGHT ACCEPTANCE TESTS

Flight acceptance thermal-vacuum tests commenced on July 25. Cycling comprised:

Temperature	Duration (Hours)
+35°C	24
- 5°C	24
+40°C	24
0°C	48

Duration total was 290 hours including transitions. (The spacecraft is shown being removed from the thermal chamber in Figure 3-VII-6.)

The following discrepancies appeared:

(1) At 25°C, a pressure burst caused spacecraft and console shutdown. The cause was considered to have been a delayed outgassing of some unspecified object in the chamber. The event caused no damage to the spacecraft.

(2) At 25°C, an inconsistency in real-time transmitter temperature telemetry was noted. This was caused by an incorrect test method, which was changed.

(3) At 25°C and 35°C, AVCS camera recorder caused a several-line dropout in picture 10. This dropout was not repeatable and the recorder was considered to be functioning properly.

(4) At 28°C, the solar proton monitor Ser. No. 004 had an incorrect word, resulting from EMI into the test suitcase.

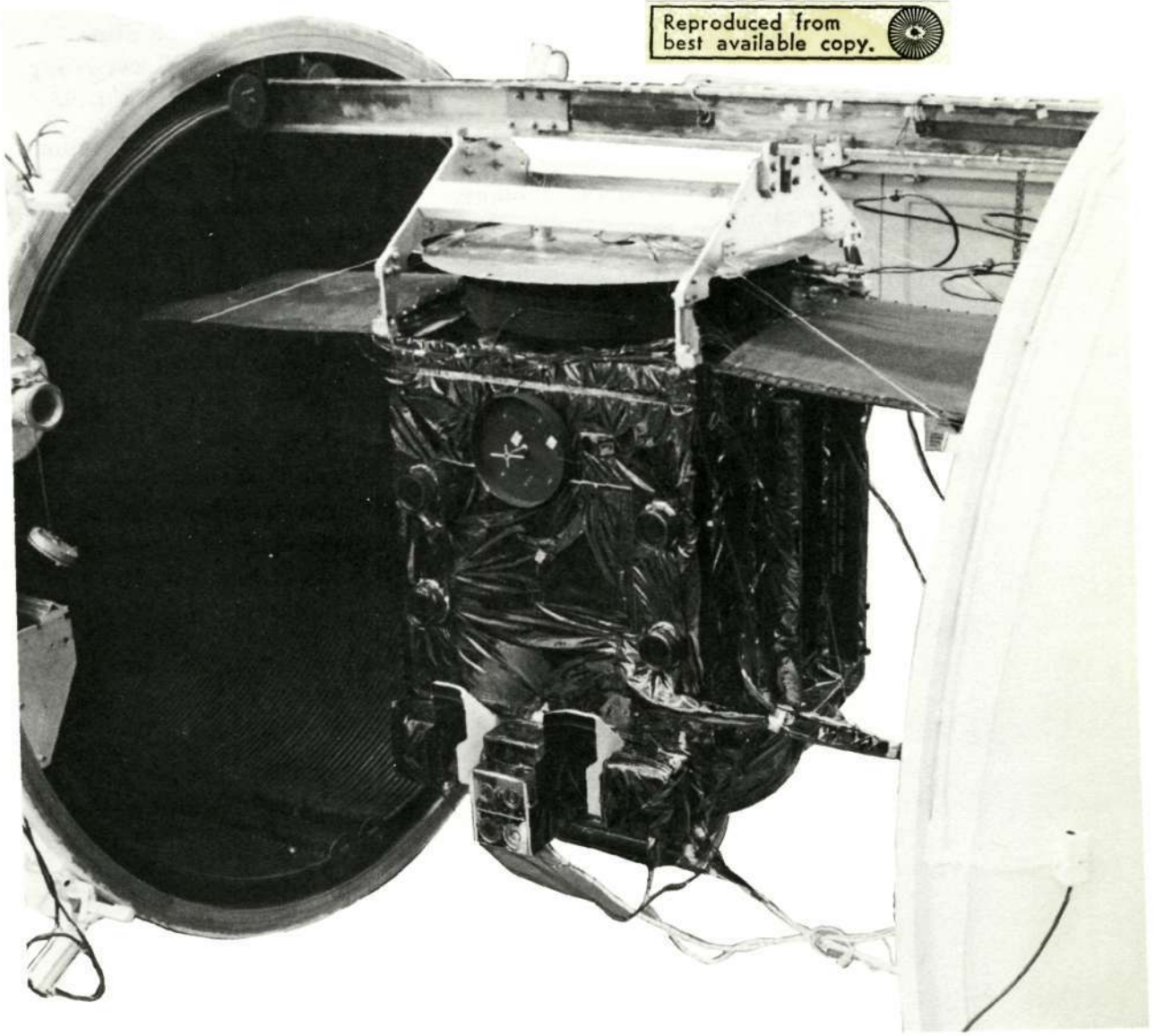

Figure 3-VII-6. TIROS M Being Removed From the 8-Foot Thermal-Vacuum Chamber

(5) At 40° C, oscillations of 3 to 5 kHz occurred in scanning radiometer recorder 2 at the beginning of playback. The SRR was replaced although the incident was not repeatable.

(6) At 40°C, beacon subcarrier oscillator 2 voltage-to-frequency transfer curve shifted. The frequency was reset.

(7) On July 27, at temperature -5°C, the flat plate radiometer words 1 and 2 had an incorrect count (194 instead of 460 to 480 ±50). The FPR was replaced and returned to the University of Wisconsin.

(8) At 0°C, scanning radiometer recorder Ser. No. 04 was slow starting, taking 12 seconds to reach proper speed. SR recorder Ser. No. 04 was replaced on August 9 by SR recorder Ser. No. 05.

(9) At -5°C, reduction of time code in orbit 2 revealed a 3.25-second discrepancy between time base unit 2 time and GSE clock time. EMI was suspected; the anomaly was overcome by command programming.

(10) On July 31, at 40°C, beacon subcarrier oscillator 2 voltage-to-frequency curve shifted; the SCO was retuned.

(11) On August 4 at -5°C, command receiver 2 sensitivity was out of specification, caused by a local oscillator shift due to temperature change. The test procedure had not taken this into account.

(12) At 0°C, playback of AVCS camera 2, recorder 2 data showed a dropout in picture 9. On previous occasions, five dropouts of less than 1-millisecond duration each were observed. These dropouts were random and did not indicate tape damage or recorder degradation.

(13) On August 5, thermal-vacuum tests were interrupted because of a sudden decrease in speed of the MWA, and the spacecraft was removed from the chamber. This deceleration occurred soon after the MWA was turned on following a period during which the spacecraft was held at cold temperatures. Investigation of the anomaly showed the most probable cause to be interference between a teflon ring in the MWA and the T-plate that carries the horizon crossing sensors. The interference is caused by hoop-stress deformation of the ring, the deformation occurring when the ring shrinks at extremely cold temperatures.

The condition was corrected by the use of a teflon ring made in eight segments. The segmented ring was incorporated on the MWA (Ser. No. 06) which was installed on the spacecraft on August 9, and thermal tests were resumed.

While the spacecraft was out of the thermal chamber, DET was conducted on the flat plate radiometer with no problems. On August 7, investigation of AVCS dropout was conducted. A total of 176 pictures were taken with both cameras. Played back data showed one small dropout in both ground stations and one dropout in one station but not in the other.

On August 8 and 9, DET was performed satisfactorily on the pitch control subsystem. MWA alignment was performed satisfactorily on August 9. DET was performed on SR recorder 2 (Ser. No. 05) successfully, also on August 9.

c. RESUMPTION OF THERMAL-VACUUM TESTS

Thermal-vacuum acceptance tests were resumed on August 9 and lasted through August 26. This cycling consisted of:

Temperature	Duration (Hours)
+40° C	12
0° C	12
5° C	29
+15° C	120
+20° C	30
+25° C	48
+40° C	12
0° C	12

Total thermal-vacuum cycling for this sequence was 366 hours including transitions. The tests were completed after the following problems were resolved.

(1) At 40°, 0°, and 25° C, APT camera contained black lines in readout. The camera was replaced later, on September 2, after failure of the vidicon tube.

(2) At 40° C, flat plate radiometer words 1 and 2 read incorrectly. This anomaly resulted from misinterpretation of calibration data supplied by the University of Wisconsin and not a failure.

On August 26, the spacecraft was removed from the thermal-vacuum chamber. A strain gage assembly was installed on the momentum flywheel. During a check of the telemetry polarity, the strain gage caused the telemetry to decrease toward zero as the motor commutator moved from a high spot to a low spot. This indicated motor brush wear. The strain gage wiring was changed to correct this. This change reversed the polarity of the strain gage to the amplifier unit allowing the correct increasingly more negative telemetry readings with brush wear.

On August 28, a strain gage amplifier compatibility check was conducted to evaluate strain gage interference with spacecraft cameras. APT camera 1 had an open filament in its vidicon tube. This camera had exhibited other trouble during thermal-vacuum tests and was replaced on September 2.

On August 28, command distribution unit Ser. No. 02 and power supply electronics Ser. No. 03 were removed and modified; they checked out satisfactorily on September 2.

The MWA (Ser. No. 06) was removed and the teflon bumper was reworked. The MWA was reinstalled and checked out satisfactorily on September 3.

d. SPECIAL BLANKET THERMAL TESTS

On September 7, thermal tests were conducted on the TIROS M spacecraft for the operational 30-degree and 60-degree beginning-of-life cases. During the first phase of the tests, all equipment except the two scanning radiometers ran close to the 127-body predicted temperatures; the radiometers ran approximately 12° to 14° C colder than predicted. To correct this condition, conductive coupling between the radiometers and the structure was increased. This change, in turn, required the closing of portions of the spacecraft radiating areas to maintain heat balance. Before the tests were rerun with the changes in configuration, temperature predictions were computer analyzed. The second phase of testing was completed with satisfactory results, all test temperatures matching the analytical predictions within a 3° C spread.

D. FINAL CALIBRATION*

The final calibration phase was performed during the period September 6 to October 4, 1969. These tests comprised the final check of system parameters and the detailed measurements to provide calibrated transfer functions. Final mechanical measurements were performed and included sensor alignment and moment-of-inertia, center-of-gravity, and spacecraft weight measurements. The major tests performed during final calibration are listed below, in roughly chronological order.

- Magnetic dipole check
- SEPET
- Battery capacity test
- Camera calibration
- SR calibration
- SPM and FPR calibration
- Sensor alignment check
- RF testing
- Fine balancing
- Moment-of-inertia and center-of-gravity measurements and final weighing

---

* For a complete report of final calibration see: RCA Corporation, Astro-Electronics Division, Alignment and Calibration Data for the TIROS M Meteorological Satellite. AED R-3468, revised December 19, 1969.

1. Magnetic Dipole Check

On September 20 and 21, the magnetic dipole moments for the various spacecraft operating modes were measured. The results are given in Table 3-VII-3. A trimming magnet having a magnetic dipole moment of +0.8631 ampere-turn-meter^2 (atm^2) was installed on the spacecraft on September 21 to produce a net spacecraft dipole moment of +0.7913 atm^2. With the trimming magnet in place, the magnetic dipole moments for the side 2 nighttime operating mode, QOMAC positive, and momentum coils were measured. The results of these measurements are listed in Table 3-VII-4.

TABLE 3-VII-3. MEASURED MAGNETIC DIPOLE MOMENTS, UNCOMPENSATED (BEFORE ADDITION OF TRIMMING MAGNET)

Operating Mode	Magnetic Moment (ampere-turns-meters^2)		
	X-Axis	Y-Axis	Z-Axis
Spacecraft Power Off (residual spacecraft dipole)	+0.9079	+0.3170	+0.3225
Side 1 Day Operation	+1.073	+0.4567	-0.0806
Side 1 Night Operation (charger)	+1.037	+0.2973	-0.03822
Side 2 Day Operation	+-.9633	+0.4324	-0.0298
Side 2 Night Operation	+0.9026	+0.3622	-0.0718

TABLE 3-VII-4. MEASURED MAGNETIC DIPOLE MOMENTS, COMPENSATED (TRIMMING MAGNET ADDED)

Operating Mode	Magnetic Moment (ampere-turns-meters^2)		
	X-Axis	Y-Axis	Z-Axis
QOMAC Positive	+ 0.9001	+0.2328	+4.6453
Momentum Coils (Negative)	+22.892	+1.2113	+0.3963
Side 2 Night Operation	+ 0.9418	+0.334	+0.7913

2. Standard Electrical Performance Evaluation Test (SEPET)

The purpose of this SEPET is to demonstrate the satisfactory performance of the spacecraft through a combination of major operational modes. The detailed measurements required to demonstrate spacecraft integrity are made during the simulated orbits. The TIROS M SEPET program was performed successfully on September 22.

3. Battery Capacity Test

A comparison of battery capacity test results, run on September 24, with earlier capacity tests, indicated a possible small reduction in the capacity of both battery packs. However, a review of battery test data showed all battery parameters to be normal and capable of meeting mission requirements. The capacity measurements differed since there were three preconditioning cycles in the earlier capacity test but only two in this final test.

4. Camera Calibration

Camera calibration was performed during September 24 and 25.

a. AVCS CALIBRATION

The scan formats for the AVCS cameras 1 and 2 are shown in Figures 3-VII-7 and 3-VII-8. The field-of-view of each of the AVCS cameras has been adjusted to 89 ±1 degrees. This is the angle subtended by the scanned area in the direction of the horizontal scan through the center of the picture. The effective focal lengths of the AVCS cameras are 5.8 millimeters for camera 1 and 5.9 millimeters for camera 2.

The distortion of the original scene caused by the AVCS lens, camera scan, and kinescope reproduction is determined from prints of test photographs of the kinescope screen while the system is imaging an accurately surveyed target. Camera orientation during the making of the test photographs and the camera scan directions as projected onto the target are shown in Figure 3-VII-9. The distortion photographs for AVCS cameras 1 and 2 are direct (not via tape) pictures. They are reproduced in Figures 3-VII-10 and 3-VII-11. Although the direct AVCS pictures are inverted as they appear on the kinescope screen, they are presented right-side-up here.

Camera response to radiant energy is shown in Figure 3-VII-12 and 3-VII-13. This data was taken using a light source that has very nearly the same spectral content as sunlight emerging from two atmospheres. The spacecraft was at room temperature for these tests.

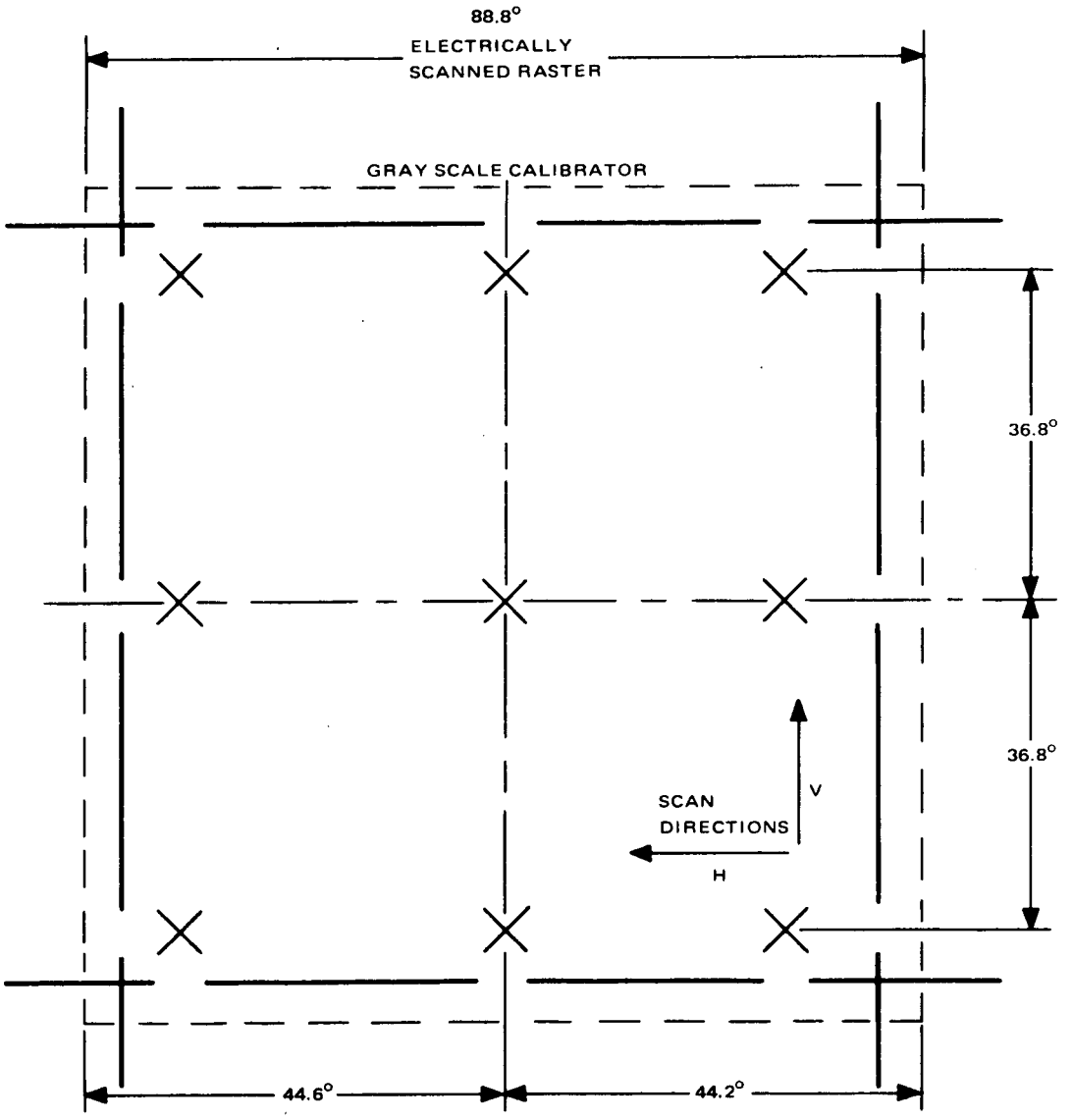

START OF HORIZONTAL SWEEP TO CENTER OF TARGET:	44.2°
CENTER OF TARGET TO END OF HORIZONTAL SWEEP:	44.6°
TOTAL:	88.8°
BOTTOM RETICLE MARK TO CENTER OF TARGET:	36.8°
CENTER OF TARGET TO TOP RETICLE MARK:	36.8°
CENTER OF TARGET TO CENTER FIDUCIAL:	
HORIZONTAL:	0°
VERTICAL:	0°

Figure 3-VII-7. AVCS Camera 1 Scan Format

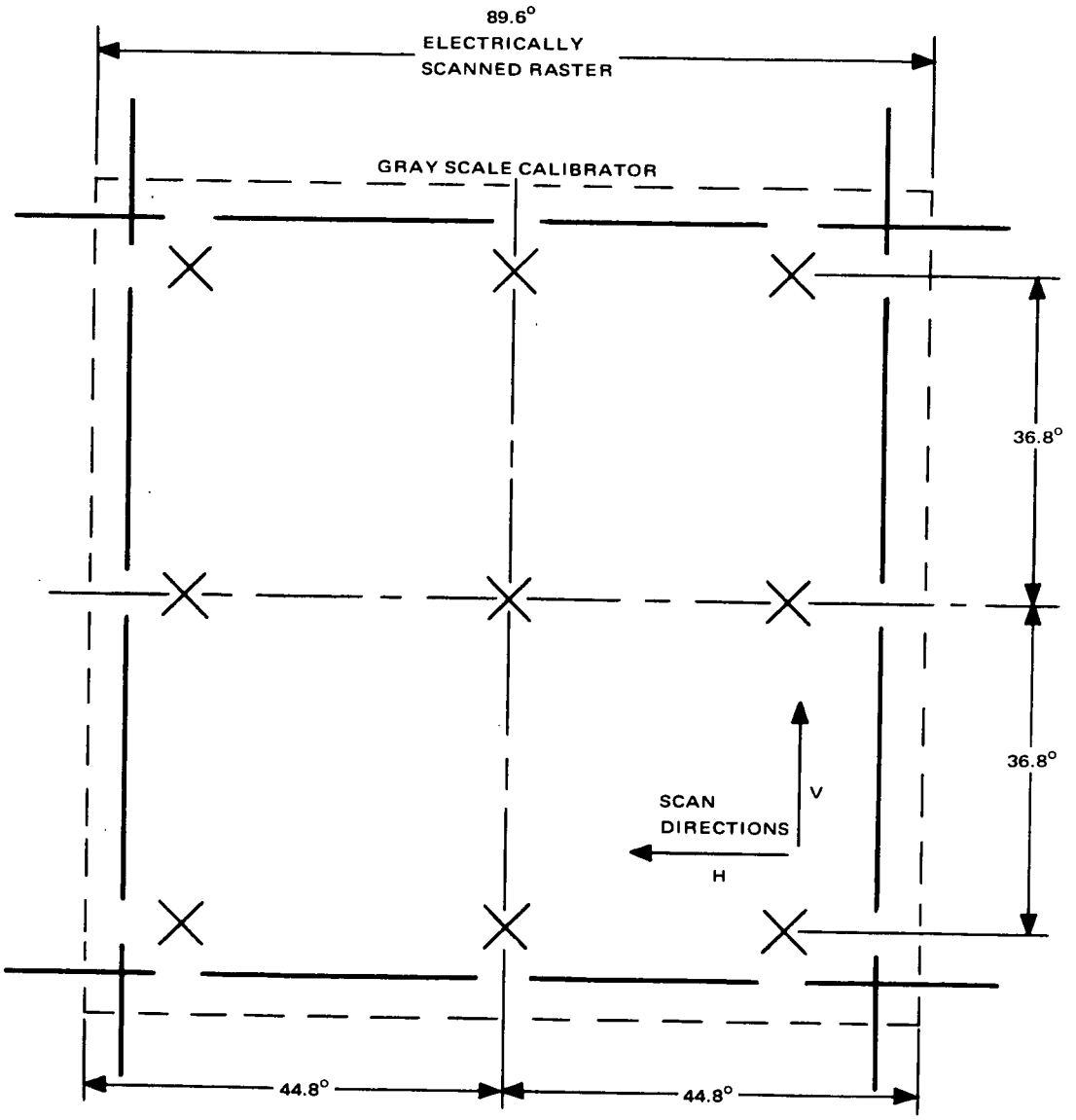

START OF HORIZONTAL SWEEP TO CENTER OF TARGET: 44.8°
CENTER OF TARGET TO END OF HORIZONTAL SWEEP: 44.8°

TOTAL: 89.6°

BOTTOM RETICLE MARK TO CENTER OF TARGET: 36.8°
CENTER OF TARGET TO TOP RETICLE MARK: 36.8°
CENTER OF TARGET TO CENTER FIDUCIAL:

HORIZONTAL: 0°
VERTICAL: 0°

Figure 3-VII-8. AVCS Camera 2 Scan Format

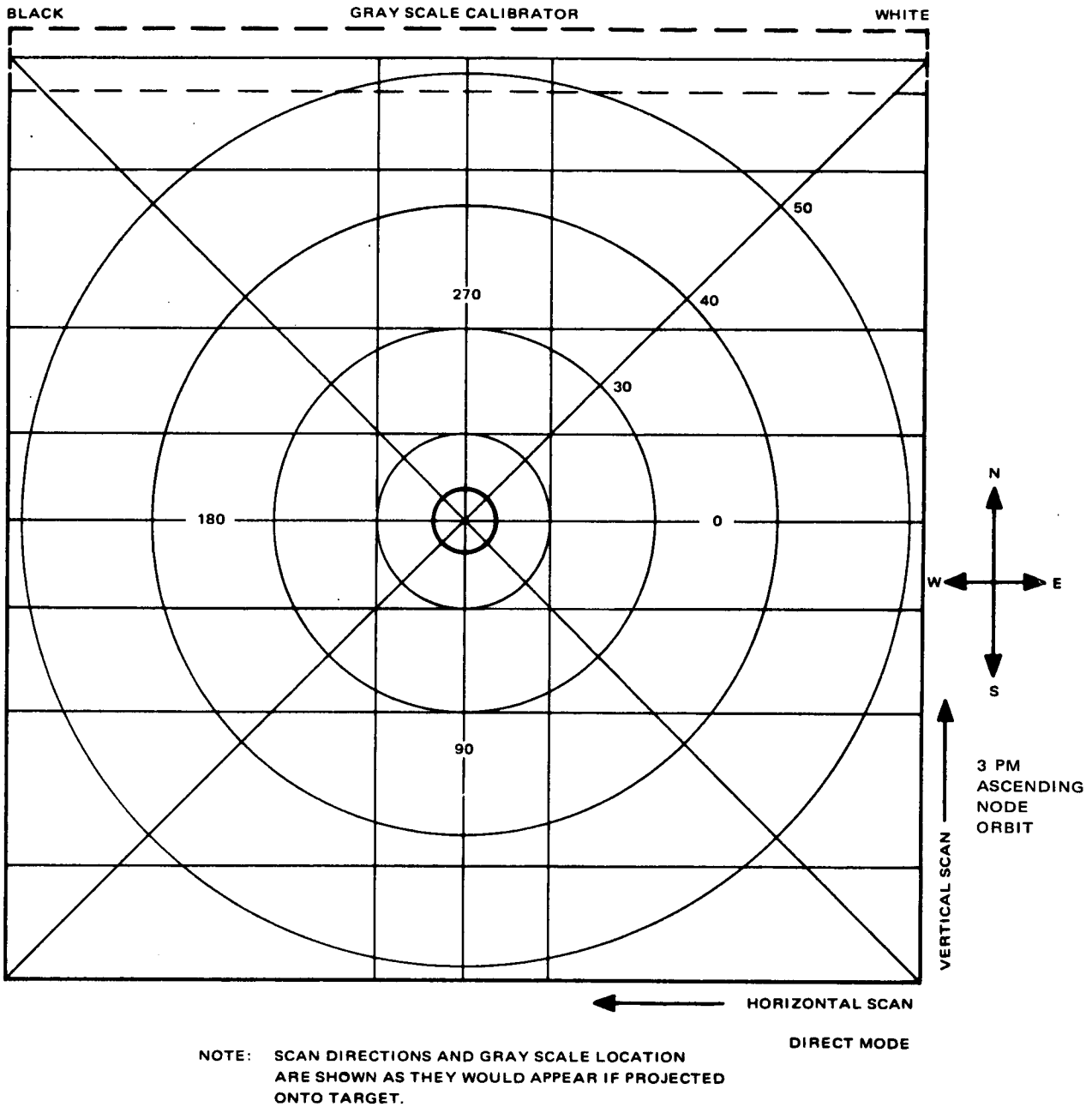

Figure 3-VII-9. Orientation of AVCS Cameras for Distortion Photographs

4

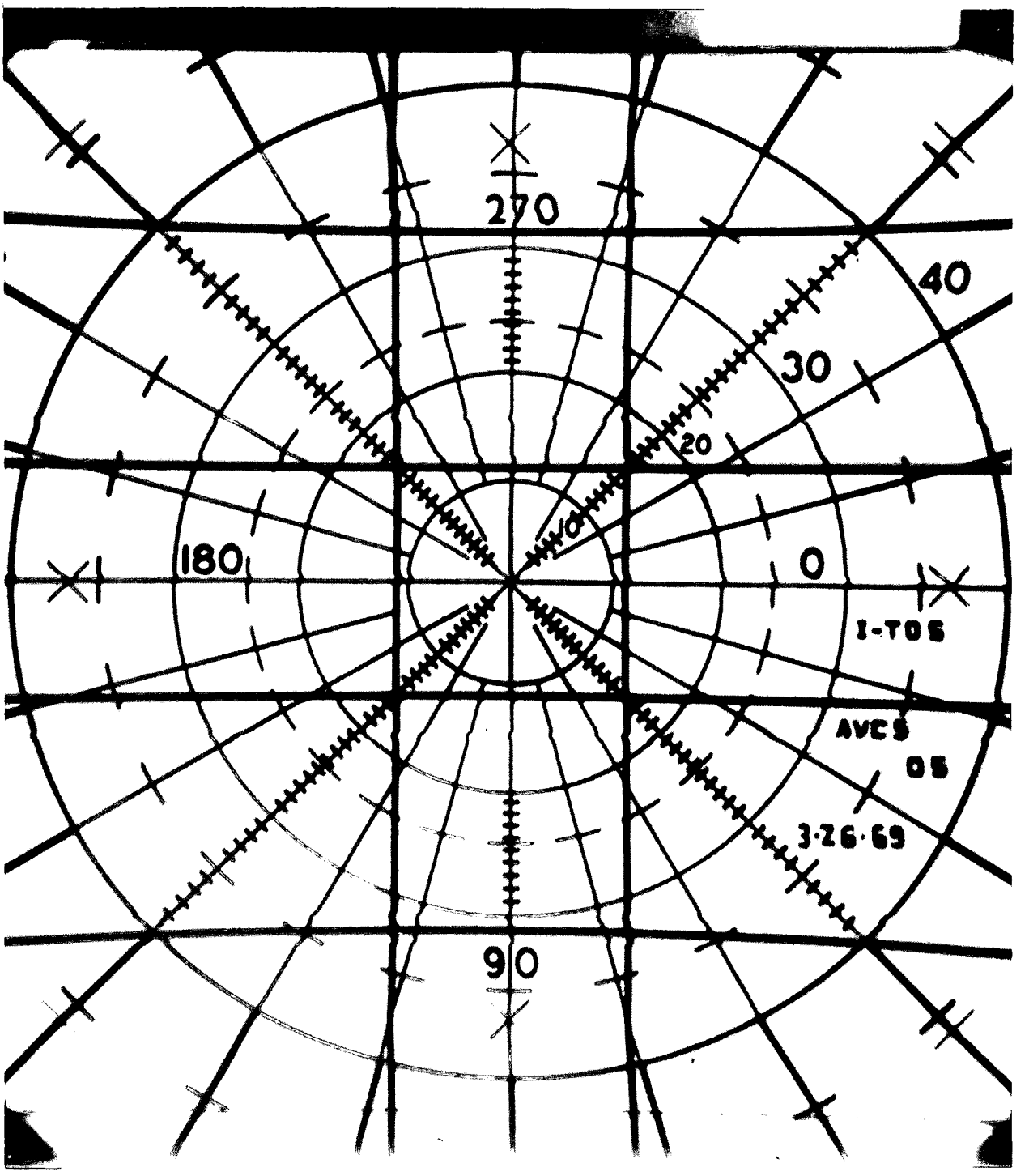

Figure 3-VII-10. AVCS Camera 1 Distortion Calibration Photograph

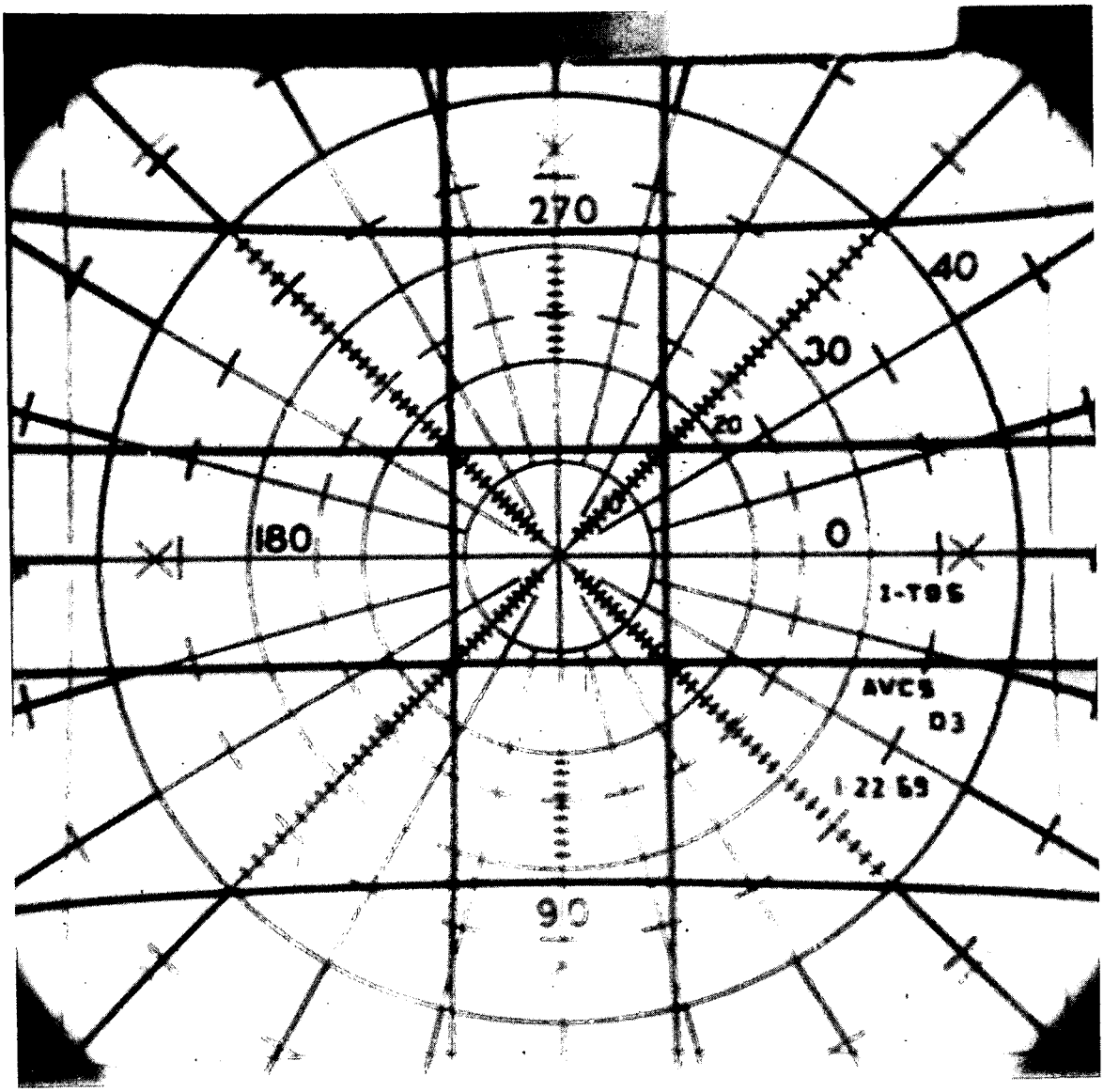

Figure 3-VII-11. AVCS Camera 2 Distortion Calibration Photograph

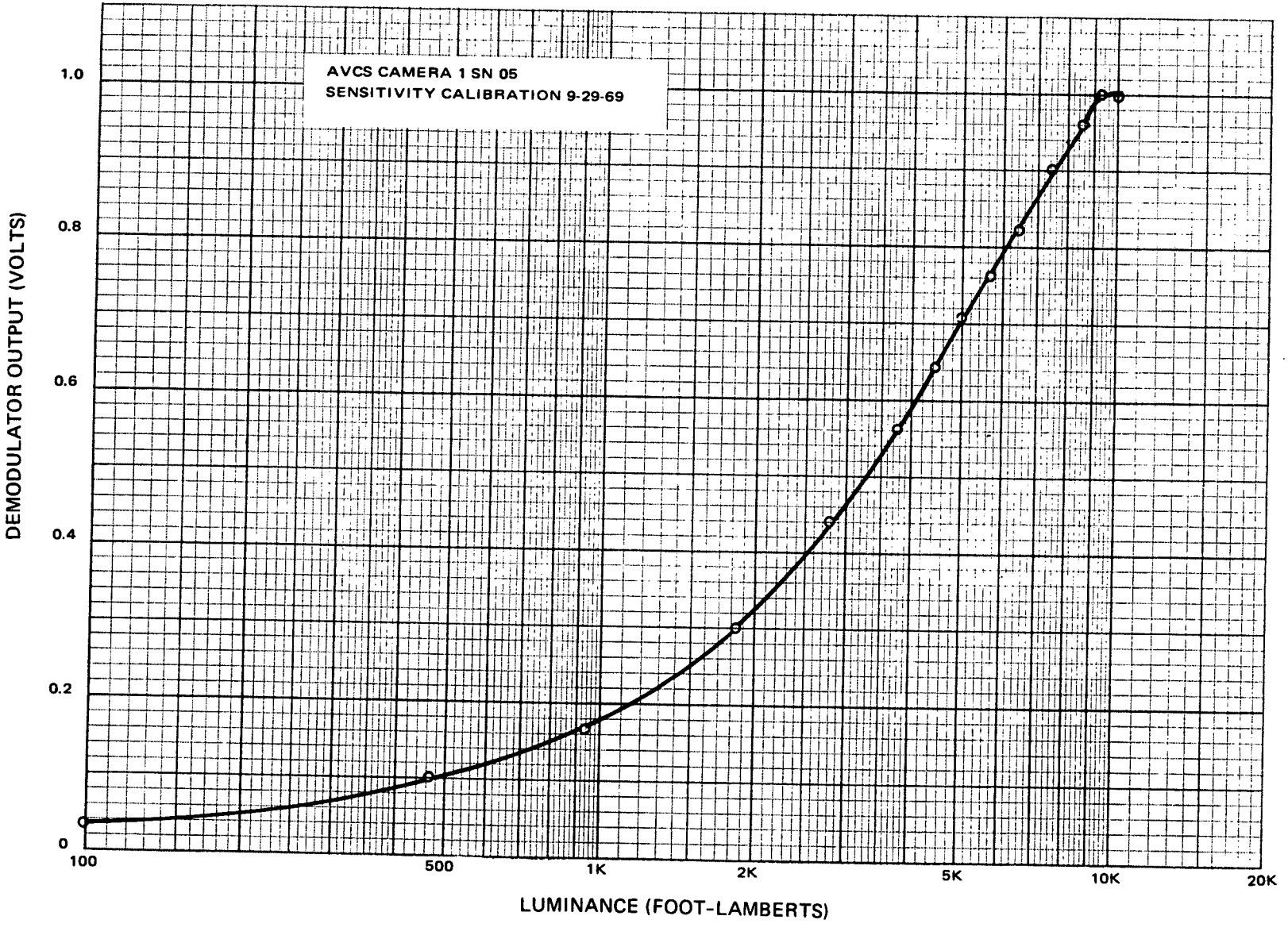

Figure 3-VII-12. AVCS Camera 1 Sensitivity Calibration Curve

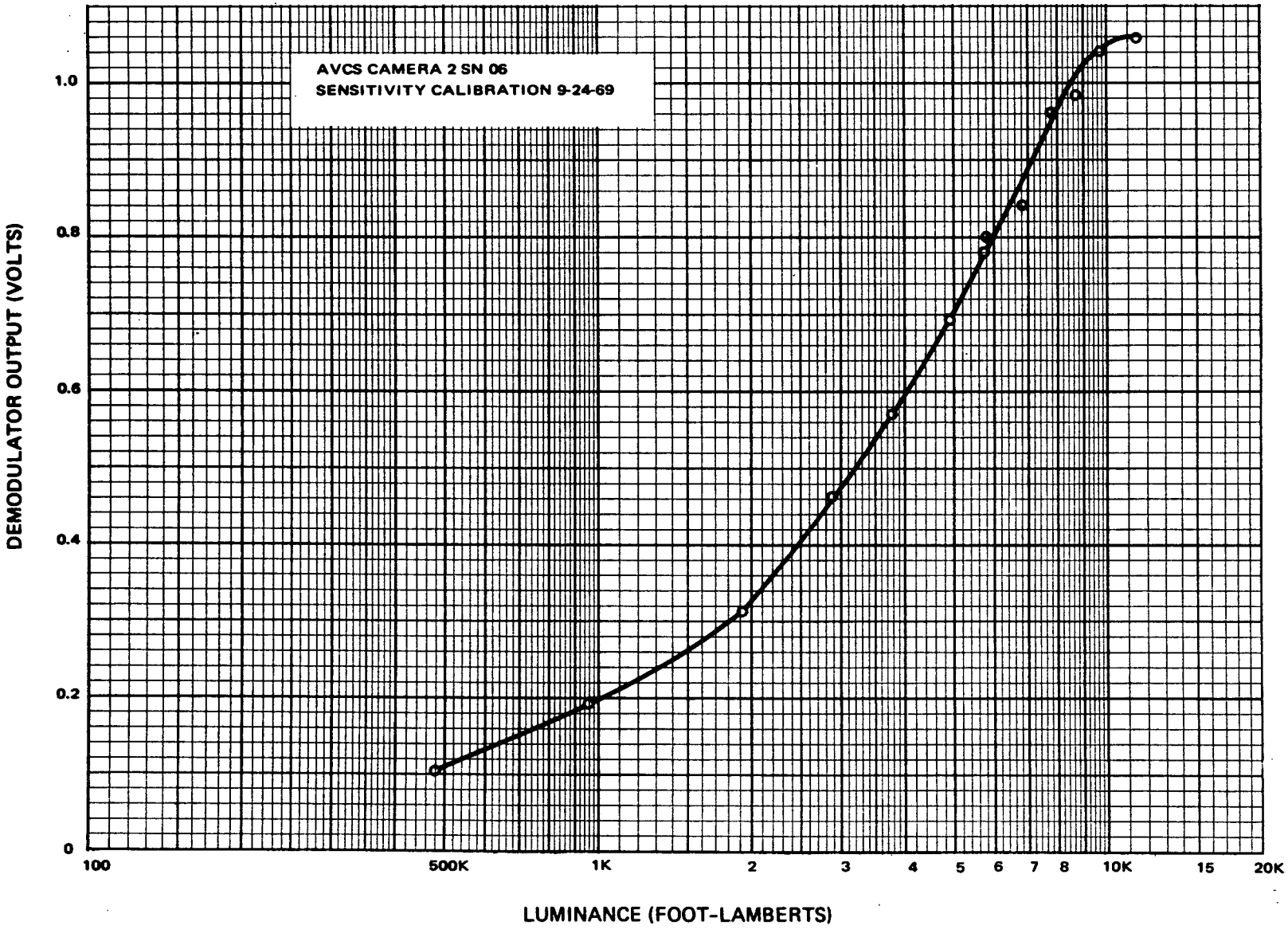

Figure 3-VII-13. AVCS Camera 2 Sensitivity Calibration Curve

b. APT CALIBRATION

The scan formats for APT cameras 1 and 2 are shown in Figures 3-VII-14 and 3-VII-15. The field-of-view of each camera was adjusted to 89 ±1 degrees. This is the angle subtended by the scanned area in the direction of the horizontal scan through the center of the picture. The effective focal length of both APT cameras is 5.95 millimeters.

APT distortion calibration photographs are made in the same manner as those for the AVCS cameras.

Orientation of the APT cameras with respect to the target for the distortion photographs is shown in Figure 3-VII-16. The camera scan directions are shown projected onto the target. Distortion photographs for APT cameras 1 and 2 are reproduced in Figures 3-VII-17 and 3-VII-18. The distance from the nodal point of the lens to the target was 58.45 inches for cameras 1 and 2. The distance from the front surface of the lens to the front nodal point was 1.32 inches for both cameras.

APT camera response to radiant energy is given in Figures 3-VII-19 and 3-VII-20. This data was taken using a light source that has very nearly the same spectral content as sunlight emerging from two atmospheres. The spacecraft was at room temperature for these measurements.

5. Scanning Radiometer Calibration

Calibration of the scanning radiometers (SR) is initially performed on the units by themselves and is verified during integrated spacecraft testing. For the original unit calibration data, refer to the "Data Book".* For the flight model TIROS M, serial number F-5 is scanning radiometer 1 and serial number F-3 is scanning radiometer 2.

The radiance calibration curves for the visible channels and infrared channels of the scanning radiometers are shown in Figures 3-VII-21 through 3-VII-24. The visible channels are calibrated in percent albedo.

While the IR channels are calibrated in degrees of scene temperature. The ordinate scale for all the curves is given in volts at the output of the radiometer. Albedo of 100 percent, as used in the calibration of the visible channels, is defined as the raliance reflected perpendicularly from a Lambertian surface having a reflectance of 1.0 that is positioned normal to the sun's rays and is

* "Data Book, Flight Model (F3 and F5), ITOS Scanning Radiometer"; Santa Barbara Research Center, Santa Barbara, California.

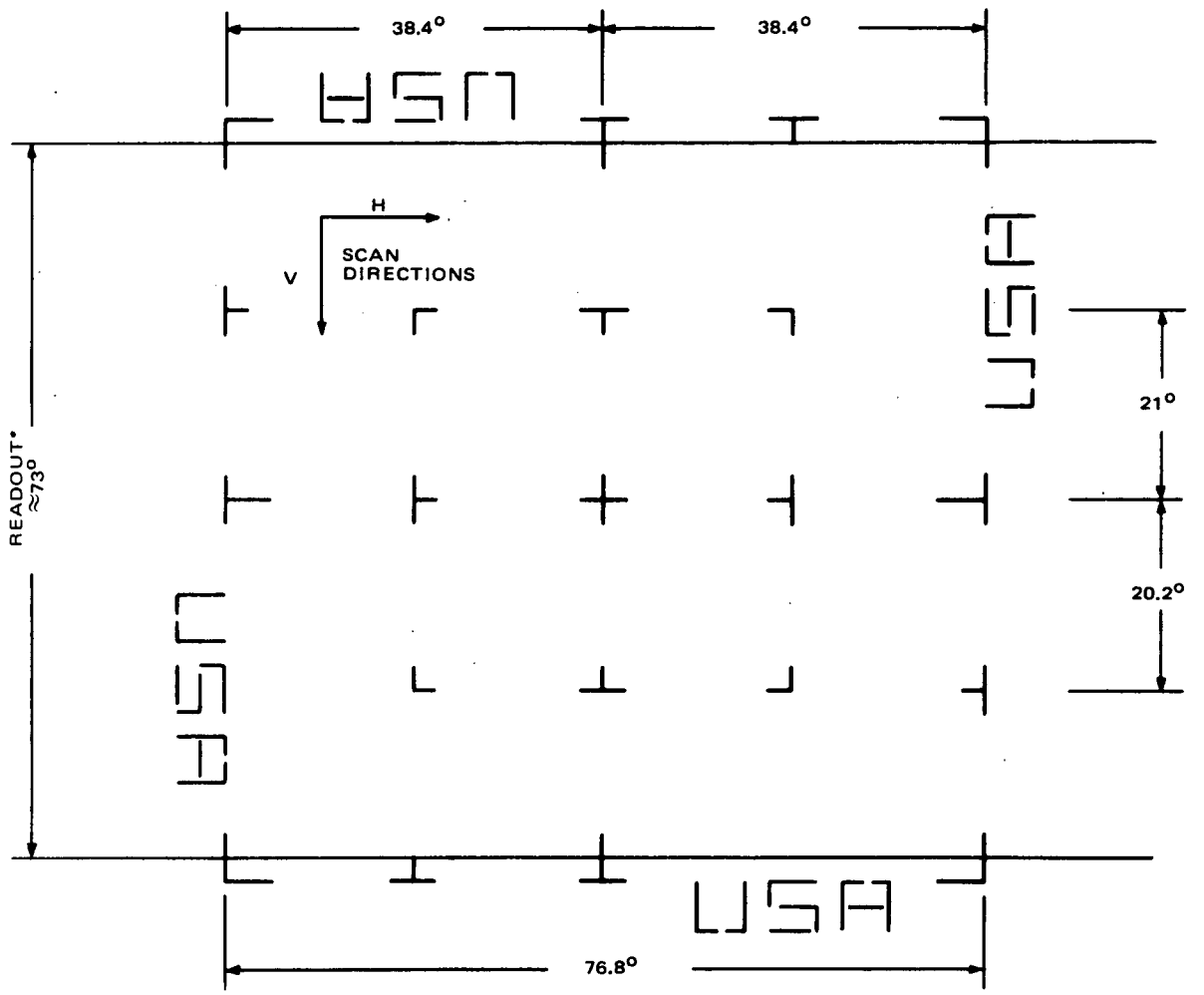

*THE READOUT LIMITS INDICATED IN THE DRAWING ARE THE APPROXIMATE LIMITS OF THE 600-LINE APT SCAN. THE PORTIONS OF THE RETICLE PATTERN OUTSIDE THE SCANNED AREA WILL NOT APPEAR IN THE APT PICTURES.

Figure 3-VII-14. APT Camera 1 Scan Format

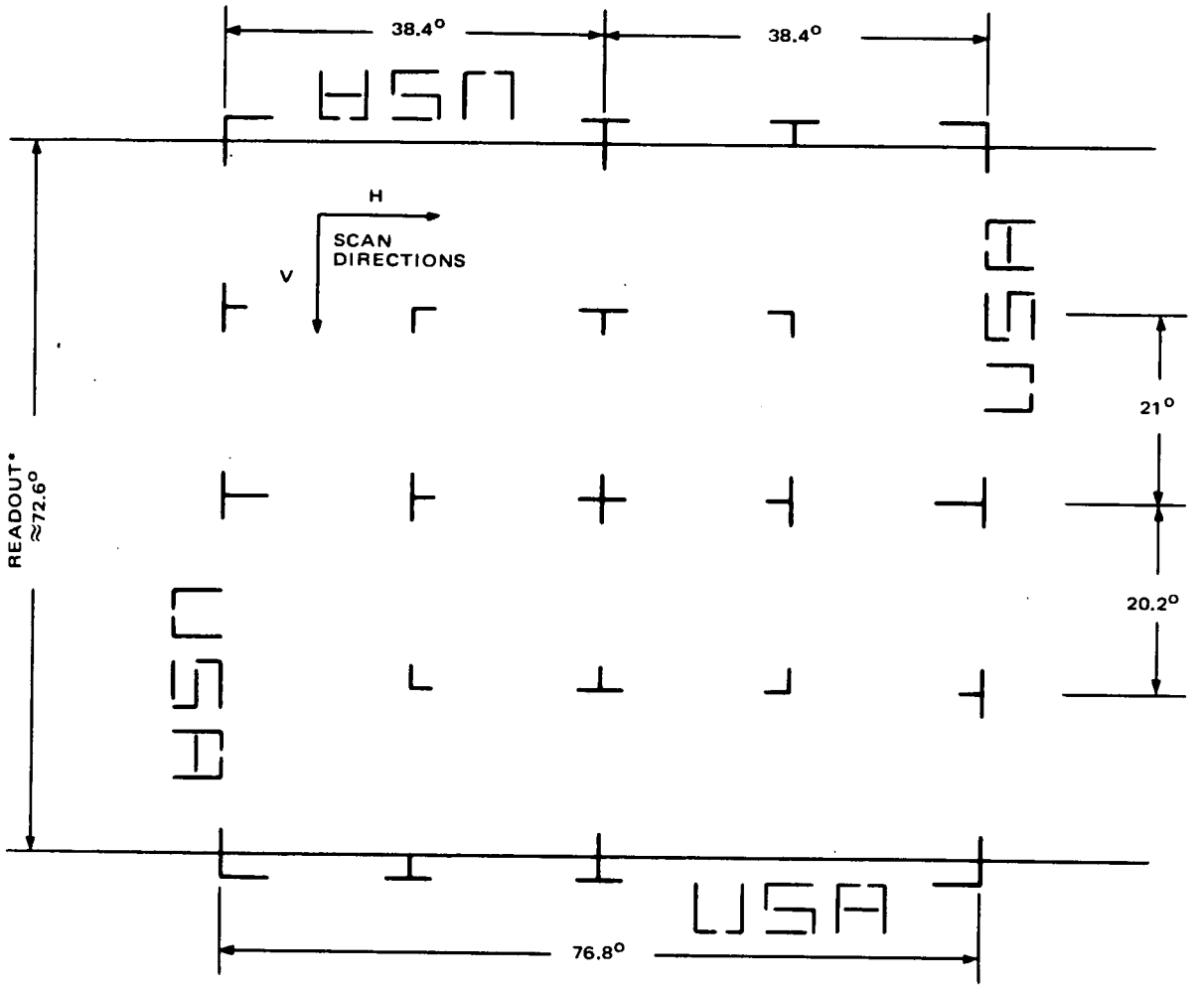

*THE READOUT LIMITS INDICATED IN THE DRAWING ARE THE APPROXIMATE LIMITS OF THE 600-LINE APT SCAN. THE PORTIONS OF THE RETICLE PATTERN OUTSIDE THE SCANNED AREA WILL NOT APPEAR IN THE APT PICTURES.

Figure 3-VII-15. APT Camera 2 Scan Format

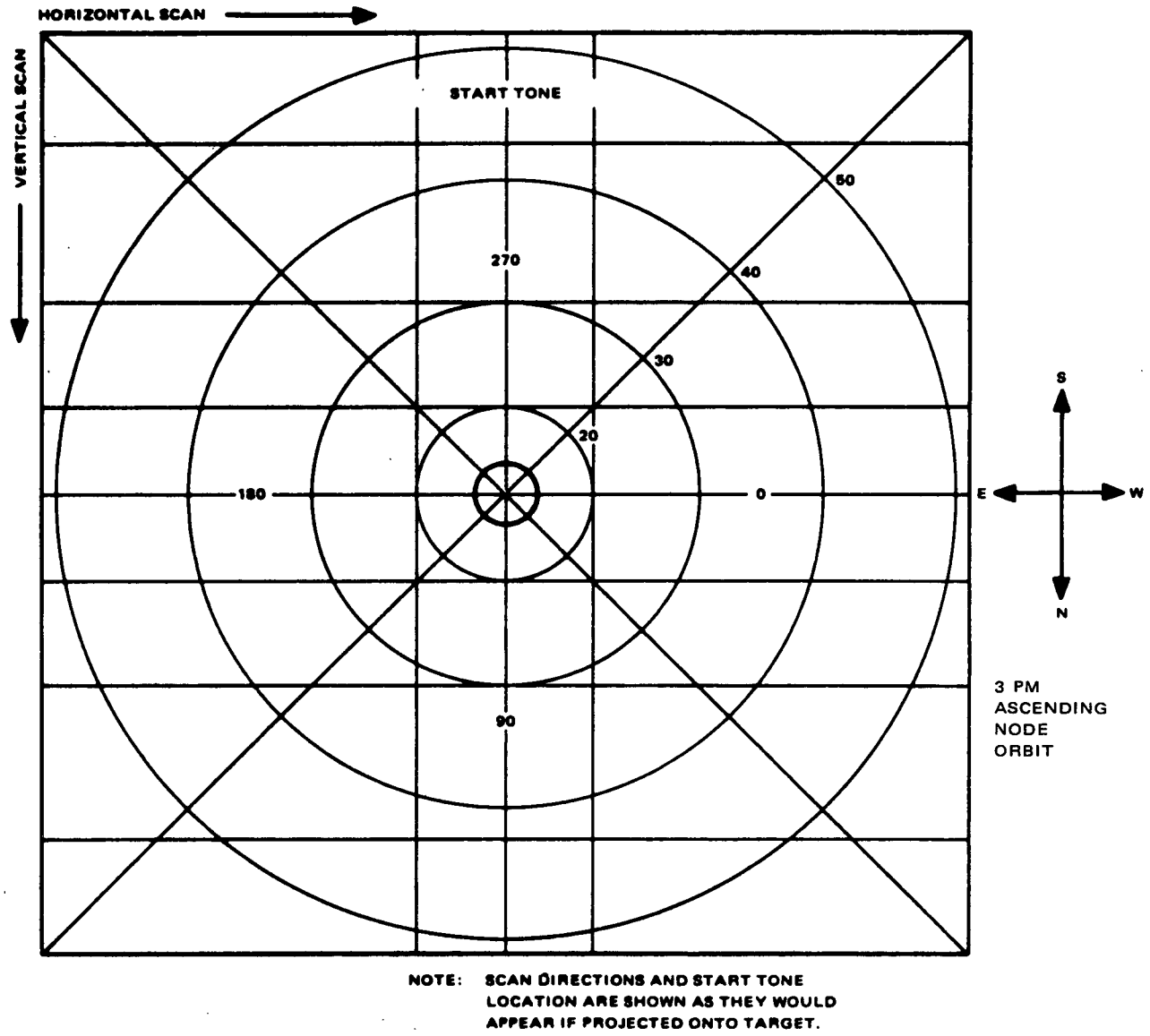

Figure 3-VII-16. Orientation of APT Cameras for Distortion Photograph

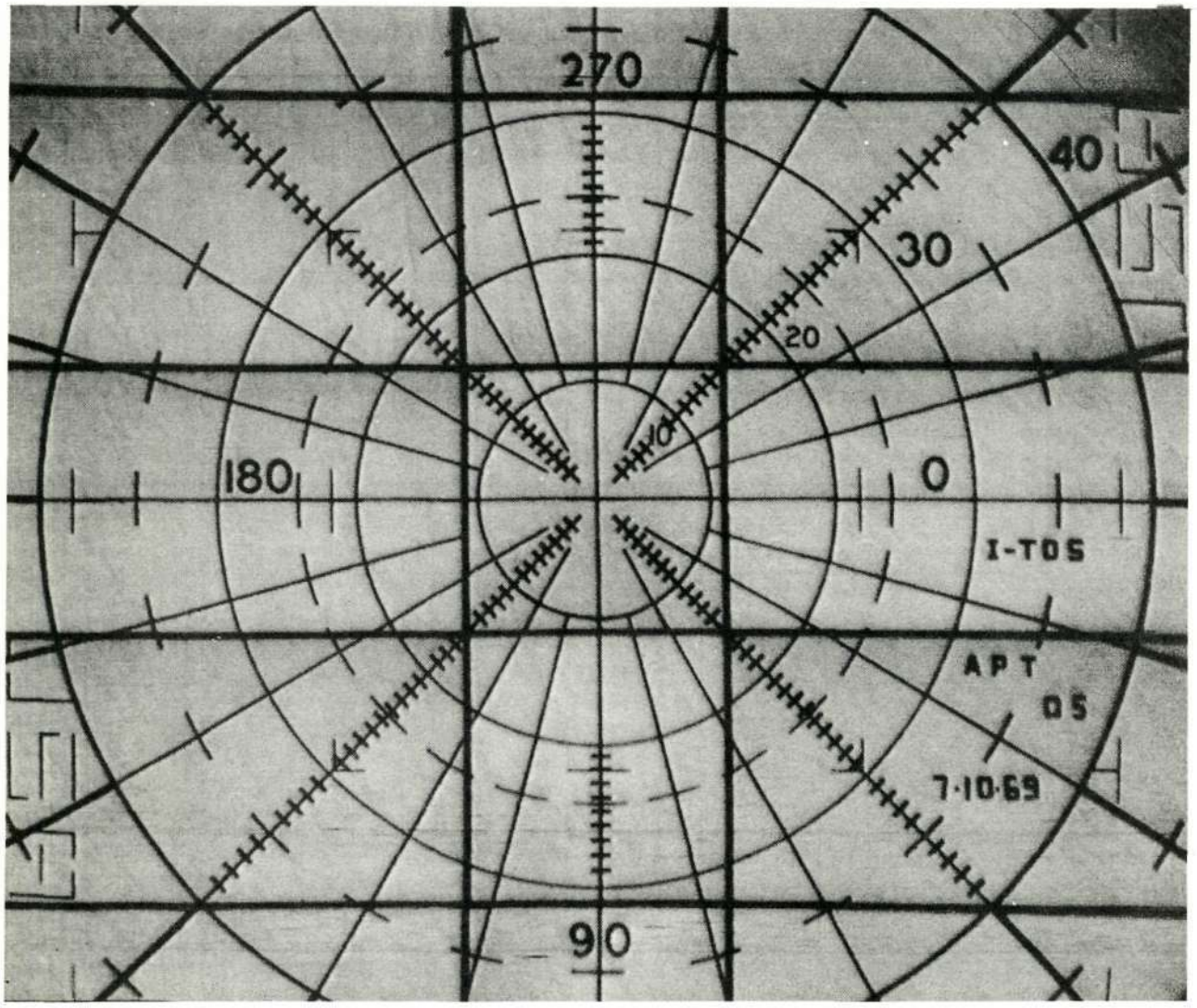

Figure 3-VII-17. APT Camera 1 Distortion Calibration Photograph

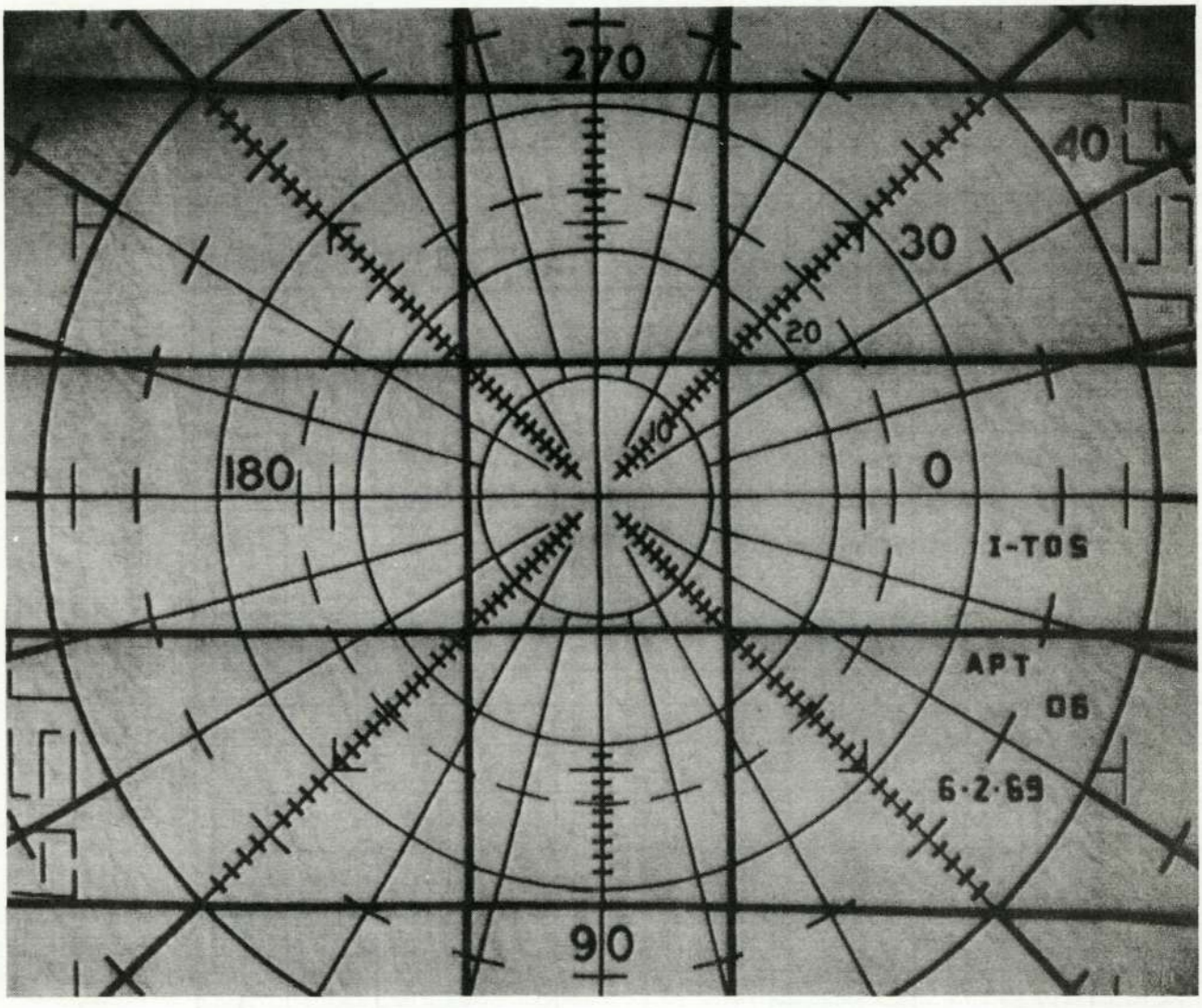

Figure 3-VII-18. APT Camera 2 Distortion Calibration Photograph

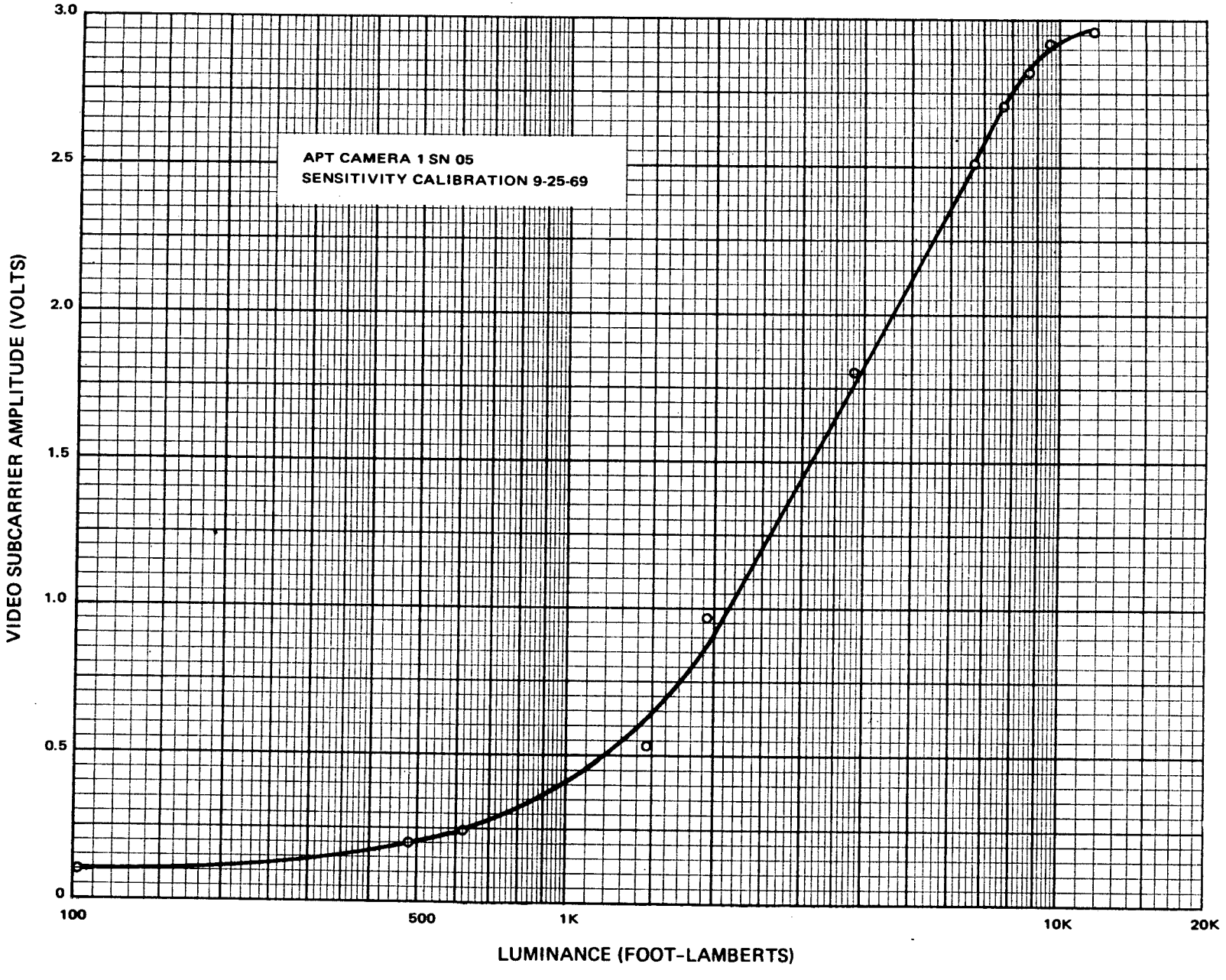

Figure 3-VII-19. APT Camera 1 Sensitivity Calibration Curve

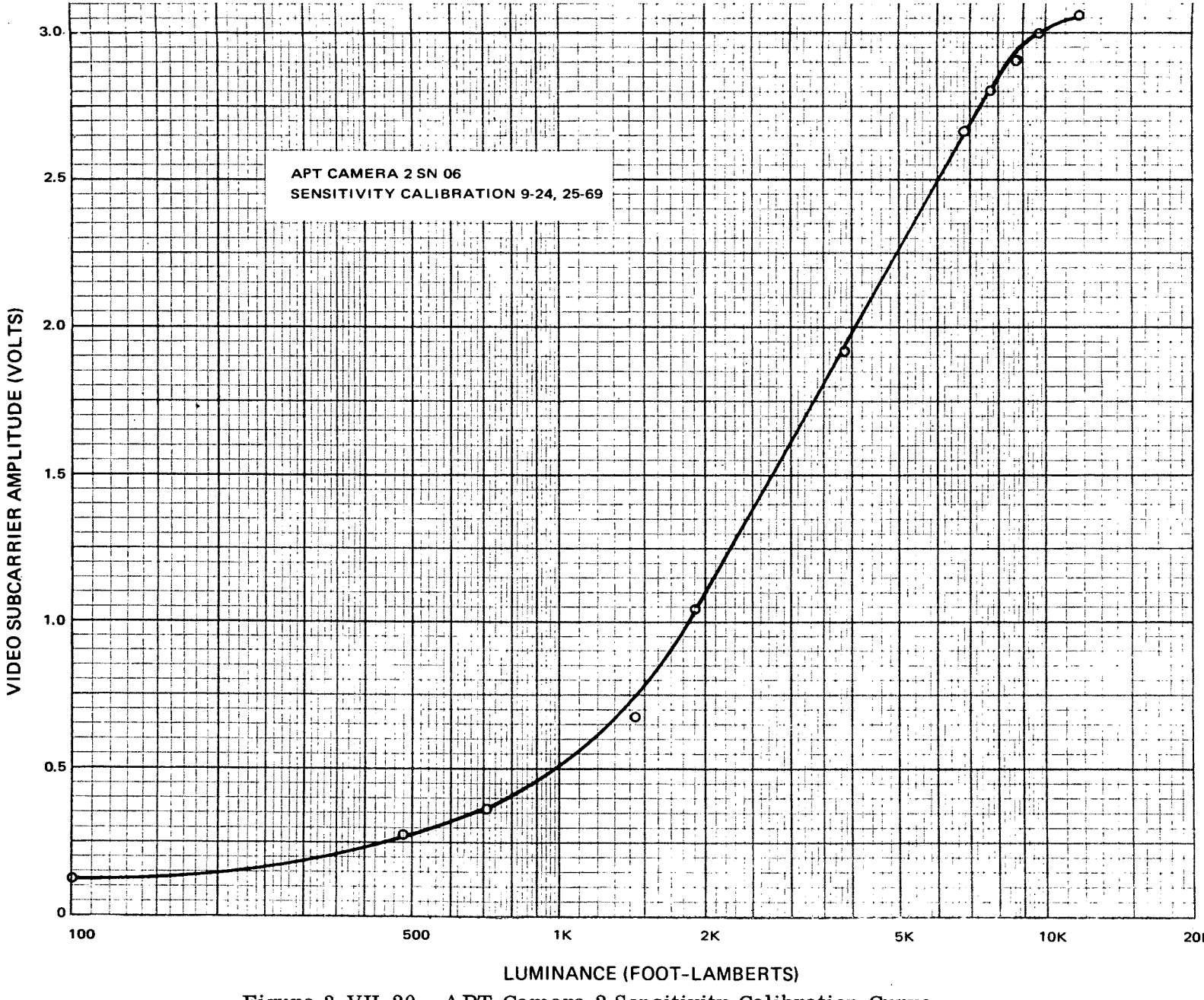

Figure 3-VII-20. APT Camera 2 Sensitivity Calibration Curve

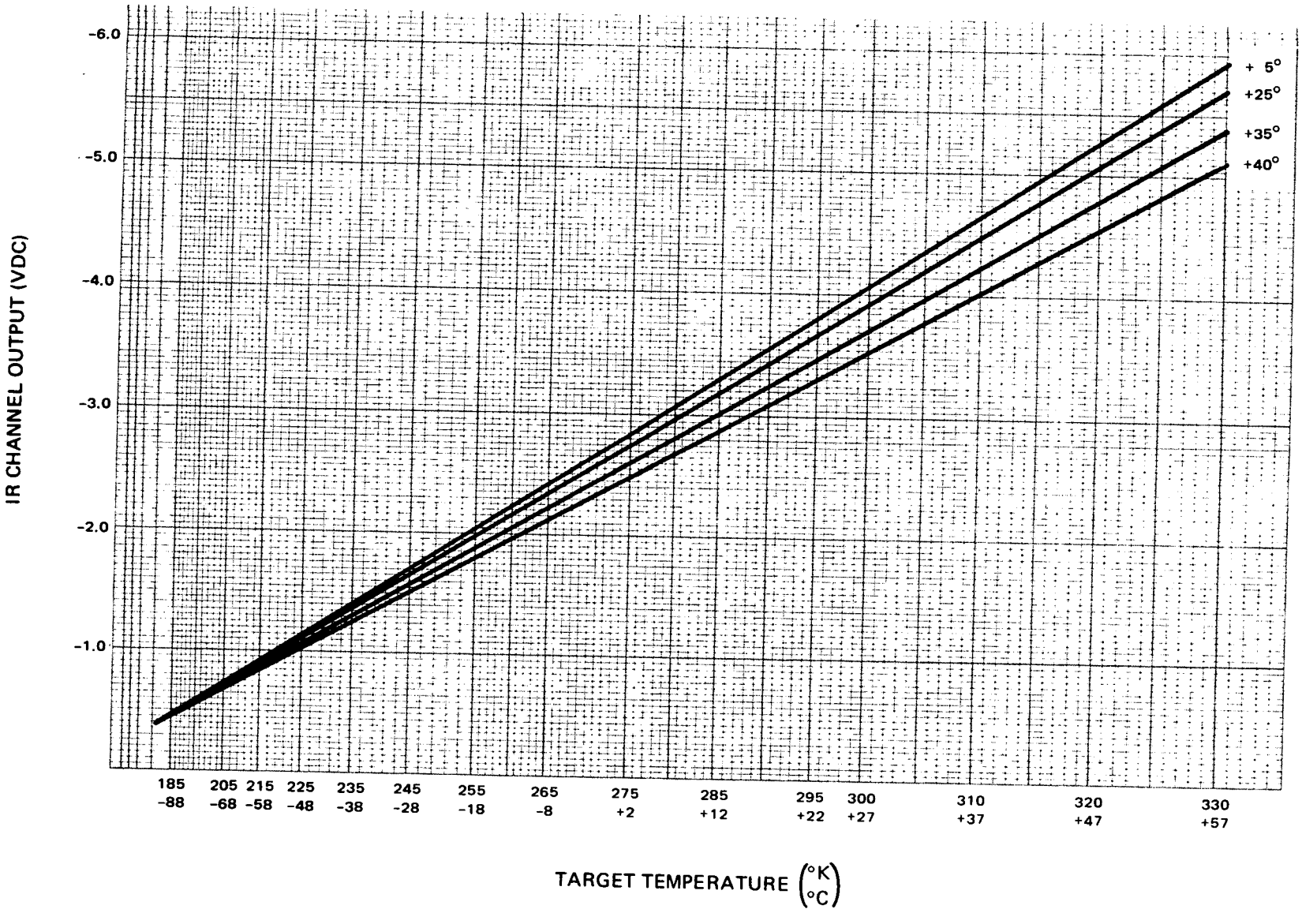

Figure 3-VII-21. Scanning Radiometer 1, IR Channel Radiance Calibration Curves

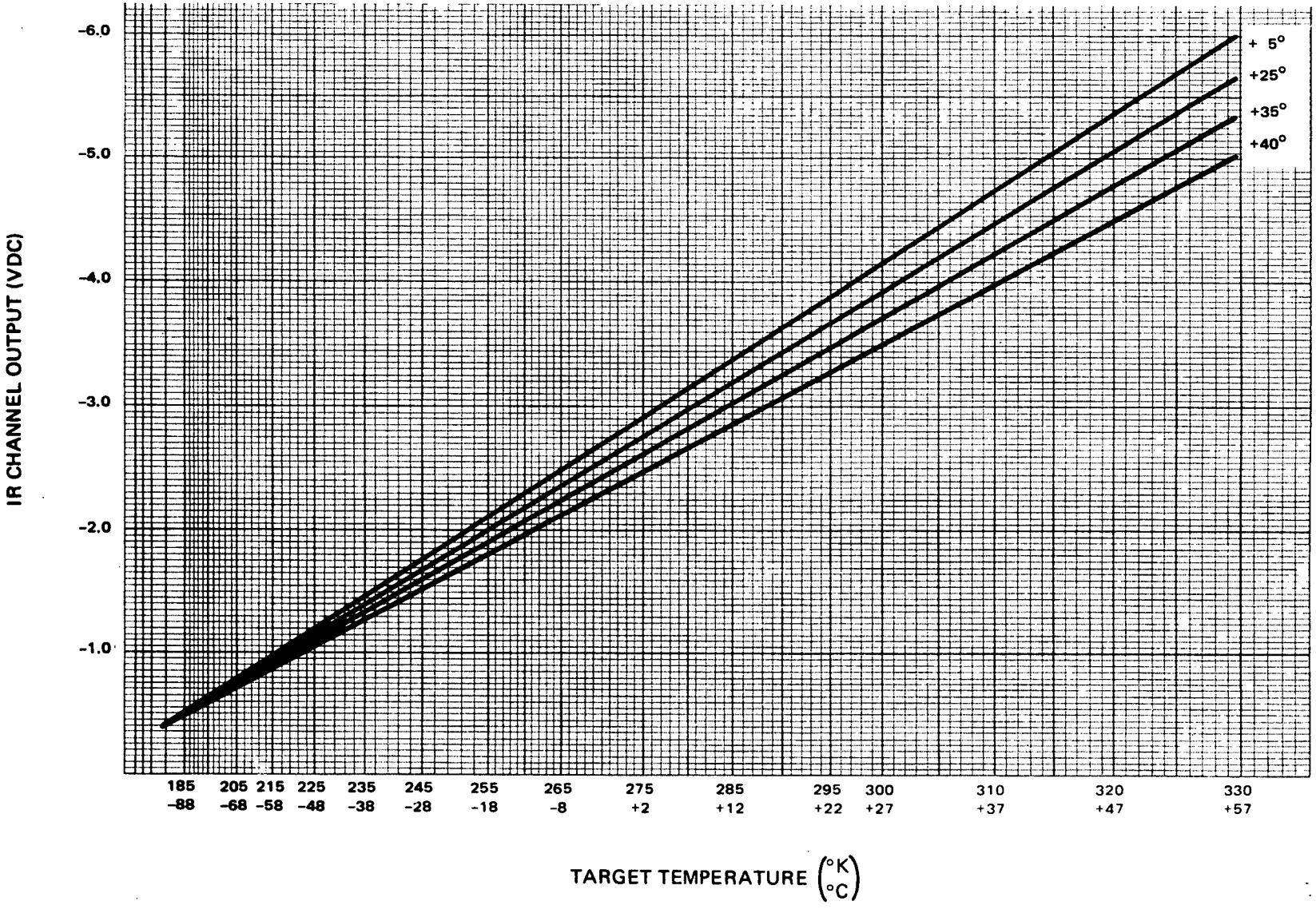

Figure 3-VII-22. Scanning Radiometer 2, IR Channel Radiance Calibration Curves

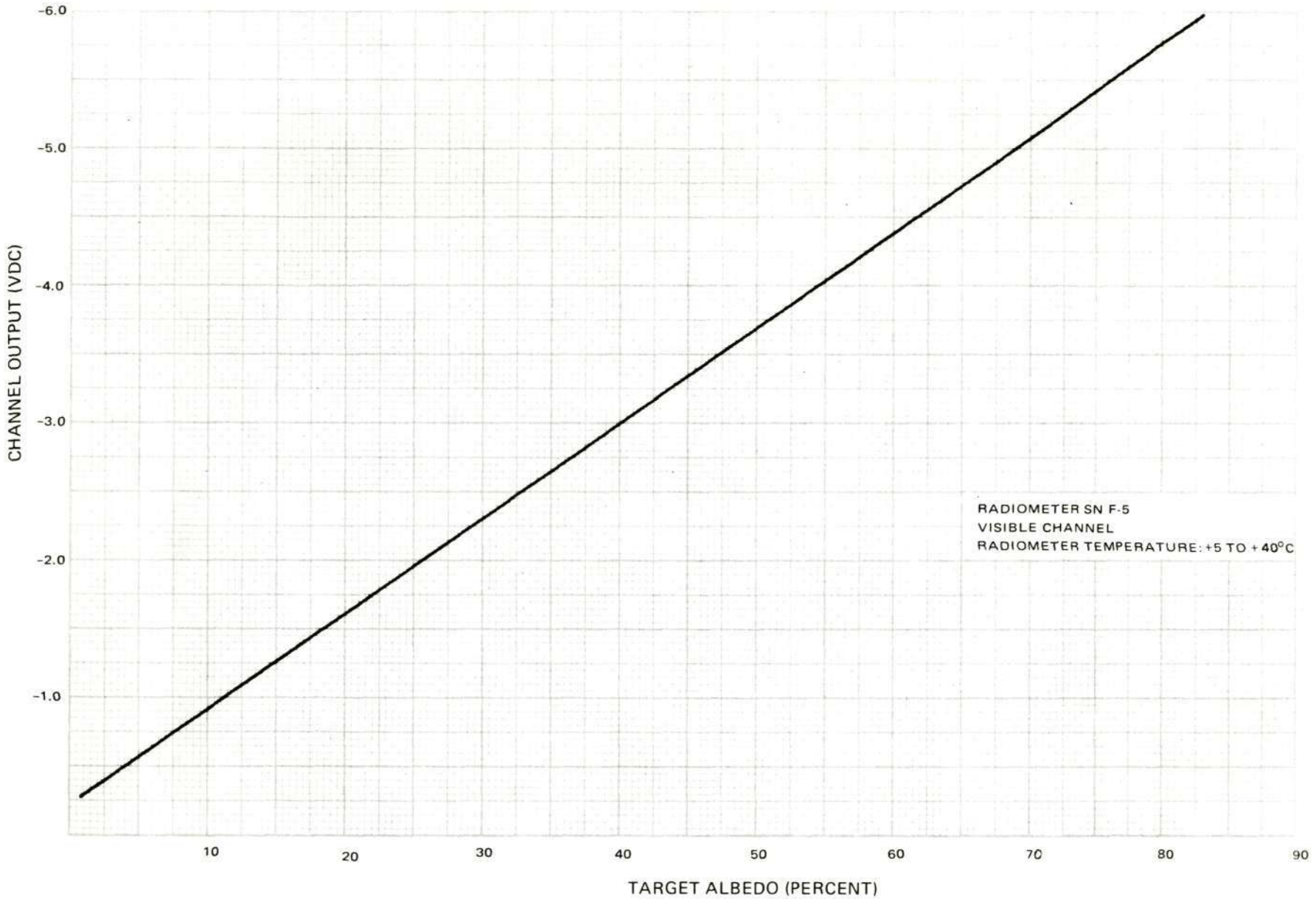

Figure 3-VII-23. Scanning Radiometer 1 Visible Channel Radiance Calibration Curve

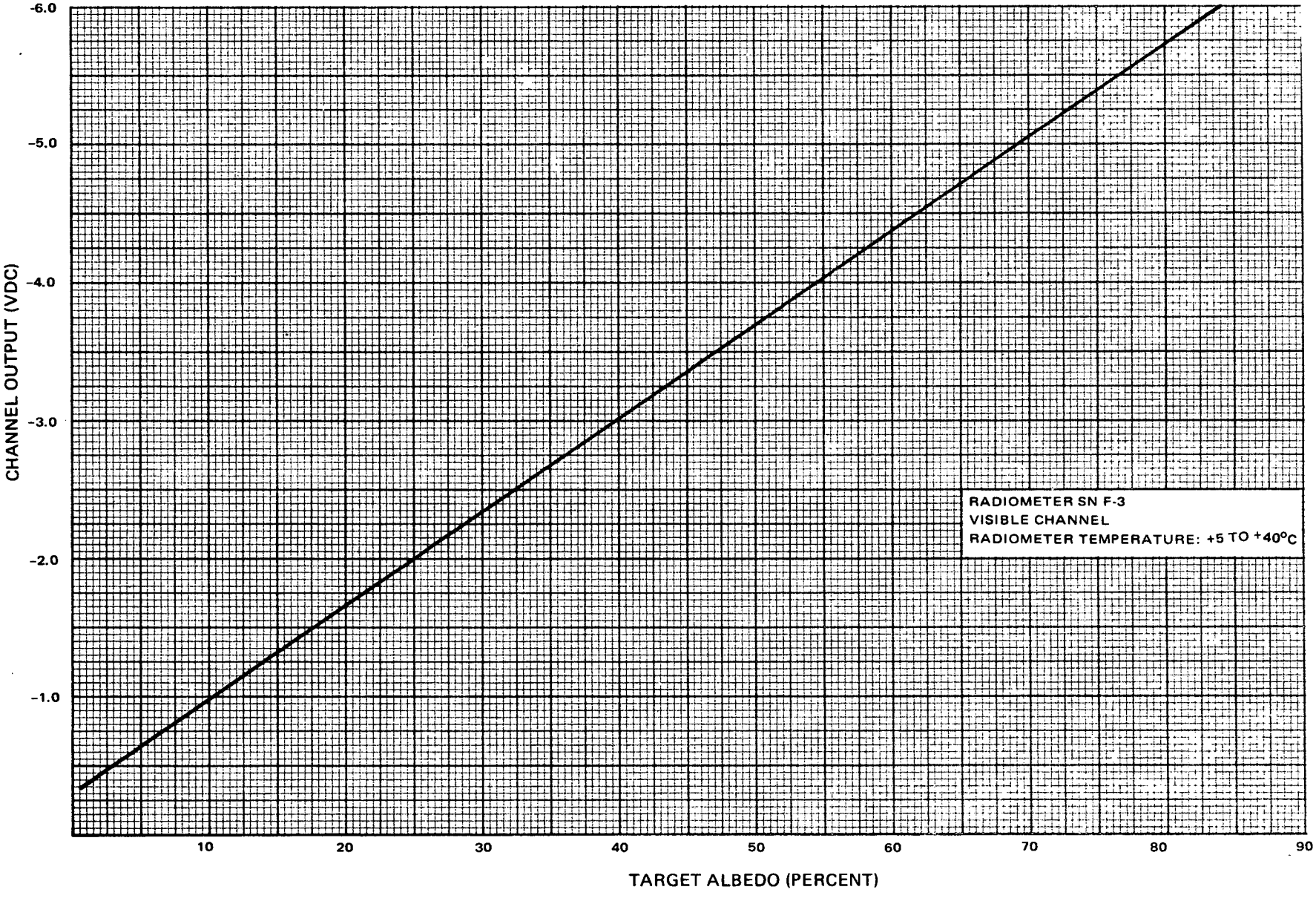

Figure 3-VII-24. Scanning Radiometer 2 Visible Channel Radiance Calibration Curve

outside Earth's atmosphere. Albedo calculations are based on the Handbook of Geophysics.* No correction is necessary in the visible channel data for different radiometer temperatures.

An ideal black body is taken as the radiance scene for IR channel calibration. The IR channel data must be corrected for the temperature of the scanner unit except for temperatures between -5° and +5° C. The magnitude of correction required increases with increasing temperature. There is a marked change in calibration between +35° and +40° C, as can be seen in Figure 3-VII-21 and 3-VII-22. The ordinate for these curves is the signal amplitude output of the scanning radiometer. Integrated spacecraft SR calibration was performed on September 25.

6. Solar Proton Monitor and Flat Plate Radiometer Calibration

True calibration of the SPM and the FPR was performed by the Applied Physical Laboratory of the John Hopkins University and the University of Wisconsin, respectively, who supplied them for the TIROS M mission. The following three special tests were conducted by RCA on September 26.

a. SPM ELECTRONICS TEST

This test was a check of SPM electronics using a test suitcase which generates specific inputs to the SPM electronics, which simulate the output of the SPM sensors. The test suitcase is used in conjunction with a decoder which prints out the numerical equivalent of each SPM word.

b. SPM SENSOR TEST

Support was provided to APL personnel to conduct a check of the SPM sensors using a radioactive source.

c. FPR TESTS

Support was provided to University of Wisconsin personnel to conduct a calibration of the FPR flight sensors in a thermal chamber.

---

*Handbook of Geophysics, First Edition 1957, Table 16-8; U.S. Air Force Cambridge Research Center.

7. Sensor Alignment Check

A system of three orthoginal axes was established as the reference system for optical and mechanical alignment on the spacecraft (see Figure 3-VII-25). The number 1 and number 2 axes are parallel to the separation plane, with their positive directions along the + yaw and + roll axes of the spacecraft, respectively. The number 3 axis coincides with the pitch axis of the spacecraft, with its positive direction along the + pitch axis. The +1, +2, and +3 axes also correspond to the +y, -x, +z axes, respectively. The optical orientations of the spacecraft sensors with respect to the reference system are also shown in Figure 3-VIII-25.

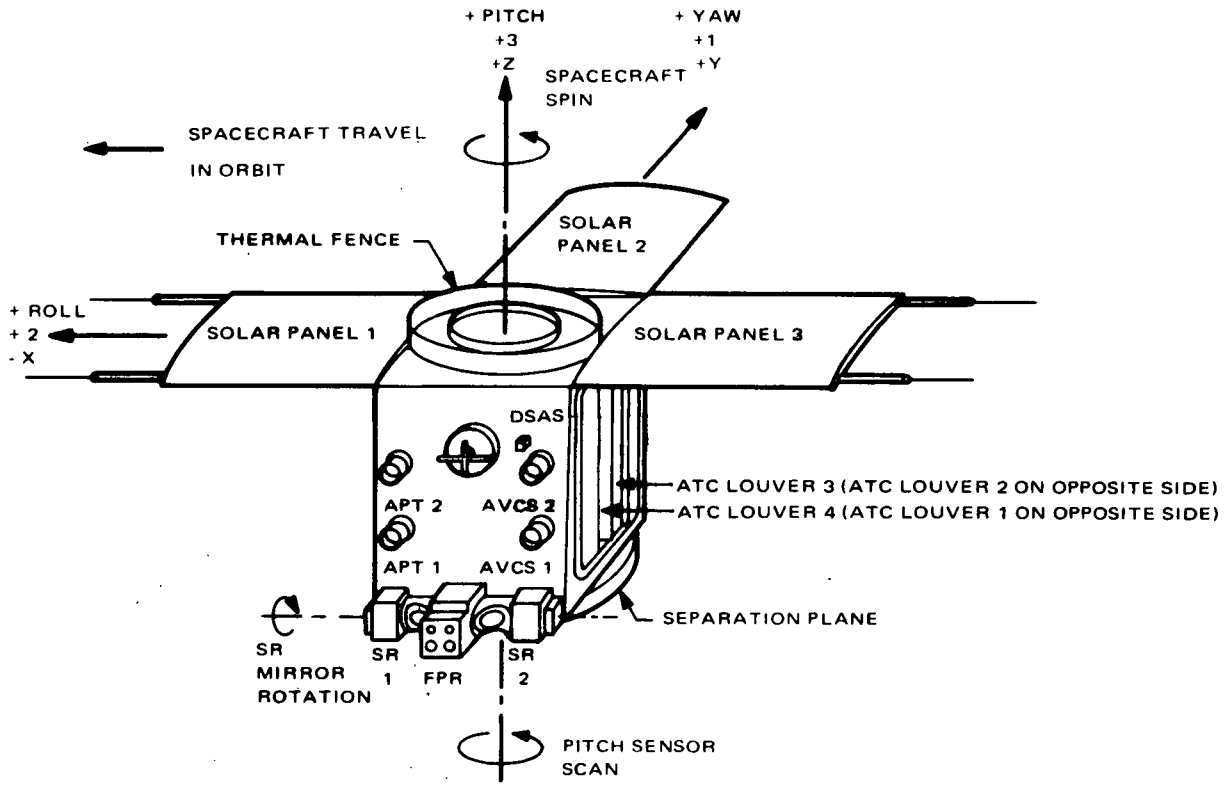

Figure 3-VII-25. Spacecraft Alignment Reference Axes

a. CAMERA ALIGNMENT

The orientation of the AVCS and the APT pictures with respect to orbit geometry is illustrated in Figure 3-VII-26. The optimum orientation of the optical axes of all four cameras is along the local vertical (i.e., parallel to the -1 axis) within a tolerance of ±14 minutes. The alignment angles are illustrated in Figure 3-VII-27.

Table 3-VII-5 lists the optical alignment measurements for all four cameras. These measurements were made on September 27.

b. SCANNING RADIOMETER OPTICAL ALIGNMENT

Figure 3-VII-28 illustrates the orientation of the pictures received during real time and playback for a 3 PM ascending node orbit, and indicates the relationship between spacecraft, orbit track, area scanned, and received pictures. The orbit is shown as viewed from a point directly above the North Pole. The geometry of the radiometer scan is shown in Figure 3-VII-29. The angles that define scan orientation (shown exaggerated) are angle A, the angle between the scanning plane and the -1 ($-\gamma$) axis of the spacecraft, and angle B, the angle between the scanning plane and the spacecraft +3 (+Z) axis. Angle A, combined with the spacecraft pitch angle, determines how far ahead of or behind the local vertical the scanning plane will cut the orbit track. Angle B, combined with the spacecraft yaw angle, determines the skew angle at which the scanning plane will cut the orbit track. Both angles are calculated from measurements made using a precision rotary table.

c. DIGITAL SOLAR ASPECT SENSOR ALIGNMENT

The angle ϕ between the 1-2 plane and the mechanical axis of the digital solar aspect sensor (DSAS) was measured and found to be 90° 2'. The orientation of the projection of the 1-2 plane of the normal to the DSAS (Angle θ) was measured to be 60° 0' as determined during final calibration.

TABLE 3-VII-5. TV CAMERAS OPTICAL ALIGNMENT SUMMARY

Axis Measured	APT Cameras				AVCS Cameras			
	No. 1		No. 2		No. 1		No. 2	
	α_1	β_1	α_2	β_2	α_3	β_3	α_4	β_4
Optical Axis	89° 59'	90° 0'	89° 59'	90° 4'	90° 0'	89° 59'	90° 0'	90° 3'
α and β are both nominally 90°.								

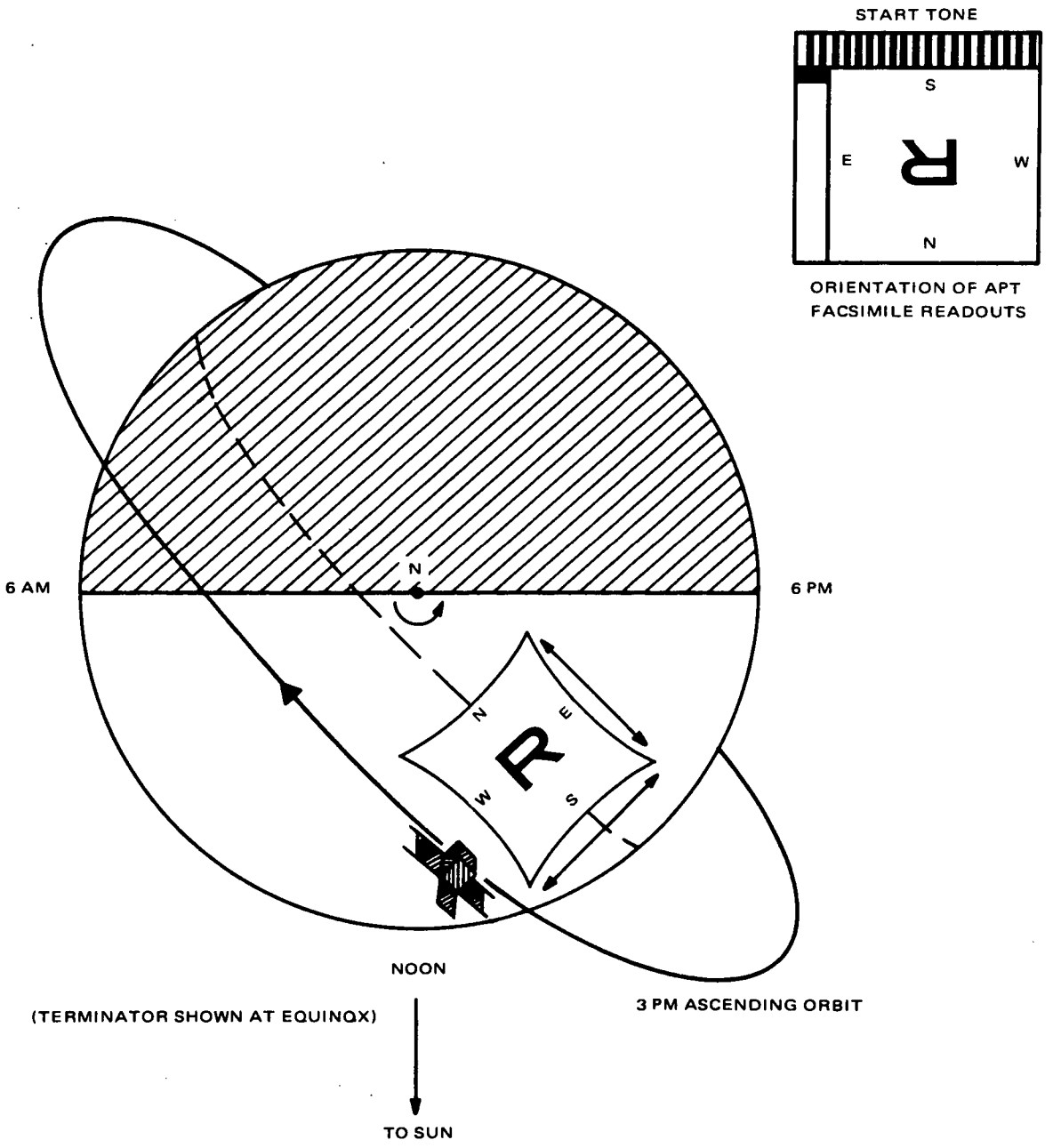

Figure 3-VII-26. AVCS and APT Picture Orientation for 3 PM Ascending Node Orbit

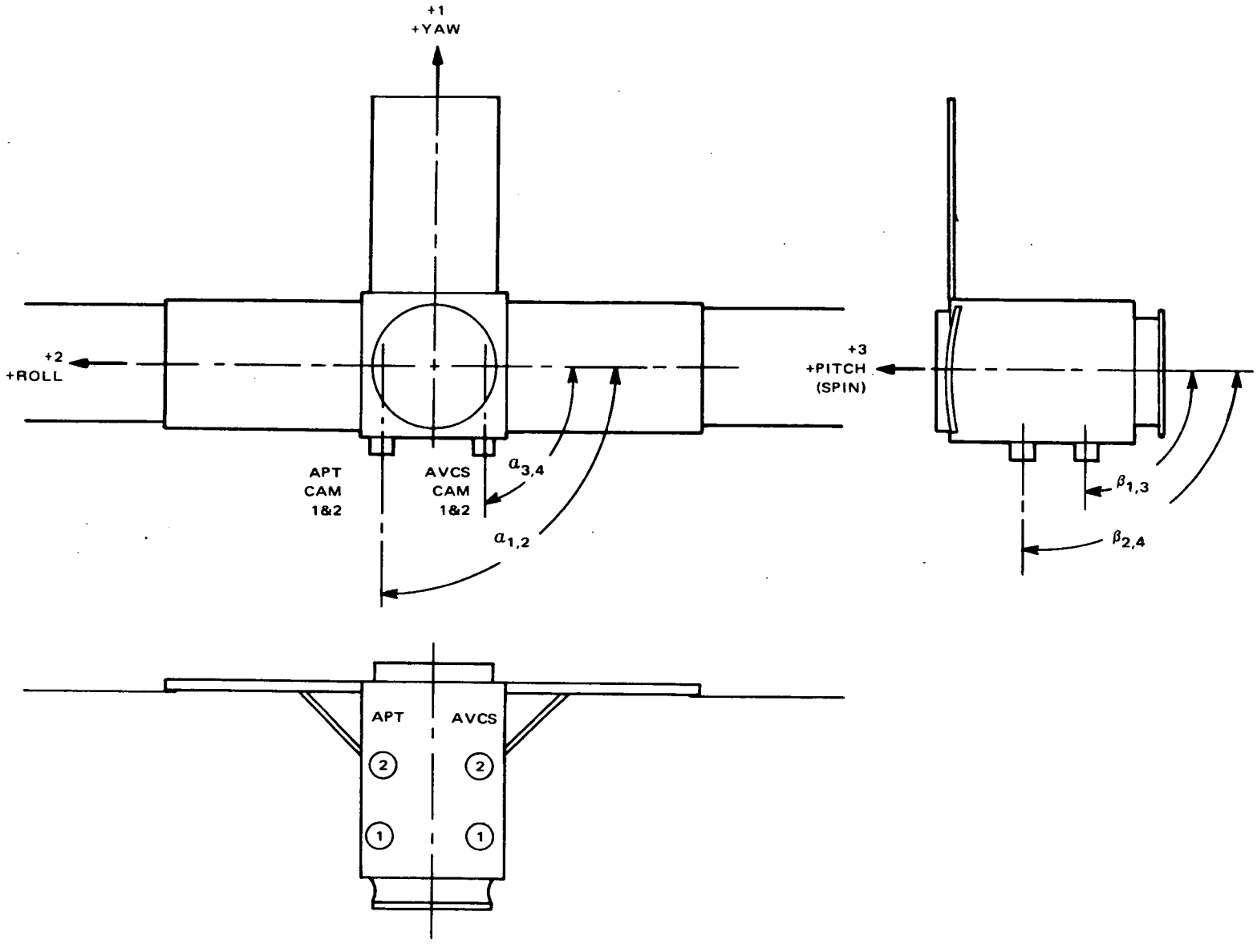

Figure 3-VII-27. Alignment AVCS and APT TV Cameras Optical Axes

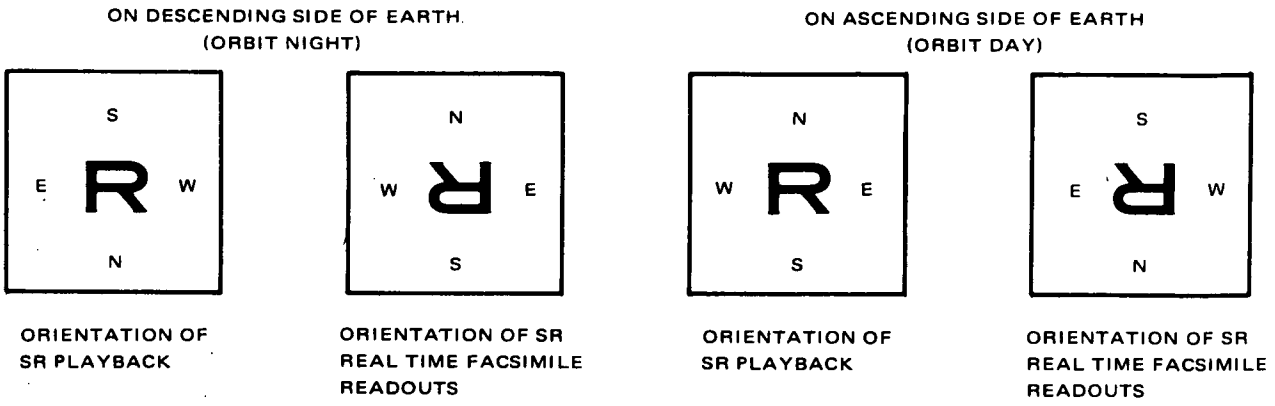

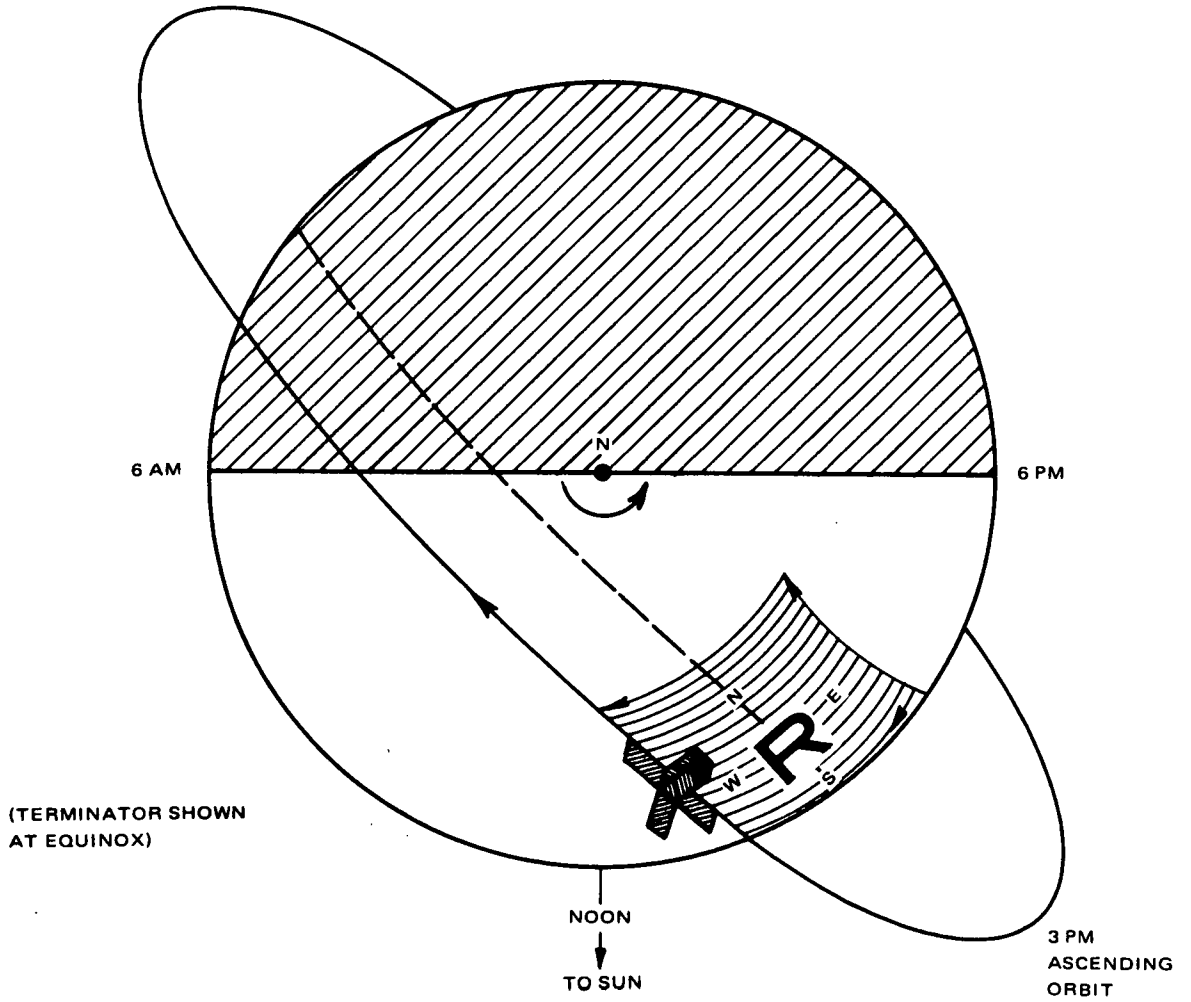

Figure 3-VII-28. SR Readout Orientation for 3 PM Ascending Node Orbit

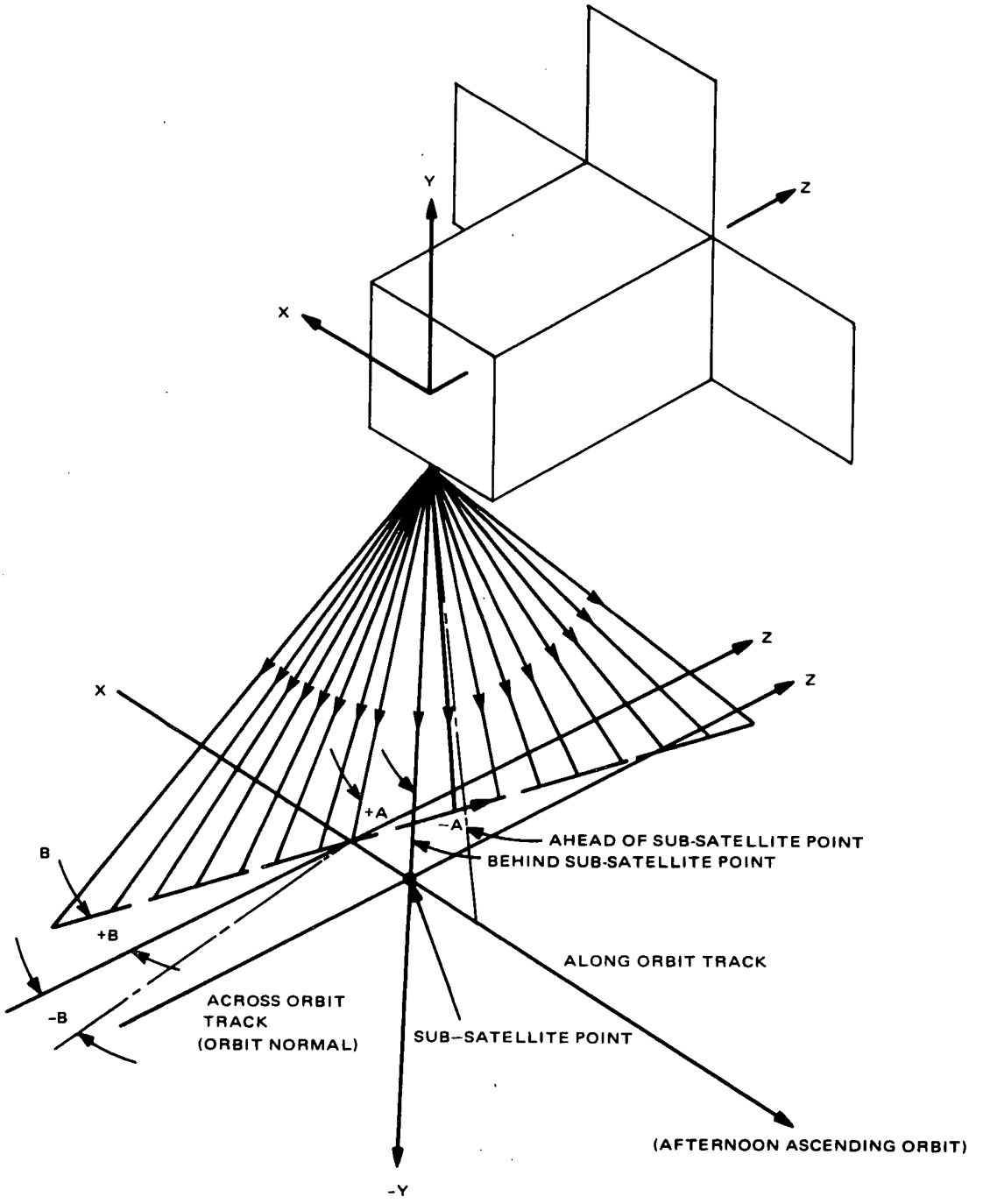

Figure 3-VII-29. Scanning Radiometer Scan Orientation

8. RF Testing

Special RF tests conducted on September 30 showed that no RF interference existed between the OSCAR and the TIROS M spacecraft. The NASA RF compatibility van was used to monitor these tests. Figure 3-VII-30 shows the TIROS M spacecraft set up inside the RCA RF tower.

9. Fine Balancing

In its launch configuration, the dynamic balancing of the spacecraft was performed on October 2. The spacecraft was dynamically balanced to within a maximum of 192 pounds-inch^2, which was within the specified limit of 200 pounds-inch.^{2}

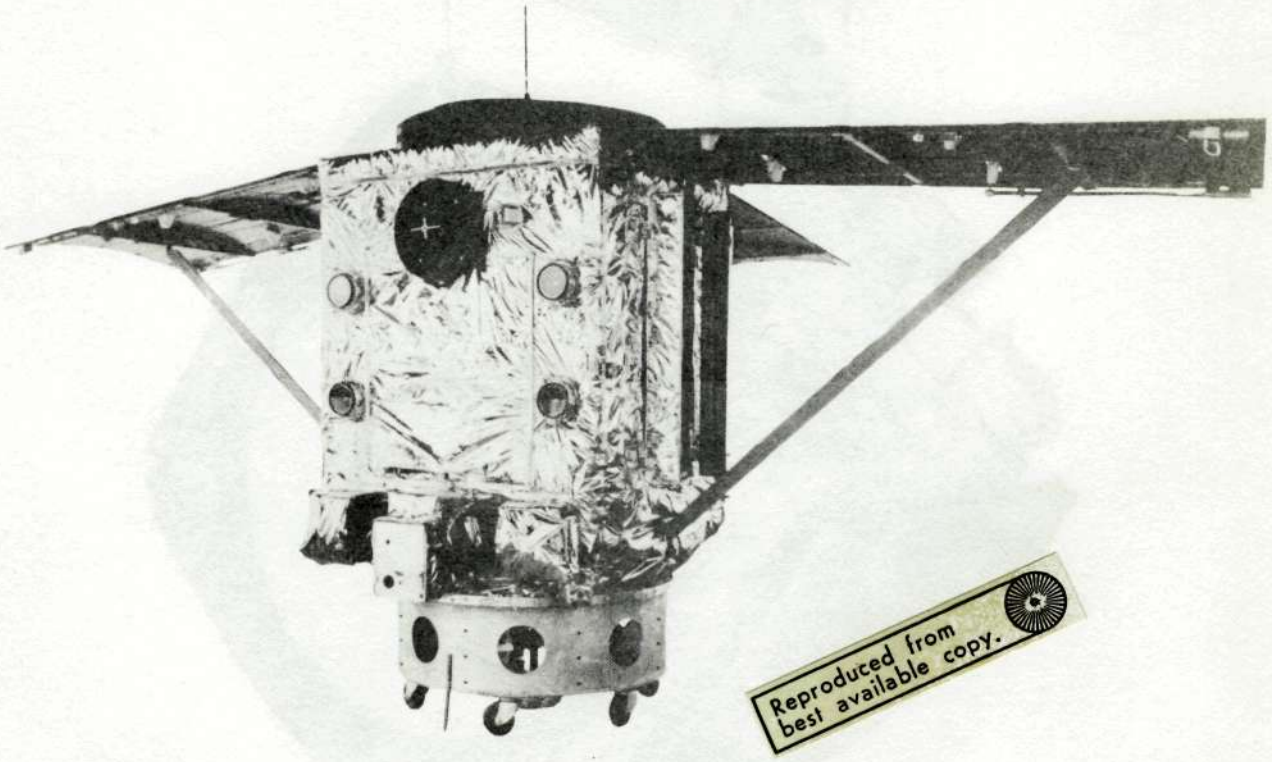

Figure 3-VII-30. TIROS M in RCA RF Test Tower

10. Moment-of-Inertia and Center-of-Gravity Measurements and Final Weighing

Moments-of-inertia of the spacecraft are measured on a bifilar pendulum. The spacecraft is suspended on the bifilar wires in the spin and transverse (pitch) modes, as in Figure 3-VII-31. Using the "standard" equation for a bifilar pendulum, and applying fixed parameters for the test set-up, the moment-of-inertia is determined from the formula:

$$I = \frac{WR^2T^2}{4\pi^2L},$$

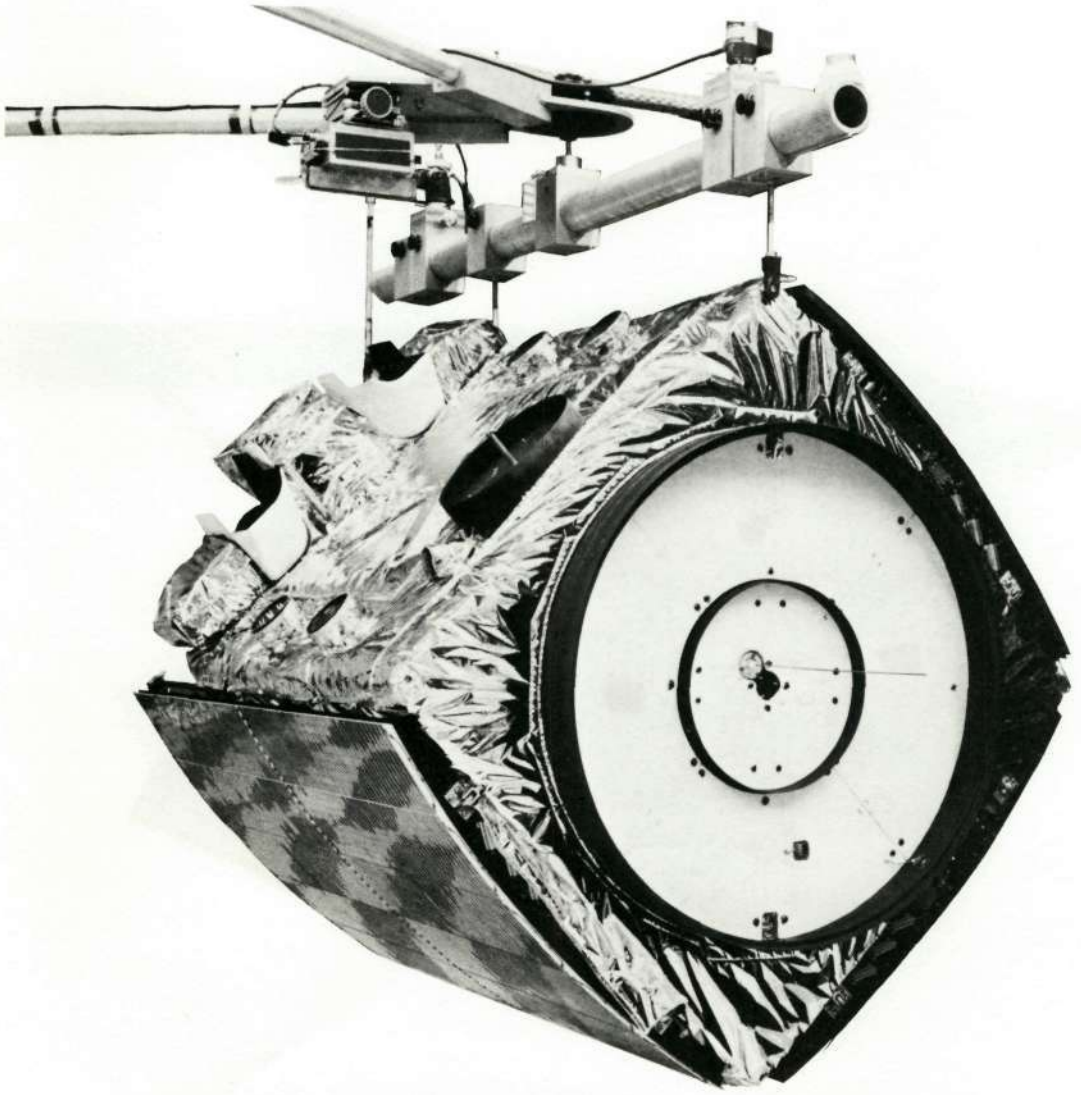

Figure 3-VII-31. TIROS M Moment-of-Inertia Measurement

I is the moment-of-inertia [lb-in-sec^2],

W is the total suspended weight [pounds],

R is half the distance between the suspension wires [inches],

T is the period of oscillation [seconds], and

L is the length of the suspension wires [inches].

The lateral center-of-gravity of the spacecraft is measured on the same bifilar pendulum. With the weight of the spacecraft equally distributed between the two suspension wires, in the transverse mode of suspension, the centroid of the wires is projected with reference to the RCA-MDAC separation plane. This is the location of the transverse center-of-gravity, usually referred to as Z.

In its launch configuration, the spacecraft's moment-of-inertia and center-of-gravity were measured on October 4 (see Table 3-VII-6).

The spacecraft moments and products-of-inertia in the operational configuration (solar panels and real-time antennas extended) were computer calculated according to transfer theorem equations and in accordance with specified test procedures. The results of the calculations are listed in Table 3-VII-6.

E. CONCLUSION OF TESTING

The flight acceptance test program for the TIROS M spacecraft was completed on October 4.

Flight acceptance was followed by a repeat of battery capacity tests and an abbreviated SEPET. All results were satisfactory.

In response to a NASA request, RCA performed tests and analyses to evaluate the effect of the higher equipment module depressurization rate resulting from the use of the two-stage launch vehicle with six solid boosters. RCA conducted the evaluation as follows:

(1) Computed accumulative orifice area and pressure differential across the thermal blankets during the launch vehicle ascent phase.

(2) Designed a sea-level depressurization test to simulate outgassing conditions equivalent to those of launch vehicle ascent.

(3) Built test fixtures to test venting time of the spacecraft and special scale thermal blankets.

(4) Performed venting tests.

TABLE 3-VII-6. MECHANICAL AND PHYSICAL PARAMETERS OF TIROS M

Parameter	Launch Configuration (Panels Folded)	Operational Configuration (Panels Deployed)
Spacecraft Weight	682.02 lb	682.02 lb
Moment-of-Inertia		
[a] About Yaw Axis I_{11}	849.46 lb-in-sec^2	1295.04 lb-in-sec^2
[b] About Roll Axis I_{22}	783.42 lb-in-sec^2	1020.65 lb-in-sec^2
[c] About Spin [Pitch] Axis I_{33}	682.09 lb-in-sec^2	1145.54 lb-in-sec^2
[d] About Roll-Yaw Plane I_{max}	849.64 lb-in-sec^2	--
I_{min}	783.24 lb-in-sec^2	--
[e] Location of I_{max} (Positive angles measured clockwise from earth side (-1) when viewed from above the baseplate)	183 degrees	--
[f] Inertia Ratio I_{max}/I_{33}	1.25	--
Product-of-Inertia		
[a] In Yaw-Roll Plane I_{12}	+3.46 lb-in-sec^2	+3.74 lb-in-sec^2
[b] In Yaw-Pitch Plane I_{13}	I_{13} and I_{23} assumed equal to zero for dynamically balanced spacecraft	+79.88 lb-in-sec^2
[c] In Roll-Pitch Plane I_{23}		-10.92 lb-in-sec^2
NOTE: Orbital moments-and-products-of-inertia are values about a set of coordinate axes which have been shifted parallel from the initial launch coordinates.		
Center of Gravity $\bar{z}$ [Above Separation Plane]	21.94 inches	24.85 inches
Dynamic Balance Residual Dynamic Imbalance [Maximum]	192 lb-in^2	See I_{12}, I_{13}, and I_{23} above.
Static Balance Residual Static Imbalance [Maximum]	15.5 lb-in	$\Delta\bar{y}$ = +0.859 inch $\Delta\bar{x}$ = -0.063 inch
NOTES: 1. Dynamic balance test was performed on October 2, 1969. 2. Moment-of-inertia test was performed on October 4, 1969.		

Tests with special blankets were performed. The evaluation results verified that the thermal blankets and their fastenings could withstand ascent depressurization with an ample safety margin.

At the end of November, the spacecraft was placed in storage awaiting shipment to the Western Test Range. The spacecraft was shipped on December 7, 1969.

PART 4. TIROS M LAUNCH-SUPPORT OPERATIONS

SECTION I. PRELAUNCH ACTIVITIES

A. INTRODUCTION

The TIROS M spacecraft and its counterpart, the Electrical Test Model (ETM) spacecraft, were shipped to the Western Test Range (WTR) after successful completion of the final environmental and calibration tests at RCA. The two spacecraft and associated launch support equipment arrived at the WTR on December 8, 1969, and were transported to the spacecraft laboratory in building 836. The launch support equipment was used during December and January in prelaunch testing and preparation for launch of TIROS M at the WTR.

After a series of mechanical and electrical inspections and tests, the TIROS M spacecraft was successfully launched on January 23, 1970. After launch, the satellite was officially designated ITOS 1.

The following paragraphs describe chronologically the operations at the WTR on both the ETM and TIROS M spacecraft. The ETM was used primarily as an RF and mechanical-assembly test model before launch. As such, it served to familiarize the RCA, McDonnell Douglas Astronautics Corporation (MDAC), and WTR personnel with the handling, testing, and operational requirements of the TIROS M spacecraft as an entity and when wedded to the Delta launch vehicle. Also, the exercises with the ETM disclosed certain facility, handling, and procedural problems in time for appropriate corrective action to be effected.

B. ETM SPACECRAFT OPERATIONS

On December 9, the ETM was removed from its shipping container at the WTR laboratory and mounted on a stand in preparation for a go/no-go electrical test. These tests were successfully completed on December 10.

On December 11, fit checks between the spacecraft and flight attach fitting were completed. The marmon clamp was torqued and found to seat properly. After these checks, the ETM was removed from the electrical test stand and installed in the ETM shipping container for storage until launch checkout tests were to be conducted.

A fairing-off and fairing-on launch checkout test was performed on the ETM spacecraft, at the spacecraft laboratory, on December 15. After these tests, the spacecraft was placed in its shipping container and transported to the launch service tower area the following day.

On December 16, the ETM was mounted on the launch vehicle second stage and the MDAC thermal shroud installed. A fairing-off launch checkout was then performed. RF signal strength was improved by the addition of external antennas and power amplifiers. The command link was periodically marginal due to other transmitters at WTR operating on the same frequency.

After the fairings were installed on December 18, a fairing-on launch checkout was performed without difficulty. At the completion of this checkout, the spacecraft was demounted, installed in its shipping container, and returned to the spacecraft laboratory.

The ETM spacecraft was shipped from the WTR on January 23 and arrived at RCA in Princeton, New Jersey on February 2, 1970.

C. TIROS M SPACECRAFT OPERATIONS

On December 8, the standard electrical performance evaluation test (SEPET) fixture was assembled, and on December 9, the TIROS M spacecraft was removed from its container and visually inspected for shipment damage. No damage was evident and the TIROS M was installed in the SEPET fixture in preparation for a go/no-go test. The test was completed satisfactorily and the spacecraft was made ready for a fit check with the flight attach fitting. The fit check was adjudged satisfactory, the breakaway connector alignment was verified, and the spacecraft was returned to its shipping container.

On December 10, the TIROS M was removed from its container, mounted on a stand, and weighed in its flight configuration. The weight was considered within tolerance. After weighing, the spacecraft was installed in the SEPET fixture and the collimators were aligned. The preliminary conditions check, backup function checkout, sensor exciter check, and pyrotechnics test, paragraphs 5.0.1, 5.0.2, 5.0.3, and 5.12, respectively, of the spacecraft SEPET were then successfully completed and reviewed.

On December 11, the pitch loop test, paragraph 5.13, and the power system tests, paragraph 5.14, of the SEPET were successfully completed and reviewed. The load bus profile test, paragraph 5.15, and the orbit 1 test, paragraph 5.1, of the SEPET were successfully performed, with a continuing review of the resulting data. Two special tests, preceding the power system test, indicated that there was no measurable momentum wheel assembly (MWA) brush wear since the end of the spacecraft qualification program and that the solar proton monitor (SPM) was performing normally.

The orbit 2 tests, paragraph 5.2, and the beginning of orbit 3 tests, paragraph 5.3, of the SEPET were completed on December 12. Data from orbits 1 and 2 continued under review. The review of the load bus profile data indicated a

difference in absolute current values in comparable steps of the side 1 and side 2 measurements. This was attributed to improper command sequencing. Portions of the load bus profile test were rerun with the proper command sequencing and the results proved satisfactory. Other sections of the load bus profile test were also rerun to substantiate questionable initial test data.

On December 13, the review of the SEPET orbits 1 and 2 test data was completed. Orbits 3, 4, 5, and 6, paragraphs 5.3, 5.4, 5.5, and 5.6 of the SEPET, respectively, were successfully completed. The orbit 7 test, paragraph 5.7 of the SEPET, was partially completed, consisting only of playing back the data recorded in the four previous orbits. The orbital test data was placed in the review cycle.

Orbits 7, 8, 9, 10, and 11, paragraphs 5.7, 5.8, 5.9, 5.10, and 5.11 of the SEPET, respectively, were completed on December 14. This completed the SEPET on the TIROS M spacecraft, except for the data review. As expected, both 3.9-kHz beacon subcarrier oscillators (SCO's) were out of their frequency specification. This fact was documented by Test Discrepancy Report (TDR) B-6295. The SCO frequency drifts slightly because of a hygroscopic effect. The SCO frequency returns to nominal in vacuum.

On December 15, the scanning radiometers (SR) were checked with the SR collimator. Applied Physics Laboratory (APL) personnel, utilizing a Cobalt 60 isotope, checked the solar proton monitor (SPM). The SR's and SPM operated satisfactorily. The spacecraft was returned to its storage container in the laboratory on December 17.

On January 5, the spacecraft was removed from its container and mounted in the SEPET fixture. The sensor exciter portion of the abbreviated SEPET was successfully performed, although IR data from SR1 exhibited random disturbances during display. Subsequent analysis indicated that no corrective action would be required.

A special SR1 warmup sequence was performed on January 6 to check on video instability after radiometer turn-on. The timed portion of the SEPET followed and was performed successfully, although two difficulties with the SPM test suitcase developed (a broken shield wire in the test cable and the 100-kHz ramp function failed late in the test). After the abbreviated SEPET, both SR's were operated while observing video at the test point without the mirrors rotating. The SR1 video exhibited the type of instability experienced when the 137D capacitor in the detector bias supply becomes noisy. Santa Barbara Research Center (SBRC) personnel confirmed this diagnosis. Spacecraft arming was performed. The arming connectors were not installed until after the pitch loop enable connector checkout was performed. This was done so that the squibs would not be armed while the separation switches were enabled for the pitch loop enable connector checkout.

On January 7, the spacecraft was removed from the SEPET fixture and installed on the special mounting fixture. The solar panel installation check was performed and a rerun was made of that portion of the abbreviated SEPET that deals with parallel motor telemetry. A special SR1 operation was conducted while monitoring the SR video test point. The SR was run for 2 hours, left off for 1 hour, and then run again for 2 hours. Relatively quiet video was exhibited at the test point during both runs. The video from the second run was comparable to the SR2 video obtained on January 6. The solar panels were preloaded for flight. Pre-tower inspections were performed and the spacecraft was removed from the fixture and installed in its shipping container.

On January 8, the spacecraft was removed from its container and mounted on the work stand. Fairing-off, fairing-on, and the final launch checks were performed successfully. A special solar panel illumination check was made to investigate the sensitivity of the panels to light-box position. After this test, the spacecraft was installed in its container, transported to the tower, and raised to the 5th level. The spacecraft was removed from its container, given a final underside check, and mated with the launch vehicle second stage. Calibrated torquing of the clamp was completed, the ballast weight and temporary shroud were removed, and the MDAC thermal shroud was installed around the spacecraft.

RF link checks were performed with the spacecraft mated to the launch vehicle, on January 9. Beacon and S-band links were good and the real-time link acceptable. The command link was marginal using the van transmitter and the screen yagi antenna on the line-of-sight tower. A special SR1 video check was performed. The video stabilized within 30 minutes and remained in this condition for the next 1-1/2 hours at which time the test was terminated. A fairing-off launch check was conducted successfully and then the spacecraft was turned on with beacons radiating for the command destruct portion of the vehicle's all-systems test.

On January 12, 13, 14, and 15, fairing-off launch tests were successfully completed. Tests on January 12 were delayed due to Mission Operations Intercom System (MOPS) loop difficulties. No more than two command dropouts occurred during tests on any given day and only minor difficulties were experienced with the GSE. Several severe losses of real-time transmitter signal strength at the van occurred on the 14th and 15th. These were attributed to other activity on the gantry.

Fairing-on tests were conducted successfully on January 17 and 18 with only minor difficulties occurring through operator error, GSE faults, or RF cabling to and oscillation in the gantry power amplifier. At the conclusion of the fairing-on test on January 18, a special real-time transmitter power telemetry check was made. Both transmitters showed stable power telemetry.

On January 19 and 20, a fairing-on launch check was performed successfully, with only minor, but readily correctable, difficulty in the GSE. Both real-time transmitter signals were adequate and steady.

A fairing-off test, with fairing on, was made successfully on January 21. The ITA transmitter was off for part of the side 1 check. The van transmitter was used until a second ITA transmitter was installed.

On January 22, a fairing-on check and a final launch check and inspection were made. Side 1 S-band signal was weaker than normal until the 23-foot dish was used. A power failure apparently caused the telemetry laboratory equipment to degrade. Side 2 signal was normal. Minor commanding difficulties at the GSE were corrected.

On January 23, final launch check was performed, the SR motors were turned on, and the launch state verified. Beacon turn-on and launch state verification were performed at the start of the terminal countdown at 0202 Pacific Standard Time (1002Z).

Liftoff of the Delta launch vehicle with TIROS M aboard occurred at 0331 Pacific Standard Time (1131 Z) on January 23, 1970. Accelerometer data at liftoff appeared normal.

SECTION II

POST-LAUNCH ACTIVITIES

A. BEGINNING OF OPERATION

Once the TIROS M was injected into the proper orbit, it was designated the ITOS 1 satellite. The ITOS 1 will remain under the control of NASA for the first few months so that they can assess its performance, then control will pass to ESSA.

The spacecraft was placed into an orbit having the following parameters:

- Altitude
  - Apogee: 798.3 nmi
  - Perigee: 773.6 nmi
- Inclination: 101.99 degrees
- Period: 115 minutes

The yaw maneuver and spinup program of the second stage injected the spacecraft into orbit with the pitch axis approximately 9.5 degrees off the orbit normal and with a total system momentum of 307 in-lb-sec. As expected, correction of total system momentum by ground-commanded commutation was required prior to establishing earth lock. Subsequent to attitude determination from orbit 1 data, a high torque QOMAC program was formulated and loaded on the orbit 2 contact. The performance of the QOMAC system was as predicted and the attitude error was less than 1 degree by orbit 4. Solar panels were deployed during orbit 5.

Momentum correction was continued until the measured value of total system momentum was below 242 in-lb-sec. This limit was established to insure operation of the pitch loop in the fine gain mode, thus permitting the avoidance of a moon conflict during earth lock-on in orbit 42.

During the period of time that momentum reduction was being accomplished, evaluation of the spacecraft telemetry indicated all temperature profiles to be within the predicted bounds with the exception of a low MWA bearing temperature. To correct for this low temperature, scanning radiometer 1 was turned on by means of programmer 1, providing an approximate 6-watt input to the baseplate. This input stopped the downward trend of the bearing temperature. A minimum temperature level of +5°C was chosen, and additional heat inputs to the baseplate were

generated by operating first one and then both housekeeping telemetry commutators in the manual mode of operation. Subsequent investigation has indicated that the published calibration curve for the temperature sensor was in error and the measured temperature should be approximately 5° C higher.

Initial operation of the spacecraft was as predicted; no serious anomalies occurred. Minor discrepancies consisted of several questionable data bursts from the DSAS, incorrect calibration curve for the MWA bearing temperature, and slight amount of noise in the pictures from scanning radiometer 2 and APT camera 2. Coarse measurements showed the spacecraft attitude and pitch error to be within the specification requirement of 1 degree and the total jitter rate to be less than the specified 0.05 degree per second.

Certain physical parameters were computed from the spacecraft orbital performance. The computed spinup of the second stage launch vehicle was 4.30 rpm. The computed pitch inertia of the spacecraft with the solar panels folded was 664 lb-in-sec^2. This value was derived from the momentum wheel spinup from 115 rpm to 150 rpm. The pitch inertia calculated from the body rate after solar panel deployment was 1142 lb-in-sec^2. The product term I_{13} was calculated to be 80 lb-in-sec^2 from the coning obtained after solar panel deployment. These values correspond closely with the prelaunch computations of 682.1 lb-in-sec^2, 1145.5 lb-in-sec^2, and 79.9 lb-in-sec^2, respectively.

B. INITIAL PERFORMANCE EVALUATION

At the end of February, ITOS 1 had completed 456 orbits in 37 days of successful operation in space. During February, all primary sensors were checked for operational capability and observed to be satisfactory. The number of APT and AVCS pictures taken through February 28, 1970 (orbit 456) is as follows:

• APT Camera 1	1083
• APT Camera 2	1361
• Total APT Pictures	2444
• AVCS Camera 1	485
• AVCS Camera 2	1994
• Total AVCS Pictures	2479

Of the 2479 AVCS pictures taken, 1998 were recovered by playback of the AVCS tape recorder. The remainder were not recovered since the tape recorders were fully loaded with other picture data when these pictures were taken.

The picture-taking time (real-time mode and record mode) for the scanning radiometers is categorized as follows:

	Hours	Minutes
• Scanning Radiometer 1*	454	38.7
• Scanning Radiometer 2*	170	43.9
• Total Scanning Radiometer Time	625	22.6
• Scanning Radiometer Recorder 1		
— Used with SR 1	146	40.2
— Used with SR 2	5	51.4
— Total Operating Time	152	31.6
• Scanning Radiometer Recorder 2		
— Used with SR 1	150	17.6
— Used with SR 2	8	46.9
— Total Operating Time	159	4.5

Figures 4-II-1 and 4-II-2 show two views of the same area: one seen through the infrared channel of the ITOS 1 scanning radiometer; the other seen through the visible channel.

An evaluation of the pitch jitter data for pitch loops 1 and 2 showed the jitter for each loop to be an order of magnitude better than the specification requirement. The data was obtained on orbit 217 for pitch loop 2 and on orbit 355 for loop 1. Ninety percent of this data showed jitter of less than 0.0022 degree per second.

At launch motor No. 1 brush reserve was 48 mils and motor No. 2 brush reserve was 39.8 mils. MWA motor brush wear was closely monitored during this initial period. From launch on January 23, 1970 to January 28, 1970, motor No. 1 was used to drive the MWA. During this period, indicated wear on motor No. 1 brush was approximately 0.8 mil and motor No. 2 brush approximately 0.4 mil. During orbit 066 on January 28, motor No. 2 was selected for checkout of pitch loop No. 2 operational capability. In the period from January 28 to February 7, brush wear of motor No. 2 was observed to be 0.33 mil per day, average rate. However, on February 8 the wear rate of motor No. 2 brush increased to approximately 3.5 mils per day. With the accelerated wear rate of motor No. 2 brush, AED recommended that two steps be taken to connect this problem. The first was to return pitch loop No. 1 (Motor No. 1) to operational mode and the second to increase MWA temperature by commanding both housekeeping telemetry commutations to operate in the manual advance mode.

* Total of real-time mode and record mode.

SR Infrared Picture of Saudi Arabia
Taken by ITOS 1 Orbit 241, Feb. 11, 1970

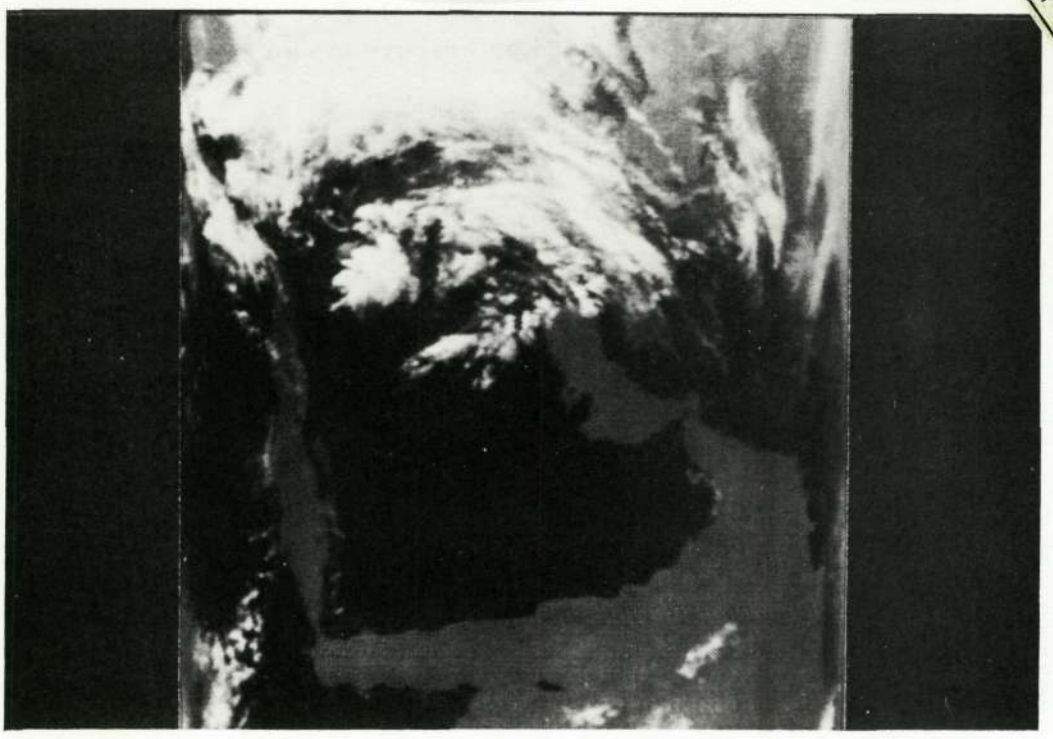

Figure 4-II-1. SR Infrared Picture of Saudi Arabia Taken By ITOS 1 Orbit 241, February 11, 1970

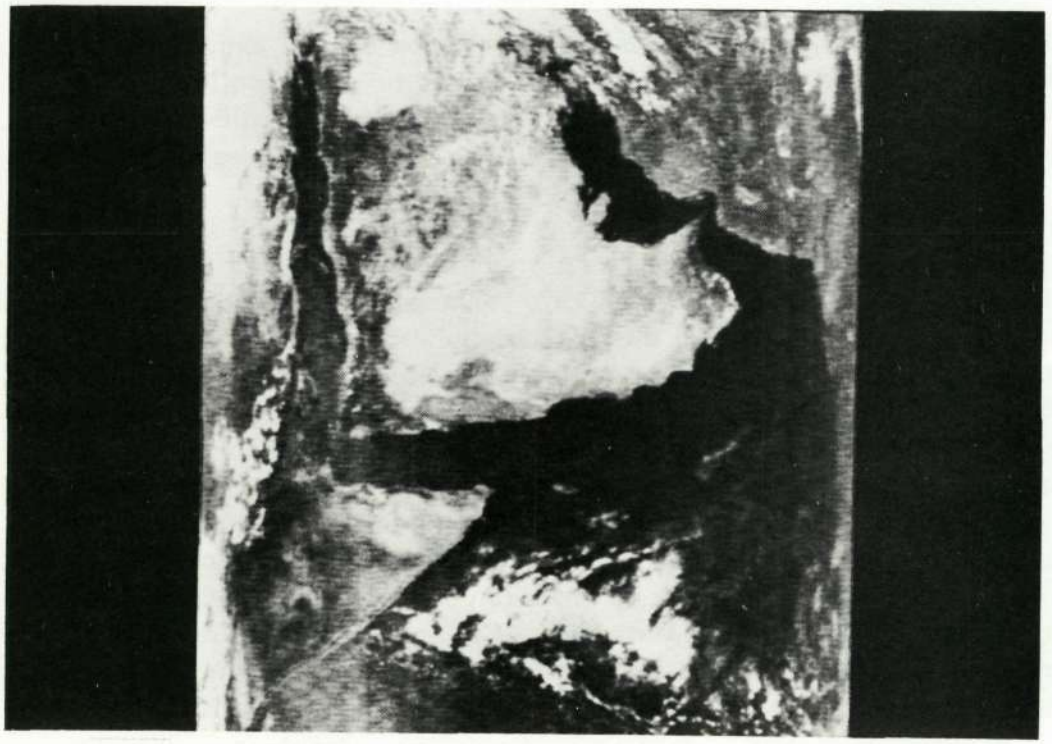

Figure 4-II-2. SR Visible Channel Picture of Saudi Arabia Taken By ITOS 1 Orbit 241, February 11, 1970

These recommendations were implemented by TEC/TCC on February 9, commencing with orbit 217. Although power to MWA motor No. 2 was commanded off during orbit 217, brush wear at the accelerated rate continued until mid-day on February 11. At this time the wear rate began to level off and by February 15 the motor No. 2 brush reserve was observed to decrease at a rate of approximately 0.7 mil per day. With increased MWA temperature on February 19 (MWA temperature increased from +10°C on February 9 to +17°C on February 19), motor No. 2 achieved a nominal brush wear rate. Motor No. 2 brush reserve on February 19 was approximately 8.0 mils, on February 23, 7.5 mils and on March 4, 7.2 mils.

During the period between January 28 and February 9 when MWA motor No. 2 was powered, MWA motor No. 1 brush reserve decreased from approximately 47.2 to 45.0 mils. When motor No. 1 was powered again on February 9, brush wear continued at an approximate rate of 0.1 mil per day until February 24 when the reserve stabilized at 43.0 mils and the wear rate decreased to a negligible value.

Factors causing rapid motor No. 2 brush wear are being investigated by AED.

On orbit 217, momentum wheel speed was monitored during switchover from pitch loop 2 to pitch loop 1. The wheel speed changed less than 2 percent and returned to within 0.25 percent of the nominal speed in 30 seconds.

The spacecraft nutation amplitude was determined to be approximately 0.06 degree half-cone angle; the nutation period, approximately 32.5 seconds. These values were derived from the scanning radiometer data obtained during orbit 392. The method used was to measure the fluctuation in the elapsed time between the insertion of the seven-pulse sync and the sky-earth transition. The roll jitter, which was also derived from this data, was approximately 0.01 degree per second.

Some difficulty was experienced in determining the attitude of the spacecraft with the desired degree of accuracy. This difficulty was a result of not being able to measure the "earth time" from the roll sensor data with consistency. Two alternate methods were developed to obtain roll angle data.

The first method was used to determine the roll angle from the scanning radiometer data. This method was already used to determine the nutation angle. The second method provided the roll angle data by measuring the time between the sky-earth pulse and the pitch index pulse instead of the time between the sky-earth and earth-sky pulse.

RCA provided engineering assistance to GSFC from February 24 to 27 for the purpose of bringing the spacecraft attitude back to the orbit normal after the roll angle

had drifted to approximately 4 degrees. The problem resulted because the attitude program was not updated to compensate for the difference between the programmed unipolar torquing orbit time and the actual orbit period.

Spacecraft temperatures corresponded closely to prelaunch predictions. The commutators were operated in a manual mode in order to compensate for the reduced power dissipation resulting from the nonoperational programming.

When the SR recorder playback command was transmitted during orbit 308, unintentional commands were executed, switching regulator 1 to regulator 2 and switching the pitch loop from normal to coarse gain. This anomaly is attributed to a problem in the CDA station command link. Command operations were normal after its occurrence.

Solar array current, battery voltages, and unregulated voltage were normal during this initial period.

The digital telemetry was processed satisfactorily at AED. A favorable report on the quality of the data from the solar proton monitor was received from Applied Physics Laboratory. To date, no report has been received from the University of Wisconsin regarding the data from the flat plate radiometer.

PART 5. GROUND STATION EQUIPMENT

SECTION I. INTRODUCTION

A. GENERAL

The ITOS ground complex is based on the use of established TOS ground facilities and equipment. Changes have been made to permit compatible ITOS/TOS operations. The additions and modifications reflect design differences between the ITOS and TOS satellite equipment. The ITOS ground complex, therefore, becomes one facet of the established and proven TOS ground operations and procedures.

B. SYSTEM DESCRIPTION

The complex of ground equipment and facilities (GSE) required to monitor and control ITOS and TOS satellite operations consists of:

(1) Command and Data Acquisition (CDA) stations located at

- Gilmore Creek, Alaska (GSE-1),
- Wallops Island, Virginia (GSE-2), and
- Princeton, New Jersey (GSE-3, used for backup receive only).

(2) Command, Programming, and Analysis Centers

- TOS Operations Center (TOC), located at ESSA's National Environmental Satellite Center (NESC) in Suitland, Maryland (GSE-4), and
- TOS Evaluation Center and TOS Checkout Center (TEC/TCC), located at the Goddard Space Flight Center (GSFC) in Greenbelt, Maryland.

(3) Microwave Link Data Transmission Equipment

(4) Satellite Checkout Equipment consisting of

- Launch Support Van (GSE-5), and
- Factory Test Set (GSE-6) at Princeton, New Jersey

(5) Other Participating Facilities and Equipment, including

- A Data Acquisition Facility (DAF) at Gilmore Creek CDA,
- A facility similar to DAF at Wallops Island CDA,
- The NESC Data Processing and Analysis Facility (DAPAF),
- The GSFC Tracking and Data Systems Directorate, and
- Automatic Picture Transmission (APT) Ground Stations.

A functional block diagram of the ITOS ground complex is shown in Figure 5-I-1.

The ITOS/TOS ground complex performs the following basic functions in the operation of the overall satellite system:*

(1) Programs ITOS satellites to record meteorological and scientific data during orbit, including AVCS television pictures, scanning radiometer (SR) data at two different wavelengths, and digitized data providing earth heat balance and proton flux level information at satellite altitude. The satellite also is programmed to take APT, SR, and secondary sensor (SS) information for real-time readout and distribution. Sensor data recorded during orbit is retrieved from the ITOS satellite, processed, and distributed over the microwave link in the ground complex.

(2) Programs operational TOS APT satellites to provide real-time meteorological data in the form of television pictures and radiometric images. Each picture is part of an overlapping pattern and occurs at an exact time and over a known location. The location and time for each picture is specified in advance through orbital-data messages generated within the ground complex and issued to the CDA stations and APT ground stations throughout the world.

(3) Programs operational TOS AVCS satellites to take and record overlapping television pictures of the earth's cloud cover and to relay the video data to the ground on command for collection and analysis within the ground complex.

---

*Detailed information concerning the ground complex is available in the following document: RCA Corporation, Astro-Electronics Division, Instruction and Operating Handbook for the Improved TIROS Operational System (ITOS) and the TIROS Operational System (TOS), AED M-2156, Contracts NAS 5-10306 and NAS 5-9034, Princeton, N.J., April 25, 1969.

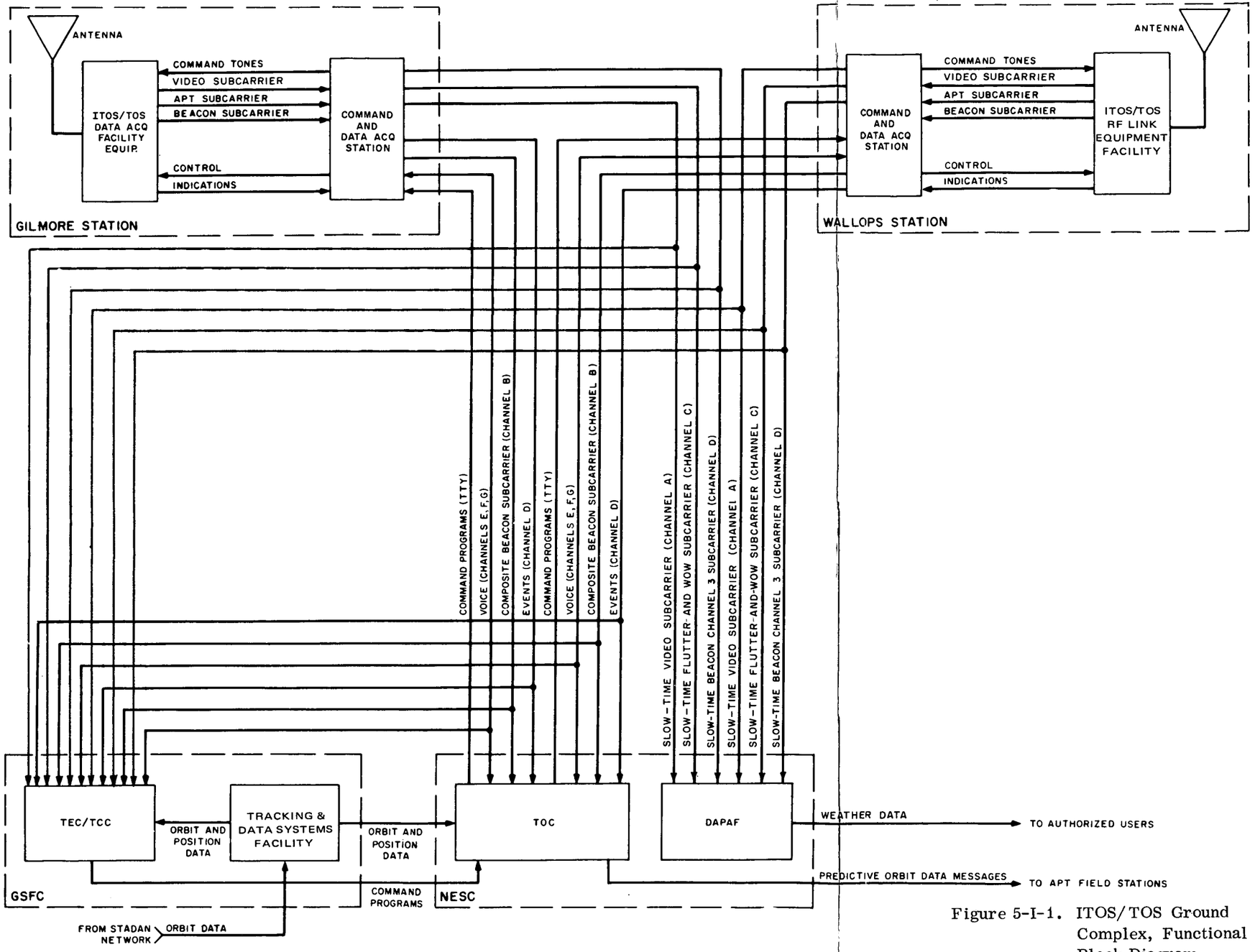

Figure 5-I-1. ITOS/TOS Ground Complex, Functional Block Diagram

FOLDOUT FRAME 1

FOLDOUT FRAME 2

(4) Monitors housekeeping telemetry and attitude data from each operational ITOS, TOS APT, and TOS AVCS satellite, and generates corrective command programs for transmission to individual satellites as required.

The major elements of the ground complex are described briefly in the following paragraphs.

C. COMMAND AND DATA ACQUISITION (CDA) STATIONS

The two primary CDA stations in the ITOS/TOS ground complex function as relay stations between the satellites and the TOS Operations Center (TOC) in Suitland, Maryland. Each station:

(1) Receives teletyped command programs from TOC,

(2) Transmits individual satellite commands in the form of a tone modulated frequency-shift keyed (FSK) RF carrier,

(3) Receives and records on magnetic tape all satellite video, SR, SS, and telemetry data. Telemetry data is relayed to TOC in real time for evaluation. Video and related data recorded during contacts with ITOS and TOS AVCS satellites are played back to the NESC Data Processing and Analysis Facility (DAPAF) over the microwave link network.

Each CDA station incorporates the equipment necessary for on-site analyses of the raw satellite telemetry data. Processed telemetry data is presented on chart recorders from which satellite attitude and other engineering data can be reduced if required. Each station also contains AVCS signal processing equipment to reconstruct the satellite recorded pictures for evaluation of the AVCS video transmission quality. Each station is equipped with the demodulators required to evaluate the performance of all the onboard primary and secondary sensor systems.

D. AUTOMATIC PICTURE TRANSMISSION (APT) GROUND STATIONS

APT ground stations located throughout the world provide fascimile reproductions of cloud-cover pictures transmitted from the onboard APT cameras. Facsimile reproduction of the transmitted scanning radiometer (SR) data is possible provided the satellite is within communication range of the station and at least 10 degrees above the horizon.

The APT video is received at the ground station by a directional antenna equipped with a low-noise preamplifier. The output is further amplified in a receiver that extracts the amplitude-modulated (AM) subcarrier from the frequency-modulated

(FM) carrier for input to a facsimile recorder. The recorder reconstructs the picture transmitted to the ground station on a line-by-line basis. The line-by-line scan produces a clear, gray-shade reproduction of the original picture transmitted by the APT camera on the satellite.

Equipment at the APT ground stations is capable of semi-automatic operation. Once the directional antenna is positioned to acquire the satellite signal, the facsimile recorder will commence recording after an adequate signal is received, and will continue to print on a line-by-line basis until the signal from the satellite is lost for the pass. The recorder then reverts to a standby condition until re-activated on the next pass by transmissions from an APT satellite.

Weekly messages from NESC that contain up-to-date orbital data required to track and orient geographically the pictures received are available to the APT ground stations. Once the facsimile pictures can be geographically oriented and gridded, meteorological data can be extracted for use in forecasting.

E. THE TOS OPERATIONS CENTER (TOC) AND TOS EVALUATION AND CHECKOUT CENTER (TEC/TCC)

The TOS Operations Center (TOC) is the central control point for overall operation of the ITOS and TOS satellite systems. The TOC facility receives requests for weather data from various agencies, and prepares routine command programs for the instrumentation available in orbit that can secure the requested data. The command programs are then teletyped to a CDA station where they are punched on paper tape. To verify correct transmission, the paper tape is used to retransmit the message back to TOC. After TOC confirms that the message has been properly recorded, both the teletype hard copy and the tape are stored at the CDA station until the orbit during which the command is to be transmitted to the satellite.

During contact between satellites and the CDA stations, TOC monitors significant CDA station events and beacon data from the satellite. This data is transmitted from the CDA station to TOC either in real time (RT) or in playback (PB) modes. In the event of unusual performance by the satellite equipment, TOC personnel advise the CDA as to the required corrective action by teletype or voice communication. The telemetry data forwarded to TOC is evaluated in near real time to permit corrective action to be taken as required.

In addition to the primary control functions mentioned above, TOC also prepares operating and maintenance schedules for the CDA stations, and collects all messages, reports, and/or data that relate to the operation of the overall system. From this and other information, TOC maintains historical records of system operation, and disseminates the meteorological and engineering outputs of the ITOS/TOS system.

The TOS Evaluation and Checkout Centers (TEC/TCC), located at GSFC, perform the functions of the TOC during prelaunch checkout and launch of new or replacement ITOS and TOS spacecraft. Once post-launch procedures have shown that the unit is operational, control is assumed by TOC. TOC monitors all TEC/TCC operations during the prelaunch, launch, and post-launch periods, and serves as a relay for all messages and commands to the CDA stations and for data from the newly orbited satellite. In the event that an operational satellite performance appears to be impaired or there are indications that the unit is failing, TOC reassigns control of the satellite to TEC/TCC for evaluation. In this way, satellites with doubtful life expectancy can be replaced to ensure that continuous weather surveillance is maintained by the overall ITOS/TOS system.

F. MICROWAVE LINK DATA TRANSMISSION EQUIPMENT

Coordination of all ITOS/TOS satellite operations is carried out by means of a microwave link ground communications network between major elements in the ground complex. The network links the CDA stations with NESC (TOC, DAPAF) and GSFC (TEC/TCC). The link relays command program data to the CDA stations from TOC or TEC/TCC and provides hard-copy for written instructions and meassages within the ground complex. The link is used for voice communications and to transmit satellite video and other sensor data from the CDA stations to the central control points within the system for evaluation and distribution. The total baseband frequency is 48 kHz; the link is divided into seven channels with the following bandwidths and functions.

Channel	Function	Baseband (Hz)
A	SR, AVCS video, secondary sensor data	13,000 to 30,000
B	Composite beacon subcarrier	1,800 to 4,400
C	Flutter-and-wow subcarriers for SR, AVCS	5,950 to 6,550
D	Multiplexed CDA events composite subcarrier, slow-time beacon playback	300 to 3,200
E	Voice communications or teletype (2)	
F,G	Voice communications	

G. OTHER PARTICIPATING FACILITIES

1. The Data Acquisition Facility (DAF)

The DAF equipment is co-located with the CDA station at Gilmore Creek, Alaska. A similar facility also exists at the Wallops Island CDA. The two facilities provide the ancilliary equipment required to establish an RF link with

the orbiting ITOS and TOS satellites. The equipment is not unique to the ITOS/TOS ground complex, and is used on other space and communication projects. DAF provides the transmitting and receiving equipment at frequencies called for by the ITOS/TOS satellites, including antennas and tracking capability necessary to acquire and follow the satellites during contacts for data readout or command transmission. The inputs from DAF to the CDA stations consist of demodulated carriers and AGC voltages. The AGC inputs are used to indicate received signal strength and to monitor the time when actual data transmission from the satellite commences.

2. The NESC Data Processing and Analysis Facility (DAPAF)

DAPAF processes all meteorological data obtained from ITOS and TOS satellite instrumentation for presentation to user agencies. The AVCS, scanning radiometer (SR), and secondary sensor (SS) data received by the CDA stations are sent via the microwave link to DAPAF where computer equipment digitizes, formats, and/or presents the satellite input data in scale-rectified map form or in related forms of meteorological significance. After a series of 12 or 13 orbits, a photographic mosaic covering the entire surface of the earth can be constructed at DAPAF from AVCS video data, complete with latitude and longitude references. The facility also prepares SR and SS information for use by other agencies, and supports TOC by processing telemetry inputs from orbiting satellites on equipment conditions and satellite attitude.

3. The GSFC Tracking and Data Systems Directorate

Operating in conjunction with the NASA STADAN network, the Directorate provides TOC and TEC/TCC with orbital parameter data on a continuous basis throughout the operational life of each ITOS and TOS satellite. These inputs are used within the ground complex to generate messages for the CDA stations, APT ground stations, and DAPAF.

SECTION II

COMMAND AND DATA ACQUISITION STATIONS

A. GENERAL

The CDA stations, operating in conjunction with radio and microwave link facilities at each installation, function as relay stations between orbiting ITOS and TOS satellites and TOC. The primary CDA stations at Gilmore Creek and Wallops Island (1) transmit command programs formulated by TOC to the satellites, (2) receive and process the data transmitted by the satellites upon command, and (3) transmit this data to other facilities within the ground complex as directed by TOC. (See Figure 5-II-1.) To carry out the above functions, the stations must be equipped to perform the following tasks:

- Convert the satellite program commands received from TOC to audio-frequency tones suitable for modulation of an RF carrier,
- Provide the RF link facilities at the installation with command messages suitable for direct transmission to the satellites,
- Record all subcarriers carrying video, secondary sensor, and data required to determine satellite orientation and condition that are received from the satellites via the RF link,
- Process and transmit this data in real time or by playback of recordings on magnetic tape to other facilities in the ground complex for reduction and evaluation, and
- Monitor and display data received from the RF link to provide a backup capability for the evaluation and reduction activity performed at other facilities.

Each of the primary CDA stations is equipped to process data from ITOS, TOS APT, and TOS AVCS satellites, and to prepare the command programs for transmission to each type of satellite in the orbiting system. Operating parameters are listed in Table 5-II-1.

The CDA station equipment is divided into the following subsystems:

- Master timing equipment
- Programming equipment
- Video processing equipment

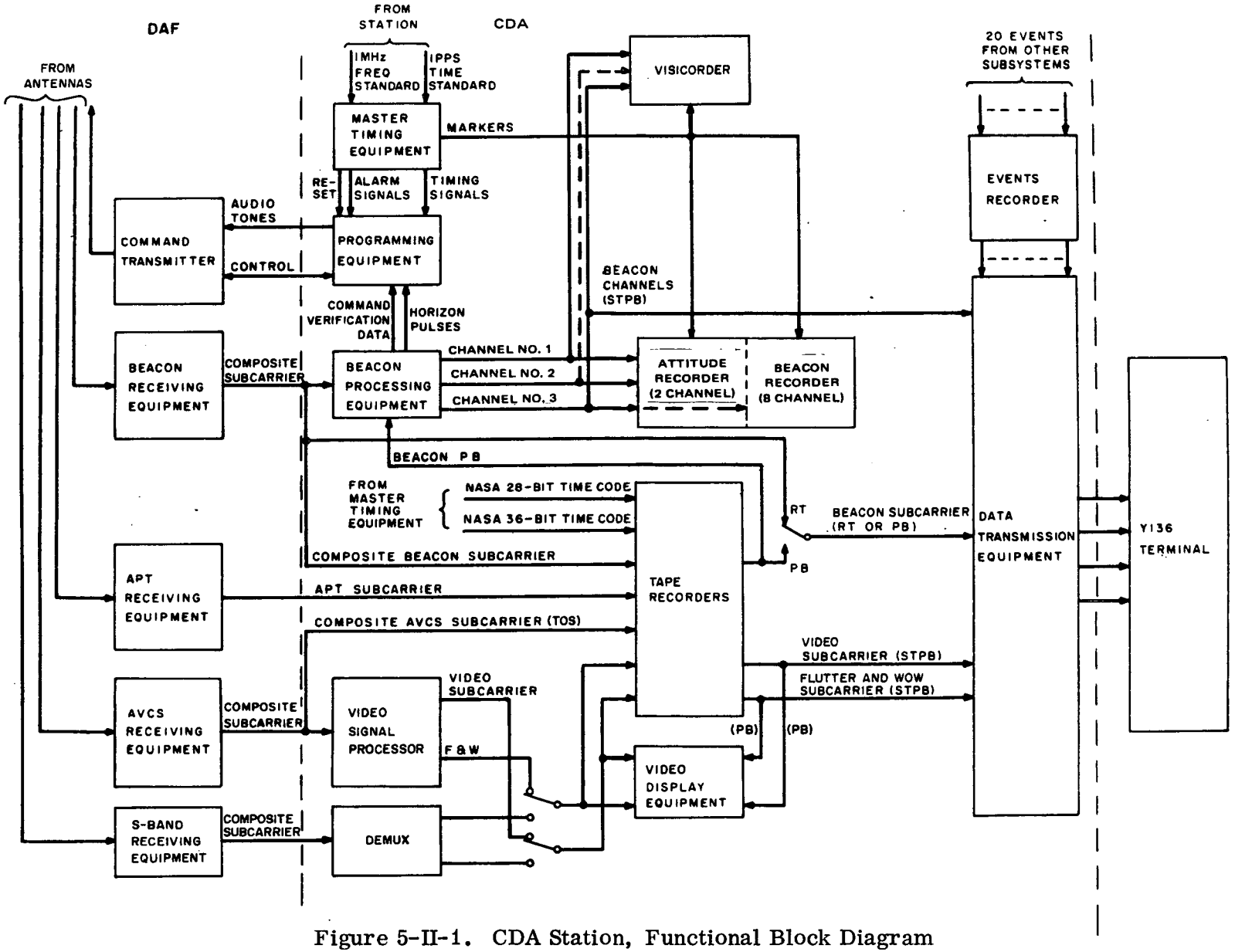

Figure 5-II-1. CDA Station, Functional Block Diagram

TABLE 5-II-1. MAJOR CDA STATION OPERATING PARAMETERS

Parameter	Specified Limits
POWER INPUTS	
AC Power	
Type	3 phase, 4 wire
Voltage	208 volts ±10 percent
Frequency	60 Hz ±1 percent
Current	30 amperes per phase
SIGNAL INPUTS	
TOS Composite Playback Signal	
Composite frequency spectrum	9 to 120 kHz
Amplitude	3 volts, peak-to-peak
Input impedance	75 ohms
APT Video Subcarrier	
Frequency spectrum	0.8 to 4.0 kHz
Amplitude	3 volts, peak-to-peak
Input impedance	75 ohms
Composite Beacon Subcarrier	
Composite frequency spectrum	2.0 to 4.4 kHz
Amplitude	3 volts, peak-to-peak
Input impedance	75 ohms
ITOS Composite Playback Signal	
Composite frequency spectrum	10 to 480 kHz
Amplitude	2.8 volts, peak-to-peak
Impedance	75 ohms
TIMING INPUTS	
Frequency Standard	
Frequency	1 MHz
Amplitude	8 to 12 volts, peak-to-peak
Input impedance	75 ohms

TABLE 5-II-1. MAJOR CDA STATION OPERATING PARAMETERS (Continued)

Parameter	Specified Limits
TIMING INPUTS (Continued)	
Time Standard	
Frequency	1 pps
Amplitude	1 volt, peak-to-peak
CDA/ DAF INTERFACES	
Control and Indicator Lines	
Command transmitter ready	28-volt indicator - DAF to CDA
Command transmitter on	28-volt control - CDA to DAF
Command transmitter plate supply	28-volt indicator - DAF to CDA
Power transmitted	28-volt indicator - DAF to CDA
Select antenna or dummy load	28-volt control - CDA to DAF
Antenna selected	28-volt indicator - DAF to CDA
Dummy load selected	28-volt indicator - DAF to CDA
Command RF from Antenna Feed	
Frequency	Command
Amplitude	-113 to -27 dBm
Impedance	50 ohms
Horizontally Polarized AVCS Receiver AGC	
Voltage range	0 to 8 volts
Corresponding RF signal strength*	thermal noise to -25 dBm
Vertically Polarized AVCS Receiver AGC	
Voltage range	0 to 8 volts
Corresponding RF signal strength*	thermal noise to -25 dBm
Horizontally Polarized APT Receiver AGC	
Voltage range	0 to 8 volts
Corresponding RF signal strength*	thermal noise to -25 dBm
Vertically Polarized APT Receiver AGC	
Voltage range	0 to 8 volts
Corresponding RF signal strength*	thermal noise to -25 dBm

*At receiver input.

TABLE 5-II-1. MAJOR CDA STATION OPERATING PARAMETERS (Continued)

Parameter	Specified Limits
CDA/ DAF INTERFACES (Continued)	
Horizontally Polarized Beacon Receiver AGC	
Voltage range	0 to 8 volts
Corresponding RF signal strength*	thermal noise to -25 dBm
Vertically Polarized Beacon Receiver AGC	
Voltage range	0 to 8 volts
Corresponding RF signal strength*	thermal noise to -25 dBm
Horizontally Polarized S-Band Receiver AGC	
Voltage range	0 to 8 volts
Corresponding RF signal strength*	thermal noise to -25 dBm
Vertically Polarized S-Band Receiver AGC	
Voltage range	0 to 8 volts
Corresponding RF signal strength*	thermal noise to -25 dBm
Command Tone Outputs	
Frequencies	Tone pair A or tone pair B
Amplitude	0 to 1.0 volt, peak-to-peak (adjustable)
Output impedance	50 ohms
CDA/ MICROWAVE LINK INTERFACES	
Channel A	
Wideband video channel	
Frequency spectrum	13 to 30 kHz
Amplitude	1 ±0.1 volt, peak-to-peak
Impedance	135 ohms, balanced
Channel B	
Composite beacon subcarrier	
Frequency spectrum	1.8 to 4.4 kHz
Amplitude	1 ±0.1 volt, peak-to-peak
Impedance	135 ohms, balanced

*At receiver input.

TABLE 5-II-1. MAJOR CDA STATION OPERATING PARAMETERS (Continued)

Parameter	Specified Limits
CDA/ MICROWAVE LINK INTERFACES (Continued)	
Channel C	
Flutter-and-wow subcarrier	
Frequency	6250 ± 300 Hz
Amplitude	1 ±0.1 volt, peak-to-peak
Impedance	135 ohms, balanced
Channel D	
Events channel	
Frequency spectrum	300 to 3200 Hz
Amplitude	1 ±0.1 volt, peak-to-peak
Impedance	135 ohms, balanced
CDA programmer events	
Frequency	2400 ±125 Hz (FSK)
Bandwidth	±350 Hz
Amplitude	1/ 3 volt, peak-to-peak (nominal)
CDA station events subcarrier	
Frequency	1300 ±125 Hz (FSK)
Bandwidth	±200 Hz
Amplitude	1/ 3 volt, peak-to-peak (nominal)
TOS STPB beacon No. 3 subcarrier	
Frequency	451 to 524 Hz (487.5 center frequency)
Amplitude	1/3 volt, peak-to-peak (nominal)

- Recording equipment
- Microwave link data transmission equipment
- Station control circuitry

The master timing equipment provides all CDA station equipment with a time reference and generates the signals required for automatic transmission of command programs to satellites in orbit. The equipment is synchronized to a 1-MHz station time standard that is external to the master timing subsystem. Signals available from the subsystem include pulse trains at frequencies of 0.1-pps, 1-pps, 10-pps, 100-pps, and 1000-pps, and standard NASA serial 28-bit and 36-bit time codes. The serial NASA codes are available as modulation on a 50-kHz carrier or in level-shift format. The 36-bit codes presently are not used in CDA station operations.

The programming equipment generates satellite commands in the proper sequence along with an enable tone, and compares the retransmission of commands received by the satellite with the original transmission from the CDA station on a bit-for-bit basis. Commands may be direct or remote, and are originated by TOC and teletyped to the CDA station well in advance of the orbit during which they will be transmitted to the satellite.

Video processing equipment at the station displays and photographs the TV pictures transmitted from TOS AVCS and ITOS satellites. The Data Processing and Analysis Facility (DAPAF) is responsible for processing AVCS video subcarrier data relayed from the station, but a local capability to process the data serves two purposes. The quality of the TV images can be evaluated, and the fidelity of the tape recorded video data can be determined. The stations do not have the facsimile equipment required to display the pictures received from the TOS APT and ITOS satellites. Facilities are provided at the stations, however, to display the APT subcarrier received from the satellite. Demodulators for the scanning radiometer (SR) and secondary sensor (SS) signals are included in the video processing subsystem to allow evaluation of the quality of the data received at the CDA station.

Four magnetic tape recorders are used to record and playback all data transmissions from the satellites. A 20-channel Esterline-Angus recorder provides a permanent record of major CDA station events that occur during a satellite contact. Two Brush chart recorders are used at the station to record attitude data received from TOS satellites (a two-channel unit), and to record beacon telemetry data from all types of satellites in the system, transmitted commands to the satellites, and signal strength information on signals received at the station from the orbiting satellites (an eight-channel unit). A Honeywell Visicorder is included for display and reduction of ITOS attitude data.

Microwave link data transmission equipment connects all facilities within the ground complex, serves as the relay for satellite data through the system and as a verbal communications link for the system, and provides hard-copy instructions and procedures for the operating facilities. The equipment is used for transmission of data in real time from the CDA station to TOC or TEC/TCC, or for playback of data recorded during the satellite pass on station magnetic tape or paper chart recorders.

In addition to the above equipment, the CDA station requires circuitry to control operating modes and to monitor the condition and status of the subsystems at the station. These functions are accomplished by the station control panel located in rack 26. The push-button switches on the panel accomplish the following as required:

- Apply power to the AVCS processing equipment and show the status of the power supplies required to operate equipment in the various station subsystems, as well as selecting the vertical sync generator to be used in processing AVCS pictures.
- Select one of the redundant command programmers for use and place the selected unit in an operating or test mode.
- Switch station equipment to an ITOS or TOS AVCS and TOS APT mode of operation.
- Decide on manual or automatic start for the CDA station events recorder in response to received signal strength, and decide on manual or automatic start of the paper tape reader in the programming equipment by the alarm timer.
- Select either the local or system calibration mode for the beacon signal processing operations. Selection of the system mode includes the RF equipment of the DAF in the calibration procedure.

The CDA station also contains the test equipment necessary to monitor and maintain the operational CDA subsystems.

To ensure that the CDA stations will be in a state of operational readiness for all satellite passes, the equipments in the stations either have been provided in redundant pairs, or two different units that perform similar functions have been included in the equipment complement.

In the programming subsystem, two complete command programmers, located in racks 35A and 35B, have been provided to ensure the satellite-commanding capability. In addition, the program of commands to the satellite can be set up by either of two methods: the primary method, using the automatic teletype tape reading system, or a secondary method that employs manually set switches on the front panels of both programmer racks.

The data subcarriers (both video and beacon), which are transmitted from the satellite to the CDA station, are permanently recorded on two of the four redundant magnetic tape recorders. During satellite interrogations, one recorder is turned on at the beginning of the pass and the other is turned on at the beginning of the video transmission.

The beacon transmissions from the satellite, besides being redundantly recorded on the Mincom recorders, are also demodulated, and the data obtained is recorded in permanent form on paper chart recorders. Should a failure occur in the tape recorders, this data would still be available. In addition, since the beacon subcarrier is normally delivered in real time to TOC via the ground complex communications network, the data would also be available at that facility.

Equipment at the Gilmore Creek and Wallops Island CDA stations consists of 11 standard equipment racks, four tape recorders, and a kinescope complex of three permanently-attached racks. The arrangement of the equipment racks at each of the stations is shown in Figure 5-II-2. The racks to which modifications and/or additions have been made for ITOS ground operations are shaded for discussion later in the section. Equipment complements for the two stations are provided in Table 5-II-2.

B. DESIGN APPROACH

1. General

The two CDA stations at Gilmore Creek, Alaska and Wallops Island, Virginia have been modified to operate with the ITOS system, without compromising their TOS capability. Switching circuitry has been installed which will permit rapid changeover from one system to the other.

Much of the equipment already installed for use with TOS is incorporated into the ITOS command and data acquisition system. Special equipment has been installed at these stations to accommodate the requirements of ITOS.

The additional equipment required for ITOS necessitated the addition of one rack of equipment and two magnetic tape recorders.

The new rack incorporates:

(1) Two demultiplexers,

(2) Two dual-mode scanning radiometer signal demodulators,

(3) A high-speed chart recorder,

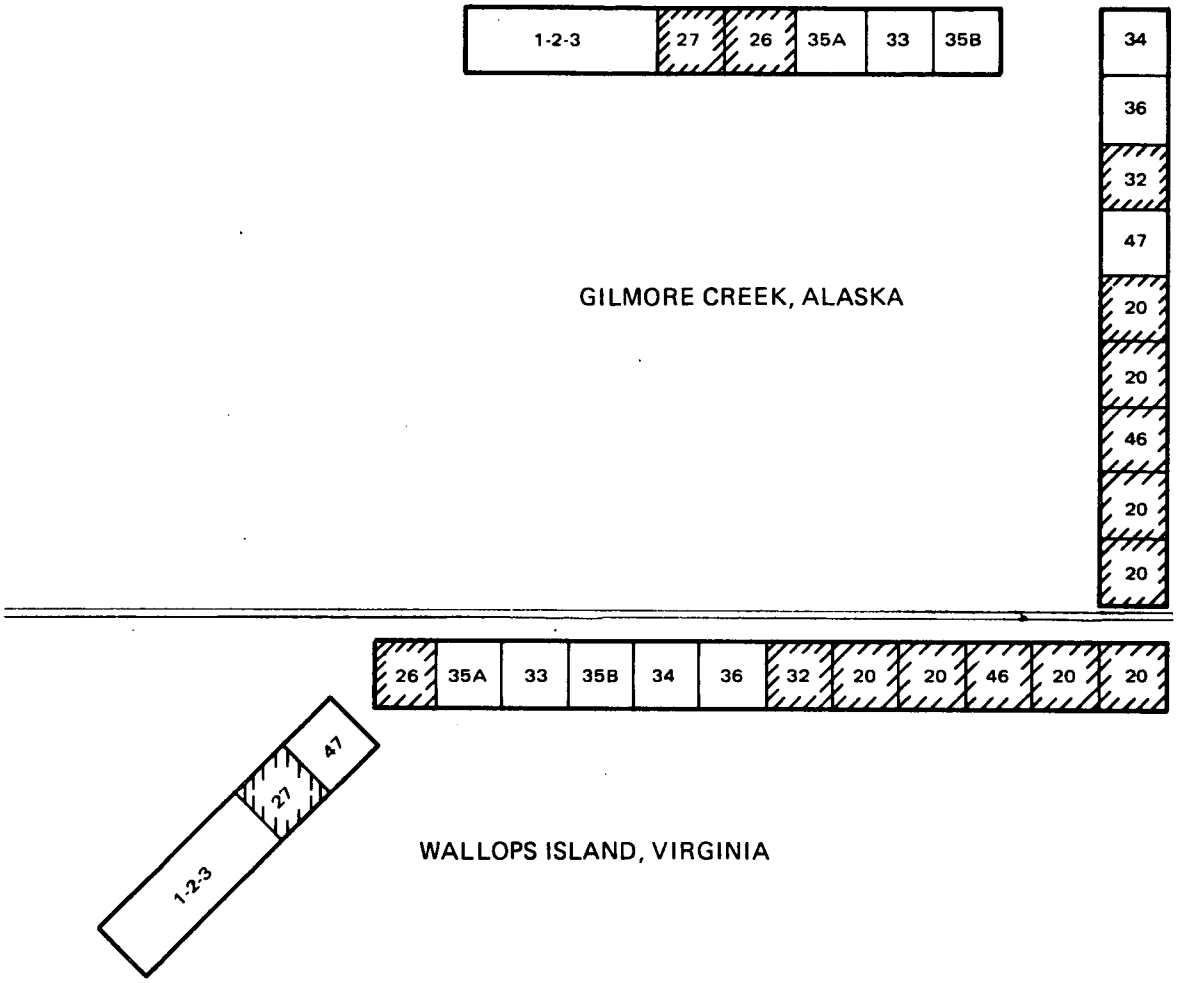

Figure 5-II-2. CDA Station Equipment Arrangements

(4) A monitor oscilloscope with signal selection switching,

(5) Monitor and control switching facilities, and

(6) Secondary sensor processing and demodulation.

The additional discriminators and calibration equipment required for use with special channel 3 beacon subcarrier are installed in the unused section of the existing subcarrier discriminator chassis (rack 32). A complete replacement station control panel with additional switching facilities has been provided for in rack 26.

Additional switching resulting from the ITOS changes is incorporated to minimize the time required to change from TOS to ITOS operation.

TABLE 5-II-2. CDA STATION EQUIPMENT

Rack No.	Rack Name	Chassis Equipment
1, 2	Kinescope Display	Polaroid Film Processor Kinescope Assembly Kinescope Display Unit
3	Kinescope Electronics	Storage Video Jack Panel Kinescope Deflection Generator Video Control Circuits High-Voltage Power Supply Blower
27	Video Signal Processor	Data Locator Control, Mincom A Data Locator Control, Mincom B Oscilloscope* Index Display Control Panel Video Signal Processor Scope Selector and Jack Panel Auxiliary Jack Panel Hewlett-Packard 200CDR Oscillator Blower
26	Station Control	AC Power Control Panel Station Control Panel Lambda +300 VDC Power Supply Lambda +22 VDC Power Supply Lambda +24.5 VDC Power Supply Lambda -24.5 VDC Power Supply

*In Gilmore station, Tektronix RM35A; in Wallops station, Tektronix RM545B.

TABLE 5-II-2. CDA STATION EQUIPMENT (Continued)

Rack No.	Rack Name	Chassis Equipment
26 (cont)	Station Control	Lambda +24 VDC Power Supply Lambda -24 VDC Power Supply Lambda -18 VDC Power Supply Blower
35A	Command A	ECCO 812 Master Clock Programmer,* Drawer A Programmer,* Drawer B Programmer,* Drawer C Programmer,* Drawer D NAVCOR 12 VDC Power Supply Blower
33	Tape Reader	Speaker Panel Esterline-Angus Events Recorder Royal McBee Tape Reader Tape Reader Electronics NAVCOR 12 VDC Power Supply Blower Relay Panel (rear of rack)
35B	Command B	Same as Rack 35A
34	Alarm Timer	Hewlett-Packard 5245L Electronic Counter Counter Selector Panel Alarm Timer

*Digital command programmer (DCP) and auxiliary command unit (ACU) share Drawers A through D of this rack.

TABLE 5-II-2. CDA STATION EQUIPMENT (Continued)

Rack No.	Rack Name	Chassis Equipment
34 (cont)	Alarm Timer	Transmitter Control Panel Quindar Scanner and Tone Transmitter (2 sets) Blower
36	Data Recorder	Beacon (8-Channel) Recorder Ampex Magnetic Tape Degausser Blower
32	Beacon	Tektronix RM504 Oscilloscope Scope Selector Panel Attitude Recorder (2-Channel) Beacon Subcarrier Discriminators and Calibrator (EMR) Command Comparator Blower
20A1 and 20A2	Magnetic Tape Recorder A	Mincom G-100 or Sangamo 4784 Magnetic Tape Recorder Relay Panel and Isolation Amplifier (at rear of rack) Blower
20B1 and 20B2	Magnetic Tape Recorder B	Mincom G-100 or Sangamo 4784 Magnetic Tape Recorder Relay Panel and Isolation Amplifier (at rear of rack) Blower
46	Demultiplexer	Control Panel Demultiplexer Jack Panel
47	Telemetry	Visicoder Chart Recorder Telemetry Jack Panel

Redundancy is provided in the CDA stations wherever an electronic failure could result in loss of information. Parallel channels are provided up to and including the magnetic tape recorders. Beyond the recorders, redundancy is not considered necessary, since information can always be recovered by replaying the recorders.

Two complete command programmers ensure command capability. In addition, the program of commands to the satellite can be set up by either of two methods: the primary method uses the automatic teletype tape-reading system; the secondary method uses manual switches on the front panels of both programmer racks.

2. AVCS Video Processing and Display Equipment

ITOS satellites utilize an S-band link to transmit AVCS video data. S-band receivers have been installed at the DAF section of the CDA station. The carrier is modulated by a composite signal containing nine channels of data.

The video handling section of the CDA station receives and processes the 10- to 480-kHz composite signal transmitted from the satellite. This composite signal contains the information shown below:

Information	No. of Channels
SR Video	2
SR Flutter-and-Wow	2
AVCS Video	1
AVCS Flutter-and-Wow	1
Secondary Sensor Data	3

The individual subcarriers are extracted from the composite signal by the CDA station demultiplexers and recorded on magnetic tape recorders. After each satellite pass, the information is retransmitted to DAPAF via the microwave link. The limited capacity of the link necessitates the sequential transmission of the video data; however, each video channel is transmitted simultaneously with its associated flutter-and-wow signal. The CDA station processes the video data (e.g., by replaying the recorders at a reduced speed) to produce compatibility between the frequency characteristics of the video signals and the microwave link. The three secondary sensor data channels are retransmitted as a composite signal over the video channel in slow-time playback.

Redundant demultiplexers and recorders are provided to minimize the possibility of loss of information. Oscilloscope display of the received subcarriers and of the demodulated signals for monitoring purposes is included.

3. APT Video Processing Equipment

APT video transmissions from an ITOS satellite are processed only by Wallops Island through separately provided GFE equipment.

4. Recorded Scanning Radiometer Data Processing Equipment

The SR data is received as a continuous signal. Each line of the signal will last 156.25 milliseconds and will include a 7.5-millisecond sync pulse. The information is received as a frequency-modulated signal, with a frequency of 26.4 kHz corresponding to cold, 21.0 kHz to hot, and 19.2 kHz to sync tip. The information baseband is 3.6 kHz. The earth-scan portion of the SR signal begins immediately after the sync pulse and ends 52 milliseconds after the sync pulse. The remainder of the video signal is time-shared among spacecraft-clock, calibration, and telemetry data.

The flutter-and-wow signal is a 6.25-kHz subcarrier, frequency-modulated by the flutter-and-wow of the spacecraft and ground tape recorders. The flutter-and-wow signal is present throughout the SR video transmission.

The SR video and flutter-and-wow signals will be played back at half the recorded rates. Their frequency characteristics are then directly compatible with those of the microwave link.

The SR video channel to be transmitted is selected by relay switching on recorder playback. Since a flutter-and-wow channel is not uniquely associated with one video channel, it will be necessary to monitor the two flutter-and-wow channels on playback to determine which is to be transmitted on the microwave link in association with a video channel.

When a flutter-and-wow signal is present on both channels, each flutter-and-wow channel is associated with its related video channel (flutter-and-wow 1 with video 1 and flutter-and-wow 2 with video 2). When a flutter-and-wow signal is present on only one channel, it is associated with both video channels. In this case, the signal can be on either flutter-and-wow channel 1 or 2, depending upon the spacecraft tape recorder in use.

5. Secondary Sensor Data Processing Equipment

The secondary sensor data frequency-modulates three multiplexed subcarriers, centered at 19, 20, and 22 kHz. The deviation of each subcarrier is ±500 Hz.

The 18-kHz subcarrier is modulated with solar proton monitor data. Each frame of data contains 180 bits divided into 20 nine-bit words. The first word is a frame

sync code (111010001). The remaining 19 words are each divided into two parts; the first four bits contain the exponent, and the remaining five contain the characteristic of the channel being sampled.

The 20-kHz subcarrier is modulated with a 125-Hz clock signal.

The 22-kHz subcarrier is modulated with flat plate radiometer (FPR), time code, and telemetry data. Each frame contains 480 bits divided into 60 words of 8 bits each. The first two words contain all "1's" and are used as a frame marker. The first bit of each of the remaining 58 words is a "0", which is used as a word marker. The allocation of the words in each frame follows:

Number of Words	Information
2	Frame sync
4	Time code
8	FPR data
7	FPR telemetry
39	Spacecraft telemetry and spares

6. Tape Recorders

Two 14-track magnetic tape recorders (A and B) were originally in use at the CDA stations. Seven of the 14 available tracks on each recorder were used for TOS. For ITOS, it was proposed that each CDA station have four 14-track recorders (operated as redundant pairs) for the following reasons:

- Data from one set of recorders would be retransmitted at one-half real time and data from the second set at one-eighth real time, minimizing the possibility of operator error.
- It would be possible to redundantly record signals from one pass simultaneously with the retransmission of data recorded from a previous pass.
- Replacement units of the same design were not available. The revised design required a change of interface, which would be simplified if all recorder-reproducers at one station were of the same design.

Therefore, four new recorders were installed at the Gilmore Creek station and two of the recorders at Gilmore Creek were moved to the Wallops Island station, so that there are four 14-track recorders at each station. For the functional description of these recorders, see Paragraph C.7.a of this section.

7. Beacon and Telemetry Data Processing Equipment

a. GENERAL

The beacon receiving equipment and the beacon data-processing equipment receive, record, and process the beacon transmission from ITOS spacecraft. The DAF equipment receives and demodulates the 136.77-MHz phase-modulated beacon carrier signal and delivers a 3-volt peak-to-peak composite beacon subcarrier to the CDA beacon data-processing equipment. Figure 5-II-3 is a block diagram of the beacon data-handling equipment.

For TOS, the composite beacon subcarrier signal consists of three frequency-multiplexed audio subcarriers on IRIG channel 7 (2.3 kHz), 8 (3.0 kHz), and 9 (3.9 kHz). The three subcarriers are demultiplexed and demodulated. The demodulated data is displayed on a two-channel attitude chart recorder (channels 7 and 8) and on an eight-channel beacon recorder (channel 9). A telemetry calibrator, consisting of a multiplexing unit and three calibration oscillators, provides a means for calibrating the discriminator/recorder operation. A loudspeaker indicates to ground station personnel that the composite beacon signal is being received.

The composite beacon signal is recorded on the magnetic tape recorders and transmitted on the microwave link in real time to TOC and TEC/TCC. The composite signal can also be played back from the recorders for transmission to TOC and TEC/TCC. In slow-time playback operations, the channel 9 subcarrier is separated from the composite subcarrier and transmitted with the video data on the microwave link.

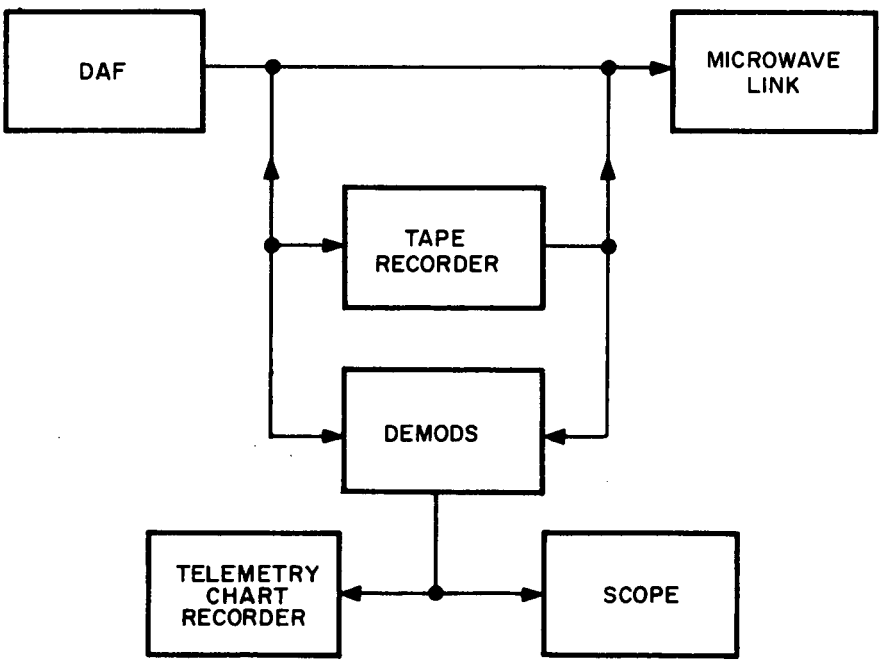

Figure 5-II-3. Beacon Data Handling, Block Diagram

The ITOS beacon subcarrier consists of two frequency-multiplexed audio subcarriers, one using IRIG channel 9 (centered at 3.9 kHz) and a second channel centered at 2.3 kHz with a deviation of ±20 percent (not IRIG standard).

IRIG channel 9 contains the following data:

(1) Command verification data,

(2) Housekeeping telemetry, and

(3) Solar aspect sensor data.

The nonstandard channel (channel 3) contains horizon crossing data and, during the satellite launch phase, accelerometer data. Channel 9 processing remains the same as for TOS. Channel 3 data is demultiplexed, demodulated, and displayed on a high-speed chart recorder. The composite subcarrier is recorded on any two of the four magnetic recorders. The subcarrier is retransmitted to TOC and TEC/TCC as it is being received from the spacecraft. For postacquisition playback, one of the recorders is replayed at the recorded rate to transmit the recorded data to TOC and TEC/TCC. Additional calibration facilities are provided.

b. BEACON PROCESSING

The existing facilities for handling TOS beacon data are not changed. A channel selector and discriminator were added to extract and demodulate the data from the subcarrier. The channel selector has a bandwidth of 1.6 to 3.0 kHz. A center frequency input (2.3 kHz) to the discriminator produces an output to 0 volt. The output voltage varies linearly with the deviation from the center frequency. For full deviation (±20 percent) the output voltage of the discriminator is ±10 volts, ±5 percent. A calibration oscillator is controlled by the existing Electro-Magnetic Research model 280A calibrator.

The calibration procedure remains unchanged.

c. BEACON DISPLAY

The demodulated data is displayed on a high-speed chart recorder. The recorder has a recording speed of at least 50 inches per second. The associated galvanometer frequency response is not less than 1 kHz. When operating in the TOS mode, the beacon display is identical to that previously employed, and the signal input to the recorder is grounded. When operating in the ITOS mode, the channel 7 and 8 inputs to the recorder are grounded, and it is possible to select the demodulated signal for display on the oscilloscope mounted on rack 32.

d. TELEMETRY

Telemetry is available from three sources. One source is the beacon telemetry subsystem. This subsystem is redundant, utilizing two subcarrier oscillators (SCO's) for each of two beacon transmitters. One SCO is a 3.9-kHz standard IRIG channel (±7.5-percent deviation) and the other is a 2.3-kHz non-standard IRIG channel (±20-percent deviation). One beacon transmitter and its associated SCO's are in operation at a time; the selection is made by ground command. The subsystem is used for the transmission of housekeeping telemetry (120 points), command data verification, pitch and roll sensor analog data, roll sensor and selected pitch index pulse data, digital solar aspect sensor (DSAS) data, real-time solar proton monitor (SPM) data, and spacecraft time code data. The data is used primarily for "quick look" analysis of the performance and status of the spacecraft; it is also used for troubleshooting operations, should problems arise in the operation of the spacecraft.

The beacon telemetry subsystem data is in real time, available only during the relatively brief CDA contact times, and its use is not recommended for investigating problems requiring trend analysis.

A second spacecraft source of telemetry is the secondary sensors subsystem, which consists of a data format converter (DFC), an incremental tape recorder (ITR), a solar proton monitor (SPM), and a flat plate radiometer (FPR). The secondary sensors subsystem data includes 39 words of digital converted telemetry in the data format recorded on track No. 3 of the ITR. The telemetry information in these words is recorded whenever the subsystem is operating (normally, throughout the orbit) and is used primarily in the evaluation of the thermal and power status of the spacecraft on an orbital basis. The data consists of samples of certain power and temperature telemetry points which are recorded once every 32 seconds. This data permits a detailed analysis of the thermal and electrical environment of the spacecraft throughout the orbit under the varying load conditions dictated by the operational modes of the spacecraft.

The third source of spacecraft telemetry is the scanning radiometer (SR) subsystem. During the period in each mirror rotation when the selected scanning radiometer is scanning its housing, an analog commutation system provides samples of certain data points for recording on the scanning radiometer recorder. Two types of data are subcommutated and recorded in this manner: data that provides continuous calibration references for use in the processing of the scanning radiometer information and analog recordings of pertinent pitch sensor, roll sensor, and selected pitch index pulse information. The latter serve as a secondary source of data for determining spacecraft attitude and for evaluating performance of the spacecraft stabilization (pitch control) system.

8. Microwave Link Transmission Equipment

The existing microwave link facilities and channel characteristics remain unchanged for ITOS. The data-handling channels are as follows:

Channel	Bandwidth (kHz)
A	13 to 30
B	1.4 to 4.4
C	4.3 to 7.4
D	0.3 to 3.4

A technique similar to that used for AVCS is employed for transmitting secondary sensor data on the microwave link. The tape recorder is replayed at one-eighth the recording speed to convert the frequency spectrum of the signal to a spectrum compatible with the characteristics of the microwave link. A secondary sensor relay selects the source of information. This relay is disabled while the system is operated for TOS.

The ITOS system requires that the secondary sensor data modulate three voltage-controlled oscillators while it is being replayed from the spacecraft incremental tape recorder. The outputs of the three oscillators are combined and transmitted as one channel of the multiplexed S-band transmission.

9. Programming Equipment

The CDA station programming equipment consists of: (1) a punched paper tape reader (PTR) and a tape reader electronics (TRE) unit; (2) dual and redundant programmer units, each containing a digital command programmer (DCP) and an auxiliary command unit (ACU); (3) a transmitter control panel that provides the interface with the data acquisition facility (DAF); and (4) a command comparator. The PTR and TRE units permit automatic processing of the satellite command programs directly from the teletype tapes prepared at the CDA station and verified with TOC. The DCP and ACU are used to generate the individual commands to be transmitted to a satellite. Each command sent to a satellite is compared on a bit-by-bit basis with the retransmission of the command from the satellite by the command comparator unit. Any commands that are erroneously received by the satellite are either manually or automatically retransmitted under the control of the comparator.

Commands for programming ITOS and TOS satellite instrumentation are transmitted from the CDA stations to the satellites in the form of audio frequency tones that amplitude modulate a radio frequency command carrier. Each command

transmission to the satellite consists of a 5.35-second transmission of a continuous, analog, audio frequency "enable" tone required as part of the access sequence for command reception, followed by a digital address and one or more sequencies of commands that are formed by frequency-shift-keying a second audio tone, the FSK tone, to form binary "1's", and binary "0's" that make up individual satellite commands.

The satellite commands fall into two classifications: direct commands and remote commands. The direct commands consist of the following: a sync pulse that resets the satellite decoder circuits; an address portion consisting of a 12-bit code that uniquely identifies the satellite for which the command is intended; a second sync pulse; and a 13-bit instructional command that either selects a satellite component for operation or performs an ON/OFF type function. The structure of the direct command is a 2-out-of-12 code plus a command termination bit, providing 64 unique command combinations for the TOS satellites. For the ITOS satellites, the command capacity is doubled by the use of 2 sets of commands which are differentiated by a one position shift in the satellite address.

Remote commands are similar to direct commands in that they contain a sync pulse, satellite address portion, a second sync pulse, and a direct command portion. However, in the remote command, the direct command portion selects one of the two redundant programmer units in the satellite for operation, and is immediately followed by 28 bits of programmer-loading data containing a program of operations for either the satellite-borne TV picture subsystem or dynamics control subsystem, to be implemented in areas remote from the CDA station.

The timing and generation of the enable tone, and the timing, sequencing, and generation of the individual commands in each command sequence are controlled by the programming equipment.

C. FUNCTIONAL DESCRIPTION

1. General

The sensor data receiving and processing equipment at each of the two CDA stations acquires, records, and processes the RF transmission from ITOS for retransmission over the microwave link to DAPAF and for system performance analysis.

The Data Acquisition Facility (DAF) equipment contains the RF receiving equipment, and the CDA equipment contains the following equipment: sensor data processing and recording; real-time data display; slow-time data transmission;

and signal monitoring. The DAF and CDA equipment is used during the satellite passes as follows:

The DAF equipment is used:

- To acquire and deomodulate the FM carrier containing the real-time amplitude-modulated APT video or scanning radiometer (SR) subcarrier; and
- To acquire and demodulate the frequency-modulated S-band carrier which is modulated by a frequency-multiplexed composite subcarrier containing the AVCS, recorded scanning radiometer (SR), and recorded secondary sensor subcarrier.

The CDA equipment is used:

- To record the real-time APT or SR subcarrier on two of the four redundant magnetic tape recorders (only at Wallops Island);
- To demultiplex the composite video subcarrier and record on two redundant tape recorders the seven channels of video and flutter-and-wow signals (AVCS video subcarrier, SR video subcarrier A, SR 1 flutter-and-wow subcarrier, SR video subcarrier B, and SR 2 flutter-and-wow subcarrier, AVCS flutter-and-wow subcarrier, and secondary sensor subcarrier); and
- To demodulate and display or monitor the above listed seven channels of video and flutter-and-wow signals.

2. Video Data Processing and Display Equipment

The sensor data signals transmitted by ITOS satellites are an S-band (1697.5 MHz), RHC polarized carrier on which an FDM baseband signal, extending from 10 to 500 kHz, and a 137.5-MHz, linearly polarized carrier with a 2.4-kHz subcarrier, are frequency modulated. The modulation baseband for the S-band carrier includes the AVCS video subcarrier, the scanning radiometer (SR) subcarriers (visible or IR), the secondary sensors FSK subcarriers (SPM, FPR, and telemetry), the AVCS flutter- and-wow subcarrier, and the SR flutter- and-wow subcarrier. The 137.5 MHz carrier is frequency modulated by the satellite's 2.4-kHz real-time subcarrier; i.e., APT picture video or real-time SR data, which has a video baseband of 1600 Hz and an RF bandwidth of 28.4 kHz.

At the ground station, the satellite signals are received by a polarization diversity receiving system which provides the CDA station equipment with a 2.4-kHz APT or real-time SR subcarrier and a composite subcarrier band of 10 to 480 kHz containing the AVCS, recorded SR, secondary sensors, time code, and flutter-and-wow subcarriers.

The 2.4-kHz APT or SR subcarrier is recorded on one or more of the four tape recorders and is available for monitoring on an oscilloscope either in real time (RT) or in real-time playback (RT PLBK) at 60 ips (at Wallops Island).

A simplified block diagram of the video data processing equipment is shown in Figure 5-II-4.

The 10- to 500-kHz composite signal is applied to the inputs of two identical demultiplexers, A and B, each of which separates the composite video subcarrier into six single subcarriers containing the AVCS and SR video and flutter-and-wow information and a seventh composite subcarrier containing the secondary sensor information and a clock channel. The AVCS video subcarrier is doubled and the SR subcarriers are divided to facilitate further processing. Each demultiplexer has its seven individual output channels routed to a pair of redundant tape recorders. Normally when sensor data is being received, two tape recorders, one connected to each demultiplexer, will be used to record the processed subcarrier, thereby ensuring that a single demultiplexer or recorder failure will not result in loss of data. The 10- to 500-kHz composite signal may be monitored on a scope in real time but is not recorded.

The AVCS filter and frequency-doubler separates the frequency-modulated AVCS subcarrier from the multiplexed output of the diversity combiner and doubles its frequency. The output of the AVCS filter and frequency-doubler is channeled to the tape recorders and, in record and monitor mode, to the FM demodulator and to the alternate vertical-sync detector as well. Each CDA station incorporates two redundant filter and frequency-doubler units, one for each of two tape recorders.

In real-time playback or in the record and monitor mode, the doubled AVCS subcarrier is applied to an FM demodulator that reduces the modulating component to a video signal. This signal voltage, comprising horizontal sync pulses and cloud cover video, is raised by the video amplifier to a level suitable for driving the kinescope grid. The output of the FM demodulator is also applied to the horizontal sync-slice amplifier. This stage removes the picture video from the composite signal and provides horizontal sync pulses to the horizontal sync detector. (See Figure 5-II-4.) Two sync-generating modes are available: "amplitude" or "flywheel".

The FM demodulator, which consists of a limiter section and a demodulator section, extracts the video from the doubled AVCS frequency-modulated subcarrier and applies it to the video amplifier and the horizontal sync-slice amplifier. The input to the demodulator is derived from the frequency-doubler during the record and monitor mode and from the tape recorder during playback mode. The video output voltage of the demodulator is a linear function of the input frequency.

3. Programming Equipment

Command programs are originated by TOC and teletyped to the CDA stations well in advance of the orbit on which they are to be transmitted to the satellite. Just prior to the satellite pass on the specified orbit, the CDA programming equipment is set up in accordance with the instructions contained in the teletyped message. The specified time of initiation of the first sequence in the program, and the start times of the other sequences (if used) are set into the alarm timer unit in the CDA timing equipment. The various operating modes specified in command program are selected by front panel switches on both the ACU and station control panels, and the specified 12-bit satellite address is set into an octal coded switch bank on the ACU front panel. The remainder of the command program (i.e., the actual binary representations of the direct and remote commands) is set into the equipment in one of the following two ways (as specified in the command program): (1) a punched paper tape containing the binary command data and received during the TOC-to-CDA teletype transmission is installed in the PTR or (2) octal coded representations of the binary command data are dialed into switch banks on the ACU.

When the first alarm set into the alarm timer occurs at the beginning of the CDA-to-satellite contact, the DCP generates the required 5.35 seconds of enable tone, and applies this tone as amplitude modulation to the DAF command transmitter. Then, after a 1.05-second period of FSK center frequency transmission, a "dummy" command, consisting of the satellite address portion (decoded from the address switch bank in the ACU), the required sync pulses, and 13 binary "0's" generated internally in the DCP are processed by the DCP and transmitted to the satellite. (Although this command will produce no change in the satellite instrumentation, it is transmitted to ensure that a good communications link exists between the CDA station and the satellite.) After proper satellite reception of the "dummy" command has been verified by the CDA comparator, the programmed commands are either read from the paper tape by the PTR, or decoded from the command switch banks in the ACU, and after processing by the DCP, are combined with the required satellite address and sync pulses and transmitted in the programmed sequence to the satellite.

At the end of the last command in the first command sequence, the programming equipment ceases transmission of commands to the satellite, but maintains contact with it. In multisequence command programs, subsequent alarms from the alarm timer will cause the subsequent programs to be transmitted, in turn, in a manner identical to the first sequence. (However, because contact is maintained with the satellite after the first sequence, transmission of the enable tone and "dummy" command is not required.) At the end of the last command in the last programmed sequence, the programming equipment resets, and returns to a quiescent condition. In addition to the digital commands, it is possible at anytime to transmit the "enable" tone manually. This may be used to command a readout of housekeeping telemetry. If operated manually, the enable tone has precedence over the FSK tone and will interrupt any digital command in progress.

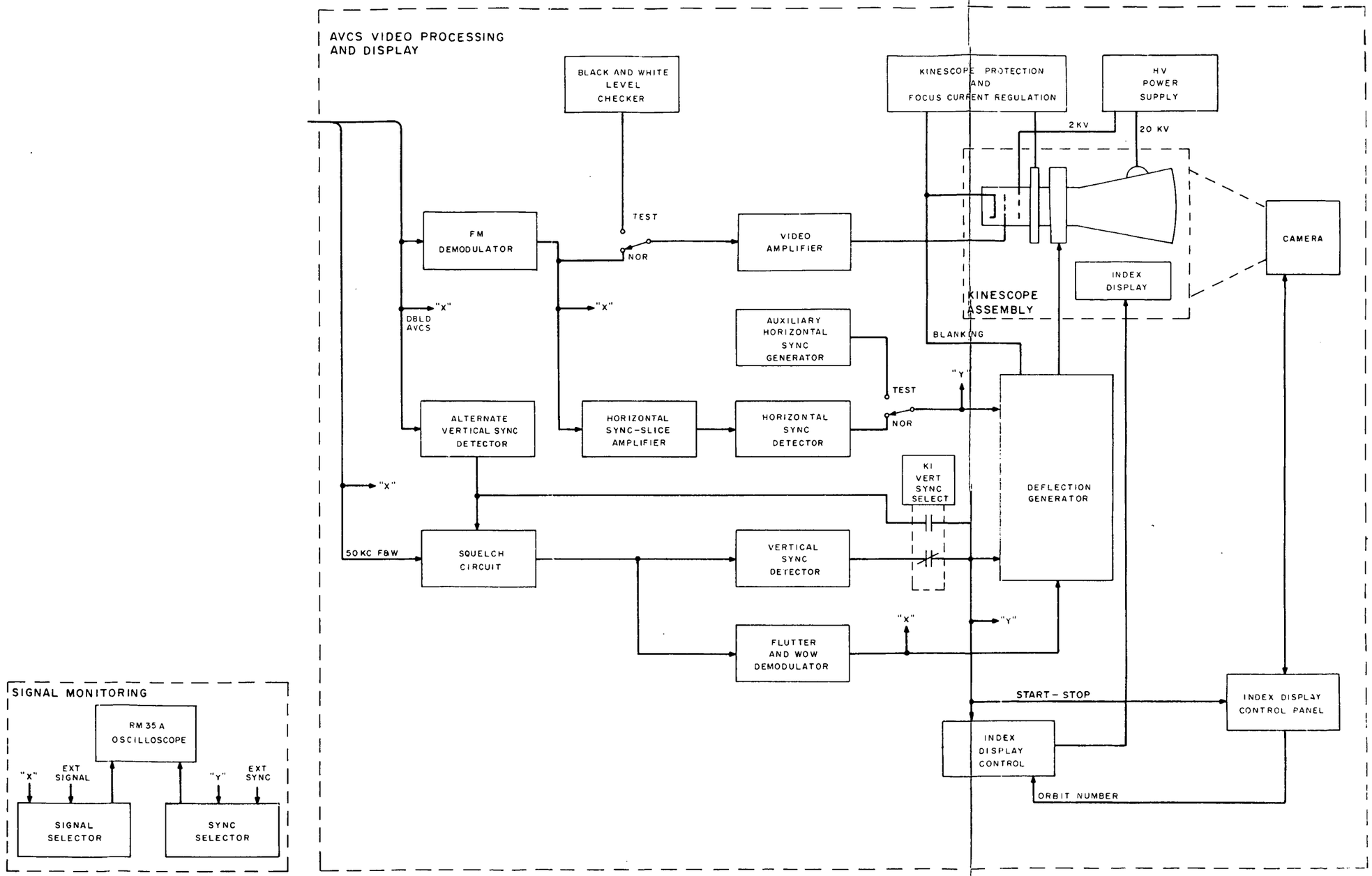

Figure 5-II-4. Video Data Processing Equipment, Simplified Block Diagram

FOLDOUT FRAME 1

FOLDOUT FRAME 2

4. Master Timing Equipment

The basic time standards for the CDA station are provided by the master timing equipment which, in turn, is synchronized by the 1-MHz time standard from the Wallops or Gilmore facility. The timing signals generated by the equipment are (1) a 36-bit and a 28-bit standard NASA serial time code modulated onto a 50-kHz carrier frequencies; (2) a 28-bit and a 36-bit level-shift, standard NASA serial time code; (3) a 20-bit binary-coded decimal, parallel time code; and (4) five pulse trains at frequencies of 0.1 pps, 1 pps, 10 pps, 100 pps, and 1000 pps, all of which are referenced to the basic 1-MHz time standard. It should be noted that, although the 36-bit NASA serial time code is generated by the master clocks, its output is disabled, and it is not used in the CDA station.

The master timing equipment is comprised basically of two master clocks, one of which is used in conjunction with each of the two redundant command programmer systems, and an alarm timer that consists of two separate channels that are used, primarily, with an associated command programmer. The equipment also includes the necessary signal processing and demodulating circuits required to condition the timing signals for compatibility with the various units of the CDA station that utilize them.

Each of the master clocks generates a 28-bit NASA time code amplitude-modulated on a 50-kHz carrier for use in recording time-reference notations on the magnetic tape recorders. The clocks also produce an unmodulated 28-bit time code, a 20-bit binary coded decimal (BCD) time-of-day code (on 20 parallel lines), and timing pulses at rates of 0.1 pps, 1 pps, 10 pps, 100 pps, and 1000 pps that provide the basic timing for all operational equipment in the CDA station.

Each master clock is a highly stable time code generator that provides precision binary-coded decimal (BCD) NASA time codes and timing pulses for use as a time standard for the ground station equipments. Each unit is synchronized with real time by an external 1-MHz reference signal available at the station. The 1-MHz standard signal of the facility is divided down to basic 1-pps timing pulses for application to accumulator circuitry. (An internal 1-MHz crystal-controlled oscillator can also be used to provide the frequency standard signal.)

The clock accumulator circuitry counts the 1-pps pulses and accumulates time from a preset time (synchronized real time), provides a direct decimal panel display of the accumulated time-of-day, and supplies the time-of-year code in parallel BCD form to the code generator sections of the clock which, in turn, produce NASA time code formats. The master clock also includes advance-retard circuitry which provides a continuous phase-shifting control that allows the basic 1-pps timing pulses to be shifted in time for synchronization with an external real-time reference signal.

5. Beacon Data Processing Equipment

The beacon receiving equipment and the beacon data processing equipment receive, record, and process the beacon transmissions from both the ITOS and TOS satellites.

The Data Acquisition Facility (DAF) equipment receives and demodulates the 136.770-MHz, phase-modulated beacon carrier signal and delivers a 3-volt, peak-to-peak, composite beacon subcarrier signal to the CDA beacon data processing equipment. For TOS, the composite beacon subcarrier signal consists of three frequency-multiplexed audio subcarriers on IRIG channels 7 (2.3 kHz), 8 (3.0 kHz), and 9 (3.9 kHz). In the ITOS mode, the composite subcarrier consists of two frequency-multiplexed subcarriers. One of these subcarriers is centered at 3.9 kHz and is the same as for TOS. The other is centerd at 2.3 kHz and had wider deviation (±20 percent). Utilization in ITOS mode is shown in Table 5-II-3.

TABLE 5-II-3. BEACON SUBCARRIER UTILIZATION, ITOS

Subcarrier	Data Content	Time of Transmission
No. 1M (2.3-kHz center frequency ±20-percent deviation) (IRIG Channel 7 special)	Roll sensor 1 or 2	Normally continuous during operational mode
	Time code	Upon command
	Roll sensor and pitch index	Upon command
	Pitch sensor 1 or 2	Upon command
No. 3 (3.9-kHz center frequency ±7.5-percent deviation) (IRIG Channel 9)	Solar proton monitor data	Normally continuous during operational mode
	Digital solar aspect sensor	Normally continuous during acquisition mode (initial condition)
	Telemetry commutator 1 or 2	Upon command
	Data verification 1 or 2	During command operation

The beacon data processing equipment consists basically of three subcarrier discriminators that separate and restore the beacon data from each frequency-modulated subcarrier. A detailed block diagram of the beacon data processing equipment is shown in Figure 5-II-5. The restored data is routed to the 2-channel attitude chart recorder, the optical chart recorder, and the 8-channel beacon recorder for direct readout. A telemetry calibrator, consisting of a multiplexing unit and four calibration oscillators, provides a means for calibrating the discriminator-recorder operation. A loud-speaker system provides an audible indication of the reception of the composite beacon subcarrier signal by the ground station.

The composite beacon signal from the beacon receiving equipment is also delivered to channel 6 of all four tape recorders for recording on magnetic tape, and to the microwave link data transmission equipment for real-time transmission to TOC or TEC/TCC. The composite beacon can also be played back from the recorders and routed to TOC or TEC/TCC in real-time playback. For TOS AVCS slow-time playback operations (i.e., during transmission of AVCS pictures to DAPAF), the No. 3 subcarrier is separated from the played-back composite and transmitted with the video data.

During satellite interrogations, the composite beacon subcarrier signal is supplied directly to all tape recorders and to the beacon processing equipment. Normally the beacon signal is relayed to TOC and TEC/TCC stations as it is received.

In the 60-inch-per-second real-time playback operating mode, the previously recorded composite beacon subcarrier is applied through the beacon select matrix to the beacon processing equipment. In slow-time TOS AVCS playback operating mode (i.e., when a recorder is played back at 1/8 the recording speed, or 7.5 inches per second), the composite beacon signal is applied to a tuned amplifier through the beacon select matrix. The tuned amplifier separates the channel 3 telemetry subcarrier, which, at the slow-time playback speed, varies over the frequency range of 450 to 524 Hz (with a 487.5 Hz center frequency), and delivers this subcarrier via the summing amplifier and BLA to the data transmission equipment for transmission with the video data.

Note that real-time beacon playback and slow-time AVCS playback may take place simultaneously using two recorders. In this case, the AVCS flutter-and-wow tone is automatically selected for transmission.

In normal operation, the real-time composite beacon subcarrier from either the beacon receiving equipment or from the recorders is applied through switching in the telemetry calibrator unit to the common input of subcarrier discriminators (SCD's) operating at center frequencies of 2.3 kHz, 3.0 kHz, and 3.9 kHz for beacon channels 1, 2, and 3, respectively. The SCD's collectively perform the

demultiplexing operation by accepting only the bands of frequencies associated with their respective channels, simultaneously rejecting the other bands. Each SCD then demodulates the associated FM subcarrier, and presents the resulting data as varying DC voltages over a range from -10 volts DC (low band edge) to +10 volts DC (high band edge). The disposition of the data from each of the SCD's is as follows:

- SCD No. 1 (2.3 kHz) — The output of SCD No. 1M which contains the attitude data from the ITOS satellite is delivered to the 2-channel (Brush) attitude recorder for routing monitoring, and to the Visicorder for display if reduction of attitude data is to be done at the station.
- SCD No. 3 (3.9 kHz) — The output of this deomodulator may be displayed on the 8-channel (Brush) beacon recorder and sent to the Visicorder for monitoring and display of telemetry and command verification. In ITOS mode, this channel may also carry solar proton monitor data.

In addition, all of the outputs from the SCD's, along with the composite beacon subcarrier, are applied to the oscilloscope selector panel in rack 32, where they are available for display on the RM504 oscilloscope. The composite subcarrier is also applied to a speaker in rack 33 for an audible indication of beacon reception.

The individual subcarrier frequencies, after separation, may be measured on the counter in rack 34 by selecting BEACON S.C. on the counter input selector, and depressing the pushbutton on the front panel of the SCD for the desired channel.

The beacon processing equipment also incorporates a built-in calibration system that provides for checking out and calibrating all units of the system and all units driven by the system. The calibrator can be operated in either a data or calibration mode. When the calibrator is operated in the data mode, the multiplexed beacon subcarrier input is routed directly through the sequencer to the discriminators and other equipment as described previously. When the calibration sequence is operated in a calibration mode, two methods of calibration are possible. In local calibration, the data line is broken, and a calibration signal, produced by two or three calibration oscillators, is supplied to the discriminators. In system calibration, the outputs of the selected oscillators are summed and routed to the DAF where the signal may be used to modulate a signal generator at the beacon RF frequency, thus making it possible to include the receiver in the calibration loop. The oscillators operate at 2.3 kHz, 3.0 kHz, and 3.9 kHz, which corresponds to the three IRIG channels used by the beacon subcarriers.

Each calibration oscillator produces five crystal controlled frequencies for a particular channel at five calibration points in the passband of the corresponding discriminator. Any of the five calibration points can be selected for a channel independently of the deviations selected for the other channels, and any channel can also be turned off independently. Three modes of automatic calibration routines are also available.

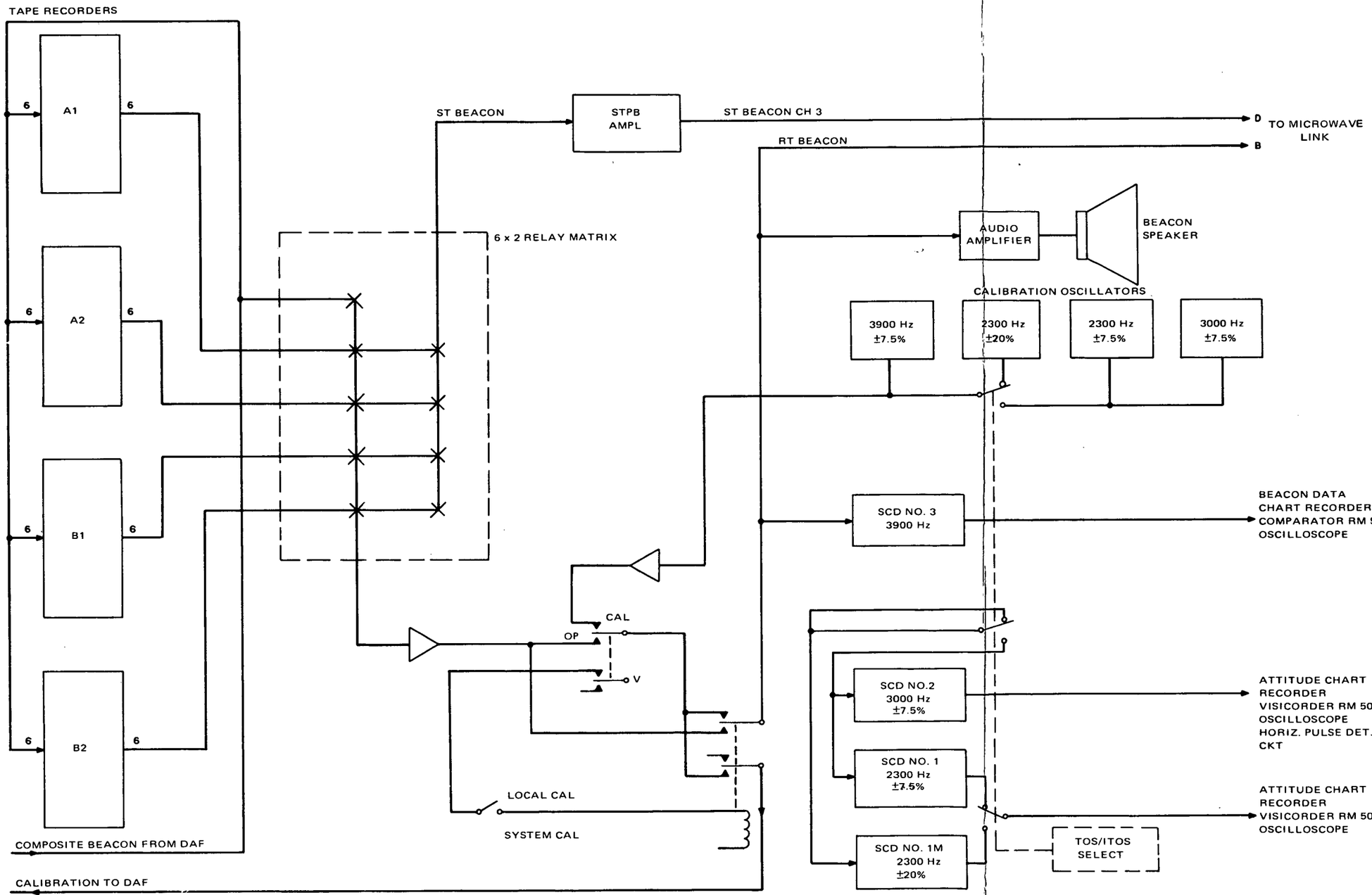

Figure 5-II-5. Beacon Data Processing

FOLDOUT FRAME 1

FOLDOUT FRAME 2

6. Microwave Link Transmission Equipment

The AVCS, SR, and secondary sensor video data (including the flutter-and-wow data) received from ITOS and TOS satellites, the beacon transmissions received from both ITOS and TOS satellites, significant commands, and CDA station events are transmitted by the CDA station to other TOS ground complex facilities over microwave link voice channels. The data transmission equipment processes the signals containing this data to make them compatible with the voice channel equipment, and deliver them to the terminal through four balanced line amplifiers that provide the necessary signal amplitude and impedance-matching characteristics.

A functional block diagram of the data transmission equipment is shown in Figure 5-II-6. The equipment consists basically of four separate audio frequency channels: one each for the video and associated flutter-and-wow data, one for real-time playback of the composite beacon subcarrier, and one which carries a multiplexed signal that combines the program events, station events, and during slow-time playback of TOS AVCS video data, the slow-time beacon channel 3 data associated with the pictures being played back.

As soon as practicable after reception of video data, the data is relayed via channels A and C to DAPAF for processing. The tape-recorded signals are replayed at reduced speed to make the signal bandwidth compatible with the frequency response of the microwave link. Channel A, with a bandwidth of 13 to 30 kHz, is used for AVCS, secondary sensor, and scanning radiometer video data. Channel C, with a bandwidth of 4.3 to 7.4 kHz, is used to relate simultaneously the associated flutter-and-wow with the video signal selected for transmission on channel A.

The microwave link signal-select relay matrix selects one of the video signals (and associated flutter-and-wow) from any one of the four recorders as selected on the demultiplexer control panel. The recorder selected for playback of video is then operated at 30 ips for replay of SR data, or 7.5 ips for replay of AVCS or secondary sensor data as shown below:

Signal	Record Frequency (kHz)	Tape Speed (ips)		Playback Frequency (kHz)
		Record	Playback	
AVCS Flutter-and-Wow	50	60	7.5	6.25
AVCS Video	108 to 248	60	7.5	13.5-31
Secondary Sensors	140 to 180	60	7.5	17-23
SR Video	30 to 60	60	30	15-30
SR Flutter-and-Wow	12.5	60	30	6.25

On playback, the secondary sensor composite signal is processed to reduce amplitude variations caused by the tape recording. This processing consists of separating the three subcarriers and passing each individual subcarrier through a limiter and low pass filter before recombining them for transmission.

The other video and flutter-and-wow signals are delivered directly to the balanced line amplifier (BLA) inputs without any processing. The outputs of the balanced line amplifiers are delivered to the terminal equipment at a level of 1 volt, peak-to-peak.

The video and flutter-and-wow signals to be sent to the link inputs are selected by a relay matrix in the rear of the demultiplexer rack. There are 16 video inputs to this matrix and 12 flutter-and-wow inputs, representing each selectable signal for channels A and C from each of the four tape recorders. A block diagram of the video-select matrix is shown in Figure 5-II-7.

During the satellite pass, the real-time beacon composite subcarrier is coupled directly from the beacon receiving equipment to the terminal through the beacon-select relay matrix, and through the beacon BLA (also located in the signal processor drawer). This BLA is adjusted to provide a 1-volt peak-to-peak signal to the terminal. Facilities are also provided for playing back prerecorded satellite beacon data in real time (i.e., at 60 ips recorder speed). The output from channel 6 of the selected recorder is applied through the beacon select relay matrix to the beacon BLA, thence to the terminal.

There are two SR recorders on the satellite, and each may contain two information signals and one flutter-and-wow signal. When the SR satellite recorder playback is commanded, there are two possible modes. In one mode, only one satellite recorder is played at a time and all three signals are transmitted to the ground station. If both satellite recorders are played simultaneously, the SR visual information is discarded and only the SR IR is transmitted, together with the flutter-and-wow. The modes of operation of the satellite recorders, toegether with the information transmission is shown below:

Satellite Playback Mode	Data Channel			
	SR 1 Video	SR1 F&W	SR2 Video	SR2 F&W
Recorder 1	SR 1 IR	Recorder 1 F&W	SR1 Visible	----------
Recorder 2	SR 1 Visible	----------	SR2 IR	Recorder 2 F&W
Both 1 and 2	SR 1 IR	Recorder 1 F&W	SR2 IR	Recorder 2 F&W

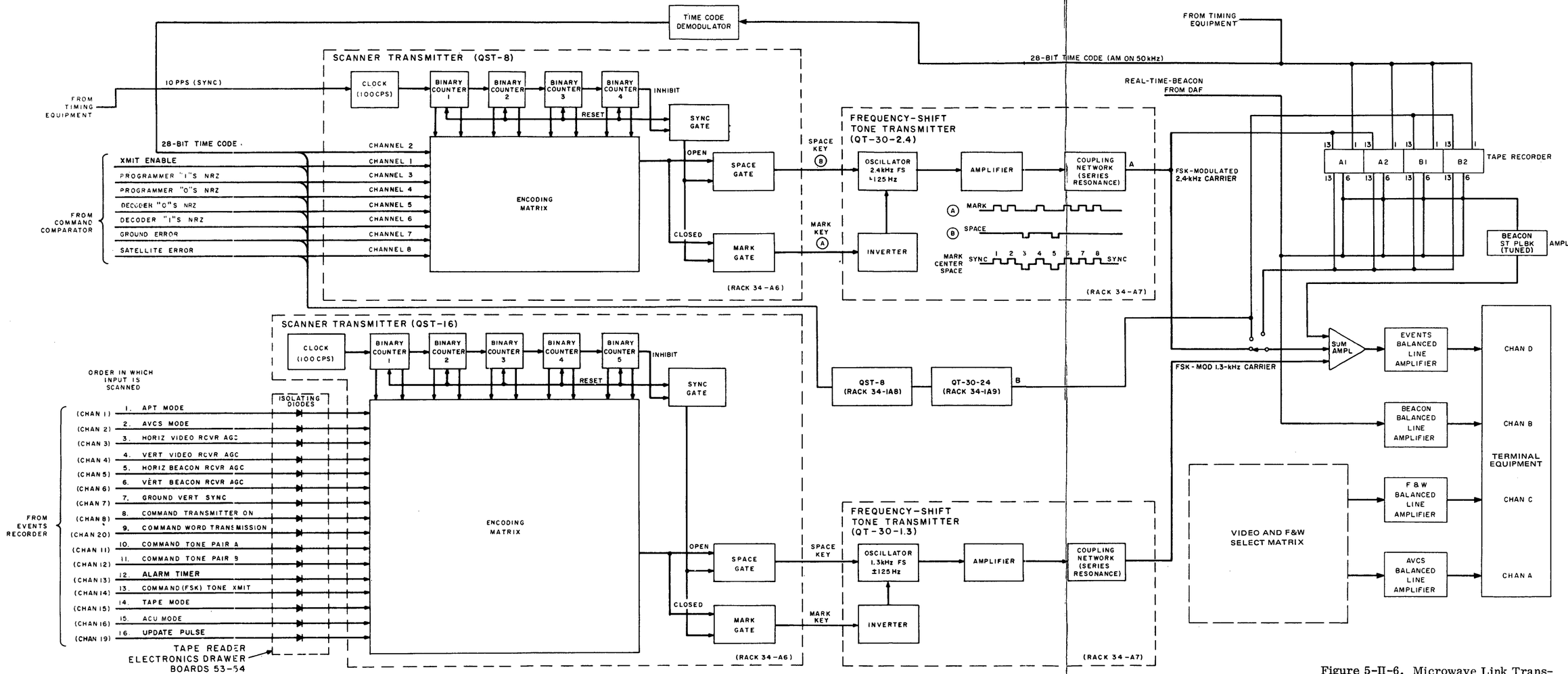

Figure 5-II-6. Microwave Link Transmission Equipment, Functional Block Diagram

FOLDOUT FRAME 1 FOLDOUT FRAME 2 FOLDOUT FRAME 3

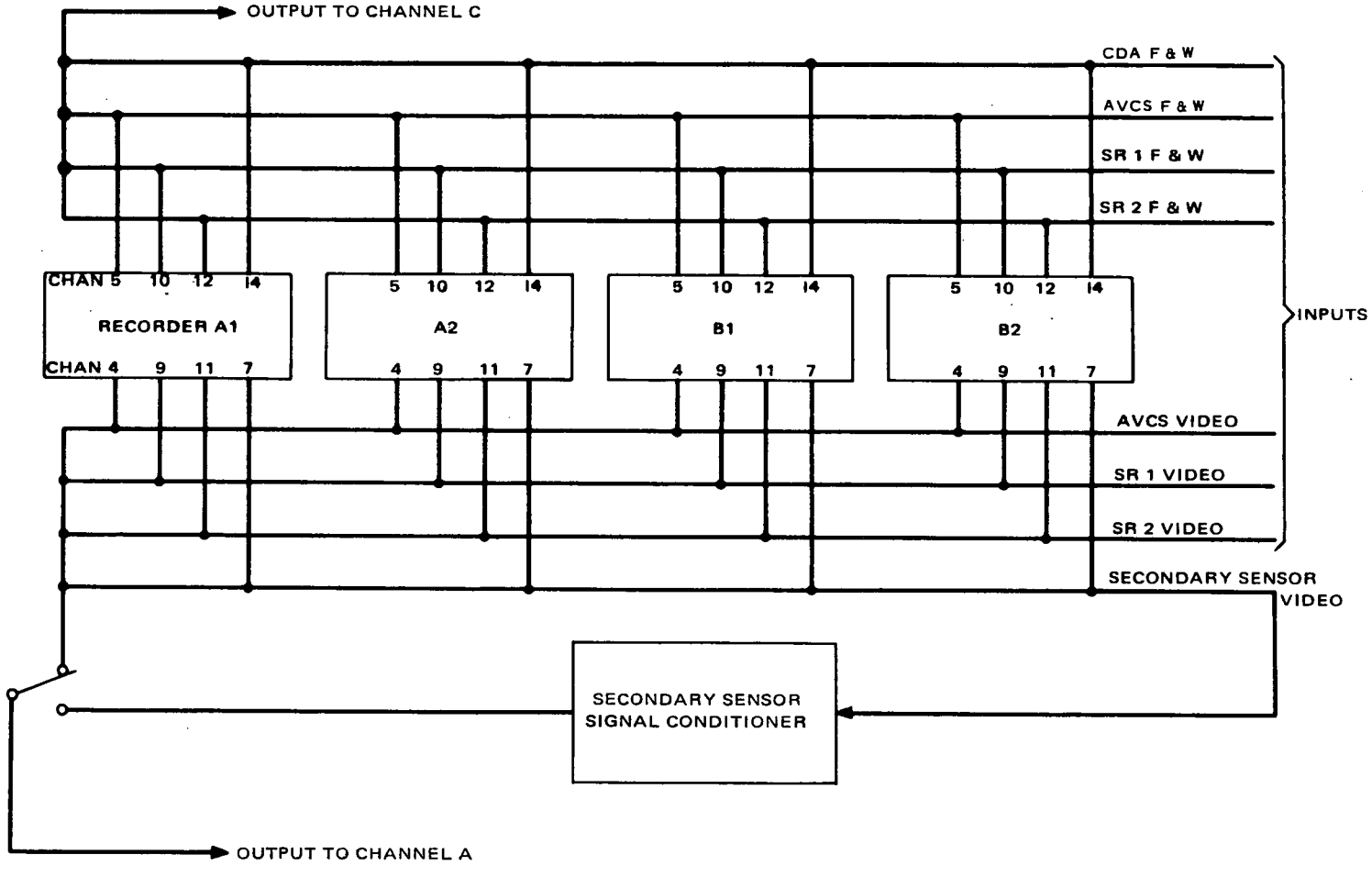

Figure 5-II-7. Microwave Link Transmission Equipment Video and Flutter-and-Wow Select Matrix

When an SR information signal is selected for input to the microwave link, the proper flutter-and-wow must also be selected. Therefore, a knowledge of the satellite playback mode is required to properly selected the correct flutter-and-wow.

During satellite interrogations, command program events are transmitted in real time to TOC and TEC/TCC over a separate voice channel. The command program events data comprises eight significant parameters used by the centers to monitor and evaluate each command as it is transmitted to the satellite. Facilities are also provided for playing back prerecorded command program events data in real time simultaneously with the playback of the satellite beacon data.

The secondary sensor signal conditioner processes the composite 18-kHz, 20-kHz, and 22-kHz signals reproduced by the CDA station tape recorder before transmission to ESSA via the microwave link. This processing is required to remove amplitude variations in the composite signal which are caused by the record-reproduce cycle of the CDA tape recorder.

The input to the signal conditioner is a frequency-division-multiplexed composite signal consisting of three frequency-shift-keyed (FSK) subcarriers. The center frequency of the subcarriers are 18 kHz, 20 kHz, and 22 kHz. Each of the subcarriers is deviated to a maximum of ±0.58 kHz at a maximum modulating frequency of 0.188 kHz. The modulating signals are from the NRZ data tracks of a digital tape recorder.

Amplitude variations introduced by the CDA recorders can produce a reduction in signal amplitude of 16 dB.

The functional block diagram of the secondary sensor signal conditioner is shown in Figure 5-II-8. The composite signal received from the CDA tape recorder is separated into the three subcarriers by means of the bandpass filters at the inputs of the channels. The filtered signals are then fed to a limiter-amplifier (Z1) to remove any amplitude variations that are present. The performance of the limiter reduces 16-dB variations at the input to less than 1 dB at the output of this signal conditioner. A second bandpass filter, identical to the input filter, but after the limiter removes the unwanted frequencies, and provides amplitude limited channel sidebands to the running operational amplifier, Z1. The potentiometers (R19) are used to adjust each of the processed channel sideband signals to equal amplitudes at the output of the operational amplifier, Z1.

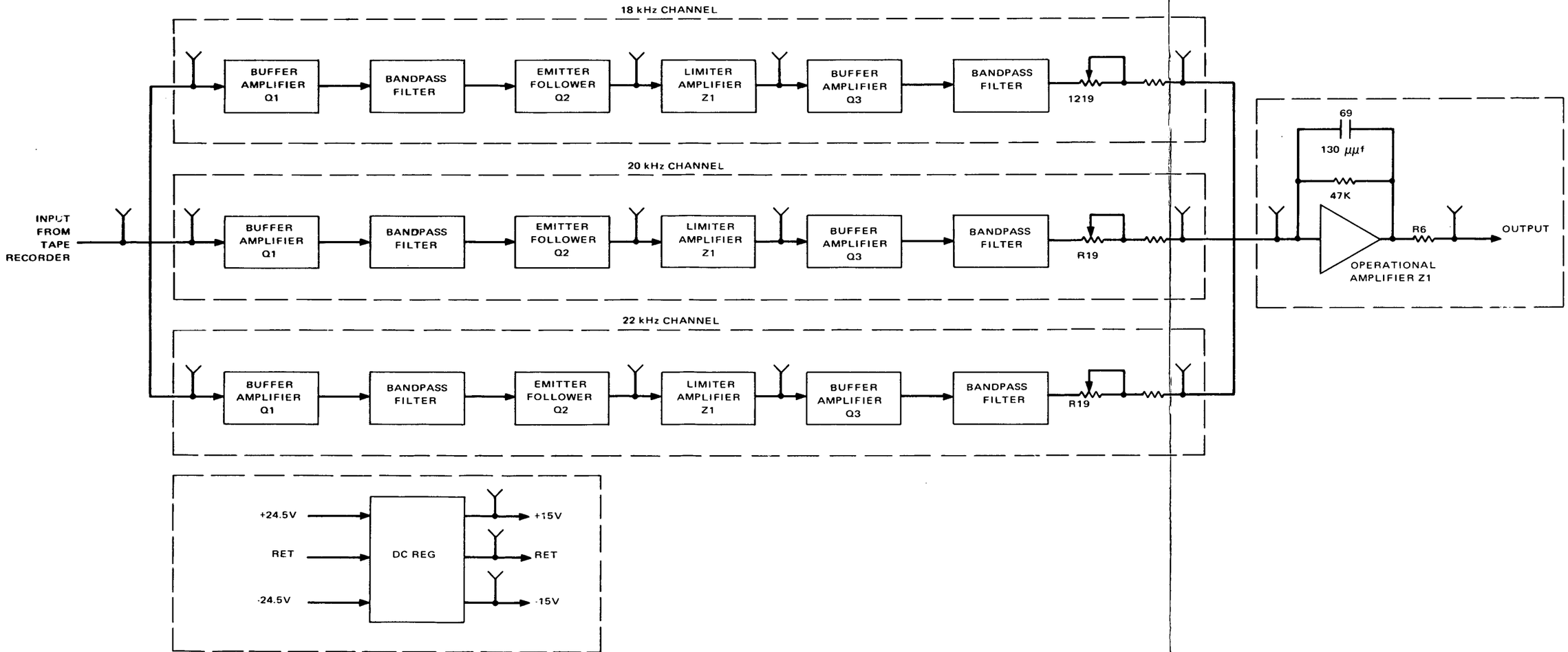

Figure 5-II-8. Secondary Sensor Signal Conditioner, Functional Block Diagram

7. CDA Station Recorders

a. TAPE RECORDERS

All data transmissions from the TOS satellites received at the CDA stations are permanently recorded, on magnetic tape, by a recording system comprising four 14-channel, magnetic tape recorders and associated control circuits. The use of two recorders during signal reception, each of which records identical data, provides an increased degree of reliability in recording all useful data. During interrogations of TOS APT satellites one or both recorders are turned on to record beacon subcarrier only when the signal strength of the beacon RF carrier from the satellite exceeds a predetermined threshold and run throughout the duration of the satellite pass. During TOS AVCS and ITOS interrogations, one of the recorders is turned on at beacon threshold as previously described; the second recorder is turned on at the start of video transmission. During all recording operations, the tape recorders are operated at a speed of 60 inches per second. The data recorded on each of the recorder channels is described in Table 5-II-4. During AVCS and ITOS recording, one A and one B recorder should be operated to take advantage of redundancy in the prerecording processing circuits.

Either recorder can be selected for playback operations, in either of two playback modes: real-time playback (RTPB) and slow-time playback (STPB). In the RTPB mode, the selected recorder is played back at 60 ips, the same speed as the recording operation. This mode permits the prerecorded data to be played back at frequencies identical to the frequencies of the recorded data. The RTPB mode is used primarily for: (1) playback of the composite beacon subcarrier, either for retransmission to TOC or TEC/TCC or for evaluation of beacon data at the CDA station; (2) displaying and photographing prerecorded AVCS pictures on the CDA video processing equipment; (3) displaying prerecorded APT subcarrier transmissions on the CDA station oscilloscope for evaluation purposes; (4) displaying the recorded SR or secondary sensor data from an ITOS satellite; and (5) general CDA station checkout and maintenance operations.

The STPB mode is used only for transmission of recorded AVCS, SR, or secondary sensor video data to DAPAF. In this operation, which is performed immediately following each AVCS or ITOS satellite interrogation, the recorders are played back at 7-1/2 ips, or one eighth the recording speed for relaying AVCS or secondary sensor data. This reduces the doubled AVCS video subcarrier frequency bandwidth from 108 to 248 kHz to 13.5 to 31 kHz, and the secondary sensor signal bandwidth from 140 to 180 kHz to 17.5 to 22.5 kHz, thereby making them compatible with the telephone equipment used in the TOS ground complex communications link. The AVCS flutter-and-wow subcarrier on channel 5 of the recorder is reduced, at the STPB rate to 6.25-kHz and also transmitted with the AVCS video. In addition (for TOS AVCS only) the beacon No. 3 subcarrier is filtered from the

TABLE 5-II-4. TAPE RECORDER CHANNEL ASSIGNMENTS

Channel	Data Recorded	Description
1	NASA 28-Bit Time Code	A digital indication of data and time of recording of the CDA station, modulated on a 50-kHz carrier.
2	APT Subcarrier	The 2.4-kHz subcarrier received from TOS APT and ITOS satellites (only) containing APT video data.
3	TOS AVCS Subcarrier	The composite AVCS subcarrier directly from the AVCS receivers (i.e., before processing by CDA) containing the 96-kHz AVCS video and 9.6-kHz AVCS recorder flutter-and-wow subcarriers.
4	Doubled AVCS Subcarrier	The doubled AVCS video subcarrier (192-kHz) from the CDA ITOS demultiplexer.
5	Flutter-and-Wow Subcarrier	The converted flutter-and-wow subcarrier (50-kHz) from the CDA ITOS demultiplexer.
6	Beacon Subcarrier	A composite of the 2.3-kHz, 3.0-kHz, and 3.9-kHz subcarriers received from all TOS satellites.
7	Secondary Sensor	The composite of 144, 160, 176-kHz subcarriers containing the ITOS secondary sensor data.
8		Channel 8 is used for the servo reference or pilot tone on the Sangamo recorders in the Gilmore station.
9	SR Video Subcarrier No. 1	The demultiplexed SR video subcarrier (45.6 kHz) from the ITOS demultiplexer.
10	SR Flutter-and-Wow Subcarrier No. 1	The demultiplexed SR flutter-and-wow tone (12.5 kHz) from the ITOS demultiplexer.

TABLE 5-II-4. TAPE RECORDER CHANNEL ASSIGNMENTS (Continued)

Channel	Date Recorded	Description
11	SR Video Subcarrier No. 2	Same as channel 9
12	SR Flutter-and-Wow Subcarrier No. 2	Same as channel 10
13	Command Events	Output of 8-channel Quindar
14	CDA Flutter-and-Wow	6.25-kHz tone derived from master clock.
NOTE: All frequencies designated are center frequencies.		

played-back composite beacon subcarrier on channel 6 of the recorder, and transmitted to DAPAF with the AVCS video data. At the STPB recorder speed, the frequency of this subcarrier is reduced from 3.9 kHz to 487.5 Hz. Operation of the recording system is controlled by switches located on the control panel in the demultiplexer rack and on each recorder (racks 20A1, 20A2, 20B1, and 20B2). The recorders are played back at 30 ips for relaying the ITOS SR data, reducing the signal spectrum of 60 to 60 kHz to 15 to 30 kHz. The SR flutter-and-wow is correspondingly reduced from 12.5 to 6.25 kHz.

The most important characteristics of the recorder from an operational point of view are the permissible operating speeds and the performance of these speeds. Although the basic transport is capable of operation over a wide range of binarily related speeds, only those speeds for which equalizer networks are included in the playback amplifiers may be used to playback data. Any record speed may be used as long as that data is usable at one of the equalized playback speeds listed in Table 5-II-5.

The actual control of the recorders is accomplished using only the switches on the recorders (or data locators at Wallops). Control of the flow of recorder input and output signals is accomplished manually using the control panel in the demultiplexer rack. Since several recorder modes are possible (e.g., at 60 ips, PLBK at 60, 30, 7 1/2 ips), the status of the recorders is displayed on the demultiplexer rack control panel. The control panel also indicates whether the status of the recorder selected for a given function is normal. Abnormal modes of operation are possible, and might be derived for some special situation; they are not prohibited, therefore, but are visually indicated on the control panel.

Two data locator panels, associated with Mincom recorders A1 and B1, are located in rack No. 46 at the Wallops station. These units provide for remote control of the Mincom recorders by incorporating control pushbuttons and indicators that duplicate identical controls on the associated recorder.

5

TABLE 5-II-5. EQUALIZED PLAYBACK SPEEDS

Tracks	Gilmore		Wallops	
	Equalized Speeds	Nominal 3-dB Bandwidth (kHz)	Equalized Speeds	Nominal 3-dB Bandwidth (kHz)
1 through 7	60	0.4 to 300	60	0.2 to 300
	7.5	0.2 to 37.5	15	0.1 to 75
	—	—	7.5	0.05 to 37.5
8 through 14	60	0.4 to 300	60	0.2 to 300
	30	0.4 to 150	30	0.15 to 150
	—	—	7.5	0.05 to 37.5

b. EVENTS RECORDER

The events recorder (mounted in rack 33) is an Esterline-Angus Model A620T paper chart recorder that provides for simultaneous recording of 20 independent channels of slow-speed on/off information. The recorder is used to monitor significant CDA station operations and to provide a hard copy record of these and certain critical programming events. The recorder is also useful in checking overall CDA station operation prior to the satellite pass. Recorder chart speed, which is controlled by a synchronous motor and gear train, is selectable in 10 steps. The writing elements are electrically-heated styluses which record on chart paper sensitive to both heat and pressure. The events recorder is capable of both manual and automatic operation. Manual operation is used during station troubleshooting and maintenance procedures, while automatic operation is employed as the normal operating mode.

The events recorder monitors the programming events involved in transmitting commands to the satellite from either program A or program B in the CDA programming equipment, indicates detection of a satellite or ground station programming error, and monitors the horizontal and vertical components of the video receiver AGC circuits and the beacon receiver AGC circuits to determine the start of data reception. Other events recorded by the unit include indication of the processing of an AVCS video frame, and the type of satellite (ITOS, AVCS, or APT) the station is set up to interrogate. Refer to Table 5-II-6 for a description of the events recorded and their recorder-channel assignments. Simplified logic diagrams of the events recorder circuitry are shown in Figure 5-II-9. The input circuitry located in the tape reader electronics drawer, rack 33, consists of 13 independent inverter-amplifiers which drive 13 of the 20 recorder channels.

TABLE 5-II-6. EVENTS RECORDER CHANNEL ASSIGNMENTS

Channel No.	Designation	Event Indicated
1	APT Operation	Station set up for TOS/APT satellite interrogation*
2	AVCS Operation	Station set up for TOS/AVCS satellite interrogation*
3	Detected Video Receiver AGC	Start of video reception**
4	Detected APT Receiver AGC	Start of APT reception †
5	Detected Beacon Receiver AGC	Start of beacon reception ††
6	Error Sensing Off	Abnormal mode of command program operation - command errors to be ignored
7	Frames	AVCS video frame being processed by video circuits
8	Command Transmitter On	Outgoing command signal above threshold of satellite-type-receiver amplifier in comparator.
9	Alarm Timer Pulse	Alarm signal activated (1-second pulse)
10	0.1 PPS Marker	Master clock timing pulses
11	Command Tone Pair A	Enable and command tone pair A selected
12	Command Tone Pair B	Enable and command tone pair B selected

* Activation of both channels 1 and 2 indicates station is set up for ITOS satellite interrogation.

** In AVCS mode, activates when AVCS receiver AGC reaches prescribed threshold-voltage level; in ITOS mode, activates when S-band receiver AGC exceeds preset threshold level.

† In APT or ITOS mode, activates when APT receiver AGC reaches prescribed threshold-voltage level.

†† Activates when beacon receiver AGC reaches prescribed threshold voltage level.

TABLE 5-II-6. EVENTS RECORDER CHANNEL ASSIGNMENTS (Continued)

Channel No.	Designation	Event Indicated
13	Enable Tone Transmission	Enable tone being transmitted
14	Command (FSK) Tone Transmission	Command tone being transmitted
15	Tape Reader Mode	Tape reader selected as the command data source
16	ACU Mode	Switch register on the command programmer ACU selected as the command data source
17	Satellite Error	Error detected in comparison of command programmer output with verification signal from satellite
18	Ground Error	Error detected in comparison of programmer output with signal at command antenna
19	Spin Count	Indicates each command updating pulse
20	Command Word Transmission	Command tone being modulated with data

In order to provide for the most efficient utilization of recorder chart paper, and yet ensure that all significant station events are properly recorded, an automatic turn-on feature for the CDA events recorder has been incorporated into the station design. The system is controlled, primarily by the AGC voltage from the beacon receiver in the RF receiving section of the station. This AGC voltage is indicative of the RF signal strength present at the receiving antenna. Threshold devices incorporated in the automatic turn-on circuitry are preset to trigger upon sensing AGC levels that correspond to usable RF signal levels. Triggering of the threshold devices actuates a time-delay relay that couples AC power to the events recorder through an AUTO-MAN pushbutton on the station control panel. In the AUTO position, the recorder is turned ON automatically at the start of satellite interrogation provided the beacon signal strength exceeds the predetermined threshold. Once started, the recorder remains ON as long as the AGC bias remains above the threshold, but if it drops below the threshold, the recorder is turned OFF after an adjustable time delay. In the MAN position, the recorder is turned ON manually with the ON-OFF pushbutton on the front panel of the recorder.

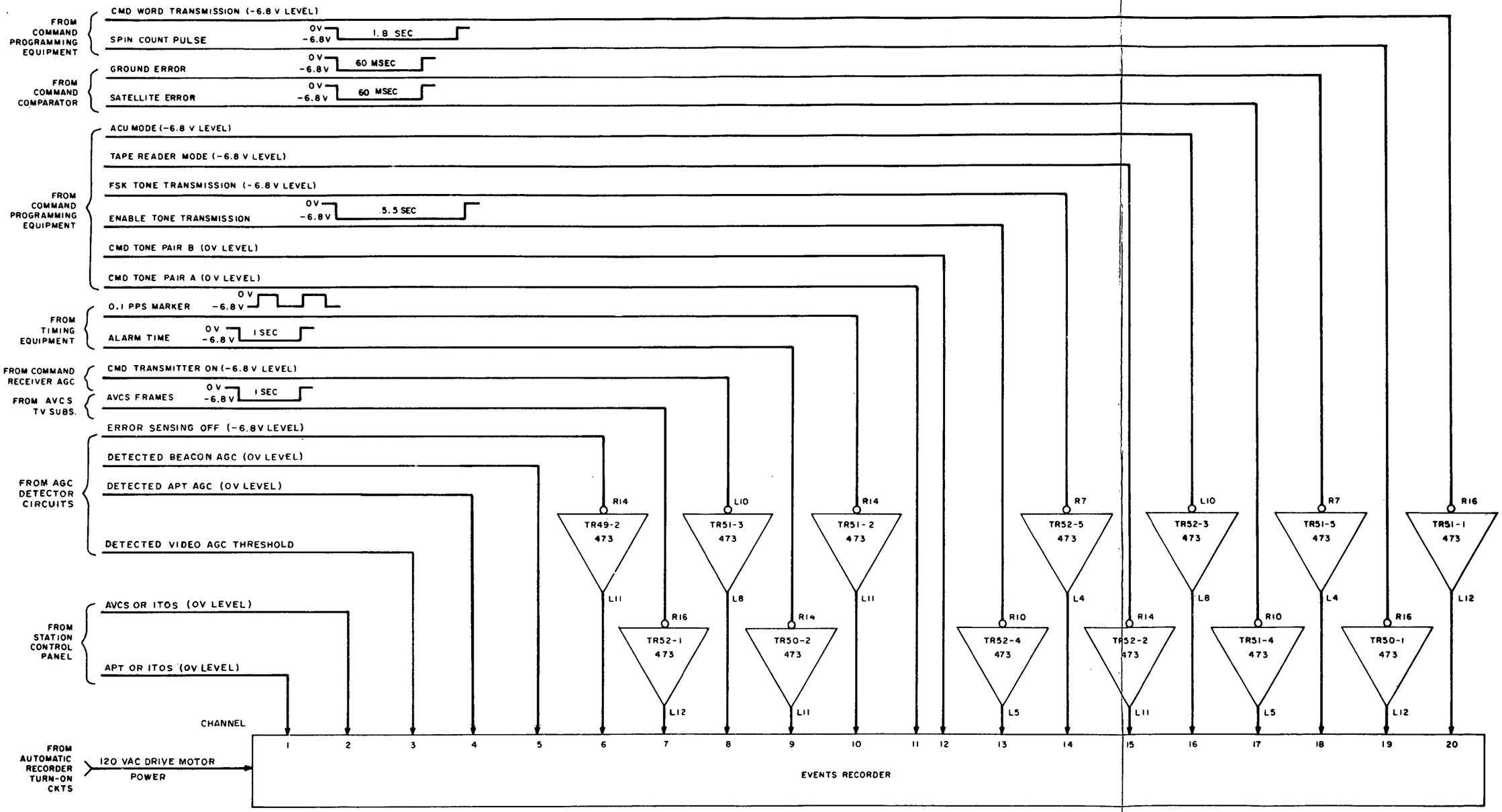

Figure 5-II-9. Events Recorder Circuitry, Logic Diagram

The AGC levels of the beacon, APT, and S-band receivers are sensed by threshold circuits which provide indications of the presence of corresponding received data in the RF section of the station. The AGC voltages from the horizontal beacon receiver (receiving horizontally polarized signals) and from the vertical beacon receiver (receiving vertically polarized signals) are applied through two buffer stages to two Schmitt trigger circuits.

Whenever the AGC voltage exceeds a prescribed threshold, a 0-volt level from the "0" side of the activated Schmitt circuit will cause the output of a NOR gate to go to -6.8 volts. This voltage is applied to solenoid drivers to provide drives for the automatic turn-on of the events recorder and for channel 5 on the events recorder, respectively.*

The output of one gate is also delivered to the comparator as a control signal to disable command comparison during conditions of weak beacon signal.

The video (APT and S-band) AGC detection circuits are identical to the beacon AGC circuits. During TOS AVCS satellite interrogations, the horizontal and vertical S-band receiver AGC's are applied to Schmitt triggers through buffer amplifiers. During TOS APT and ITOS satellite interrogations, the APT receiver AGC's are applied to these circuits. Switching is accomplished by a relay as selected by the ACQUISITION MODE switches on the station control panel. When either the horizontal or vertical AGC voltage exceeds the preset threshold, the 0-volt level from the "0" side of the Schmitt trigger is applied to a NOR gate, causing a -6.8-volt level to be applied to one input of the gated solenoid drivers.

When the station is in the TOS AVCS mode, the second input causes the detected video AGC to activate channel 3 on the events recorder, and to light the AVCS AGC indicator on the status and control panel in the demultiplexer rack.

When the station is not in the TOS AVCS mode, it causes the detected APT AGC to be indicated on channel 4 of the events recorder, and the APT AGC indicator to be lit on the status and control panel.

The AGC's from the horizontal and vertical S-band receivers are applied to a high-input impedance threshold detector. This circuit may be used to detect either negative- or positive-going AGC signals, depending on the position of the switch (S1) mounted on the handle of the circuit card. With this switch in the (+) position, and when either AGC is more positive than the preset threshold, the output will be low at -6.8 volts. Similarly, when the switch is in the (-) position, and when either AGC is more negative then the preset threshold, the output will be low.

---

*The channel 5 indication is paralleled to an indicator on the status and control panel in the demultiplexer rack.

Channel 3 indicates the detected AGC of the AVCS receiver in TOS AVCS mode, and the detected AGC of the S-band receiver in ITOS mode.

c. BEACON DATA RECORDER

The beacon data recorder (mounted in rack 36-A2) is a Brush Mark 200 high-speed paper chart recorder which provides simultaneous recording of eight channels of analog data and two events markers. The recorder channel assignments are indicated in Figure 5-II-10. The recorder is normally operated at 20 millimeters per second. A pressurized fluid writing system is used with a true rectilinear presentation. The recorder channel width is 40 millimeters (50 divisions) and trace width is 0.01 inch. The frequency response is:

- 50-millimeter p-p deflection, 0 to 55 Hz;
- 40-millimeter p-p deflection, 0 to 60 Hz;
- 15-millimeter p-p deflection, 0 to 100 Hz; and
- 4-millimeter p-p deflection, 0 to 200 Hz.

The sensitivity is 2.5 volts full scale and AC or DC linearity is 0.05 percent full scale.

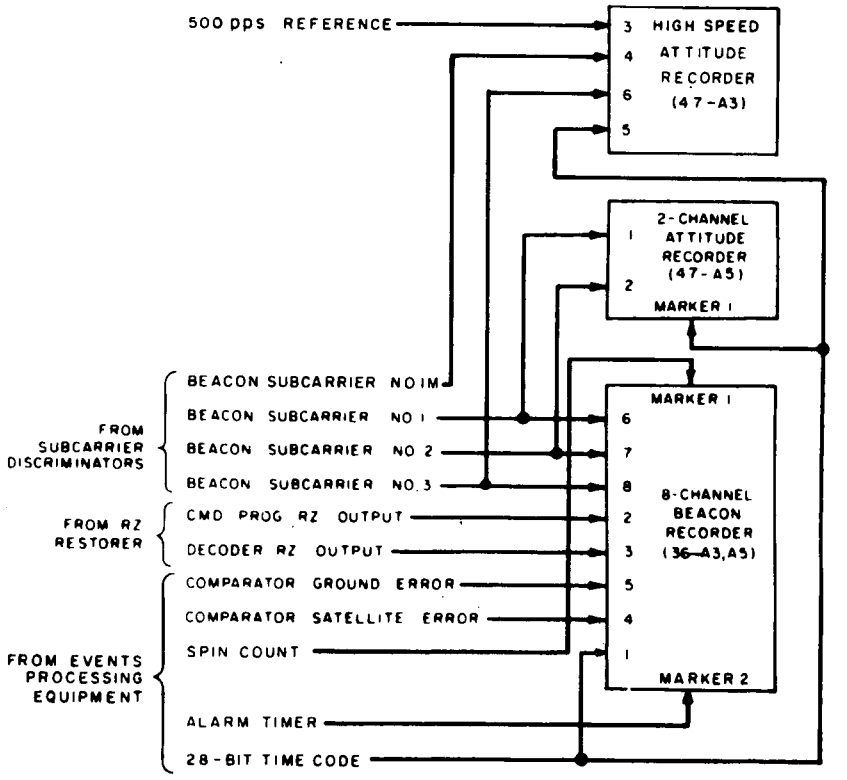

Figure 5-II-10. Beacon and Attitude Recorders, Block Diagram

d. ATTITUDE DATA RECORDER

The attitude data recorder (see Figure 5-II-10), which is mounted in rack 32-A4, is a Brush Mark Model 280 high-speed paper chart recorder which provides simultaneous recording of two channels of analog data and two events markers. The recorder is used to display the attitude-sensor data carried on beacon channels 1 and 2 and, on recorder channels 1 and 2, respectively. The two events markers of the recorder are used to display the 10-pps timing pulses and the 28-bit time code. The 10-pps timing pulses are utilized in the computation of the spin period and the 28-bit time code is used as a real-time reference. The recorder is operated at 50 millimeters per second to optimize the resolution of attitude pulses and, hence, optimize the accuracy of the attitude-sensor data reduction since it is directly related to the accuracy involved in reading pulse locations from the chart.

The recorder writing system is pressurized fluid used to produce a true rectilinear presentation. The recorder channel width is 80 millimeters (50 divisions) and trace width is 0.01 inch. The frequency response is:

- 80-millimeter p-p deflection, 0 to 35 Hz;
- 40-millimeter p-p deflection, 0 to 60 Hz;
- 15-millimeter p-p deflection, 0 to 100 Hz; and
- 4-millimeter p-p deflection, 0 to 200 Hz.

The sensivity is 25 millivolts full scale and linearity is 0.25 percent full scale.

e. VISICORDER

The Visicorder, mounted in rack 47, is a high-speed paper chart recorder using optical writing and capable of handling up to 12 individual data channels with response characteristics determined by the individual galvanometers, which are listed below.

Channel	Nominal Galvanometer Response (Hz)	Maximum Deflection (inches)	Normal Input Signal
1	13,000	±1	Spare
2	1,000	±4	28-bit time code
3	4,800	±2	500-pps marker
4	1,000	±4	Beacon channel 1
5	1,000	±4	Beacon channel 2
6	1,000	±4	Beacon channel 3

Drive currents for the galvanometers are supplied by a 6-channel amplifiter and attenuator chassis included in the same rack. The inputs to the galvanometer driver-amplifiers are connected through a jack panel permitting recording of signals other than the normal ones. The recorder is capable of operation at speeds from 0.1 to 80 ips.

8. Station Control Circuits

The AC power control panel, mounted in rack 26, supplies AC power to all racks of the CDA ground station through their respective rack circuit breakers located in the AC power control panel drawer, and to the master clock units through fused lines. The control panel also provides an indication of the blower status in each rack and an indication of a fault in the AC power supplied to either master clock unit.

Simplified schematic diagrams of the AC power control circuitry are shown in Figure 5-II-11. The circuitry shown applies to the power supply rack (rack 26) but is typical of the circuit breaker and indicator lamp circuitry for all other racks. In the other racks, however, only one phase of the AC power is utilized while two phases are applied to the power supply rack. In addition, the power supply rack circuit breaker and indicator lamp circuitry is tied in with the corresponding circuitry for the kinescope display rack and video signal processor rack, enabling it to sense a blower fault condition in either of these two other racks.

Overall control of CDA station operating modes, and facilities for monitoring the status of the major subsystems in the station, are incorporated in the switches and indicators located on the station control panel in rack 26. Pushbutton switches on the panel provide for control of the following:

- Application of DC power to the AVCS video processing equipment,
- Selection of either of the two redundant command programmers for operation,
- Placement of the selected command programmer into an operating or test mode,
- Interconnection of the station equipment for either ITOS or TOS APT or TOS AVCS satellite interrogation,
- Selection of either of two vertical sync generators (normal or alternate) for use in processing AVCS pictures,
- Selection of the CDA station events recorder for manual or automatic starting in response to received signal strength of the satellite transmissions,

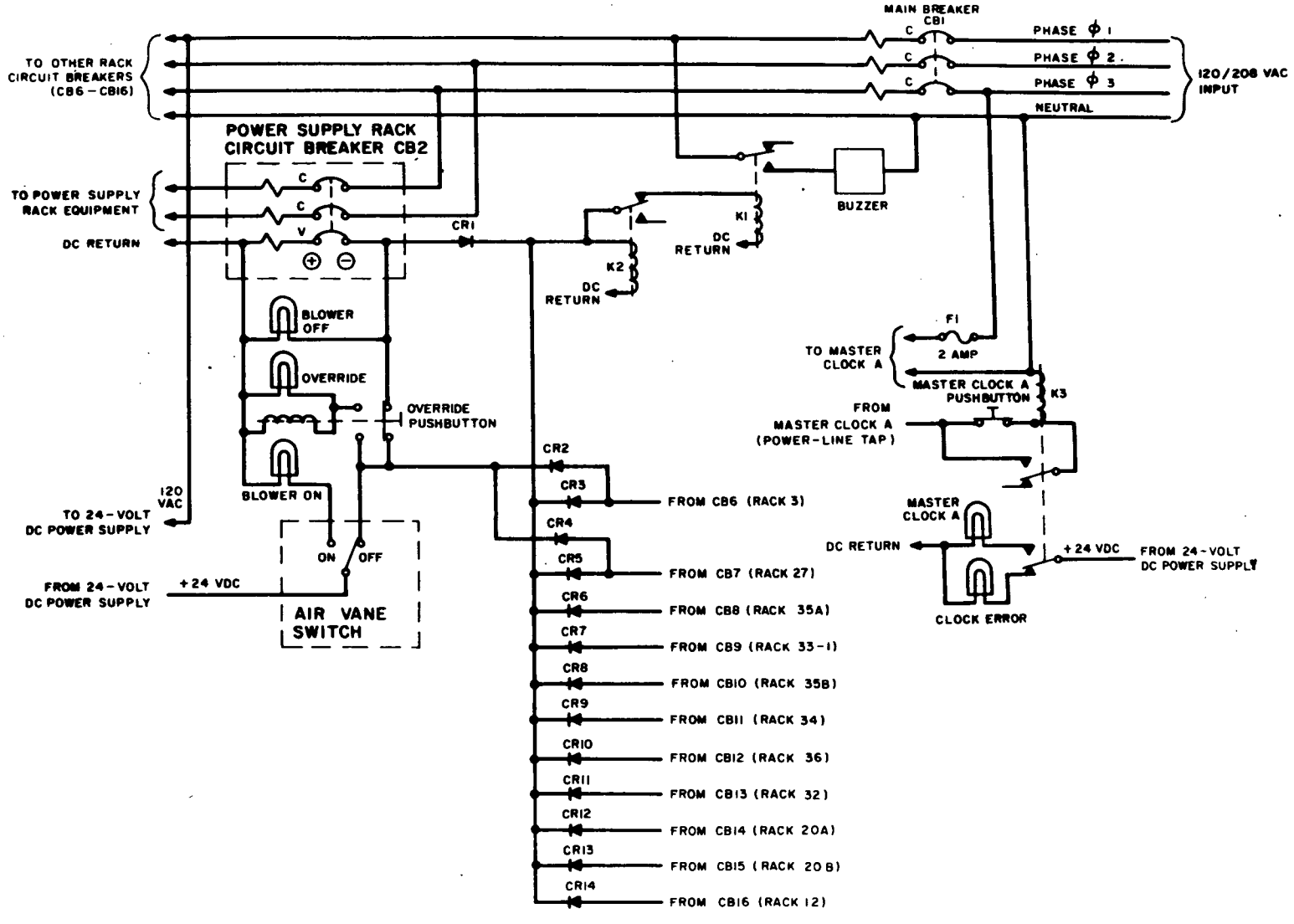

Figure 5-II-11. AC Power Control, Simplified Schematic Diagram

- Selection of the paper tape reader (PTR) for manual or automatic starting by the alarm timer, and
- Selection of local or system calibration mode for beacon system.

Indicators associated with each of the previous controls provide a visual indication of the selected mode. Other indicators on the station control panel provide indications of:

- The status of the +24- and -24-volt power supplies in rack 26,
- The status of all DC supplies required for operating command programmer A (or 1) and command programmer B (or 2),
- The status of the power supply for the beacon processing equipment subcarrier discriminators (SCD's),
- The status of the ±18-volt DC supplies for the SR and secondary sensors (SS) demodulators,
- The status of all DC power applied to the video processing equipment,
- The status of the beacon processing equipment, either the operating or calibration mode, and
- The status of DC power supplies in the two demultiplexers.

The station control panel provides control of the application of DC power to the kinescope video circuits by the video power supplies (i.e., the +300-, +24.5-, +22-, and -24.5-volt supplies mounted in rack 26). It also indicates the on-off status of the video power, kinescope high-voltage power, and kinescope low-voltage power supplied to the kinescope video circuits; and indicates a fault condition in video power if there is a loss of output from any one of the video power supplies.

Eight switch indicators that control the various operating modes of the CDA station equipment are located on the station control panel. Descriptions of these switch indicators and the associated control circuitry for each, are given below.

The COMMAND A/B switch indicator (Figure 5-II-12A) selects one of the two redundant command programmers in the CDA station for use in command programming operations. In the normally open A position, the switch portion of the device maintains program-select relays R13 on the relay panel at the rear of rack 33 in the deenergized condition, thereby coupling significant power, timing and signal lines to command programmer A; i.e., to the command programming equipment in rack 35A. Placement of the switch in the A position also selects the master clock in rack 35A for use in all CDA station timing operations. Placing

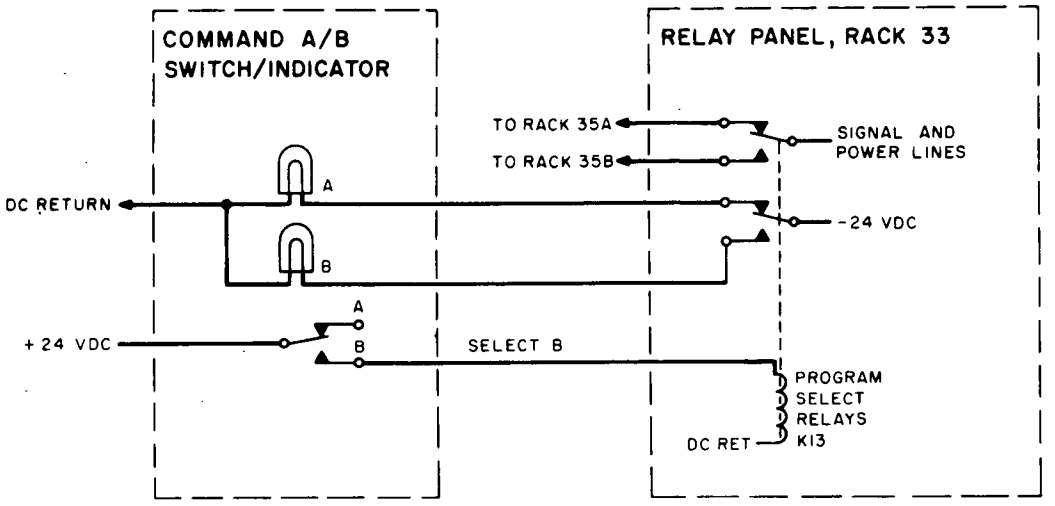

A. COMMAND A/B SWITCH INDICATOR CIRCUIT

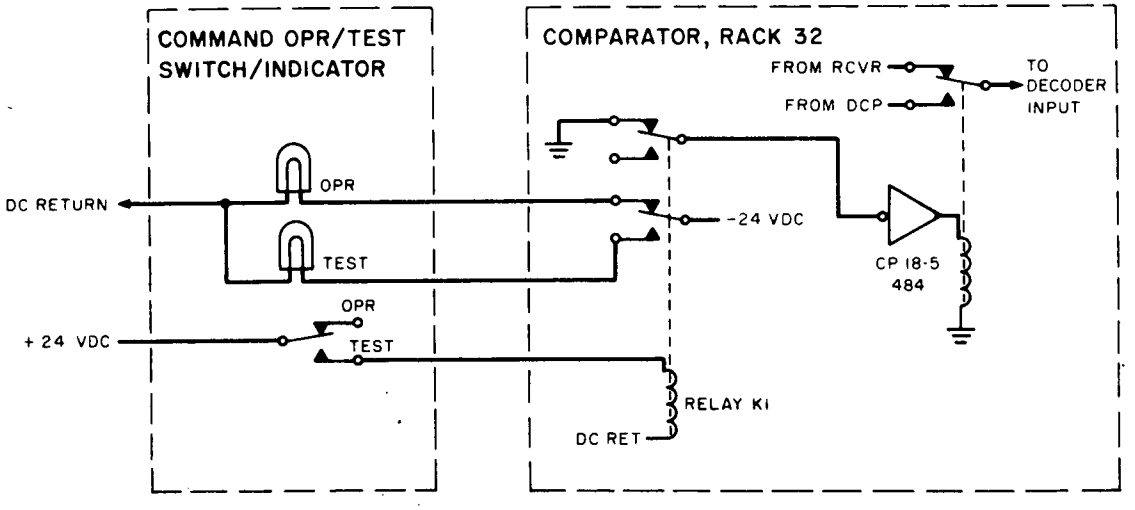

B. COMMAND OPR/TEST SWITCH INDICATOR CIRCUIT

Figure 5-II-12. CDA Station Equipment Control Circuits, Simplified Schematic Diagram

the switch in the B position energizes the program-select relays, switching the signal and power lines to the command programming equipment in command programmer rack 35B and thereby selecting that programmer and associated master clock for use. A set of transfer contacts on relay K13 couples a 24-volt level to the COMMAND A/B indicator lamp corresponding to the selected programmer.

The COMMAND OPR/TEST (operate/test) switch indicator (Figure 5-II-12B) places the command programming equipment in either its normal operational configuration, or in a test configuration. In the normally open OPR position, a relay, K1, in the comparator is held deenergized. A ground (0-volt) level from a normally closed contact of the relay is applied to relay driver CP 18-5 in the unit, inhibiting the driver. The relay associated with the driver is held deenergized and the output of the command receiver is applied through normally closed contacts of the relay to the decoder section of the calibrator. When the COMMAND OPR/TEST switch is placed to the TEST position, relay K1 in the comparator picks up and removes the inhibiting ground level from CP 18-5. The CP 18-5 relay energizes and switches the input of the decoder from the command receiver to the output of the DCP in use. This creates a direct loop from programmer output to comparator input, enabling CDA internal tests of the command programming equipment. A second set of transfer contacts on K1 are used to light the OPR or TEST indicator lamps on the station control panel according to the mode selected.

The TOS/ITOS, AVCS/APT mode switches are the most important controls on the station control panel, determining the mode of station operation during command and data acquisition operations.

The following functions are controlled by these switches (see Figure 5-II-13):

- Command programmer mode - selects rate for spin synchronization circuits in TOS mode; disables spin synchronization circuit in ITOS mode and causes commands to be sent with minimum delay (200 milliseconds) between commands.
- Selects AVCS video and flutter-and-wow signals from TOS doubler and converter circuits or ITOS demultiplexer, as appropriate.
- Selects the proper SCD's and calibration oscillators for beacon processing.
- Selects the video receiver AGC signal to be recorded on the beacon chart recorder (8 channel, brush).

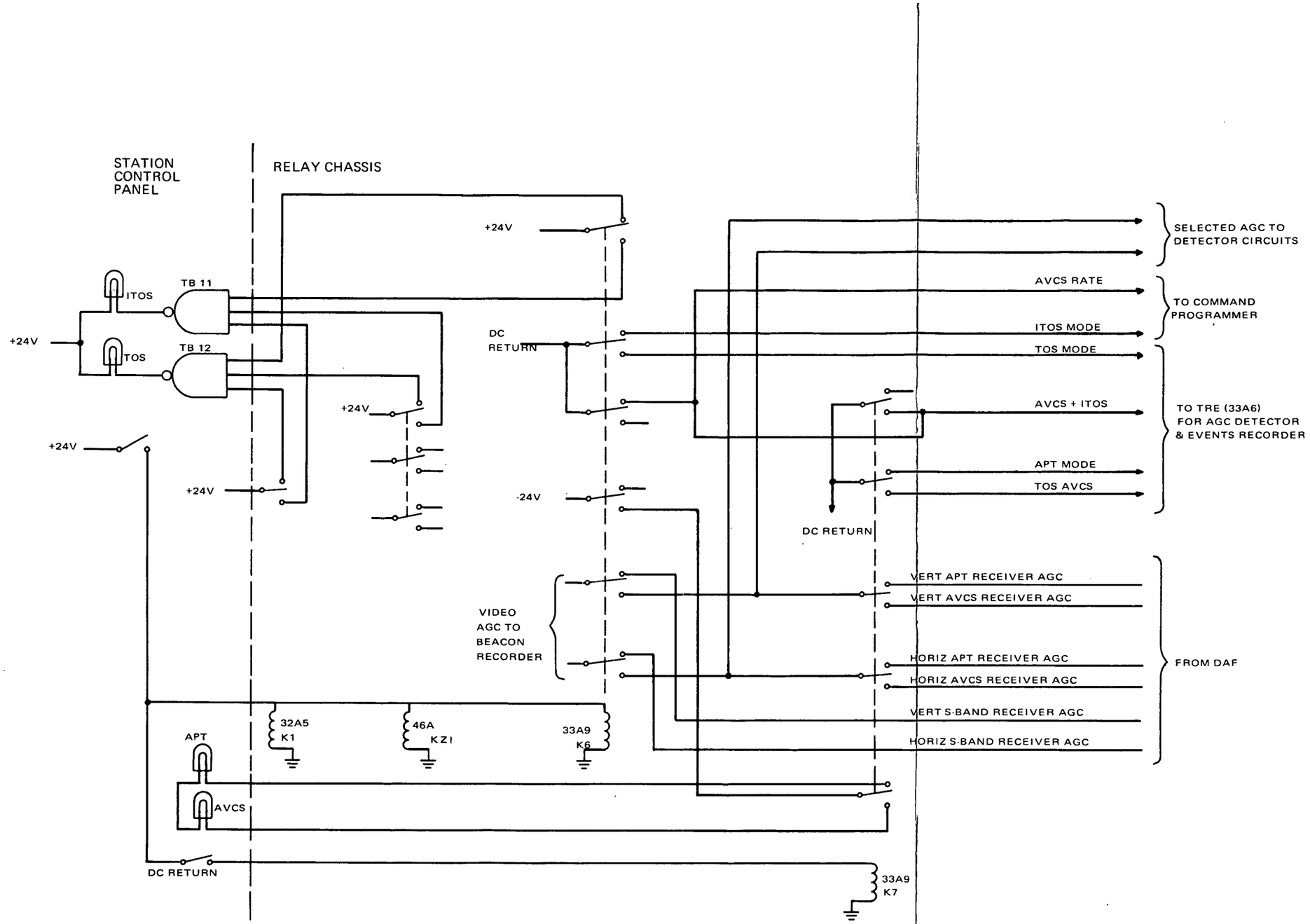

Figure 5-II-13. CDA Station Acquisition Mode Control Circuits, Schematic Diagram

- Indicates the selected station acquisition mode on channels 1 and 2 of the events recorder:

Events Recorder Channel	Indicated Mode
1	TOS APT
2	TOS AVCS
3	ITOS

Actual signal switching is accomplished by relays K6 and K7 in the rack 33 relay chassis, relay KZ1 in the demultiplexer rack and relay K1 in the beacon SCD chassis. The status of each relay is fed back over two lines to diode gates on TB11 and TB12 in the station control chassis. ITOS mode is the normal (deenergized) position for each of the relays. When all three relays are energized, the cathodes of CR 35, CR 36, CR 37 are at +24 volts allowing Q3 and Q4 to turn on the TOS light. If any one of the three relays should fail to operate, the resistor connected from -24 volts to that input would hold the base of Q3 below 0 volt, preventing the TOS light from being turned ON.

The VERT SYNC NOR/ALT (normal/alternate) switch indicator (Figure 5-II-14) selects which of two vertical sync detectors in the AVCS video display equipment are to be used. The "start" pulses and "stop" pulses from both the vertical sync detector and the alternate vertical sync detector are applied to relay K1 in the video signal processor; the alternate pulses applied to normally open contacts, the normal pulses to normally closed contacts. When the VERT SYNC NOR/ALT switch is placed in the normally open NOR position, relay K2 is deenergized, and the "start" and "stop" pulses for the AVCS video display equipment are supplied by the vertical sync detector.

When the VERT SYNC NOR/ALT switch is placed in the ALT position relay K1 is energized by the +24 volts applied through the switch, and the "start" and "stop" pulses from the alternate vertical sync detector are applied to the system. A set of transfer contacts on K1 delivers +24 volts to the NOR/ALT indicator lamp corresponding to the selected mode.

The PTR MANUAL/ALARM TIME switch and indicator control 33A9K2 which is part of the command system.power status circuit. In the manual position, it energizes 33A9K1 which applies AC power to the paper tape reader. With the switch in the ALARM TIMER position 33A9K1 is energized automatically by the alarm timer at the present time. (See Figure 5-II-15.)

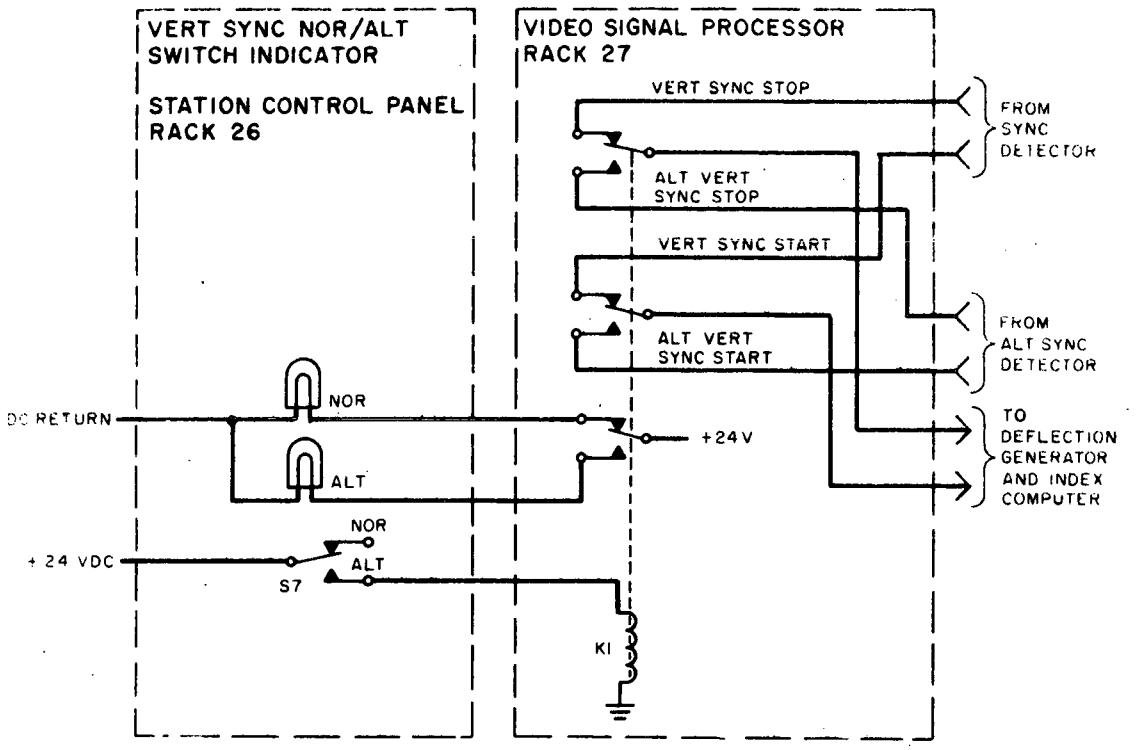

Figure 5-II-14. VERT SYNC NOR/ALT Switch-Indicator Circuit

The EVENTS RECORDER AUTO/MANUAL switch indicator is similar in operation to the PTR manual/alarm timer switch. In the AUTO position (see Figure 5-II-16) the events recorder is controlled by the beacon AGC detector circuits. When K4 is energized, K3 is deenergized, supplying AC to S1 on the events recorder panel. When K4 is deenergized, 24-volt power is applied to K3 which pulls in after an adjustable delay of from 1.0 to 180 seconds, removing AC from the events recorder. In the MANUAL position of the EVENTS RECORDER AUTO/MAN switch, K4 is energized regardless of the status of detected beacon AGC. The AUTO or MAN sections of the switch indicator are lighted green or red depending on whether the ON/OFF switch on the events recorder panel is in the ON or OFF position, respectively.

There are two modes of beacon calibration (Figure 5-II-17), local and system, controlled by the DATA-CAL switch on the EMR calibration control module in the beacon SCD chassis, and the SYSTEM/LOCAL switch on the station control panel. When the EMR control is in the DATA position, the SYSTEM/LOCAL switch is disabled and has no effect. When the EMR control is in a calibrate mode, the position of the LOCAL/SYSTEM switch determines whether the RF equipment in the DAF is to be included in the calibration.

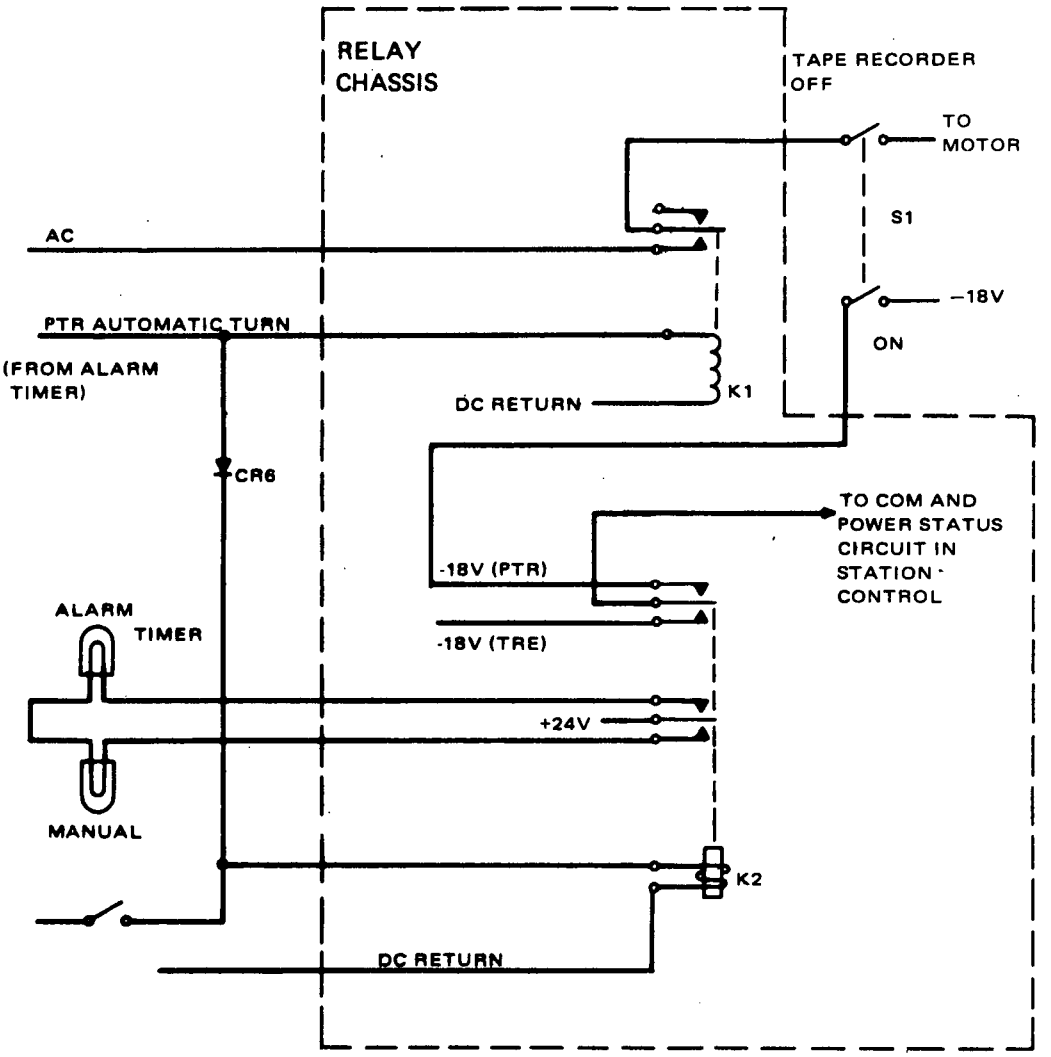

Figure 5-II-15. PTR Manual/Alarm Timer Switch Indicator

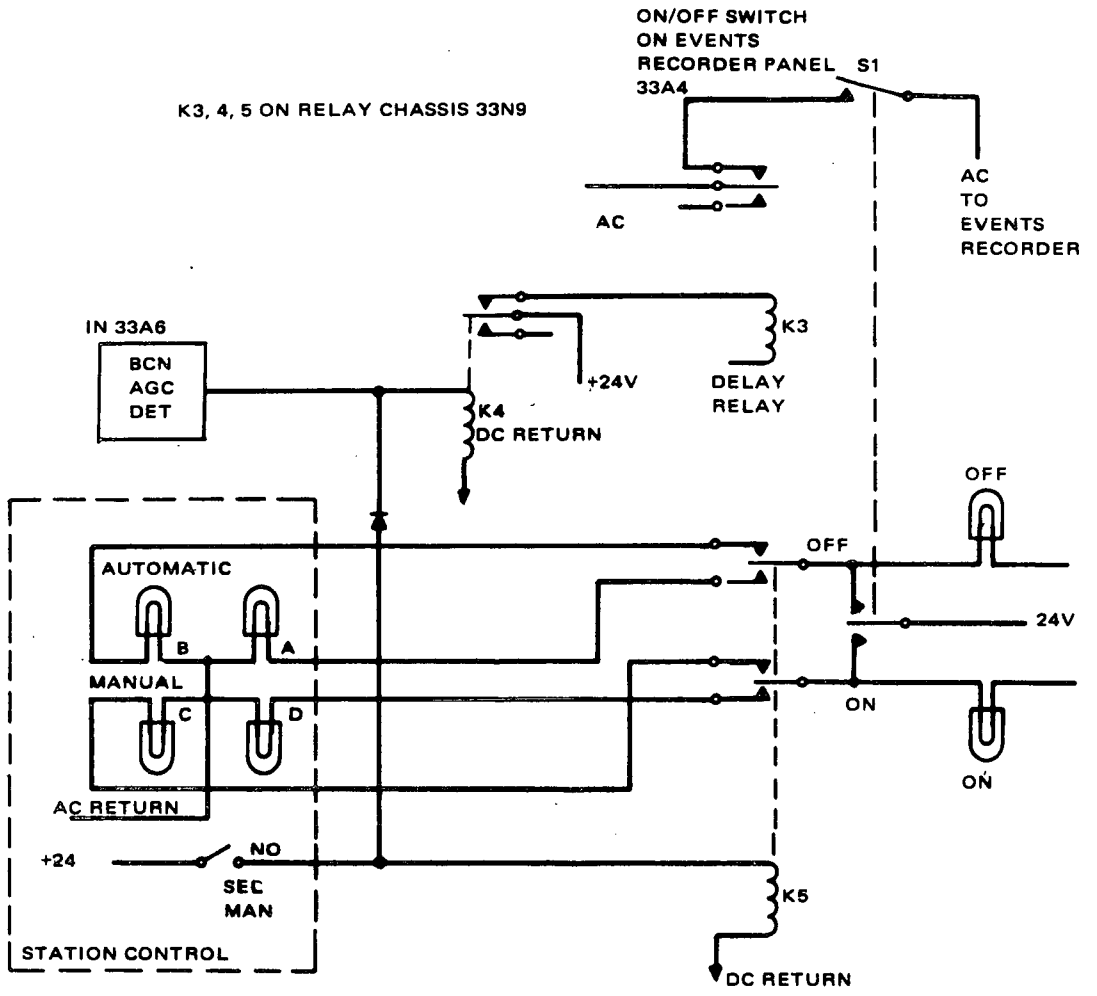

Figure 5-II-16. Events Recorder AUTO/MAN Control Circuit, Schematic Diagram

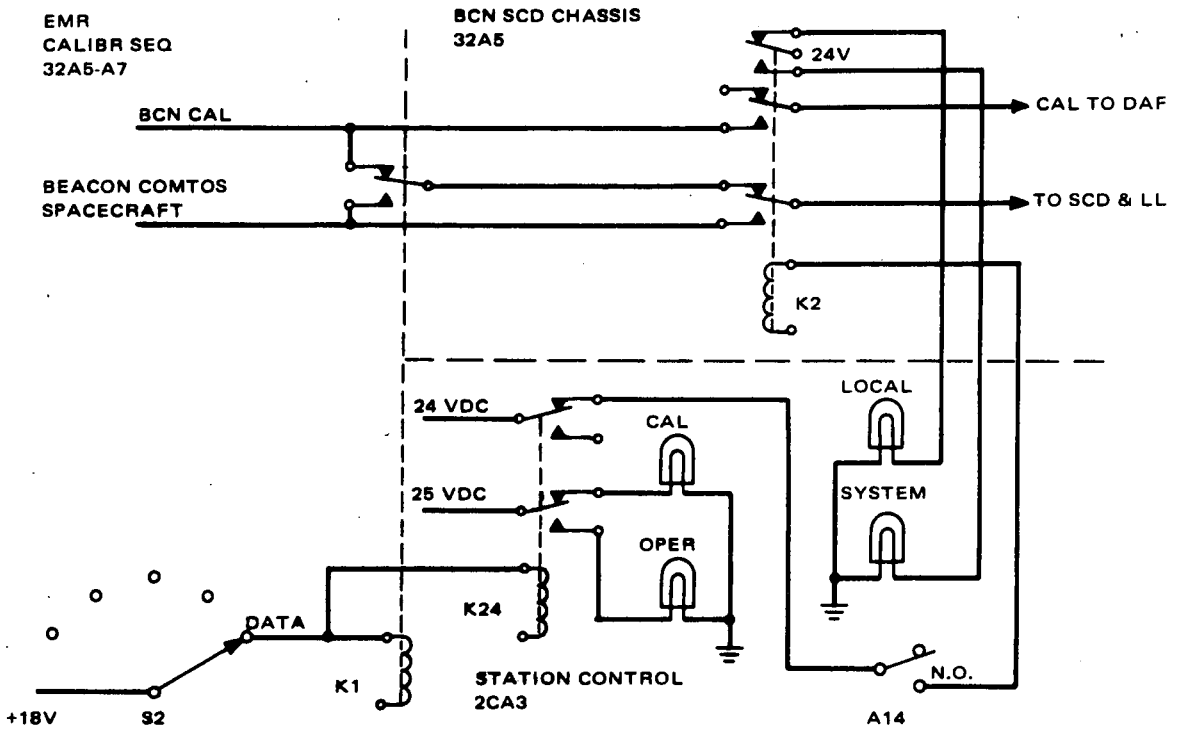

Figure 5-II-17. Beacon OPR/CAL Switch Indicator

When the AVCS video simulator is in the ON mode, a switch closure in the video simulator causes the CAL indicator to light. When the indicator is lighted, the simulator is either in the Standby or OFF mode, and the station is ready for normal operation.

SECTION III

TOS OPERATIONS CENTER (TOC)

A. GENERAL

A principal operating feature of the ITOS and TOS systems is the establishment of centralized remote control of the CDA stations by the TOS Operations Center (TOC) located at the National Environmental Satellite Center (NESC) in Suitland, Maryland. TOC is a part of the Operations Division at NESC and is solely responsible for ITOS/TOS ground system operation and ITOS/TOS satellite operation, after launch and checkout by the TOS Evaluation Center and TOS Checkout Center (TEC/TCC). During prelaunch checkout, launch, and postlaunch checkout, TOC monitors all TEC/TCC operations.

The duties of TOC include real-time monitoring and assessment of satellite and CDA station operation; near real-time system evaluation; origination of satellite command programs upon consideration of engineering factors involved; attitude determination; magnetic attitude and momentum control programming; and maintenance of engineering and other data records.

The equipment at TOC is capable of real-time data processing and display from only one CDA station at a time, although simultaneous receipt of data from both stations is possible. When simultaneous transmissions are received, one set of data is processed on-line and displayed on the chart recorders, and both sets are recorded on tape. At the conclusion of the simultaneous transmission, the tape recorder can be rewound and replayed so that the second set of data can be processed.

For two weeks preceding a scheduled ITOS launch, TOC directs TEC/TCC in simulated launch operations, and the entire ground system participates as scheduled by TOC. During these tests, TEC/TCC transmits simulated command programs to TOC for relay to the CDA stations.

During launch and the initial maneuver, TOC acts as a relay station between TEC/TCC and the CDA stations, while monitoring all TEC/TCC messages.

During postlaunch checkout of the satellite, TOC monitors all operations of the newly launched ITOS or TOS satellite. When the manager of the NESC Operations Division and the ITOS or TOS project manager determine that the new satellite has been fully checked out and is operational, TOC assumes all control of the satellite operations.

The TOC station personnel, using orbital and satellite attitude predictions supplied by the NASA T&DS Facility, generate satellite command programs to obtain TV pictures that will provide the weather data requested by NESC or any other authorized agency. These command programs are transmitted to the CDA stations by teletype. CDA station personnel then set up the station equipment for transmitting the command program to the satellite when it comes into communication range of the CDA station. TOC monitors the CDA station transmission during the satellite pass to determine that the correct commands are transmitted by the CDA station and that the satellite interprets the commands correctly (command verification). Satellite telemetry data is recorded by TOC for satellite evaluation.

During satellite operation, beacon and events data is supplied to TOC by the CDA stations. This data is transmitted from the CDA stations to TOC over the microwave link either in real time (RT) or in playback (PB), depending upon the mode of operation. In the PB mode, the data is transmitted in the real-time playback (RTPB) speed of 60 onches per second or in the slow-time playback (STPB) speed of 7.5 inches per second. When the data is received in STPB speed, it must be recorded on a tape recorder at TOC and then play back at RT speed before it is in the correct format to be processed by the TOC equipment.

In the event that the performance of a satellite degrades so that its operational capabilities are impaired and its operational life is doubtful, TOC assigns control of the satellite to TEC/TCC for evaluation. In this way, such satellites can be replaced before the end of their useful operating lives and continuous weather surveillance can be maintained.

B. RCA-SUPPLIED EQUIPMENT

As shown in Figure 5-III-1, the RCA-supplied portion of TOC consists of four racks of equipment, as follows:

- Discriminator rack, No. 37,
- Data recorder rack, No. 36,
- Decommutator rack, No. 38, and
- Telemetry rack No. 47.

The TOC equipment is housed in standard equipment racks 72 by 24 by 24 inches, and the racks containing the RCA-supplied equipment are installed side-by-side.

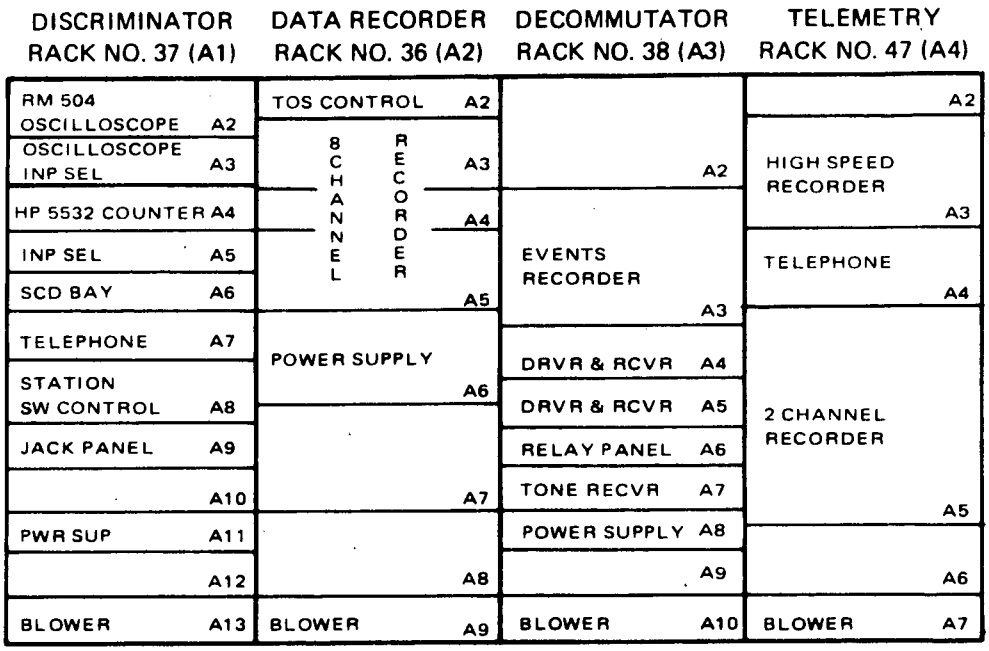

Figure 5-III-1. TOC Equipment Racks, Front Panel Elevation

The discriminator rack 37, the left rack in Figure 5-III-1, contains the following assemblies (from top to bottom):

- A1: cabinet frame,
- A2: RM 504 oscilloscope, Tektronix,
- A3: oscilloscope input selector, RCA 1843145-503,
- A4: HP-5532A electronic counter,
- A5: counter input selector, RCA 1843145-504,
- A6: subcarrier discriminator, EMR,
- A7: telephone,
- A8: station switching control, RCA 1759134,
- A9: jack panel,
- A10: blank panel,
- A11: power supply Lambda Model 50-OBBM-1383-1,
- A12: blank panel, and
- A13: blower, McLean.

The principal functions performed in the discriminator rack are (1) processing of the composite beacon subcarrier received over the microwave link into its components for recording on the chart recorders (racks 36, 38, and 47) and for

display on the oscilloscope, (2) providing the composite beacon subcarrier as an input to the electronic counter unit, and (3) providing switching control for the TOC equipment.

The primary function performed in the data recorder rack 36 is to provide an 8-channel hard copy of the ITOS/TOS beacon subcarriers, the command verification signals, and the satellite and ground error signals. The rack contains the following assemblies (from top to bottom):

- A1: cabinet frame,
- A2: TOS control,
- A3 through A5: 8-channel recorder,
- A6: Quindar power supply,
- A7 and A8: blank panels, and
- A9: blower, McLean.

The primary function performed in the decommutator rack 38 is the demultiplexing and processing of the events data, the ground and satellite error data, the command verification signals, and the 28-bit timing code, to make the data compatible for recording on the chart and events recorders and for display of the decoder and programmer RZ (events) data on the oscilloscope. The rack contains the following assemblies (from top to bottom):

- A1: cabinet frame,
- A2: blank panel,
- A3: events recorder,
- A4 through A7: Quindar tone receivers, demultiplexing equipment, and relay panels,
- A8: Quindar power supply,
- A9: blank panel, and
- A10: blower, McLean.

The primary function performed in the telemetry rack 47 is to provide a hard copy record of the two ITOS beacon subcarriers. The rack contains the following assemblies (from top to bottom):

- A1: cabinet frame,
- A2: blank panel,
- A3: high speed chart recorder,

- A4: telephone panel,
- A5: 2-channel recorder,
- A6: blank panel, and
- A7: blower, McLean.

C. MAJOR TOC SUBSYSTEMS

The TOC equipment consists of four major subsystems, as follows, and the blower fault protection circuits:

- Station switching control equipment,
- Beacon data processing equipment,
- Events processing equipment, and
- Recording and display equipment.

The station switching control subsystem consists of the station switching control panel, relays, and a patch panel, located in rack 37. This subsystem controls the application of AC and DC power to all TOC racks and convenience outlets. The subsystem also provides for the selection of the station input source (Wallops or Gilmore), the type of input (direct or playback), and the type of input signals (TOS or ITOS). The playback mode permits playback of microwave link data recorded at TOC. Remote or local control of the recorders is provided by this subsystem. In the remote mode of control, turn-on of all recorders is accomplished by one switch on the station switching control panel provided the individual power switches have been turned on. In addition, the station switching control panel provides facilities for monitoring the status of the blowers in all four TOC racks, for providing aural and visual indications of blower faults, and for overriding blower faults. Front panel MAIN POWER ON and CONVENIENCE OUTLETS ON indications are provided by this subsystem. The jack panel permits a selection of auxiliary attitude signals originating from either the tape recorder in playback mode, or one of the CDA stations. The signals are displayed on either the 2-channel recorder (TOS) or the high speed chart recorder (ITOS) while the normal signals are displayed on other recorders.

The beacon data processing subsystem separates the composite beacon signal into its subcarriers and supplies the discriminated subcarriers to the proper recording and display (oscilloscope) equipment. This subsystem also supplies the composite beacon signal to the input selector for application to the electronic counter and to the input selector for display on the oscilloscope.

The events processing subsystem receives the FSK tones from the selected CDA station (via the microwave link and processes the signals for application

to the events and beacon data recorders to provide hard copy records and to the oscilloscope input selector for visual display on the oscilloscope.

The recording and display equipment provides hard copy records of the following: (1) the beacon data from the beacon subcarriers, (2) the 19 channels of station events data, (3) the satellite and ground error indications, and (4) the command verification signals (decoder RZ signals and programmer RZ signals). This subsystem provides for visual displays of the beacon subcarriers and the two RZ command verification signals (decoder and programmer). Provisions are also available for supplying the composite beacon data to the electronic counter.

The blower fault protection subsystem provides visual and aural indications of blower faults in any of the four TOC racks. This subsystem provides for overriding a fault indication in case of an emergency.

D. OVERALL FUNCTIONAL DESCRIPTION

TOC is composed primarily of two information processing and recording chains; i.e., the beacon data chain and the CDA station (events) data chain. The beacon data chain consists of a telemetry calibrator, four subcarrier discriminators, a 2-channel chart recorder, a high speed chart recorder, and 3 channels of an 8-channel recorder. The CDA station data chain consists of a FSK-tone receiving and demultiplexing device, a switching unit, an RZ (return-to-zero) restorer, an events recorder, and 5 channels of an 8-channel chart recorder. Figure 5-III-2 is a block diagram of the TOC equipment.

As shown in this illustration, the input to TOC from the microwave link consists of (1) multiplexed beacon signals containing 2.3-, 3.0-, and 3.9-kHz subcarriers and (2) multiplexed CDA station signals containing 1.3- and 2.4-kHz FSK tones. Signals are selected from either the Wallops or Gilmore CDA stations and may be real-time (RT) data directly from the CDA station or tape-recorded (TR) playback (PB) data from a tape recorder. The station switching control panel provides facilities for switching the TOC equipment on the proper line to receive the signal present at any given time, and the following inputs to TOC are provided:

- Real-time beacon and events data from the Wallops station,
- Tape-recorded beacon and events data from the Wallops station,
- Real-time beacon and events data from the Gilmore station, and
- Tape-recorded beacon and events data from the Gilmore station.

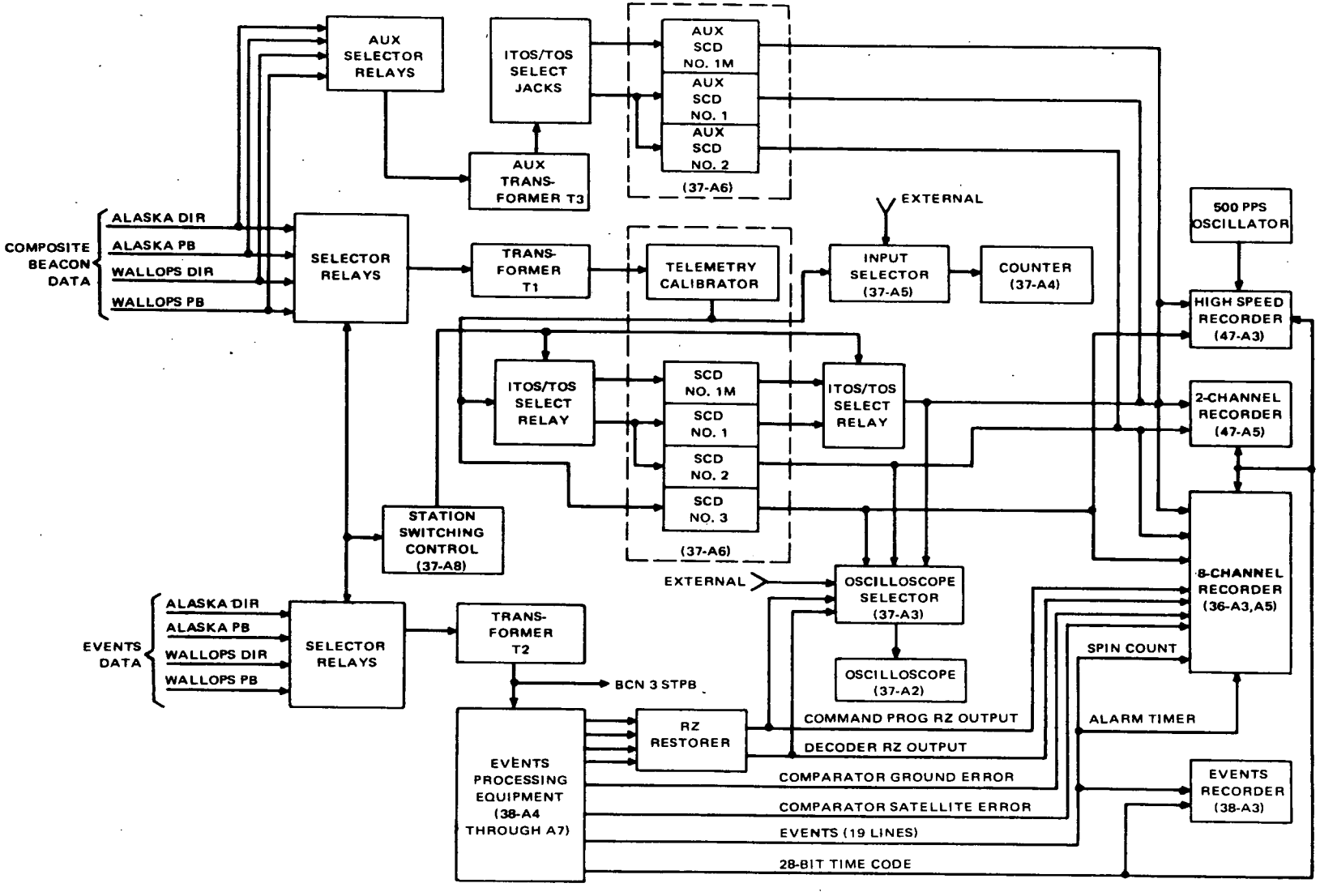

Figure 5-III-2. TOS Operations Center (TOC), Block Diagram

The station switching control panel also provides the facilities for either automatically or manually switching the TOC equipment into the TOS or ITOS mode.

As shown in Figure 5-III-2, the selected composite beacon data is applied to impedance matching transformer T1. The composite beacon output from transformer T1 is coupled, through switching in the ITOS/TOS select relays, to the common input of either three TOS subcarrier discriminators (SCD's), operating at center frequencies of 2.3, 3.0, and 3.9 kHz (beacon channels 1, 2, and 3, respectively) or two ITOS subcarrier discriminators that operate at center frequencies of 2.3 and 3.9 kHz (beacon channels 1M and 3). The 3.9-kHz SCD is used for both TOS and ITOS. The individual SCD's demultiplex the composite beacon signal by accepting only the band of frequencies ±7.5 percent above the respective center frequencies for beacon channels 1, 2, and 3 and ±20 percent for beacon channel 1M.

Each SCD demodulates the associated FM subcarrier for recording on the 2-channel (beacon) recorder (beacon channels 1 and 2 only), on the 8-channel (attitude) recorder (all three TOS beacon channels) and on the high speed (attitude) recorder (both ITOS beacon channels). The outputs from the three SCD's are also applied to the oscilloscope input selector to provide a visual display on the oscilloscope. The composite beacon subcarrier is also supplied to the input selector for application to the electronic counter.

The jack panel, shown in Figure 5-III-3, provides a means of manually patching an auxiliary signal from the microwave link equipment to impedance matching transformer T3 and to the required auxiliary SCD's and recorders. However, the CDA input, selected on the station switching control panel as the primary TOC input, is automatically excluded from the auxiliary signal channel to avoid disrupting the primary TOC input.

The selected CDA data signals are applied to impedance matching transformer T2 (see Figure 5-III-2). (An auxiliary output from T2 is also routed to NESC.) The output from the transformer (composite 1.3- and 2.4-kHz FSK tones) is applied to the demultiplexing equipment, which recovers the events data from the two tones and supplies this data on separate lines to the RZ restorer, the events recorder, and the 8-channel recorder. The programmer and decoder NRZ "1's" and "0's" recovered from the FSK tones are converted to RZ signals in the RZ restorer. The decoder and programmer RZ outputs from the RZ restorer are supplied to the 8-channel recorder and to the oscilloscope input selector for presentation on the oscilloscope.

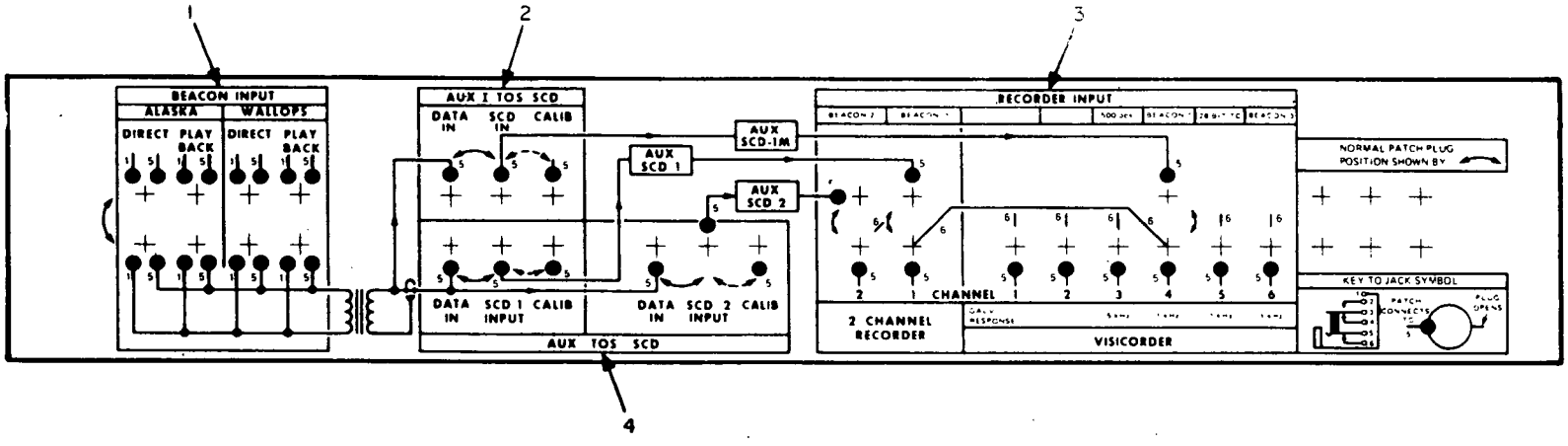

LEGEND

1. BEACON INPUT: Input jacks for connection from either the Alaska or Wallops CDA to impedance matching transformer.

2. AUX ITOS SCD: Patch jacks permit either direct or PB ITOS Beacon subcarrier to be applied to the auxiliary SCD 1M.

3. RECORDER INPUT: Patch jacks permit demodulated subcarrier from selected CDA long line to be applied to either the 2-channel high speed recorder or the Visicorder.

4. AUX TOS SCD: Patch jacks permit either direct or PB TOS beacon subcarrier to be applied to the appropriate auxiliary SCD.

Figure 5-III-3. Jack Panel Front Elevation (Rack 37)

E. STATION SWITCHING CONTROL EQUIPMENT

The station switching control equipment consists of the station switching control panel, assembly A8 in the discriminator rack No. 37, relays 37-K1, 37-K2, and 37-K3 located in the bottom rear of the rack, and the -24-volt DC power supply (assembly 37-A11). Refer to Figure 5-III-4 for additional detail.

The station switching control circuitry controls the AC power to the four TOC racks, provides for the selection of the CDA station data to be processed by the TOC equipment, and selects the mode of operation (direct or playback and TOS or ITOS). This circuitry also provides for local or remote control of the TOC recorders. Blower status is indicated on the panel and faults may be overriden in emergency cases. Indicators on the station switching control panel provide visual indications of all functions controlled. In addition to the visual indications, a buzzer is energized when a blower fault occurs.

F. BEACON DATA PROCESSING EQUIPMENT

The beacon data processing equipment provides for demultiplexing and processing of the beacon transmissions from the selected CDA to convert this data into the proper format for application of the recording equipment and to the oscilloscope. The composite beacon signal is applied through an impedance matching transformer to the TOC beacon processing equipment. The composite beacon subcarrier signal consists of three subcarriers on IRIG channels 7 (2.3 kHz), 8 (3.0 kHz), and 9 (3.9 kHz) for TOS and IRIG channel 9 (3.9 kHz) and a nonstandard IRIG 2.3-kHz channel for ITOS. The utilization of these three subcarriers for TOS/APT, TOS/AVCS, and ITOS satellites is given in Tables 5-III-1, 5-III-2, and 5-III-3, respectively. (See also Figure 5-III-2.)

The beacon processing equipment employs three subcarrier discriminators for TOS and two subcarrier discriminators for ITOS that separate and restore the beacon data from each FM subcarrier. The restored TOS data is routed to the 2-channel (attitude) recorder and the 8-channel (beacon) recorder for direct readout. ITOS data is routed to the high speed (attitude) recorder and the 8-channel (beacon) recorder for direct readout. A telemetry calibrator, consisting of a sequencing unit and four calibration oscillators, provides a means for calibrating the discriminator/recorder operation.

The real-time TOS composite beacon subcarrier from the selected CDA or from the Mincom recorders via the impedance matching transformer is applied through switching in the telemetry calibrator and the ITOS/TOS select relays to the common input of three SCD's operating at center frequencies of 2.3, 3.0, and 3.9 kHz (beacon channels 1, 2, and 3, respectively). The three SCD's collectively

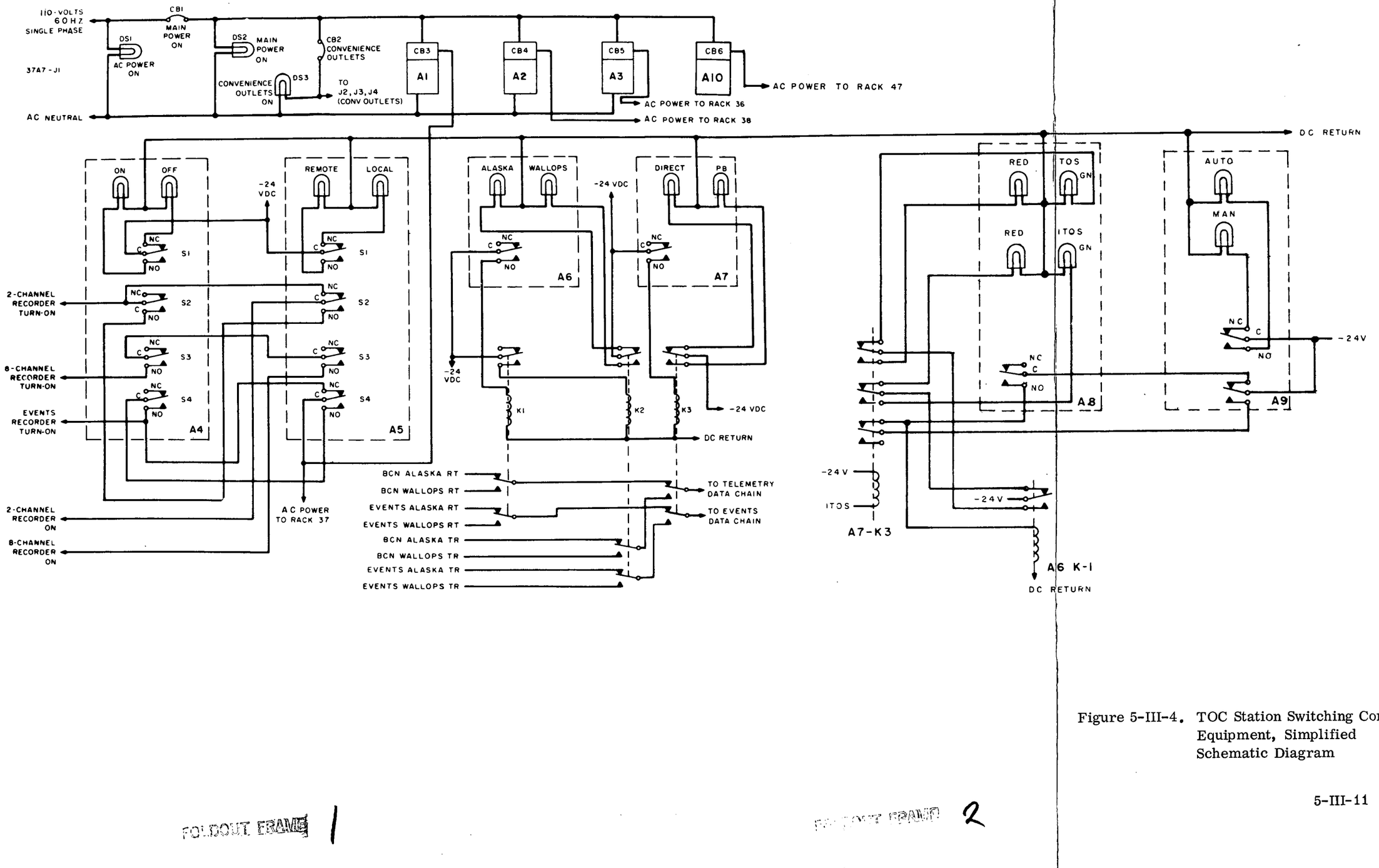

Figure 5-III-4. TOC Station Switching Control Equipment, Simplified Schematic Diagram

FOLDOUT FRAME 1

FOLDOUT FRAME 2

TABLE 5-III-1. BEACON SUBCARRIER UTILIZATION, TOS/APT

Beacon Subcarrier	Data Content	Time of Transmission
No. 1 (2.3-kHz center frequency, ±7.5 percent deviation) (IRIG Channel 7)	Up-looking V-head attitude sensor data	Continuously transmitted.
	Booster separation indication (by a return to center frequency)	Only during satellite launch phase.
No. 2 (3.0-kHz center frequency, ±7.5 percent deviation) (IRIG Channel 8)	Down-looking V-head attitude sensor data and horizon crossing data from horizon crossing indicator No. 1	Continuously transmitted. The two signals time-share this channel because of sensor location on the spacecraft.
No. 3 (3.9-kHz center frequency, ±7.5 percent deviation) (IRIG Channel 9)	Horizon crossing indicator data	Continuously transmitted, unless other data is present.
	Command verification data	Present whenever commands are being transmitted to satellite.
	Housekeeping telemetry data	On command
	Solar aspect indicator data	On command
	APT camera "prepare" and "expose" markers	Just prior to APT picture transmission.
	MASC coil polarity switching indications	Whenever MASC system is activated.

TABLE 5-III-2. BEACON SUBCARRIER UTILIZATION, TOS/AVCS

Beacon Subcarrier	Data Content	Time of Transmission
No. 1 (2.3-kHz center frequency, ±7.5 percent deviation) (IRIG Channel 7)	Up-looking V-head attitude sensor data	Continuously transmitted.
	Booster separation indication (by a return to center frequency)	Only during satellite launch phase.
No. 2 (3.0-kHz center frequency, ±7.5 percent deviation) (IRIG Channel 8)	Down-looking V-head attitude sensor data and horizon crossing data from horizon crossing indicator No. 1	Continuously transmitted. The two signals time-share this channel because of sensor location on the spacecraft.
No. 3 (3.9-kHz center frequency, ±7.5 percent deviation) (IRIG Channel 9)	Horizon crossing indicator data	Continuously transmitted unless other data is present.
	Command verification data	Present whenever commands are being transmitted to satellite
	Housekeeping telemetry data and picture time code	On command and during transmission of each AVCS picture. The picture time code occurs during the first 1.2 seconds of the command telemetry readout.
	Solar aspect indicator data	On command.
	MASC coil polarity switching indications	Whenever MASC system is activated.

TABLE 5-III-3. BEACON SUBCARRIER UTILIZATION, ITOS

Subcarrier	Data Content	Time of Transmission
No. 1M (2.3-kHz center frequency, ±20 percent deviation) (IRIG Channel 7 special)	Roll sensor 1 or 2	Normally continuous during operational mode
	Time code	Upon command
	Roll sensor and pitch index	Upon command
	Pitch sensor 1 or 2	Upon command
No. 3 3.9-kHz center frequency ±7.5 percent deviation (IRIG Channel 9)	Solar proton monitor data	Normally continuous during operational mode
	Digital solar aspect data	Normally continuous during acquisition mode (initial condition)
	Telemetry commutated data	Upon command
	Data verification	During command operations

perform the discrimination operation by accepting only the band of frequencies associated with the particular channel (i.e., deviations of ±7.5 percent about the center frequency) and rejecting all others.

Each SCD individually demodulates the associated FM subcarrier, and presents the resulting data as varying DC voltages over a range from -10 volts DC (upper band edge) to +10 volts DC (lower band edge). The disposition of the data from each of the SCD's is as follows:

- SCD No. 1 (2.3 kHz): The output from SCD No. 1 which represents the horizon crossing information from channel 2 of the V-head attitude sensor in the spacecraft, is fed to channel 1 of the 2-channel attitude recorder, to channel 4 of the high speed attitude recorder to channel 6 of the 8-channel beacon recorder, and to the oscilloscope input selector.

- SCD No. 2 (3.0 kHz): The output of SCD No. 2, which contains the composite of horizon crossing information from channel 1 of the V-head attitude sensor and from the No. 1 horizon crossing indicator, is applied to channel 2 of the attitude recorder, to channel 7 of the beacon recorder, and to the oscilloscope input selector.

- SCD No. 3 (3.9 kHz): The output of SCD No. 3, which contains the switched telemetry data from the spacecraft (see Tables 5-III-1 and 5-III-2) is applied to channel 8 of the beacon recorder, channel 6 of the high speed attitude recorder, and to the oscilloscope input selector.

The real-time ITOS composite beacon subcarrier is processed in a manner similar to the TOS composite beacon subcarrier, with the exception that there are only two beacon subcarrier channels with center frequencies of 2.3 and 3.9 kHz (beacon channels 1M and 3). SCD No. 3 is used for both TOS and ITOS and accepts deviations of ±7.5 percent about the center frequency, while SCD No. 1M accepts deviations of ±20 percent about the center frequency. The disposition of the data from these SCD's is as follows:

- SCD No. 1M (2.3 kHz): The output from SCD No. 1M, which contains the attitude information, is fed to channel 4 of the high speed attitude recorder, to channel 1 of the 2-channel attitude, to channel 6 of the beacon recorder, and to the oscilloscope input selector.

- SCD No. 3 (3.9 kHz): The output of SCD No. 3, which contains the switched telemetry data from the spacecraft (see Table 5-III-3) is applied to channel 8 of the beacon recorder, to channel 6 of the high speed attitude recorder, and to the oscilloscope input selector.

In addition, the telemetry calibrator output is applied to the electronic counter input selector.

The beacon processing equipment incorporates a built-in telemetry calibration system that provides for checking and calibrating all units of the system and all units driven by the system. The calibrator can be operated in either the data mode or the calibration mode. When the calibrator is operated in the data mode, the composite beacon subcarrier input is routed directly through the sequencer to the discriminators and other equipment, as described above. When the calibration sequencer is operated in the calibration mode, the data line is broken, and a calibration signal produced by the four calibration oscillators (operating at 2.3, 3.0, and 3.9-kHz, as well as one for the special 2.3-kHz discriminator, corresponding to the channels used by the beacon subcarriers) is supplied to

the discriminators. Each oscillator produces five crystal-controlled frequencies for calibration of a particular channel at five points in the passband of the corresponding discriminator. Any of the five calibration points can be selected for a channel independently of the deviations selected for the other channels, and any channel can also be turned off independently. Three modes of automatic calibration routines are also available.

G. EVENTS PROCESSING EQUIPMENT

The events processing equipment demultiplexes and processes the events FSK tones from the selected CDA station to convert them into the proper format for application to the recording equipment and to the oscilloscope.

The events processing equipment employs two data processing chains, the 1.3-kHz data chain and the 2.4-kHz data chain, comprised as follows:

2.4-kHz Data Chain	1.3-kHz Data Chain
• 2.4-kHz tone receiver	• 1.3-kHz tone receiver
• Scanner receiver	• Scanner receiver
• Receive register (8-channel)	• Two receive registers (total of 16 outputs)
• Relay panel (8-channel)	• Two relay panels (total of 16 outputs)

The events processing equipment also contains an RZ restorer unit. This unit converts the decoder and programmer "1's" and "0's" outputs from the 2.4-kHz data chain from NRZ to RZ signals before they are applied to the recording equipment and to the oscilloscope. A block diagram of the events processing equipment is shown in Figure 5-III-5.

H. RECORDING EQUIPMENT

1. Events Recorder

The events recorder (mounted in rack 38-A3) is an Esterline-Angus Model A620T paper chart recorder that provides for simultaneous recording of 20 independent channels of slow speed, ON-OFF information. The events recorder is normally operated at a chart speed of 3 inches per minute. The recorder is used to record significant CDA station operations that have been transmitted via microwave link and to provide a hard copy record of these and certain critical programming events. Chart speed, controlled by a synchronous motor and a gear train,

is selectable in 10 steps. The writing elements are electrically heated styluses which record on chart paper sensitive to both heat and pressure. The event recorder is capable of both manual and remote operation.

The events recorder (1) records the programming events involved in transmitting commands to the satellite from either programmer A or programmer B in the CDA programming equipment, (2) indicates detection of a satellite or ground station error, and (3) monitors the diversity combined AGC outputs of both video receivers and the beacon receiver to determine the start of data reception. Other events recorded by the unit include indication of the processing of an AVCS video frame, and the type of satellite (TOS AVCS, TOS APT, or ITOS) the station is set up to interrogate. Refer to Table 5-III-4 for a description of the events recorded and their recorder channel assignments.

When the RECORDER REMOTE-LOCAL switch on the station switching control panel is in the LOCAL position, power to the events recorder is controlled by an alternate action ON-OFF switch on the recorder front panel. If the REMOTE-LOCAL switch on the station switching control panel is in the REMOTE position and the alternate action ON-OFF switch on the recorder panel is ON, power to the events recorder is controlled by the RECORDER ON-OFF switch on the station switching control panel.

For detailed information on the Esterline-Angus A620-T events recorder, refer to the appropriate instruction manual.

2. Beacon Data Recorder

The 8-channel beacon data recorder (mounted in rack 36-A3, A4, and A5) is a Brush Model Mark 200, high speed, paper chart recorder which provides simultaneous recording of 8 channels of analog data. The recorder channel assignments are indicated in Figure 5-III-6.

The recorder is normally operated at a chart speed of 20 millimeters per second and utilizes a pressurized fluid writing system with rectilinear presentation. Each recorder channel chart width is 40 millimeters (50 divisions) and trace width is 0.01 inch. The frequency response is as follows:

- 50-mm p-p deflection 0 to 55 Hz,
- 40-mm p-p deflection, 0 to 60 Hz,
- 15-mm p-p deflection, 0 to 100 Hz, and
- 4-mm p-p deflection, 0 to 200 Hz.

For a detailed dexcription of the beacon data recorder, refer to the appropriate instruction manual.

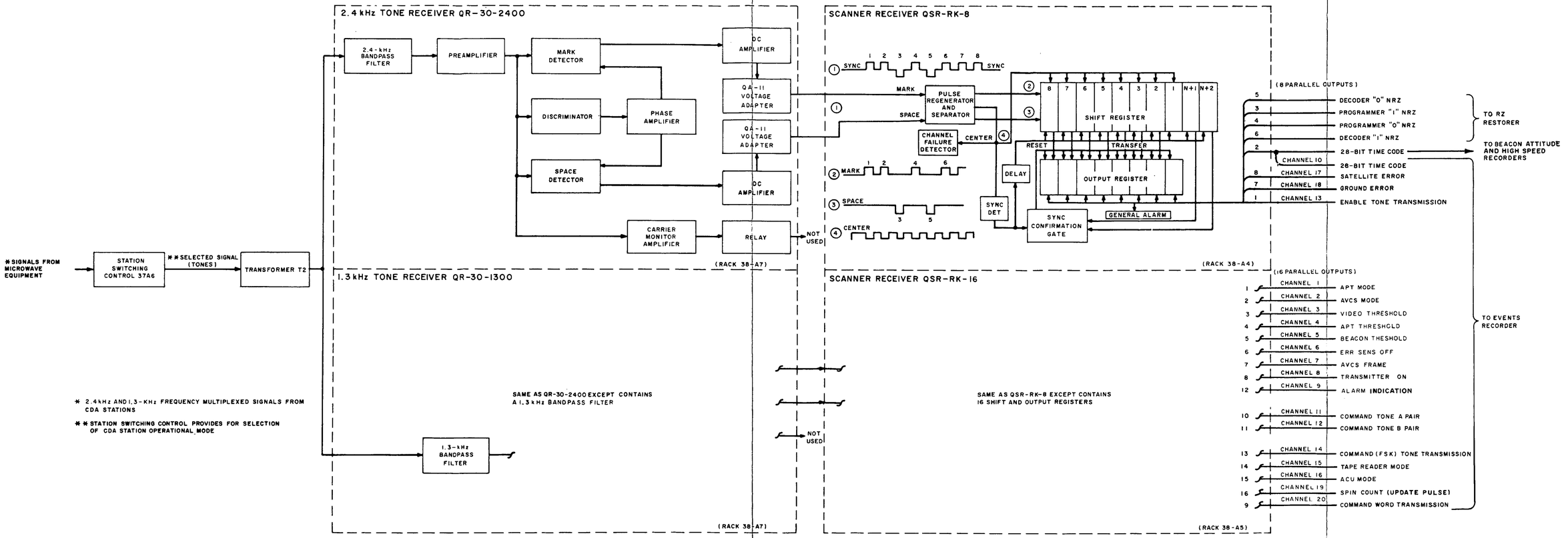

Figure 5-III-5. Events Processing Equipment, Functional Block Diagram

TABLE 5-III-4. EVENTS RECORDER CHANNEL ASSIGNMENTS

Channel No.	Designation	Event Indicated
1	APT MODE	Station set up for TOS/APT satellite interrogation*
2	AVCS MODE	Station set up for TOS/AVCS satellite interrogation*
3	VIDEO AGC	Start of video reception**
4	APT AGC	Start of APT video reception †
5	BCN AGC	Start of beacon reception † †
6	ERROR SENS OFF	Activates when satellite error verification from comparator is ignored.
7	AVCS	AVCS video frame being processed by video circuits
8	CMD XMTR ON	Outgoing command signal above threshold of receiver in comparator
9	ALARM TIMER	Alarm signal activated (1-second pulse)
10	28-BIT TIME CODE	Real-time reference for CDA recording
11	CMD TONE A	Enable and command tone pair A selected

*Both present indicates ITOS

**In TOS mode, activates when AVCS receiver AGC reaches +1.5-volt level. In ITOS mode, activates when S-band receiver AGC reaches +1.5-volt level.

† Activates when APT receiver AGC reaches +1.5-volt level.

† † Activates when beacon receiver AGC reaches +1.5-volt level.

TABLE 5-III-4. EVENTS RECORDER CHANNEL ASSIGNMENTS (Continued)

Channel No.	Designation	Event Indicated
12	CMD TONE B	Enable and command tone pair B selected
13	ENABLE TONE	Enable tone being transmitted
14	FSK TONE	Command tone being transmitted
15	PTR MODE	Tape reader selected as the command data source
16	ACU MODE	Switch register on the command programmer ACU selected as the command data source
17	SAT ERROR	Error detected in comparison of command programmer output with verification signal from satellite
18	GRND ERROR	Error detected in comparison of programmer output with signal from CDA command transmitter
19	SPIN COUNT	Occurrence of command update pulse
20	XMT CMD	Command tone being modulated with data word

3. Attitude Recorders

The 2-channel attitude recorder (mounted in rack 47-A5) is a Brush Mark 280, high speed, paper chart recorder which provides simultaneous recording of two channels of analog data and a marker trace. The recorder channel assignments are indicated in Figure 5-III-6. The 28-bit time code is used as a real-time reference when the CDA station is recording. In playback, it indicates the time the data was recorded at the CDA station. The recorder is normally

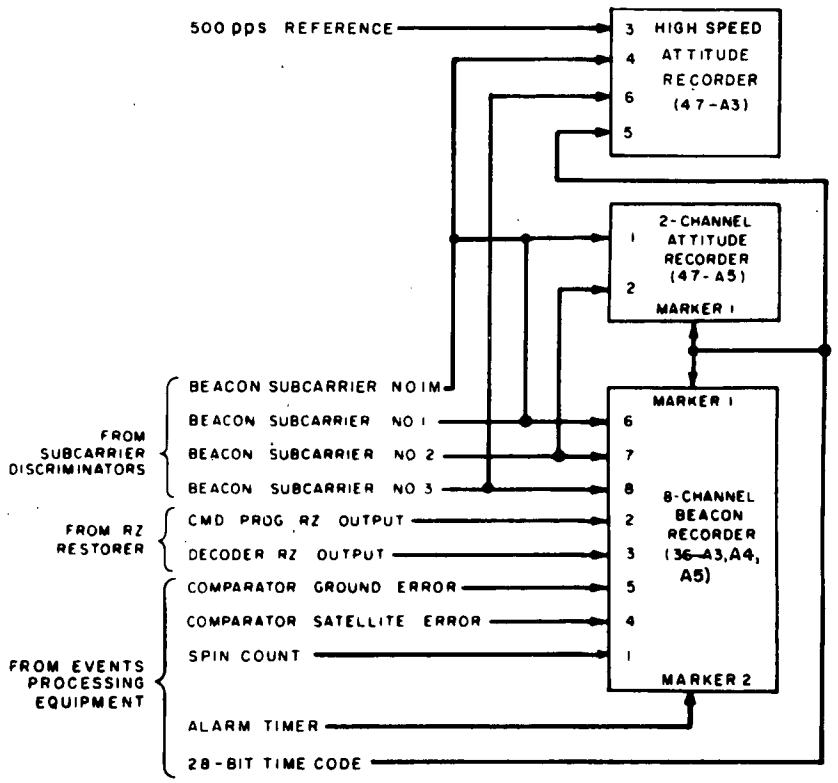

Figure 5-III-6. Beacon and Attitude Recorders, Block Diagram

operated at a chart speed of 50 millimeters per second and utilizes a pressurized fluid writing system with a true rectilinear presentation. Each recorder channel chart width is 8 millimeters (50 divisions) and trace width is 0.01 inch. The frequency response is as follows:

- 80-mm p-p deflection, 0 to 35 Hz,
- 40-mm p-p deflection, 0 to 60 Hz,
- 15-mm p-p deflection, 0 to 100 Hz, and
- 4-mm p-p deflection, 0 to 200 Hz.

The sensitivity is 25 millivolts full-scale, and linearity is 0.25 percent full-scale.

For a detailed description of the attitude recorder, refer to the appropriate instruction manual.

The high speed attitude recorder (mounted in rack 47-A3) is a Honeywell Model 1508 Visicorder, high speed, direct recording oscillograph. The recorder is equipped with 4 analog channels. The recorder channel assignments are indicated in Figure 5-III-6. It is normally operated at a speed of 20 inches per second and utilizes an ultraviolet light beam to record on sensitized paper.

For a detailed description of the high speed attitude recorder, refer to the appropriate instruction manual.

I. AC DISTRIBUTION AND BLOWER FAULT PROTECTION CIRCUITRY

The AC distribution and blower fault protection circuits in the four TOC equipment racks are identical (refer to Figure 5-III-7). Whenever AC power is supplied to the rack, the red POWER ON indicator lamp, located at the rear of the rack on the terminal blocks, will be lit. AC power is applied to the blower when the MAIN POWER circuit breaker is placed in the ON position. The air vane switch is initially closed and the red FAULT lamp lights and the buzzer sounds. The air vane switch associated with the rack blower remains closed until the blower reaches a speed which provides the necessary air flow to mechanically force the vane extension of the microswitch to the open position and to hold it there. The open state of the air vane switch causes the delay relay to deenergize which, in turn, causes the power relay to operate.

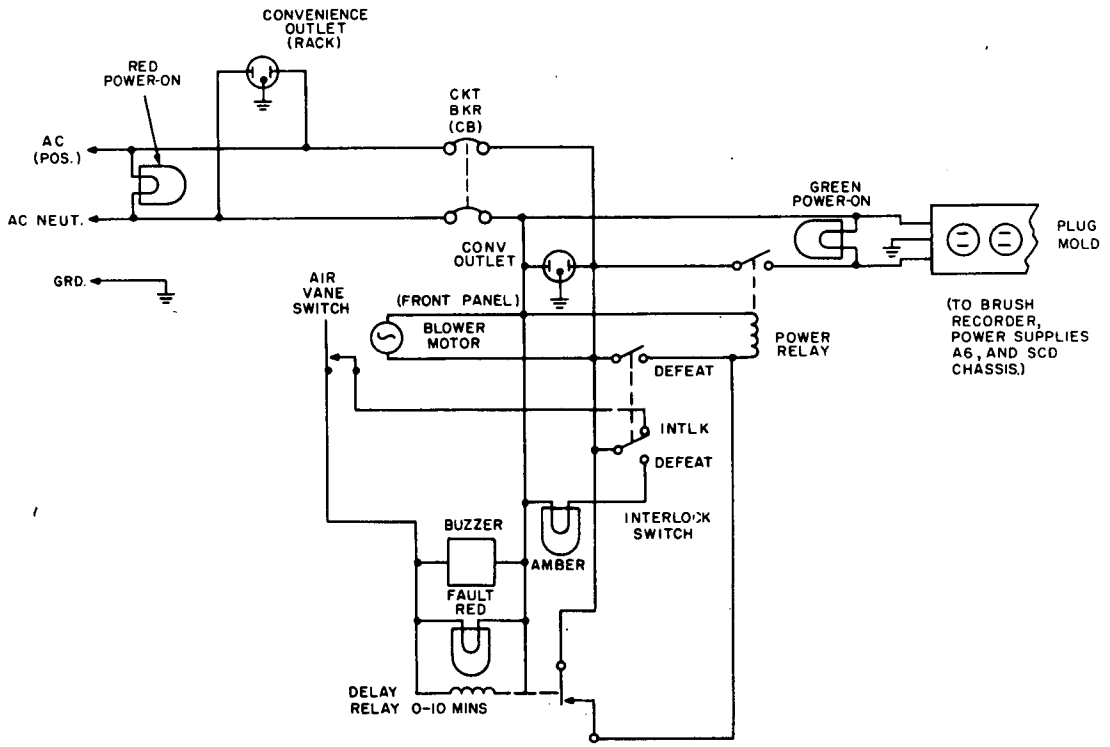

Figure 5-III-7. AC Distribution and Blower Fault Protection Circuits, Simplified Schematic Diagram

A reducation of approximately 50 percent of the rated blower output will cause the air vane switch to revert to its closed state, which after a delay determined by the delay relay will cause the power relay to drop out, shutting off power to all rack equipment.

During the normal power on state, the green POWER ON lamp on the front panel will be illuminated, and the convenience outlets at the front of the rack and at the front and rear on the bottom of the rack will be powered. An overload in the rack will cause the main power circuit breaker to shut off.

When the interlock switch is in the DEFEAT position the delay relay is bypassed, power is supplied to the rest of the rack, and the amber light is lighted.

SECTION IV

TOS EVALUATION CENTER AND TOS CHECKOUT CENTER

A. GENERAL

During the checkout and launch phases of the ITOS and TOS systems, centralized remote control of the CDA stations is performed by the TOS Evaluation Center and TOS Checkout Center (TEC/TCC), located at the Goddard Space Flight Center (GFSC), Suitland, Maryland. TEC/TCC is solely responsible for the pre-launch checkout, launch, and postlaunch checkout of the ITOS and TOS satellites. During these phases all TEC/TCC operations are monitored by the TOS Operations Center (TOC).

For two weeks preceding a scheduled ITOS or TOS launch, TEC/TCC is directed by the TOS Project office to perform simulated launch operations, and the entire ITOS/TOS ground system participates as scheduled by TOC. During these exercises, TEC/TCC generates and transmits simulated initial maneuver and checkout command programs to the CDA stations via TOC.

During launch and the initial maneuver, TEC/TCC generates satellite command programs and CDA station pass operating instructions for relay to the CDA station via TOC. TEC/TCC coordinates CDA station schedules with TOC during the initial maneuver phase.

The TEC/TCC station personnel using orbital and satellite attitude predictions supplied by the NASA T&DS Facility generate satellite command programs to obtain the data required to check out and determine the operational capabilities of the newly launched ITOS or TOS satellite. These command programs are transmitted to the CDA stations via TOC. CDA station personnel then set up the station equipment for transmitting the command program to the ITOS or TOS satellite when it comes into communication range of the CDA station. TEC/TCC monitors the CDA station transmission during the satellite pass to determine that the correct commands are transmitted by the CDA station and that the satellite interpreted the commands correctly (command verification).

During satellite checkout, beacon and events data is supplied to TEC/TCC by the CDA stations. This data is transmitted from the CDA stations to TEC/TCC over the microwave link either in real time (RT) or in playback (PB); the real-time playback (RTPB) contains all beacon data and also station time code events data.

When the manager of the NESC Operations Division and the ITOS or TOS project manager determine that the new satellite has been fully checked out and is operational, TOC assumes all control of the satellite operations.

In the event that the performance of a satellite degrades so that its operation capabilities are impaired and its operational life is doubtful, NESC may assign control of the satellite to TEC/TCC for evaluation. This aids in the establishment of data for improvement of future satellite systems.

B. RCA-SUPPLIED EQUIPMENT

The RCA-supplied portion of the TEC/TCC equipment is installed in five standard 72 by 24 by 24 inches equipment racks; all remaining racks, bays, and cabinets contain GFE equipment. Figure 5-IV-1 shows seven racks of equipment; the additional racks (second and third racks from the left) are: (1) the test and monitor rack and (2) the communications and patch bay rack. The complete rack complement and other equipment which make up the TEC/TCC complex are shown in the TEC/TCC equipment room arrangement diagram of Figure 5-IV-2.

The five RCA-supplied equipment racks are designated as follows:

- Secondary sensor subsystem data display rack (Mod 27),
- Telemetry rack, No. 47,
- Discriminator rack, No. 37,

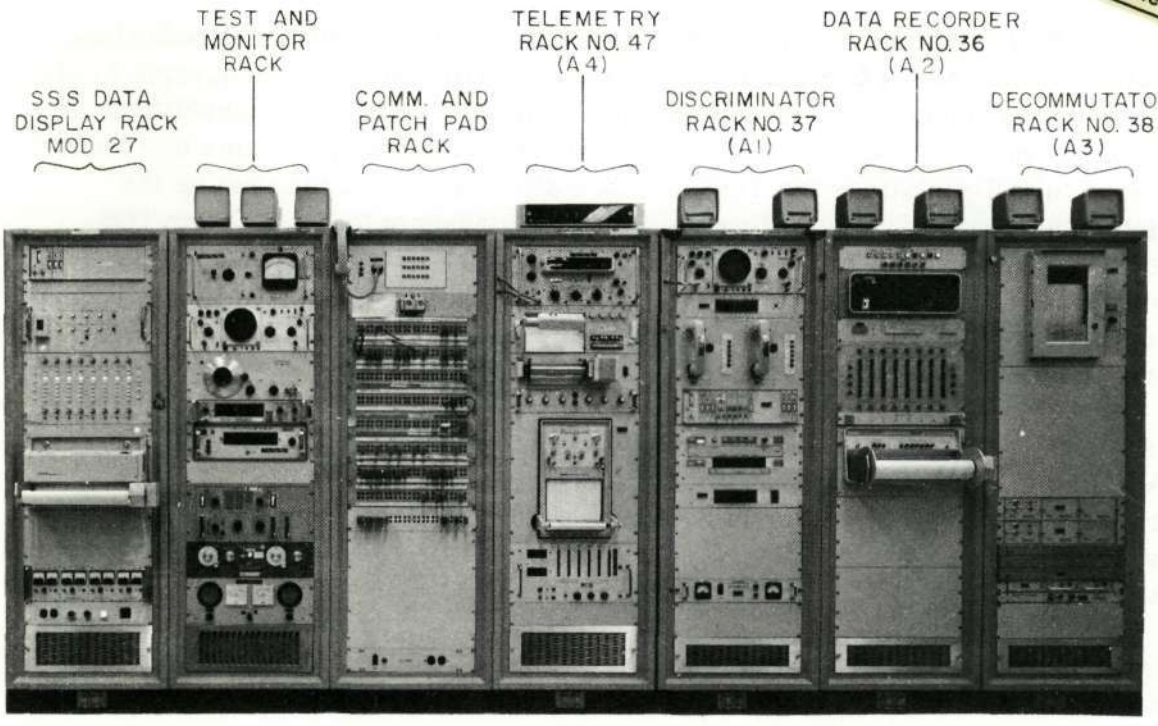

Figure 5-IV-1. TEC/TCC Station Equipment Racks, Front Panel Elevations

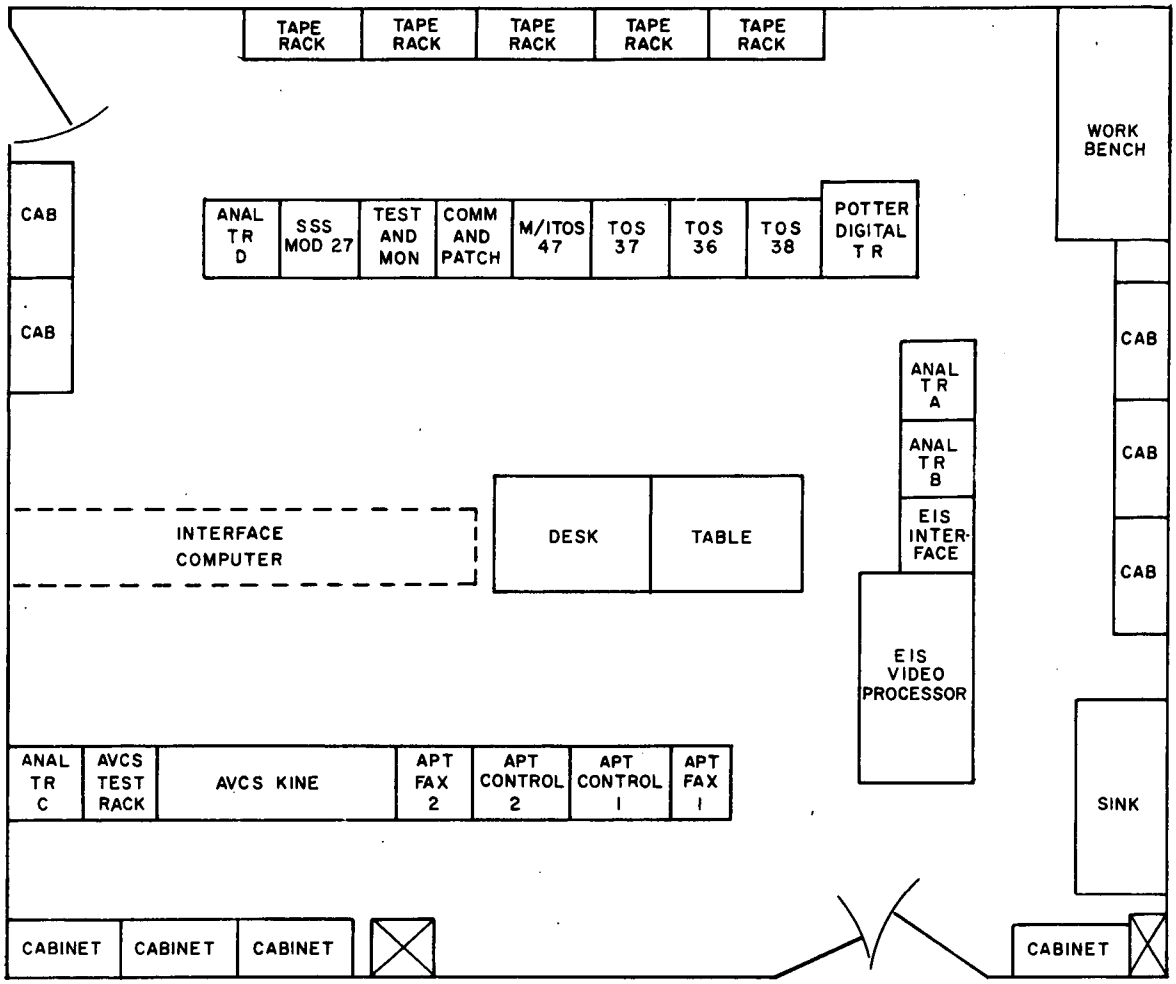

Figure 5-IV-2. TEC/TCC Station Equipment Arrangement Diagram

- Data recorder rack, No. 36, and
- Decommutator rack, No. 38

The primary function of the secondary sensor subsystem (SSS) data display rack (Mod 27) is to provide an 8-channel hard copy display of the data contained in the track 2 and track 3 frequency modulated IRIG 17B and IRIG 19B subcarriers. In addition to track 3 data, scanning radiometer signals are also demodulated in the subcarrier discriminator chassis. The rack contains the following assemblies (from top to bottom):

- A1: cabinet frame,
- A2: subcarrier discriminator chassis, EMR,
- A3: blank panel,
- A4: logic chassis,

- A5: Brush Mk 200 attenuator panel and driver amplifiers,
- A6: Brush Mk 200 8-channel recorder,
- A7: power supply chassis (blank panel),
- A8: power supply meter panel,
- A9: ac control panel, and
- A10: blower, McLean.

The primary function performed in telemetry rack 47 is to provide a hard copy record of the two ITOS beacon subcarriers. The rack contains the following assemblies (from top to bottom):

- A1: cabinet frame,
- A2: HP 523 C/D counter,
- A3: Honeywell 1508 Viscorder,
- A4: take up unit for Viscorder
- A5: galvanometer amplifiers for Visicorder
- A6: Brush Mk 280 2-channel recorder
- A7: Beckman preset counter
- A8: blank panel
- A9: blower, McLean

The discriminator rack (rack No. 37) contains the following assemblies (from top to bottom):

- A1: cabinet frame,
- A2: RM 504 oscilloscope, Tektronix,
- A3: oscilloscope input selector, RCA 1843145-503,
- A4: telephone panel,
- A5: subcarrier discriminator, EMR,
- A6: station control panel,
- A7: counter input selector, RCA 1843145-504,
- A8: blank panel,
- A9: power supply, Lambda Model 50-OBBM-1383-1,

- A10: blank panel, and
- A11: blower, McLean

The principal functions performed in the discriminator rack are (1) processing of the composite beacon subcarrier received over the microwave link into its components for recording on the chart recorders (racks 36, 38, and 47) and for display on the oscilloscope, (2) providing the composite beacon subcarrier as an input to the electronic counter unit, and (3) providing switching control of the TEC/TCC equipment.

The primary function performed in data recorder rack 36 is to provide an 8-channel hard copy of the ITOS/TOS beacon subcarrier, the command verification signals, and the satellite and ground error signals. The rack contains the following assemblies (from top to bottom):

- A1: cabinet frame,
- A2: TOS control,
- A3: Navcor A/D converter
- A4: digital control panel,
- A5: Brush Mk 200 attenuator and driver panel,
- A6: Brush Mk 200 8-channel recorder,
- A7: blank panel,
- A8: blank panel, and
- A9: blower, McLean.

The primary function performed in decommutator rack 38 is the demultiplexing and processing of the events data, the ground and satellite error data, the command verification signals, and the 28-bit timing code to make the data compatible for recording on the chart and events recorders and for display of the decoder and programmer RZ (events) data on the oscilloscope. The rack contains the following assemblies (from top to bottom):

- A1: cabinet frame,
- A2: 20-channel events recorder,
- A3: blank panel,
- A4 through A7: Quindar tone receivers, demultiplexing equipment, and relay panels,

- A8: Quindar power supply,
- A9: blank panel, and
- A10: blower, McLean.

C. MAJOR TEC/TCC SUBSYSTEMS

The TEC/TCC equipment consists of five major subsystems, as follows, and the blower fault protection circuits:

- Station switching control equipment,
- Beacon data processing equipment,
- Events processing equipment,
- Recording and display equipment, and
- Secondary sensor data display equipment.

The station switching control subsystem consists of the station switching control panel and relays located in rack 37. This subsystem controls the application of AC and DC power to all TEC/TCC racks and convenience outlets and also provides for the selection of the station input source (Wallops or Gilmore), the type of input (direct or playback), and the type of input signals (TOS or ITOS). The playback position is for the playback of beacon and events data available on analog recording tapes at TCC. Remote or local control of the recorders is provided by this subsystem. In the remote mode of control, turn-on of all recorders is accomplished by one switch on the station switching control panel provided the individual power switches have been turned on. In addition, the station switching control panel provides facilities for monitoring the status of the blowers in all five TEC/TCC racks, for providing aural and visual indications of blower faults, and for overriding blower faults. Front panel MAIN POWER ON and CONVENIENCE OUTLETS ON indications are provided by this subsystem.

The beacon data processing subsystem separates the composite beacon signal into its subcarriers and supplies the discriminated subcarriers to the proper recording and display (oscilloscope) equipment. This subsystem also supplies the composite beacon signal to the input selector for application to the electronic counter and to the input selector for display on the oscilloscope.

The events processing subsystem receives the FSK tones from the selected CDA station (via the microwave link) and processes the signals for application to the events and beacon data recorders to provide hard copy records and to the oscilloscope input selector for visual display on the oscilloscope.

The recording and display equipment provides hard copy records of the following: (1) the beacon data from the three beacon subcarriers, (2) the 19 channels of station events data, (3) the satellite and ground error indications, and (4) the command verification signals (decoder RZ signals and programmer RZ signals). This subsystem provides for visual displays of the three beacon subcarriers and the two RZ command verification signals (decoder and programmer). Provisions are also available for supplying the composite beacon data to the electronic counter.

The secondary sensor (data disply) subsystem contains three subcarrier discriminators (SCD's) which demodulate (1) the ITR track 2 clock and track 3 telemetry data and (2) the scanning radiometer signals for hard-copy display through the facility of the remote patch panel. The SCD's operate at center frequencies of 144 kHz, 160 kHz, and 45.6 kHz, corresponding to the frequency-modulated IRIG 17B and 19B subcarriers and the scanning radiometer subcarrier, respectively.

The demodulated output from the scanning radiometer subcarrier discriminator is routed directly to the remote patch panel for display on the high-speed recorder (Visicorder) in rack No. 47. The output data from the subcarrier discriminators for IRIG 17B and IRIG 19B subcarriers are routed through the rack internal logic chassis to the patch panel for display on the Brush chart recorder in the SSS data display rack along with the timing information. The output from each SCD is also routed to the bottom of the rack assembly where connections to the remote patch panel may be made for monitoring purposes, such as to an oscilloscope. Data test points and front panel frame sync error and system clock error indicators are also provided in the SSS data display rack.

The blower fault protection subsystem provides visual and aural indications of blower faults in any of the five TEC/TCC racks. This subsystem provides for overriding a fault indication in case of an emergency.

D. OVERALL FUNCTIONAL DESCRIPTION

Figure 5-IV-3 is an overall functional system block diagram of the TEC/TCC equipment, and comprises the following:

- Beacon data and CDA (events) data chains (real time and tape-recorded playback)
- Secondary sensor and scanning radiometer system equipment,
- AVCS kinescope system equipment,
- APT facsimile system equipment,

- Electronics image system (EIS) video display system equipment, and
- Test and monitor rack equipment.

The detailed functional block diagram for the beacon and events data chains is shown in Figure 5-IV-4.

As shown in Figure 5-IV-4, the TEC/TCC is composed primarily of two information processing and recording chains; i.e., the beacon data chain and the CDA station (events) data chain. The beacon data chain consists of a telemetry calibrator, four subcarrier discriminators, a 2-channel attitude recorder, a high-speed attitude recorder, and 3 channels of an 8-channel attitude recorder. The CDA station data chain consists of a FSK tone receiving and demultiplexing device, a switching unit, an RZ (return-to-zero) restorer, an events recorder, and 5 channels of an 8-channel beacon recorder.

The input to TEC/TCC from the microwave link equipment consists of (1) multiplexed beacon signals containing 2.3, 3.0, and 3.9 kHz and (2) multiplexed CDA station signals containing 1.3 and 2.4 kHz FSK tones. Signals are selected from either the Wallops or Gilmore CDA stations and may be real-time (RT) data directly from the CDA station or tape-recorded (TR) playback (PB) data from a tape recorder. The station switching control panel provides facilities for switching the TEC/TCC equipment on the proper line to receive the signal present at any given time, and the following TEC/TCC inputs are provided:

- Real-time beacon and events data from the Wallops station,
- Tape-recorded beacon and events data from the Wallops station,
- Real-time beacon and events data from the Gilmore station, and
- Tape-recorded beacon and events data from the Gilmore station.

The station switching control panel also provides the facilities for either automatically or manually switching the equipment into the TOS or ITOS mode.

As shown in Figure 5-IV-4, the selected composite beacon data is applied to impedance matching transformer T1. The composite beacon output from transformer T1 is coupled, through switching the ITOS/TOS select relays, to the common input of either three TOS subcarrier discriminators (SCD's), operating at center frequencies of 2.3, 3.0, and 3.9 kHz (beacon channels 1, 2, and 3, respectively) or two ITOS subcarrier discriminators that operate

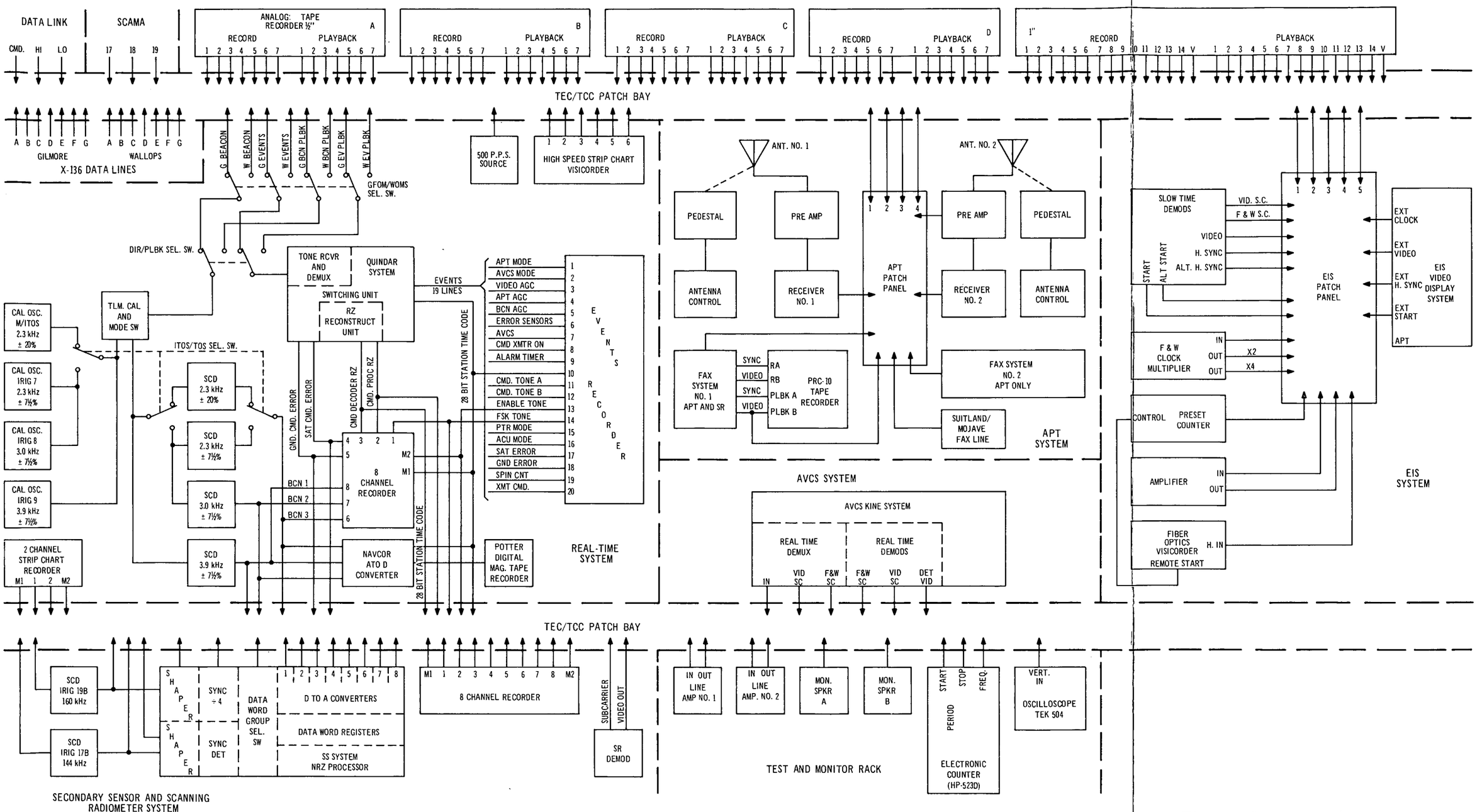

Figure 5-IV-3. TEC/TCC Station Overall System, Functional Block Diagram

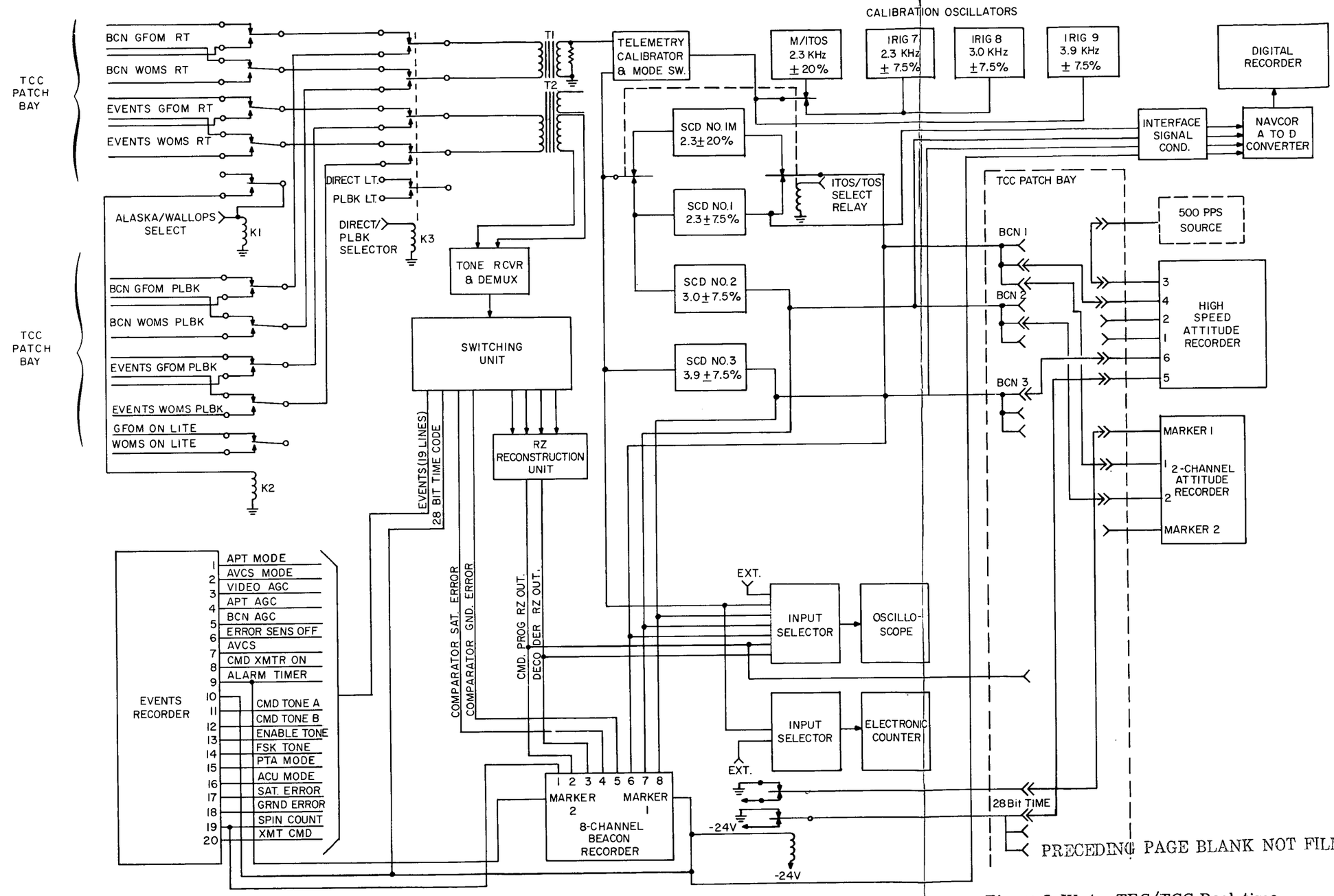

Figure 5-IV-4. TEC/TCC Real-time Beacon and Events Data Recorders, Functional Block Diagram

at center frequencies of 2.3 and 3.9 kHz (beacon channels 1M and 3). The 3.9-kHz SCD is used for both TOS and ITOS. The individual SCD's demultiplex the composite beacon signal by accepting only the band of frequencies ±7.5 percent about the respective center frequencies for both channels 1, 2, and 3 and ±20 percent for beacon channel 1M. Each SCD demodulates the associated FM subcarrier for recording on the 2-channel (beacon) recorder (beacon channels 1 and 2 only), and on the 8-channel (attitude) recorder (all three beacon channels). The outputs from the three SCD's are also applied to the oscilloscope input selector to provide a visual display on the oscilloscope. The composite beacon subcarrier from the secondary of the transformer T1 is also supplied to the input selector for application to the electronic counter.

The selected CDA events data signals are applied to impedance matching transformer T2 (see Figure 5-IV-4). (An auxiliary output from T2 is also routed to NESC.) The output from the transformer (composite 1.3- and 2.4-kHz FSK tones) is applied to the demultiplexing equipment, which recovers the events data from the two tones and supplies this data on separate lines through the switching unit to the RZ restorer, the events recorder, and the 8-channel recorder. The programmer and decoder NRZ "1's" and "0's" recovered from the FSK tones are converted to RZ signals in the RZ restorer. The decoder and programmer RZ outputs from the RZ restorer are supplied to the 8-channel recorder and to the oscilloscope input selector for presentation on the oscilloscope.

E. STATION SWITCHING CONTROL EQUIPMENT

The station switching control equipment consists of the station switching control panel, assembly A6 in discriminator rack No. 37, relays 37-K1, 37-K2, and 37-K3 located in the bottom rear of the rack, and the -24-volt DC power supply (assembly 37-A9). Refer to Figure 5-III-4 for additional detail.*

The station switching control circuitry controls the AC power to the five TEC/TCC racks, provides for CDA station selection of the data to be processed by the TEC/TCC equipment, and the mode of operation (direct or playback and TOS or ITOS). This circuitry also provides for local or remote control of the TEC/TCC recorders.

Blower status is indicated on the control panel and faults may be overriden in emergency cases. Indicators on this panel also provide visual indication of all functions controlled. In addition to the visual indications, a buzzer is energized when a blower fault occurs.

*To avoid duplication the illustrations appearing in Section III of this report are not repeated in this section.

F. BEACON DATA PROCESSING EQUIPMENT

The beacon processing equipment provides for demultiplexing and processing of the beacon transmissions from the selected CDA to convert this data into the proper format for application to the recording equipment and to the oscilloscope. The composite beacon signal is applied through an impedance matching transformer to the beacon processing equipment in the TEC/TCC. The composite beacon subcarrier signal consists of three subcarriers on standard IRIG channels: 7 (2.3 kHz), 8 (3.0 kHz), and 9 (3.9 kHz) for TOS, and IRIG channel 9 (3.9 kHz) and a nonstandard IRIG 2.3-kHz channel for ITOS.

The utilization of these three subcarriers for TOS/APT, TOS/AVCS, and ITOS satellites is given in Tables 5-IV-1, 5-IV-2, and 5-IV-3, respectively.

The beacon processing equipment employs three subcarrier discriminators for TOS and two subcarrier discriminators for ITOS that separate and restore the beacon data from each FM subcarrier. The restored TOS data is routed to the 2-channel (attitude) recorder and the 8-channel (beacon) recorder for direct readout. ITOS data is routed to the high speed (attitude) recorder and the 8-channel (beacon) recorder for direct readout. A telemetry calibrator, consisting of a sequencing unit and four calibration oscillators, provides a means for calibrating the discriminator recorder operation.

The real-time TOS composite beacon subcarrier from the microwave link equipment, or from the Mincom recorders via the impedance matching transformer, is applied through switching in the telemetry calibrator and mode switch unit to the common input of three SCD's operating at center frequencies of 2.3, 3.0, and 3.9 kHz (beacon channels 1, 2, and 3, respectively). (See Figure 5-IV-4). The three SCD's collectively perform the discrimination operation by accepting only the band of frequencies associated with their particular channel (i.e., deviations of ±7.5 percent about the center frequency) and rejecting all others. Each SCD individually demodulates the associated FM subcarrier, and presents the resulting data as varying DC voltages over a range from -10 volts DC (upper band edge) to +10 volts DC (lower band edge).

The disposition of the data from each of the SCD's is:

- SCD No. 1 (2.3 kHz): The output from SCD No. 1, which represents the horizon crossing information from channel 2 of the V-head attitude sensor in the spacecraft, is fed to channel 1 of the 2-channel attitude recorder, to channel 4 of the high-speed attitude recorder, to channel 6 of the 8-channel beacon recorder, to the oscilloscope input selector, and to the digital recorder via the NAVCOR converter.

TABLE 5-IV-1. BEACON SUBCARRIER UTILIZATION, TOS/APT

Beacon Subcarrier	Data Content	Time of Transmission
No. 1 (2.3-kHz center frequency, ±7.5 percent deviation) (IRIG Channel 7)	Up-looking V-head attitude sensor data	Continuously transmitted.
	Booster separation indication (by a return to center frequency)	Only during satellite launch phase.
No. 2 (3.0-kHz center frequency, ±7.5 percent deviation) (IRIG Channel 8)	Down-looking V-head attitude sensor data and horizon crossing data from horizon crossing indicator No. 1	Continuously transmitted. The two signals time-share this channel because of sensor location on the spacecraft.
No. 3 (3.9-kHz center frequency, ±7.5 percent deviation) (IRIG Channel 9)	Horizon crossing indicator data	Continuously transmitted, unless other data is present.
	Command verification data	Present whenever commands are being transmitted to satellite.
	Housekeeping telemetry data	On command (immediately following verification).
	Solar aspect indicator data	On command (immediately following verification).
	APT camera "prepare" and "expose" markers	Just prior to APT picture transmission.
	MASC coil polarity switching indications	Whenever MASC system is activated.

TABLE 5-IV-2. BEACON SUBCARRIER UTILIZATION, TOS/AVCS

Beacon Subcarrier	Data Content	Time and Transmission
No. 1 (2.3-kHz center frequency, ±7.5 percent deviation) (IRIG Channel 7)	Up-looking V-head attitude sensor data	Continuously transmitted.
	Booster separation indication (by a return to center frequency)	Only during satellite launch phase.
No. 2 (3.0-kHz center frequency, ±7.5 percent deviation) (IRIG Channel 8)	Down-looking V-head attitude sensor data and horizon crossing data from horizon crossing indicator No. 1	Continuously transmitted. The two signals time-share this channel because of the sensor location on the spacecraft.
No. 3 (3.9-kHz center frequency, ±7.5 percent deviation) (IRIG Channel 9)	Horizon crossing indicator data	Continuously transmitted unless other data is present.
	Command verification data	Present whenever commands are being transmitted to satellite.
	Housekeeping telemetry data and picture time code	On command (after verification) and during transmission of each AVCS picture. The picture time code occurs during the first 1.2 seconds of the command telemetry readout. (When real-time pictures are received, the time code indicates real-time; when pictures are played back from the satellite recorder, the time code indicates time of picture taking)
	Solar aspect indicator data	On command (immediately following verification)
	MASC coil polarity switching indications	Whenever MASC system is activated.

- SCD No. 2 (3.0 kHz): The output of SCD No. 2, which contains the composite of horizon crossing information from channel 1 of the V-head attitude sensor and from the No. 1 horizon crossing indicator, is applied to channel 2 of the attitude recorder, to channel 7 of the beacon recorder, to the oscilloscope input selector, and to the digital recorder via the NAVCOR converter.

- SCD No. 3 (3.9 kHz): The output of SCD No. 3, which contains the switched telemetry data from the spacecraft (see Table 5-IV-1 and 5-IV-2) is applied to channel 8 of the beacon recorder, channel 6 of the high-speed recorder, to the oscilloscope input selector, and to the digital recorder via the NAVCOR converter.

TABLE 5-IV-3. BEACON SUBCARRIER UTILIZATION, ITOS

Subcarrier	Data Content	Time of Transmission
No. 1M (2.3-kHz center frequency, ±20-percent deviation) (IRIG Channel 7 special)	Roll sensor 1 or 2	Normally continuous during operational mode.
	Time code	Upon command
	Roll sensor and pitch index	Upon command
	Pitch sensor 1 or 2	Upon command
No. 3 (3.9-kHz center frequency, ±7.5 percent deviation) (IRIG Channel 9)	Solar proton monitor data	Normally continuous during operational mode
	Digital solar aspect data	Normally continuous during acquisition mode (inital condition)
	Telemetry commutated data	Upon command
	Data verification	During command operations

The real-time ITOS composite beacon subcarrier is processed in a manner similar to the TOS composite beacon subcarrier, with the exception that there are only two beacon subcarrier channels with center frequencies of 2.3 and 3.9 kHz (beacon channels 1M and 3). SCD No. 3 is used for both TOS and ITOS and accepts deviations of ±7.5 percent about the center frequency, while SCD No. 1M accepts deviations of ±20 percent about the center frequency. The disposition of the data from these SCD's is as follows:

- SCD No. 1M (2.3 kHz): The output from SCD No. 1M, which contains the attitude information, is fed to channel 4 of the high-speed attitude recorder, to channel 1 of the 2-channel attitude recorder, channel 6 of the beacon recorder, and to the oscilloscope input selector.

- SCD No. 3 (3.9 kHz): The output of SCD No. 3, which contains the switched telemetry data from the spacecraft (see Table 5-IV-3) is applied to channel 8 of the beacon recorder, to channel 6 of the high-speed attitude recorder, to the oscilloscope input selector, and to the digital recorder via the NAVCOR converter.

In addition, the telemetry calibrator output is applied to the electronic counter input selector.

The beacon processing equipment incorporates a built-in telemetry calibration system that provides for checking and calibrating all units of the system and all units driven by the system. The telemetry calibrator can be operated in either the data mode or the calibration mode. When the telemetry calibrator is operated in the data mode, the composite beacon subcarrier input is routed directly through the sequencer to the discriminators and other equipment, as described. When the calibration sequencer is operated in the calibration mode, the data line is broken, and a calibration signal produced by four calibration oscillators operating at 2.3, 3.0, and 3.9 kHz, as well as one for the special 2.3-kHz discriminator corresponding to the channels used by the beacon subcarriers is supplied to the discriminators.

Each oscillator produces five crystal-controlled frequencies for calibration of a particular channel at five points in the passband of the corresponding discriminator. Any of the five calibration points can be selected for a channel independently of the deviations selected for the other two channels, and any channel can also be turned off independently. Three modes of automatic calibration routines are also available.

G. EVENTS PROCESSING EQUIPMENT

The events processing equipment demultiplexes and processes the events FSK tones from the selected CDA station to convert them into the proper format for application to the recording equipment and to the oscilloscope.

The events processing equipment consists basically of two data processing chains, the 2.4-kHz data chain and the 1.3-kHz data chain, comprising the following items:

2.4-kHz Data Chain	1.3-kHz Data Chain
• 2.4-kHz tone receiver	• 1.3-kHz tone receiver
• Scanner receiver	• Scanner receiver
• Receive register (8-channel)	• Two receive registers (total of 16 outputs)
• Relay panel (8-channel)	• Two relay panels (total of 16 outputs)

The events processing equipment also contains an RZ restorer unit. This unit converts the decoder and programmer "1's" and "0's" outputs from the 2.4-kHz data chain from NRZ to RZ signals before they are applied to the recording equipment and to the oscilloscope. A block diagram of the events processing equipment is shown in Figure 5-III-5.

H. RECORDING EQUIPMENT

1. Events Recorder

The events recorder (mounted in rack 38-A2) is an Esterline-Angus Model A620T paper chart recorder that provides for simultaneous recording of 20 independent channels of slow speed, ON-OFF information. The events recorder, normally operated at a chart speed of 3 inches per minute, is used to record significant CDA station operations that have been transmitted via microwave link and to provide a hard copy recorded of these and certain critical programming events. Chart speed, controlled by a synchronous motor and a gear train, is selectable in 10 steps. The writing elements are electrically heated styluses which record on chart paper sensitive to both heat and pressure. The events recorder is capable of both manual and remote operation.

The events recorder (1) records the programming events involved in transmitting commands to the satellite from either Programmer A or Programmer B in the CDA programming equipment, (2) indicates detection of a satellite or ground station error, and (3) monitors the diversity combined components of both video receiver AGC circuits and the beacon receiver AGC circuits to determine the start of data reception. Other events recorded by the unit include indication of the processing of an AVCS video frame, and the type of satellite (TOS AVCS, TOS APT, or ITOS) the station is set up to interrogate. Refer to Table 5-IV-4 for a description of the events recorded and their recorder channel assignments.

When the RECORDER REMOTE-LOCAL switch on the the station switching control panel is in the LOCAL position, power to the events recorder is controlled by an alternate action ON-OFF switch on the recorder front panel. If the REMOTE-LOCAL switch position is in REMOTE and the alternate action ON-OFF switch on the recorder panel is ON, power to the events recorder is controlled by the RECORDER ON-OFF switch on the station switching control panel.

For detailed information on the Easterline-Angus A620-T events recorder, refer to the appropriate instruction manual.

2. Beacon Data Recorder

The 8-channel beacon data recorder (mounted in rack 36-A5, and A6 is a Brush Model Mark 200, high speed, paper chart recorder which provides simultaneous recording of 8 channels of analog data. The recorder channel assignments are indicated in Figure 5-III-6.

The recorder is normally operated at a chart speed of 20 millimeters per second, and utilizes a pressurized fluid writing system with rectilinear presentation. Each recorder channel chart width is 40 millimeters (50 divisions) and trace width is 0.01 inch. The frequency response is as follows:

- 50-mm p-p deflection, 0 to 55 Hz,
- 40-mm p-p deflection, 0 to 60 Hz,
- 15-mm p-p deflection, 0 to 100 Hz, and
- 4-mm p-p deflection, 0 to 200 Hz.

For a detailed description of the beacon data recorder, refer to the appropriate instruction manual.

TABLE 5-IV-4. EVENTS RECORDER CHANNEL ASSIGNMENTS

Channel No.	Designation	Event Indicated
1	APT MODE	Station set up for TOS/APT satellite interrogation*
2	AVCS MODE	Station set up for TOS/AVCS satellite interrogation*
3	VIDEO AGC	Start of video reception**
4	APT AGC	Start of APT video reception †
5	BCN AGC	Start of beacon reception ††
6	ERROR SENS OFF	Activities when satellite error verification from comparator ignored
7	AVCS	AVCS video frame being processed by video circuits
8	CMD XMTR ON	Outgoing command signal above threshold of receiver in comparator
9	ALARM TIMER	Alarm signal activated (1-second pulse)
10	28-BIT TIME CODE	Real-time reference for CDA recording
11	CMD TONE A	Enable and command tone pair A selected
12	CMD TONE B	Enable and command tone pair B selected
13	ENABLE TONE	Enable tone being transmitted

* Both present indicates ITOS

** In TOS mode, activates when AVCS receiver AGC reaches +1.5-volt level. In ITOS mode, activates when S-band receiver AGC reaches +1.5-volt level.

† Activates when APT receiver AGC reaches +1.5-volt level.

†† Activates when beacon receiver AGC reaches +1.5-volt level.

TABLE 5-IV-4. EVENTS RECORDER CHANNEL ASSIGNMENTS (continued)

Channel No.	Designation	Event Indicated
14	FSK TONE	Command tone being transmitted
15	PTR MODE	Tape reader selected as the command data source
16	ACU MODE	Switch register on the command programmer ACU selected as the command data source
17	SAT ERROR	Error detected in comparison of command programmer output with verification signal from satellite
18	GRND ERROR	Error detected in comparison of programmer output with signal from CDA command transmitter
19	SPIN COUNT	Occurrence of command update pulse
20	XMT CMD	Command tone being modulated with data word

3. Attitude Recorder

The 2-channel attitude recorder (mounted in rack 47-A6) is a Brush Mark 280, high speed, paper chart recorder which provides simultaneous recording of two channels of analog data and a marker trace. The recorder channel assignments are indicated in Figure 5-III-6. The 28-bit time code is used as real-time reference when the CDA station is recording; in playback, it indicates the time the data was recorded at the CDA station is recording; in playback, it indicates the time the data was recorded at the CDA station. The recorder is normally operated at a chart speed of 20 millimeters per second, and utilizes a pressurized fluid writing system with rectilinear presentation. Each channel chart width is 8 millimeters (50 divisions) and trace width is 0.01 inch. The frequency response is as follows:

- 80-mm p-p deflection 0 to 35 Hz,
- 40-mm p-p deflection, 0 to 60 Hz,

- 15-mm p-p deflection, 0 to 100 Hz, and
- 4-mm p-p deflection, 0 to 200 Hz.

The sensitivity is 25 millivolts full-scale, and linearity is 0.25 percent full scale.

For a detailed description of the attitude recorder, refer to the appropriate instruction manual.

The high speed attitude recorder (mounted in rack 47-A3, A4, and A5) is a Honeywell Model 1508 Visicorder, high speed, direct recording oscillograph. The recorder is equipped with 4 analog channels. The recorder channel assignments are indicated in Figure 5-III-6. It is normally operated at a chart speed of 20 inches per second and utilizes ultraviolet light beam to record on sensitized paper.

For a detailed description of the high speed attitude recorder, refer to the appropriate instruction manual.

I. SECONDARY SENSOR SUBSYSTEM DATA DISPLAY EQUIPMENT

The secondary sensor subsystem (SSS) data display rack (Mod 27) equipment provides for demodulating and processing of (1) the spacecraft ITR track 2 clock and track 3 telemetry data and (2) the scanning radiometer data, and converting this data into the proper format for hard copy display on the high-speed Brush Model 200 paper chart recorder in the SSS data display rack and on the high-speed, four-channel Visicorder in rack No. 47, respectively. The composite ITR subcarrier signal consists of two added audio subcarriers, one for IRIG channel 17B (144 kHz) and the other for IRIG channel 19B (160 kHz). The composite scanning radiometer signal contains an audio subcarrier with center frequency of 45.6 kHz. The demodulator portion of the SSS data display equipment contains three subcarrier discriminators that separate and restore the display data from each FM subcarrier. The demodulated scanning radiometer data is routed to the four-channel Visicorder via the remote patch panel for direct readout. The track 3 demodulated data along with the spacecraft ITR track 2 clock signal is routed through the SSS rack logic chassis to the patch panel and back to the Brush chart recorder in the SSS data display rack.

The ITR track 3 data composition comprises 60-word data frames; each data frame contains 8 blocks of data, each block containing 8 data words, and each data word containing 8 bits. The bit rate is 2000 ±300 bits per second. The content of the 60-word data frame is detailed in Table 5-IV-5. A block diagram of the equipment is shown in Figure 5-IV-5.

TABLE 5-IV-5. ITR TRACK 3 DATA FRAME CONTENT

Word No.	Telemetered Signal for Track 3 Data
1,2	Frame marker
3-6	Time code
7-21	Flat plate radiometer
22	Calibration data: code 95 = -3.73
23	Calibration data: code 64 = -2.52
24	Calibration data: code 32 = -1.27
25-27	Solar array current
28	Solar array voltage
29	Unregulated bus voltage
30	Battery pack No. 1 voltage
31	Battery pack No. 1 current
32	Battery pack No. 2 voltage
33	Battery pack No. 2 current
34	Power supply electronics temperature
35-37	Temperature of solar array panels
38-40	Temperature of shunt limiter dissipators
41	Command receiver no. 1 AGC voltage
42	Command receiver No. 2 AGC voltage
43-46	Active thermal controller, position of flaps

TABLE 5-IV-5. ITR TRACK 3 DATA FRAME CONTENT (Continued)

Word No.	Telemetered Signal for Track 3 Data
47	Active thermal controller reservoir No. 1 temperature
48	Active thermal controller reservoir No. 3 temperature
49	Thermal control fence temperature
50	Alzak reflector temperature
51	Command decoder No. 1 enable tone detector output
52	Command decoder No. 1 FSK tone detector output
53	Command decoder No. 2 enable tone detector output
54	Command decoder No. 2 FSK tone detector output
55	Pitch loop No. 1 or No. 2 gain switch state
56	Pitch loop No. 1 motor voltage
57	Pitch loop No. 2 motor voltage
58	Housekeeping telemetry commutator No. 1 output in manual operating mode
59	Housekeeping telemetry commutator No. 2 output in manual operating mode
60	Spare

J. AC DISTRIBUTION AND BLOWER FAULT PROTECTION CIRCUITRY

The AC distribution and blower fault protection circuits in the five TEC/TCC equipment racks are identical (refer to Figure 5-III-7).

Whenever AC power is supplied to the rack the red POWER ON indicator lamp, located at the rear of the rack on the terminal blocks, will be lit. AC power is applied to the blower when the MAIN POWER circuit breaker is placed in the ON position. The air vane switch is initially closed and the red FAULT lamp lights and the buzzer sounds. The air vane switch associated with the rack blower remains closed until the blower reaches a speed which provides the necessary air flow to mechanically force the vane extension of the micro-switch to the open position and to hold it there. The open state of the air vane switch causes the delay relay to deenerigz which, in turn, causes the power relay to operate.

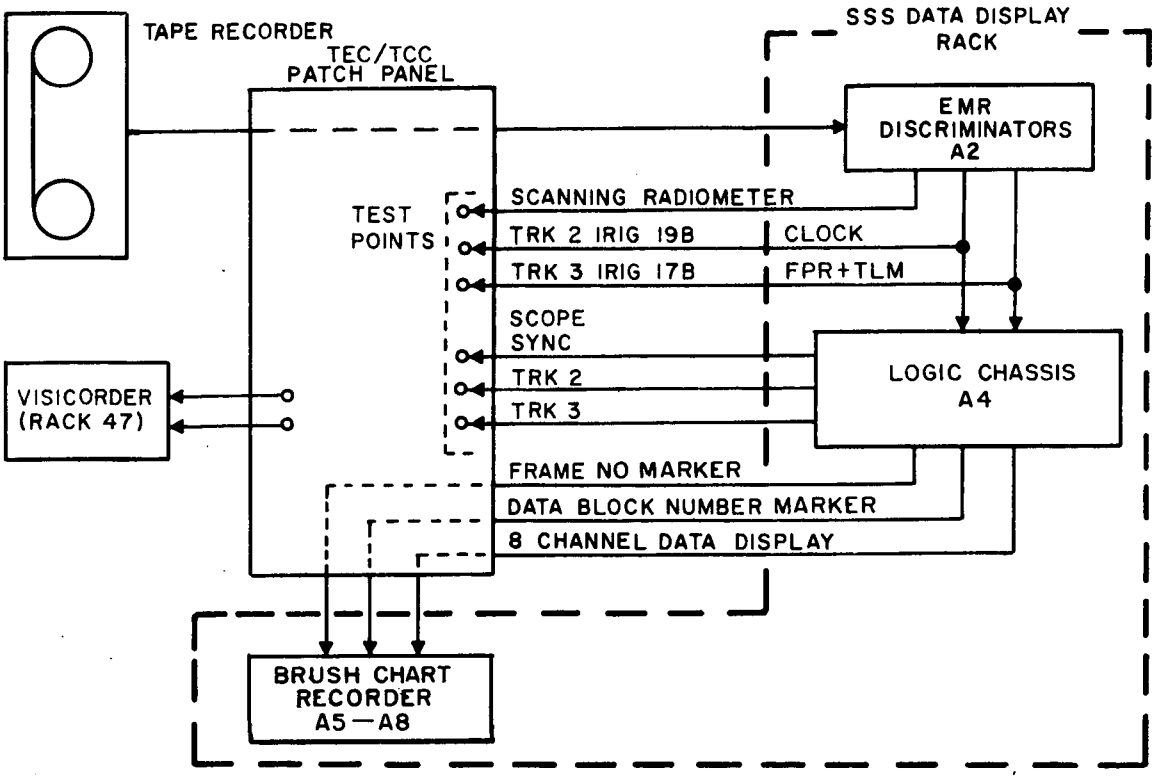

Figure 5-IV-5. Secondary Sensor Subsystem Data Display Signal Flow, Simplified Block Diagram

A reduction of approximately 50 percent of the rated blower output will cause the air vane switch to revert to its closed state, which after a delay determined by the delay relay will cause the power relay to drop out, shutting off AC power to all rack equipment.

During the normal power on state, the green POWER ON lamp on the front panel will be illuminated, and the convenience outlets at the front of the rack and at the front and rear on the bottom of the rack will be powered. An overload in the rack will cause the main power circuit breaker to shut off.

When the interlock switch is in the DEFEAT position the delay relay is bypassed, power is supplied to the rest of the rack, and the amber light is lighted.

SECTION V

SPACECRAFT CHECKOUT EQUIPMENT

A. GENERAL

The spacecraft checkout equipment includes the AED checkout facility (factory test set), the AED backup CDA ground station, and the go/no-go launch support van.

1. AED Checkout Equipment

The AED checkout facility and the AED ground station are each a complete set of ground-support equipment, which, with some additional facilities, permit the functioning of the spacecraft to be fully checked out. In addition to most of the facilities included in the CDA station, it was necessary to include equipment simulating the operation of the DAF station and facilities for the display of APT, SR, and secondary sensor information in the checkout stations. Since a failure in either of the AED stations would not be operationally catastrophic, it is not necessary to include the redundant features that are incorporated in the CDA stations.

The checkout stations include equipment for converting the transmitted signals from the spacecraft into the frequency bands and signal levels supplied to the CDA stations from RF equipment. Equipment for the reception of beacon data and APT/SR signals had been installed. An S-band receiver was added to convert the S-band signals into a multiplexed signal in the 10- to 480-Hz frequency, with an amplitude of 3 volts peak-to-peak across a 75-ohm load. Facilities are installed for transmitting command data to the spacecraft.

Changes which were made to the CDA stations at Gilmore Creek and Wallops Island were also made at the checkout stations. These changes include:

- An additional demultiplexer for the data on the S-band signal
- An additional discriminator and calibrator for the beacon wideband channel
- A modified station-control panel
- Modified beacon and video oscilloscope inputs

Table 5-V-1 lists the equipment in the modified backup CDA station (GSE-3) and Table 5-V-2 lists the factory test set equipment (GSE-6).

Facilities have been provided to demultiplex the composite secondary sensor subcarrier and subsequently demodulate the subcarriers into one clock and two data channels.

Circuits are provided to generate frame and word timing pulses for each of the data channels. These are used for oscilloscope trigger purposes so that, by use of the delayed sweep facility of the display oscilloscope, any word in a frame can be displayed.

A high-speed chart recorder is provided for the display of secondary sensor data. The synchronizing signals previously referred to as well as the clock channel data are displayed on the recorder.

2. Go/No-Go Launch Support Van

The go/no-go van includes the ground station equipment necessary to check out the spacecraft prior to launch. In addition to providing most of the facilities included in the CDA stations, it also includes equipment for simulating the operation of the DAF station and facilities for the display of the APT and SR information.

The changes described for the AED checkout stations also apply to the go/no-go van, with the following exceptions:

(1) A redundant S-band receiver is provided.

(2) The magnetic tape recorder facility has been expanded to its full 14-track capability. Table 5-V-3 lists the equipment in the go/no-go launch support van (GSE-5).

B. FUNCTIONAL DESCRIPTION OF GSE EQUIPMENT

1. Patching Equipment

Patching between the various units in the backup CDA station (GSE-3) and in the factory test set (GSE-6) is performed by the modified station control panel installed in each of these facilities. These panels are the same as those installed in the CDA stations at Gilmore Creek and Wallops Island.

TABLE 5-V-1. BACKUP CDA STATION (GSE-3) EQUIPMENT

Rack No.	Title	Unchanged	Modified	New
1, 2 and 3	Kinescope display assembly	x		
20-1	Magnetic tape recorder - AVCS	x		
20-2	Magnetic tape recorder - AVCS	x		
26	Power supply		Note 1	
27	Signal Processor		Note 2	
30	APT receiver		Note 3	
31	Chart recorder	x		
32	Beacon		Note 4	
33	Tape reader	x		
35	Command	x		
44	AVCS receiver		Note 5	
45	Beacon receiver	x		
20-3	Magnetic tape recorder - SR			Note 6
51	SR signal processor			Note 7

Note 1 - Modified station control panel

Note 2 - Modified oscilloscope input selector

Note 3 - Modified facsimile drive circuits

Note 4 - Modified oscilloscope input selector
Additional channel selector and demodulator
Additional calibration unit

Note 5 - S-band receiver added

Note 6 - Fourteen track capability, fitted with seven tracks of electronics; equalization for 60 ips only

Note 7 - SR signal processor contains demultiplexer, SR video processing circuits, data locator, high-speed chart recorder, and secondary sensor processor chassis

TABLE 5-V-2. FACTORY TEST SET (GSE-6) EQUIPMENT

Rack No.	Title	Unchanged	Modified	New
1, 2 and 3	Kinescope display assembly	x		
20-1	Magnetic tape recorder - AVCS	x		
26	Power supply		Note 1	
27	Signal processor		Note 2	
30	APT receiver		Note 3	
31	Chart recorder	x		
32	Beacon		Note 4	
33	Tape reader	x		
35	Command	x		
44	AVCS receiver		Note 5	
45	Beacon receiver	x		
51	SR signal processor			Note 6
20-2	Magnetic tape recorder - SR			Note 7

Note 1 - Modified station control panel

Note 2 - Modified oscilloscope input selector

Note 3 - Modified facsimile drive circuit

Note 4 - Modified oscilloscope input selector
Additional channel selector and demodulator
Additional calibration unit

Note 5 - S-band receiver added

Note 6 - SR signal processor contains demultiplexer, SR video processor, high-speed chart recorder, and secondary sensor processor chassis

Note 7 - Fourteen-track capability with seven tracks of electronics

TABLE 5-V-3. LAUNCH SUPPORT VAN (GSE-5) EQUIPMENT

Rack No.	Title	Unchanged	Modified
1, 2, and 3	Kinescope display assembly	x	
20	Magnetic tape recorder		Note 1
26	Power supply		Note 2
27	Signal processor		Note 3
30	APT receiver		Note 4
31	Chart recorder	x	
32	Beacon	x	Note 5
33	Tape recorder	x	
35	Command	x	
44	AVCS receivers		Note 6
45	Beacon receiver	x	
51	SR signal processor		Note 7

Note 1 - Modified to accept 14 signal inputs

Note 2 - Modified station control panel

Note 3 - Modified oscilloscope input selector

Note 4 - Modified facsimile drive circuits

Note 5 - Modified oscilloscope input selector

Additional channel selector and demodulator

Additional calibration unit

Note 6 - S-band receiver added. Second S-band receiver for redundancy.

Note 7 - SR signal processor contains demultiplexer, SR video processor, high-speed chart recorder, secondary sensor processor chassis, and S-band receiver.

Interconnection between the factory test set and the spacecraft while undergoing tests depends on the specific requirements for each test.

When the spacecraft is mounted on the launch vehicle communication is maintained to and from the launch support van (GSE-5) by an RF link. The spacecraft antennas are used to receive and transmit appropriate data. The antennas at the launch support area are mounted on a 420-foot tower, and are connected to the launch support van by RG-58 coaxial cables. Because of the orientation of the mounted spacecraft to the launch support area antennas, it is necessary to install intermediate RF links. The S-band antenna is fed into a horn antenna mounted on the launch tower. A coaxial cable connects the horn to a dish antenna which is aimed at the launch support area antenna.

Real-time transmission from the launch-mounted spacecraft is received on a whip antenna, amplified, and relayed to the support area by a yagi antenna. Command and beacon links are direct.

Power to charge the spacecraft batteries is supplied and controlled from the blockhouse. A battery charger, operated by RCA launch support personnel, is connected to the spacecraft via the second stage umbilical.

Sensor exciters are mounted on a frame attached to the spacecraft handling lugs. These exciters are powered and controlled by the launch stand test set. The following equipment is required at the spacecraft for launch checkout:

- Camera light. These are small boxes with lights mounted behind a piece of frosted glass. There is one box for each camera.
- Radiometer targets. These are heated metal plates mounted next to an unheated plate which simulates space temperature. There is one target for each radiometer.
- Digital solar aspect sensor (DSAS) light. This is a high intensity light mounted on a bracket in front of the DSAS.
- Pitch sensor/roll sensor target. This is a small heated plate that is manually placed in the sensor field of view while the momentum flywheel is running.
- Power enable box. This box mounts on the target support fixture. It is attached through cables to the spacecraft main enable plug and pitch loop enable plug. This box, on signals from the launch stand test set, controls the spacecraft power system and pitch loop motors.
- Launch stand test set. This is a suitcase size unit which mates through appropriate cables to the power enable box and the target support fixture. It controls and monitors the

spacecraft power system, the pitch loop motors and the various targets. It derives its power from commercial 120 volts AC on the launch stand.

- Solar proton monitor source. This is a weak radioisotope supplied and under direct control of Applied Physics Lab personnel. It is used for a final checkout of the SPM experiment.
- Varian 620i computer. Used to reduce housekeeping, telemetry, secondary sensor telemetry, and FPR and SPM data.

2. APT Receiving and Processing Equipment

The APT receiving and processing equipments in the CDA backup station at AED are standard Mufax and Fairchild APT ground station units.

The factory test set equipment and the launch support van contain no provisions for transmission of the recorded data.

Processing of APT data consists of recording the signal on the Mincom tape recorder and display of the video information on the facsimile recorder.

3. AVCS Receiving and Processing Equipment

AVCS data received at each of the spacecraft checkout centers is processed in the same manner as in the CDA stations.

4. SR Receiving and Processing Equipment

SR data is received and processed at the spacecraft checkout equipment in the same manner as in the CDA stations. Additional magnetic tape recorders have been added to the CDA backup station and the factory test set equipments. Electronics has been added to the recorder in the launch support van to utilize the previously unused seven channels for recording of SR data.

5. Secondary Sensor Receiving and Processing Equipment

Secondary sensor data is demodulated from the S-band composite signal and recorded on magnetic and chart recorders in the same manner as in the CDA stations. A redundant S-band receiver is provided in the launch support van.

6. Beacon Receiving and Processing Equipment

The beacon carrier is received by the support stations and modulated with the composite beacon subcarrier. The composite subcarrier is recorded on a magnetic recorder. The subcarrier discriminators separate the two channels of data for recording on a chart recorder. No processing of the signal for transmission is performed at these stations.

7. Command Support Console

The spacecraft checkout stations include facilities to transmit commands to the spacecraft. These commands can be derived from prepunched tape or they can be manually set up on the control panel in the station. Programming is identical to the CDA stations. Transmitters are installed as part of each equipment complex.

8. Spacecraft Support Console

The spacecraft support console is used to conduct tests on the spacecraft during the construction and prelaunch preparation phases. In conjunction with the SEPET test fixture, the console performs collimation and calibration of the spacecraft sensors. It is also used to monitor test points in the spacecraft.

The support console is used with the factory test set at AED. It is shipped to the WTR as part of the launch support equipment to check out the spacecraft prior to installation on the launch vehicle.

When the spacecraft is mounted on the launch vehicle, the launch checkout test set and on-stand checkout equipment are used to perform some of the functions of the spacecraft support console and SEPET.

The support console contains provision for battery charging and spacecraft power supply during testing operations. An oscilloscope, test data readout instruments, and a chart recorder are included in the console. The SEPET test fixture controls are also part of the console. Figure 5-V-1 shows the spacecraft support console.

9. Varian 620i Computer

This computer is used in GSE No. 4, 5, and 6. It performs data reduction on the satellite housekeeping telemetry, secondary sensor telemetry and the FPR

and SPM data. The program is controlled via an ASR-33 teletype. Output of the computer is on a 20-line per second, 16-characters per line printer. The 620i is rack mounted along with an RCA-designed interface drawer, which interfaces between the external inputs and the computer.

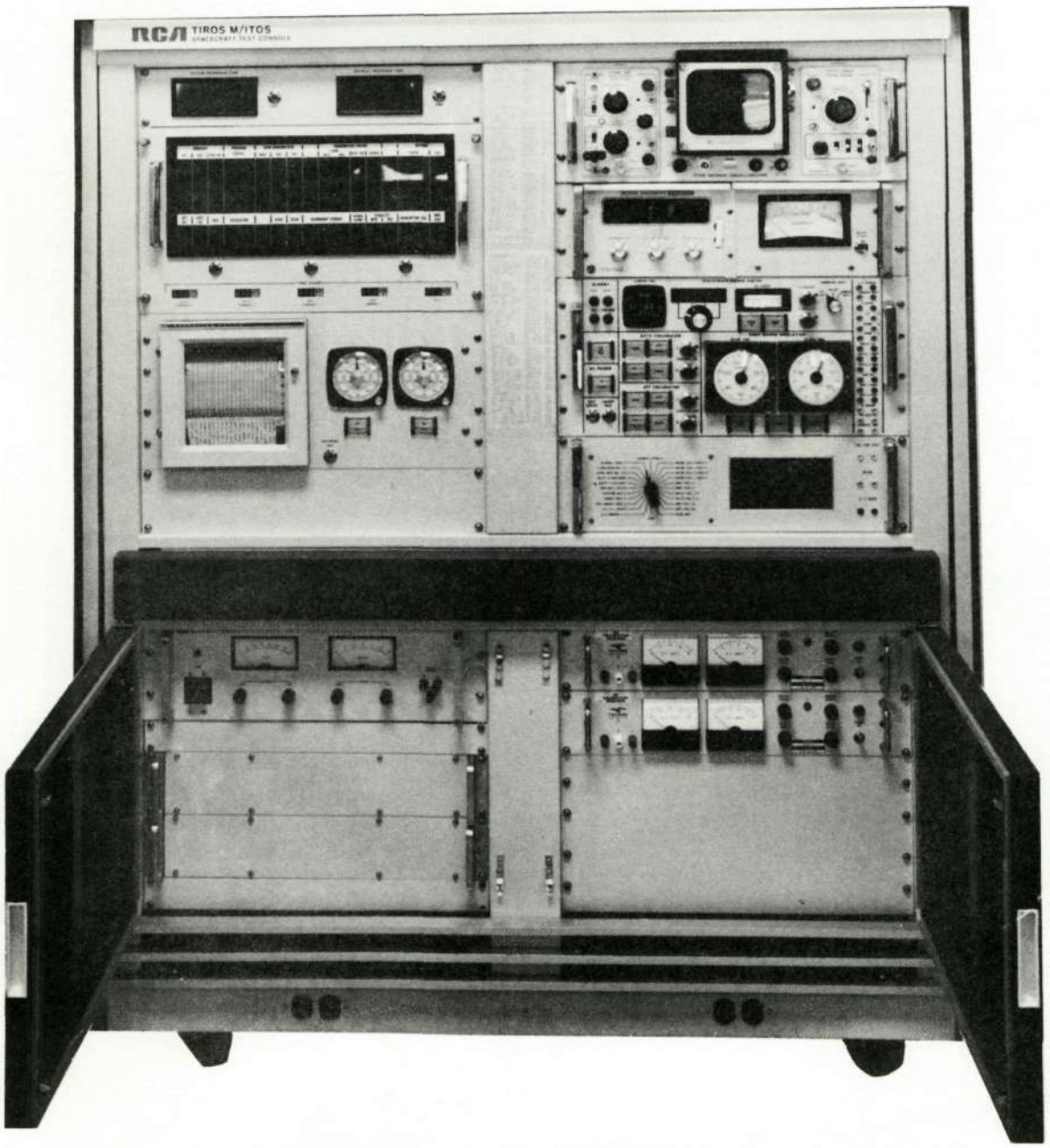

Figure 5-V-1. Spacecraft Test Console

SECTION VI

DESIGN DEVELOPMENTS

A. GENERAL

Much of the ground equipment used with the ITOS system was previously installed as part of the TOS complex, as described in the preceding section. Facilities that are unique to the ITOS system have been added to the CDA stations and control centers. These changes are designed in a manner which enables rapid changeover between the TOS and ITOS modes of operation. The following paragraphs detail the areas of equipment change in the ground equipment.

B. S-BAND COMMUNICATIONS LINK

The S-band communications link between the satellite and the CDA stations was used originally with the ESSA 7 and ESSA 9 satellites. For ITOS, the data processing characteristics of this link have been expanded to accommodate the multiplicity of sensors carried on the spacecraft.

The 1700-MHz signal from the spacecraft carries a composite subcarrier in the 10- to 480-kHz band. An 85-foot parabolic reflector antenna, in conjunction with redundant pairs of S-band receivers and demodulators, receives the signal from the spacecraft and extracts the subcarrier for presentation at the DAF/CDA interface.

The video-handling section of the CDA station receives and processes the 10- to 480-kHz composite signal. This composite signal contains the following information:

Information	No. of Channels
SR Video	2
SR Flutter-and-Wow	2
AVCS Video	1
AVCS Flutter-and-Wow	1
Secondary Sensor Data	3

The individual subcarriers are extracted from the composite signal by the CDA station demultiplexers and recorded on magnetic tape recorders. After each satellite pass, the information is retransmitted to DAPAF via microwave link. The limited capacity of the microwave link necessitates the sequential transmission of the video data; however, each video channel is transmitted simultaneously with its associated flutter-and-wow signal. The CDA station processes the video data (e.g., by replaying the recorders at a reduced speed) to produce compatibility between the frequency characteristics of the video signals and the microwave link. The three secondary sensor data channels are retransmitted as a composite signal over the video channel in slow-time playback.

Redundant demultiplexers and recorders are provided to minimize the possibility of loss of information. An oscilloscope display of the received subcarriers and of the demodulated signals is available for monitoring purposes.

Table 5-VI-1 shows the function, input channel frequency band, output channel frequency band, and peak deviation for each of the signals present on the composite subcarrier received at the CDA ITOS station from DAF.

TABLE 5-VI-1. COMPOSITE SUBCARRIER SIGNALS

Channel No.	Function	Demux Input Frequency (kHz)	Demux Output Frequency (kHz)	Peak Deviation (kHz)
1	AVCS Video	24 - 128	108 - 248	72 - 120
2	SR No. 1 F&W	10.5 - 14.5	10.5 - 14.5	12.5 ±1%
3	AVCS F&W	198 - 202	48.5 - 51.5	50 ±1%
4	SR No. 1 Data	225 - 270	31.2 - 60	38.4 - 52.6
5	Pilot Tone	300	*	
6	SR No. 2 Data	330 - 375	31.2 - 60	38.4 - 52.6
7	SR No. 2 F&W	398 - 402	10.5 - 14.5	12.5 ±1%
8	Secondary Sensors	440 - 480	140 - 180	**

* The 300-kHz pilot tone is used as the reference for the demultiplexer local oscillators used in translating the other frequency spectra. The local oscillator frequency is available for monitoring.

** The secondary sensor channel contains three multiplexed subcarriers centered at 144, 160, and 176 kHz, respectively. The deviation of each subcarrier is ±4 kHz.

C. DEMULTIPLEXER

The input voltage to the ITOS demultiplexer at the DAF/CDA interface is 3 volts peak-to-peak at an impedance of 75 ohms. The nominal output from each channel of the demultiplexer is 3.0 volts peak-to-peak at an impedance of 75 ohms. Two identical demultiplexers are provided, the input signal being derived from a common interface connection. The outputs of the two demultiplexers are separate.

The demultiplexer receives the frequency-multiplexed signal from the S-band receiver and demultiplexes this signal to obtain eight subcarrier frequencies. These subcarrier frequencies contain AVCS, scanning radiometer, flutter-and-wow, and secondary sensor data. Seven of the subcarrier frequencies are recorded on the AVCS and SR magnetic recorders for playback at a later time; the eighth subcarrier frequency, the 300-kHz reference signal (pilot tone) is used within the demultiplexer as a mixer frequency and is used externally to the demultiplexer at the oscilloscope. The following paragraphs provide a description of the operation of the demultiplexer. A block diagram of the demultiplexer is shown in Figure 5-IV-1.

The baseband signal is supplied to the CDA from the S-band diversity combiner in the DAF, and is applied to the multiplexers in parallel. Except for the 300-kHz pilot tone, the outputs of each demultiplexer are recorded on redundant magnetic tape recorders.

The AVCS flutter-and-wow signal, at 200 ±2 kHz, is converted to a nominal 100 kHz. This signal is filtered to eliminate unwanted signals and harmonics, and is divided by a factor of two. It is again filtered, then amplified, and is recorded at a nominal 50 kHz.

AVCS video data is separated from the baseband by a 24- to 130-kHz filter, phase corrected, rectified, and doubled in frequency. The doubled frequency is filtered, amplified, and recorded. The recorded frequency range is 108 to 248 kHz.

Data from the SR Channel 1 recorder, together with its associated flutter-and-wow signal, is filtered from the baseband and injected into a balanced mixer. The filter bandpass is 197 to 270 kHz. The mixing frequency from the phase-locked oscillator is 300 kHz. The SR No. 1 flutter-and-wow signal is filtered and amplified to remove other data signals.

The SR video data in the frequency band from 225 to 270 kHz is converted by the balanced mixer to a difference signal in the range from 31.2 to 60 kHz. It is phase-corrected, limited, filtered to remove the unwanted sideband, and amplified for recording.

SR Channel 2 data is processed in a manner similar to SR Channel 1. The input frequency range is 330 to 403 kHz. The flutter-and-wow data is at a nominal 400 kHz and the video data range is from 330 to 375 kHz. Mixing with the 300-kHz oscillator frequency, with subsequent filtering, produces difference frequencies of 100 kHz for the flutter-and-wow data, and 31.2 to 60 kHz for the video signal. Further processing is the same as for SR Channel 1 data, except that the flutter-and-wow signal is divided by 8 to obtain 12.5 kHz.

Secondary sensor data is filtered from the baseband by a 440- to 480-kHz filter. The signal is mixed with the oscillator frequency, and produces a difference frequency in the range from 140 to 180 kHz. This signal is a composite subcarrier, containing three multiplexed subcarriers centered at 144, 160 and 176 kHz, respectively. The deviation of each subcarrier is ±4 kHz. The composite subcarrier is recorded directly on the magnetic tape recorders, and is further processed to separate the data channels for presentation on the chart recorders.

The 300-kHz pilot tone is not recorded on magnetic tape. It is separated from the baseband by a bandpass filter at 300 ±1 kHz. This signal is used to phase-lock the oscillator for the mixing operations. It is also available at the monitor oscilloscope.

D. ITOS BEACON DISPLAY

In the ITOS system, the composite beacon subcarrier consists of only two individual subcarriers, which correspond to Channels 1M and 3 of the three TOS subcarriers. One channel, using IRIG channel 9 centered at 3.9 kHz, is used to carry command verification data, housekeeping telemetry, and solar aspect sensor data on three subchannels.

The other channel, centered at 2.3 kHz with a deviation of ±20 percent (not IRIG standard) contains horizon crossing data. This data is demultiplexed, demodulated, and displayed on a high-speed chart recorder. The composite subcarrier is recorded on all four magnetic tape recorders, and is retransmitted in real time to TOC and TCC/TEC.

A calibration oscillator, controlled by the Electro-Magnetic Research model 280A calibrator, is used to calibrate the nonstandard channel. It produces five crystal-controlled frequencies, as follows:

1. LBE,

2. $\text{LBE} + \frac{\text{CF} - \text{LBE}}{2}$

3. CF,

4. $CF - \frac{UBE - CF}{2}$,

5. UBE.

where

LBE is the lower band edge,

CF is the center frequency, and

UBE is the upper band edge.

The calibration procedure remains unchanged.

The demodulated channel 4 data is displayed on a high-speed chart recorder. The recorder has a recording speed of at least 50 inches per second. When operating in the TOS mode, the signal input to the recorder is grounded. When operating in the ITOS mode, the channel 7 and 8 inputs to the recorder are grounded, and it is possible to select the demodulated channel 4 signal for display on the oscilloscope mounted on rack 32. The demodulated signals may also be displayed on the Visicorder, although the primary use is reduction of attitude data, when required.

E. MICROWAVE LINK INTERFACE

The AVCS, SR, and secondary sensor video data (including the flutter-and-wow data) received from TOS and ITOS satellites, the beacon transmissions, significant commands, and CDA station events are transmitted by the CDA station to other ground complex facilities over microwave channels. The data transmission equipment processes the signals to make them compatible with the voice channel equipment, and delivers them to the X136 terminal through four balanced line amplifiers that provide the necessary signal amplitude and impedance-matching characteristics. The existing microwave facilities and channel characteristics remain unchanged for ITOS operations. However, the CDA station interface equipment has been modified to provide a secondary sensor data bandwidth that is compatible with the characteristics of the microwave link.

The ITOS communication system requires that the secondary sensor data modulate three voltage-controlled oscillators during replay from the spacecraft incremental tape recorder. The outputs of the three oscillators are combined and transmitted as one channel of the multiplexed S-band transmission.

A technique similar to that used for AVCS is employed for transmitting secondary sensor data via microwave relay. The tape recorder is replayed at one-eighth the recording speed to convert the frequency spectrum of the

signal to a spectrum compatible with the characteristics of the voice channels. A secondary sensor relay will select the source of information.

The possibility of errors in the secondary sensor data as a result of noise was investigated and qualitative rather than quantitative approach was taken because of the restricted amount of data available.

It would be advantageous to establish and maintain the nominal signal level at the input to the link. However, the form of the signal (a composite subcarrier) is such that limiting at the output of the tape recorder is impracticable and the level changes are too rapid to permit an AGC circuit to be used. The alternative is to demultiplex the three subcarriers, pass each of them through an amplitude limiter, filter each channel to reestablish the transmission bandwidth, and then recombine them for transmission.

This alternative was implemented for the ITOS system. Although multiplexed subcarrier transmission has been previously used on TOS for the transmission of beacon data, errors due to impulse noise were not obvious. The reasons for this are as follows:

(1) The primary mode of data transmission is in real time; i.e., there is no intermediate recording carried out at the CDA stations.

(2) The data rate is much lower.

(3) Because the signal is essentially analog, noise is less likely to destroy information. In a digital signal, noise can invalidate a whole word or frame.

The secondary sensor signal conditioner processes the composite 18-kHz, 20-kHz, and 22-kHz signals reproduced by the CDA station tape recorder before transmission to ESSA. This processing is required to remove amplitude variations in the composite signal which are caused by the record-reproduce cycle of the CDA tape recorder.

The input to the signal conditioner is a frequency-division-multiplexed composite signal consisting of three frequency-shift-keyed (FSK) subscribers. The center frequencies of the subcarriers are 18 kHz, 20 kHz and 22 kHz. Each of the subcarriers is deviated to a maximum of ± 0.58 kHz at a maximum modulating frequency of 0.188 kHz. The modulating signals are from the NRZ data tracks of a digital tape recorder.

Amplitude variations introduced by the CDA recorders can produce a reduction in signal amplitude of 16 dB.

The functional block diagram of the secondary sensor signal conditioner is shown in Figure 5-II-8. The composite signal received from the CDA tape recorder is separated into the three subcarriers by means of the bandpass filters at the inputs of the channels. The filtered signals are then fed to a limiter-amplifier (Z1) to remove any amplitude variations that are present. The performance of the limiter reduces 16-dB variations at the input to less than 1 dB at the output of this signal conditioner. A second bandpass filter, identical to the input filter but after the limiter, removes the unwanted harmonics, and provides amplitude limited channel sidebands to the operational amplifier, Z1. The potentiometers (R19) are used to adjust each of the processed channel sideband signals to equal amplitudes at the output of the operational amplifier, Z1.

The operational amplifier feedback network consisting of R4 and C9 provides a fixed gain and frequency rolloff above the highest sideband of 22.58 kHz. This provides an additional reduction in noise bandwidth of the signal conditioner. Resistor R6 ensures additional stability in the presence of load variations.

The video and flutter-and-wow signals are delivered directly to the balanced line amplifier (BLA) inputs without any processing. The outputs of the balanced line amplifiers are delivered to terminal equipment at a level of 1 volt, peak-to-peak.

Each balanced line amplifier consists of a two-stage, capacitance-coupled amplifier with transformer output, which provides a 1-volt peak-to-peak signal and a matching output impedance of 135 ohms to the terminal equipment.

F. STATION CONTROL

Much of the equipment installed at the CDA for use with the TOS satellites is also incorporated in ITOS operations. The increased amount of data to be handled, the different techniques necessary for handling the signals, and experience gained in the operation of the TOS ground stations, have led to a change in station control.

Consideration was given to extending the automatic controls installed for TOS operation; however, this would lead to a complex and inflexible system. It was decided to use a system of manual switching, with station operation being automatically monitored to detect abnormal operation in either the ITOS or the TOS mode. The operator selects the required station operating mode, the operating modes for the magnetic tape recorders, and the microwave link interface switching.

Overall control of the CDA operating modes and facilities for monitoring the status of major subsystems in the station is incorporated in the switches and indicators located on the station control panel (rack 26) and the signal processing rack. Switches provide for control of the following:

- Application of DC power to the video processing equipment.
- Selection of either of the two redundant command programmers.
- Selection of either the operating or test mode for the command programmer.
- Setting up of the station equipment for TOS APT, TOS AVCS, or ITOS satellite interrogation.
- Selection of either of two vertical sync generators (normal or alternate) for processing of AVCS pictures.
- Selection of one of the four magnetic tape recorders for playback operations.
- Selection of playback of AVCS, secondary sensor, scanning radiometer information Channel 1 or 2, and scanning radiometer, flutter-and-wow 1 or 2 for transmission via the microwave link.
- Selection of real-time or playback beacon transmission.
- Selection of real-time or real-time playback input to AVCS display.

Indicators are also provided for the status of the following functions:

- Beacon system OPERATE or CALIBRATE.
- Video simulator.
- All power supplies.

The versatility of the control circuitry allows the station to record data from a satellite while playing back data from a previous pass. The actual rate at which data is played back and the channel from which the signals are obtained depend upon the nature of the signals being processed and on the spacecraft from which the signals originate.

The station operator selects the required station operating mode and the operating modes for the magnetic tape recorders and microwave link interface switching. A warning light will illuminate when the mode selected for the recorders or the interface is not compatible with the station operating mode. A warning light does not necessarily indicate that the station is not operational. For example, when ITOS signals are being received, all four magnetic tape recorders should be recording data from the spacecraft. If one of the recorders is not working,

the warning light will be illuminated. All data will be recorded; however, the channel which is associated with the defective recorder will not be redundantly recorded.

The station operating modes are divided into two on-line groups: spacecraft contact record data and playback. When a conflict exists between the two modes, the spacecraft contact mode will take precedence. The various operating modes and the related magnetic tape recorder and microwave relay requirements are shown below. Indicators associated with each of the controls provides visual monitoring of the selected mode.

(1)

Spacecraft Contact Record	
Operating Mode	Requirements
TOS/APT	Either recorders A and B at 60 ips or recorders C and D at 15 ips
TOS/AVCS	Recorders A and B at 60 ips
ITOS	Recorders A, B, C, or D at 60 ips.

(2)

Data Playback	
Operating Mode	Requirements
AVCS	Either recorder A, B, C, or D at 7-1/2 ips
SR Channel 1	Either recorder A, B, C, or D at 30 ips Channel 1 selected SR F&W Channel 1 or 2 selected
SR Channel 2	Either recorder A, B, C, or D at 30 ips Channel 2 selected SR F&W Channel 1 or 2 selected
Secondary Sensors	Either recorder A, B, C, or D at 7-1/2 ips Secondary sensors selected
Beacon	Either recorder A, B, C, or D at 60 ips (For TOS, either A, B, C, or D at 7-1/2 ips).

The TOS events recorder was retained. It is a paper-chart recorder that provides for simultaneous recording of 20 independent channels of slow-speed on/off information. The recorder is used to monitor significant CDA station operations and to provide a hard copy of these and certain critical programming events. The recorder is also useful in checking overall CDA operation prior to the satellite pass. The 8-channel beacon recorder also has inputs from the

video AGC, command comparator, and digital command programmer. During a satellite interrogation, certain station-events indications are transmitted to TOC and TEC/TCC command-program events are also transmitted over the same channel.

G. SUBCARRIER SIGNAL MONITORING

Three separate transmissions are received at the CDA station from ITOS satellites: real-time APT or SR sensor data, S-band sensor data, and the beacon signal. Each of these signals is received separately, and the information subcarriers are demodulated at DAF. The subcarriers are then presented to the CDA for processing and monitoring.

The APT or SR subcarrier at a frequency of 2400 Hz is recorded on one of the redundant pairs of magnetic tape recorders and is available for monitoring on an oscilloscope, either in real-time or in real-time playback.

The 10- to 500-kHz composite subcarrier signal from the S-band receivers is applied to the inputs of two identical redundant demultiplexers, each of which separates the composite video subcarrier into six single subcarriers containing the AVCS and SR video and flutter-and-wow information, and a seventh composite subcarrier containing the secondary sensor information and a clock channel. The output of each demultiplexer is recorded on one of a redundant pair of magnetic tape recorders.

The 10- to 500-kHz composite signal may be monitored on an oscilloscope in real-time, but is not recorded. The CDA station modification includes provision for the oscilloscope monitoring. The video data may be applied to the kinescope, either in real time or in a playback mode, and a photographic record of the data may be obtained by use of a Polaroid camera, which is part of this equipment.

The beacon composite subcarrier is demultiplexed and the data is either recorded on magnetic tape or recorded on chart recorders. The 3.9-kHz and 2.3-kHz subcarriers are sent over the microwave link in real time.

Although the three sources of data may be displayed on the kinescope, oscilloscope, or facsimile recorders, the principal monitoring equipment at the CDA consists of four strip chart recorders as follows:

(1) Events recorder — Esterline-Angus Model A620T.

(2) Beacon data recorder — Brush Mark 200.

(3) Attitude data recorder — Brush Mark 280.

(4) Visicorder.

The events recorder is used to monitor CDA station events. It consists of 20 channels of slow-speed on/off information. The writing elements are electronically heated styluses, which record on chart paper that is sensitive to both heat and pressure. Either automatic or manual operation is available. The latter is used during station troubleshooting and maintenance procedures. Figure 5-II-9 is a simplified logic diagram of the recorder, showing data inputs to each of the channels.

The beacon data recorder is a high-speed paper chart recorder, which provides simultaneous recording of eight channels of analog data and two events markers. It is normally operated at 20 millimeters per second. A pressurized fluid writing system is used, and the presentation is true rectilinear. The recorder channel width is 40 millimeters and the trace width is 0.01 inch. The frequency response is:

- 50-millimeter p-p deflection, 0 to 55 Hz;
- 40-millimeter p-p deflection, 0 to 60 Hz;
- 15-millimeter p-p deflection, 0 to 100 Hz;
- 4-millimeter p-p deflection, 0 to 200 Hz.

The sensitivity is 2.5 volts, full scale, and AC or DC linearity is 0.05 percent, full scale. Figure 5-II-10 shows data inputs to the beacon data recorder.

The attitude data recorder (Figure 5-II-10) is a high-speed paper chart recorder, which provides simultaneous recording of two channels of analog data and two events markers. It is used to display the attitude-sensor data from beacon channels 1 and 2 and, from recorder channels 1 and 2, respectively. The two events markers of the recorder are used to display the 10-pps timing pulses and the 28-bit time code. The recorder is operated at 50 millimeters per second to optimize the resolution of attitude pulses and, hence, optimize the accuracy of the attitude-sensor data reduction since it is directly related to the accuracy involved in reading pulse locations from the chart.

The recorder writing system is pressurized fluid used to produce a true rectilinear presentation. The recorder channel width is 80 millimeters and trace width is 0.01 inch. The frequency response is:

- 80-millimeter p-p deflection, 0 to 35 Hz;
- 40-millimeter p-p deflection, 0 - 60 Hz;
- 15-millimeter p-p deflection, 0 - 100 Hz; and
- 4-millimeter p-p deflection, 0 - 200 Hz.

The sensitivity is 25 millivolts full scale and linearity is 0.25 percent full scale.

The Visicorder is a high-speed paper chart recorder using optical writing and capable of handling up to 12 individual data channels with response characteristics determined by the individual galvanometers. The Visicorder in the CDA station is equipped with 6 galvanometers. The characteristics of each galvanometer and the channel data inputs are listed below.

Channel	Nominal Galvanometer Response (Hz)	Maximum Deflection (inches)	Normal Input Signal
1	13,000	±1	Spare
2	1,000	±4	28-bit time code
3	4,800	±2	500-pps marker
4	1,000	±4	Beacon channel 1
5	1,000	±4	Beacon channel 2
6	1,000	±4	Beacon channel 3

Drive currents for the galvanometers are supplied by a 6-channel amplifier and attenuator chassis included in the same rack. The inputs to this galvanometer driver-amplifiers are connected through a jack panel permitting recording of signals other than the normal ones. The recorder is capable of operation at speeds from 0.1 to 80 ips. Figure 5-II-10 shows data inputs to the Visicorder.

H. COMMAND TRANSMISSION RATE AND ADDRESS SHIFT

The TOS command equipment is also used to command the ITOS satellites. Commands are transmitted from the CDA stations to the satellites in the form of FSK amplitude modulation of an RF command carrier. Each command transmission to the satellite consists of a 5.35-second transmission of an enable tone followed by one or more sequences of commands formed by frequency-shift-keying a second audio tone.

The satellite commands fall into two classifications: direct and remote. The direct commands consist of a sync pulse that conditions the satellite for receipt of data, an address portion consisting of a 12-bit code that identifies the satellite for which the command is intended, a second sync pulse, a 12-bit instructional command that either selects a satellite component for operation or performs an on/off function, and a single command-termination bit. Remote commands are similar to direct commands; however, in a remote command, the direct command is immediately followed by 28 bits of program data to be implemented from the CDA station after a delay in orbit.

Because the basic timing of the TOS satellite's television picture-taking operations (and, to a lesser extent, the QOMAC operations) is dependent on the satellite's spin rate, two features have been incorporated in the design of the programming equipment. One, using spin data from the satellite's beacon transmission, a count of all spins occurring during the period from the time of the first alarm until the transmission of remote commands is kept, and the data contained in the remote command is automatically updated with this count prior to its transmission. And, two, the initiation of each command transmission is delayed for a specific period following the completion of a satellite spin, in order to obviate a possible 1-spin ambiguity in the spin count. (Because of the differing spin rates in TOS/APT and TOS/AVCS satellites, different delay periods are employed during command operations.)

Since the ITOS satellite is earth stabilized, no delay between commands is necessary. When in ITOS mode, the commands in each sequence are transmitted in rapid succession with an interval of only 200 milliseconds between commands. In this mode, remote commands in Set I are updated prior to transmission using a counter that counts at 1 pulse every 6.5 seconds starting at the first alarm. Set II commands are not updated.

At the end of the last command in the first command sequence, the programming equipment ceases transmission of commands to the satellite, but maintains contact with it. In multisequence command programs, subsequent alarms from the alarm timer will cause the subsequent programs to be transmitted, in turn, in a manner identical to the first sequence. (However, because contact is maintained with the satellite after the first sequence, transmission of the enable tone and "dummy" command is not required.) At the end of the last command in the last programmed sequence, the programming equipment resets, and returns to a quiescent condition. In addition to the digital commands, it is possible at anytime to transmit the "enable" tone manually. This may be used to command a readout of housekeeping telemetry. If operated manually, the enable tone has precedence over the FSK tone and will interrupt any digital command in progress.

When an ITOS spacecraft is being controlled, the 6.5-second internally generated timing pulse is used to update the remote command word. This arrangement requires a "not AVCS" ($\overline{\text{AVCS}}$) signal to be applied to the digital command programmer. Also, the horizon-crossing signal input from subcarrier discriminator No. 2 in the digital command programmer is grounded to prevent faulty operation due to noise.

The auxiliary command unit contains two sets of dials which are used for the remote command section of a command word. These are designated "programmer 1" and "programmer 2" (these refer to spacecraft programmers). The contents of the programmer 1 dials are transmitted whenever the direct command set on the dial contains the code 4200_8 (load programmer 1 for TOS), and similarly the contents of the programmer 2 dials are transmitted whenever the direct com-

mand code is 1020_8 (load programmer 2 for TOS). The division of commands into two groups for ITOS permits the two sets of dials to be used to provide four remote commands, subject to the following restrictions:

(1) The remote command must be preceded by one of the two codes.

(2) During any one command transmission each of the codes can be used only once.

There are no restrictions on valid remote commands transmitted from a tape input.

I. TOC AND TEC/TCC EQUIPMENT

New facilities added to the TOC and TEC/TCC equipment include the following:

(1) An attitude channel selector which is a bandpass filter to extract the attitude data subcarrier from the composite beacon subcarrier. The filter bandwidth is 1.6 to 3.0 kHz.

(2) An attitude channel discriminator which extracts information from the 2.3-kHz subcarrier.

(3) An attitude channel calibrator which is a modification of the existing calibrator, for use with the 2.3-kHz ± 20-percent subcarrier used with ITOS. The calibration procedure will remain unchanged.

(4) An attitude channel chart recorder capable of recording at a speed of at least 50 inches per second with a frequency response of at least 1 kHz.

(5) A switch/indicator marked TOS-ITOS was added to the switching control panel. When the switch indicates TOS operation, station operation will be identical to the previous TOS operation. In the ITOS mode, the station will be modified for ITOS operation.

(6) A spare input on the oscilloscope input-selector front panel connected to the output of the attitude channel discriminator. The legend plate on the switch has been modified to indicate the additional input.

The attitude channel selector, discriminator, and calibrator are incorporated into the subcarrier subunit (rack 37). The recorder is installed in rack 36 below the original 8-channel recorder. The magnetic tape degausser at the TOC station has been moved from rack 36 to rack 37.

Spacecraft beacon data, AVCS video and flutter-and-wow signals, SR video and flutter-and-wow signals, associated telemetry and time code data, and certain timing signals generated at the CDA stations will be received, recorded, and processed at DAPAF at the National Environmental Satellite Center (NESC). DAPAF can receive and distribute data simultaneously from the CDA stations at Gilmore Creek, Alaska, and Wallops Island, Virginia. Some data will be processed on-line as it is received; other data will be stored temporarily before processing.

The AVCS video data is received as discrete frames of 834 active lines each and is preceded by a time code. The first 33 lines of each frame is at black level; the remaining 834 lines contain video data and are preceded by a 5-millisecond sync pulse. Approximately 12 seconds elapses after each frame. Transmission of each line requires 60 milliseconds.

The information is received as a frequency-modulated signal, with a frequency of 29.4 kHz corresponding to white, 21 kHz to black, and 18 kHz to the tip of the sync pulse. The baseband of the signal is approximately 7.5 kHz.

The time code contains 24 return-to-zero bits and is repeated at least three times prior to each frame. The code is coherent with picture timing. The rate is 7.5 bits per second; the duration of a bit is 66-2/3 milliseconds. The first bit of the code is the most significant digit, and the time code resolution is 0.5 second.

The flutter-and-wow signal is a 6.25-kHz subcarrier, frequency-modulated by the flutter-and-wow of the spacecraft and ground tape recorders. The flutter-and-wow signal is present during the 834 lines of each frame and during the time code.

The SR data is received as a continuous signal. Each line of the signal lasts 156.25 milliseconds and includes a 7.5-millisecond sync pulse. The information is received as a frequency-modulated signal, with a frequency of 26.4 kHz corresponding to cold, 21.0 kHz to hot, and 19.2 kHz to sync tip. The information baseband is 3.6 kHz. The earth-scan portion of the SR signal begins immediately after the sync pulse and ends 52 milliseconds after the sync pulse. The remainder of the video signal is time-shared among spacecraft-clock, calibration, and telemetry data.

The flutter-and-wow signal is a 6.25-kHz subcarrier, frequency-modulated by the flutter-and-wow of the spacecraft and ground tape recorders. The flutter-and-wow signal is present throughout the SR video transmission.

The SR video and flutter-and-wow signals are played back at half the recorded rates. Their frequency characteristics are then directly compatible with those of the microwave link.

The SR video channel to be transmitted is selected by relay switching on recorder playback. Since a flutter-and-wow channel is not uniquely associated with one video channel, it is necessary to monitor the two flutter-and-wow channels on playback to determine which is to be transmitted in association with a video channel.

When a flutter-and-wow signal is present on both channels, each flutter-and-wow channel is associated with its related video channel (flutter-and-wow 1 with video 1, and flutter-and-wow 2 with video 2). When a flutter-and-wow signal is present on only one channel, it is associated with both video channels. In this case, the signal can be on either flutter-and-wow channel 1 or 2, depending upon the spacecraft tape recorder in use.

The secondary sensor data frequency-modulates three multiplexed subcarriers, centered at 19, 20, and 22 kHz. The deviation of each subcarrier is ±500 Hz.

The 18-kHz subcarrier is modulated with solar proton monitor data. Each frame of data contains 180 bits divided into 20 nine-bit words. The first word is a frame sync code (111001001). The remaining 19 words are each divided into two parts; the first four bits contain the exponent, and the remaining five contain the characteristic of the channel being sampled.

The 20-kHz subcarrier is modulated with a 125-Hz clock signal.

The 22-kHz subcarrier is modulated with flat plate radiometer (FPR), time code, and telemetry data. Each frame contains 480 bits divided into 60 words of 8 bits each. The first two words contain all "1's" and are used as a frame marker. The first bit of each of the remaining 58 words is a "0", which is used as a word marker. The allocation of the words in each frame follows:

Number of Words	Information
2	Frame sync
4	Time code
8	FPR data
7	FPR telemetry
39	Spacecraft telemetry and spares

The beacon data is carried on two multiplexed subcarriers centered at 2.3 and 3.9 kHz. The lower-frequency subcarrier is deviated up to ±20 percent by the attitude sensor; the upper-frequency subcarrier contains housekeeping telemetry and other data and is deviated up to ±7.5 percent (IRIG channel 9).

During satellite interrogations, command program and CDA station events are received as commutated signals modulating subcarriers centered at 2.4 and 1.3 kHz, respectively. This transmission is identical to that received during TOS interrogations.

Signals are received from the CDA stations via a 48-kHz microwave link baseband subdivided into seven subgroups, designated channels A through G. The bandwidth and function of each channel are shown in Table 5-VI-1. Where a channel is required to carry more than one form of information signal, the selection is made by the CDA station under the direction of NESC.

J. SPACECRAFT CHECKOUT FACILITIES

Changes to the Spacecraft Checkout Facilities are the same as those at the CDA stations. These facilities are covered in Section V of this part of the report.

SECTION VII

PROGRAM MILESTONES

Table 5-VII-1 gives a chronological account of the major ground station events.

TABLE 5-VII-1. PROGRAM MILESTONES

Date	Milestone
4/25/67	TIROS M contract signed by NASA/GSFC
6/67	Demultiplexer design started
12/67	Installation of new recorder at Gilmore Creek completed
2/16/68	Design review for spacecraft checkout station
7/68	Launch Support Van (GSE-5) equipment completed
8/30/68	Launch Support Van modification completed
8/68	Backup CDA Station (GSE-3) modification completed
10/24/68	Modification of CDA station at Gilmore Creek (GSE-1) completed
11/13/68	Modification of TEC/TCC station completed
11/22/68	Modification of CDA station at Wallops Island (GSE-2) completed
11/27/68	Modification of TOC station completed
11/68	Second Spacecraft Checkout Console completed
2/69	Third Spacecraft Checkout Console completed
5/69	CDA Station modifications per Contract Modification No. 45 completed

APPENDIX A

THE ITOS RADIATION HARDENING PROGRAM

1. INTRODUCTION

During the design phase of the ITOS spacecraft program, a procedure for radiation hardening was adopted to avoid the possibility of significant performance degradation in orbit that might result from radiation damage effects in sensitive components. The purpose of the procedure was to provide adequate allowances for radiation-induced degradation under worst-case conditions, but to avoid prescribing a larger safety factor than actually needed. The procedure and its effectiveness in accommodating anticipated radiation damage effects in electronic components on ITOS are outlined in the following paragraphs.

2. THE ITOS RADIATION ENVIRONMENT

The major sources of radiation that will affect ITOS components in space are the high energy electrons and protons trapped in the Earth's Van Allen belt and encountered by the satellite along its orbit path. Estimates of the total numbers of these particles bombarding the satellite over the mission period are based on data listed in NASA publications.* The spacecraft launch date was an important factor in estimating the total number of electrons because of the gradual decay in the number of trapped electrons in the belt following the enormous increase resulting from the 1962 "Starfish" experiments. In contrast, the proton population in the belt has remained relatively constant. Although the effect of the 1962 nuclear explosions has largely disappeared, there are still substantial short and long term variations from the average levels as given by the published data. To provide a margin of safety for such variations as well as for unexpected contributions to the total dose from solar flares, and possible errors in orbit altitude, the radiation environment forming the basis for ITOS dose calculations was taken as that of January 1965, when the electron population in the belt was very much higher than it is at present (1969).

In the discussion of radiation hardening in the ITOS Design Study Report,** the margin of safety provided by using the environment of January 1965 as the basis for

---

*Models of the Trapped Radiation Environment; NASA Publication NASA SP-3024.

**Design Study Report for the Improved TOS (ITOS) System, June 7, 1968; Volume III, Appendix A.

predicting worst-case damage effects was examined in detail. A need for re-estimating the anticipated ITOS dose levels arose from two changes in the environmental conditions. The first was an increase in orbit altitude to 790 nautical miles. Originally specified as 750 nautical miles, the orbit altitude was raised to 775 nautical miles, and later to 790 nautical miles. The second change was the updating of the proton flux data in the energy range from 4 to 30 MeV to reflect the NASA data released in 1968. While neither change was of major proportions, the combination was expected to result in significant increases in estimated dose levels.

Based on the revised data for the 790-nautical-mile sun-synchronous orbit, the energy distribution of both the proton and the electron fluxes integrated over a 1-year mission period were recalculated. In comparing the results listed in Table A-1 with earlier data, increases in the total integrated flux are evident, especially in the energy range from 10 to 30 MeV. However, in no case does the increase in any energy bracket exceed 20 percent. The data in Table A-1 formed the basis for the revised version of the ionization damage profile in Figure A-1 for the overall 1-year 1968 data (790-nautical-mile orbit). The corresponding curve for 6 months' exposure in the 1965 environment is also plotted in Figure A-1.

The procedure for deriving the profiles from environmental data of the type listed in Table A-1 is described in detail in the TOS Radiation Program Report* issued in September 1965. The profiles show the relationship between the dose affecting a component at the center of a uniform sphere of aluminum and the thickness of the aluminum shell in mils. The dose levels affecting individual components within a complex spacecraft are determined from the profile by applying a technique called "Sector Analysis", also described in the TOS Radiation Program Report. In following this procedure, the total solid angle surrounding a given component location is divided into a number of sectors over each of which the amount of shielding material is essentially uniform. The contribution to the total dose from each sector is derived from the profile by determining first the total dose within a sphere of the same equivalent thickness as the sector and then applying a factor equal to the ratio of the sector to the total solid angle of 4π radians. The total dose is simply the sum of the contributions from all the sectors.

Calculations of dose levels for the ITOS Design Study Report, based on the 1965 environment, showed that in an exposed location, within but close to an outer wall of the spacecraft, the dose level would reach 1×10^5 rads. In a more protected location, within a subsystem fastened on only one side to an outer wall, the dose level is not expected to exceed 2×10^4 rads. These dose levels formed the basis for estimates of component degradation from ionization effects. In only a few instances was it necessary to add the effect of bulk damage to the predominating effect from ionization.

The margin of safety provided by using the more severe environment of January 1965 in this manner can be estimated from the relationship of the two overall

* NASA Accession No. X65 20853 - ADW 67603

curves in Figure A-1. The two vertical dotted lines in Figure A-1 correspond to shield thicknesses of 170 and 270 mils of aluminum. In the 1965 environment, uniform shielding of these amounts would provide the same protection as the highly complex shielding surrounding internal components in the previously defined "exposed" and "protected" locations. The differences between the dose levels determined by the intersection of the dotted lines and the two overall profiles indicate approximately the margin of safety provided by using the 1965 environment. For components in the exposed locations, the ratio of the two dose levels is about 5 to 1, and in the protected location the ratio is about 2 to 1. These margins of safety for 1 year in orbit are believed sufficient to accommodate almost any possible variations in the Van Allen Belt particle population from natural causes, excluding, of course, the effects from a repetition of the "Starfish" experiments.

TABLE A-1. ITOS RADIATION ENVIRONMENT

One Year Mission - 790-Nautical-Mile Circular Sun-Synchronous Orbit
(Post 1969 Launch Date) Inclination 102 Degrees

Protons		Electrons	
MeV Range	Integrated Flux	MeV Range	Integrated Flux
4 - 5	7.00×10^{10}	0 - 0.25	9.52×10^{14}
5 - 6	4.22×10^{10}	0.25 - 0.50	1.58×10^{14}
6 - 7	2.80×10^{10}	0.50 - 0.75	2.82×10^{13}
7 - 8	2.00×10^{10}	0.75 - 1	6.42×10^{12}
8 - 9	1.49×10^{10}	1 - 2	3.40×10^{12}
9 - 10	1.16×10^{10}	2 - 3	3.16×10^{11}
10 - 11	0.942×10^{10}	3 - 4	5.84×10^{10}
11 - 12	0.758×10^{10}	4 - 5	2.28×10^{10}
12 - 13	0.622×10^{10}	5 - 6	1.49×10^{10}
13 - 14	0.530×10^{10}	6 - 7	1.10×10^{10}
14 - 15	0.456×10^{10}	> 7	4.40×10^{10}
15 - 30	3.06×10^{10}		
30 - 100	2.39×10^{10}		
> 100	0.830×10^{10}		

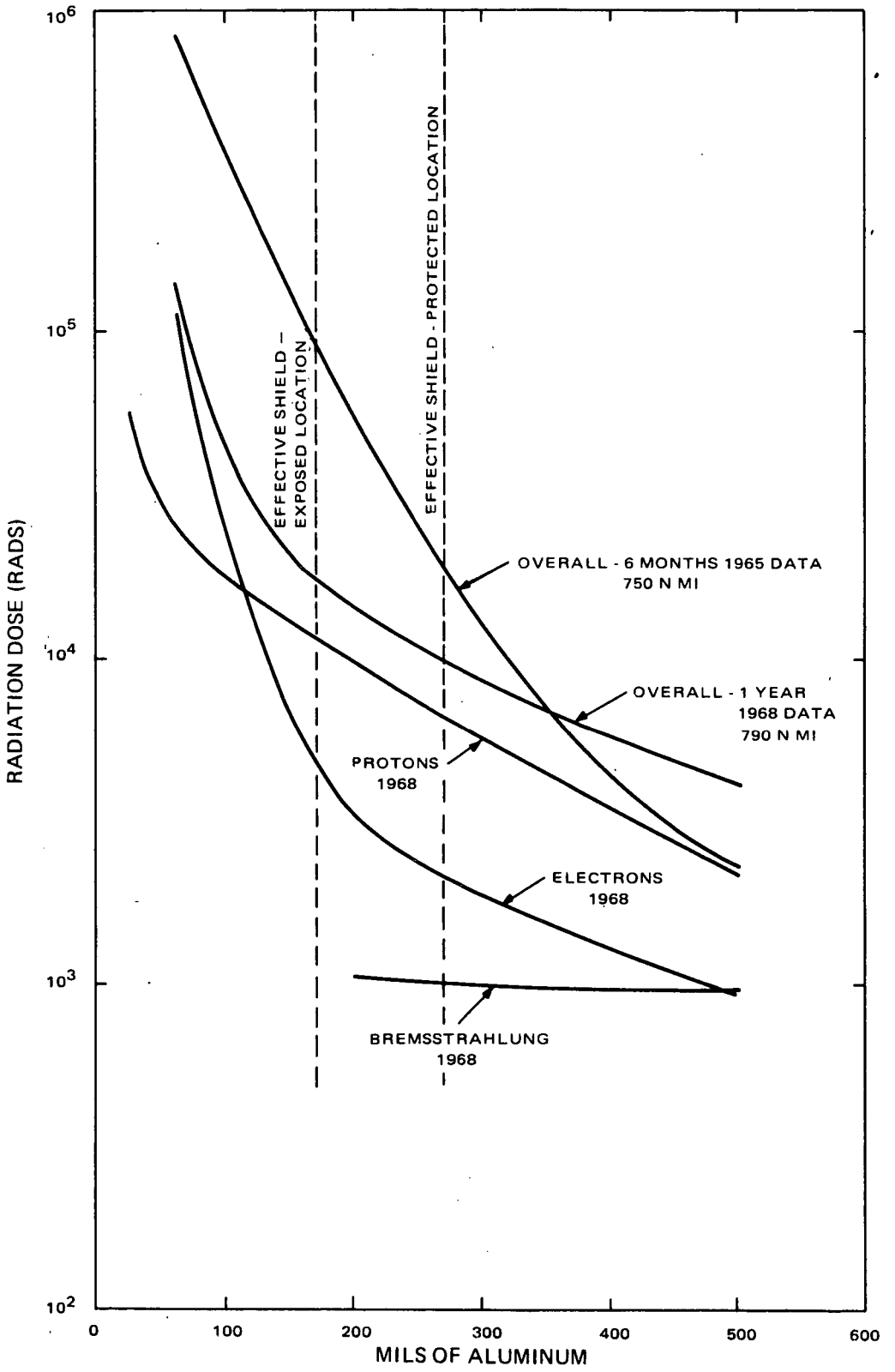

Figure A-1. Comparison of ITOS Ionization Damage Profiles

3. ITOS RADIATION HARDENING PROCEDURE

As indicated previously, the dose levels determined for the January 1965 environment provided the basis for internal component degradation information. All components on the approved standard parts list were reviewed from the standpoint of susceptibility to radiation damage. This review showed that relatively few component types on the list (primarily semiconductor devices) would be significantly affected by exposure to the estimated dose levels.

Fortunately, space radiation under normal conditions does not cause catastrophic failures in such components as bipolar transistors but only a gradual change in component parameters, primarily a decrease in the forward current gain (Beta) and an increase in leakage current (I_{CBO}). By using conservative estimates of anticipated parameter changes from exposure in the specified space radiation environment, design engineers can provide the allowances needed in their circuit design to prevent significant deterioration in performance. No unusual effort is required since similar derating allowances are routinely made for the effects of temperature, aging and the normal variation in parameters expected in the products as received from the manufacturer.

In preparing the radiation degradation data needed for this purpose, the most satisfactory method is to base such predictions on the results of exposing representative samples to radiation from sources that will produce essentially the same effect as exposure to space radiation. A large body of such data was collected during late 1964 and early 1965 as part of the TOS radiation program. Similar tests reported by other organizations, such as the MIT Lincoln Laboratory, have provided much additional useful data. Occasionally data from one component type can be adapted to other types similar in construction and processing. Tests since 1965 for the TIROS program, as well as a number of other programs including a large IR and D effort, have helped provide radiation test data useful in predicting the effect of space radiation on the more recently developed semiconductor devices such as MOS transistors and integrated circuits.*

Figure A-2 illustrates a convenient method for combining all the worst-case data related to the Beta of a particular transistor type, the 2N930, in a useful graphical form. The curves in Figure A-2 show the dependence of Beta on collector current (I_C) for four different conditions. The upper curve, designated No. 1, indicates the mininum values of Beta at -10°C still considered acceptable from the vendor. Curve No. 2 was derived from curve No. 1 by applying a correction factor to take

---

* W.J. Poch and A.G. Holmes-Siedle "A Prediction and Selection System for Radiation Effects in Planar Transistors", IEEE Transactions on Nuclear Science NS 15(6) Dec 1968.
W.J. Poch and A.G. Holmes-Siedle "Permanent Radiation Effects in Complementary - Symmetry MOS Integrated Circuits", IEEE Transactions on Nuclear Science NS 16(6).

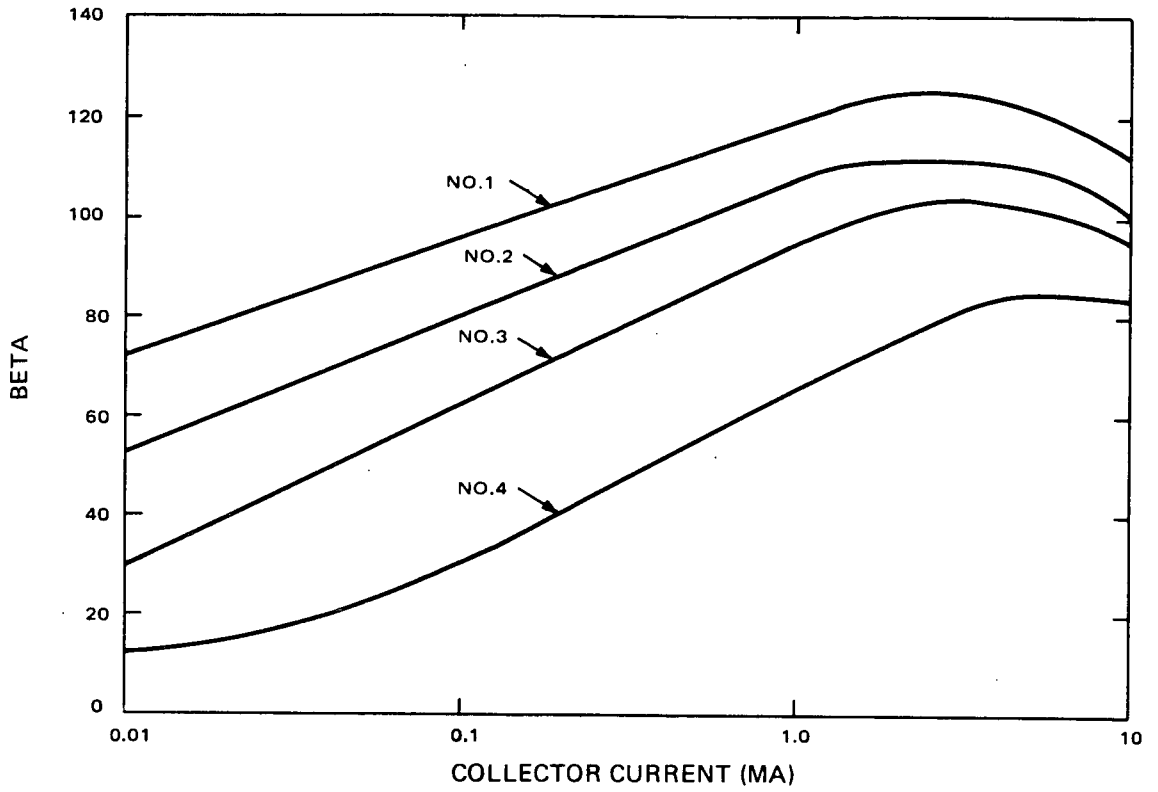

Figure A-2. Worst-Case Beta Values for Transistor 2N930

into account possible Beta reduction from all sources other than radiation. The predicted effect of radiation corresponding to the end-of-mission dose levels in combination with all other degradation factors is given by curves No. 3 and No. 4 Curve No. 3 shows the anticipated worst-case Beta for a 2N930 in a protected location corresponding to an ionizing dose level of 2×10^4 rads. Curve No. 4 provides similar data for the exposed location at the 1×10^5 rad dose level.

Curves No. 3 and No. 4 show that the effect of radiation is more severe if the 2N930 is operated with relatively low values of collector current. Using these curves, the circuit designer can optimize the tradeoff between collector current, transistor location, and minimum acceptable value of Beta.

Data of the kind shown in Figure A-2 for the 2N930 was provided for a large number of transistor types. For those types generally used over a limited range of collector current, data of the same nature was supplied in tabular form. Most of the power transistors were in this category. Data indicating the anticipated increases in transistor leakage current was also presented in tabular form.

The effectiveness of the radiation hardening procedure as outlined in this appendix depends in a large measure on the design engineer who has the responsibility for providing the necessary allowances in his circuits to prevent failure from all sources including radiation. Worst-case analyses based on data of the kind outlined in this discussion were presented at the regularly held design reviews to ensure that

all measures needed to prevent failure had been taken. Since such procedures have been in effect at the RCA Astro-Electronics Division, no in-flight failures traceable to radiation damage have occurred.

4. RADIATION TESTING SINCE 1965

In the period since the major test program in 1965, many new semiconductor devices have become available and many of the older types have become obsolete. To keep pace with these new developments, a modest continuing test program has been underway to evaluate those devices of particular interest for space applications from the radiation viewpoint. Funding for IR and D, in addition to other spacecraft projects has provided major support for this program. Only a few highlights from this effort are presented here, since a detailed account of the results is beyond the scope of this report.

The development of the MOS transistor was of particular importance from the space viewpoint. Its low power drain, adaptability to logic circuitry, and the relative ease of incorporating MOS devices in large scale arrays are major advantages. For space applications, however, adequate allowances must be made for the shift in threshold voltage characteristic of these devices when subjected to ionizing radiation. Tests in 1967 of the MEM 2009, which is used on ITOS, showed that its threshold voltage could shift as much as 10 volts in the ITOS environment. In designing the associated circuitry, therefore, measures were taken to accommodate at least a 20-volt shift in threshold without causing a significant change in performance.

More recent tests of MOS devices indicate that changes in the gate insulator material and in the processing methods have greatly reduced the threshold shift problem. In Figure A-3 the results of testing samples of six-channel switches from four different manufacturers show that even with 15 volts bias applied to the switch electrode during irradiation (a worst-case condition), the maximum shift at the 1×10^5 rad level is only about 3 volts. Information of this kind has been supplied to design engineers so that full advantage can be taken of available MOS devices in new circuit designs.

Integrated circuits of various kinds incorporating the equivalent of conventional bipolar transistors as active elements have also proved attractive for space applications. Tests of individual transistors on integrated circuit chips have shown that the behavior under irradiation is much the same as their discrete counterparts. Data of this kind has helped to evaluate the effect of radiation on complex devices. In addition, samples of complete units have been subjected to ionizing radiation under normal operating conditions. A number of Fairchild type μA741C Operational

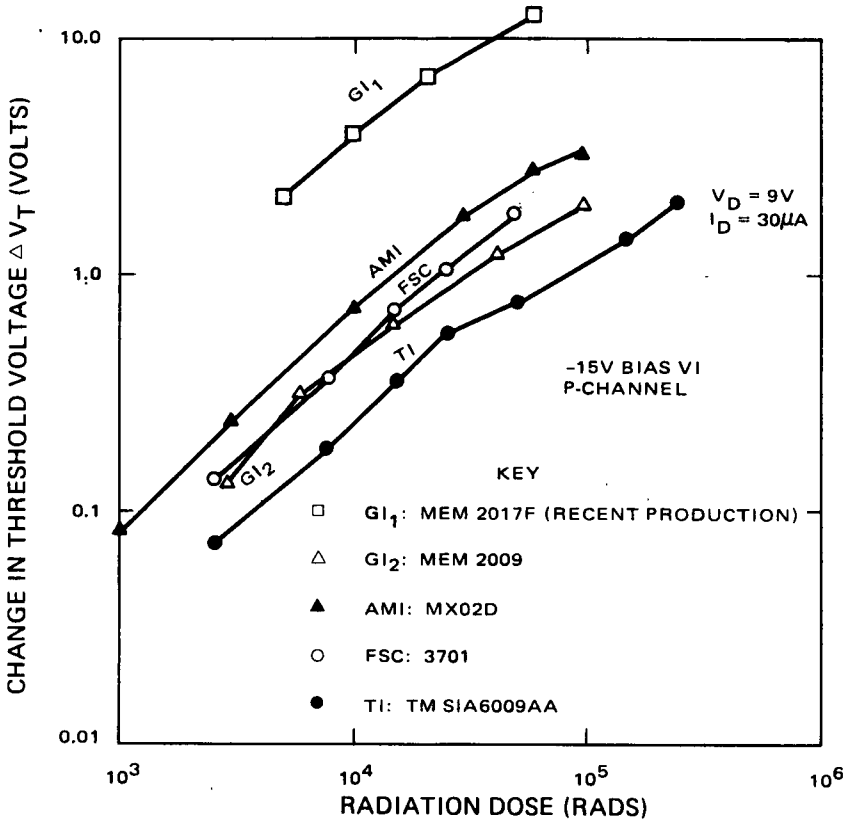

Figure A-3. Comparison of MOS Six-Channel Switches From Four Different Manufacturers

Amplifiers were included in a recent test which showed that these devices are only slightly affected by radiation at the 1×10^5 rad dose level.

Occasionally, items other than semiconductors have been evaluated for their susceptibility to space radiation. Front surface mirrors of the type used for IR radiometers on ITOS were subjected to bombardment by 1 MeV electrons to simulate the effect of high energy particles in space. Measurements of reflectance over the wavelength range of interest before and after irradiation showed very little change, even at dose levels an order of magnitude greater than those expected at the end of 1 year in orbit.

5. CONCLUSIONS

The procedure adopted for radiation hardening subsystems used on ITOS has provided an adequate margin of safety for a 1-year mission without imposing unusual or difficult-to-meet requirements on design engineers. The success of this approach to radiation hardening depends on having up-to-date information on the radiation susceptibility of components included in the spacecraft subsystems.

APPENDIX B

BATTERY LIFE CYCLING TEST

1. INTRODUCTION

The objective of the battery life cycling test was to confirm that a 23-cell, 4-ampere-hour, nickel-cadmium storage battery will maintain a minimum voltage of 26.5 volts when subjected to the cycling requirements for the spacecraft. In addition, a study was made of the cell-charging characteristics as a function of life, to improve the data used in the computer analysis of the power subsystem.

The test program completed in the AED battery laboratory consisted of testing 40 nickel-cadmium storage cells under conditions simulating a worst-case ITOS mission power profile. The test schedule was based upon the battery requirements as given in performance specification for a 23-cell battery.

The test data, including its analysis, are presented in this appendix. The 23-cell battery exceeds the system requirements, even though the test cells performed at an average end-of-discharge voltage slightly below the estimated value. This is attributed to the fact that the cell temperature was maintained relatively high (32° C to 35° C) for the first four months of test, whereas the estimate was based on a linear reduction of temperature from 35° C to 25° C over a six-month test period. It is also indicated that operating at the lower limit of the voltage-temperature charge control curve caused a reduction in end-of-discharge cell voltage.

The duration of the test program was extended from six months to seven months to obtain additional cell and reliability data.

2. TEST PROCEDURE

The nickel-cadmium storage cells tested are identified by serial number and age in Table B-1. These cells were all manufactured by the General Electric Company Battery Products Group. The 40 cells listed in Table B-1 are part of a 50 cell group available for the engineering test program. All cells were subjected to a reconditioning cycle, and 46 of the cells were subjected to the ITOS acceptance tests. The number of test cells was then reduced to 40 and these cells were subjected to an overcharge test to verify the maximum overcharge currents specified in the battery performance specification prior to the start of the cycling program.

TABLE B-1. STORAGE CELLS TESTED FOR OVERCHARGE

Cell Position	New Cells		Date (Yr/Wk)	Old Cells		Date (Yr/Wk)
	Channel	Ser. No.		Channel	Ser. No.	
1	1	1-33	6706	29	5-10	6506
2	2	1-44	6706	30	5-20	6506
3	3	2-7	6706	31	5-28	6506
4	4	2-11	6706	32	5-45	6506
5	5	2-32	6706	33	5-128	6511
6	6	3-16	6706	34	7-53	6521
7	7	3-33	6720	35	9-22	6525
8	8	3-35	6720	36	9-25	6525
9	9	3-36	6720	37	14-17	6533
10	10	4-21	6720	38	14-19	6533
11	11	4-25	6720	39	25-8	6615
12	12	4-28	6720	40	25-9	6615
13	13	5-1	6720	41	25-12	6615
14	14	5-25	6720	42	25-14	6615
15	15	6-2	6720	43	25-17	6615
16	16	6-3	6720	44	25-19	6615
17	17	6-4	6720	45	25-22	6615
18	18	6-5	6720	46	25-23	6615
19	19	6-7	6720	47	25-26	6615
20	20	6-9	6720	48	25-28	6615

Twenty cells were taken from the 1967 cell shipments and 20 cells were older, the oldest of which was manufactured in February 1965, and was, therefore, 30 months old at the start of the test. The date shown is etched on the cell and indicates the year and week in which the cell was manufactured.

The seven-month battery life cycling program is summarized in Table B-2. Each month of testing consisted of 381 electrical cycles at the cell temperatures indicated.

TABLE B-2. SEVEN-MONTH BATTERY LIFE CYCLING TEST SUMMARY

Cycle No.	Temp (° C)	Discharge		Charge		Voltage Limit (volts)
		Time (minutes)	Rate (Amperes)	Time (minutes)	Rate (Amperes)	
1-381	35	22	1.64	91.5	0.95	27.90
382-762	34	23.5	1.56	90.0	0.95	27.96
763-1143	33	24.5	1.52	89.0	0.95	28.04
1144-1524	32	26.2	1.51	87.3	0.95	28.12
1525-1905	28	29.0	1.51	84.5	0.95	28.46
1906-2286	25	31.0	1.46	82.5	0.95	28.64
2287-2667	25	31.0	1.46	82.5	0.95	28.64

3. TEST RESULTS

The nickel-cadmium battery life cycling test results are presented in graphical form in Figures B-1 through B-31 and summarized narrative form in Paragraphs 3.a through 3.h as follows.

a. Data Summary

Figure B-1 presents an overall summary of the test with the cell parameters shown as a function of cycle number (time).

On several occasions between cycles 500 and 600 the temperature exceeded 34° C by as much as 6° C due to equipment malfunction. The equipment was repaired and the ± 2° C temperature control was subsequently restored. Although these temperature excursions did effect the end-of-discharge voltage of the specific cycle in which they occurred, they apparently had no significant permanent effect.

At the beginning of the sixth month, the discharge current was inadvertently allowed to remain at the value used during the fifth month for a depth of discharge of 19.5% instead of 18.9%. This additional discharge is reflected in a lower average end-of-discharge cell voltage as shown in Figures B-1 and B-2 for cycles 1905 to 1973. The correction of the discharge current produced higher average end-of-discharge cell voltages thus there appears to have been no significant program effect.

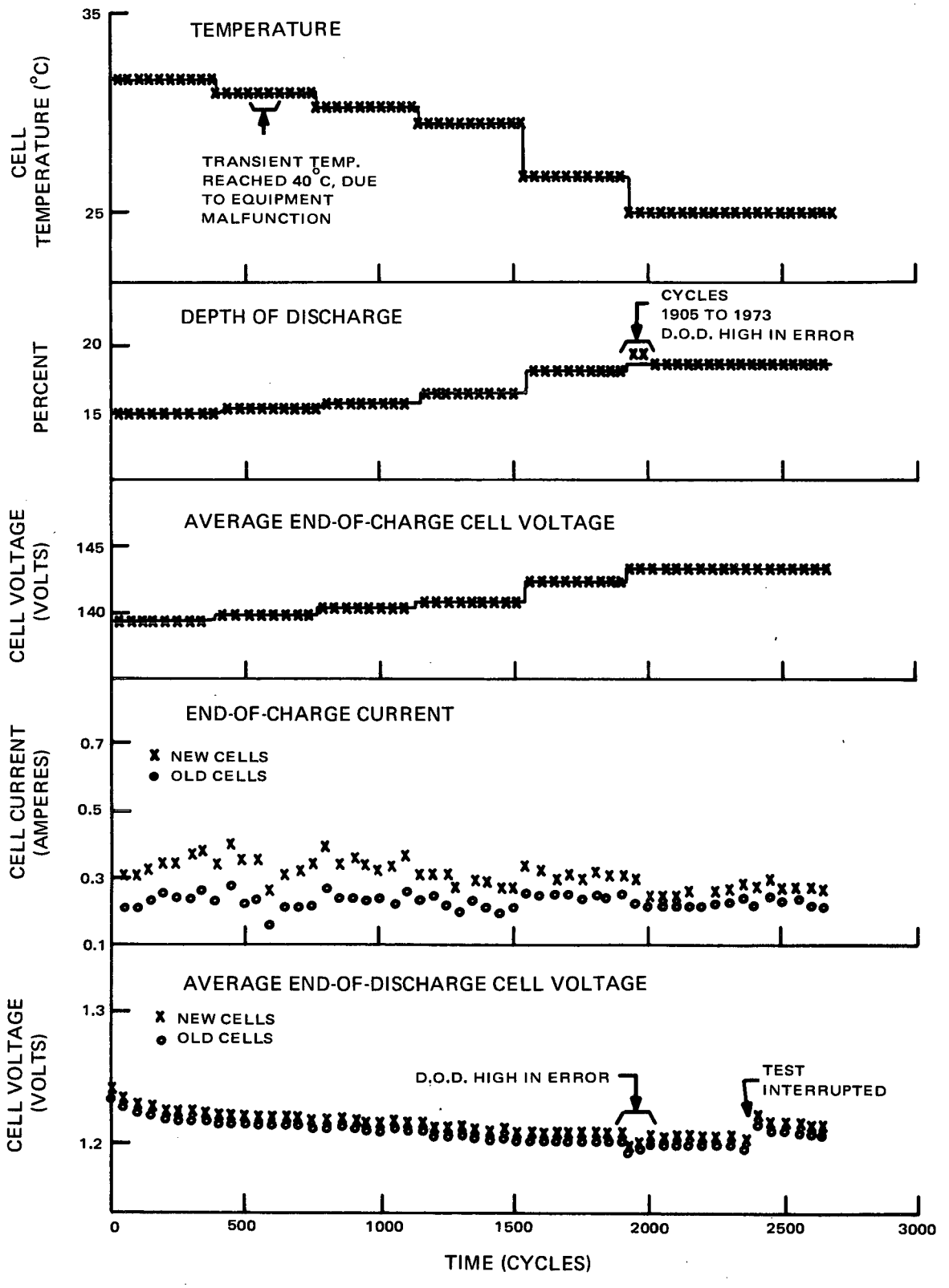

Figure B-1. Battery Test Parameters Versus Life Cycling

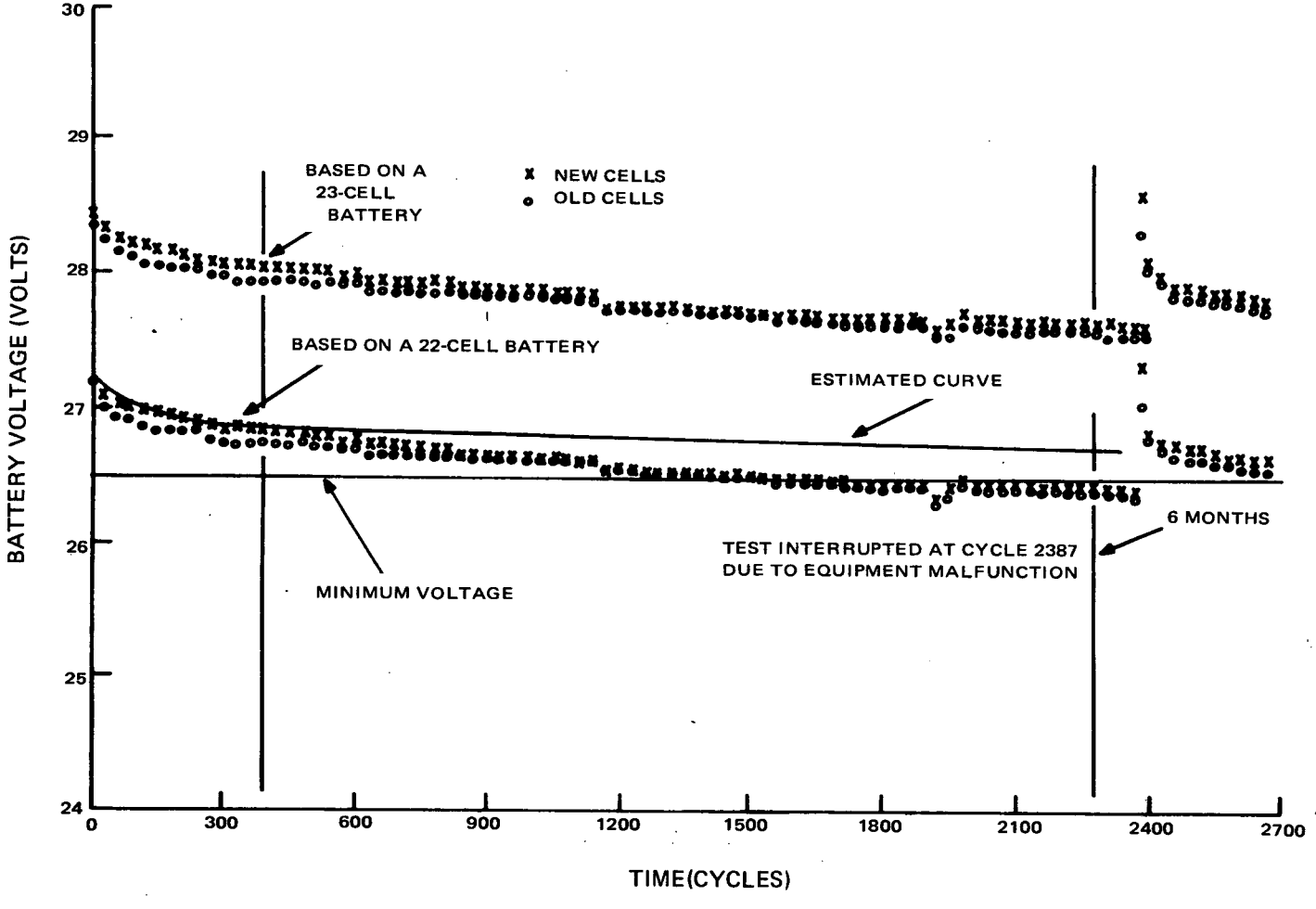

Figure B-2. Battery End-of-Discharge Voltage Versus Life Cycling

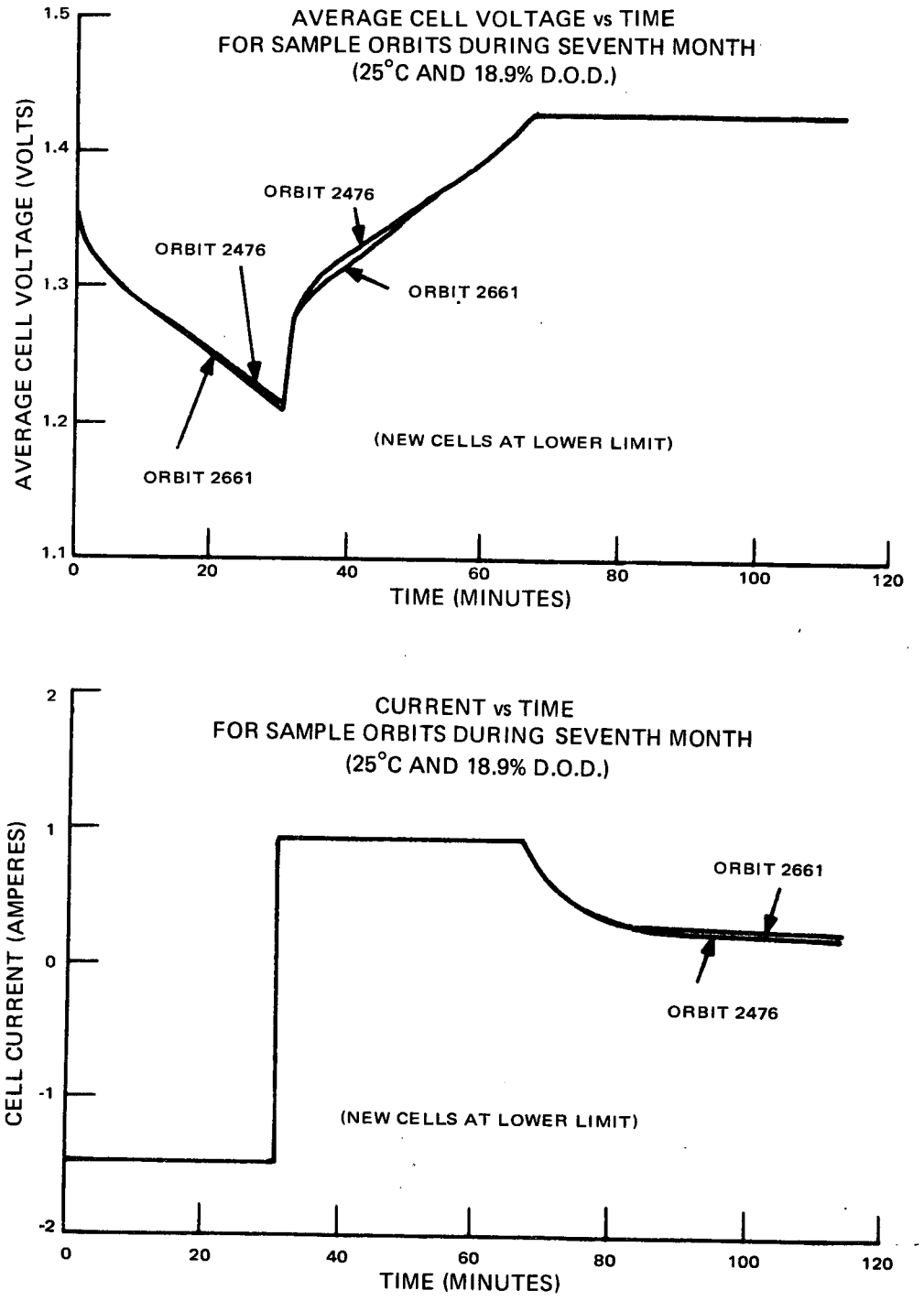

Figure B-3. Cell Current and Average Cell Voltage Versus Time (New Cells Tested-Orbit Cycles 2476 and 2661)

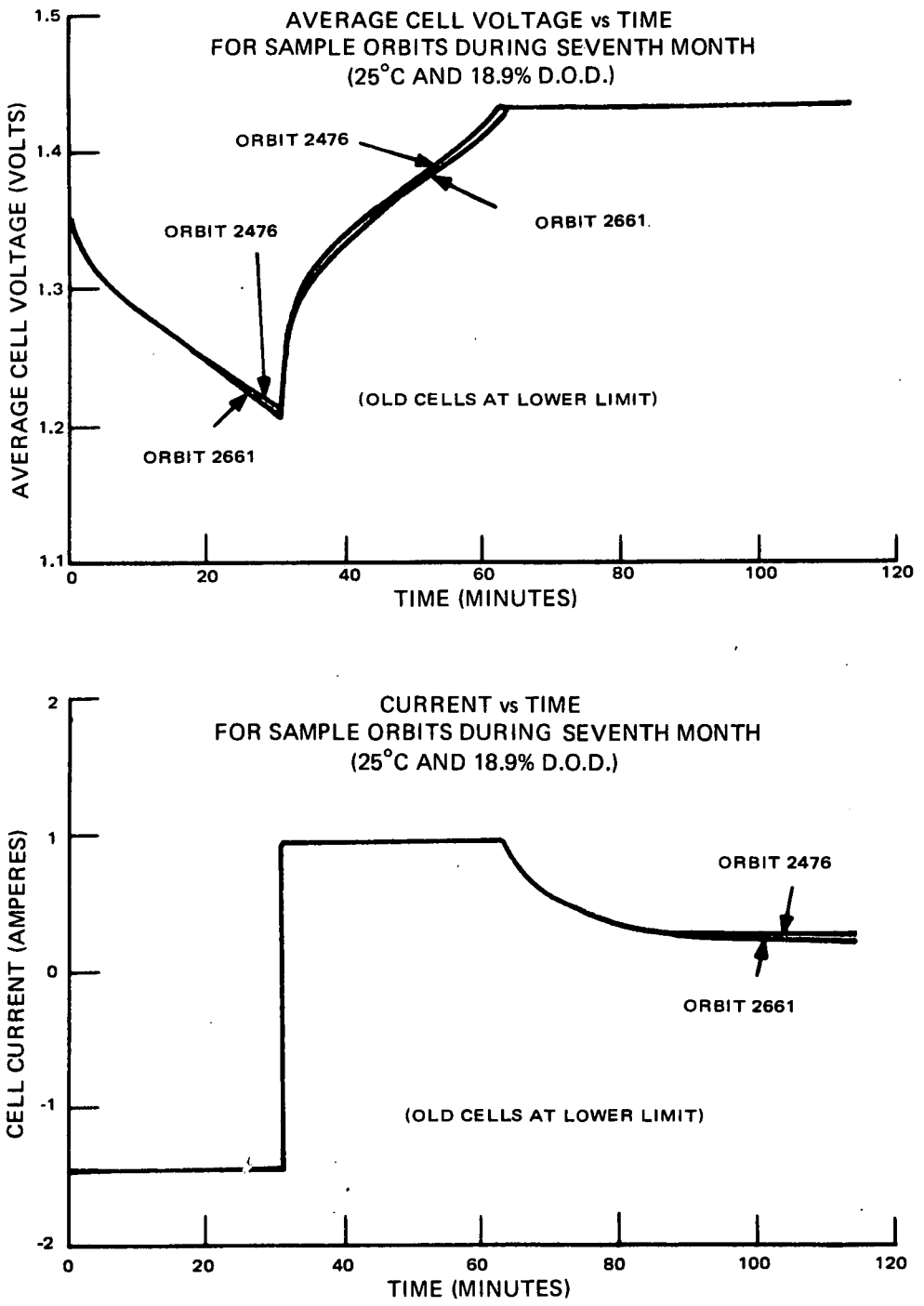

Figure B-4. Cell Current and Average Cell Voltage Versus Time (Old Cells Tested-Orbit Cycles 2476 and 2661)

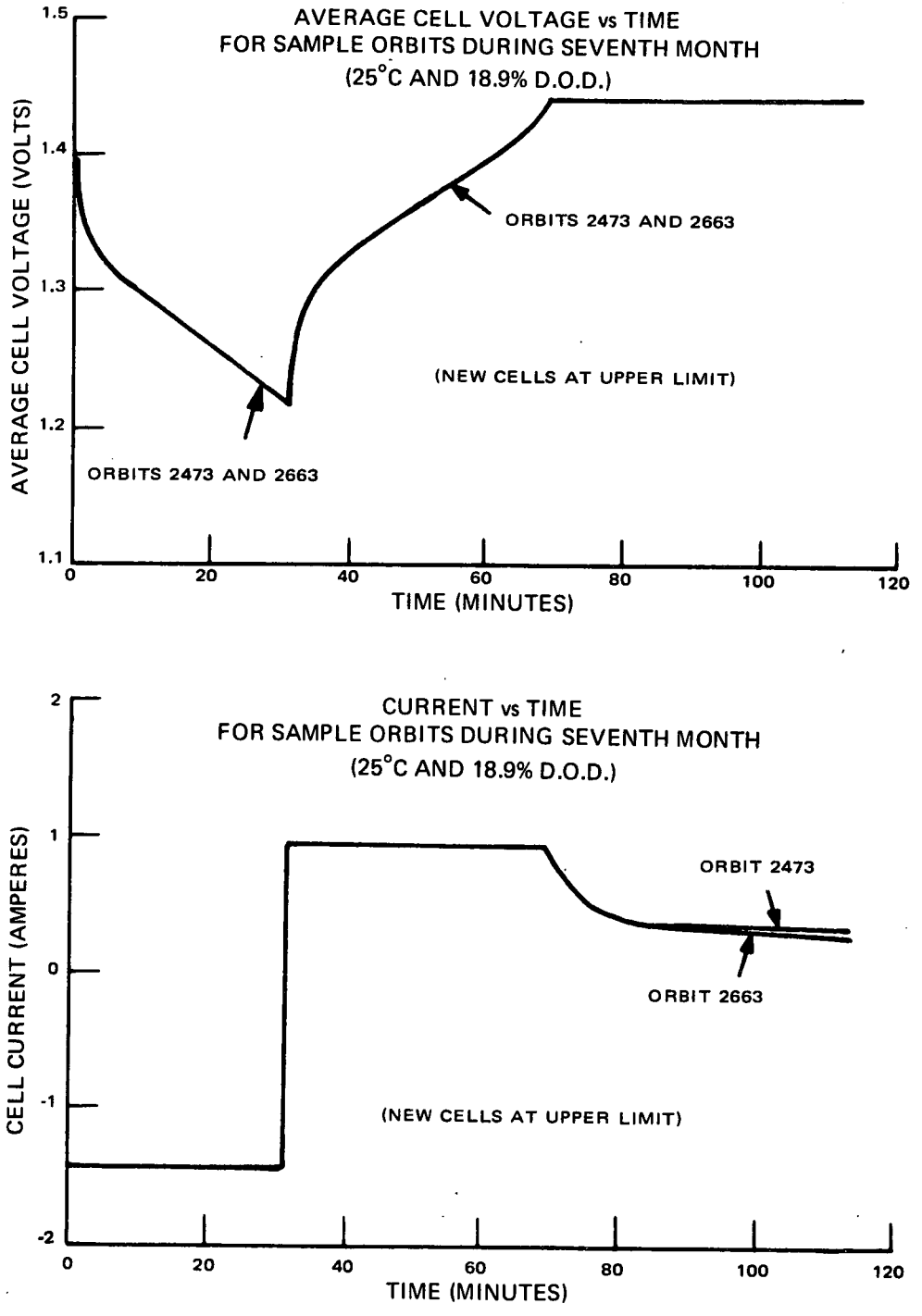

Figure B-5. Cell Current and Average Cell Voltage Versus Time (New Cells Tested-Orbit Cycles 2473 and 2663)

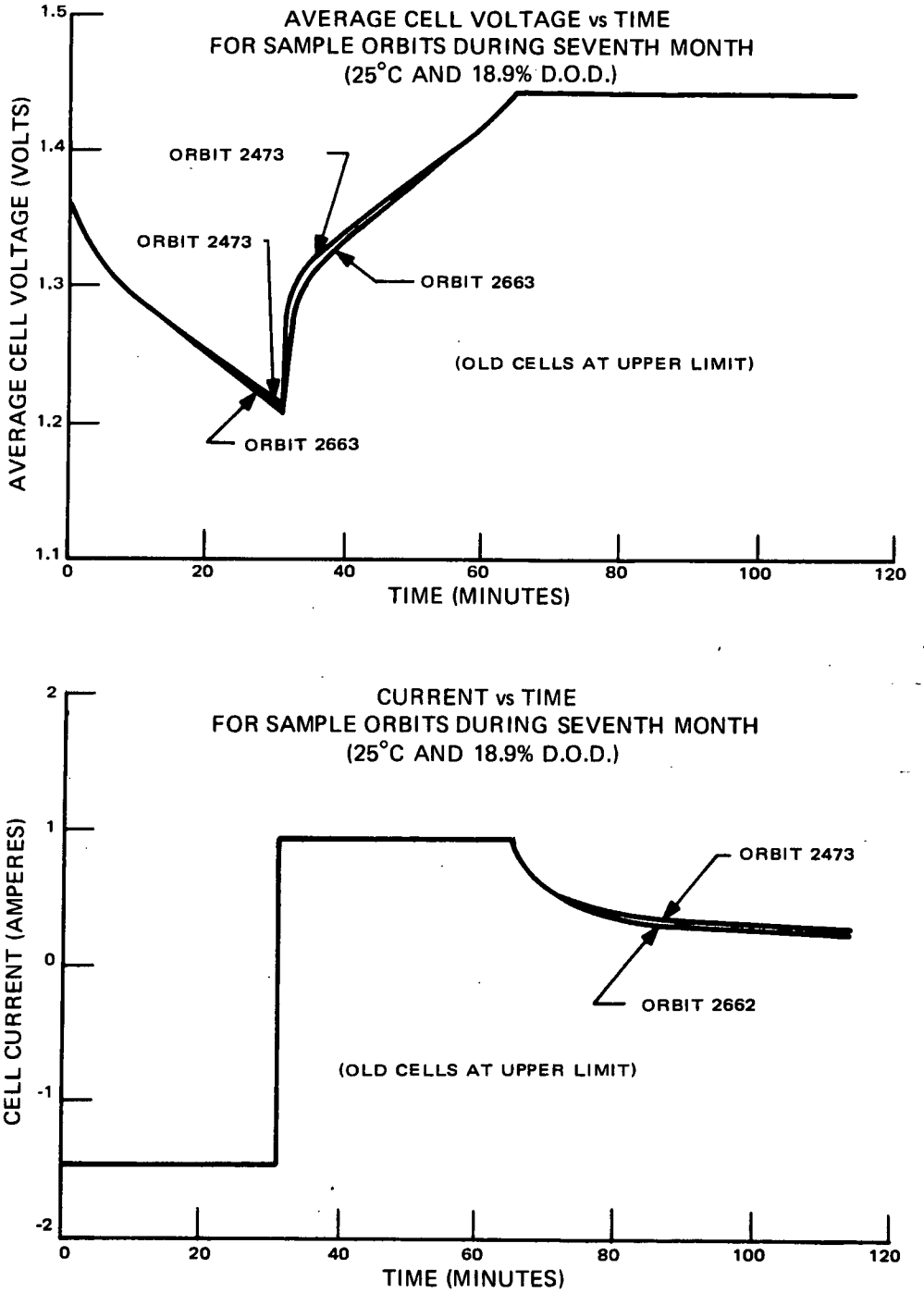

Figure B-6. Cell Current and Average Cell Voltage Versus Time (Old Cells Tested-Orbit Cycles 2473 and 2663)

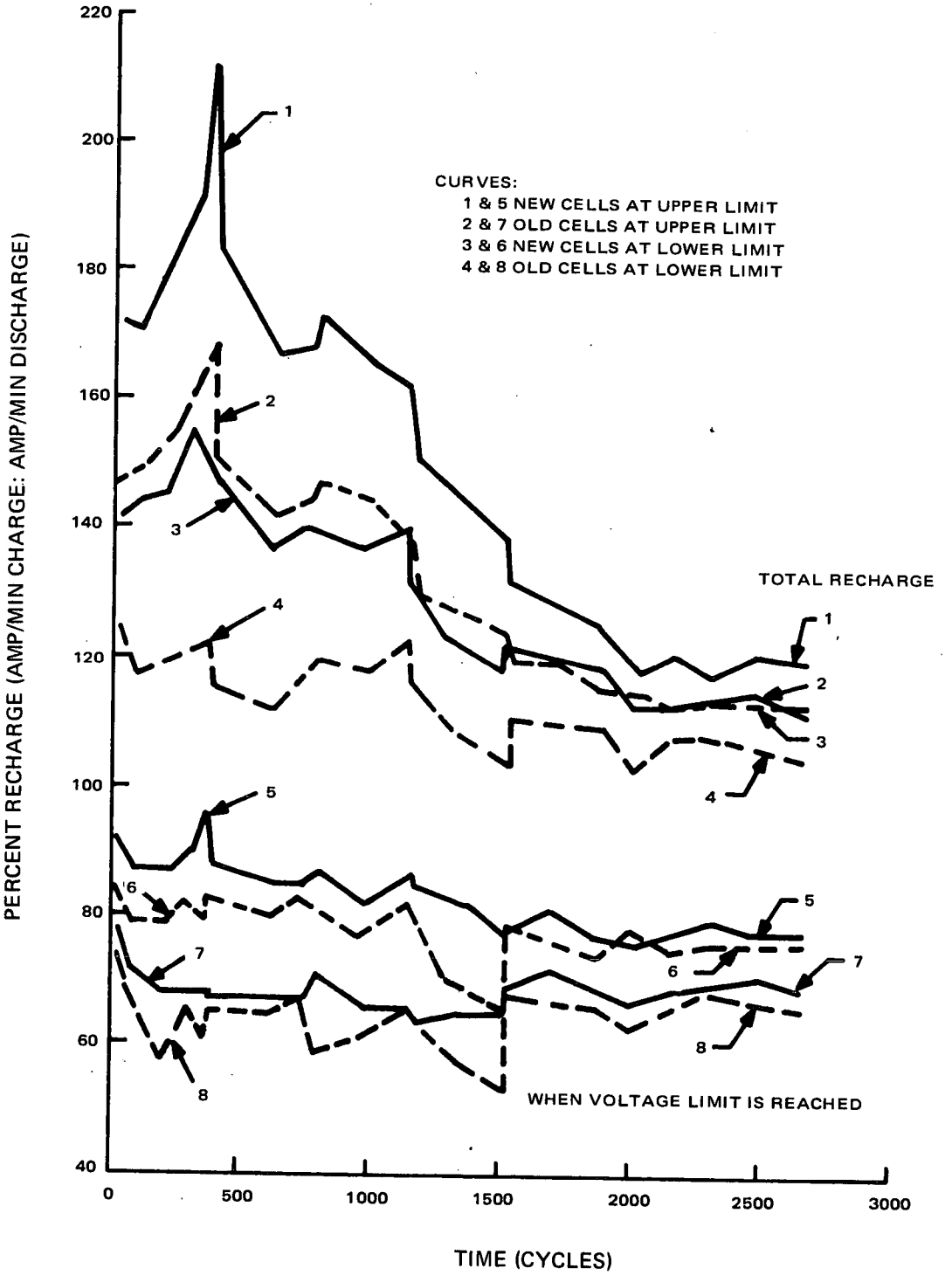

Figure B-7. Percent Recharge Versus Sample Cycling at Lower and Upper Voltage Limits

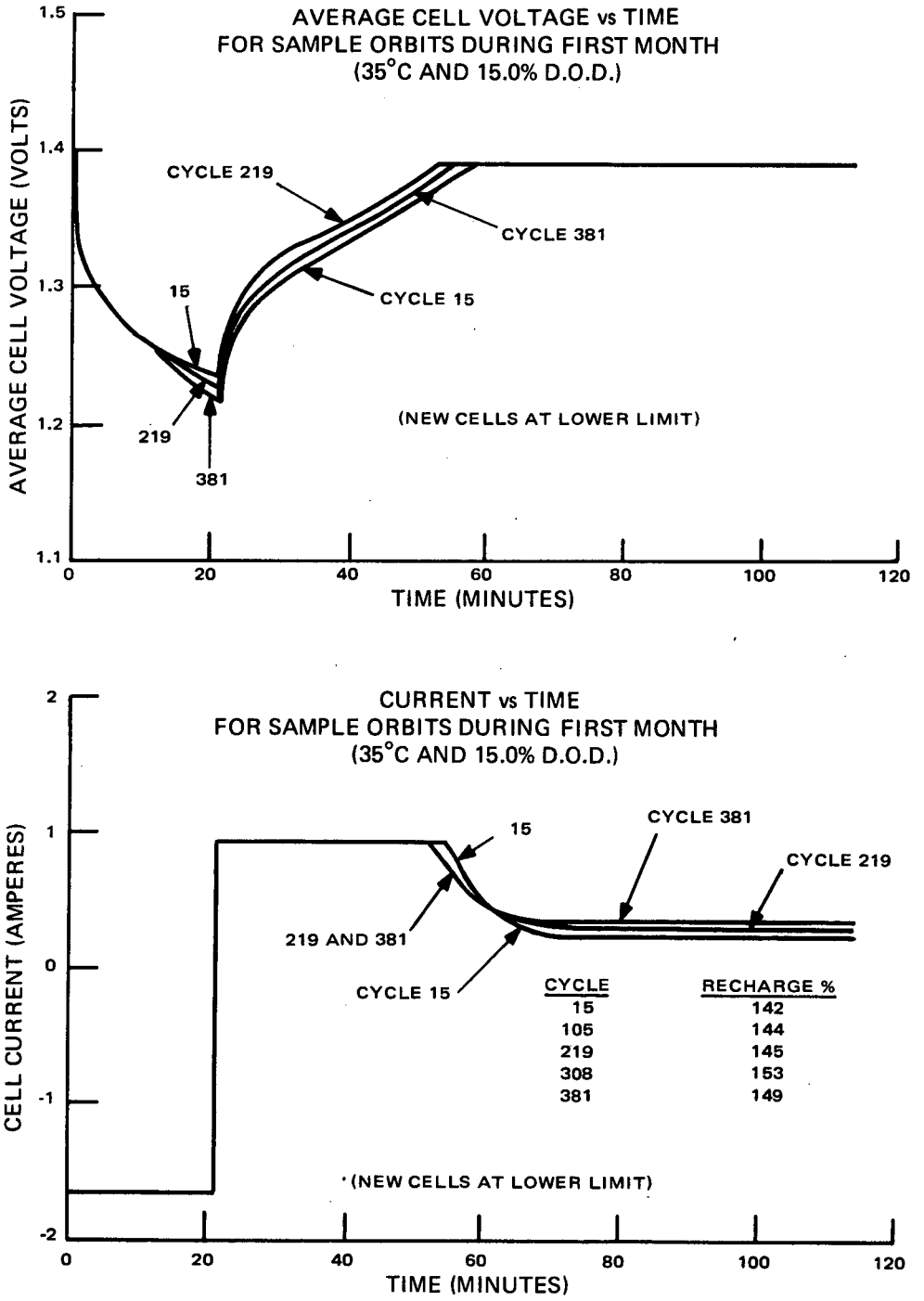

Figure B-8. Cell Current and Average Cell Voltage Versus Time (New Cells Tested-Orbit Cycles 15, 219, and 381)

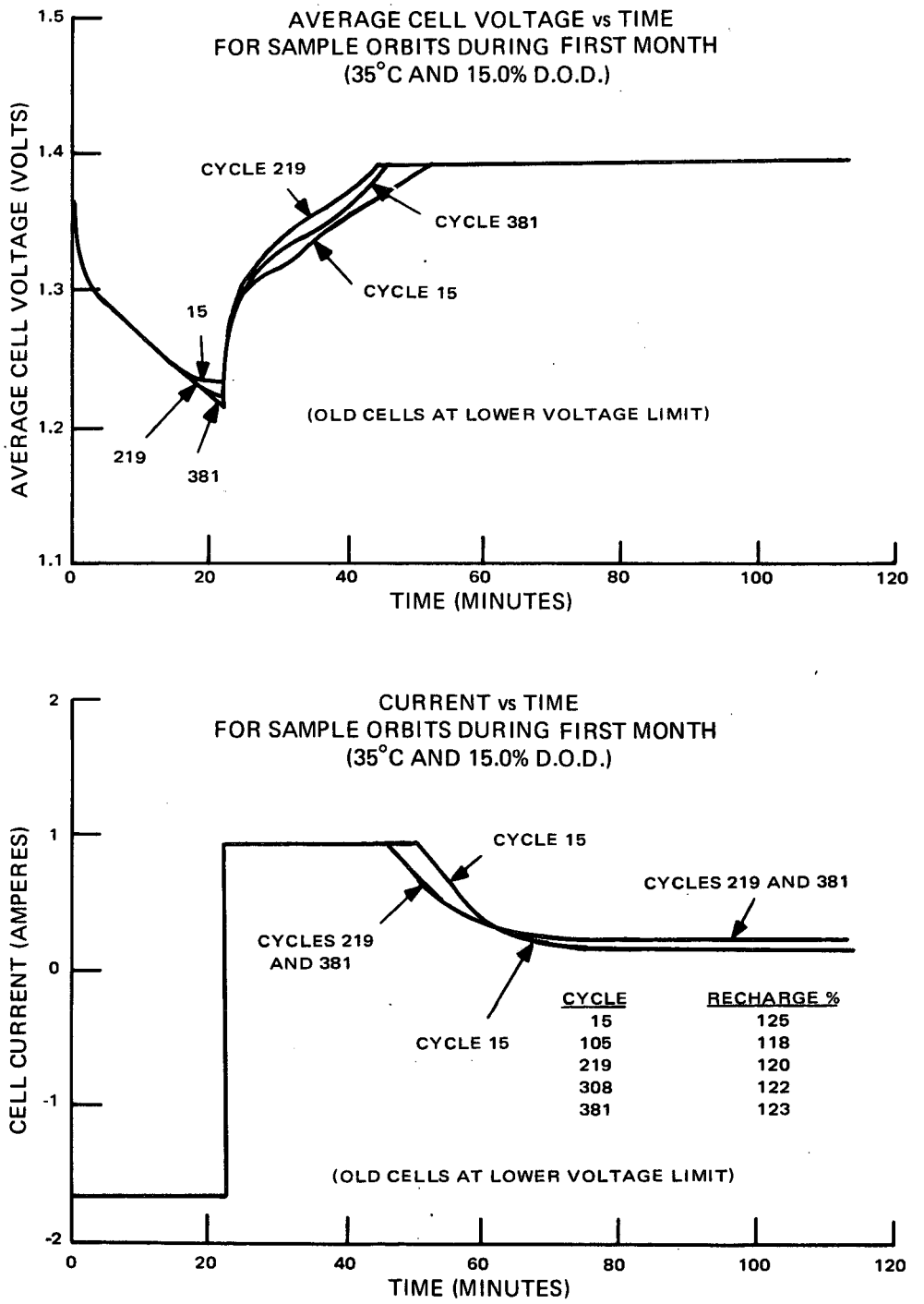

Figure B-9. Cell Current and Average Cell Voltage Versus Time (Old Cells Tested-Orbit Cycles 15, 219, and 381)

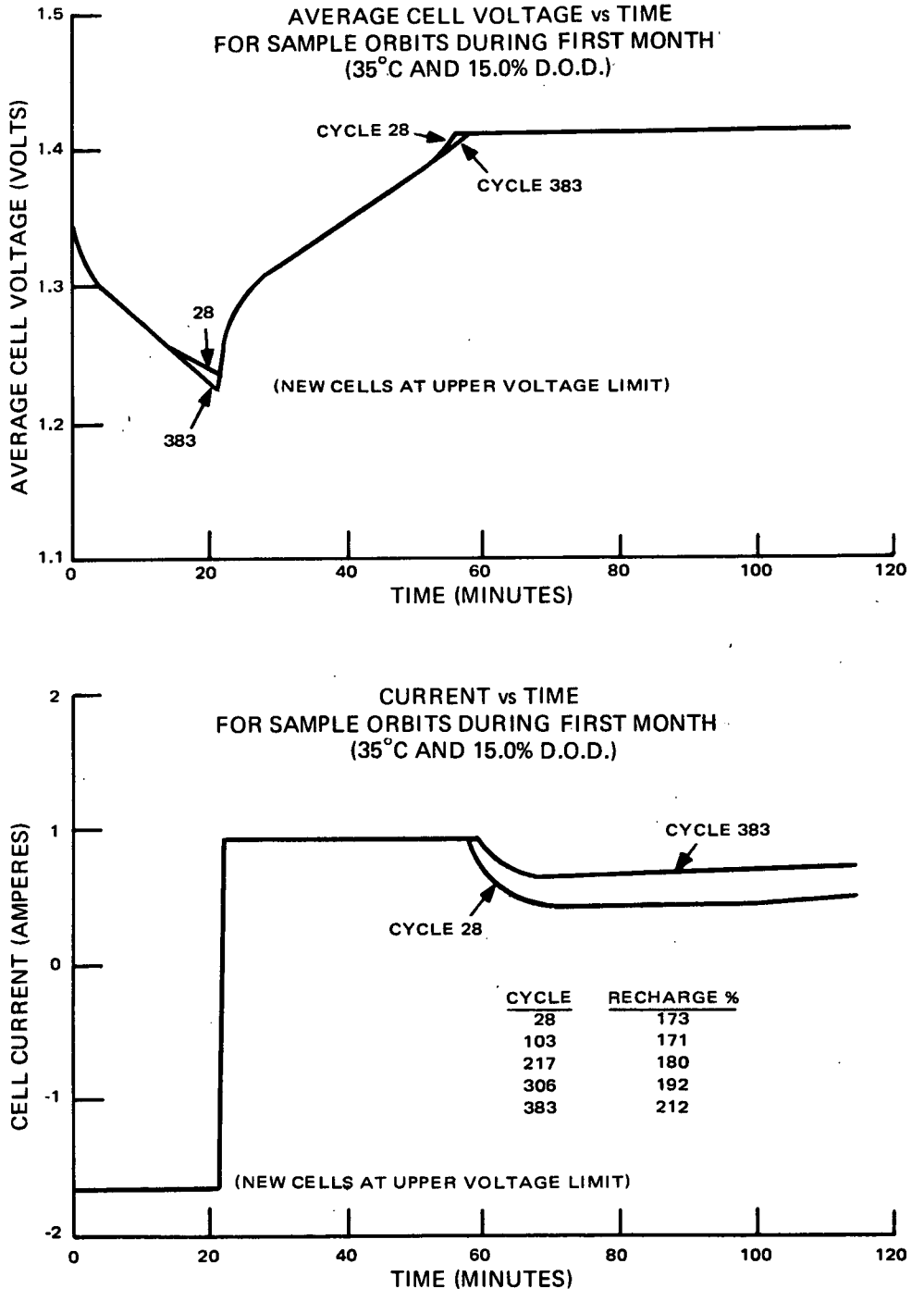

Figure B-10. Cell Current and Average Cell Voltage Versus Time (New Cells Tested-Orbit Cycles 28 and 383)

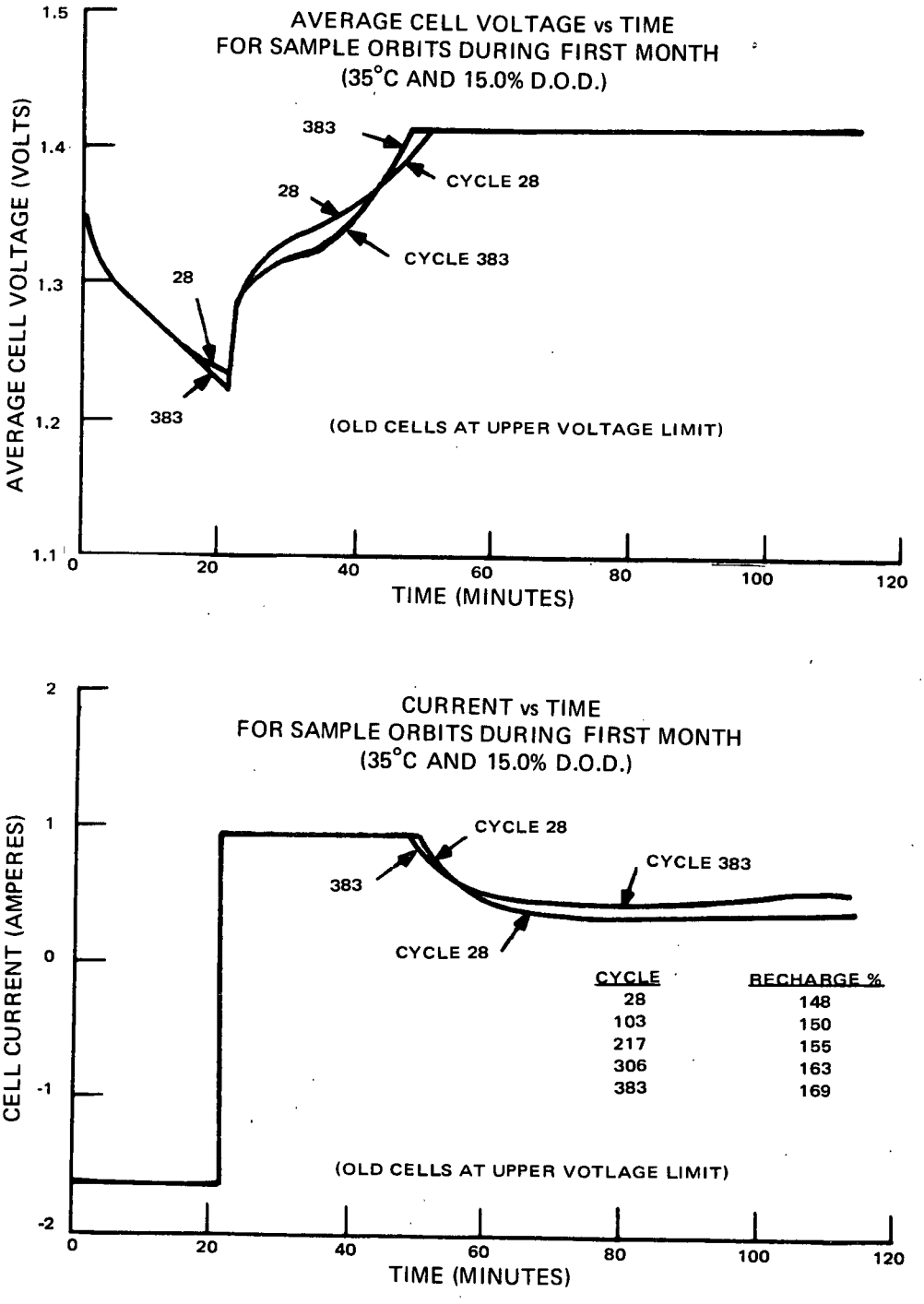

Figure B-11. Cell Current and Average Cell Voltage Versus Time (Old Cells Tested-Orbit Cycles 28 and 383)

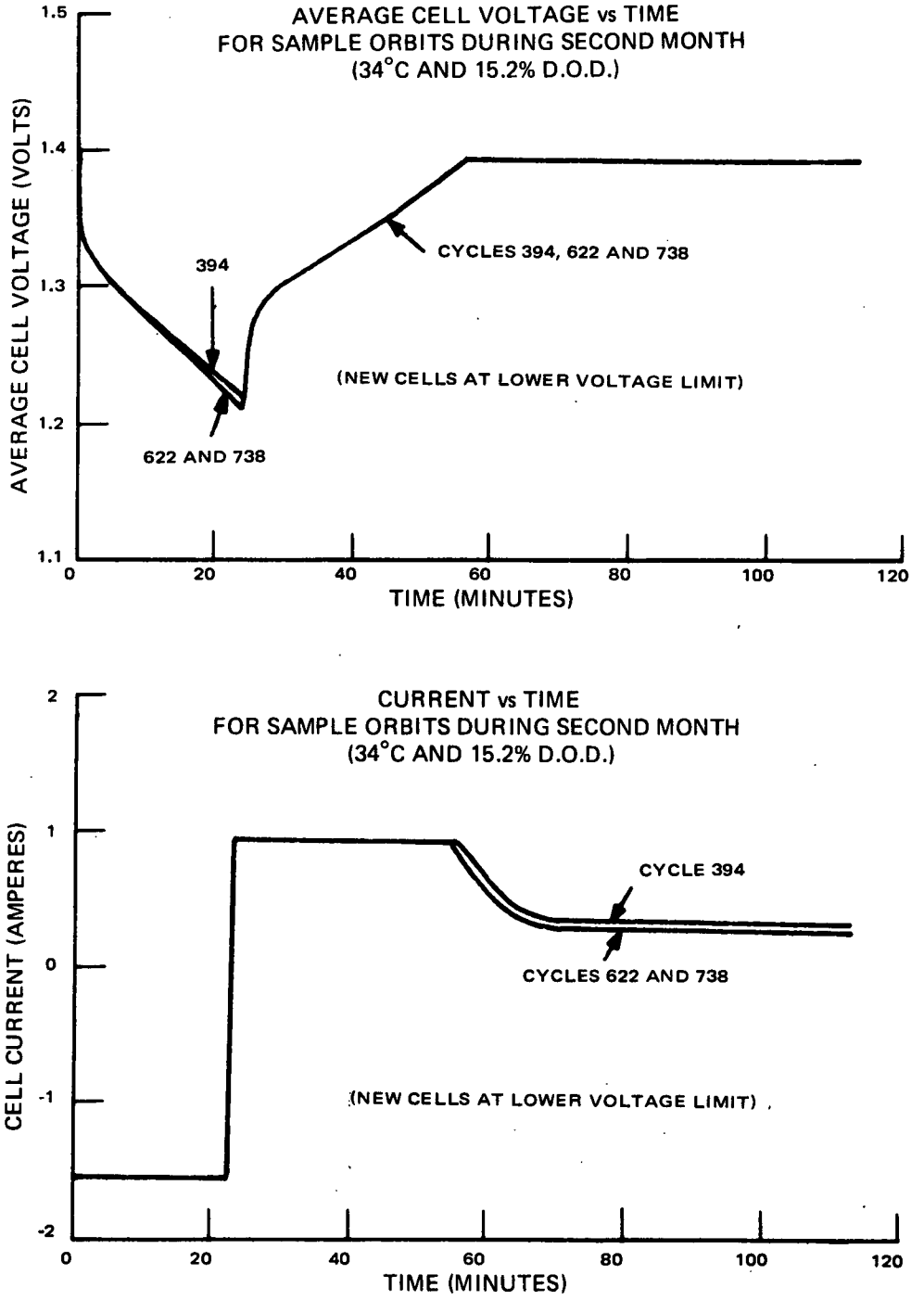

Figure B-12. Cell Current and Average Cell Voltage Versus Time (New Cells Tested-Orbit Cycles 394, 622, and 738)

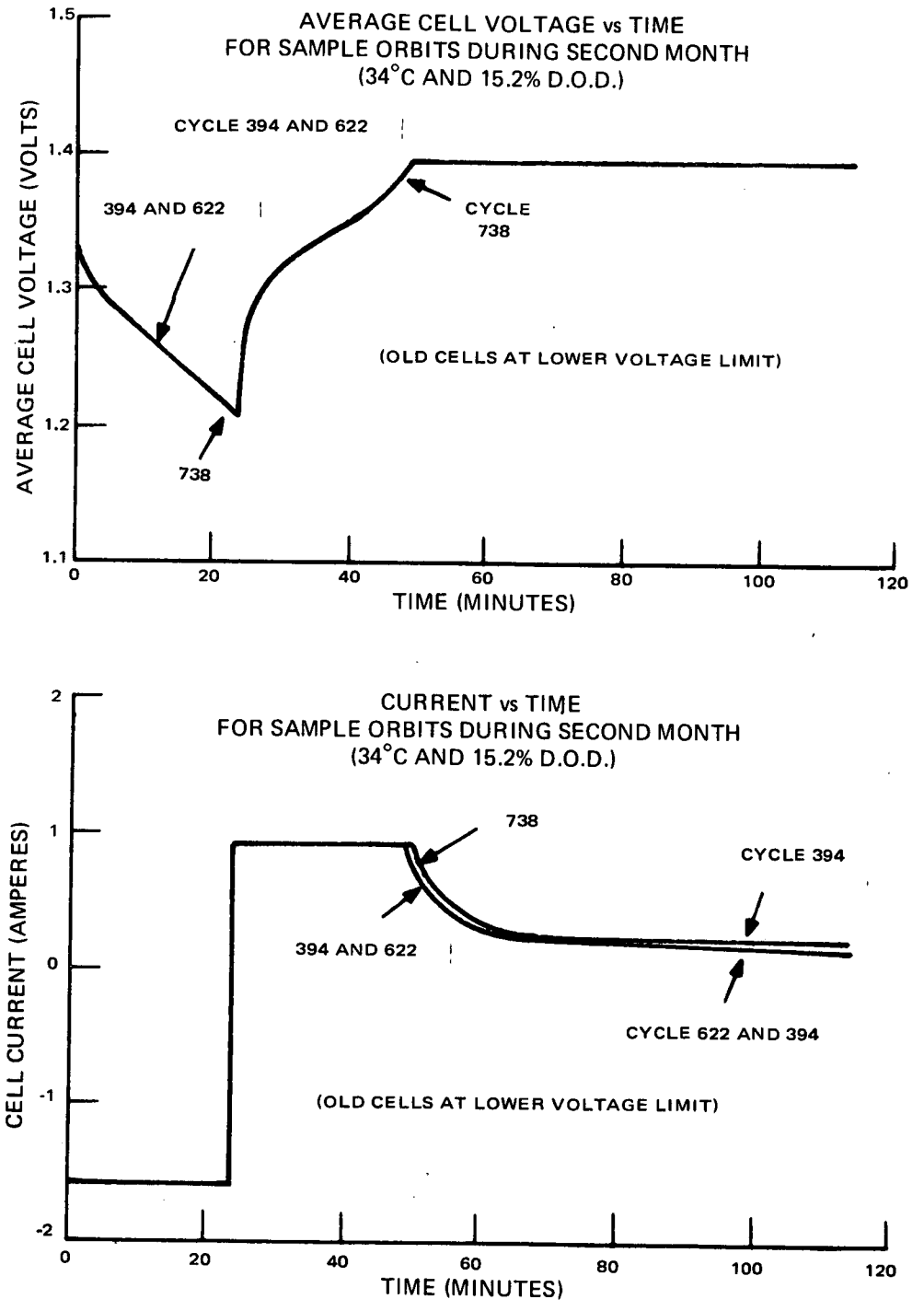

Figure B-13. Cell Current and Average Cell Voltage Versus Time (Old Cells Tested-Orbit Cycles 394, 622, and 738)

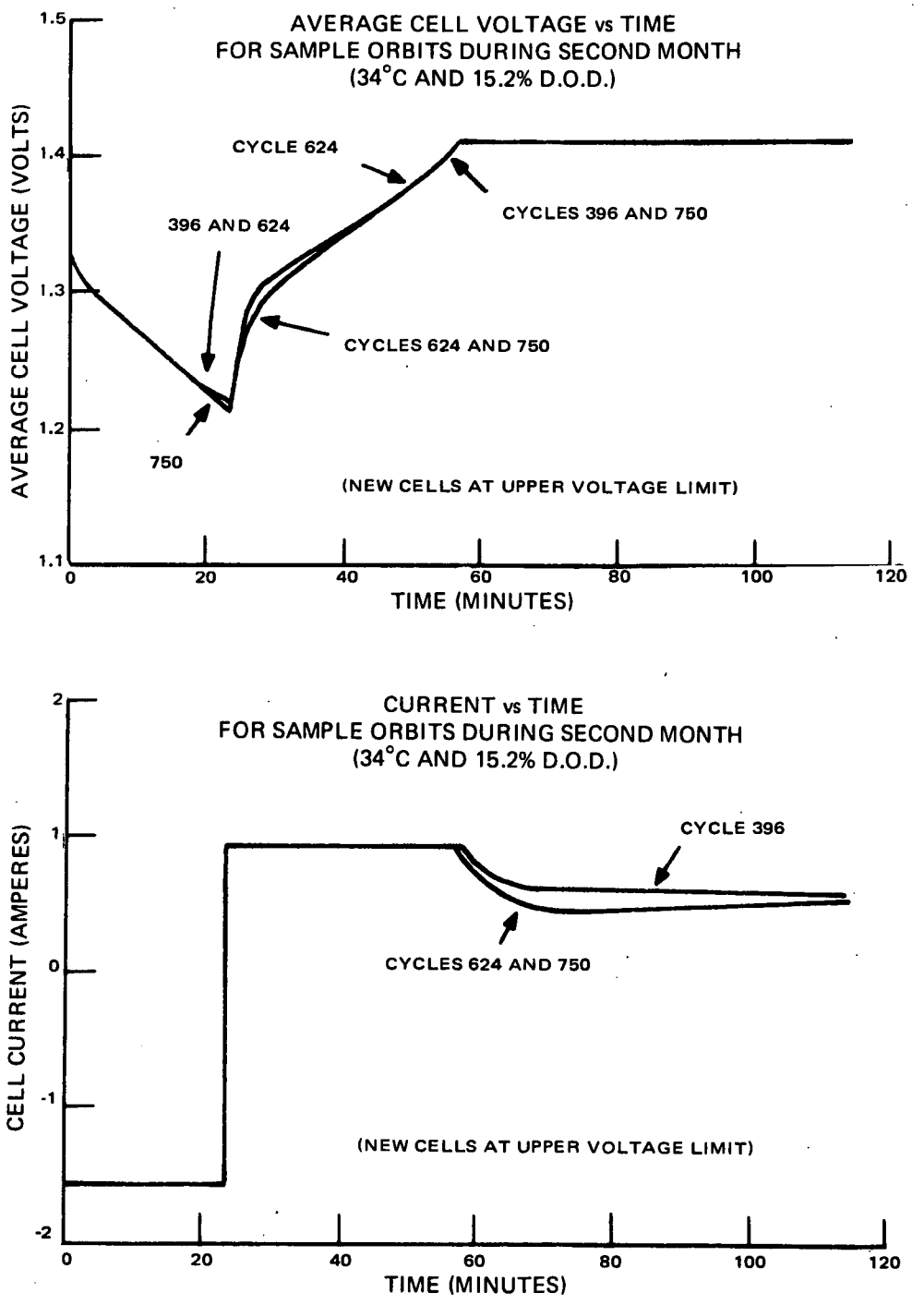

Figure B-14. Cell Current and Average Cell Voltage Versus Time (New Cells Tested-Orbit Cycles 396, 624, and 750)

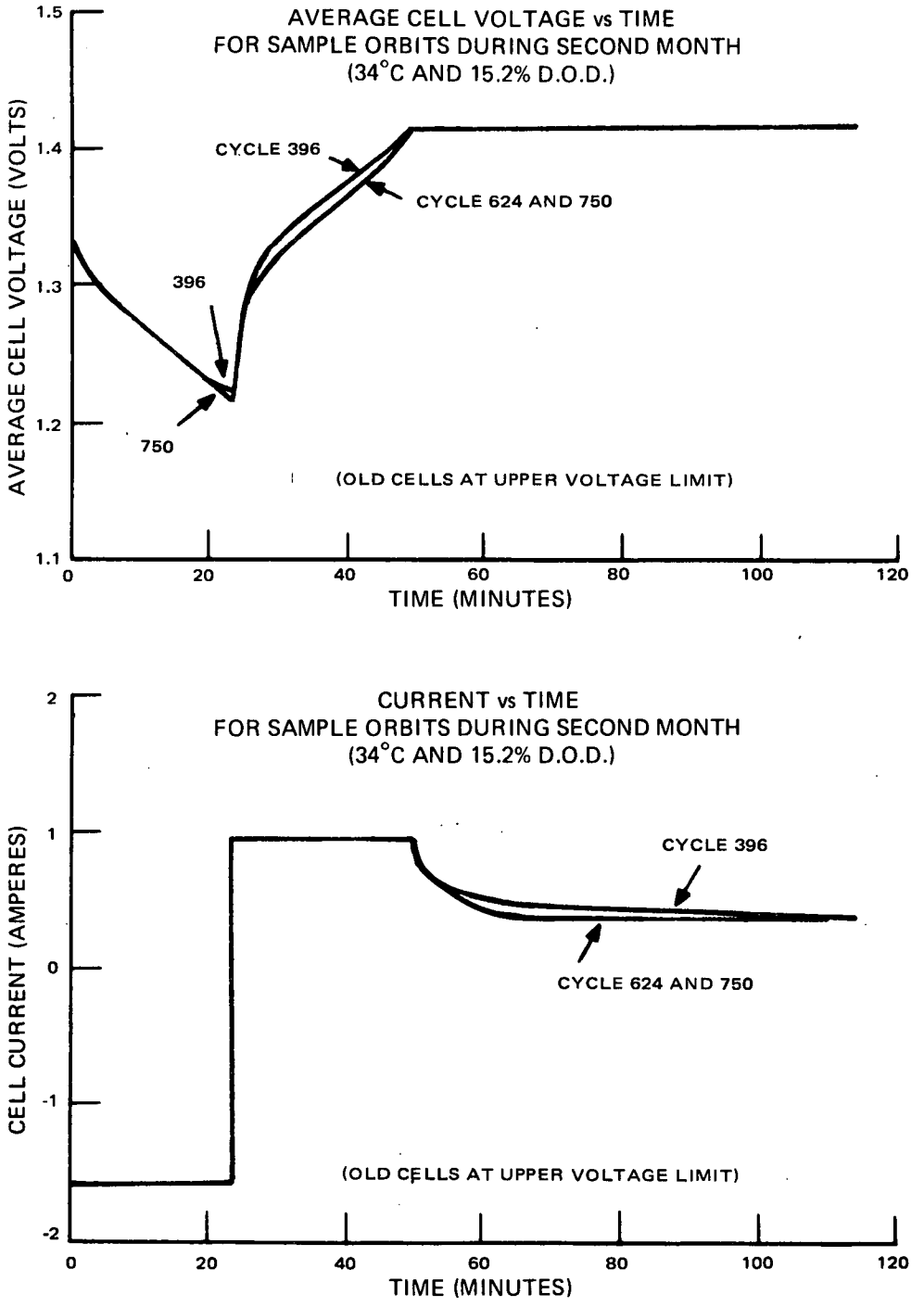

Figure B-15. Cell Current and Average Cell Voltage Versus Time (Old Cells Tested-Orbit Cycles 396, 624, and 750)

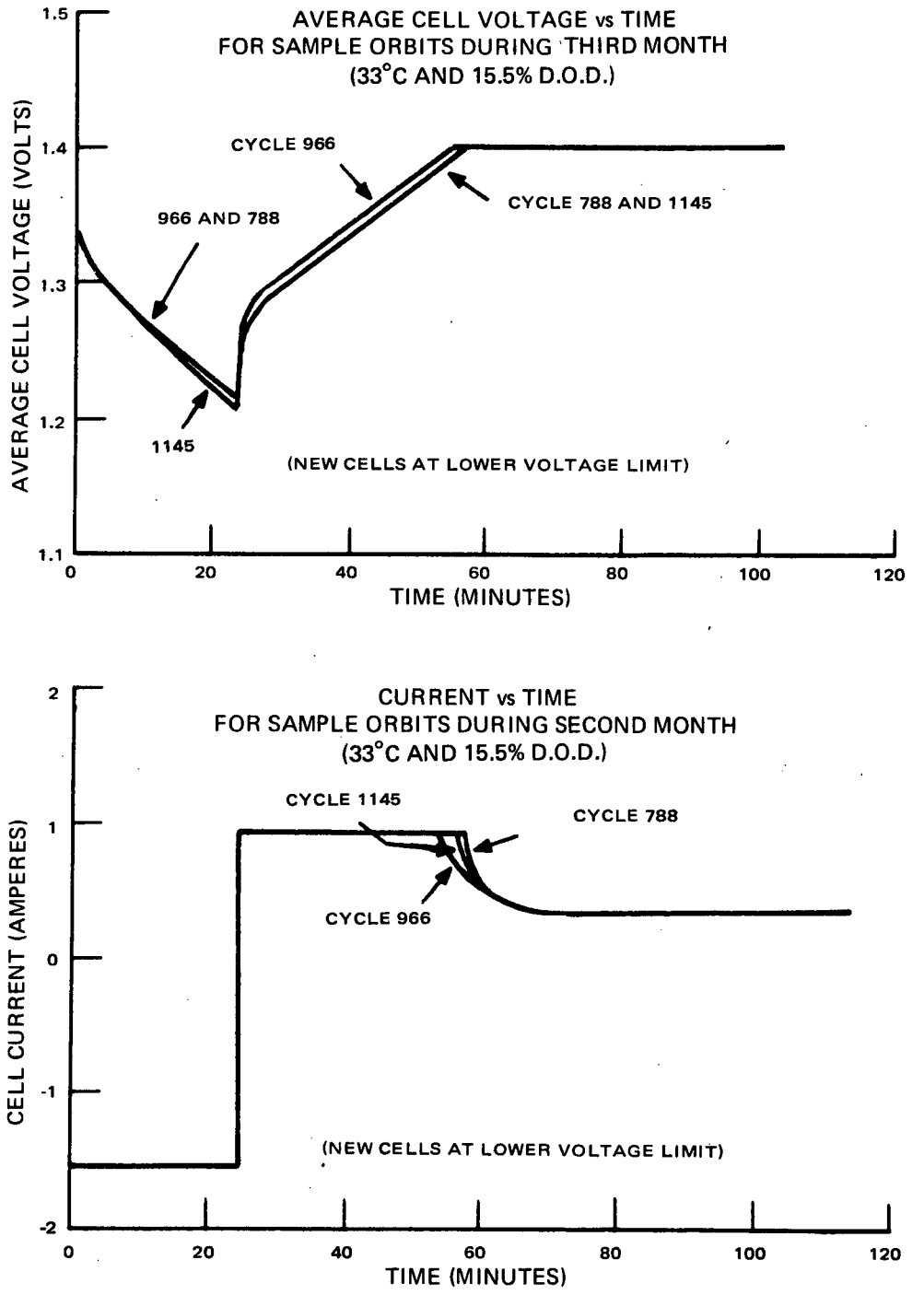

Figure B-16. Cell Current and Average Cell Voltage Versus Time (New Cells Tested-Orbit Cycles 788, 966, and 1145)

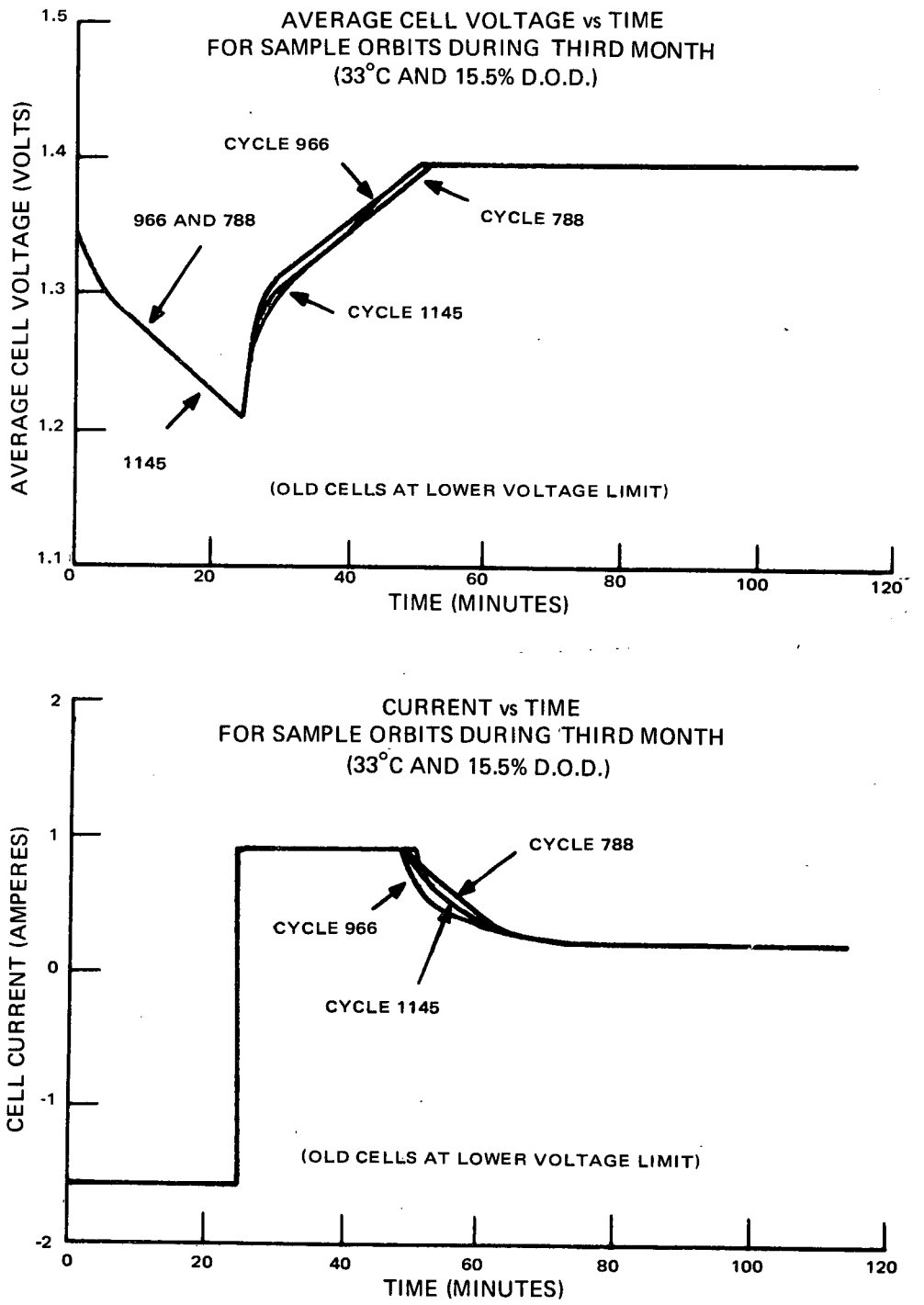

Figure B-17. Cell Current and Average Cell Voltage Versus Time (Old Cells Tested-Orbit Cycles 788, 966, and 1145)

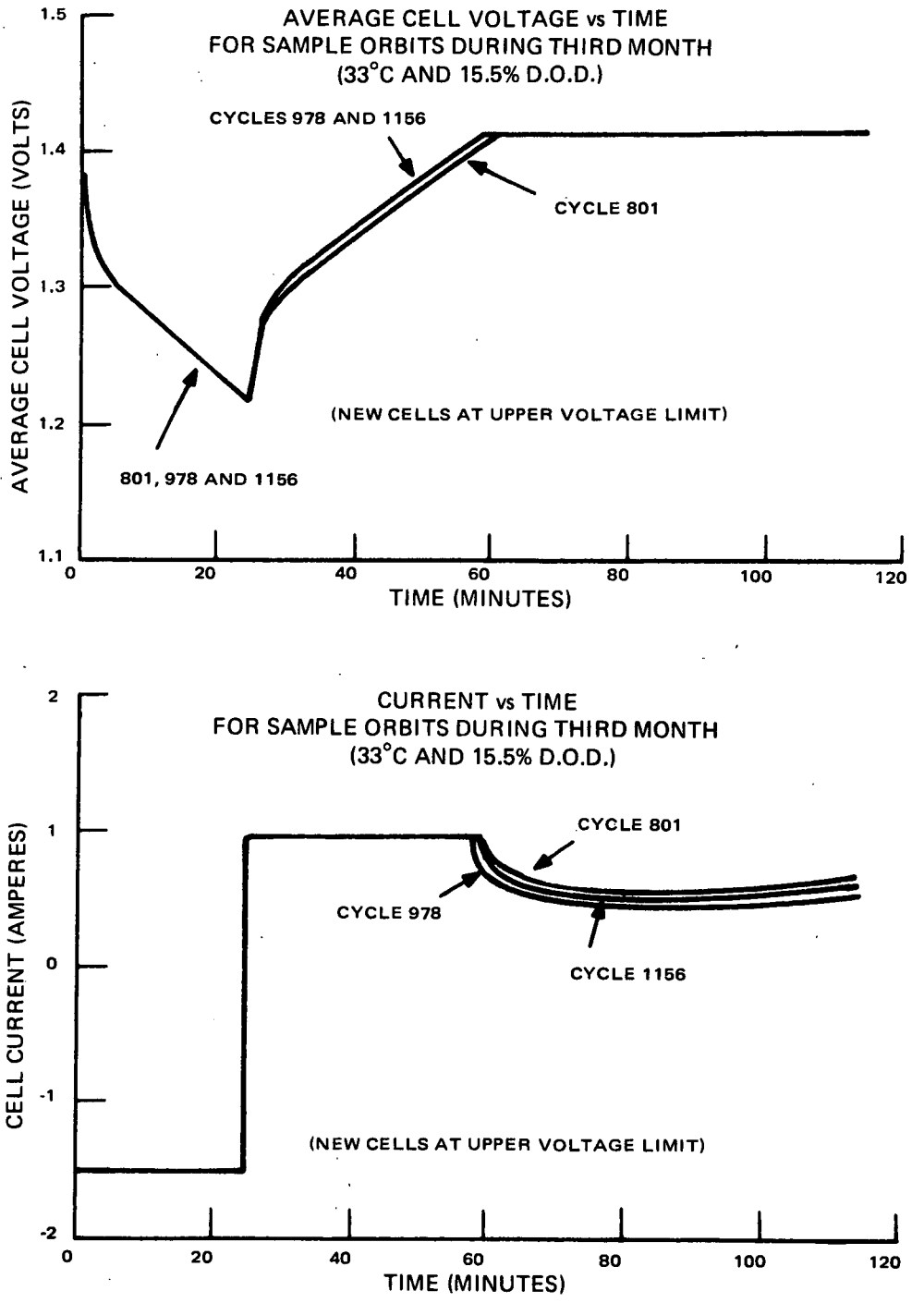

Figure B-18. Cell Current and Average Cell Voltage Versus Time (New Cells Tested-Orbit Cycles 801, 978, and 1156)

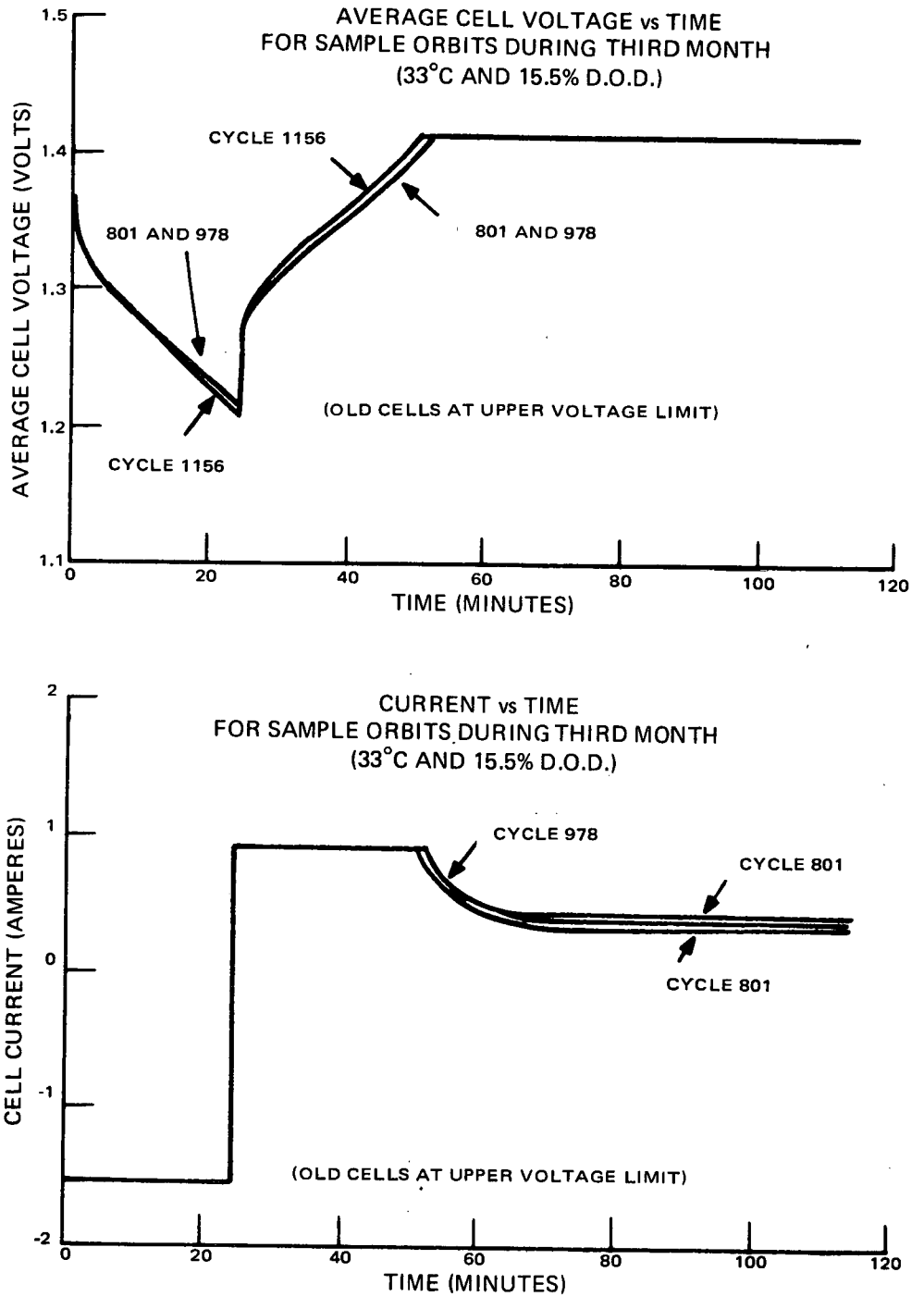

Figure B-19. Cell Current and Average Cell Voltage Versus Time (Old Cells Tested-Orbit Cycles 801, 978, and 1156)

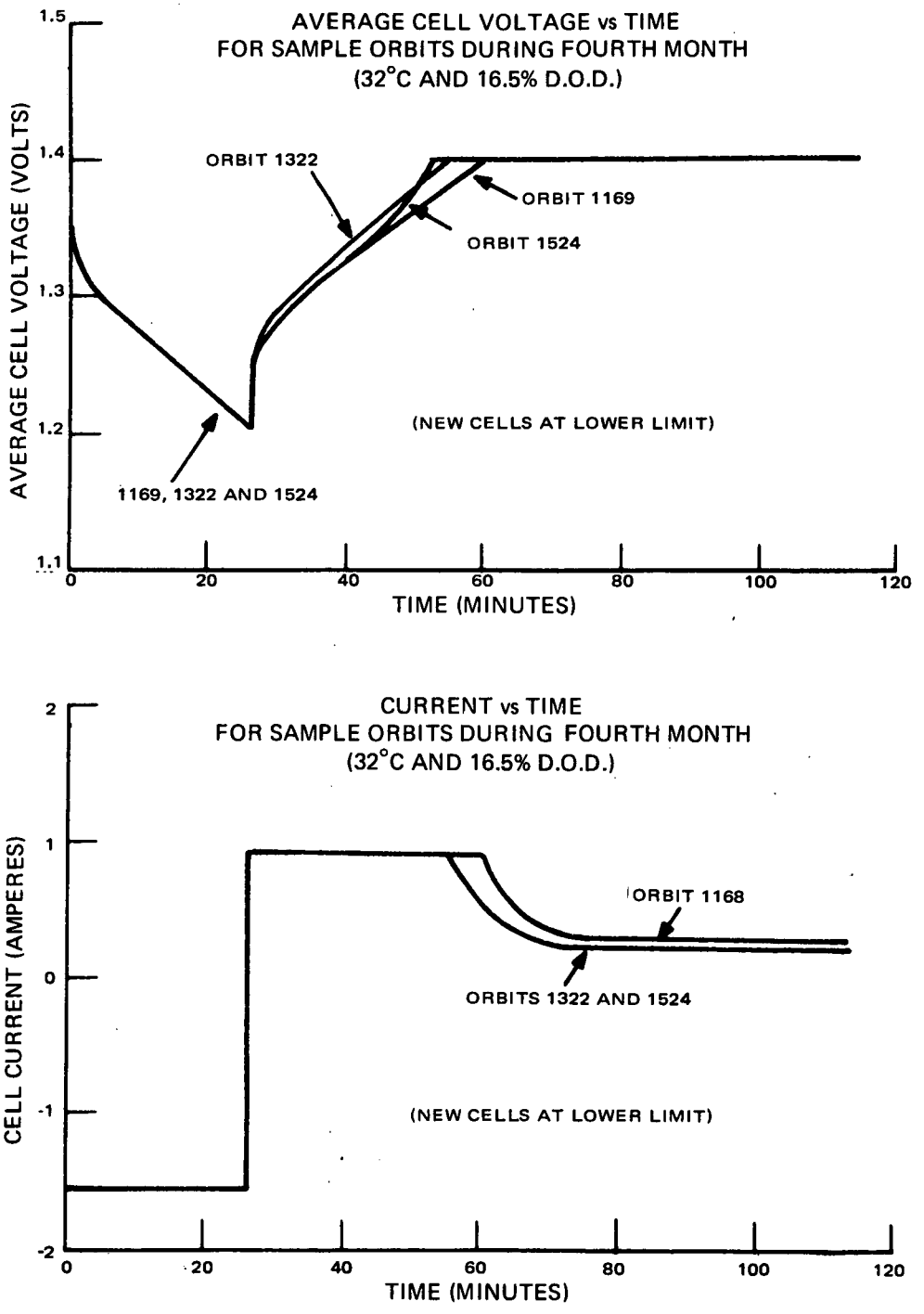

Figure B-20. Cell Current and Average Cell Voltage Versus Time (New Cells Tested-Orbit Cycles 1169, 1322, and 1524)

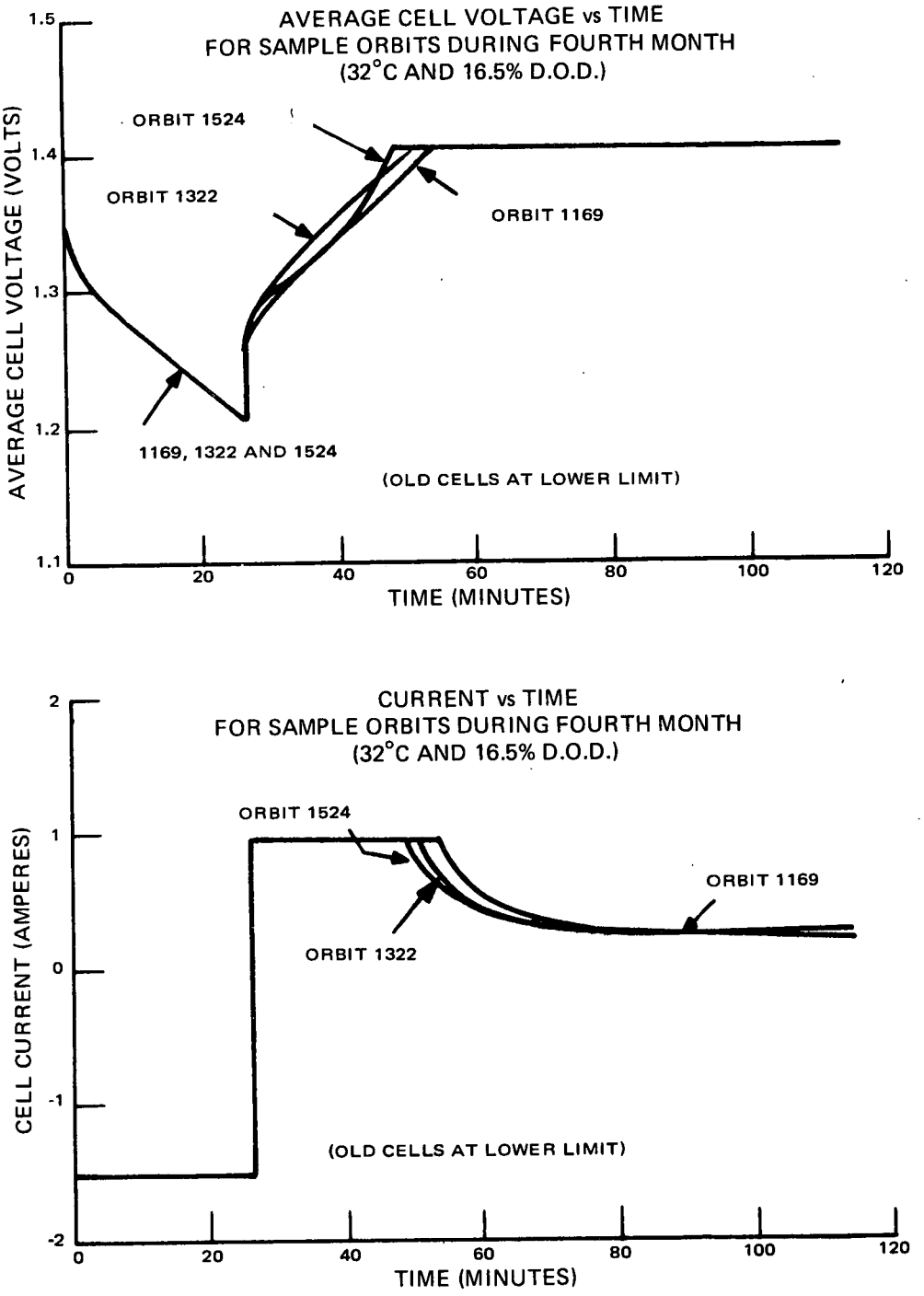

Figure B-21. Cell Current and Average Cell Voltage Versus Time (Old Cells Tested-Orbit Cycles 1169, 1322, and 1524)

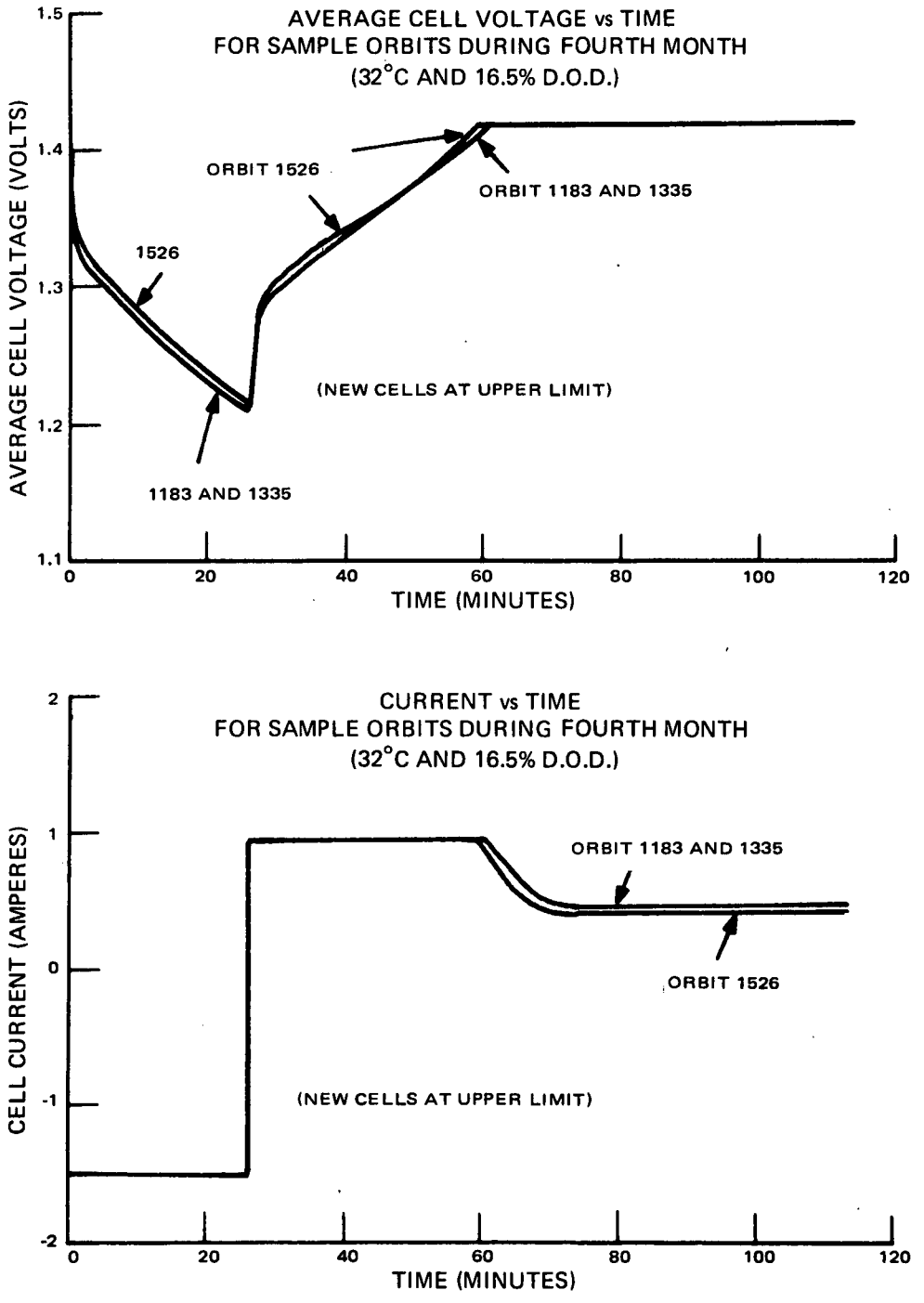

Figure B-22. Cell Current and Average Cell Voltage Versus Time (New Cells Tested-Orbit Cycles 1183, 1335, and 1526)

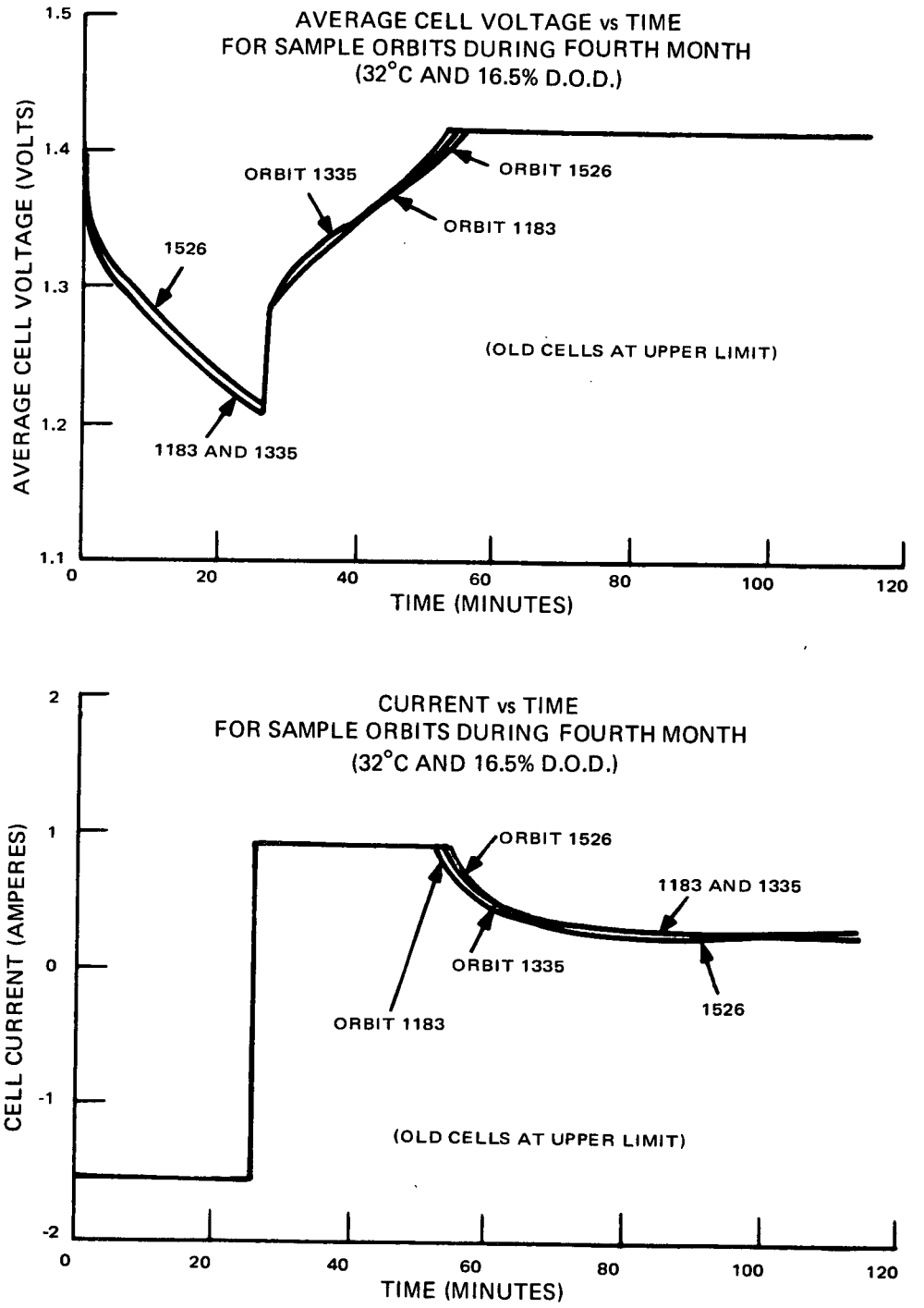

Figure B-23. Cell Current and Average Cell Voltage Versus Time (Old Cells Tested-Orbit Cycles 1183, 1335, and 1526)

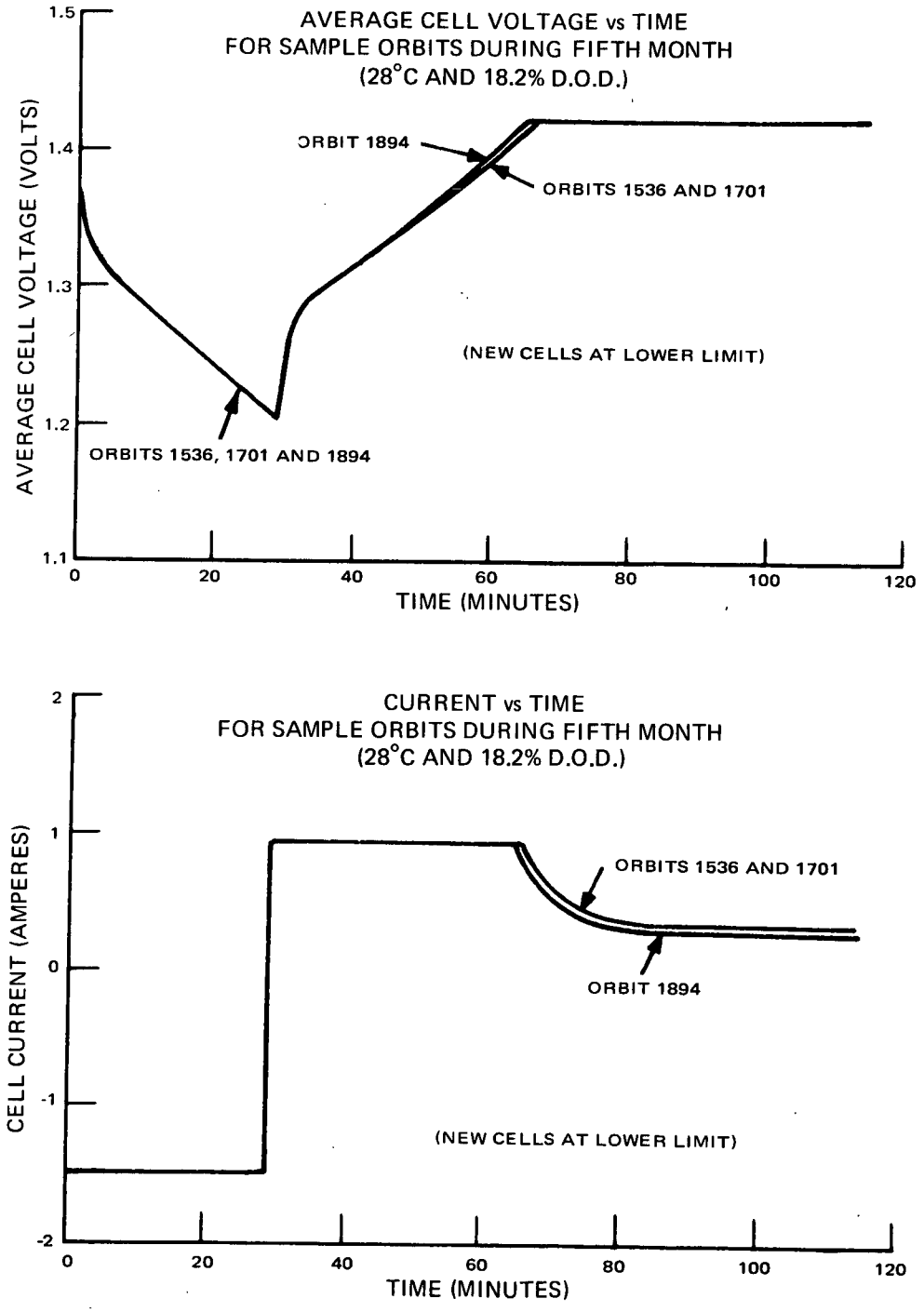

Figure B-24. Cell Current and Average Cell Voltage Versus Time (New Cells Tested-Orbit Cycles 1536, 1701, and 1894)

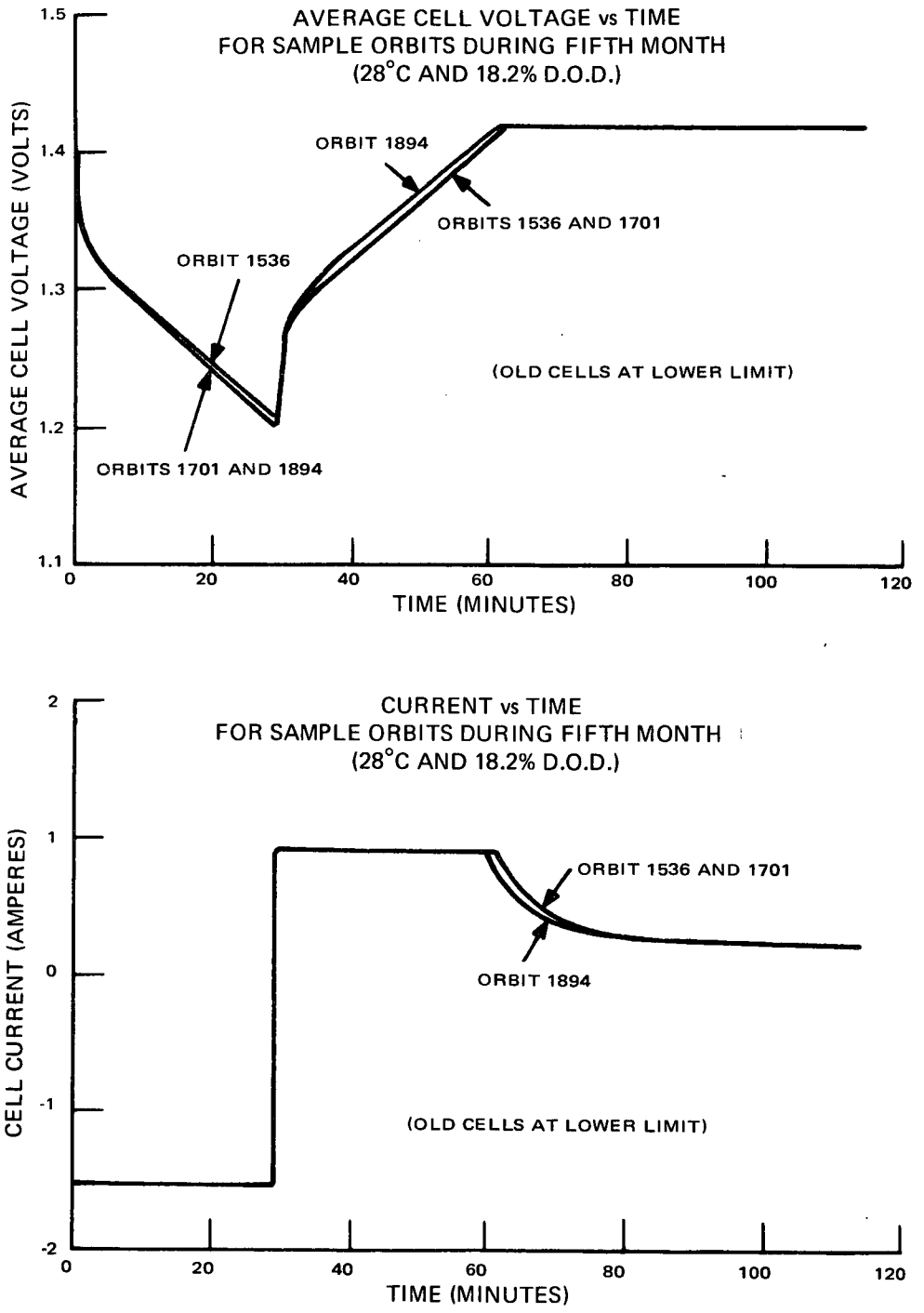

Figure B-25. Cell Current and Average Cell Voltage Versus Time (Old Cells Tested-Orbit Cycles 1536, 1701, and 1894)

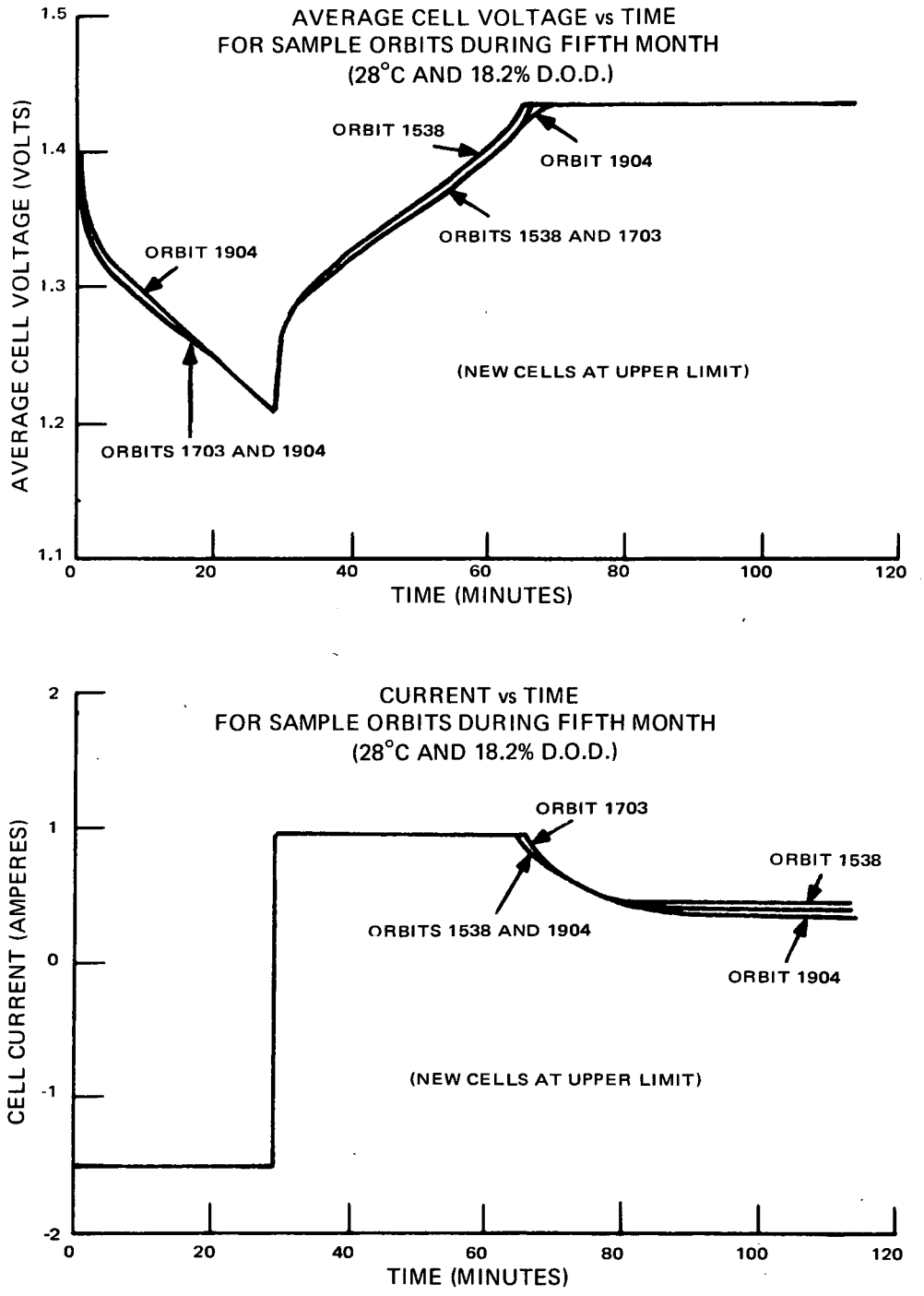

Figure B-26. Cell Current and Average Cell Voltage Versus Time (New Cells Tested-Orbit Cycles 1538, 1703, and 1904)

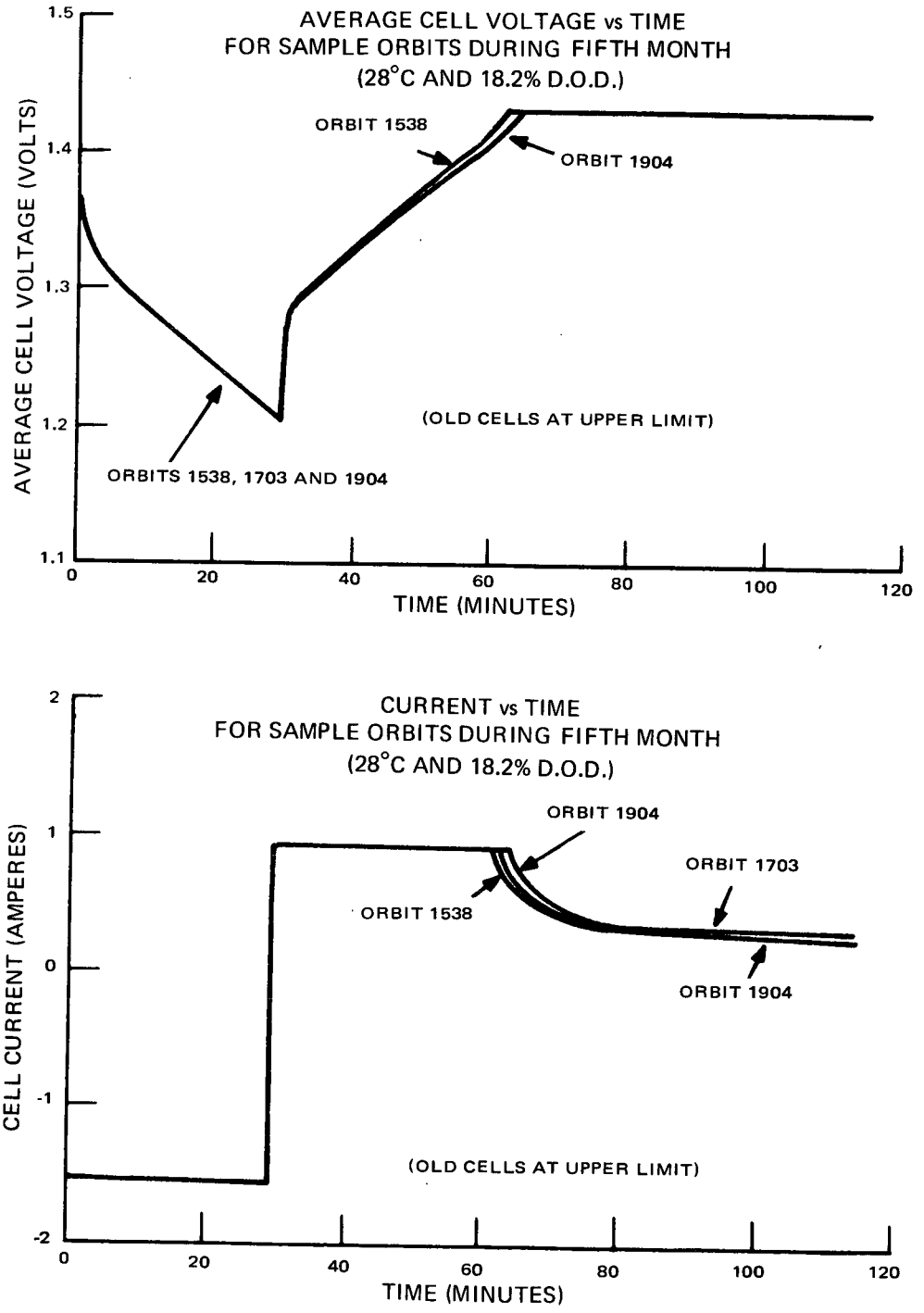

Figure B-27. Cell Current and Average Cell Voltage Versus Time (Old Cells Tested-Orbit Cycles 1538, 1703, and 1904)

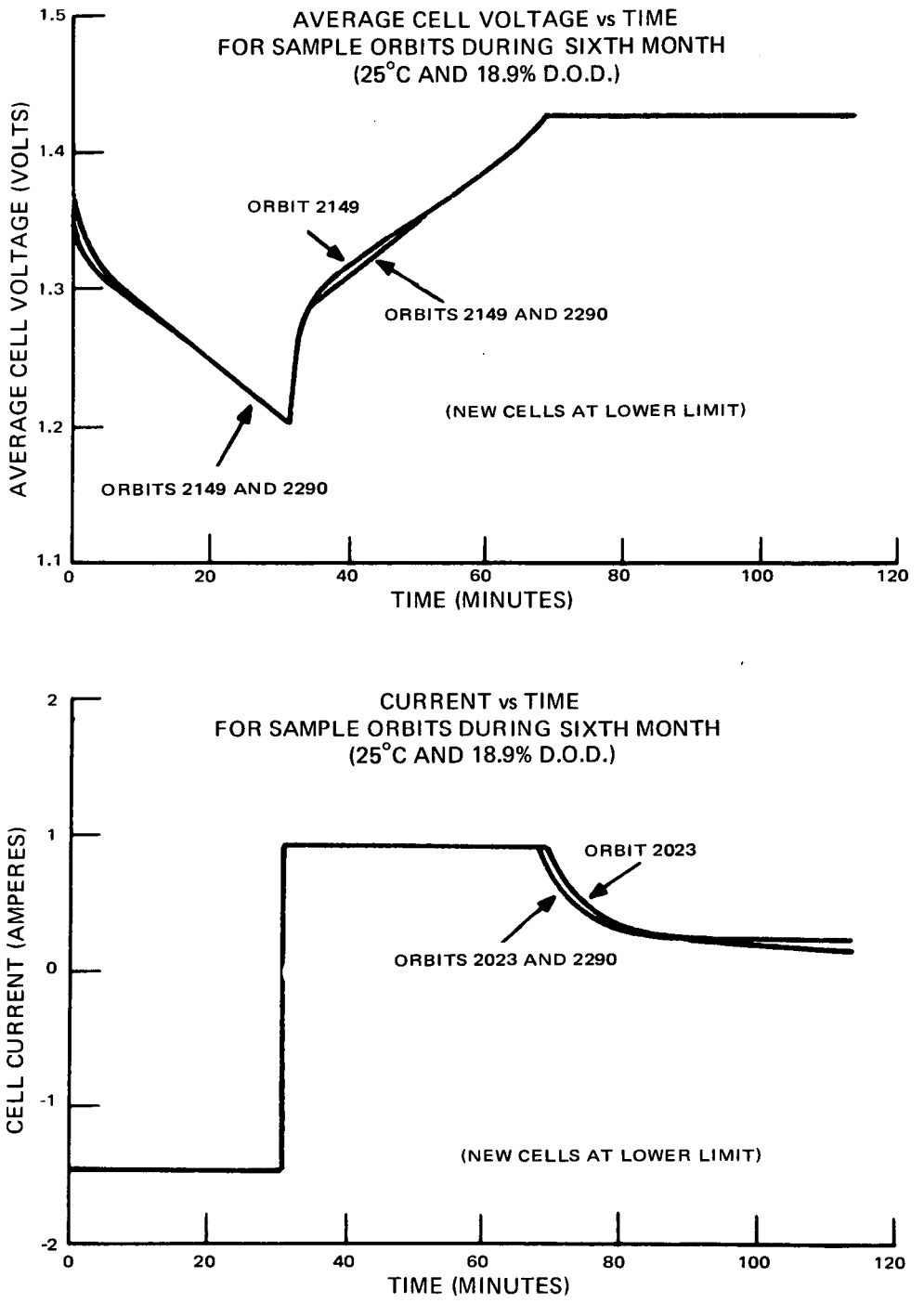

Figure B-28. Cell Current and Average Cell Voltage Versus Time (New Cells Tested-Orbit Cycles 2023, 2149, and 2290)

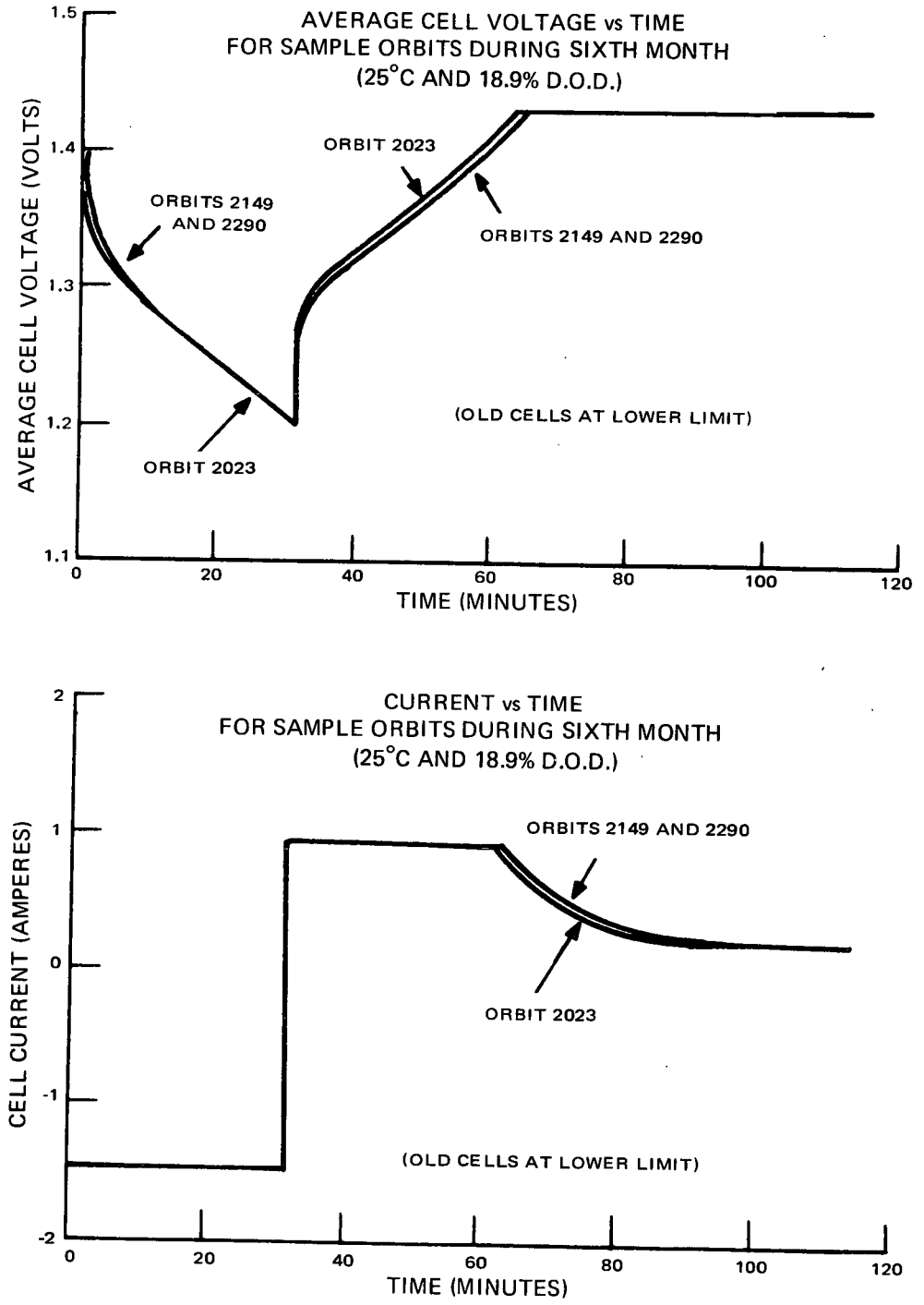

Figure B-29. Cell Current and Average Cell Voltage Versus Time (Old Cells Tested-Orbit Cycles 2023, 2149, and 2290)

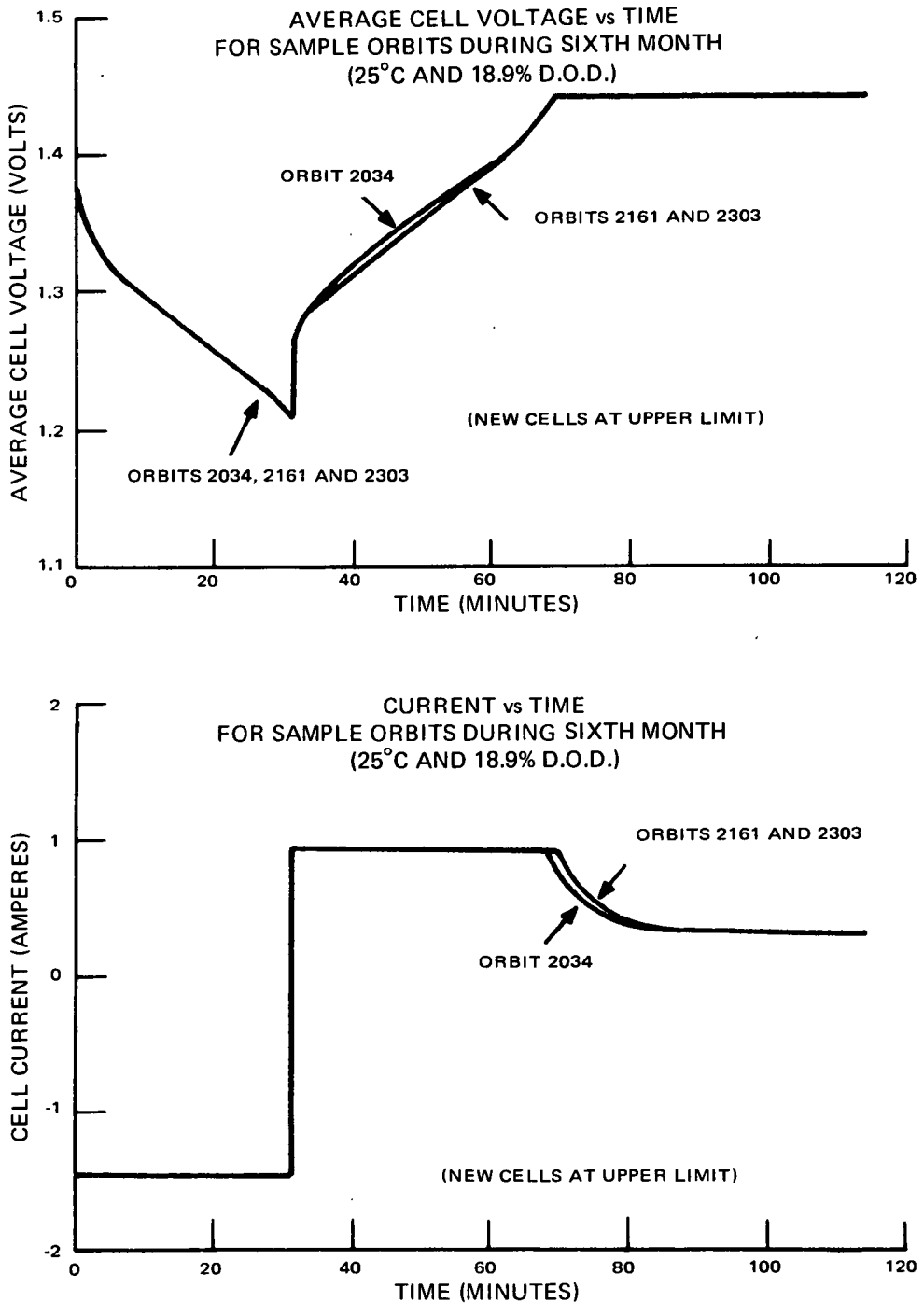

Figure B-30. Cell Current and Average Cell Voltage Versus Time (New Cells Tested-Orbit Cycles 2034, 2161, and 2303)

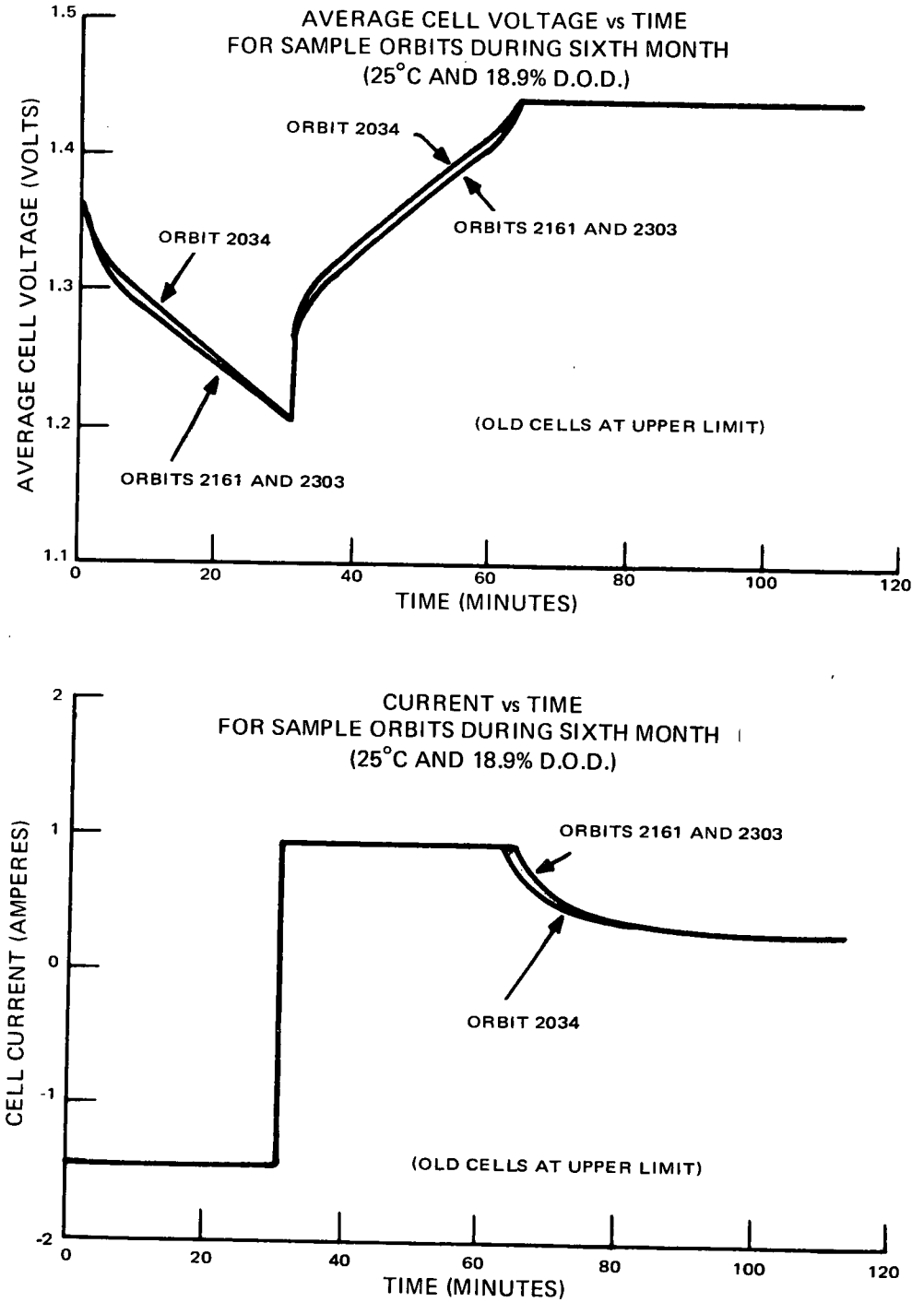

Figure B-31. Cell Current and Average Cell Voltage Versus Time (Old Cells Tested-Orbit Cycles 2034, 2161, and 2303)

The end-of-charge current is a measured variable, and for old cells is less than for new cells. During the first month, end-of-charge current was increasing, but during the second month this trend reversed. This current is affected by cell aging and temperature change, which is believed to explain the trend reversal and differences between old and new cells.

At orbit number 2387, the timing equipment malfunctioned such that the discharge continued until the cells had discharged approximately 30 percent of rated capacity. The lowest cell terminal voltage when this discharge was manually terminated was 1.08 volts. After the repair of the equipment, the cells were charged for 234 minutes rather than the scheduled 82-minute recharge, and the test resumed.

This extended discharge and charge cycle radically effect the end-of-discharge voltage for the subsequent cycles as plotted on Figure B-1 and Figure B-2. The end-of-discharge voltages reverted to the levels of the second month of the test program but, more significantly, the voltages decrease more rapidly than during the second month. As a result of this test interruption, the average end-of-discharge cell voltages were higher (1.212 volts for new cells and 1.208 volts for old cells) at the end of the seventh month than at the end of the sixth month. The minimum requirement for the spacecraft mission using a 22-cell battery is 1.205 volts, and for a 23-cell battery 1.152 volts. The range of end-of-discharge cell voltages for the new cells after seven months was 1.184 to 1.231 volts and the range for the old cells was 1.145 to 1.222 volts.

b. End-of-Discharge Voltage for 22- and 23-Cell Batteries

The data shown on Figure B-2 is identical to the bottom graph on Figure B-1 except that the voltage is based on either a 22-cell battery or a 23-cell battery. A curve is also shown to represent the design estimate for the six-month mission with a 22-cell battery.

c. Two-Minute Sample Cycle Data for New Cells

In addition to obtaining test data at the end of each charge, discharge period, data was also recorded during sample cycles at two-minute intervals. In Figure B-3 these data are plotted for new cells for the 2476th and 2661 cycles. From these same data, the ratio of ampere-minutes charge to ampere-minutes discharge was calculated and is plotted in Figure B-7. After showing an increasing trend during the first month, the "percent recharge" decreased each month through the sixth month. The seventh month shows the same percent recharge as the sixth month, however, indicating that the decline was due mainly to temperature change.

d. Two-Minute Sample Cycle Data for Old Cells

The same data is presented for old cells in Figure B-4 as was presented for new cells in Figure B-3.

e. Sample Cycle Data for New Cells, Using Upper Voltage Limit

During the test program the voltage limit placed on the cells was as indicated on Table B-2. This limit is the lower voltage limit of the battery performance specification. During sample cycles, however, the voltage limit was raised to the upper limit of the battery performance specification, and cell data was recorded at two-minute intervals. This data is presented in Figure B-5 for the new cells. Not only are the end-of-charge currents and the "percent recharge" substantially higher than for the lower voltage limit, but the end-of-discharge voltages are also higher.

f. Sample Cycle Data for Old Cells, Using Upper Voltage Limit

The same data as is shown in Figure B-5 for the new cells is shown in Figure B-6 for old cells.

g. Calculated Recharge Percentages for Sample Cycles

The "percent recharge" which was calculated for each sample cycle at both the lower and the upper voltage limit is shown as a function of the cycle number (time). In addition to the total recharge, the "percent recharge" of the cells was also calculated for the time period before the cells reached the imposed voltage limit.

h. Cell Voltage and Current Profiles for Sample Cycles

Figures B-8 through B-31 show the average cell voltage - current profiles for sample cycles during the first six months of test. Since the temperature, depth of discharge, and limiting charge voltage were varied in each month, it is difficult to make an accurate assessment as to the changes in charge and discharge characteristics that are directly related to age or number of cycles. A direct comparison can be made, however, from the beginning of the sixth month to the end of the seventh month since these two months were run under identical conditions. In comparing Figures B-3, B-4, B-5, and B-6 with Figures B-28, B-29, B-30, and B-31, note that there is no significant change for the charging

characteristics over this period of approximately 540 cycles. However, there was a difference between new cells and old cells throughout the test program and AED believes a gradual change in both charge and discharge voltage characteristics related directly to aging and cycling does occur.

4. CONCLUSIONS

It is concluded that under the worst-case conditions of temperature, depth of discharge, and charge voltage limitation, the 23-cell nickel cadmium battery will support a seven-month spacecraft mission. It is also concluded that a 22-cell battery cannot reliably support a six-month mission under similar worst-case conditions but could so do under nominal conditions of temperature, depth of discharge, and charge voltage limitation. It is indicated that if the voltage limit were raised to the level originally proposed for the system, the 22-cell battery would maintain a minimum voltage of 26.5 volts.

The charge - discharge characteristics curves in Figures B-3 through B-6 and B-8 through B-31 were used to adjust the characteristic cell data used in the power system computer program.

APPENDIX C

ITOS MAGNETIC TAPE EVALUATION

1. Introduction

This appendix describes the tests performed and results obtained on the 3M-551 and Memorex-161 magnetic tapes for the purpose of evaluating the two in order to select the ideal tape for use in the ITOS SR and AVCS tape recorders. The original requirement was that the tape recorders for ITOS perform within specification up to +60°C. In the present state of the art, magnetic tapes deteriorate at this high temperature and this requirement could not be met. The object of this test program, therefore, was to determine the high temperature limits for the magnetic tape which was presently in stock and in sufficient quantities for the ITOS program.

The 3M-551 magnetic tape evaluation report was completed on August 2, 1968, followed by the Memorex 161 magnetic tape evaluation report, completed on February 28, 1969. Magnetic tape for the incremental tape recorder (ITR) was not included as part of this evaluation as it is a special thin tape and the motion of the ITR is completely different from that of the SR and AVCS recorders.

A summary of the test results indicates that the 3M-551 magnetic tape can be used on the ITOS program up to +45°C. The tape showed appreciable damage after an exposure of only 10 record-playback cycles of operation at +55°C, and considerable damage was evident after 100 cycles of operation at +55°C. However, after an additional 100 cycles of operation at +45°C, the amount of damage to the tape was reduced to such a point that it can be safely stated that the ITOS tape recorders should provide reliable performance if the tape recorder qualification and flight acceptance tests do not expose the recorders to temperatures higher than +45°C.

The Memorex 161 magnetic tape test results show that this tape is a valid back-up tape for use on the ITOS program up to +45°C. In contrast to the 3M-551 magnetic tape, which showed some damage after 100 cycles of operation at +45°C, the Memorex 161 tape did not show any damage after similar cycling. Some specks of mylar were observed close to the ends of tape travel, and this was attributed to scuffing of the tape by the levers on the end-of-tape microswitches.

Though the Memorex 161 tape successfully passed the test at +45°C, it was learned soon after the conclusion of the tape test program that the Memorex 161 magnetic tape was no longer commercially available as the manufacturer ceased to market tape suitable for this application.

2. Description of 3M-551 Magnetic Tape Test

a. TEST SETUP

A block diagram of the test setup for testing the 3M-551 magnetic tape is shown in Figure C-1.

(1) BREADBOARD MODEL

The breadboard model of the SR servo recorder was used as the test bed. This breadboard was chosen because it records at a lower speed than the AVCS recorder, and past history has shown that the lower the speed, the more susceptible the tape is to damage. The tape path of the SR breadboard recorder is the same as that of the AVCS recorder and slightly more severe on the tape than is the SR recorder itself, because the end-of-tape posts constantly rub the tape in the AVCS configuration, but only rub near the ends of tape in the SR configuration. Figure C-2 is a top view of the SR recorder breadboard model.

The tape recorder assembly consisted of the following:

- Breadboard transport from the QRA-5 engineering model.
- DC motor and encoder assembly, replacing the original QRA-5 synchronous motor and belt drive.
- Breadboard electronics, which is functionally similar to the SR engineering model electronics.

(2) TEST EQUIPMENT AND INSTRUMENTATION

The test equipment used in instrumenting the ITOS magnetic tape test is listed in Table C-1.

(a) Dropout Detector

The dropout detector (see Figure C-3) consists of a level detector (Schmitt Trigger) and a sawtooth generator which controls an "AND" gate. When the level of the input signal is below a certain level, the gate is closed and the output of the sinusoidal oscillator triggers the counter. The oscillator was set at the playback frequency (60 kHz) and the detector was set at 300 millivolts. Any value below this level was measured as a dropout.

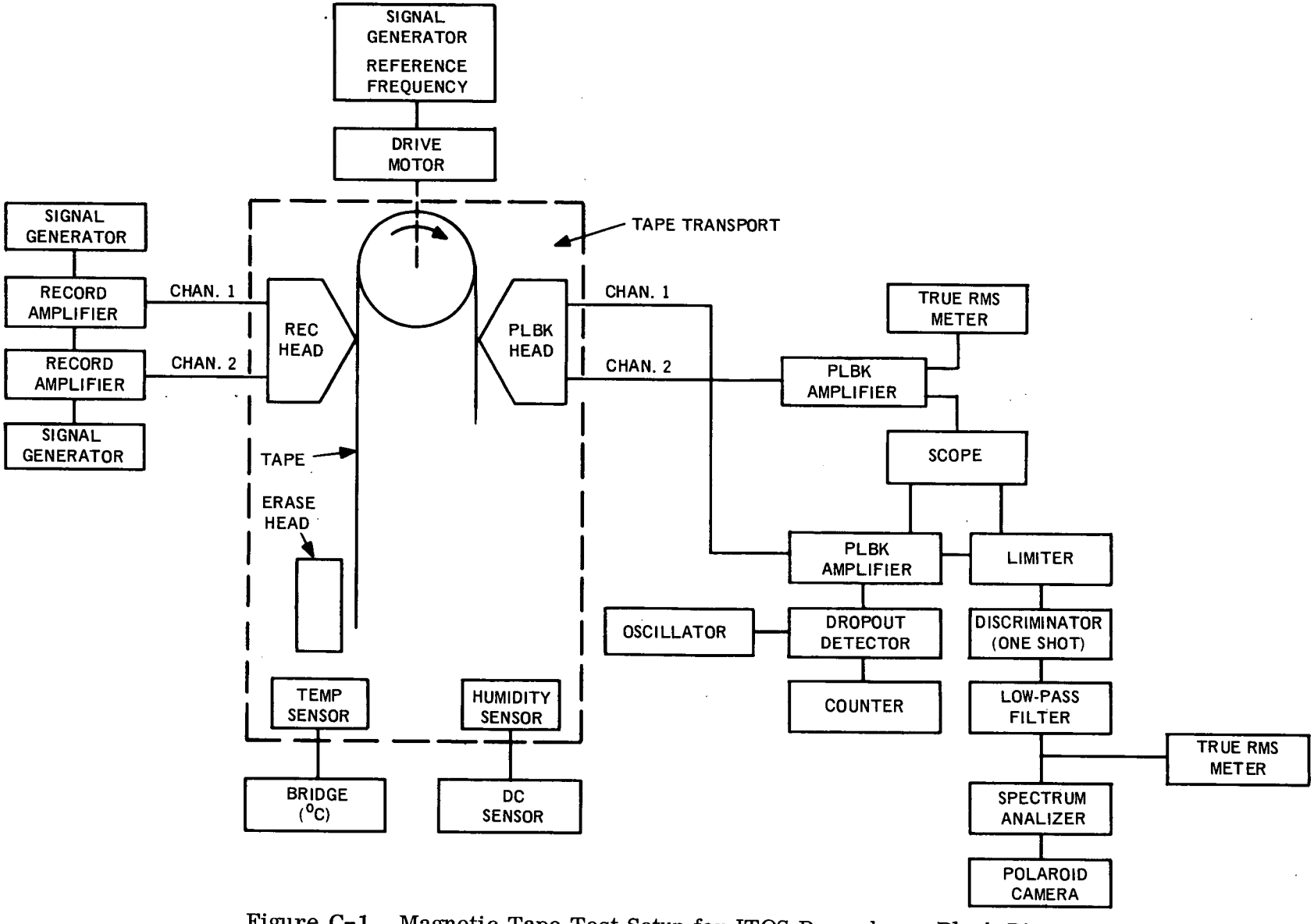

Figure C-1. Magnetic Tape Test Setup for ITOS Recorders, Block Diagram

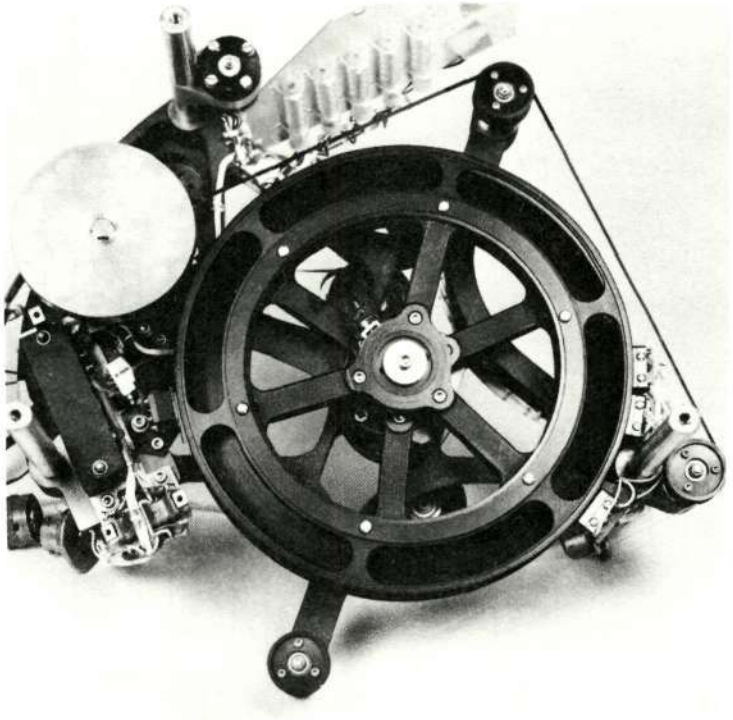

Figure C-2. SR Tape Recorder Breadboard Model, Top View

TABLE C-1. TEST EQUIPMENT FOR ITOS MAGNETIC TAPE TEST

Test Equipment	Manufacturer/Model
Frequency Meter and Discriminator	General Radio Co., Type 1142-A
True RMS Meters (2)	Ballantine Labs, Type 320-A
Signal Generators (3)	Hewlett-Packard Square Wave Generator, Model 211A
Oscillator	Hewlett-Packard Wide Range Oscillator, Model 200CD
Spectrum Analyzer	Nelson Ross Plug-In Spectrum Analyzer, used with Tektronix 535
Low Pass Filter	SKL, Variable Electronic Filter, Model 308A
Bridge	Temperature Potentiometer Leeds & Northrup, Type 8692
Counter	Hewlett-Packard, Model 523D
Electric Hygrometer Indicator	Hygrodynamics, Inc., Model 15-3001
Dropout Detector	(See Figure C-3.)

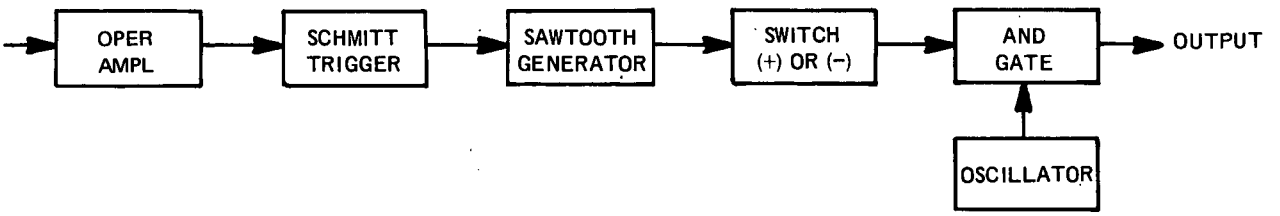

NOTE:

IF THE SAWTOOTH GENERATOR SIGNAL GROWS ABOVE A CERTAIN LEVEL, THE SWITCH BECOMES POSITIVE AND CLOSES THE AND GATE. EACH TIME THE SCHMITT TRIGGER IS TRIGGERED, THE SAWTOOTH SIGNAL STARTS GROWING FROM ZERO.

Figure C-3. Dropout Detector Circuit, Block Diagram

The test was conducted in the tape recorder laboratory and a noisy electrical environment created by neighboring interfering equipment caused a number of dropouts that was not consistent during weekdays. Information is, therefore, furnished for weekend readings only.

(b) Flutter Measurements

The readings in the true rms meter are directly proportional to the cumulative flutter percent rms. The conversion formula from millivolts rms to flutter percent rms is:

$$\text{Flutter \% (rms)} = \frac{\dfrac{\text{maximum frequency}}{\text{max. deviation (mV)}} \ \text{output (mV)} \times 100 \times \begin{pmatrix}\text{filter}\\ \text{attenuation}\\ \text{factor}\end{pmatrix}}{\text{f (carrier, Hz)}}$$

$$= \frac{1000 \times \text{output (mV)} \times 30/11}{60{,}000 \text{ Hz}} = \frac{\text{output (mV)}}{22}$$

In general, the flutter figures with new tape at +25° C have been above (outside) specification (0.3 percent). This is believed to be caused by the breadboard quality tape recorder that has been used for the test.

The low-pass filter was set at 7.2 kHz; therefore the cumulative flutter involves components from DC to the above mentioned frequency.

b. TEST PROGRAM

It was decided that a test program consisting of 100 cycles (record/playback) at the temperature of interest would be sufficient to provide meaningful data. The number of cycles (100) was determined by computing the expected number of cycles that a recorder would experience during flight testing, both as a subsystem and during the spacecraft level tests. This number of cycles was then multiplied by a safety factor of 2-1/2, an arbitrary number (which was used merely to supply greater confidence) providing the final figure of 100 cycles.

The tape recorder was loaded with 3M-551 tape (1/4-inch width) and the erase, record, and reproduce heads aligned. The recorder was then tested for proper electrical performance, after which it was put into a sealed container. The humidity was then measured to ensure that it was 30 percent relative humidity (±5 percent) at room temperature. If necessary, water or dessicant was added until satisfactory humidity readings were obtained.

A test cycle was then run, consisting of the following:

(1) Measurement of performance at +25° C.

(2) Stabilize at desired test temperature, and run to destruction or to 100 record/playback cycles, whichever is less. Measurement of performance was taken periodically.

(3) Stabilize at +25° C and remeasure performance.

The following parameters were measured: cumulative flutter percent (rms), number of dropouts, frequency response (two points), record motor currents, temperature, humidity, and record and playback times.

On track I, the record frequency was 3.75 kHz and the playback frequency was 60 kHz (16:1 ratio).

Track II was used to measure frequency response. The selected record frequencies were 1.95 kHz and 3.75 kHz which yield, on playback, 31.2 kHz and 60 kHz respectively. These two frequencies correspond to limits of the FM signal spectrum.

The amplitude of the signal was 5 milliamperes (peak-to-peak) from a 750-ohm source.

c. TEST RESULTS

(1) 3M-551 TAPE TEST RESULTS AT +55°C

This test consisted of five cycles at stabilized room temperature (+25°C) and 10 cycles at +55°C. The results of the test are summarized in Table C-2.

TABLE C-2. 3M-551 TAPE TEST RESULTS AT +25°C AND +55°C

Temp. (°C)	Track I		Track II (volts)		Motor Currents (mA)	
	Cumulative Flutter (% rms)		1.95 kHz	3.75 kHz	Record	
	Start*	End*			Start*	End*
+25	6 mV/0.27	6 mV/0.27	2.5	1.75	13	28
+55	100 mV/4.5	9 mV 0.41	2.2	1.4	12	38
+25 (after test)	6 mV/0.27	6 mV/0.27	2.5	1.6	8	30
*Start = Start of tape End = End of tape						

(a) Comments

At the end of the test, the tape was found in extremely bad condition, particularly at end-of-tape record, and there were oxide binder and mylar deposits on the heads.

Excessive flutter was measured at the start of playback (end-of-tape record). Figure C-4 shows the condition of the tape with severe oxide binder pullouts. Figure C-5 shows the record head condition after the +55°C test run.

(b) Conclusion

The 3M-551 magnetic tape cannot meet the performance requirements at +55°C.

(2) 3M-551 TAPE TEST RESULTS AT +50°C

The test consisted of two test runs, each of 50 cycles at +50°C. The results of each test run are summarized in Tables C-3 and C-4, respectively.

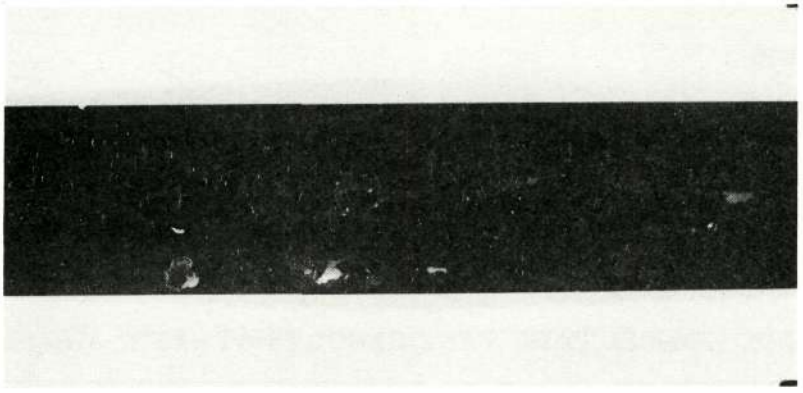

Figure C-4. 3M-551 Magnetic Tape Condition After +55 °C Test Run, Showing Severe Oxide Binder Pullouts

The average number of dropouts at the beginning and end of test at +50 °C was 150 and 700, respectively.

(a) Comments

After the end of each test run of 50 cycles at +50 °C, the heads and tape were inspected. At the time of the first inspection, there were some

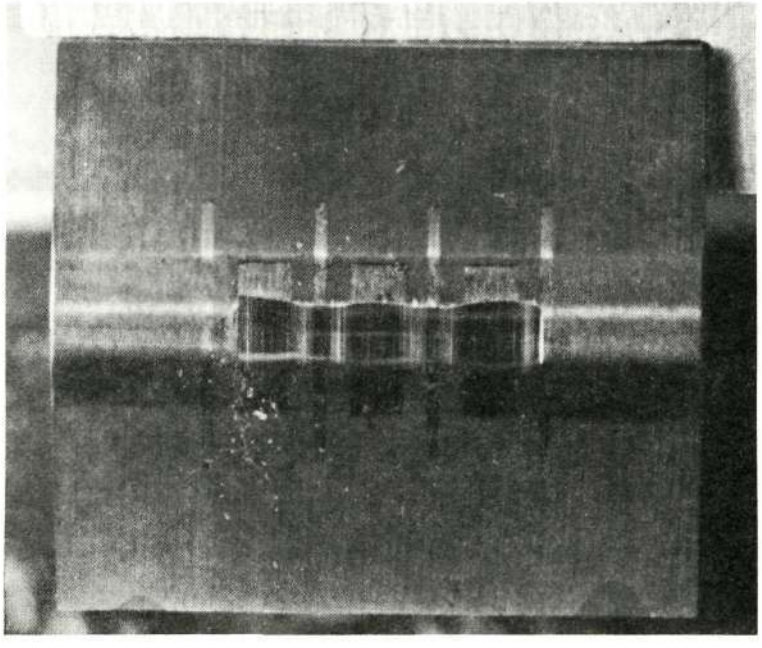

Figure C-5. Record Head, After +55° C Test Run of 3M-551 Tape

TABLE C-3. 3M-551 TAPE TEST RESULTS AT +50°C FOR FIRST 50 CYCLES

Temp. (°C)	Track I		Track II (volts)		Motor Currents (mA)	
	Cumulative Flutter (% rms)		1.95 kHz	3.75 kHz	Record	
	Start*	End*			Start*	End*
+25	5 mV/0.23	5 mV/0.23	2.4	1.5	8	24
+50	12 mV/0.55	11 mV/0.5	2.4	1.4	15	42
*Start = Start of tape End = End of tape						

TABLE C-4. 3M-551 TAPE TEST RESULTS AT +50°C FOR SECOND 50 CYCLES

Temp. (°C)	Track I		Track II (volts)		Motor Currents (mA)	
	Cumulative Flutter (% rms)		1.95 kHz	3.75 kHz	Record	
	Start*	End*			Start*	End*
+25	8 mV/0.36	7 mV/0.32	2.1	1.15	12	34
+50	10 mV/0.45	8.5 mV/0.39	2.2	1.25	15	38
+25 (after test)	8.5 mV/0.39	8.5 mV/0.39	2.5	1.5	14	36
*Start = Start of tape End = End of tape						

deposits on the heads but the tape did not show any damage from end-of-tape playback through the middle of the tape. In the second half of the tape (to end-of-tape record), some signs of damage were found.

At the end of the 100th cycle, there was no significant increase in the amount of head deposits, but the tape showed increasing signs of damage at the end-of-tape record.

Comparing the results at +55°C and at +50°C, a substantial improvement in performance was noticed at the latter temperature. The decrease of cumulative flutter percent rms during the second part of the test was probably caused by a difference in the head alignment. This test showed that electrical performance is not a sensitive enough indicator of tape damage.

Figure C-6 shows the condition of the 3M-551 tape at end-of-tape record for the +50° C test run. Figure C-7 shows the record head with some accumulated deposits after the test run at +50° C.

(b) Conclusion

As the 3M-551 tape is substantially damaged when subjected to 100 cycles at +50°C, the tape was not considered satisfactory for use at this temperature, even though the electrical tests indicated proper performance.

(3) 3M-551 TAPE TEST RESULTS AT +45°C

This test consisted of two test runs, the first of 57 cycles, and the second test of 43 cycles, both at +45°C. The results of the two test runs are summarized in Tables C-5 and C-6, respectively.

The average number of dropouts at the beginning of the test at +45°C was 300.

(a) Comments

After the first test run of 57 cycles, the only sign of deterioration appeared at the end-of-tape record, but it was very slight. The record heads showed debris deposits during both inspections (after the 57- and 43-test run operations). At the end of the 100th cycle of operation at +45°C, the tape was still in good condition, except for a small zone at both ends of the tape, that showed damage. However, the damage did not affect the tape recorder operation.

No trends were observable in the electrical performance measurements with regard to forecasting incipient or progressive damage.

Figure C-8 shows the condition of the 3M-551 tape at end-of-tape record (after 100 cycles operation at +45°C). Figures C-9 and C-10 show the debris on the record head after 57 cycles and 100 cycles of operation, respectively, at +45°C.

The record and playback times were fairly constant throughout both test runs. The typical values were:

- Record time = 8540 seconds (8485 min; 8557 max)
- Playback time = 534 seconds (531 min; 535 max)

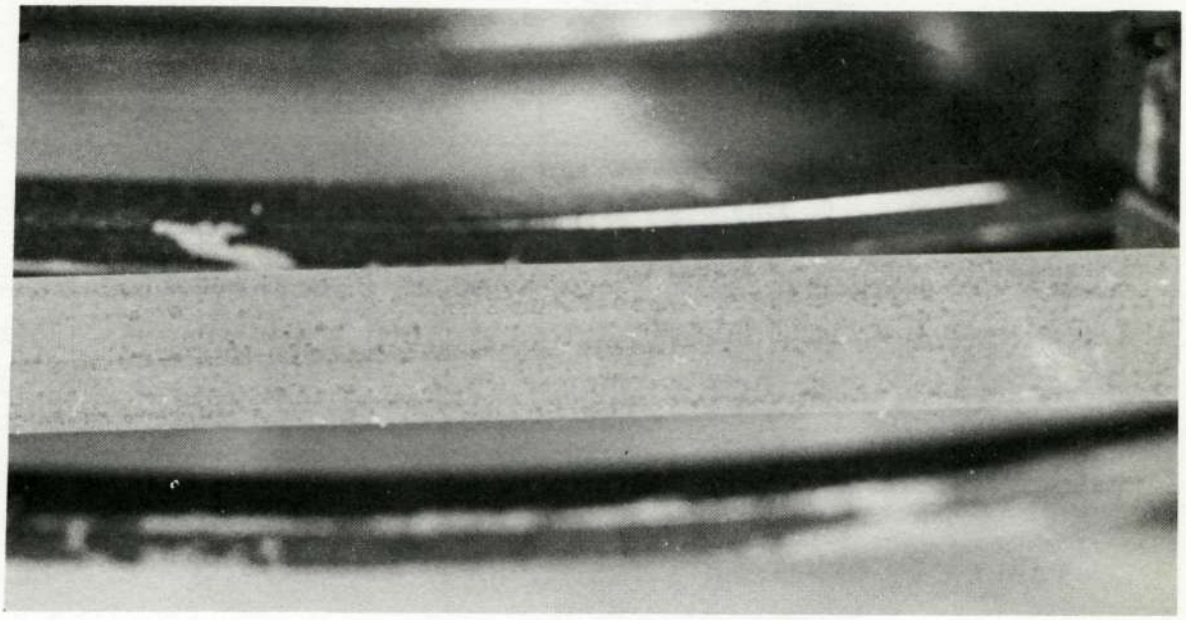

Figure C-6. 3M-551 Magnetic Tape Condition After +50° C Test Run, Showing Damage at End-of-Tape Record

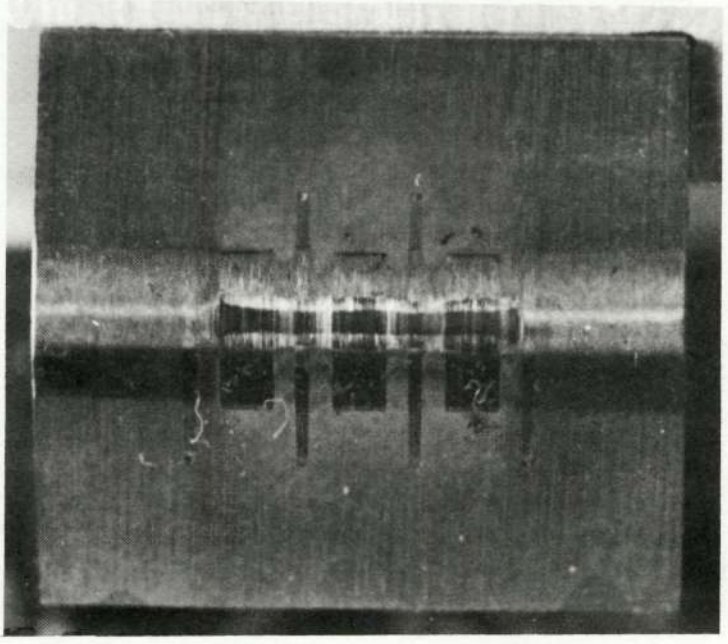

Figure C-7. Record Head with Accumulated Deposits After +50° C Test Run of 3M-551 Tape

TABLE C-5. 3M-551 TAPE TEST RESULTS AT +45°C FOR 57 CYCLES (FIRST TEST RUN)

Temp. (°C)	Track I		Track II (volts)		Motor Currents (mA)	
	Cumulative Flutter (% rms)		1.95 kHz	3.75 kHz	Record	
	Start*	End*			Start*	End*
+25	10 mV/0.45	9 mV/0.41	2.6	1.7	15	42
+45	11 mV/0.5	8.5 mV/0.39	2.6	1.5	16	50
*Start = Start of tape End = End of tape						

TABLE C-6. 3M-551 TAPE TEST RESULTS AT +45°C FOR 43 CYCLES (SECOND TEST RUN)

Temp. (°C)	Track I		Track II (volts)		Motor Currents (mA)	
	Cumulative Flutter (% rms)		1.95 kHz	3.75 kHz	Record	
	Start*	End*			Start*	End*
+25	8 mV/0.36	7.5 mV/0.34	2.6	1.7	14	45
+45	10 mV/0.45	9 mV/0.41	2.45	1.4	18	52
+25 (after test)	9.2 mV/0.42	8.5 mV/0.39	2.6	1.45	16	48
*Start = Start of tape End = End of tape						

(b) Conclusion

Acceptance testing to +45° C on ITOS SR and AVCS recorders was possible without a high probability of creating a latent failure mode which would cause subsequent failure in orbit. This conclusion was based on the following:

(1) A much greater damage was sustained by the tape at +50° C without performance failure.

Figure C-8. 3M-551 Magnetic Tape Condition After 100 Cycles of Operation at +45° C

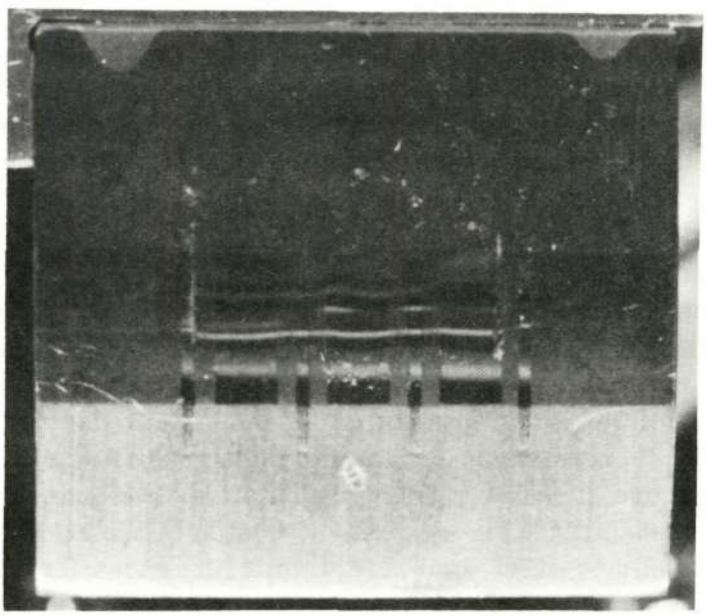

Figure C-9. Record Head, Showing Debris on Head After 57-Cycle Test Run of 3M-551 Tape at +45° C

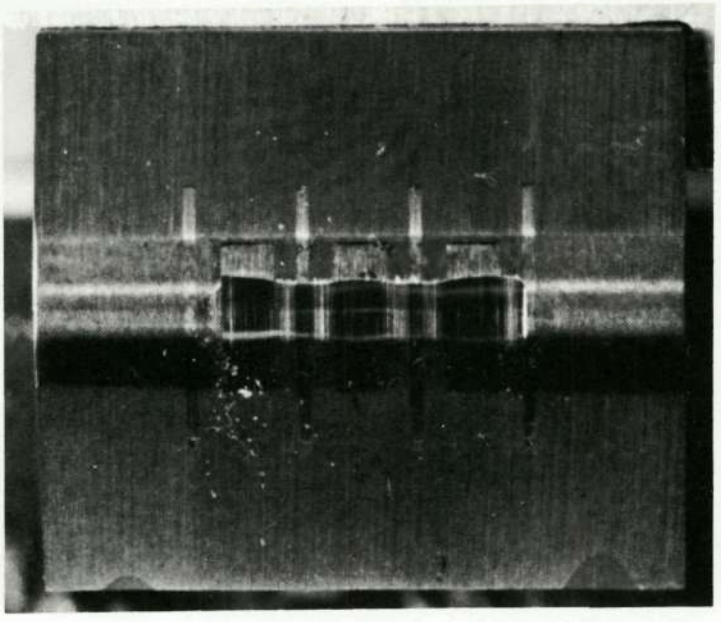

Figure C-10. Record Head, Showing Debris on Head After Completing 100-Cycle Test Run of 3M-551 Tape at +45°C

(2) After the +45°C test was completed, a motor life test was performed leaving the same tape on the recorder. This motor life test consisted of running the transport the same number of passes it would experience in one year of orbital operation, but it was cycled continuously at 37.5 ips for both record and playback rather than normal operation which would be 1.875 ips record (30 ips playback). Thus, the life test was completed in one month. Flutter was measured during the test; although it increased 50 percent at the middle and 100 percent at the end-of-tape (compared to the flutter readings at the beginning of the life test), there was no catastrophic failure. There was an increase in the amount of loose mylar particles along the surface of the tape at the end of this test, but no noticeable increase in damage (pullouts). Although the record speed was nonrepresentative, the ends-of-tape (the most critical areas) were subjected to the correct number of stops and starts, an action which degrades the tape because it enhances the possibility of oxide-binder pullouts.

(3) The SR engineering model was loaded with 3M-551 tape and soaked for 12 hours at +50°C, to simulate the conditions during spacecraft testing. At the end of the test the tape was inspected and no imperfections were observed.

(4) FLUTTER VARIATION FOR TAPE TESTS AT +55°C, +50°C, AND +45°C

Variation of flutter for the 3M-551 tape tests at +55° C, +50° C, and +45° C is shown in Figures C-11, C-12 and C-13, respectively. No clear and easily interpreted trend is apparent, although further testing might have revealed that a slight positive slope might be readable.

The motor current readings varied, but like the flutter, not in any clearly defined manner.

3. Description of Memorex 161 Magnetic Tape Test

a. TEST SETUP

The test setup for testing the Memorex 161 magnetic tape was similar to that for the 3M-551 tape test, including the breadboard model, test equipment, and instrumentation.

b. TEST PROGRAM

The record and playback heads were first reground and polished to remove the wear track present from previous tests. The head assembly was then reworked to update it to the present configuration used on the AVCS and SR recorders.

The recorder was then loaded with 1400 feet of Memorex 161 magnetic recording tape. This recorder was then installed in an airtight container. After 24 hours elapsed, during which time the recorder was cycled once, the humidity was seen to have stabilized at 25 percent relative humidity, an acceptable value.

The performance of the recorder was measured at +25° C, then during 117 record-playback cycles at +45° C, and finally at +25° C.

The following parameters were measured: accumulative flutter (percent rms), number of dropouts, record motor currents, temperature, and humidity. On track 1, the record frequency was 3.75 kHz and the playback frequency was 60 kHz (16:1 ratio).

c. TEST RESULTS

Test measurements were recorded at four different times during the 117 record-playback cycles at +45° C. The results of these tests are summarized

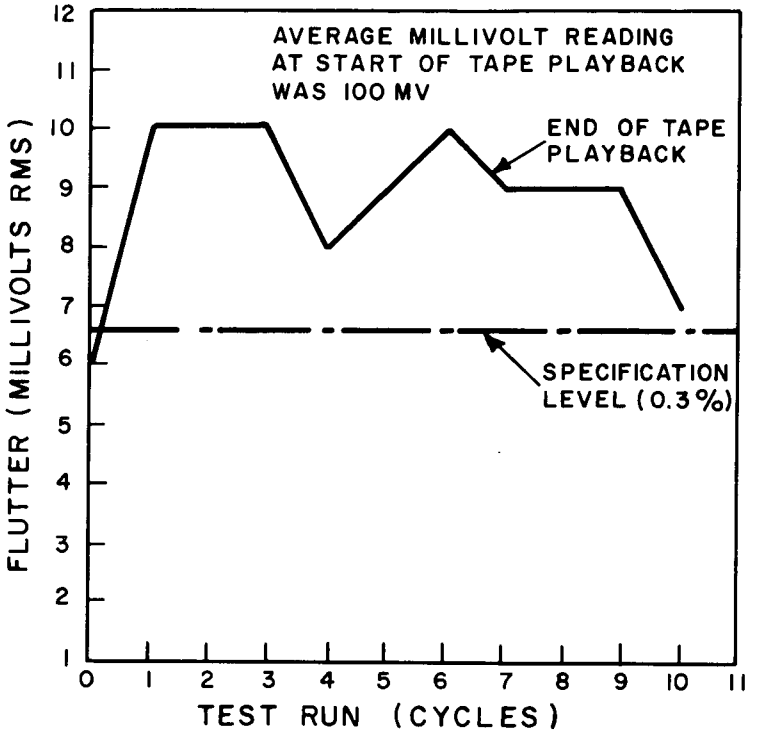

Figure C-11. Flutter Variation in 3M-551 Tape at +55°C (10 Cycles)

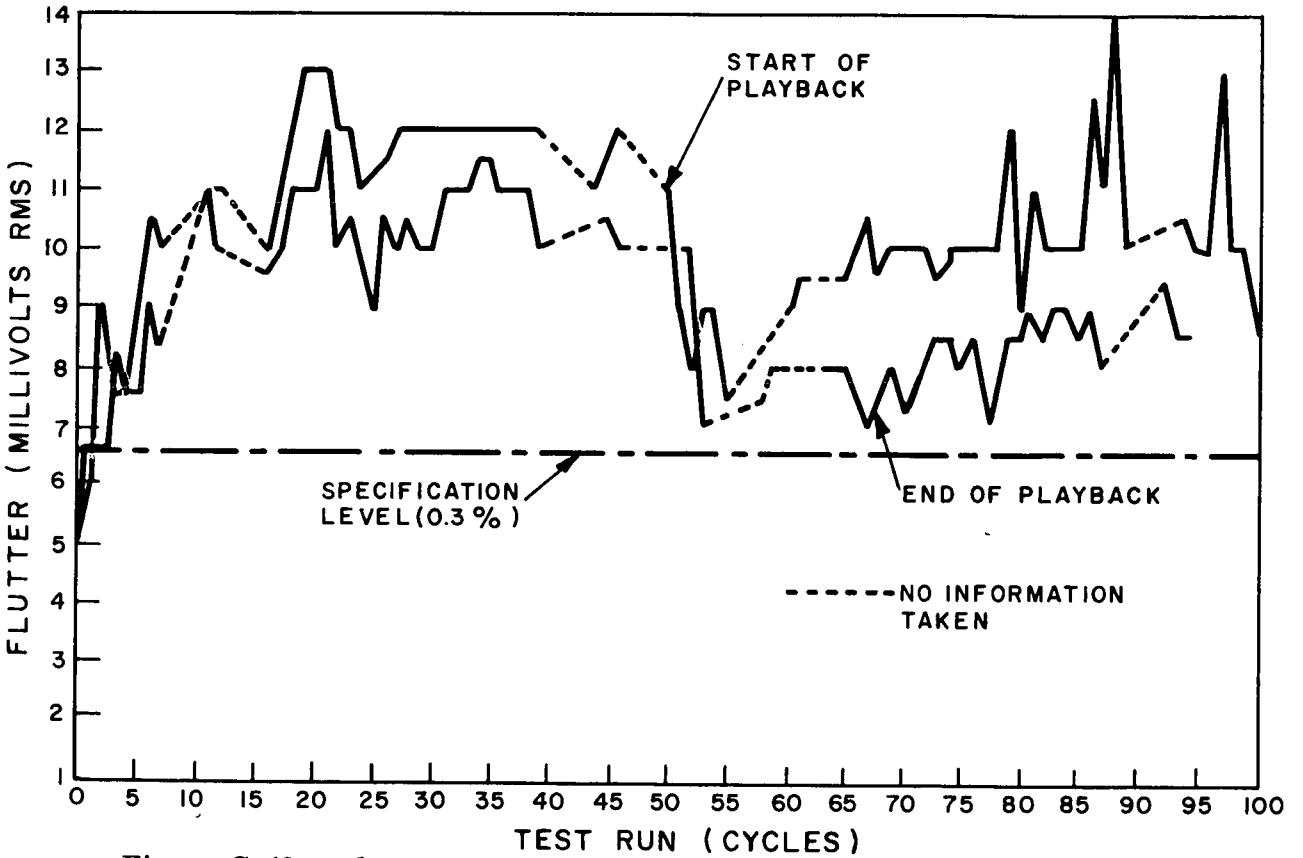

Figure C-12. Flutter Variation in 3M-551 Tape at +50°C (100 Cycles)

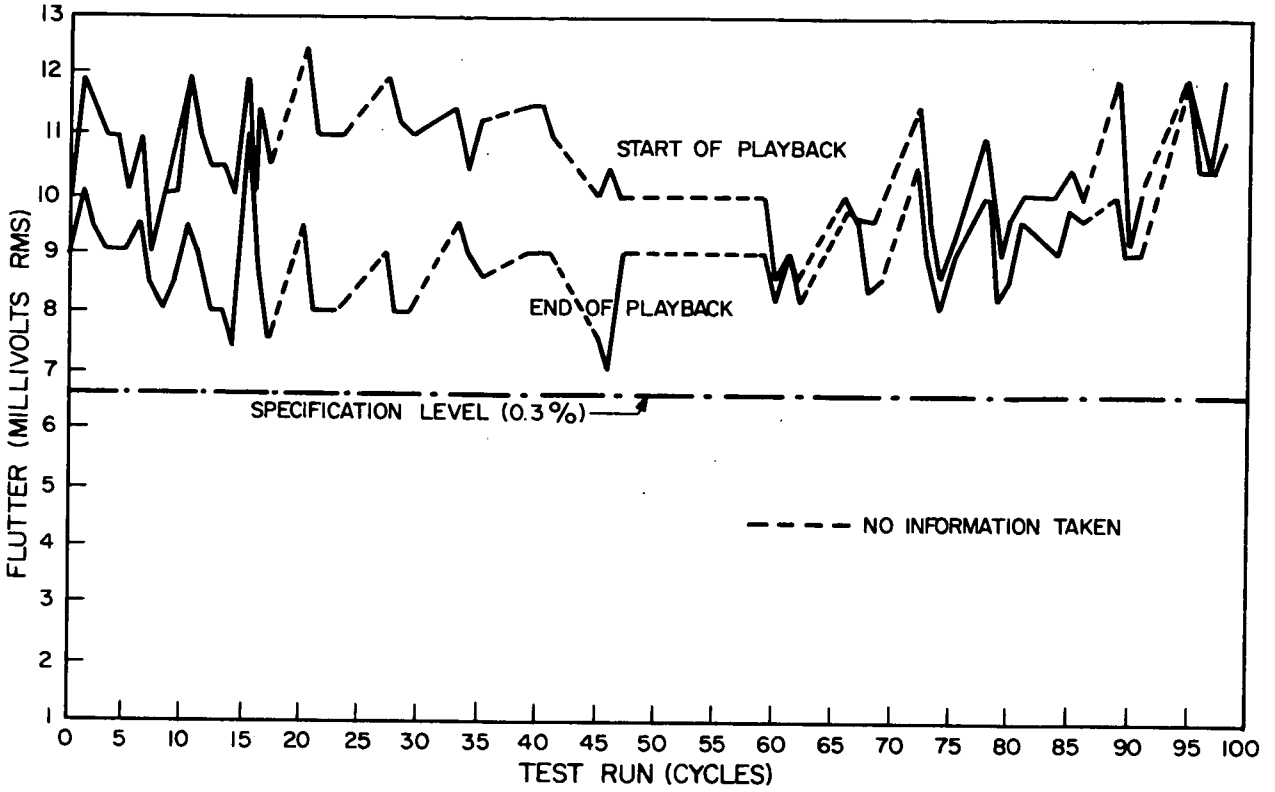

Figure C-13. Flutter Variation in 3M-551 Tape at +45° C (100 Cycles)

in Table C-7. (Detailed data is recorded in RCA Laboratory Notebook No. 35176, pages 48 through 50, and in RCA equipment log book, Tape Evaluation Test Log No. 5, pages 1 through 25.)

TABLE C-7. MEMOREX 161 TAPE TEST RESULTS AT +45° C

Temperature (°C)	Cumulative Flutter (% rms)		Dropouts	Motor Current (mA)	
	Start*	End*		Start*	End*
+25	0.29	0.32	0	12	32
+45 1st Cycle	0.4	0.4	Not taken	12	34
+45 53rd Cycle	0.32	0.31	326	12	36
+45 61st Cycle	0.37	0.26	Varies from	12	36
+45 117th Cycle	0.4	0.38	567 to 34,281	12	36
+25	0.72	0.68	13466	12	38

*Start = Start of playback End = End of playback

Figure C-14 shows the condition of the Memorex 161 tape after the 117th cycle of operation at +45° C. Figure C-15 shows the condition of the record and playback heads after completion of the Memorex 161 tape test at +45° C.

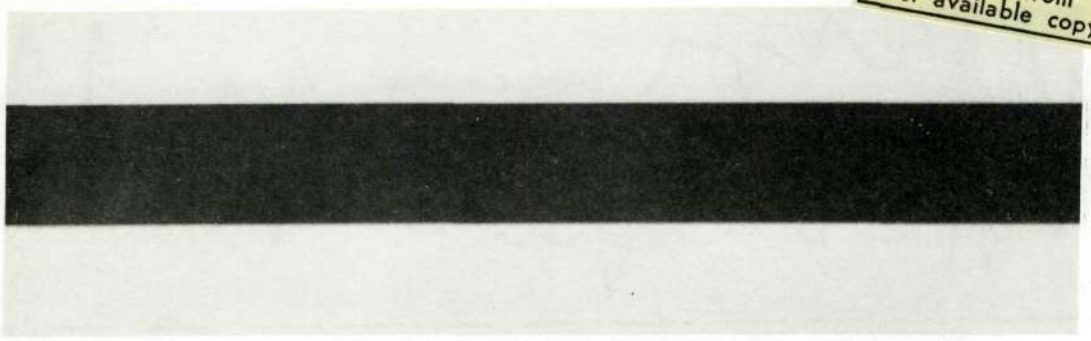

Figure C-14. Memorex 161 Magnetic Tape Condition After 117th Record-Playback Cycle at +45° C

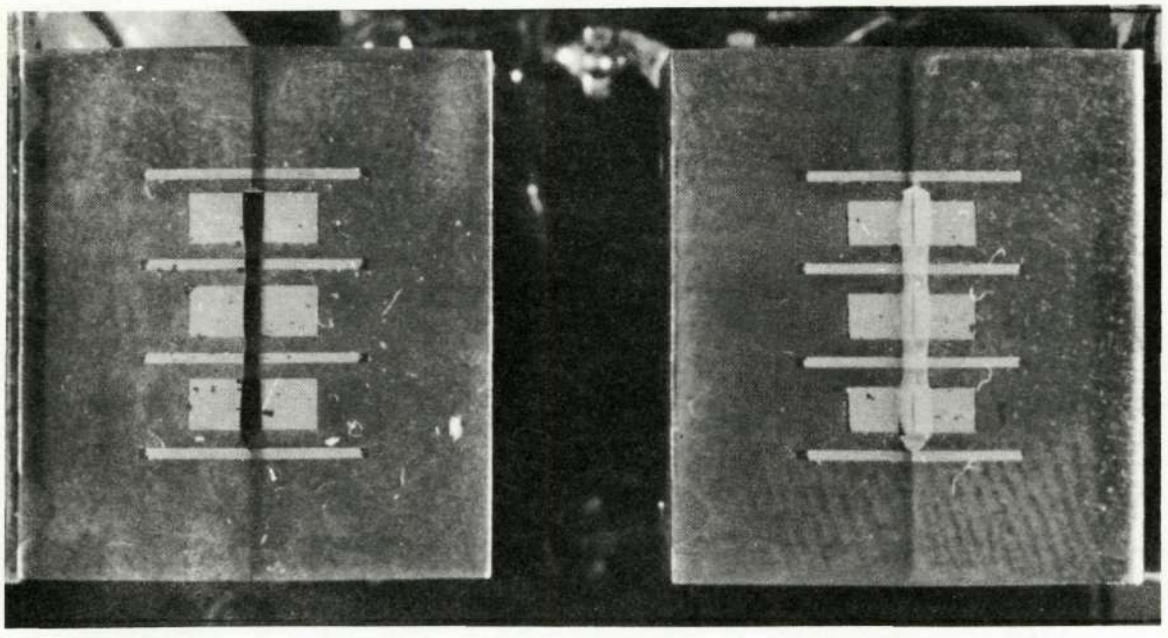

Figure C-15. Record (Left) and Playback Heads, Shown After Completion of Memorex 161 Magnetic Tape Test at +45° C

d. SUMMARY

(1) CAUSE FOR SIGNAL STRENGTH DETERIORATION AND DROPOUTS

Approximately halfway through the Memorex 161 tape test, the recorded signal dropped to about one half of its original strength, and continued to deteriorate until, at the end of the test, the signal strength was less than one third original strength. In addition to this, dropouts began varying widely from one run to another. Upon completion of the test, the heads were examined and it was discovered that the heads were so badly worn (due to extensive use, refinishing, and reuse) that the gaps were opening up. This would certainly

cause the drop in signal strength, and would also be likely to cause increased susceptibility to dropouts. There was no debris evident on either the tape or the heads to have caused this type of dropout performance. Thus the tape is assumed to have successfully passed the test. Flutter and motor current appeared to remain unchanged throughout the test.

(2) TAPE FLUTTER

The sudden rise in flutter shown in the final run at +25° C has not been explained, as the tape was removed before further testing could be accomplished. It was noticed that the humidity was relatively stable during the cycling at +45° C (20.3 to 26.8 percent) but shot up to 38.9 percent when returned to ambient for the final run. Perhaps this amount of humidity caused increased tape head friction, which caused head tape scrape flutter. The flutter spectrum taken during this run showed strong components in the range (3.8 kHz) associated with head tape scrape flutter.

APPENDIX D

COMPONENT BOX SERIAL NUMBERS

The serial numbers of the component boxes installed on the TIROS M Spacecraft are given in Table D-1.

TABLE D-1. TIROS M COMPONENT SERIAL NUMBERS

Component	Serial No.
Command and Control Subsystem	
Dual Command Decoder	02
Dual Command Programmer	02
Command Distribution Unit A	03
Command Distribution Unit B	02
Dual Time Base Unit	02
Power Supply Subsystem	
Battery 1	02
Battery 2	03
Power Supply Electronics	03
Solar Array Panel 1	02
Solar Array Panel 2	03
Solar Array Panel 3	05
Solar Array Actuator 1	103G
Solar Array Actuator 2	105G
Solar Array Actuator 3	104G
Solar Panel Pin Puller 1	26890, 26893
Solar Panel Pin Puller 2	26900, 26917
Solar Panel Pin Puller 3	26897, 26894

TABLE D-1. TIROS M COMPONENT SERIAL NUMBERS (Continued)

Component	Serial No.
Communications Subsystem	
Command Receiver	02
Beacon and Command Antenna	02
Beacon Xmtr and SCO Assembly	05
Dual SCO Assembly	05
Beacon Xmtr 1	08
Beacon Xmtr 2	10
Telemetry Conditioner	02
Commutator 1	2489
Commutator 2	2481
Multiplexer	02
S-Band Xmtr 1	10
S-Band Xmtr 2	13
S-Band Coupler	03
S-Band Antenna	03
Real-Time Xmtr 1	03
Real-Time Xmtr 2	05
Command Hybrid Coupler	193
RF Cable Assembly	02
RF Switch	02
Real-Time Antennas 1 (AVCS Panel)	09, 09
Real-Time Antennas 2 (APT Panel)	10, 10
Antenna Hybrid Coupler 1	50
Antenna Hybrid Coupler 2	71
148 MHz Notch Filter 1	04
148 MHz Notch Filter 2	05
136 MHz Notch Filter 1	02
136 MHz Notch Filter 2	03
Band Pass Filter	04

TABLE D-1. TIROS M COMPONENT SERIAL NUMBERS (Continued)

Component	Serial No.
Primary Sensor Subsystems	
AVCS Subsystem	
AVCS Camera and Electronics 1	04
AVCS Camera and Electronics 2	03
AVCS Recorder and Electronics 1	02/03
AVCS Recorder and Electronics 2	03/04
APT Subsystem	
APT Camera and Electronics 1	05
APT Camera and Electronics 2	06
SR Subsystem	
Scanning Radiometer and Electronics 1	F5
Scanning Radiometer and Electronics 2	F3
SR Recorder and Electronics 1	02
SR Recorder and Electronics 2	05
SR Processor	04
Secondary Sensors Subsystem	
Flat Plate Radiometer	03
Solar Proton Monitor Sensor	04
Solar Proton Monitor Electronics	05
Data Format Converter	03
Incremental Tape Recorder	03
Vehicle Dynamics Subsystem	
Momentum Wheel Assembly	06
Pitch Control Electronics	04
Momentum Coil	04

TABLE D-1. TIROS M COMPONENT SERIAL NUMBERS (Continued)

Component	Serial No.
Vehicle Dynamics Subsystem (Continued)	
QOMAC Coil	05
Magnetic Bias Switch	01
Digital Solar Aspect Sensor and Electronics	02
Nutation Damper 1 (APT Panel)	25
Nutation Damper 2 (AVCS Panel)	24
Accelerometer Control Unit	02
Accelerometer Assembly	02
Accelerometer (X - X)	2579
Accelerometer (Y - Y)	2973
Thermal Control	
Active Thermal Control 1	07
Active Thermal Control 2 (AVCS Panel)	08
Louver Assembly 1	07, 07
Louver Assembly 2	08, 09
Active Thermal Control 3 (APT Panel)	09
Active Thermal Control 4	
Spacecraft	
Separation Switch	09
Separation Switch	12
Wiring Harness	02
Strain Gage Amplifier	02